Innovations in Chemical Biology

Bilge Şener
Editor

Innovations in Chemical Biology

Springer

Editor
Bilge Şener
Gazi University
Ankara
Turkey

ISBN 978-1-4020-6954-3 e-ISBN 978-1-4020-6955-0

Library of Congress Control Number: 2008936994

Printed on acid-free paper

9 8 7 6 5 4 3 2 1

springer.com

Foreword

Before this book went to press; sad news was received of the sudden death, on November 5, 2006, of Professor Hitoshi Ohtaki.

Professor Dr. H. Ohtaki was one of the founders of the Eurasia series of conferences. His enormous service to organize this series of conferences have been aimed to deepen the friendship of chemists in the Eurasia continent, supporting scientific researches of chemists from other continents. This significant amount of voluntary work has earned great respect to him in the chemical community around the world.

The contribution to the latest Eurasia conference, *9th Eurasia Conference on Chemical Sciences* was tremendous and the conference proceedings will be an important memorial action of Hitoshi's Eurasia initiative.

Therefore, I would like to share this opportunity with you and his friends by adding tributes and messages in the book.

Preface

Modern life is complex and evolution went a long way starting from very simple organic molecules to larger biomolecules and they interact with other classes of molecules in the environment.

The growing role of chemistry and the contribution of chemical and pharmaceutical industries to the science of mankind are enormously going on. Next century will witness more tremendous achievements of chemistry as well as its application of different fields for the benefit of mankind life in terms of healthy, good, productive and comfortable long life.

The system for training researchers in the various areas of chemistry has maintained a largely traditional and single disciplinary focus. Although many investigators have broadened their selection of research techniques at the level of organized and integrated programs. The Eurasia region has increased its profile in chemistry, particularly chemical biology over the last 20 years.

Chemical Biology is one of the fastest areas of science as a multidisciplinary during this century. The interdisciplinary study of molecules in living systems at a health science campus helps to integrate the traditional disciplines of chemistry and biology by understanding the molecular mechanisms of biological processes provides an opportunity to manipulate them in a defined and predictable way.

The source of this book is the *9th Eurasia Conference on Chemical Sciences* (EuAs C_2S-9) held in Antalya-Turkey during September 9-13, 2006 under auspices of the IUPAC organized by the Society of Biological Diversity, Ankara-Turkey. This conference was part of a series Eurasia conferences that are held every two years since 1988 initiated by Professor Dr. Hitoshi Ohtaki, Professor Dr. Michael Rode and Professor Dr. Ivano Bertini. Eurasia conference is one of the dreams for realizing the development of chemical sciences in Asia with the cooperation of European countries. Therefore, this book belonged to the Proceedings of the 9th Eurasia Conference will give an excellent overview of the progress being made in the field of Chemical Biology.

This book will be an excellent issue for a rich scientific diversity in the field of Chemistry and Biology. The interpretation of chemistry for biology is probably slightly broader than what commonly is referred to as Chemical Biology, thus also including topics related to molecular biology, biochemistry, ecology, semiochemicals, environmental and material sciences.

This book includes 49 chapters presented as plenary, invited lectures and posters at the conference. Six plenary lectures have published in an issue of *Pure and Applied Chemistry,* Vol. 79, No. 12, 2007; the titles of these presentations are given as an Annex at the end of the book.

I thank all contributors for the preparation of their presentations.

It is sad to report that Professor Hitoshi Ohtaki, one of the founders of the Eurasia conferences and contributors passed away on November 5, 2006. Professor Ohtaki enthusiastically promoted international cooperation and took it upon himself to publicize Japanese science to the wider world. His contribution in this book will serve as a memorable contribution to that goal. He will be missed by all of us.

This book is dedicated to his memory.

Professor Dr. Bilge Şener
Editor

Memorial Tribute to Professor Dr. Hitoshi Ohtaki

Curriculum Vitae of Hitoshi Ohtaki

Date of Birth	September 16, 1932
Place of Birth	Tokyo, Japan
Date of Decease	November 5, 2006 (at the age of 74)
Address	3-9-406 Namiki-2-chome, Kanazawa-ku, Yokohama, Japan
Institution	Chair Professor of The Research Organization of Science and Engineering, Ritsumeikan University
	Guest Professor of Yokohama City University
Education	Bachelor of Science, Nagoya University, 1955
	Master of Science, Nagoya University, 1957
	Doctor of Science, Nagoya University, 1961

Professional Career

April	1959	Research Associate of Research Laboratory of Nuclear Reactors, Tokyo Institute of Technology
January	1965	Lecturer of Faculty of Science, Nagoya University
February	1967	Associate Professor of Faculty of Science, Nagoya University
August	1970	Associate Professor of Faculty of Engineering, Tokyo Institute of Technology
June	1973	Professor of Faculty of Engineering, Tokyo Institute of Technology
April	1975	Professor of Graduate School at Nagatsuta, Tokyo Institute of Technology
April	1988	Professor of the Institute for Molecular Science, Okazaki National Research Institutes
June	1988	Director of Coordination Chemistry Laboratories, Institute for Molecular Science, Okazaki National Research Institutes
October	1988	Professor of Faculty of Physical Sciences, Graduate University for Advanced Studies (Concurrent Post)
April	1992	Dean of Faculty of Physical Sciences, Graduate University for Advanced Studies
April	1993	Professor Emeritus of Tokyo Institute of Technology Professor Emeritus of Graduate University for Advanced Studies Professor of Faculty of Science and Engineering, Ritsumeikan University
April	1994	Director of Institute of Science and Engineering of Ritsumeikan University (until March 2000)
April	1998	The Leader of the Scientific Frontier Project “Analyses and Control of Specific Selectivities in Various Fields of Science and Technology” (until March 2003)
March	2003	Guest Professor of Yokohama City University
April	2003	Guest Professor of the Institute for COE Promotion, Ritsumeikan University

Awards

1976	The Matsunaga Prize (Matsunaga Science Foundation)
1989	The Tejima Memorial Award (Tejima Educational Foundations)
1990	Takei Prize of Electrochemical Society of Japan (Electrochemical Society of Japan)
1995	National Medal of Purple Ribbon (Japanese Government)

2000 The Prize for Scientific Merits of Electrochemical Society of Japan (Electrochemical Society of Japan)
2003 Medal for the Contribution to the Development of Science and Technology (Vietnam Union of Science and Technology Association)
2005 Kato Memorial Award (Kato Memorial Science Foundation)
2007 The Order of the Sacred Treasure, Gold Rays with Neck Ribbon (Japanese Government, posthumous award)

Honors

1999 Kato Memorial Lectureship (Electrochemical Society of Japan)
2002 17th M. H. Khundkar Memorial Lectureship 2002 (University of Dhaka, Bangladesh)
Honorary Professor of St. Petersburg University, Russia
Honorary Member of Japan Society of Coordination Chemistry
2003 Honorary Member of Japan Association of Solution Chemists
Medal of Vietnam Union of Science and Technology Associations

Science Council of Japan

July 1994–July 1997	Member of the 4th Division (Pure Science)
July 1997–July 2000	Vice President of the 4th Division
July 2000–July 2003	President of the 4th Division
1988–1991	Member of National Committee for IUPAC
1991–2003	Member of National Committee for Chemistry
	Secretary (1984–1991, 1994–1997)
	Chairman of Committee for Inorganic Chemistry (1997–2003)

International Activities

International Union of Pure and Applied Chemistry (IUPAC)
Chairman of Commission of Equilibrium Data
Member of Inorganic Chemistry Division
Coopted Member of Analytical Chemistry Division
Bureau Member
Chairman of Membership Developing Committee
Chairman of International Conferences in Developing Countries
Executive Committee Member

Science Council of Asia (SCA)
Organizing Committee Member (1994–2005)
Representative Delegate of Science Council of Japan (1998–2005)

Federation of Asian Chemical Societies (FACS)
Delegate of Chemical Society of Japan (1993–2001)
President Elect (1995–1997)
President (1997–1999)
Past President (1999–2001)

Eurasia Conference on Chemical Sciences (EuAs C_2S)
One of the Three Founders: Established in 1988
International Organizing Committee Member (1988–present)
Permanent General Coordinator (2003–2006) (equivalent to the President)
Chairman of International Organizing Committee of EuAs C_2S
1990 (Seoul, Korea)
1994 (Kuala Lumpur, Malaysia)
2002 (Karachi, Pakistan)
2006 (Antalya, Turkey)

PACIFICHEM
1989 PACIFICHEM
Organizing Committee Member
Chairman of Program Committee
Chairman of the National Steering Committee
1995 PACIFICHEM
Vice President
Chairman of Protocol and Public Relation Committee

Guest Professors in Other Countries
University of Innsbruck, Austria
Chulalongkorn University, Thailand
University of Valladolid, Spain

Number of Papers and Books
Number of Original Papers: 210
Number of Reviews: 88
Number of Books (including Editorial): 11
Number of Books Contributes in Chapters: 12
Number of Students Who Received Ph.D. 11

International Conferences Organized
VI International Symposium on Solute-Solute-Solvent Interactions, 1982, Minoo, Osaka (as Secretary General. Chairman: Professor Nobuyuki Tanaka of Tohoku University)
International Symposium on Molecular and Dynamic Approaches to Electrolyte Solutions, 1988, Tokyo (Chairman)
45th Okazaki Conference on Chemistry of Intra- and Intermolecular Charge Transfer of metal Complexes 1993 (Co-organizer)
30th International Conference on Coordination Chemistry, 1994 Kyoto (Chairman)

26th International Conference on Solution Chemistry, 1999, Fukuoka (Chairman)
International Symposium on New Horizons of Coordination Chemistry towards the 21st Century, 2001, Kusatsu, Shiga (Chairman)
2nd Eurasia Conference on Chemistry in Seoul, Seoul, Korea, 1900 (IOC Chairman. NOC Chairman: M. S. Jhon)
4th Eurasia Conference on Chemical Sciences, Kuala Lumpur, Malaysia, 1994 (IOC Chairman. NOC Chairman, M. M. Sign)
7th Eurasia Conference on Chemical Sciences, Karachi, Pakistan, 2002 (IOC Chairman. NOC Chairman: Atta-ur-Rahman)
8th Eurasia Conference on Chemical Sciences, Hanoi, Vietnam, **2003** (General Coordinator. IOC Chairman, Ivano Bertini; NOC Chairman, H. S. Thoang)
9th Eurasia Conference on Chemical Sciences, Antalya, Turkey, **2006** (General Coordinator. IOC Chairman, H. Ohtaki, NOC Chairman, B. Sener)

September 11, 2006 Antalya-Turkey

Dear IOC members and Fellows of EuAs C_2S,

I should inform you of very sad news that Professor Hitoshi Ohtaki, Permanent General Coordinator, PGC, passed away due to myocardial infarction in the morning on November 5th. I would like to pray with you for the repose of Hitoshi's soul.

Sincerely yours
Susumu Kitagawa
IAB member of EuAs C_2S

Message from Associate Professor Dr. Michitaka OHTAKI (His son)

My father, Hitoshi Ohtaki, passed away at his second home (used as his office) by myocardial infarction in the early morning of November 5th (Sunday), 2006.
My mother, Ei Ohtaki, coming with anxious for his no-show at the morning service at their home church, found him, who had already lost the warmth in his bed.
It was really a sudden loss, because there had been no obvious symptom about his heart. The EuAs C_2S-9 was the last occasion for me to see him in life.
We, Hitoshi's family, Ei (his wife), Michitaka (eldest son), Yu (eldest daughter), and Tamao (second daughter), deeply appreciate your friendship with him.
It is my great regret that I have no skills for expressing our sincere gratitude to you in English properly.
All correspondence will be received by:

Mrs. Ei Ohtaki
Yokohama Baywest 304, 7-225 Tobe-cho,
Nishi-ku, Yokohama 220-0042, Japan
Phone and fax: +81-45-316-4680

With greatest regards,
Representing Hitoshi's Family,
Michitaka Ohtaki

Tribute to Professor Dr. Hitoshi Ohtaki
by Bernd M. Rode, Austria

My scientific co-operation and personal friendship with Professor Ohtaki started in 1979, when I stayed as a guest professor at Tokyo University and met him on the occasion of a visit to his department at the Tokyo Institute of Technology. Understanding that his experimental and our theoretical work ideally complemented each other we agreed on a close co-operation, and only a year later I was invited as a guest professor to his University, and he to mine. Joint publications followed and together with Professor Ivano Bertini we initiated the EURASIA Conference Series in the 1980s. Through the continuous joint activities and contacts we developed a deep friendship, which also gave me a much closer access to Japanese culture – after some years Hitoshi preferred to talk with me in his mother tongue and to consider me 'almost a Japanese'….

When Hitoshi retired from the Tokyo Institute of Technology and moved to the Institute for Molecular Science in Okazaki, I continued my co-operation with him there, and when he moved again to Ritsumeikan University, this did not make any difference to our relationship either.

We still had so many plans for further activities, in particular related to the organisation of EURASIA Conferences, and thus his sudden passing away meant a deep shock for me. After so many years of working together in deep mutual appreciation and friendship I feel a strong, uncompensatable loss and my mourning is only consoled by the knowledge that the memory of Hitoshi will be a long-lasting one, not only for me but also for so many other friends and colleagues who have not only enjoyed his spirit of hard work but also his strong social character and dedication to good personal relationships, in good and hard times. This memory brings all of us closer to each other, a last achievement of Hitoshi's endeavours!

REQUIESCAT IN PACE!

Tribute to Professor Dr. Hitoshi Ohtaki
by Ivano Bertini, Italy

I met Professor Hitoshi Ohtaki in 1978 in Vienna at a conference on Solute-Solute-Solvent Interactions organized by the late Victor Gutmann. I organized the following meeting in Florence in 1980 which was attended by Hitoshi and our friend Bernd Michael Rode. In 1985 I visited him at the Tokyo Institute of Technology. I reported the wish of Michael Rode to organize a scientific meeting in Bangkok as he was regular visiting professor there. Hitoshi, Michael and myself decided to start a series of meetings called Eurasia with the first event in Bangkok. Hitoshi suggested that I visited Salag Dhabanandana, vicerector of the Chulalongkorn University in Bangkok during my trip back. Salag and myself agreed on the details of the organization of the first Eurasia Conference on Chemical Sciences to be held

in Bangkok on January 4-8 of 1988. Hitoshi was organizing the 10th in Manila when he passed away. Hitoshi, Michael and myself had organized all the Eurasia meetings together (except the 9th which I did not attend).

I visited Hitoshi in Okazaki in 1989 when he was Director of the Coordination Chemistry Laboratories of the Institute for Molecular Science and I was invited speakers at the following meetings organized by him: International Symposium on Molecular and Dynamic Approaches to Electrolyte Solutions, Tokyo, 1988; Okazaki Conference, 1990; XXX International Conference on Coordination Chemistry, Kyoto, 1994; 26th International Conference on Solution Chemistry, Fukuoka, 1999. He has visited me several times and I was at the meeting celebrating him at the Ohtaki Symposium in Kusatsu in 2003. I write all of this to underline the degree of our friendship and the close feelings in the policy of the development of chemistry that we had.

Hitoshi dedicated his life to Science and to the organization of Science. As a scientist, I remember the studies by X-ray of the coordination compounds in solution of metal ions with monodentate ligands which constituted milestones in the field. Eventually, he started simulating through informatic tools the interaction of solvents and ligands with metal ions.

Now, I feel more lonely in my scientific activity and in my daily work. Hitoshi was a great man and a real Maestro (sensei). I used to call him “Shogun”.

We all will remember him.

Professor Hitoshi Ohtaki in Memoriam

It was really sad and so unexpected to receive the news that Professor Hitoshi Ohtaki passed away November 5th. Just a couple of weeks earlier we had been in contact, to explore and follow up some ideas put forward during lively discussions at the 9th Eurasia Conference on Chemical Sciences, $EuAsC_2S$, which we both attended in Antalya, Turkey, in the middle of September.

During this conference Hitoshi was in full blossom. As chair of the International Organizing Committee for the conference, he had been actively involved in developing the scientific programme as well as inviting lecturers. Among the plenary lecturers he succeeded to attract was HRH Princess Chulabhorn Mahidol of Thailand, who Professor Ohtaki received and hosted with experience and confidence and with the respect and gratitude required. But he also dared to show some of his characteristic social warmth and scientific enthusiasm that contributed so much to make this solemn occasion a conference high-light. What a memorable imprint to leave behind!

By Professor Ohtaki’s unexpected death, a tremendous career in chemistry has come to an end. He received his education from the Faculty of Science at Nagoya University where he obtained his Dr.Sc. degree in 1961. Then followed several years (1961-1964) as a Postdoctoral Research Fellow in Professor Lars G. Sillén’s group at the Royal Institute of Technology in Stockholm, Sweden, years he often talked about with sincere enthusiasm to someone coming from that part the world. During the stay in Stockholm his research interests were shaped and firmly directed towards solution chemistry and coordination chemistry, and when he returned to

Japan, he pursued research in this field of chemistry with considerable success at several institutions (Nagoya University, Tokyo Institute of Technology, Okazaki National Research Institutes, and Ritsumeikan University) and advanced through the ranks from lecturer to full Professor and also Research Director. Through his career he published more than 300 research papers and reviews and authored and coauthored contributions to more than 20 books. It should also be mentioned that he translated several books into Japanese.

The research activities of Professor Hitoshi Ohtaki gave him a name in the international chemical community, but his reputation is much greater than his important scientific contributions can account for. The reason for this is his long-standing and unselfish participation in voluntary work through several international organizations and on an independent basis. His work in the International Union of Pure and Applied Chemistry is particularly note-worthy; in this union he served in various capacities and was an active Commission member, Division member, and Bureau member for a number of years, and for 2 years, 2002–2003, he was a member of the IUPAC Executive Committee. For a period of time I also enjoyed working closely with Hitoshi in the Membership Committee; when we were out in the field, it was really an experience to see him using his friendly charm and enormous enthusiasm to recruit new IUPAC members.

But just as important were his significant contributions as a congress organizer, in particular his service to the Eurasian series of conferences, which was founded by Hitoshi and two of his friends, Professor Bernd M. Rode from the University of Innsbruck, Austria, and Professor Ivano Bertini from the University of Florence, Italy. These conferences on Chemical Sciences were close to his heart because in addition to present and discuss the latest research results, the EuAs C_2S meetings have always been aiming at engaging chemists from developing and disadvantaged countries in cooperation and networking, thereby supporting the chemical communities in these countries. This was a long-term goal for Hitoshi to achieve, so he never gave up in spite of the fact that the progress often was slower than he had hoped. In fact, when he gathered the International Advisory Board for the next EuAs C_2S meeting at the end of the conference in Antalya, he argued with optimism for new initiatives directed especially towards young chemists in developing countries in the Eurasian continent. Now, when Hitoshi is no longer among us, it is up to all of us to continue this important work.

Over the years Professor Ohtaki's significant scientific achievements earned him a number of important distinctions and prizes, among which are the National Medal of Purple Ribbon and the Prize for Scientific Merits of the Electrochemical Society of Japan. However, during the same period of time his significant amount of voluntary work for the common good has earned great respect in the chemical community around the world.

For all his contributions he will be remembered for years to come!

Leiv K. Sydnes
Past President of IUPAC and Member of the International Advisory Board for EuAs C_2S

In memory of H. Ohtaki

"Today I received beautiful photos along with kind note from you. After reading your note in the faculty meeting room, I was again quite impressed by not only how thoughtful and organized person you are but also how physically strong person you are. To have you as the General Coordinator of the EuAs C_2S is certainly our luck. I like the photos you sent very much. Although my visit to Karachi was short, my memory of Pakistan will last forever thanks to you."

The above is the quotation of my letter that was sent on May 14, 2002 to Professor Hitoshi Ohtaki at the Department of Chemistry, Faculty of Science and Engineering, Ritsumeikan University, Japan. The following is one of the very photos taken on March 12, 2002 during the closing ceremony of the 7th EuAs C_2S held in Karachi, Pakistan: Ohtaki (center), Rode (left), Do (right) and invisible Bertini who left earlier. This photo delivers a special message regarding Ohtaki's strong will on the EuAs C_2S because the organization of the Pakistan meeting, originally scheduled on November 11–13, 2001, confronted near cancellation due to, among others, September 11 World Trade Center Tragedy of 2001.

Looking back, my first encounter with Ohtaki was made in 1988 in Seoul right after the 1st EuAs C_2S held in Bangkok, Thailand. He was then the Chairman of the International Organizing Committee of the 2nd EuAsC_2S held in Seoul, Korea. Since then, I have been sharing and enjoying all the forthcoming EuAsC_2S meetings with Ohtaki: 1992 3rd in Bangkok, 1994 4th in Kuala Lumpur, 1996 5th in Guangzhou, 1999 6th in Brunei Darussalam, 2002 7th in Karachi, 2003 8th in Hanoi, 2006 9th in Antalya and the initiation of 2008 10th in Manila. During this course, I had an honor in 1994 to be invited by Ohtaki to join the International Organizing Committee of EuAs C_2S and take the Secretary role. In 1999, after the Brunei Darussalam's meeting, he extended me an offer to become a member of the

International Organizing Committee of EuAs C_2S but I returned him with my role of the Secretary. He served the Chairmanship of the EuAs C_2S meeting many times that earned him General Coordinator followed by Permanent General Coordinator of the International Organizing Committee of EuAs C_2S.

Yes! Permanent General Coordinator of the EuAs C_2S! Among the many titles Ohtaki hold, I would like remember him as Permanent General Coordinator of the EuAs C_2S! Saga of the EuAs C_2S should be continued because of the widely understood and accepted aim of the EuAs C_2S. Let me quote the aim of the EuAs C_2S provided by Ohtaki, Rode and Bertini: "… the creation of an international conference called Eurasia Conference on Chemistry of Solution (EuAs C_2S) with the aim at deepening the friendship of chemists in the Eurasia continent, at supporting scientific researches of chemists in the continent with the help of chemists in other continents such as America, Canada, and Australia, and at organizing a world-top class international conference in a developing country of Asia with the help of their world-wide friendship network through which we invite world-leading scientists, with whom scientists, especially young scientists in developing countries, could exchange information to emphasize scientific activities of their countries."

I strongly believe that Ohtaki himself and his spirit and philosophy on the EuAs C_2S will be remembered by all of us and serve as everlasting driving force to keep the EuAs C_2S going. Dear Ohtaki! Please allow me to spread this writing as a tribute of my respect to you!

March 8, 2007

Youngkyu Do
Secretary
IOC of the EuAs C_2S
Professor of Chemistry
KAIST, Korea

A Tribute to Professor Hitoshi Ohtaki; A Great Scientist and Friend

Amal Al-Aboudi

It didn't come to my mind that when we said good bye, at the end of the 9th Eurasia conference in Antalya, that this is going to be the last time to see Professor Ohtaki!! The news of his death was a devastating shock that took me some time to believe!

Professor Ohtaki was one of the kindest people I have ever known. I first met him during the 7th Eurasia conference held in Karachi 2002, and I had the chance to set next to him during the dinner, when he explained to me the aim of Eurasia conference. I felt his sincere devotion for opening doors for young scientist in the developing countries to learn top science. That was evident not only in his participation in organizing world-top class international conferences in the developing countries, but also in his activities in many international scientific organizations such as IUPAC and FACS. He shared with me his ideas about the excitement of knowledge, and more important the dedication to spread and share knowledge through what he referred to – with his peaceful smile – "knowledge loving groups".

Professor Hitoshi was a highly respected scientist; he had visionary leadership towards a brighter future for chemistry. He was a brilliant thinker, an inspiring mentor who affected the life of many of his students, and above all he was a great friend. He will always be remembered for his sincerity, spontaneity in giving help and advice, and for his passion of photography and nature.

Hitoshi, we will always remember you, and miss your beautiful company. May you rest in peace.

Tribute to Professor Dr. Hitoshi Ohtaki

Athar Ata

On November 5, 2006, I heard extremely sad news regarding the sudden departure of Professor Hitoshi Ohtaki. This is a big loss for all of us. He is one of the eminent scientists in the area of solution chemistry in this era and made a significant contribution to the chemical literature in his field. His efforts to develop a high quality research program in the developing countries of Asia will be remembered for ever. He was the permanent chair of International Organizing Committee for Eurasia Conference on Chemical Sciences. In this capacity, he played a model role in bringing scientists from Europe and Asia together on a table to think about joint innovative research programs between two Continents. We also share this sorrow with his family and pray for his soul to be in peace and patient for his family to afford this great loss. I would like to dedicate my paper entitled "Novel Bioactive Natural Products from Marine and Terrestrial sources" in the memory of Professor Hitoshi Ohtaki.

Messages received from his colleagues after November 5, 2007

It is indeed very sad news, especially considering how active and full of life he was in Antalya. Yes, it is wholly appropriate to extend one's condolences. I might write to his son who was a participant of the Antalya meeting and whom I had a chance to talk on the last day.

Such events are very tragic and the family is left totally bewildered. It is like the lightening striking without warning. For the person self it is not long and drawn out which may be some solace; but others family and friends are left to cope with the loss as best as they can which is not easy. The first news about Hitoshi came from your letter. After that there was a message from the Isobe's and then further news started pouring in; including one from the IUPAC office from Fabienne. I did write a short note to be added to my report on EURASIA 9 and asked Fabienne if that would be appropriate. She replied within minutes saying she had thought exactly the same and could use my text.

Ohtaki had been very active in the IUPAC and I am sure that the office in Raleigh will take appropriate note of and initiate due action in the matter. My contacts with him were mainly when as the President of Division III, I participated in the meetings of the IUPAC Bureau. In connection with the 9th Eurasia in Antalya, and considering Ohtaki's role in the series of these meetings which I believe he initiated perhaps you may wish to have some tribute to Ohtaki in the book on the Antalya congress.

With my expression of condolences on the demise of a good and noble friend.

Upendra K. Pandit

***

The sad news that Hitoshi Ohtaki suddenly passed away in a myocardial infarction was shocking and came completely unexpectedly. He was such an inspiring personality and did a lot for the chemical community and in particular for IUPAC and similar organizations. I really hope that someone will continue his work for the Eurasia initiative. Your contribution to the latest Eurasia conference was tremendous and your work on the conference proceedings will be an important memorial action of Hitoshi's Eurasia initiative.

Thank you for rapidly sending me the tragic news. I will forward the news to the present head of the inorganic chemistry. It was in this laboratory Hitoshi worked as a postdoc, when we first met. I express my sincere condolence with you on the unexpected death of Hitoshi Ohtaki.

Torbjörn Norin

***

I fully understand of how difficult it was for you to make the announcement of the passing away of the late Professor H. Ohtaki. In fact I was already informed on the event by Professor Haruhiko Yokoyama, to whom I also sent my condolescence as well as to Mrs. Ohtaki.

It was really a sudden and unexpected event, since Ohtaki looked very well in his health, only a month and half ago, in Antalya. He had also proposed me to organize the 12 Eurasia conference, in Greece in 2012, which I had accepted. This may remind us all of how easy is to pass to the other side (away) at any moment!

I indeed share your prayers for the soul of Professor Ohtaki.

Nick Hadjiliadis

***

It was a true shock to Astrid and myself when we learned last Sunday night that Hitoshi has passed away. This is a tremendous loss for our whole community. As you correctly state, we had seen him in Tokyo twice, namely at October 12 and 13, when he attended both of my lectures. He was in good mood and spirit and we had in fact intense scientific discussions about the chelate effect and this continued until November 3, when he sent me his last mail. We all definitely lost a very dear friend. Of course, Astrid and I have immediately written to his wife Ei… and as you say, at this time we can only pray for his soul.

Helmut Sigel

***

The only thing that I can say at the moment is that I am still shocked for this very sad news and it is difficult for me to react. My wife cried yesterday for long time and I also was unable to retain the tears. My collaborators at the University can't believe that.

He was a fantastic scientist and a very nice person. We all will keep his memory for ever.

Fernando Rull Perez

***

Thank you very much for your kind letter, informing me of the sudden death of Hitoshi Ohtaki.

I have, indeed, known Hitoshi for many years, sitting together on committees, attending conferences, and sharing scientific interests. I strongly share your sentiments concerning Hitoshi's personality and involvement in international cooperation. We will all miss his enterprise and good advice and his friendly attitude towards his colleagues all over the world.

Yizhak Marcus

***

I cannot believe how you and I have thought of each at the same moment! I was just going to write to you about this unbelievable sad news which I heard from Professor Yokoyama. I cannot still believe this. Neither can Albert. Albert is very happy to have met him and heard from many people at the conference so many good things about him. Hitoshi seemed to be in good health and quite active during the conference in Antalya and when he said good bye to me and Albert on the last day, I thanked him and you for inviting me to the conference. I cannot believe how life can be taken away by God so suddenly. The only consolation is that he had a quick departure, after a very successful and fruitful life on Earth. I have always seen him in god mood and good and respectable terms with all people he knew. As you have written, we send our best thoughts on him to his soul, now with God.

It must have been a very great shock for his wife and large family. I wrote to his son asking him to convey my sympathies and condolences to all in the family. I join you in mourning his loss from the scientific and human world. After working closely with him for nearly 10 months recently, I can imagine you must be feeling quite dazed. I send you my comfort to bear the sorrow.
Raji Heyrovska

***

It was indeed a very depressing and very sad news to hear.

I have told Mathuros to inform HRH Princess Chulabhorn about this terrible news. HRH Princess Chulabhorn and Mathuros left for India this morning.
Somsak Ruchirawat

***

It was so sad news that Hitoshi has passed away. He was so healthy and pleasant in Antalya, and I can hear his clear and loud speaking voice even now.

He had been working for Eurasia Conference as the permanent committee member. I was with him in the previous conference in Hanoi, Vietnam, where he decided to transfer the next conference in Turky to be organized by you. Hitoshi was also a leader in other meetings of IUPAC activities since many years ago. I join you to send my deep condolences to his family (his son being in Antalya) and chemistry colleagues for Professor Hitoshi Ohtaki.
Minoru Isobe

***

I am now staying in China. Yesterday, I got the e-mail that Professor Ohtaki passed away from his son. I am very surprised to hear that. I am now the vice-president of Japan Society of Coordination Chemistry. We are discussing about the ceremony for late Professor Ohtaki.

Anyway, Professor Ohtaki was too young (about 72 years old). All members in Japan Society of Coordination Chemistry are surprised and sad.

Thank you for your kind cooperation.

Masahiro Yamashita

***

I am surprised to hear that Professor Hitopshi ohtaki passed away.

I can not find words to say. I am very sad. He was a great man in every points as research and humanity. I am expected him. He was a honorable leader for us. I also wish to pray with you for the peaceful sleep of Hitoshi's soul.

Mitsutaka Kitamura

***

Professor Hitoshi Ohtaki told me that he was very glad to know the big success of 9th Eurasia Conference on Chemical Sciences and appreciate your big contribution. He really enjoyed not only the conference but also trip in Turkey. Although his death was very sad to us, I think that we have to take over his intention and continue the Eurasia Conference.

Today I will attend his funeral and pray for the repose of his soul.

Hiroki Oshio

***

Thank you very much for your e-mail, offering your condolences to the untimely demise of Professor Ohtaki. I heard the sad news yesterday in Tokyo, when we were having a meeting in the Chemical Society of Japan for our IUPAC activity. He was a key person of many international activities such as Eurasian Conference, IUPAC, Pacifichem, etc. and we all miss him and his services.

I would like to thank you very much for your king arrangement for my very first trip to Turkey last September, which I also owe much to the late Professor Ohtaki. I had a great time in Antalya with the people of the Eurasia Conference and with Professor Ohtaki.

It was just 2 months ago, and I feel a life as transitory.

Kaz Tatsumi (Nagoya)

***

I already heard the sad news from one of the Japanese professor yesterday morning.

I have known him for more than 15 years. I even met him this summer twice in Cape Town and Antalya. He was, as you know, active and healthy all the time, and I have never expected that this would happen to him.

I would like to share my condolences with you. I will pray for his soul.

Myunghyun Paik Suh

***

All of us have been surprised to hear of the sudden and sad news about the passing away of Hitoshi.

Hitoshi has been a good friend of mine for a long time since I started my scientific career.

I have been fostered by him as well as my professor in our community of solution chemistry in Japan.

I have been to Yokohama to attend the funeral held in a small church yesterday.

Many of us who were in Antalya gathered there to regret the loss of the great scientist and leader in our field and to encourage his family. I remember very well how happy Hitoshi was working together with you for the 9th Eurasia Conference held in your hometown, Antalya. Your town is fantastic with many historical spots. I enjoyed them. After you closed the conference, we Japanese delegates took dinner together in the beautiful hotel to appreciate his great contribution to your successful Eurasia Conference.

Your hometown was the last place where I saw Hitoshi and chattered with him without noticing the time passage. He was so wonderful in personality that he could attract so many nice people around him without noticing the time passage.

He was very proud of your success in organizing the Eurasia Conference.

Masaru Nakahara

***

I am deeply saddened by the unexpected news of the passing of Professor Hitoshi Ohtaki. Recently, during the Conference in Antalya he was so active and appeared to be in a perfect health. We shall all remember him as outstanding scientist and noble person. I have, as many others, admired his wisdom and gracious personality. Since you have worked with Professor Hitoshi Ohtaki closely for many months you feeling of the lose is no doubt particularly intense. Please accept my sincere sympathy for you in your sorrow.

Osman Achmatowicz

***

I am greatly saddened by the news of the untimely death of Hitoshi Ohtaki. It is our great loss. You have misinterpreted the warmth of my relationship with Hitoshi. We met for the first time in Istanbul only the week before your meeting, and shared the same seat in the coach tours through Cappadocia. So we became good friends very rapidly.

I append the letter I have just sent to Kyoki Isobe, whose e-mail reached my just before yours today. (I have been travelling again).

Michael Blackburn

***

I share your distress and expression of sentiments at the sad news about Hitoshi Ohtaki. He was an outstanding scholar and IUPAC colleague, and his sudden death has deprived us of his wise council and his selfless devotion to many duties.

I hope that we can derive some consolation from the knowledge that he has left an indelible legacy of achievement. Not least, the successful passage of Eurasia-9 will remind us of his constructive contributions to this and other worthy enterprises that he identified as opportunities to advance science and its societal responsibilities. Thank you for sharing your thoughts and recollections with me.

James Bull

***

Tribute to Professor Dr. Hitoshi Ohtaki
by

Bilge Şener, *NOC Chair of the 9th Eurasia Conference on Chemical Sciences, Turkey*

I would like to extend my condolences to all of you for the distinguished professor Hitoshi Ohtaki and for this great loss.

The sad news that Hitoshi Ohtaki suddenly passed away in a myocardial infarction was shocking and came completely unexpectedly. He was such an inspiring personality.

I just had multiple exchanges with Professor Ohtaki on October 23 and 25 as he informed me that he sent me a CD belonged to several photographs taken by him during the conference. During these days, I was waiting to get this CD from him !!

Hitoshi seemed to be in good health and quite active during the conference in Antalya. He was so healthy and pleasant, it was just 2 months ago, he was in Antalya-Turkey and I felt a life as transitory!

My first encounter with Professor Hitoshi Ohtaki was made in 2002 during the 7th EuAs C_2S held in Karachi, Pakistan. He has extended me an offer to become a member of the International Advisory Committee of EuAs C_2S. Since 2004, I had closely worked with him for the preparation of the 9th Eurasia Conference, he was the Permanent General Coordinator of the International Organizing Committee of EuAs C_2S.

September 13, 2006 Antalya-Turkey

After this course, I had an honor in 2006 to be invited by Professor Hitoshi Ohtaki to join the International Organizing Committee of EuAs C_2S.

I appreciated his leadership very much. He has shared and advised all details (by starting to design the Eurasia emblem, rosette, awards, guidelines and many more…) with me during this period.

Looking back, he was a most important Japanese who worked for IUPAC, Eurasia and many societies. He was always a dependable leader. He himself has a fighting spirit in rather conservative Japanese Society. His last lecture will be a good representation to explain his idea for Japan and Japanese chemists presented by him in Antalya on September 13, 2006 at 2.30 p.m.

Our contribution to the latest Eurasia conference was tremendous and our work on the conference proceedings will be an important memorial action of Hitoshi's Eurasia initiative. I would like to share this opportunity with you and his friends by adding tributes and messages in this book which is dedicated to Professor Hitoshi Ohtaki.

I think that we have to take over his intention and continue the Eurasia Conferences. Professor Hitoshi Ohtaki and his services will be remembered for years by all of us.

September 13, 2006 Antalya-Turkey

Contents

Contributors

Amirul A. Abdullah
Universiti Sains Malaysia, School of Biological Sciences, 11800 Penang, Malaysia
E-mail: amirul@usm.my

Şaziye Abdurrahmanoğlu
Dr., Marmara University, Faculty of Arts and Sciences, Department of Chemistry, 34722 Göztepe-Istanbul, Turkey
E-mail: sabdur@marmara.edu.tr

Rohana Adnan
School of Chemical Sciences, Universiti Sains Malaysia, 11800 Penang, Malaysia

Hüseyin Afşar
Yıldız Technical University, Faculty of Arts and Sciences,
Department of Chemistry, Davutpasa, 34220, Istanbul, Turkey

Alper Akıncı
Yıldız Technical University, Faculty of Arts and Sciences,
Department of Chemistry, 34220, Esenler-Istanbul, Turkey

Özlem Aksu Dönmez
Yıldız Technical University, Faculty of Arts and Sciences,
Department of Chemistry, 34220 Davutpaşa Campus, Esenler-Istanbul, Turkey
E-mail: oziaksu@yahoo.com

Güzin Alpdoğan
Yıldız Technical University, Faculty of Arts and Sciences,
Department of Chemistry, 34210 Davutpaşa-Istanbul, Turkey

Serkan Angi
Esenler Primary School, Esenler, Istanbul, Turkey

Mitsuhiro Arisawa
Graduate School of Pharmaceutical Sciences, Hokkaido University, Kita 12, Nishi 6, Kita-ku, Sapporo, 060-0812, Japan

Bürge Aşçı
Dr., Yıldız Technical University, Faculty of Arts and Sciences,
Department of Chemistry, 34220 Davutpaşa Campus, Esenler-Istanbul, Turkey
E-mail: burgeasci@yahoo.de

Athar Ata
Associate Professor Dr., The University of Winnipeg, Department of Chemistry,
515 Portage Avenue, Winnipeg, MB R3B 2E9 Canada
E-mail: a.ata@uwinnipeg.ca

Ulvi Avcıata
Yıldız Technical University, Faculty of Arts and Sciences,
Department of Chemistry, 34210 Esenler, Istanbul, Turkey

Feray Aydoğan
Associate Professor Dr., Yildiz Technical University, Faculty of Arts
and Sciences, Department of Chemistry, 34220 Davutpaşa Campus,
Esenler-Istanbul, Turkey
E-mail: feray_aydogan@yahoo.com

Erol Ayrancı
Akdeniz University, Faculty of Arts and Sciences, Department of Chemistry,
07058 Antalya, Turkey

Mohd N. M. Azizan
School of Biological Sciences, Universiti Sains Malaysia,
11800 Penang, Malaysia

Emine Bağdatlı
Yıldız Technical University, Faculty of Arts and Sciences,
Department of Chemistry, 34220 Davutpaşa Campus, Esenler-Istanbul, Turkey
E-mail: e_bagdatli@yahoo.com

Aslı Barla
Istanbul University, Faculty of Pharmacy, 34116, Beyazit, Istanbul, Turkey

Edip Bayram
Akdeniz University, Faculty of Arts and Sciences, Department of Chemistry,
07058 Antalya, Turkey

Özer Bekaroğlu
Marmara University, Department of Chemistry, 34722
Göztepe-Istanbul, Turkey

H. Kerim Beker
Yıldız Technical University, Faculty of Arts and Sciences,
Department of Chemistry, 34220, Esenler-Istanbul, Turkey

Elena Yu. Blishchenko
Shemyakin-Ovchinnikov Institute of Bioorganic Chemistry, Russian
Academy of Sciences Moscow, Russia

Stacey J. Borg
School of Chemistry, Faculty of Science, University of Melbourne, Australia

Stefan Bossmann
Lehrstuhl für Umweltmesstechnik, Universität Karlsruhe,
76128 Karlsruhe, Germany

Abdürrezak Bozdoğan
Yıldız Technical University, Department of Chemistry, 34210 Davutpasa, Istanbul, Turkey

Mustafa Bulut
Marmara University, Department of Chemistry, 34722 Göztepe-Istanbul, Turkey

Wanda Buzgariu
National Institute of Research and Development for Biological Sciences,
Center for Bioanalysis, 296, Spl. Independentei Bucharest, Romania

Mevlüde Canlıca
Dr., Yıldız Technical University, Faculty of Arts and Sciences,
Department of Chemistry, 34220 Davutpaşa Campus, Esenler-Istanbul, Turkey
E-mail: mc1111@e-kolay.net

Emily Valentin Castriciones
Assistant Professor Dr., University of the Philippines, Institute of Chemistry,
Inorganic Synthesis and Computational Research Laboratory, Diliman, Quezon City, 1101, Philippines
E-mail: ecastriciones@gmail.com

A. Dar
International Center for Chemical Sciences, H.E.J. Research Institute
of Chemistry, University of Karachi, Karachi-75270, Pakistan

Leonard Dela Cruz
Natural Sciences Research Institute, University of the Philippines, Diliman,
Philippines, Inorganic Synthesis and Computational Research Laboratory,
Institute of Chemistry, University of the Philippines, Diliman, Quezon City,
1101, Philippines

Nebahat Demirhan
Yıldız Technical University, Faculty of Arts and Sciences,
Department of Chemistry, 34210 Esenler- Istanbul, Turkey

Mirela Diaconu
National Institute of Research and Development for Biological Sciences,
Center for Bioanalysis, 296, Spl. Independentei Bucharest, Romania

Şule Dinç
Yıldız Technical University, Faculty of Arts and Sciences, Department of Chemistry,
34220 Davutpaşa Campus, Esenler-Istanbul, Turkey
E-mail: sule_dinc@yahoo.com

Mehmet Dişbudak
Istanbul University, Department of Forensic Medicine, Istanbul, Turkey

Ali Erdoğmuş
Yıldız Technical University, Faculty of Arts and Sciences,
Department of Chemistry, 34220 Davutpaşa Campus, Esenler-Istanbul, Turkey
E-mail: erdogmusali@yahoo.com

Ahmet C. Gören
Tubitak, Ulusal Metroloji Enstitüsü (UME), Group of Chemistry, P.O. Box 54,
41470, Gebze - Kocaeli, Turkey

Ahmet Gül
Istanbul Technical University, Department of Chemistry, Maslak, Istanbul, Turkey

Gülşah Gümrükçü
Yıldız Technical University, Faculty of Arts and Sciences,
Department of Chemistry, 34220 Davutpaşa Campus, Esenler-Istanbul, Turkey
E-mail: gumrukcugulsah@yahoo.com

Sotiris K. Hadjikakou
Section of Inorganic and Analytical Chemistry, Department of Chemistry,
University of Ioannina, 45110, Ioannina, Greece

Nick Hadjiliadis
Professor Dr., University of Ioannina, Section of Inorganic and Analytical
Chemistry, Department of Chemistry, 45110, Ioannina, Greece
E-mail: nhadjis@uoi.gr

Takayuki Hara
Department of Mechanical and System Engineering, University of Hyogo,
2167 Shosha, Himeji, 671-2201, Japan

Raji Heyrovska
Professor Dr., Academy of Sciences of the Czech Republic,
Institute of Biophysics, Královopolská 135, 612 65 Brno, Czech Republic
E-mail: rheyrovs@hotmail.com

Numan Hoda
Associate Professor Dr., Akdeniz University, Faculty of Arts and Sciences,
Department of Chemistry, 07058 Antalya, Turkey
E-mail: nhoda@akdeniz.edu.tr

Filiz İmer
Associate Professor Dr., Yildiz Technical University, Faculty of Arts
and Sciences, Department of Chemistry, 34220 Davutpaşa Campus,
Esenler-Istanbul, Turkey
E-mail: filizimer@yahoo.com

Vadim T. Ivanov
Professor Dr., Russian Academy of Sciences, Shemyakin-Ovchinnikov Institute of Bioorganic Chemistry, Moscow, Russia
E-mail: ivavt@mail.ibch.ru

Sajid Jahangir
Dr., Neubaugasse 66-1-3, Graz 8020, Austria
E-mail: sajid318@gmail.com

Şeniz Kaban
Yıldız Technical University, Faculty of Arts and Sciences,
Department of Chemistry, 34220, Esenler-Istanbul, Turkey

Andrey A. Karelin
Shemyakin-Ovchinnikov Institute of Bioorganic Chemistry, Russian Academy of Sciences Moscow, Russia

M. Jain Kassim
School of Chemical Sciences, Universiti Sains Malaysia, 11800 Penang, Malaysia

Dieter E. Kaufmann
Clausthal Technical University, Institute of Organic Chemistry, Leibnizstr 6,
D-38678 Clausthal-Zellerfeld, Germany

Bahadır Keskin
Yıldız Technical University, Faculty of Arts and Sciences, Department of Chemistry,
34220 Davutpaşa Campus, Esenler-Istanbul, Turkey
E-mail: bkeskin@hotmail.com

K. M. Khan
International Center for Chemical Sciences, H.E.J. Research Institute of Chemistry,
University of Karachi, Karachi-75270, Pakistan

Mahmud Tareq Hassan Khan
Dr., University of Tromsø, Institute of Medical Biology, School of Molecular and Structural Biology, Department of Pharmacology, 9037 Tromsø, Norway
E-mail: mahmud.khan@fagmed.uit.no

Hasan Kılıç
Marmara University, Department of Chemistry,
34722 Ziverbey, Istanbul, Turkey

Turgut Kılıç
Balikesir University, Faculty of Science and Letters, Department of Chemistry,
10100 Balikesir, Turkey

David. G. I. Kingston
Virginia Polytechnic Institute and State University, Department of Chemistry,
M/C 0212, Blacksburg, Virginia 24061, USA

Mitsutaka Kitamura
Professor Dr., University of Hyogo, Department of Mechanical and System Engineering, 2167 Shosha, Himeji, 671-2201, Japan
E-mail: mkitamura@eng.u-hyogo.ac.jp

Sevgi Kocaoba
Yıldız Technical University, Faculty of Arts and Sciences, Department of Chemistry, 34210 Esenler, Istanbul, Turkey

Arnie R. de Leon
Natural Sciences Research Institute, University of the Philippines, Diliman, Quezon City 1101, Philippines

Mohd I. A. Majid
Malaysian Institute of Pharmaceuticals and Nutraceuticals, MOSTI, Malaysia

Mohamad Nasir Mohamad Ibrahim
Dr., Universiti Sains Malaysia, School of Chemical Sciences, 11800 Minden, Pulau Pinang, Malaysia
E-mail: mmm@usm.my

M. Mohammad
International Center for Chemical Sciences, H.E.J. Research Institute of Chemistry, University of Karachi, Karachi-75270, Pakistan

Noor Hamdah Musa
School of Chemical Sciences, Universiti Sains Malaysia, 11800 Penang, Malaysia

M. Y. Nor Nadiah
School of Chemical Sciences, Universiti Sains Malaysia, 11800 Minden, Pulau Pinang, Malaysia

Masako Nakagawa
Professor Dr., Kanagawa University, Faculty of Science, Department of Chemistry, Hiratsuka, Kanagawa, 259-1293, Japan
E-mail: nakagawa@chem.kanagawa-u.ac.jp

Atsushi Nishida
Graduate School of Pharmaceutical Sciences, Chiba University, 1-33 Yayoi -cho, Inage-ku, Chiba, 263-8522, Japan

M. S. Norliyana
School of Chemical Sciences, Universiti Sains Malaysia, 11800 Minden, Pulau Pinang, Malaysia

Nüket Öcal
Yıldız Technical University, Department of Chemistry, Davutpasa Campus, 34210, Esenler-Istanbul, Turkey

Hitoshi Ohtaki
Late Professor, Ritsumeikan University, Faculty of Science and Engineering, Department of Applied Chemistry, Kusatsu, 525-8577, Japan

Ilkay Orhan
Associate Professor Dr., Gazi University, Faculty of Pharmacy, Department of Pharmacognosy, 06330, Etiler-Ankara, Turkey
E-mail: iorhan@gazi.edu.tr

Mahmure Üstün Özgür
Yıldız Technical University, Department of Chemistry, Davutpaşa Campus, 34220 Esenler, Istanbul, Turkey

İbrahim E. Özyiğit
Yıldız Technical University, Faculty of Arts and Sciences, Department of Chemistry, 34220, Esenler-Istanbul, Turkey

Leon M. Jr. Payawan
Associate Professor Dr., University of the Philippines, Institute of Chemistry, Diliman 1101 Q.C., Philippines
E-mail: lmpayawan@yahoo.com

Emel Pelit
Yıldız Technical University, Faculty of Arts and Sciences, Department of Chemistry, Davutpasa Campus, 34210, Esenler-Istanbul, Turkey

G. I. Radu
National Institute of Research and Development for Biological Sciences, Center for Bioanalysis, 296, Spl. Independentei Bucharest, Romania

Afidah A. Rahim
Universiti Sains Malaysia, School of Chemical Sciences, 11800 Penang, Malaysia
E-mail: afidah@usm.my

Eva Marie Ratilla
Institute of Chemistry, University of the Philippines, Diliman 1101 Q.C., Philippines

Raymond V. Rivera-Virtudazo
Materials Science Engineering Program-College of Engineering, University of the Philippines,- Diliman, Philippines

Alexandrina Rugina
National Institute of Research and Development for Biological Sciences, Center for Bioanalysis, 296, Spl. Independentei Bucharest, Romania
E-mail: rina@zappmobile.ro

Ivan Salamon
Associate Professor Dr. Presov University, Faculty of Humanities and Natural Sciences, Department of Ecology, 01, 17th November St., SK- 081 16 Presov, Slovakia
E-mail: salamon@fhpv.unipo.sk

Ümit Salan
Dr., Marmara University, Faculty of Arts and Sciences, Department of Chemistry, 34722, Göztepe-Istanbul, Turkey
E-mail: usalan@marmara.edu.tr

Ayfer Saraç
Yildiz Technical University, Faculty of Arts and Sciences, Department of Chemistry, Davutpasa Campus, 34220 Esenler- Istanbul, Turkey

Mehmet Şenel
Fatih University, Department of Chemistry, 34500 B. Çekmece, Istanbul, Turkey

Bilge Şener
Department of Pharmacognosy, Faculty of Pharmacy, Gazi University, 06330, Ankara, Turkey

S. Shuib
School of Mechanical Engineering, USM Engineering Campus, Universiti Sains Malaysia, 14300 Nibong Tebal, Pulau Pinang, Malaysia

Geoff L. A. Sims
Manchester Materials Science Centre, UMIST and University of Manchester, Grosvenor Street, Manchester M1 7HS, UK

Coswald Stephan Sipaut
Dr., Universiti Sains Malaysia, School of Chemical Sciences, 11800, Penang, Malaysia
E-mail: c_sipaut@usm.my

Girlie Naomi N. Sison
Assistant Professor Dr., University of the Philippines, Institute of Chemistry, Diliman, Quezon City 1101, Philippines
E-mail: girlie_naomi.sison@up.edu.ph

J. Steinmetz
Laboratoire de Chimie du Solide Mineral-Universite Henri Poincare-Nancy I, BP 239-54506 Vandoeuvre Les Nancy, France

M. S. Subhani
Department of Chemistry, Quaid-i-Azam University, Islamabad, Pakistan

Kumar Sudesh
School of Biological Sciences, Universiti Sains Malaysia, 11800 Penang, Malaysia

Sidika Sungur
Yildiz Technical University, Department of Chemistry, 34210 Davutpasa, Istanbul, Turkey

Ingebrigt Sylte
School of Molecular and Structural Biology, and Department of Pharmacology, Institute of Medical Biology, University of Tromsø, 9037 Tromsø, Norway

A. Tahiri
Department of Chemistry, Quaid-i-Azam University, Islamabad, Pakistan, Department of Chemistry, Federal Urdu University of Arts Science and Technology, Gulshan- i-Iqbal Campus Karachi, Pakistan

Alvin Karlo G. Tapia
Materials Science Engineering Program-College of Engineering, University of the Philippines, Diliman, Philippines, Materials Physics Laboratory, Physics Division, IMSP, CAS University of the Philippines-Los Baños, Laguna, Philippines

Eugenia Teodor
National Institute of Research and Development for Biological Sciences, Center for Bioanalysis, 296, Spl. Independentei Bucharest, Romania

Gülaçti Topçu
Professor Dr., Istanbul Technical University, Faculty of Science and Letters, Department of Chemistry, Maslak, Istanbul, Turkey
E-mail: topcugul@itu.edu.tr

Gülendam Tümen
Balıkesir University, Faculty of Science and Letters, Department of Chemistry, 10100 Balikesir, Turkey

Fikriye Tuncel Elmalı
Yıldız Technical University, Faculty of Arts and Sciences, Department of Chemistry, 34220 Davutpaşa Campus, Esenler-Istanbul, Turkey
E-mail: nebahatdemirhan@gmail.com

Fatma Turak
Yıldız Technical University, Faculty of Arts and Sciences, Department of Chemistry, 34220 Davutpaşa Campus, Esenler-Istanbul, Turkey
E-mail: fturak2005@yahoo.com.tr

Zuhal Turgut
Associate Professor Dr., Yıldız Technical University, Faculty of Arts and Sciences, Department of Chemistry, 34220 Davutpasa Campus, Esenler-Istanbul, Turkey
E-mail: zturgut@yildiz.edu.tr

Kadir Turhan
Yıldız Technical University, Faculty of Arts and Sciences,
Department of Chemistry, 34220 Davutpaşa Campus, Esenler-Istanbul, Turkey
E-mail: turhankadir@yahoo.com

Metin Tülü
Dr., Fatih University, Faculty of Arts and Sciences, Department of Chemistry,
34500 B. Çekmece, Istanbul, Turkey
E-mail: metin@fatih.edu.tr

Zeynep Türkmen
Istanbul University, Faculty of Pharmacy, 34116, Beyazit, Istanbul, Turkey

Ahmet Lütfi Uğur
Yildiz Technical University, Faculty of Arts and Sciences, Departmant of Chemistry, 34210, Davutpasa, Istanbul, Turkey

Jesus Felix B. Valenzuela
Materials Physics Laboratory, Physics Division, IMSP, CAS University
of the Philippines-Los Baños, Laguna, Philippines

Ayhan Ulubelen
Em. Professor Dr., Istanbul University, Faculty of Pharmacy,
Beyazit-Istanbul, Turkey
E-mail: aulubelen@yahoo.com

Süheyla Uzman
Yıldız Technical University, Department of Chemistry, Davutpaşa Campus,
34220 Esenler-Istanbul, Turkey

Ahmad R. M. Yahya
School of Biological Sciences, Universiti Sains Malaysia, 11800 Penang, Malaysia

Çiğdem Yolaçan
Assistant Professor Dr., Yıldız Technical University, Faculty of Arts and Sciences,
Department of Chemistry, 34220 Davutpaşa Campus, Esenler-Istanbul, Turkey
E-mail: yolacan@yildiz.edu.tr

Chapter 1
Development of Chemistry in Asia with the Cooperation of European Countries

Hitoshi Ohtaki

Abstract The development of science and technology of Asia, mainly Japan, is briefly reviewed. The reasons are discussed why science and technology of Japan could develop after the serious damage of the Second World War. It is emphasized that *Three S's*, "*Spirit*", "*Scope*" and "*Sincerity*" are important factors in order to contribute to the international community. *Honesty* and *Diligence* are essential in the work of science and technology. *Originality* is indispensable in the scientific works. An aspect is presented how we should step forward to the development of science and technology in Asia in the 21st century.

Keywords Development of chemistry, Japan, science, technology

Introduction

Japan was an underdeveloped country in science and technology 150 years ago. Japan had no automobile and no train, and the most convenient transportation system was *Kago* (Palanquin) and the fastest one was horse. Guns were introduced to *Tanegashima island* in the 16th century by a Portuguese. Japan was isolated from other countries in the *Tokugawa Period* for 300 years until the *Meiji Era* started in 1852. During the isolation period, Japan had practically no contact with European and American cultures. On the other had, the characteristic culture of Japan had been blooming in the period. It was fortunate and unfortunate.

Other Asian countries, which were controlled by their Suzerain States at that time, were much more enriched in modern sciences (e.g., medical science) and technologies (e.g., cars and railways) than Japan. In many Asian countries modern science and technology had already been introduced and used for practical purposes

Department of Applied Chemistry, Faculty of Science and Engineering, Ritsumeikan University, Kusatsu, 525-8577, Japan

B. Sener (ed.), *Innovations in Chemical Biology*, doi: 10.1007/978-1-4020-6955-0

around 16th–17th centuries, but these modern science and technology had been usually exclusively used by the only suzerains, and native people had been isolated from the benefits of science and technology.

Modern Chemical Sciences of Japan

Each country has its own culture from the ancient time. There were many great successes in technology in old Asia. *Moenjo-Daro* in Pakistan shows us surprisingly high technology of architecture and city plans 5,000 year ago. Chinese architecture for building many old beautiful buildings and palaces is another examples. *The Great Wall* constructed in the 17th century could be observed from the moon. The architectural technology of Japan has mostly been introduced from China. *Todai-ji Temple* built in Nara in 752, Japan is the existing largest wooden building in the world, in which the Great Buddha Statue of 14.7 m tall is sitting. The Buddha statue was also built in 752.

Gunpowder is one of the chemical products originated in China already in the 7th century, which is much earlier than the production of gunpowder in Europe in the 13th century. The introduction of gunpowder to Japan was made, together with guns, by a Portuguese. Japan had at that time already a high level technology for the production of high quality iron, which had been used for making Japanese swards, and therefore, the production of guns in Japan was rapidly spread over the country. Further improvement of gunpowder by *Dr. Masachika Shimose* (1859–1911) using picric acid instead of nitrocellulose brought the winning of Japan at the battle of the Yellow Sea between Lushun Fleet and Fleet of Japan and another battle of Japan Sea between Baltic Fleet of Russia and the Combined Fleet of Japan commanded by General Togo in 1905 at the end of *Russo-Japanese War*.

Pre-historical Period of Modernization of Japan

The systematic investigation of chemical sciences of Japan was started by *Yoan Udagawa* (1798–1846), who was influenced by the books of A. L. Lavoisier (translated into Dutch) and W. Henry (in English, translated into Germany). These books were imported from European countries to Nagasaki, which was only the gate opened to outside during the period of Isolation of Japan. He published the first textbook of chemistry in Japanese entitled "*Seimi-Kaiso*" (Opening of Chemistry: "*Seimi*" comes from the pronunciation of Chemie in Dutch) in 1837. At that time, however, Japan was much behind Europe in chemical sciences and unaware of the advance made by Atomic Theory developed by J. Dalton and J. J. V. Berzelius due to the National Isolation Policy of the Japanese Government.

The life of Japanese at that time was not so poor, especially Governors including Shogun, Local Governors, and their Samurais, and merchants were relatively rich, although farmers were poor, and most of them lived in wooden houses. Japanese

arts grew to a noticeable level. It is a famous story that Japanese woodcut prints influence to painters of impressionism. However, the development of science and technology were very limited.

The Isolation Policy of Japan started from the beginning of the 17th century and ended in 1854 when four *Black Ships* directed by Commodore M. C. Perry (1794–1858) of USA visited *Uraga*, a small town near Yokohama in 1853 and concluded *the Treaty of the Peace and Amity* in Yokohama in 1854. The big Black Ships constructed with iron, which can float on water, brought a big surprise to all Japanese, and Japanese Government had to open the country for trade and other exchanges to all foreign countries under the power of big cannons, which Japanese had never seen. Then, the Isolation Policy of Japan ended.

Foreign Teachers of Science and Technology Employed by the Japanese Government at Modernization

Soon after the end of *Tokugawa Period* (*Edo Era*), the new government under *Meiji Emperor* started in 1867. In the *Meiji Era*, Japanese Government intended to follow up the modern European culture, especially European science and technology, and established *The Imperial University of Tokyo* having Faculties of Law, Science, and Literature in 1868. This is the first university of Japan.

Before the establishment of the Imperial University of Tokyo, Japan had some private schools. *Kaisei School*, the former Imperial University of Tokyo, is one of them. Medical treatments have been already made by some people with the help of textbooks brought by Dutch who came to Nagasaki, which was the center of medical sciences of Japan in the latter half of the 19th century.

Many Japanese visited Nagasaki to learn medical science and methods of medical treatments by foreigners. The foreigners are, for instance, *J. K. Van den Broek* (Dutch in Nagasaki, medical science), *P. F. Siebold* (German in Nagasaki, medical science and botany, coming from Holland in 1823), *J. L. C. Pompe van Meerdervoort* (Dutch in Nagasaki, medical science), and *A. F. Bauduin* (Dutch in Nagasaki, medical science).

When the modern Japan started, the Japanese Government employed many foreign scientists and engineers. The number of the foreign teachers became about 3,000. Their monthly payments could be compared with those of Ministers. They whose names appearing in the history of chemical and medical sciences are *A. J. C. Geerts* (Dutch, pharmaceutical science), *G. Wagener* (German, chemistry and ceramics in Tokyo and Kyoto after Nagasaki), *K. M. Gratama* (Dutch in Nagasaki, and then, in Tokyo, chemistry and physics), *H. Ritter* (German in Tokyo, chemistry and physics), *T. Antisell* (American, engineer for printing), *W. H. Griffis* (American in Fukui, chemistry), *W. H. Clark* (American in Shizuoka, mathematics, physics and chemistry), *R. W. Atkinson* (British in Tokyo, chemistry), *E. Divers* (British in Tokyo, chemistry, the supervisor of *Dr. Shimose,* aforementioned), *F. F. Jewett* (American in Tokyo, chemistry), and *J. F. Eijkman* (Dutch in Tokyo, pharmacy and chemistry). Their names are listed in Table 1.1.

Table 1.1 Foreign teachers in science and technology at the beginning of modernization of Japan in the 19th century

Name	Country	Field	Place of teaching
W. Van den Broek	Holland	Chemistry, physics, mathematics	Nagasaki
J.L.C. Pompe van Meerdervoort	Holland	Medical science	Nagasaki
A.F. Bauduin	Holland	Medical science	Nagasaki
P.H. Siebold	Germany	Medical science, botany	Nagasaki
K.M. Gratama	Holland	Chemistry, physics	Nagasaki, Tokyo
W. Wagner	Germany	Chemistry, ceramics	Nagasaki, Tokyo, Kyoto
W.H. Griffis	USA	Chemistry	Fukui
W.H. Clark	UK	Chemistry	Shizuoka
E. Divers	UK	Chemistry	Tokyo
F.F. Jewett	USA	Chemistry	Tokyo
G. Martin	Germany	Pharmacy, chemistry	Tokyo
J.F. Eijkman	Holland	Pharmacy, chemistry	Tokyo
A.J.C. Greets	Holland	Pharmacy, chemistry	Kyoto
H. Ritter	Germany	Chemistry, physics	Tokyo
T. Antisell	USA	Print engineering	Tokyo
R.W. Atkinson	UK	Chemistry	Tokyo

Textbooks of Science and Technology Written by Japanese at the Beginning of Modernization

Textbooks of chemistry were introduced to Nagasaki by Dutch, German, and French doctors. Some of them were translated into Japanese. *Yoan Udagawa* (1798–1846) is one of the frontiers of chemistry of Japan. *Komin Kawamoto* (1810–1871) published "*Kagaku Shinsho* (New Chemistry)" in 1861, which is a Japanese translation of "The School of Chemistry" (published in 1846) written by J. A. Stöckhardt (Germany), which was translated from the Dutch book "Inorganic and Organic Chemistry" by J. W. Genning (Holland) in 1850. *Teizo Kono* (1817–1871) published 14 volumes of "*Seimi Binran* (Handbook of Chemistry)" in 1856, five years before the publication of Kawamoto's book. The book is a translation of "Qualitative Analysis with a Table of Systematic Analytical Processes" written by H. Kramer Hommes (1845), which was possessed by a Dutch medical doctor Van den Broek in Nagasaki. The Japanese book is well colored for showing precipitates.

Young Students Sent Abroad by the Japanese Government to Study Science and Technology at the Modernization

In the Meiji Period, many young students were sent to European countries for their studies in various fields. The investment for these educational activities of Japan at that time became about one-third of the total budget of the Ministry of Education.

The students studied in Europe became leaders of modern Japan in the Eras of *Meiji* (1868–1912) and *Taisho* (1912–1926, the Era between *Meiji* and *Showa*). Among them, *Nagayoshi Nagai* (1845–1922) studied chemistry in the laboratory of A. W. Hoffmann (1819–1892) in the University of Berlin, Germany and discovered ephedrine ($C_{10}H_{15}NO$) in *mahuang*, a Chinese medicine and succeeded the synthesis of this compound in 1885.

Jokichi Takamine (1854–1922) went to the University of Glasgow, and then, to the United States to investigate the phosphatic manure, and he established the first company of phosphatic manure in Japan. He produced *Takadiastase*, a digestive agent containing various digestive enzymes, ribonuclease and cellulase. Amylase was extracted from *Takadiastase*. In a narrow sense, *Takadiastase* is one of the carboxyoroteases. He discovered *Adrenaline* in 1900.

Keitaro Matsumoto (1850–1877) learned Dutch language and science from Pompe van Meerdervoort and Bauduin and later from Gratama in Nagasaki. When Bauduin went back to Holland, he went to Utrecht at the age of 17 together with Bauduin. He studied chemistry under the supervision of G. J. Mulder of the University of Utrecht. He and *Ichiro Kishimoto* (1849–1878) were the first Japanese students who learned chemistry in Europe. He returned to Japan due to the *Meiji Restoration* in 1869 and worked at the *Seimi-Kyoku* (The Institute of Chemistry) in Osaka with Gratama. He taught chemistry, geology, and mineralogy. When Gratama finished his term in Japan and left to Holland, Matsumoto again went to Europe to study chemistry at the laboratory of Hofmann of the University of Berlin. He investigated synthesis of phenyloxycrotonic acid and products from reactions of protocatechuic acid (3,4-dihydroxybenzoic acid). Confirmation of production of dimethylprotocatechuic acid from *Veratrum maackii* var. *japonicum* (*Shuro-so* in Japanese) is one of his noticeable contributions.

Joji Sakurai (1858–1939) is one of the leaders of science at the beginning of the Modernization period of Japan. He was selected as one of the students send abroad by the Japanese Government at the second selection and went to London in 1878 to study chemistry under the supervision of A. W. Williamson (1824–1904). When he returned to Japan in 1881, he was immediately appointed a lecturer and soon promoted to a professor of the Imperial University of Tokyo.

His works concerning the improvement of the method of measurement for the boiling point of liquids (so-called improved Beckman method) and the measurement of molar conductivities of aminosulfonic acids are known as the pioneering works of physical chemistry or solution chemistry of Japan.

His contribution to the development of chemistry, especially his leadership as the President of Chemical Society of Japan, which was established in 1878, and as the President of Japan Academy (established in 1879) should be noted.

Kikunae Ikeda (1864–1936) was interested in physical chemistry, a new and rapidly progressing field of chemistry in Europe, and studied reaction kinetics and catalytic reactions in the laboratory of F. W. Ostwald (1853–1932) of the University of Leipzig, Germany, from 1899 to 1901. He also stayed in London for a half a year at the end of his stay in Europe. He became the professor of physical chemistry of the Imperial University of Tokyo.

His works are known in studies on osmotic pressures and vapor pressures of solutions, but he is much better known as the discoverer of glutamic acid extracted from sea tangle (*Konbu*, a seaweed, in Japanese) and the producer of the seasoning "*Aji-no-Moto*" (sodium glutamate). His wife, *Sada*, is a younger sister of the wife of Joji Sakurai.

Umetaro Suzuki (1874–1943) graduated from the Agricultural College of the Imperial University of Tokyo. After the appointment of Associate Professor of the Agricultural College, he first went to ETH of Zurich, Switzerland to work with E. A. Schlze in 1900, and then, he moved to the laboratory of E. Fischer (1852–1910) of the University of Berlin in 1901 to stay there until 1906. He was appointed to be a professor of the Agricultural High School of Morioka. His observation of chicken's beriberi resulted in the discovery of *Oryzanin* (the name is coming from rice, *Oryza sativa*, *Vitamin* B_1 at present) from the extract of rice bran in 1910. He reported the result at the Annual Meeting of Chemical Society of Japan and published in 1911 in the *Journal of the Chemical Society of Tokyo*. In the same year he reported the result in *Zentralbladt für Biochemie und Biophysik* in Germany.

In 1912 a Polish scientist C. Frank published a paper in *Journal of Physiology*, in which he also reported an extracted compound from rice bran with the same procedure as Suzuki reported and named the extracted substance *Vitamin* (which means vital amine). The compound is the same as that found by Suzuki. The Nobel Prize for Medicine and Physiology in 1929 was awarded to C. Eijkman and F. G. Hopkins for their discovery and contributions to *Vitamin*, but it is obvious that the discoverer of *Vitamin* is Suzuki. *Vitamin A* was isolated in 1914, four years after the discovery of *Oryzanin* (*Vitamin* B_1).

At the end of the 19th century to the beginning of the 20th century, European people had a strong prejudice to Japanese, maybe, to all Asian people. A typical example is seen in the case of the first Nobel Prize of Medicine and Physiology in 1901, when E. von Behring received it for his contribution to the medical treatments for diphtheria after a strong argument. The Nobel Committee first considered to award the Nobel Prize to both of von Behring (German, 1854–1917) and Shibasaburo Kitazato (1853–1931), who succeeded the cultivation of *tetanus bacilli* (*Clostridium tetani*) in 1889, together with Behring and discovered *Yersinia pestis* (*Pasteurella pestis*) in 1894. However, because he was a yellow race, the Nobel Committee excluded Kitazato from the awarding. This is a well-known fact as a negative history of the Nobel Prize.

The author would like to introduce *Yuji Shibata* (1882–1980), the second son of *Keisho Shibata* (1849 or 1950–1910) and the younger brother of *Keita* (1877–1949) at the end of this section.

He was sent by the Japanese Government to Europe in 1910. He first stayed in the laboratory of A. Hantzsch in Leipzig, and soon moved to the laboratory of A. Werner (1866–1919) in Zurich to learn Coordination Chemistry. He also stayed in the laboratory of G. Urban of the University of Paris to study spectroscopy. He returned from Europe in 1913 with a spectrometer made by Adam Hilger Co. in England, which is the first equipment to be able to measure spectra of solution in Japan, and he used the equipment for the measurements of spectra of coordination

compounds in solution. He became a professor of the Imperial University of Tokyo and he is the founder of Coordination Chemistry of Japan.

He found the method for the determination of the composition of unstable coordination compounds formed in solution in 1921 [1], which was later proposed by P. Job [2] and is known as the continuous variation method or Job's method. Shibata's discovery of the method was much prior than that of Job, but it was not well recognized by chemists around the world, because his report was written in Japanese. He was the Dean of the Faculty of Science of Nagoya University, and then, the President of the Tokyo Metropolitan University. He was appointed to be the President of Japan Academy.

He is the supervisor of *Ryutato Tsuchida* (1903–1962), who discovered the *Spectrophotometric Series*, which was later explained in terms of the *Ligand Field Theory*, and *Kazuo Yamasaki* (1911–), who is the founder of *Chemical Archaeology*. The latter is the supervisor of the author.

The names of some of the pioneering scientists of Japan who were sent abroad by the Japanese Government are listed in Table 1.2.

Chemical Sciences in Japan Before the End of World War II

The Japanese Government in the Meiji Era promoted science and technology with the aim at strengthening of wealth and military power of the nation in order to approach the level of European culture and power. The policy led Japan to the *Sino-Japanese* (1894–1895) and *Russo-Japanese* (1904–1905) *Wars*. Fortunately Japan won both wars and the Government intended further promotion of science and technology owing to the victories. Science and gymnastics (physical education) became the most essential subjects to be learned by students in primary and middle high schools in Japan.

As one of the results of the promotion policy of education for science and technology, Japanese Government established additional Imperial Universities in various places in Japan after Tokyo. They are Kyoto (Kyoto Imperial University, it took about 20 years after the establishment of the Imperial University of Tokyo), Sendai (Tohoku Imperial University), Sapporo in Hokkaido (Imperial University of Hokkaido), Fukuoka (Imperial University of Kyushu), Osaka and Nagoya. Owing to the promotion policy a relatively large amount of budget was provided to these universities and they played the role as centers of scientific researches of Japan.

The importance of fundamental research works, which may not be directly connected to industrial application of tomorrow, was well recognized by the Government. On the basis of such fundamental researches, technologies for producing high quality aircrafts, tanks, weapons and warships were achieved during the time of World War II. *Zero-Fighters* and warships *Musashi* and *Yamato* may be well-known names for old people who experienced World War II. Japan became one of the most powerful countries of militarism around 1935–1940, and Japan run into the World War II. Finally Japan had to receive the attacks of atomic bombs on Hiroshima and Nagasaki in 1945.

Table 1.2 Pioneering scientists and engineers of Japan who were sent by the Japanese government

Name	Place of stay in abroad	Remarks
Takato Ohshima (1826–1901)	Visit to USA and Europe and stay in Freiburg (1871) for half a year	Study of mineralogy and analytical chemistry of minerals Production of iron from the ore
Takeaki Enomoto (1836–1908)	Rotterdam (1862–1867)	Ministers of education, telecommunications, and commerce and industry. The ambassador extraordinary in Russia. President of Engineering Chemical Society of Japan (five times)
Nagayoshi Nagai (1845–1929)	Berlin (1870–1874)	Study of organic chemistry. Pioneer of pharmaceutical science of Japan. Discoverer of ephedrine
Ichiro Kishimoto (1849–1878)	London (1866–1869)	Study of chemistry. Development of printing technology of banknotes by the Cooperation of T. Antisell
Keitaro Matsumoto (1850–1877)	Utrecht (1867–1869) Berlin (1871–1877)	Study of chemistry Study of organic chemistry
Toyokichi Takamatsu (1852–1937)	Manchester, Berlin (1879–1882)	One of the founders of the Society of Industrial Chemistry of Great Britain. One of the founders of applied chemistry and faculty of engineering of Japan. President of Tokyo Gas Company. President of Chemical Society of Japan and Japan Society for Applied Chemistry
Toranosuke Nishikawa (1854–1929)	London (1869–1879)	Study of applied chemistry. Originator for the production of soda industry in Japan and the development of other chemical industries
Mitsune Kuhara (1855–1919)	Baltimore (John Hopkins University) (1879–1881)	Study of organic chemistry. Study on Beckman transformation. Pioneer of theoretical organic chemistry in Japan
Joji Sakurai (1858–1939)	London (1876–1881)	Improvement of Beckman's method. President of Chemical Society of Japan. Creator of physical chemistry of Japan. President of Japan Academy/the first president of JSPS, Baron
Jokichi Takamine (1854–1922)	Visit to EXPO in New Orleans	Creation of industry of phosphatic manure. Discoverer of *Takadiastase*. Development of whisky in USA. Discoverer of *Adrenaline*
Kikunae Ikeda (1864–1936)	Leipzig (1899–1901)	Discoverer of glutamic acid in seaweeds. Production of a seasoning of "*Aji-no-Moto*". Introduction of "*Umami*" into the classification of tastes
Umetaro Suzuki (1874–1943)	Zurich, Berlin (1900–1906)	Discoverer of *Orizanin* (vitamin B_1). The first president of the Society for Agricultural Chemistry of Japan
Keita Shibata (1877–1949)	Leipzig and Frankfurt am Main (1910–1912)	Founder of phytological physiology and the faculty of pharmacy of the Imperial University of Tokyo
Yuji Shibata (1882–1980)	Leipzig, Zurich, Paris (1910–1913)	Founder of coordination chemistry of Japan. The president of Japan Academy

Science and Technology of Japan After the World War II

The damage caused by atomic bombardments of US forces was so serious in all parts of Japan that functions of schools and universities were almost completely stopped. No research work was possible to continue for several years after the World War II. Very limited budgets were provided to universities and no research funds were available. Equipments were damaged and chemical materials were not supplied to laboratories. Even foods and clothes were not sufficient and everyone in Japan was hungry. Japan was fully controlled under US forces.

Then, supports from US started to help Japanese people, and materials for daily use were distributed to Japanese people through organizations of the United States. Such kinds of supports were extended to scientific studies. One of the most well-known organizations of US in scientific supports was Fulbright Foundation and many young and middle age scientists were invited by the Fulbright Fellowship. After one or two years stay in US as postdoctoral research fellows or students, they came back and continued their research works in their laboratories in such ways as learned in the US. The tradition of Japanese researchers produced from the Fulbright Fellowship Programme and other similar ones is sometimes called US-School researchers. The trend was different from that at the Modernization period at the end of the 19th to the beginning of the 20th centuries. Most of Japanese scientists at that time were researchers of the European-School. Probably more than 80% of Japanese researchers went to US to study science and technology after the World War II.

At the end of the World War II, Japan was almost completely destroyed and no function was possible in researches in universities of Japan. The economical situation was so low that a monthly thoroughly of a university research associate at about 30 years old was only US$30 in 1955. The rapid recovery of Japanese economy achieved in1970s was supported the development of science and technology of Japan. The present stage of science and technology of Japan was established in these 60 years after the end of the World War II and only three to four decades after the economical growth.

In these years, Japanese Government still understands the importance of fundamental researches, as well as that of applied sciences and technologies, and the promotion of these fields has been attempted. The role of *Science Council of Japan* (*SCJ*) was very important to give advice and suggestions to the Government for giving good directions for the policy of science and technology. The fund subsidy for promotion of scientific researches provided by the *Japan Society for Promotion of Sciences (JSPS)*, an organization under the Ministry of Education and Sciences, became 188 billion Yen (US$1.65 billion) in 2005. Although the increment of the total budget is slowing down in these years, the increment of 2005 was +2.7%, which is compared with that of GDP of Japan (~+2.4% in 2005).

Recently the policy of Japanese Government slightly turned towards the direction of applications which are smoothly used for industrialization. The university system was changed and national universities were restructured to universities of Independent Corporation. Nobody knows about the result of the restructuring of the university system, and we will see results after a decade.

Students Entering Universities

In Japan about 660 universities are there, including about 60 national universities (now, *universities of Independent Corporation*) and about 600 private universities. More than 98% of Junior High School students go to Senior High Schools, and more than 55% Senior High School students go to universities. The total capacity of universities in Japan is sufficient to accept all high school students who want to enter universities. The literacy of Japanese is 100%. The average level of education of Japan should be high, but often Japanese are criticized that they are not creative although they have a good ability for improvement or modification.

The Reason of the High Level of Education and Scientific Standard of Japan

Japan has a tradition of admiring educated people and Japanese are essentially "*Knowledge-Loving People*". There are many theories and assumptions to clarify the reason. One says that we have good four seasons, spring with many flowers, summer with nice sunshine, autumn with red leaves and many fruits and winter with white snow. The four seasons polish the sensitivities of Japanese to love nature. Our temperament is, in general, moderate as the climate of the country, which makes people interest in literature and science, especially fundamental sciences. Influences from old Chinese philosophies, which were taught at high schools, may not be ignored. Longing to European cultures learned after the Modernization may still be beard in mind of Japanese. Shortage of natural resources of Japan has to make Japanese to improve imported raw materials to high quality products by adding extra values for exporting them.

To learn high technologies of European and American countries was essentially necessary for the improvement of materials producing in Japan or imported raw materials. In 1960s it was said that Japanese products were cheap but in low quality. This is completely turned out to be high quality but expensive. We can hardly see cameras produced in countries other than Japan now. The car industry of Japan may be another example.

The growth of science and technology, as well as economy, of Japan after the World War II was said "miracle". *Honesty* and *Diligence* are the virtue of Japanese.

Japan has long been believed to be one of the safest countries in the world. These characters of Japanese may play an essential role for the development of science and technology, and due to the scientific and technological development Japanese economy has also been developed. Large investments for education and research from the beginning of Modernization may bring good fruits after 100 years. Although the total budget provided to scientists of Japan may be smaller than that of US, the money distributed to fundamental researches may be more than that of

US. Financial supports for fundamental research works are essentially important for further development of science and technology which can be applied to industries. We should not see the development of science and technology of a country with short sights. *Beautiful flowers will not bloom without manure*, or *a tall building can only be built on a sound and strong basis.*

An Aspect for the Development of Chemical Sciences in Asia in the Near Future

In Asia, many countries were not free from the control of European nations and US until 1945–1946. European cultures and technologies have influenced to those of the Asian countries, but after independence of these countries the culture and technologies brought to Asian countries had not well been succeeded to native people in Asia. Therefore, industries of the Asian countries have not been developed until the economy of the countries has been developed to a certain level by the effort of the native people. The modern education system of Asian countries has been applied to almost only suzerains, and most of native people could not receive the benefit of the European education systems. Religious regulations sometimes prevent the introduction of the modern education system to some countries. Education of children and young students is one of the most important factors for the development of science and technology in Asia. The education for females must be enhanced. The gender problem in research works and in any other parts of works must be solved.

Enhancement of the System of the Fundamental Education of Asian Countries

Children must go to school. Many families in Asian countries ask their children to work to support the economy of their family. In Japan we had a similar situation before the economical development until 1950s. My grandmother could not write letters. Nowadays the literacy of Japan is so high as the author mentioned in a previous section.

Sufficient Financial Supports by the Government for Scientific Researches

Government should financially support scientific researches, especially fundamental research works. The development of good technologies and industries needs

sound fundamental researches of sciences. Enhancement of chemical sciences is one of the shortest routes to achieve the development of industries, and thus, economy of their countries.

Enhancement of the University System

It is not necessary to say about the enhancement of the university system for the scientific and technological development of a country. In many countries in South-Eastern Asia, Natural Product Chemistry is one of the strongest chemical sciences in the world. However, other chemical sciences should also be strengthened.

Introduction of Good Scientists from Other Countries as Teachers

Invitation of good teachers from other countries may be one of the ways to strengthen the education systems of universities, as Japan made such a way at the modernization. Since many Asian countries English is commonly used beside their native languages, the introduction of foreign teachers may not be a difficult problem. Supports from other countries are important. Programmes of JICA or JSPS may be some examples.

International Activities

It is needless to say about the importance of international activities for the development of science and technology of countries. To join international communities as their members is essentially important to contribute to the world. Difficulties arising from membership fees must be solved by the cooperation with industries and their governments.

Concluding Remarks

Activities of Chemical Sciences in Asia must be enhanced much more than the present stage. Japan has aimed at strengthening international relationship by joining international organizations such as IUPAC etc., but the aim might not be fully successful due to characters of Japanese.

It was often said in the international communities that Japan is an important country to be a member of the communities due to her economical strength, but the contribution of Japanese to the community, on the other sides, was not very

significant so far, because of *Japanese Three S's*. The Three S's means *Smile*, *Silence*, and *Sleep*. Japanese must say "Goodbye the Three S's".

Smile is important for the establishment of friendship among people. However, meaningless smile is meaningless. For most Asian people, especially people in colonized countries of UK and USA, English speaking is easy. They are usually eloquent and they do not *sleep* at the meetings and conferences. Now, the author would like to propose *New Three S's: Spirit*, *Scope* and *Sincerity* to be active members in international societies.

Of course, we have to keep strong *spirits* to continue scientific studies. It can be a challenging spirit to the future, can be a fighting spirit to difficulties, and can be an attacking spirit to authorities.

A wide *scope* to look over the world should be prepared by each scientist and politician. A scope limited to look at their own nation cannot be enough and not expectable for the further development of science and technology of the country.

Sincerity is the most important factor among the New Three *S*'s and it is essential for the human relationship. At contacts between scientists, *sincerity* plays the most important role for promoting scientific and technological developments.

It is nothing to say that *Honesty* is indispensable for making research works. Framing up data is a crime.

Originality is another factor which is important for the establishment of good scientific research works.

Japan has long been criticized as a country of imitation with a lack of originality. This criticism is no more correct, because many Japanese received Nobel Prize in recent years. *Originality* does not simply mean to create something from nothing. Improvement of existing matters and methodologies needs the originality. The Nobel Prize in Chemistry is awarded to persons who achieve new findings in chemistry and a remarkable improvement in chemical techniques.

The *leadership* is also quite important to lead scientists and engineers of the nation and the world. A sound and wide scope and clear and prompt decisions are indispensable for good leadership. To follow a subject of a large group and a fashionable theme does not make a new way for a further development of science and technology. A proverb in England tells us

Better be the Head of a Dog than the Tail of a Lion (England)

The same expression is given in China and Japan:

Better be the Head of Chicken than the Tail of a Cow (China and Japan)

It had been said that the 21st century is the Century of Asia. The extension of this recognition has been slightly delayed after the economical crush happened in 1997, but recent economical development of China, India and Malaysia are very much remarkable. Korea and Singapore are no more developing countries after 1990 and they are now economical leaders in Asia. In many countries in Asia, the international relationship is strengthened through economical cooperation and discussions at many international conferences. Besides APEC and many other political conferences, *Science Council of Asia (SCA)* intends to play a leading role

for the development of fundamental social and natural sciences and technologies through the discussions at the meetings. Activities of *Eurasia Conference of Chemical Sciences (EuAs C_2S)* and *Asian Chemical Congress (ACC)* organized by the *Federation of Asian Chemical Societies (FACS)* are other examples for the supports of chemical sciences in Asia. We are expecting that many other countries in Asia will organize international conferences of particular fields of chemistry which may be strong in their own countries. The IUPAC Programme of the financial supports for international conferences organized in developing and economical disadvantaged countries may be helpful for the organization of international conferences in Asian countries. Since this program can be used only the member countries, we are expecting that more countries in Asia will join IUPAC. When we see the world map, we see many countries not joining IUPAC. In the near future, it is expected that most of these countries will become members of international community of chemistry. Then, the international relationship of Asian countries will be much more enhanced.

The 21st century is called the Century of Asia. Cooperation between Asian and European countries, including USA, is essentially important for establishing the Asian Century. The **Eurasia Conference** is one of the dreams for realizing the development of chemical sciences in Asia with close cooperation of European countries.

Acknowledgments The author thanks Professor Tetsuo Shiba and Professor Akio Yamamoto who described the History of Chemistry of Japan in "Chemistry Archives" published from the Chemical Society of Japan in 2004. "History of Solution Chemistry of Japan" [3] is also referred to.

References

1. Shibata, Y., Inoue, T. and Nakatsuka, Y., 1921, *Nippon Kagaku Kaishi*, 42, 983; *Jpn. J. Chem.,* **1,** 1 (1922).
2. Job, P., 1925, *C. R. Acad Sci.,* **180,** 828 ; *Ann. Chem.*, 9, 113 (1928).
3. Ohtaki, H., 2005, *J. Solution Chem.,* **33,** 575.

Chapter 2
Functional Peptidomics: Recent Developments and State of Art

Vadim T. Ivanov, E. Yu. Blishchenko, and Andrey A. Karelin

Abstract Peptidomic research recently reviewed in is gradually establishing its position among other branches of biomolecular science, such as genomics and proteomics dealing with progressive stages of transformation of primary genetic information. Scope and limitations of modern analytical techniques in total screening of biological objects for endogenous peptides will be discussed. New data will be presented on peptide generation by microorganisms, cell cultures and plants. Considerable attention will be afforded to the biological role of peptides formed *in vivo* by proteolysis of precursor proteins with other, well defined functions, such as hemoglobin or actin.

Peptidomic research provides access to a huge number of potentially or factually active components which is an invaluable source of peptide drug leads. The first steps in medically oriented peptidomic studies will be discussed.

Keywords Antiproliferative effect, biomolecules, cancer, genom, peptides, peptidome, transcriptome

Introduction

Rapid development of modern analytical, primarily chromatographic and mass-spectral techniques coupled with growing availability of genomic sequences provided conditions for total screening of biological samples for any given class of biomolecules participating in metabolism. As a result several new branches of chemical biology, based on postgenomic technological platforms have emerged dealing with such analysis and carrying in their names common suffix "omics", such as proteomics, lipidomics, metabolomics, etc. This paper refers to one of such branches, peptidomics that deals with comprehensive structural and functional study of peptides in biological samples. By analogy with proteome, the term "peptidome" embraces the

Shemyakin-Ovchinnikov Institute of Bioorganic Chemistry,
Russian Academy of Sciences, Moscow, Russia

B. Sener (ed.), *Innovations in Chemical Biology*, doi: 10.1007/978-1-4020-69550

entire multitude of endogenous peptides present in a given biological sample. It is considered as a final step in the metabolic sequence of transformation of primary genetic information:

genome→transcriptome→proteome→peptidome

In that sense peptides represent a paramount example of how Nature diversifies from one single gene to generate multiple sets of biomolecules resulting from degradation of proteins by a complex network of proteases present in a living cell.

Besides broadening our basic knowledge of regulatory networks there are several practical incentives for systematic peptidomic studies of biological objects. Peptides are known to participate in a variety of physiological functions in nervous, endocrine, immune and other systems. In fact, they comprise the most abundant and ubiquitous group of low molecular bioregulators, serving in many cases as leads for development of new drugs. Accordingly, discovery of new endogenous peptides is expected to serve as a valuable source of information for creating new biopharmaceuticals. On the other hand, since formation of the peptidome is mechanistically linked to the state of the proteome, the amount and the repertoire of peptides must change dynamically according to the physiological or pathological state of the individual organism. Therefore it is expected that comprehensive peptide analysis (i.e. exploitation of the peptidome) may lead to discovery of novel disease biomarkers and new medical diagnostic approaches.

A broad range of biological samples, mostly of animal origin have been subjected in the past 5–10 years to peptidomic analysis by chromatographic, mass-spectral and Edman degradation techniques. Hundreds of new peptides were discovered and sequenced (Table 2.1). Both, specialized protein precursors and proteins with other functions (enzymes, structural and transport proteins, etc.) were found to contribute to the formation of peptide pools (peptidomes) of biological tissues, organs and fluids. Peptide compositions obtained at normal conditions proved conservative, showing no detectable individual difference. At the same time, as expected, peptidomes underwent characteristic shifts as a result of pathology [1–26], impact of stress [27–29], genetic modification [30], action of pharmacological agents [31] or other external factors [29, 32].

As a young, rapidly evolving branch of postgenomic technologies pepdidomics poses a number of yet unresolved questions and tasks. Some of them are briefly discussed below.

Where to Stop?

The currently attainable level of sensitivity allows to isolate and sequence peptides with ca. 0.1 nmol/g or higher concentrations in the biological sample. The number of peptides present at these concentrations is typically of the order of 10^2. Mass-spectral data indicate that the number dramatically increases at lower concentrations as

Table 2.1 Objects and short summary of the results of peptidomic studies

Tissue/organ/cell culture	Organism	Number of identified peptides	Reference
Brain	Human	20	[1]
	Bovine	107	[2]
	Rat	61	[3]
	Mouse	105	[4]
	Mouse	430	[5]
	Pig	48	[6]
	Ground squirrel	25	[7]
Hypothalamus	Rat	41	[8]
	Mouse		
Pituitary	Mouse	79	[4]
Pancreas	Frog and newt	21	[9]
Entire body	Hydra	300	[10]
		427	[11]
B-lymphocytes	Human	200	[12]
Erythrocytes	Human	51	[13]
Neurons	Drosophila	28	[14]
	Locust	44	[15]
	Crab	28	[16]
Blood plasma	Human	340	[17]
		250	[18]
		1,200	[19]
		650	[20]
Urine	Human	96	[21]
Cerebrospinal fluid	Human	35	[22]

shown in Fig. 2.1. Accordingly increases the probability that such peptides belong to "metabolic trash" which as will be discussed below is further degraded to amino acids utilized for the *de novo* protein synthesis. Still, we believe that there is always a chance that the low-abundance peptide nonetheless has a specific function if it originates in a limited cellular compartment or has extreme affinity to the biological target. Therefore, peptidomic analysis should be carried out at highest possible sensitivities of analytical techniques.

Endogenous or Artifact?

It has been noted [13, 33] that in several early publications describing total screening of biological extracts for peptide material insufficient care has been taken to avoid the *ex vivo* (or *post mortem*) formation of peptides in the extract where all proteases of the initial sample are released from the cellular compartments and are free to contact with the endogenous protein and peptide components. The resultant products with sometimes quite interesting activities should be formally considered

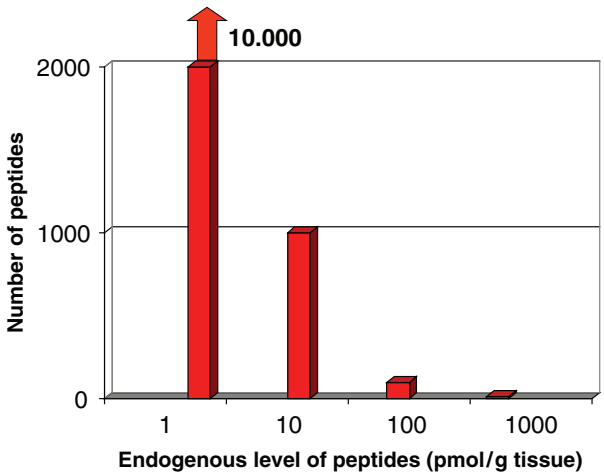

Fig. 2.1 Concentration dependence on peptide diversity (estimate)

as artifacts not participating directly in the normal homeostasis. To avoid their formation measures should be taken to minimize the hydrolysis of proteins and peptides in the extract, e. g. by preparing it at possibly lower temperatures [24, 25] or inhibiting the activity of proteases by specific inhibitors [13, 22], denaturation in boiling water [6], by microwave irradiation [33] or using organic solvents [15]. The effect of using the cocktail of protease inhibitors is illustrated in Fig. 2.2. The extract prepared in the absence of inhibitors contains several peptides (with masses 2,225, 2,323, 2,432) absent in the extract where the *ex vivo* proteolysis was inhibited. On the other hand, several peptides survived in the presence of the cocktail have disappeared in the sample with active proteases (masses 2,001, 2,092, 2,199, 2,303). Considerable part of peptides is present in both samples (with masses 1,865, 2,155, 2,428, 2,528, 2,621, 2,659, 2,734, 4,966).

How General?

All entries of Table 2.1 belong to samples representing the animal kingdom. In order to demonstrate the generality of peptidome concept we analyzed the extract of *Avenasativa* oat acrospires [34]. Table 2.2 provides the list of peptides found in that plant as well as their tentative protein precursors. Peptide formation in this case seems somewhat less intensive and on the average the peptides are longer than in animal samples. We consider this result as a proof of peptidome formation in plants. Still peptidomics of plants is apparently in its embryonic state and more results are expected in the near future. Procaryotes are not yet studied for generation of peptide pools.

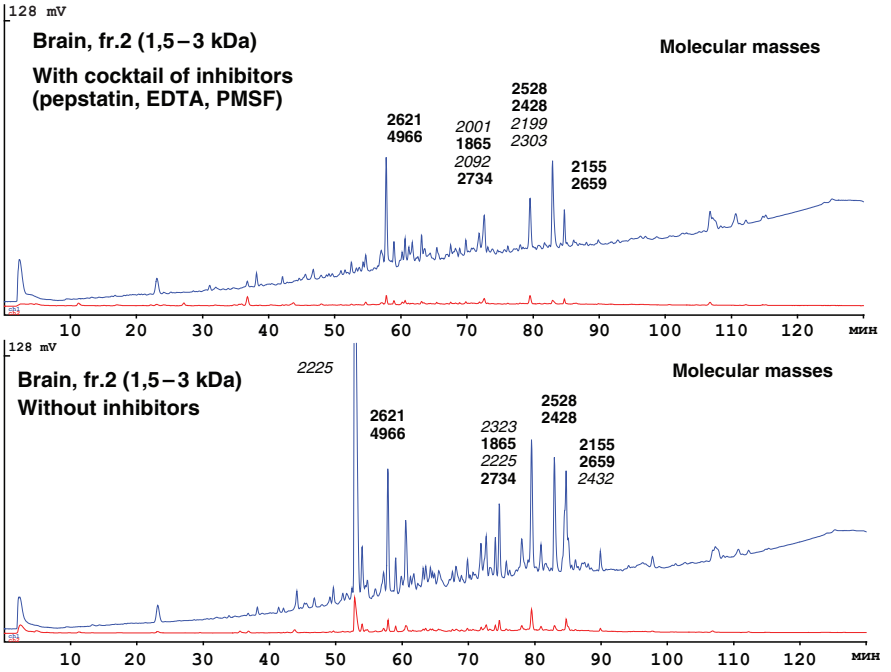

Fig. 2.2 Comparative chromatographic profiles of low molecular weight fraction isolated from rat brain

Table 2.2 Molecular masses and amino acid sequences of peptides isolated from the extract of acrospires of *Avena sativa* oat

#	MM	N-terminal sequence	Precursor/fragment/source/homology	Content (nmol/g tissue)
1	7,092	ATXDASNLVAXAGP	Acidic class III chitinase OsChib3a/219-288/*Oryza sativa* 64%	0.2
2	5,283	NT	Undetermined	0.1
3	4,864	DD	Undetermined	0.2
4	3472	XSXGSPXGGNG	Pectinesterase-like protein/394-426/*Arabidopsis thaliana* 82%	0.1
5	3,379	GSXGSPPXPGNN	Putative lateral organ boundaries (LOB) domain protein 37/177-210/*Oryza sativa*/75%	0.3
6	5,283	XXTKDDIARNN	Leaf thionin Asthi3/30-75/*Avena sativa*/82%	0.05
7	4,458	GYGGGXHRGXGLRLR	Putative alcohol oxidase/521-561/*Oryza sativa*/67%	0.05
8	3,305	EXDVXXGXPPAA	Delta-aminolevulinic acid dehydratase, chloroplast precursor (porphobilinogen synthase) (ALADH) (ALAD)/60-94/*Selaginella martensii*/100%	0.05

(continued)

Table 2.2 (continued)

#	MM	N-terminal sequence	Precursor/fragment/source/homology	Content (nmol/g tissue)
9	3,322	AIFKGXVSNNLXXFP	NADH dehydrogenase subunit F/172-201/(*Helianthostylis sprucei*/53%	0.2
10	8,983	AIFPGQVSNAL	gi|52353532|gb|AAU44098.1| hypothetical protein/11-99/*Oryza sativa*/58%	0.2
11	7,264	FPWSPXG	Sterol 4-alpha-methyl-oxidase 1/223-283/*Arabidopsis thaliana*/86%	0.2
12	3,284	ALNXGQVDTXLAPXV	Probable phospholipid transfer protein – oat (fragment) | alpha-amylase inhibitor, Oat-B {N-terminal}/1-27/*Avena sativa*(73%	0.3
13	7,188	APYNPSSLLF	Tyrosine decarboxylase (EC 4.1.1.25)/65-130/70%	0.2
14	4,401	APPPDDDTGN	Gi|50949009|ref|XP_493862.1| hypothetical protein/60-102/*Oryza sativa*/70%	0.1
15	8,663	MQIFVXTLTGXTITL	Ubiquitin/100%	0.05
16	3,400	ASRSSPPGGG	gi|37530720|ref|NP_919662.1| unknown protein/20-53/*Oryza sativa*/80%	0.1
17	3,450	ASRSSP	gi|37530720|ref|NP_919662.1| unknown protein/20-54/*Oryza sativa*/80%	0.1
18	3,290	ASRSSPPGGG	gi|37530720|ref|NP_919662.1| unknown protein/20-52/*Oryza sativa*/80%	0.1
19	3,268	ASRSSPP	gi|37530720|ref|NP_919662.1| unknown protein/20-51/*Oryza sativa*/80%	2.5
20	3,312	APSSGGP	P0506B12.19/217-251/*Oryza sativa*/100%	0.3
21	3,324	APSSGGGG	Acidic ribosomal protein P2-like/76-108/*Arabidopsis thaliana*/100%	0.2
22	3,441	VPAANA	gi|50253325|dbj|BAD29593.1| hypothetical protein/165-199/*Oryza sativa*/100%	0.2
23	3,478	APSSGGX	P0506 B12.19/217-253/*Oryza sativa*/100%	0.1

Source of Peptides: Cell Cultures as Preferred Model Systems

Living organisms, their organs and tissues represent a complex, heterogeneous system of interacting parts and cells. Therefore tracing the origin of individual peptides in the peptidome in these cases (most of the entries in Table 2.1) is a daunting, hardly attainable task. Similar problem arises in the case of biological fluids which collect the information on the metabolic state of remote parts of the organism. To reduce that difficulty cell cultures should be recommended as a much simpler object of peptidomic studies, each type of cells contributing its share to the total peptidomes (indeed, peptide pools) of more complex structures.

Bearing in mind the frequent presence of hemoglobin derived peptides in tissue extracts we studied generation of peptides by the primary culture of human red blood cells [13, 35]. It was shown that inside the erythrocytes α- and β-globin chains give rise to large families of relatively long (up to the 94-membered α-globin 1–94) of which 37 α-chain fragments and 15 β-chain fragments have been sequenced. At the same time erythrocytes release to the culture medium shorter 2–20 membered fragments (32 of them sequenced) by a metabolic energy dependent mechanism [36–38]. Further studies, when transformed myelomonocytes (WEHI-3) and human erythroleukemia K562 cells were also shown to secrete to the supernatant specific sets of peptides, confirmed the general nature of the phenomenon of peptide release by individual animal cell cultures [38].

Biological Activity of Peptide Pool Components

Even cursory inspection of peptides collected in Table 2.1 provides compelling evidence that the diversity of endogenous peptides is comprised of a much broader set of components than traditional hormones, neuromodulators and antibiotics. In spite of the availability of scattered data on the activity of selected pool components the principal question on the biological role of peptide pools remains unanswered: does the bulk of pool peptides represent transient products of protein substrate destruction on their way to reusable amino acid building blocks? Or do these peptides perform a useful regulatory function? The answer to these questions requires systematic study of a large number of samples in adequate biological test systems.

We have chosen animal cell cultures for that purpose, bearing in mind the following advantages of such system: (i) the action of peptide results in a limited number of integral responses, when a variety of biochemical mechanisms gives rise to uniform effects, such as cell death or stimulation/inhibition of cell proliferation rate; (ii) the test requires low, picomolar amounts of peptides; (iii) the results are treated by simple and reliable statistic methods.

Over 300 peptides isolated in our laboratory were studied in one or more tumor or normal cell cultures [39–44]. Part of the results obtained is summarized in Table 2.3. Over 75% of the peptides showed pronounced proliferative or antiproliferative activity in at least one cell type (Fig. 2.3). As a rule, tumor cells are more sensitive to peptide action. Besides the cell type, experimental conditions such as cell density or composition of the culture medium also affected the overall effect. In several cases (13%, Fig. 2.3) even the sign of the effect was peptide concentration dependent. Generally, experiments with cell cultures conform with the view that the main physiological function of cell and tissue peptidomes is control of long term processes and the homeostatic balance (i.e. cell differentiation, proliferation and elimination). The overall effect of peptide pools is achieved by concerted action of total sets of peptides rather than by single components. The molecular mechanisms of peptide action in cells requires concrete study in each individual case and are the subject of current research.

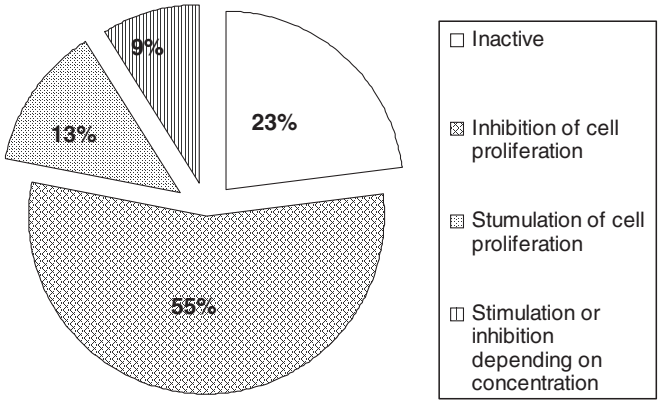

Fig. 2.3 Classification of peptide pool components exhibiting different types of activity

Table 2.3 Activity of endogenous fragments of functional proteins in tumor and normal fibroblasts. The peptides were tested for their impact on the number of cells after 24 h of incubation in serum-deficient culture medium. The active peptides affect the cell number by 25% and more

			Activity	
#	Sequence	Protein precursor	Tumor fibroblasts	Normal fibroblasts
1	VLSPADKTNVKAAWGKVGAHAGEYG AEALERMFLSFPTTKYFPHFDLS	α-globin (1–49)	NA	NT
2	VLSPADKTNVKAAWGKVGAHAGEYG AEALERMFLSFP	α-globin (1–37)	+	NT
3	VLSPADKTNVKAAWGKVGAHAGEYG AEALERMF	α-globin (1–33)	NA	NT
4	VLSPADKTNVKAAWGKVGAHAGEYG AEALERM	α-globin (1–32)	+/–	NT
5	VLSPADKTNVKAAWGKVGAHAGEY GAEALER	α-globin (1–31)	+/–	NT
6	VLSPADKTNVKAAWGKVGAHAGEY GAEAL	α-globin (1–29)	NA	NT
7	VLSPADKTNVKAAWGKVGAHAGEYG	α-globin (1–25)	NA	NT
8	VLSPADKTNVKAAWGKV	α-globin (1–17)	—	NT
9	AAWGKVGAHAGEYG	α-globin (12–25)	–/+	NT
10	AAWGKVGAHAGEY	α-globin (12–24)	–/+	NT
11	AAWGKVGAHAGE	α-globin (12–23)	NA	NT
12	AWGKVGAHAGEYG	α-globin (13–25)	—	NT
13	VGAHAGE	α-globin (17–23)	NA	NT
14	LVTLAAHLPAEFTPAVHASLDKFLASV TVLTSKYR	α-globin (106–141)	+	NT
15	VTLAAHLPAEFTPAVHASLDKFLASV TVLTSKYR	α-globin (107–141)	NA	NT
16	TLAAHLPAEFTPAVHASLDKFLASVT VLTSKYR	α-globin (108–141)	+	NT
17	AAHLPAEFTPAVHASLDKFLASVTVL TSKYR	α-globin (110–141)	+	NT
18	STVLTSKYR	α-globin (133–141)	+	NT
19	TVLTSKYR	α-globin (134–141)	+	+

(continued)

Table 2.3 (continued)

#	Sequence	Protein precursor	Activity	
			Tumor fibroblasts	Normal fibroblasts
20	VLTSKYR	α-globin (135–141)	+	NT
21	TSKYR	α-globin (137–141)	+	+
22	TVLTSKY	α-globin (134–140)	+	NT
23	STVLTS	α-globin (133–138)	+	NT
24	TSKY	α-globin (137–140)	+	NT
25	TS	Multiple precursors	+	NT
26	VHLTPEEKSAVTALWGKVNVDEVG GEALGRLLVVYPWTQRFFESFGD	β-globin (1–47)	NA	NT
27	VHLTPEEKSAVTALWGKVNVDEVG GEALGRLLVVYPWTQRF	β-globin (1–41)	NA	NT
28	TALWGKVNV	β-globin (12–20)	—	NT
29	TALWGKVN	β-globin (12–19)	—	NT
30	LVVYPWTQRY	β-globin (32–41)	—	NT
31	LVVYPWTQRF	β-globin (32–41)	—	NT
32	LVVYPWTQR	β-globin (32–40)	—	NT
33	LVVYPWTQ	β-globin (32–39)	—	NT
34	LVVYPWT	β-globin (32–38)	—	NT
35	VVYPWTQRF	β-globin (33–41)	—	NT
36	VVYPWTQR	β-globin (33–40)	–/+	NT
37	VVYPWTQ	β-globin (33–39)	—	NA
38	VVYPWT	β-globin (33–38)	—	NT
39	VYPWTQRF	β-globin (34–41)	—	NT
40	YPWTQRF	β-globin (35–41)	—	NT
41	LKYPIEHGIVTNWDDMEKIWHHT	β-actin-(67–89)	—	NT
42	IVTNWDDMEKIWHHTF	β-actin-(75–90)	—	NA
43	NWDDMEKIWHHT	β-actin-(78–89)	—	NT
44	NWDDMEKIWHH	β-actin-(78–88)	—	NT
45	NWDDMEKIWH	β-actin-(78–87)	—	NA
46	WDDMEKIWHHT	β-actin-(79–89)	—	NA
47	WDDMEKIWH	β-actin-(79–87)	—	NT
48	DDMEKIWH	β-actin-(80–87)	—	NT
49	YPIERGIVT	β-actin-(69–77)	—	NA
50	EEEEG	Multiple precursors	—	NA
51	DAE	Multiple precursors	—	NA
52	EAE	Multiple precursors	—	NT
53	EAD	Multiple precursors	—	NT
54	EADQ	Multiple precursors	—	NT
55	EADN	Multiple precursors	—	NT
56	SQIFV	Melastatin 1 (319–408)	NA	NT
57	PYQYPALTPE	Aldolase A (1–67)	NA	NT
58	SQIFE	Melanophilin (339–390)	NA	NT
59	SQIFXSL	Carbonic anhydrase XI (278–327)	NA	NT
60	APIFVXT	Cadherin EGF LAG seven-pass G-type receptor 2 (163–201)	NA	NT

$p < 0.01$; NT – Not tested; NA – Not active; + – Proliferative effect; — – Antiproliferative effect; +/- – Proliferative effect at higher concentration, antiproliferative effect at lower concentration; -/+ – Antiproliferative effect at higher concentration, proliferative effect at lower concentration

Applied Aspects

As already mentioned in the introduction, composition of the peptidome undergoes distinct shifts from the normal to the pathological state. Figure 2.4 shows the hemoglobin derived peptides that change their relative content at various pathologies, thereby lending themselves as new potential biomarkers. At present considerable effort is being directed at exploitation of blood serum and plasma peptidomes for development of early tumor diagnostics based on discovery of new peptide biomarkers [45–47]. In spite of formidable technical difficulties related to extensive *ex vivo* peptide formation, tight binding of peptides by large excesses of albumin or other blood proteins, etc. it is obvious that peptidomic studies hold considerable promise for providing useful new tools in practical diagnostics.

As a logical step in studies of the antiproliferative action of pool components in tumor cells we studied the antitumor activity of peptides in combination with standard antitumor chemotherapeutic agents (vincristin, metatrexate, cis-platin, epirubicin) [48].

Considerable synergism was found in the action of the two types of agents, both *in vitro* and *in vivo*. Figure 2.5 shows the dramatic increase of epirubicin efficacy in mice breast carcinoma in the presence of β-globin derived heptapeptide, the so called VV-hemorphin-5. The data accumulated allow to consider endogenous antiproliferative peptides or their synthetic derivatives as promising second line pharmaceuticals for combined application with other drugs in cancer therapy.

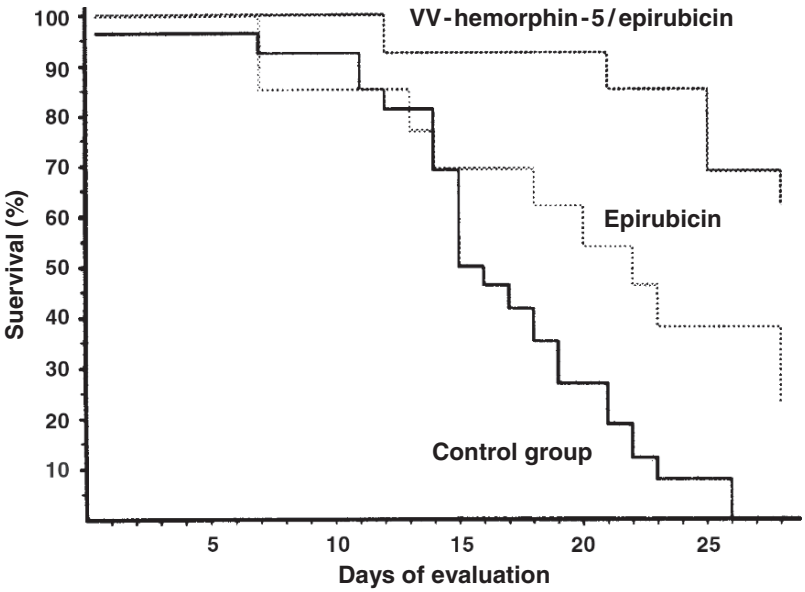

Fig. 2.4 Survival of mice with the breast cancer subjected to treatment with test substances

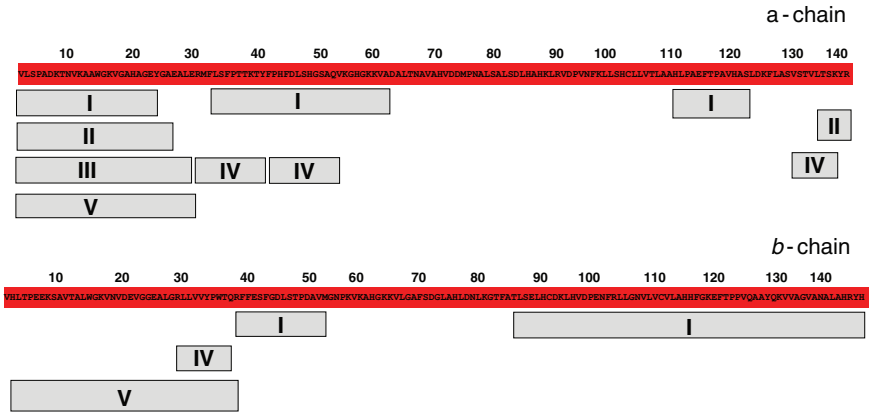

Fig. 2.5 Endogenous hemoglobin fragments responding by concentration changes in human tissues to pathologies of different genesis. I – Alzheimer's desease; II – lung carcinoma; III – Hodgkin's desease; IV – brain ischemia; V – lymphosarcoma

References

1. Slemmon, J.R., Wengenack, T.M. and Flood, D.G., 1997, *Biopolymers,* **43,** 157–170.
2. Karelin, A.A., Philippova, M.M., Karelina, E.V., Strizhkov, B.N., Grishina, G.A., Nazimov, I.V. and Ivanov, V.T., 1998, *J. Pept. Sci.,* **4,** 211–225.
3. Karelin, A.A., Philippova, M.M.,Yatskin, O.N., Kalinina, O.A., Nazimov, I.V., Blishchenko, E. Yu. and Ivanov, V.T., 2000, *J. Pept. Sci.,* **6,** 345–354.
4. Che, F.Y., Yan, L., Li, H., Mzhavia, N., Devi, L.A. and Fricker, L.D., 2001, *Proc. Natl. Acad. Sci. USA,* **98,** 9971–9976.
5. Minamino, N., Kuwahara, H., Kuwahara-Matsui, Y., Isoyama-Tanaka, J., Kibara, T., Matsubae, M., Katafuchi, T., Takao, T. and Isoyama, M., 2005, *J. Pept. Sci*., *2004* (Y. Shimohigashi, ed.), The Japanese Peptide Society, Osaka, pp 29–32.
6. Minamino, N., Tanaka, J., Kuwahara, H., Kihara, T., Satomi, Y., Matsubai, M. and Takao, T., 2003, *J. Chromatogr. B Analyt. Technol. Biomed. Life Sci.,* **792,** 33–48.
7. Ziganshin, R.Kh., Sviryaev, V.I., Vas'kovskii, B.V., Mikhaleva, I.I., Ivanov, V.T., Kokoz, Y.M., Alekseev, A.E., Korystova, A.F., Sukhova, G.S. and Emel'yanova, T.G., 1994, *Bioorg. Khim.,* **20,** 899–918.
8. Svensson, M., Skold, K., Svenningson, P. and Andren, P.E., 2003, *J. Proteome Res.,* **2,** 213–219.
9. Conlon, J.M., Kim, J.B., Johansson, A. and Kikuyama, S., 2002, *J. Endocrinol.* **175,** 769–777.
10. Bosch, T.C. and Fujisawa, T., 2001, *Bioassays,* **23,** 420–427.
11. Fujisawa, T., Hayakawa, E. and Takahashi, T., 2005, *J. Pept. Sci. 2004* (Y. Shimohigashi, ed.), The Japanese Peptide Society, Osaka, pp 21–24.
12. Hickman, H.D., Luis, A.D., Buchli, R., Few, S.R., Sathiamurthy, M., VanGundy, R.S., Giberson, C.F. and Hildebrand, W.H., 2004, *J. Immunol.,* **172,** 2944–2952.
13. Ivanov, V.T., Karelin, A.A. and Yatskin, O.N., 2005, *Biopolymers,* **80,** 332–346.
14. Baggerman, G., Cerstiaens, A., De Loof, A. and Schoofs, L., 2002, *J. Biol. Chem.,* **277,** 40368–40374.
15. Clynen, E., Baggerman, G., Veelaert, D., Horst, D. Van der, Harthoorn, L., Derua, R., Waelkens, E., De Loof, A. and Schoofs, L., 2001, *Eur. J. Biochem.,* **268,** 1929–1939.

16. Huybrechts, J., Nusbaum, M.P., Bosch, L.V., Baggerman, G., De Loof, A. and Schoofs, L., 2003, *Biochem. Biophys. Res. Commun.,* **308,** 535–544.
17. Richter, R., Schulz-Knappe, P., Schrader, M., Standker, L., Jurgens, M., Tammen, H. and Forssman, W.G., 1999, *J. Chromatogr. B Biomed. Sci. Appl.,* **726,** 25–35.
18. Koomen, J.M., Li, D., Xiao, L., Liu, T.C., Coombes, K.R., Abbruzzese, J. and Kobayashi, R., 2005, *J. Proteome Res.,* **4,** 972–981.
19. Lowenthal, M.S., Frogale, K., Al Mehta, K., Bandle, B.W., Araujo, R.P., Hood, B.L., Veenstra, T.D., Conrads, T.P., Goldsmith, P., Fishman, D.A., Petricoin, E.F. and Liotta, L.A., 2005, *Clin. Chem.,* **51,** 1933–1945.
20. Villanueva, J., Shaffer, D.R., Philip, J., Chaparro, C.A., Erdjument-Bromage, H., Olshen, A.B., Fleisher, M., Lilja, H., Brogi, E., Boyd, J., Sanchez-Carbayo, M., Holland, E.C., Cordon-Cardo, C., Scher, H.I., Tempst, P., 2006, *J. Clin. Invest.,* **116,** 271–284.
21. Cutillas, P.R., Norden, A.G., Cramer, R., Burlingame, A.L. and Unwin, R.J., 2003, *Clin. Sci. (Lond).,* **104,** 483–490.
22. Stark, M., Danielson, O., Griffiths, W.J., Jornvall, H. and Johansson, J., 2001, *J. Chromatogr. B Biomed. Sci. Appl.,* **754,** 357–367.
23. Pivnik, A.V., Rasstrigin, N.A., Philippova, M.M., Karelin, A.A. and Ivanov, V.T., 1996, *Leuk. Lymphoma,* **22,** 345–349.
24. Slemmon, J.R. and Flood, D.G., 1992, *Neurobiol. Aging,* **13,** 649–660.
25. Slemmon, J.R., Hughes, C.M., Campbell, G.A. and Flood, D.G., 1994, *J. Neurosci.,* **14,** 2225–2235.
26. Zhu, Y.X., Hsi, K.L., Chen, Z.G., Zhang, H.S., Fang, P., Guo, S., Kao, Y. and Tsou, K., 1986, *FEBS Lett.,* **208,** 253–257.
27. Karelin, A.A., Blishchenko, E. Yu. and Ivanov, V.T., 1999, *Neurochem. Res.,* **24,** 1117–1124.
28. Glamsta, E.M., Morkrid, L., Lantz, I. and Nyberg, F., 1993, *Regul. Pept.,* **49,** 9–19.
29. Che, F.Y., Yuan, Q., Kalinina, E. and Fricker, L.D., 2005, *J. Biol. Chem.,* **280,** 4451–4461.
30. Che, F.Y., Biswas, R. and Fricker, L.D., 2005, *J. Mass Spectrom.,* **40,** 227–237.
31. Karelin, A.A., Philippova, M.M., Karelina, E.V., Strizhkov, B.N., Nazimov, I.V., Ivanov, V.T., Danilova, R.A. and Ashmarin, I.P., 2000, *J. Peptide Sci.,* **6,** 168–174.
32. Uttenweiler-Josef, S., Moniatte, M., Lagueux, M., Van Dorsselaer, A., Hoffmann, J.A. and Bulet, P., 1998, *Proc. Natl. Acad. Sci. USA,* **95,** 11342–11347.
33. Swensson, M., Skold, K., Svenningsson, P. and Andren, P.E., 2003, *J. Proteome Res.,* **2,** 213–219.
34. Gara, O.G., Yatskin, O.R., Shvets, V.I., Karelin, A.A. and Ivanov, V.T., 2006, *Bioorg. Khim.,* **32,** 211–220.
35. Ivanov, V.T., Karelin, A.A., Philippova, M.M., Nazimov, I.V. and Pletnev, V.Z., 1997, *Biopolymers,* **43,** 171–188.
36. Ivanov, V.T., Karelin, A.A., Blishchenko, E.Yu., Philippova, M.M. and Nazimov, I.V., 1998, *Pure, Appl. Chem.* **70,** 67–74.
37. Karelin, A.A., Philippova, M.M., Yatskin, O.N., Blishchenko, E.Yu., Nazimov, I.V. and Ivanov, V.T., 1998, *Bioorg. Khim.* **24,** 271–281.
38. Ivanov, V.T., Yatskin, O.N., Sazonova, O.V., Talmazova, A.G., Leontiev, K.V., Philippova, M. M., Karelin, A.A. and Blishchenko, E.Yu., 2006, *Pure Appl. Chem.,* **78,** 963–976.
39. Ivanov, V.T., Yatskin, O.N., Kalinina, O.A., Phillipova, M.M., Karelin, A.A. and Blischenko, E.Yu., 2000, *Pure Appl. Chem.,* **72,** 355–363.
40. Blishchenko, E.Yu., Kalinina, O.A., Sazonova, O.V., Khaidukov, S.V., Egorova, N.S., Surovoi, A.Yu., Philippova, M.M., Vass, A.A., Karelin, A.A. and Ivanov, V.T., 2001, *Peptides,* **22,** 1999–2008.
41. Blishchenko, E.Yu., Sazonova, O.V., Kalinina, O.A., Yatskin, O.N., Philippova, M.M., Surovoy, A.Yu., Karelin, A.A. and Ivanov, V.T., 2002, *Peptides,* **23,** 903–910.
42. Blishchenko, E. Yu. Sazonova, O.V., Surovoy, A. Yu. Khaidukov, S.V., Sheikine, Yu.A., Sokolov, D.I., Freidlin, I.S., Philippova, M.M., Vass, A.A., Karelin, A.A. and Ivanov, V.T., 2002, *J. Peptide Sci.,* **8,** 438–452.
43. Sazonova, O.V., Blishchenko, E.Yu., Kalinina, O.A., Egorova, N.S., Surovoy, A.Yu., Philippova, M.M., Karelin, A.A. and Ivanov, V.T., 2003, *Protein Pept. Lett.,* **10,** 386–395.

44. Ivanov, V.T. and Karelin, A.A., 2005, *Expert Rev. Proteomics,* **2,** 463–473.
45. Liotta, L.A. and Petricoin, E.F., 2006, *J. Clin. Invest.,* **116,** 25–30.
46. Diamandis, E.P., 2006, *J. Proteome Res.,* **5,** 2079–2082.
47. Orvisky, E., Drake, S.K., Martin, B.M., Abdel-Hamid, M., Ressom, H.W., Varghese, R.S., An, Y., Saha, D., Hortin, G.L., Loffredo, C.A. and Goldman, R., 2006, *Proteomics,* **6,** 2895–2902.
48. Blishchenko, E.Yu., Sazonova, O.V., Kalinina, O.A., Moiseeva, E.V., Vass, A.A., Karelin, A.A. and Ivanov, V.T., 2005, *Cancer Biol. Ther.,* **4,** 118–124.

Chapter 3
Structural Bioinformatics in the Discovery of Novel Drugs

Mahmud Tareq Hassan Khan and Ingebrigt Sylte

Abstract There have been extensive advancements in structural genomics during the last years, especially after the sequencing of the human genome. With the augment of computational power, the *in silico* systems afford detailed insights into the structure-function relationships (SFR). The *in silico* analysis includes, prediction, virtual-engineering and modeling of mechanism, stability, specificity, and protein-protein and protein-drug (small molecule ligands) interactions as well as screening of drug candidates, both *in silico* and *in vitro*. During the last two decades, in the post-genomic era, the number of sequence-known proteins has increased rapidly. Several of these are possible "druggable" targets. A large number of recent methods and tools for the structural bioinformatics and computational chemistry have been published which provide the means to exploit the wealth of new informatics in drug discovery approaches. Not surprisingly, the biopharmaceutical industry has been quick to recognize the benefits of these new maturities and starting to accept them. In this review, some of the recent methods discussed briefly concerning their aspects of docking, virtual screening and virtual library design in drug discovery.

Keywords Docking, drug discovery, genomics, HIV-1 TAR RNA, molecular modelling, proteomics, thermolysin, transcription factors, tyrosinase virtual high-throughput screening, virtual ligand screening

Abbreviations 3D: *Three-dimensional*; HTS: *High-throughput screening*; NFκβ: *Nuclear factor kappa beta*; PDB: *Protein Databank*; QSAR: *Quantitative structure-activity relationship*; SMPI: *Streptomyces metalloproteases inhibitor*; VCL: *Virtual combinatorial library*; vHTS: *Virtual high-throughput screening*; VLS: *Virtual ligand screening*

Department of Pharmacology, Institute of Medical Biology, University of Tromsø, 9037 Tromsø, Norway

B. Sener (ed.), *Innovations in Chemical Biology*, doi: 10.1007/978-1-4020-6955-0

Introduction

Large amounts of comprehensive genome sequences are motivating the terra-scale bioinformatics, and structural and functional proteomics endeavours intended to accelerate the identification and characterization of novel drug targets, which is a critical pre-requisite for the development of new therapeutics. The number of known 3D structures of protein is increasing very rapidly, which is considered as valuable for accelerating the drug discovery processes [1, 2]. Moreover the advancements in the sequencing of whole genome, high-throughput technologies, robotics and bioinformatics in last couple of years have drastically renovated the prospects. Many possible "druggable" targets, such as proteins, enzymes, receptors, genes, DNAs, RNAs, etc., have been identified by genome analyses, and structurally detected by X-ray diffraction or NMR spectroscopy [1, 3].

Protein-structure information has traditionally played only a supporting role in many pharmaceutical drug discovery programs. With huge investments in "high-throughput screening (HTS)" and combinatorial chemistry technologies, many pharmaceutical companies aren't willing to put structural information in front in the drug discovery process. Proteins are among the most unpredictable molecules in nature. As genes are translated into proteins, an essentially digital store of information becomes a 3D language of folds and motifs, helices and sheets that we only dimly understand [4].

In the early 1980s, the 3D structures of the relevant "drug targets" were not usually available directly from X-ray crystallography, and comparative models based on homologues began to be exploited in lead optimization [5, 6]. A limited number of the accessible protein sequences from the human genome has so far been solved structurally regardless of the major developments in structural proteomics [7]. The residual, inexplicable 3D structures of proteins of the human genome will hold an affluence of information of significance meant for the appreciative of how cells work and how we can treat diseases. One of the most central roles of computational biology is to predict 3D structures of proteins by homology or comparative modelling to wrap the gap between the number of sequences and known 3D structures [7, 8]. Simple comparative modelling tools have been used for more than three decades and are well established [6, 9, 10].

In the present report we are reviewing some aspects of structural bioinformatics, some of its essential components, and their proper and efficient utilization on drug discovery process to foster the speed.

Target Identification: From Genomics Efforts to Homology Modelling

One of the key intentions of genomic researches is to discover and functionally illustrate the protein constituents of the human organism, thus providing a valuable basis for therapeutic intervention into pathophysiological mechanisms, currently

unexploited by approved medicines. A putative disease-associated protein is either identified by database-mining technologies (i.e. bioinformatics), or by protein profiling of cells or tissues (i.e. proteomics). Until now all the molecules used clinically or being in the shelf of pharmacies target about 500 proteins. So the search for new target proteins for different clinically important diseases is the certainly the dominant bottleneck of these days' pharmaceutical interest. Different aspects of genomics could be one major field of their interest. Structural and functional genomics, has recently become a reality, and there are several worldwide initiatives to define 3D structures of representative protein family members of several genomes [3, 11–14]. Structures defined by these structural genomics initiatives are useful not only as a basis for ligand design but also for homology recognition on the basis of structural comparisons [3]. In general, the putative relatives are recognized, the sequences aligned, and the 3D structures modelled. This is especially helpful for predicting binding sites and molecular functions if key residues are conserved [15, 16]. Up to now there are around 38,320 structures available in the Protein Databank (www.rcsb.org/pdb/) [17]. Several important drug targets are membrane proteins, and still only a few membrane proteins have been solved by X-ray crystallography, and mainly from bacteria. Table 3.1 is showing some statistical data of PDB at present.

Once a homologue of known structure has been identified, the targeted protein/receptor can be modelled using a variety of comparative or homology modelling procedures. Examples are:

- Fragment-assembly approach, such as Composer [18] or SWISS-MODEL [19]
- Restraint-based approach, such as Modeller [20]

These approaches typically provide high-quality models if the overall sequence identity is >30%, but the accuracy falls off sharply when it is lower, mainly because of the complications in acquiring superior alignments, in calculating shifts of core residues and in building loops [21].

Figures 3.1 and 3.2 are showing the different steps of a discovery approach, with the putative time duration. Figure 3.3 is showing a model of vibriolysin which is typical example of a homology model generated by homology with thermolysin.

Table 3.1 Statistical data from the Protein Databank (PDB) at present [17]

	Molecular types				
Experimental method	Protein	Nucleic acids	Protein-nucleic acid complexes	Others	Total
X-ray	30,147	922	1,379	33	**32,481**
Electron Microscopy	4,782	720	121	6	**5,629**
NMR	90	10	29	0	**129**
Other	74	4	3	0	**81**
Total	**35,093**	**1,656**	**1,532**	**39**	**38,320**

Figure 3.4 is showing the modern drug discovery approaches using combined approaches of *in silico* and *in vitro* sequentially.

The eventual significance of a prospective target protein can only be confirmed by discriminatory modulation of its utility in subsequent disease models by either knockout or antisense experimentations, or otherwise utilizing bioorganic methods embracing tailor-made inhibitory or antagonistic ligands.

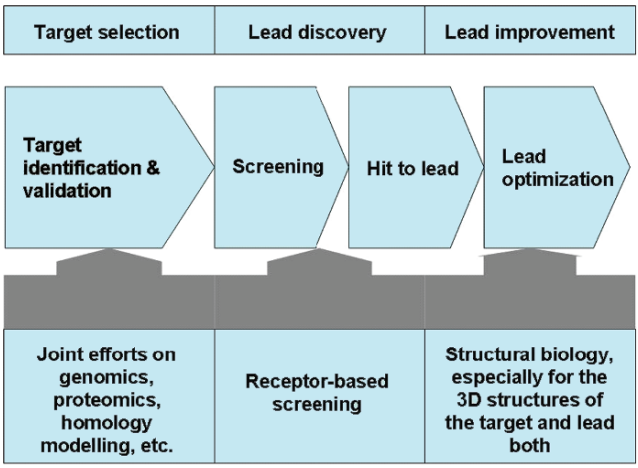

Fig. 3.1 Steps involved in drug discovery approach – a typical example. Joint efforts of classical genomics, proteomics, homology modelling, receptor- or structure-based screening approaches, and finally the structural biology efforts to determine the 3D structures of target receptor and receptor-ligand complex to get structural insight into their interactions

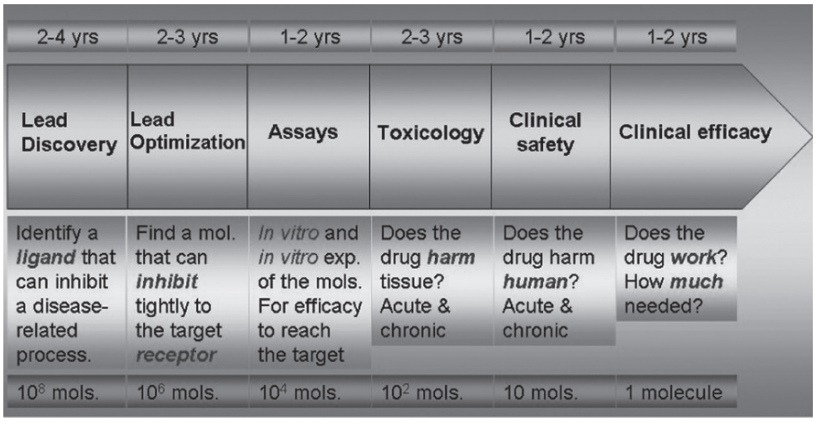

Fig. 3.2 A more detailed example of the different steps involved in a classical drug discovery approach. Different steps, duration, and number of molecules involved are shown for comparison

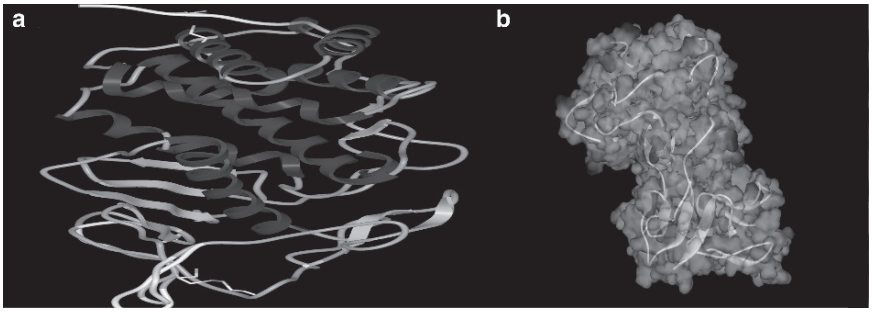

Fig. 3.3 A typical example of a homology model of vibriolysin. (A) Cartoon of the model, and (B) the transparent vdw electro-potential surface of the model. (A) has been created with ICM Pro™ (www.molsoft.com) and (B) has been created with DS visualizer™ (www.accelrys.com)

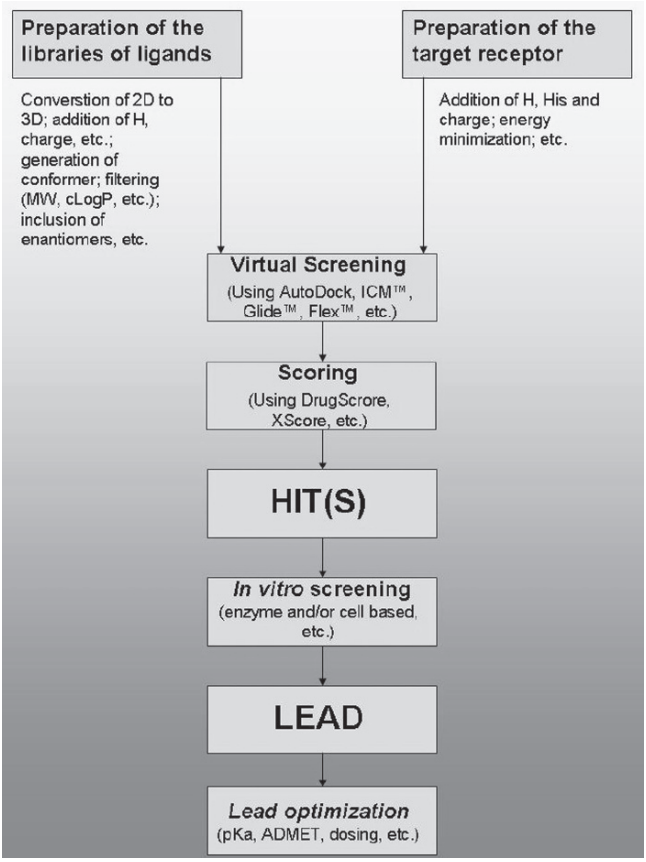

Fig. 3.4 Modern methods in drug discovery and development. The different in silico and in vitro approaches have been combined in the figure

Molecular Docking of Ligands Against Target Receptors

Once the 3D structures have been obtained, either by experimental studies or by modelling, the target receptors (mostly protein, enzyme, etc.) are ready for *in silico* studies against different ligands. These ligands can be found either by virtual high-throughput screening (vHTS)/virtual ligand screening (VLS) or by experimental *in vitro* screening to explain their possible molecular interactions with the receptors. Molecular docking tries to envisage the structure of the intermolecular complex formed between two or more constituent molecules. Understanding the ruling principles whereby protein receptors recognize, interact, and associate with molecular substrates and inhibitors is of the principal importance in drug discovery efforts [22, 23]. These principles need to be included by the docking programs.

The protein–ligand docking endeavors to predict the affinity and rank the ligand structure(s) based on the association between a given ligand and a target protein of known 3D structure. Regardless of the huge progresses over the last decades and the extensive appliances of docking procedures, there are still numerous drawbacks to be solved. Especially, protein flexibility – a significant facet for a systematic perceptive of the philosophy that direct ligand binding in proteins – is the key impediment in present-day protein–ligand docking exertions that desires to be further professionally accounted for [22]. From the preliminary efforts concerning the docking of both protein and ligand as rigid bodies [24], protein–ligand docking has evolved to a level where full or at least partial flexibility on the ligand is commonly employed. Over the last years several important steps beyond this point have been given [22, 25]. Table 3.2 is presenting some of the most commonly used molecular docking programs.

The docking procedures can be expressed as a combination of a search algorithm and a scoring function. Fairly large and continually growing number of search algorithms and scoring functions are accessible. Rationally, the perfect resolution would be to merge the most excellent searching algorithm with the preeminent scoring function [22]. Although most of the docking algorithms are regarded highly unambiguous concerning both the binding site of the target protein and the nature of the ligands [25], the nature of the molecular system must be taken into account when choosing the docking tool(s) for the study [24, 26–31]. For superior accuracy it is better to compare the docking results using multiples tools. Similar situation is also seen for the scoring functions.

Table 3.2 Most commonly used molecular docking programs [22]

ADAM	DOCK	FlexX	Hammerhead	MCDOCK	SANDOCK
AutoDock	DockVision	FLOG	ICM	Prodock	SFDock
DARWIN	EUDOC	FTDOCK	LIGIN	PRO_LEADS	Soft docking
DIVALI	FlexE	GOLD	LUDI	QXP	

Targeted Receptor-Based Virtual Ligand Screening

In spite of early pledge, high-throughput screening (HTS) procedures were not able to deliver a foremost breakthrough in the effectiveness of drug discovery [32]. The explanation for that this could be that, historically, HTS was focused on finding drug-like compounds, rather than lead-like compounds [33–35]. Therefore, new technologies are important to get new "Lead" molecule(s) in faster ways, and may be without utilizing the HTS type physical, expensive and time consuming technologies. HTS remains the most widely used method for obtaining lead compounds, and in parallel the newest technology called "virtual screening", continues to gain prominence and credibility as an alternative source of chemical starting points for the drug discovery process [30, 36–38].

Virtual screening by molecular docking, using a protein with an experimentally determined structure as a target, has become a recognized and well-known method for lead discovery and for enhancing the competence in lead optimization. Simplifications of the quantitative structure-activity relationship (QSAR) perception have led to approaches for virtual screening in the absence of a protein target structure, instead relying upon ligand-based models as surrogates of protein active sites. Recently reported methods for ligand-based virtual screening can achieve similar enrichment rates to those obtained using molecular docking [39]. Now there are number of molecules whose advancements was profoundly influenced by or based on structure-based design and screening strategies, such as HIV protease inhibitors [38].

Virtual combinatorial compound libraries can be constructed and docked against the target [40–42]. This latter approach is likely to be more suitable for the fragment-optimization phase of a project, when the virtual library can be constructed around an initial fragment hit, with varying substitution patterns on pre-defined attachment points. The compounds can then be docked either in an unrestrained fashion, or, more usefully, using the 3D structure of the initial hit as a constraint or restraint [35].

Fragment-based ligand screening can be a highly effective strategy for drug discovery. In general, fragment hits interact efficiently with the target, and although the potency of these small binders is often low, their optimization into potent leads is tractable. For a hit optimization phase to take full advantage of a good quality fragment binder, it is believed to be essential to obtain reliable structural data for the hits [35].

Combinatorial Library Design

One of the key issues in vHTS is the design of the screening library. Libraries can be two types: (a) targeted (or biased); and (b) general-purpose libraries.

Targeted libraries are developed from knowledge of natural substrates or known inhibitors, which might venture to introduce some desirable physical properties [35].

In contrast to targeted libraries, general-purpose libraries are intended for use against a variety of protein active sites. For example, Fejzo et al. describe the SHAPES methodology, which uses a small library of compounds containing only common drug scaffolds and side chains. This library was screened using a ligand-based NMR procedure, and the binders were used to select compounds from larger libraries for enzymatic assaying [35, 43].

It is also possible to design and construct a customized virtual combinatorial library (VCL) for virtual screening, using different template as scaffold that take into account the effect one is looking for and the nature of the active site of the targeted receptor. The advantage of constructing virtual combinatorial libraries, as opposed to allowing the *de novo* design algorithm decide which groups are to be added, is that the libraries can be built around known chemistry and available reactants, making the synthesis of the selected compounds more tractable [35].

Concluding Remarks

During the recent years, considerable hi-tech advances have resulted in improved VLS methods. These developments include advances made in conformational searching, greater accuracy in prediction of protein-ligand binding affinity, the generation and use of pharmacophore and interaction filters, and the inclusion of binding site flexibility considerations [37, 39, 44, 45]. Validation of these methods has been achieved through examinations of docking accuracy and enrichment of known actives in random sets of drug-like compounds, and through *in vitro* screening of VLS predicted hits. The validation has confirmed that these methods represent a plausible alternative to high-throughput screening campaigns of large compound libraries [23, 36, 46].

A major challenge in VLS is the appropriate treatment of ionization and tautomerization statuses in the input data. Currently there are no software that is able to deal the required corrections automatically [47]. Another utmost dispute remains the simultaneous optimization of both binding affinity and pharmacokinetic properties [39, 46, 48].

Due to an increase in computational power and improved algorithms, protein–ligand docking has undergone great changes over the past decades. Today, ligands are commonly treated with partial or full flexibility, and the inclusion of some levels of protein flexibility is becoming a reality. One might envision that in the near future, the treatment of the receptor with full flexibility will be a routine procedure. Despite the very promising picture drawn, docking still holds several hidden drawbacks, and the so-called docking problem is far from being solved. The lack of a suitable scoring function, able to efficiently combine both accuracy and speed, is perhaps the most detrimental weakness. The results of a docking experiment should therefore not be taken as the end result of a structural study, but rather as a good starting point for a deeper and more accurate analysis [22, 25].

In near future, the handling of the receptor with full flexibility will be seen as everyday approach [22, 25, 49]. The whole advancement harmonizes the evolution

of currently pursued genomics projects in that the function of distinct members of protein-superfamilies can be probed by small organic molecules, which are systematically derived from the toolbox of privileged ligand mimetics. This immensely interdisciplinary perception attempts to provide an operational association between the world of protein sequence data and the disease-relevance of biochemically attractive target proteins.

References

1. Berman, H. M., Bhat, T. N., Bourne, P. E., Feng, Z., Gilliland, G., Weissig, H. and Westbrook, J., 2000, *Nat. Struct. Biol.,* **7** Suppl, 957–959.
2. Westbrook, J., Feng, Z., Chen, L., Yang, H. and Berman, H. M., 2003, *Nucleic Acids Res.,* **31,** 489–491.
3. Congreve, M., Murray, C. W. and Blundell, T. L., 2005, *Drug Discov. Today,* **10** (13), 895–907.
4. Thiel, K. A., 2004, *Nat. Biotech.,* **22** (5), 513–519.
5. Blundell, T. L., 1996, *Nature,* **384,** 6604 Suppl, 23–26.
6. Altman, R. B. and Klein, T. E., 2002, *Annu. Rev. Pharmacol. Toxicol.,* **42,** 113–133.
7. Andreini, C., Banci, L., Bertini, I. and Rosato, A., 2006, *J. Proteome Res.,* **5** (1), 196–201.
8. Andreini, C., Banci, L., Bertini, I., Luchinat, C. and Rosato, A., 2004, *J. Proteome Res.,* **3** (1), 21–31.
9. Brive, L. and Abagyan, R., 2002, *Ernst Schering Res. Found Workshop,* **38,** 149–166.
10. Altman, R. B. and Dugan, J. M., 2003, *Methods Biochem. Anal.,* **44,** 3–14.
11. Service, R. F., 2002, *Science,* **298** (5595), 948–950.
12. Heinemann, U., Bussow, K., Mueller, U. and Umbach, P., 2003, *Acc. Chem. Res.,* **36** (3), 157–163.
13. Rupp, B., 2003, *Acc. Chem. Res.,* **36** (3), 173–181.
14. Lesley, S. A., Kuhn, P., Godzik, A., Deacon, A. M., Mathews, I., Kreusch, A., Spraggon, G., Klock, H. E., McMullan, D., Shin, T., Vincent, J., Robb, A., Brinen, L. S., Miller, M. D., McPhillips, T. M., Miller, M. A., Scheibe, D., Canaves, J. M., Guda, C., Jaroszewski, L., Selby, T. L., Elsliger, M. A., Wooley, J., Taylor, S. S.,Hodgson, K. O., Wilson, I. A., Schultz, P. G. and Stevens, R. C., 2002, *Proc. Natl. Acad. Sci. USA,* **99** (18), 11664–11669.
15. Blundell, T. L., Sibanda, B. L., Montalvao, R. W., Brewerton, S., Chelliah, V., Worth, C. L., Harmer, N. J., Davies, O. and Burke, D., 2006, *Philos. Trans. R. Soc. Lond. B Biol. Sci.,* **361** (1467), 413–423.
16. Ananthalakshmi, P., Samayamohan, K., Chokalingam, C., Mayilarasi, C. and Sekar, K., 2005, *Appl. Bioinformatics,* **4** (2), 141–145.
17. Berman, H. M., Westbrook, J., Feng, Z., Gilliland, G., Bhat, T. N., Weissig, H., Shindyalov, I. N. and Bourne, P. E., 2000, *Nucleic Acids Res.,* **22,** 235–242.
18. Sutcliffe, M. J., Haneef, I., Carney, D. and Blundell, T. L., 1987, *Protein Eng.,* **1** (5), 377–384.
19. Guex, N., 1999, *Trends Biochem. Sci.,* **24,** 364–367.
20. Sali, A. and Blundell, T. L., 1993, *J. Mol. Biol.,* **234,** 779–815.
21. Venclovas, C., Zemla, A., Fidelis, K. and Moult, J., 2003, *Proteins,* **53,**585–595.
22. Sousa, S. F., Fernandes, P. A. and Ramos, M. J., 2006, *Proteins,* **65**(1), 15–26.
23. Alvesalo, J. K., Siiskonen, A., Vainio, M. J., Tammela, P. S. and Vuorela, P. M., 2006, *J. Med., Chem.* **49** (7), 2353–2356.
24. Kuntz, I. D., Blaney, J. M., Oatley, S. J., Langridge, R. and Ferrin, T. E., 1982, *J. Mol. Biol.,* **161,** 269–288.
25. Apostolakis, J. and Caflisch, A., 1999, *Comb. Chem. High Throughput Screen.,* **2** (2), 91–104.
26. Schulz-Gasch, T. and Stahl, M., 2003, *J. Mol. Model.* (online), **9**(1),47–57.

27. Charifson, P. S., Corkery, J. J., Murcko, M. A. and Walters, W. P., 1999, *J. Med. Chem.,* **42** (25), 5100–5109.
28. Clark, R. D., Strizhev, A., Leonard, J. M., Blake, J. F. and Matthew, J. B., 2002, *J. Mol. Graph., Model.* **20** (4), 281–295.
29. Stahl, M. and Rarey, M., 2001, *J. Med. Chem.,* **44** (7), 1035–1042.
30. Halperin, I., Ma, B., Wolfson, H. and Nussinov, R., 2002, *Proteins,* **47** (4), 409–443.
31. Bissantz, C., Bernard, P., Hibert, M. and Rognan, D., 2003, *Proteins,* **50** (1), 5–25.
32. Hird, N., 2000, *Drug Discov. Today,* **5** (8), 307–308.
33. Hann, M. M., Leach, A. R. and Harper, G., 2001, *J. Chem. Inf. Comput. Sci.,* **41** (3), 856–864.
34. Teague, S. J., Davis, A. M., Leeson, P. D. and Oprea, T., 1999, *Angew. Chem. Int. Ed. Engl.,* **38** (24), 3743–3748.
35. Verdonk, M. L. and Hartshorn, M. J., 2004, *Curr. Opin. Drug Discov. Devel.,* **7** (4), 404–410.
36. McInnes, C., 2006, *Curr. Opin. Drug Discov. Devel.,* **9** (3), 339–347.
37. Abagyan, R. and Totrov, M., 2001, *Curr. Opin. Chem. Biol.,* **5** (4), 375–382.
38. Kitchen, D. B., Decornez, H., Furr, J. R. and Bajorath, J., 2004, *Nat. Rev. Drug Discov.,* **3** (11), 935–949.
39. Alvarez, J. C., 2004, *Curr. Opin. Chem. Biol.,* **8** (4), 365–370.
40. Jones, G., Willett, P., Glen, R. C., Leach, A. R. and Taylor, R., 1999, *Rational Drug Design, Novel Methods and Practical Applications. ACS Symposium Series* **719,** 271–291.
41. Rarey, M. and Lengauer, T., 2000, *Perspect. Drug Discov. Design* **20** (1), 63–81.
42. Sun, Y., Ewing, T. J., Skillman, A. G. and Kuntz, I. D., 1998, *J. Comput. Aided Mol. Des.,* **12** (6), 597–604.
43. Fejzo, J., Lepre, C. A., Peng, J. W., Bemis, G. W., Ajay, A., Murcko, M. A. and Moore, J. M., 1999, *Chem. Biol.,* **6** (10), 755–769.
44. Ahlstrom, M. M., Ridderstrom, M., Luthman, K. and Zamora, I., 2005, *J. Chem. Inf. Model.,* **45** (5), 1313–1323.
45. Allu, T. K. and Oprea, T. I., 2005, *J. Chem. Inf. Model.,* **45** (5), 1237–1243.
46. Alonso, H., Bliznyuk, A. A. and Gready, J. E., 2006, *Med. Res. Rev.,* **26** (5), 531–568.
47. Oprea, T. I. and Matter, H., 2004, *Curr. Opin. Chem. Biol.,* **8** (4), 349–358.
48. Oprea, T. I., 2002, *Molecules,* **7,** 51–62.
49. Aronov, A. M. and Bemis, G. W., 2004, *Proteins,* **57** (1), 36–50.

Chapter 4
Chemical and Biological Studies with an *Aconitum* and a *Delphinium* Species

Ayhan Ulubelen and Ufak Kolak

Abstract Recently, we have investigated *Aconitum cochleare* Woroschin and obtained three new alkaloids cochleareine, acoleareine from the aerial parts of the plant and cochleareinine from the roots. Cochlearenine exhibited antioxidant activity against DPPH free radical scavenging assay. The cardio active effect of has also have been studied on isolated heart preparations.

Two new norditerpene alkaloids linearilobin and linearilin were isolated from *Delphinium linearilobum* (Trautv.) N. Busch. The antioxidant activity was established by using DPPH and metal chelating activity tests.

Keywords Alkaloids, antioxidant activity, *Aconitum cochleare*, *Delphinium linearilobum*, diterpen, norditerpen, spectroscopy

Introduction

There is a long history of the use of *Aconitum*, *Delphinium* and *Consolida* species as the source of poisons and medicinals [1]. These three genera in Ranunculaceae family yield diterpenoid and norditerpenoid alkaloids. The name *Delphinium* derived from dolphine-delphine due to the shape of their flower buds [2]. *Aconitum* has an evil reputation from the antiquity [3]. The plant was used as poison in old Greece, also in north-west Pacific the natives used it to poison the whales and also as arrow poison. In England in the ancient times the plant was used against wolves, boars, tigers as well as against rodents, and it was also a homicide material [4].

The history of *Delphinium* is more peaceful, although, due to its poisinous property it was used against mammals. Crushed seeds of *Delphinium staphisagria* L. was used against body lice [5]. British army used the plant for this aim in Waterloo war as well as in the Great War. Medicinal use of *Aconitum* and *Delphinium* spans

Faculty of Pharmacy, Istanbul University, Istanbul, Turkey

B. Sener (ed.), *Innovations in Chemical Biology*, doi: 10.1007/978-1-4020-6955-0

many centuries [6]. *Aconitum* preparations have been used as cardiotonics, febrifuges, and as sedative agents and anodynes [7]. *Aconitum* were also employed in aphrodiasic preparations. Due to its toxic effects it contributed toward a sensation of flying, therefore used by witches in potions [8]. The plant was used as anticancer agent, but this value remains unproved [7]. *Delphinium* extracts have been employed in analgesic balms. In the old days the name "King's consound" was the preparation of *Consolida regalis* or *Delphinium consolida*, this preparation was not only analgesic but also sedative, emetic and antihelmintic [9]. The pharmacological activities of a few individual alkaloids were given below:

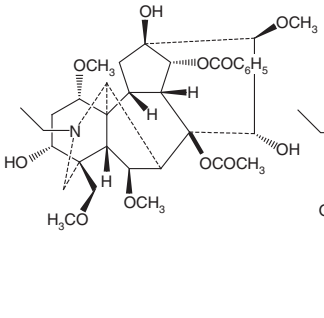

Aconitine (1)

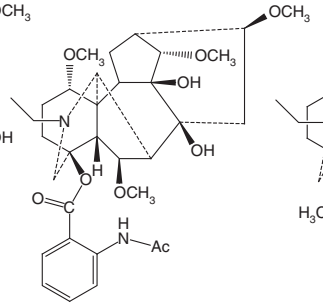

Lappaconitine (2)

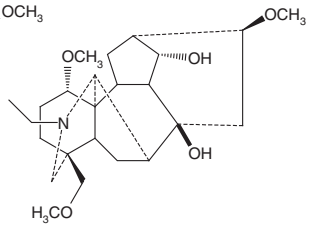

Talatisamine (3)

Aconitine (**1**): is highly toxic, when administered to anesthetized cats, it produced bradycardia, larger doses tachycardia and cardiac irregularities terminating cardiac arrest [10].

Lappaconitine (**2**): this compound is 40 times less toxic than aconitine (**1**). In anesthetized rabbits it induced cardiac arrhythmias, preceded by bradycardia and fall in blood pressure [11].

Talatisamine (**3**): causes brief hypotention and intestinal contractions [11, 12].

Karakoline (**4**): induces muscular weakness and death from respiratory depression [12, 13].

Delsemine (**5**) is a neuromuscular blocker and a hypotensive agent [12, 14].

Lycoctonine (**6**): death occur in mice from respiratory paralysis, by loss of motor control and convulsions [15].

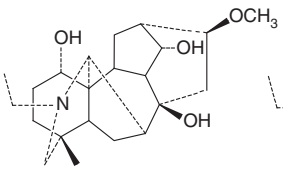

Karakoline (4)

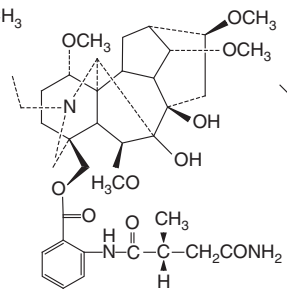

Delsemine (5)

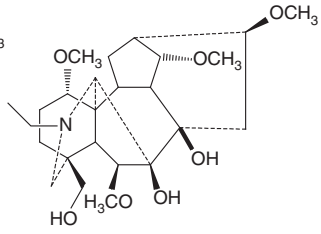

Lycoctonine (6)

We also have studied insect repellent activity of some selected alkaloids (29 of them) against *Tribolium casteneum* adults [16]. Table 4.1 shows the results, venuluson (**7**) and hetisine (**8**) were found to be the most active alkaloids.

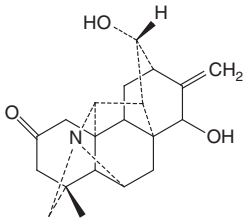

Venuluson (7)

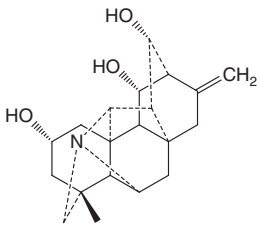

Hetisine (8)

The pharmacological activities of many more *Delphinium* alkaloids were studied by various authors, but not included in this article.

Table 4.1 Insect repellent activity of some selected alkaloids

Substances	Average repellency (%)	Mean repellency class
14-Acetylneolin	53.12	III
14-Methylperegrin	46.87	III
Peregrine	53.12	III
Delsoline	37.50	II
Condelphine	40.62	III
Karakoline	37.50	II
Ajaconine	53.12	III
Peregrine alcohol	37.50	II
N-Deacetyl lappaconit	50.00	III
Acorientinine	46.87	III
Benzoyldavisinol	46.87	III
Talatisamine	34.37	III
Orientinine	46.87	III
Hetisinone	37.50	II
14-Acetylvirescenine	43.75	III
Browniine	46.87	III
N-Deethyl-14-Me-pereg	40.62	III
Venulol	31.25	II
Venudelphine	40.62	III
Lycoctonine	46.87	III
Delphiguenerin	53.12	III
Lappaconitine	34.37	II
Venuluson	56.25	III
Gigoktonine	43.75	III
Hetisine	59.12	III
Delsemin B	37.50	II
14-Acetyltalatisamine	46.87	III
3-Hydroxytalatisamine	53.12	III
14-Demethylajacine	40.62	III

In Turkey there are about 31 *Delphinium*, 8 *Consolida* and only 4 *Aconitum* species. So far we had studied 17 *Delphinium*, 7 *Consolida* and 3 *Aconitum* species. From these studies we have obtained more than 100 alkaloids, about 50 of them were new compounds [17].

Recently we have studied the fourth Turkish *Aconitum* species namely *A. cochleare* Woroschin. The aerial parts and the roots were investigated separately. From the aerial parts four alkaloids talatisamine, 14-acetyltalatisamine, cochleareine (**9**) and acoleareine (**10**) were isolated [18].

In this study the alkaloids were separated by centrifugally accelerated radial TLC (Chromatotron) using Al_2O_3 plates (E. Merck Art 1092), and further cleaned on preparative TLC plates. The structures were determined by 1D and 2D NMR experiments including ^{1}H-^{1}H COSY, HMQC, HMBC and NOESY. The new compounds were cochleareine (**9**) C_{20} and the other acoleareine (**10**) C_{19} alkaloids.

The HRMS of cochleareine (**9**) indicated the molecular formula $C_{22}H_{37}NO_4$ *m/z* 379.2658. ^{13}C NMR (DEPT and APT) findings showed the presence of 2 methyl quartets, 11 methylene triplets,

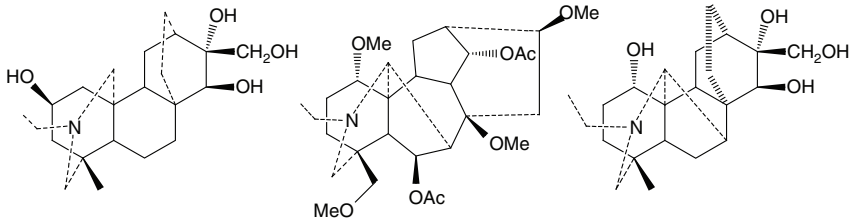

Cochleareine (9) **Acoleareine (10)** **Cochlearenine (11)**

5 methine doublets and 4 quaternary C singlets, correlating with 22 C atoms in the molecule. ^{1}H and ^{13}C NMR data is given in Table 4.2.

The molecular formula of acoleareine (**10**) is $C_{29}H_{45}NO_8$ *m/z* 535.1045 as observed from its HRMS and as correlated by ^{13}C NMR data, seven methyl quartets, seven methylene triplets, ten methine doublets and five quaternary carbon singlets. Table 4.3 gives the NMR data of acoleareine (**10**).

The roots of the same plant has yielded one new alkaloid together with two known compounds lycoctonine and lappaconitine. The structure of the new alkaloid (cochlearenine) (**11**) is quite similar to that of cochleareine (**9**). Due to this resemblance the structure determination of the compound **11** was carried out not only by spectral data but also by single-crystal x-ray diffraction studies [19].

^{1}H and ^{13}C NMR connectivities were established by HMBC technique. Relative stereo-chemistry of **11** was unambiguously assigned on the basis of x-ray diffraction studies. The antioxidant activity of compound **11** was established by DPPH scavenging assay (IC_{50} = 218.46 μM) while standard antioxidant BHA had an IC_{50} = 44.2 ∓ 0.2 μM (Figs. 4.3; 4.4).

Cochlearenine (**11**) was tested on isolated heart preparations and caused a dose-dependent (0.3–3.0 mg/ml) fall in heart rate, while a mild increase in the atrial force

Table 4.2 NMR data of cochleareine **(9)** (in CD_3OD, J values (Hz) in parentheses)

	^{13}C	^{1}H	COSY	HMBC	NOESY
1	33.82 *t*	1.70 *m*	H-2α		
2α	67.38 *d*	3.89 *dd* (6.6, 11.1)	H-1α, H-1β	C-10, C-4, C-5	H-22α, H-3α
3	41.88 *t*	1.95 *m*	H-2α		H-22α, H-6α
4	37.74 *s*	–			
5β	35.42 *d*	1.70 *m*	H-6α, H-6β	C-18, C-6, C-9	H-11β, H-12β
6	30.70 *t*	1.30 *m*	H-5β		
7	27.27 *t*	1.25 *m*	H-6α, H-6β		
8	41.76 *d*	–			
9	42.98 *d*	2.20 *d* (4.9)	H-11α, H-11β		
10	52.00 *s*	–			
11	21.30 *t*	1.35 *dd* (8.0, 17.3)	H-9, H-12		H-21β
12	41.67 *d*	2.06 *m*	H-11α, H-11β		
13	23.19 *t*	1.22 *m*	H-14		
		1.34 *m*			
14	23.79 *t*	2.30 *m*	H-13	C-12	
15α	85.01 *d*	3.93 *s*			
16	79.40 *s*	–			
17	66.56 *t*	4.02 *d* (11.5)			H-17′
17′		3.63 *d* (11.5)			H-17
18	24.96 *q*	0.79 *s*			
19	51.32 *t*	1.3 *m*			
20	57.05 *t*	2.50 *d* (12.0)		C-2, C-6	H-20′
20′		2.80 *d* (12.0)			H-20
21	51.94 *t*	2.75 *dd* (7.5, 13.8)			H-22, H-11α
21′		2.96 *dd* (7.5, 13.8)			
22	11.42 *q*	1.19 *t* (7.0)			

Table 4.3 NMR data of acoleareine (10) (in $CDCl_3$, J values (Hz) in parentheses)

	^{13}C	^{1}H	COSY	HMBC
1β	84.0 *d*	3.20 *dd* (10.0, 7.0)	H-2α, H-2β	C-6, C-17
2	27.3 *t*		H-1β, H-3α	
			H-3β	
3	37.5 *t*		H-2α, H-2β	
4	34.1 *s*			
5β	56.4 *d*	1.40 *brs*	H-6α	
6α	73.4 *d*	5.27 *t* (7.0)	H-5β, H-7β	
7β	42.0 *d*	2.62 *d* (7.2)	H-6α	
8	78.5 *s*			
9	40.9 *d*			C-10
10	45.9 *d*			C-9, C-12
11	48.4 *s*			
12	27.9 *t*			C-9, C-13
13	39.0 *d*			C-12
14β	76.4 *d*	4.80 *t* (4.5)	H-13	C-16, C-10
15	35.6 *t*			C-16
16α	83.9 *d*			C-15
17	63.8 *d*	2.92 *d* (2.0)		

(continued)

Table 4.3 (continued)

	^{13}C	^{1}H	COSY	HMBC
18	80.1 *t*	3.65 *d* (10.0)		
18′		3.50 *d* (10.0)		
19	57.4 *t*	3.04 *d* (12.7)		
19′		2.59 *d* (12.7)		
20	48.5 *t*	2.25 *m*		
21	13.4 *q*	0.83 *t* (7.0)		
OMe-1	56.0 *q*	3.15 *s*		
OMe-8	47.9 *q*	3.29 *s*		
OMe-16	56.4 *q*	3.19 *s*		
OMe-18	59.2 *q*	3.29 *s*		
OAc-6	171.0 *s*	1.99 *s*		
	22.0 *q*			
OAc-14	172.1 *s*	2.10 *s*		
	21.5 *q*			

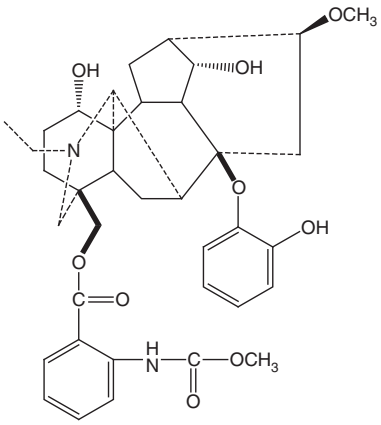

Linearilobin (12)

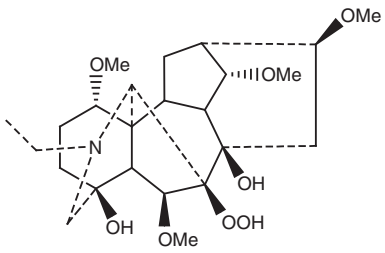

Linearilin (13)

on contraction at the dose range 0.3–1.0 mg/ml, followed a suppressant effect at the higher dose of 3.0 mg/ml (Fig. 4.1).

The data indicated that cochlearenine (**11**) exhibited dose dependent bradycardiac effect along with mild positive inotropic effect followed by cardiac suppression at higher dose, which is an interesting observation, as the drugs with bradycardiac effect without accompanying negative effect is considered relatively safe for its use in cardioactive disorders like hypertension, palpitations and ischemic heart disease.

The last *Delphinium* species we have investigated was *D. linearilobum* (Trautv.) N.Busch [20], from this plant we have isolated six known and two new compounds. The known alkaloids were lycoctonine, 14-acetyltalatisamine, browniine, cammaconine, talatisamine and cochlearenine, the new alkaloids were named as linearilobin (**12**) and linearilin (**13**).

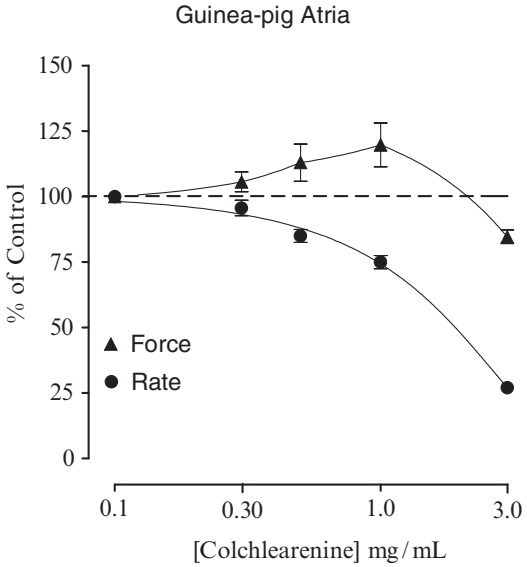

Fig. 4.1 Guinea-pig atria of colchlearenine **(11)**

Mass spectrum of compound **12** indicated a molecular ion peak at *m/z* 662.3200 for $C_{37}H_{46}N_2O_9$. ^{13}C NMR findings correlated the given formula with 1 methyl, 2 methoxyl, 8 methylene, 17 methine and 9 quaternary C signals. Figure 4.2 shows the fragmentation of linearilobin (**12**), indicating the presence of a complex side chain, at *m/z* 603 $[M\text{-}COOCH_3]^+$ (a), at *m/z* 454 $[M\text{-}C_{10}H_{10}NO_4]^+$ (b) and the peak at *m/z* 569 showed the presence of a second aromatic ring *m/z* 569 $[M\text{-}C_6H_5O]^+$ and *m/z* 553 $[M\text{-}C_6H_5O_2]^+$.

^1H and ^{13}C NMR spectra correlated with the suggested structure of **12** (Table 4.4).

The second new compound linearilin (**13**) was an amorphous powder with $[\alpha]_D$ = + 18.35° The HRMS of the compound *m/z* 469.2669 and ^{13}C NMR with one methyl, four methoxy, six methylene, nine methine and four quaternary carbon atoms indicated the molecular formula $C_{24}H_{39}NO_8$.

The compound has a lycoctonine type structure. It has six degrees of unsaturation which accounted for its skeleton. The spectral data of linearilin is given in Table 4.5.

The presence of a peroxy group was proven by iodine test, and its placement was decided by the ^{13}C NMR values of C_5, C_7 and C_8 atoms, when there is a hydroxyl group at C_7 or at C_8 the chemical shift should be around δ 88–89 for C_7 and δ 77–79 for C_8 respectively. In the ^{13}C NMR spectrum of linearilin (**13**) there is a signal at δ 78.79 (s) indicating a hydroxy group at C_8 another signal at δ 109.99 (s) for the peroxy group which could only be at C_7. Another possible place for the peroxy group could be at C_5 but the signal at δ 43.22 (d) shows the given placement is correct.

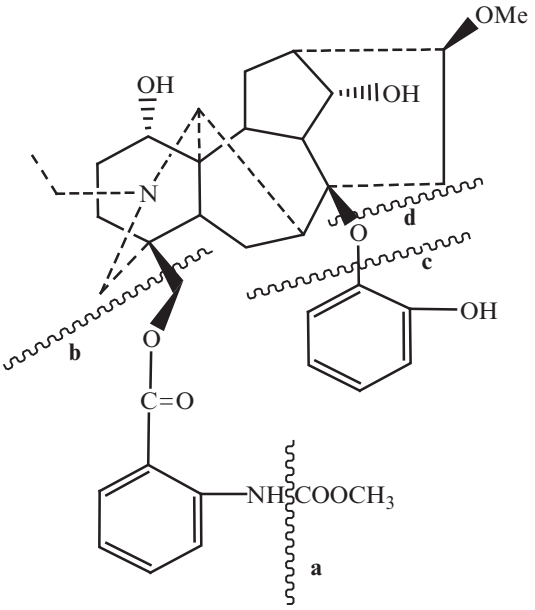

Fig. 4.2 Mass fragmentation of linearilobin **(12)**

Table 4.4 ^{1}H (500 MHz) and ^{13}C (125 MHz) NMR data of alkaloid **12** in $CDCl_3$

	δ_H (m, J Hz)	δ_C		δ_H (m, J Hz)	δ_C
1	3.76 (*t*, 3)	72.52 (*d*)	1-OMe	–	–
2	1.60 (*m*)	29.25 (*t*)	6-OMe	–	–
	1.58 (*m*)		14-OMe	–	–
3	1.85 (*m*)	31.43 (*t*)	16-OMe	3.56 (*s*)	57.40 (*d*)
	1.64 (*m*)		Ar-C = O	–	167.35 (*s*)
4	–	37.60 (*s*)	Ar-NH	11.4 (*s*)	–
5	1.75 (*d*, 8)	43.22 (*d*)	Ar-NH C = O	–	169.00 (*s*)
6	1.79 (*dd*, 14,8)	25.43 (*t*)	$COOCH_3$	3.60 (*s*)	51.0 (*s*)
	1.56 (*m*)		1′	–	114.72 (*s*)
7	2.42 (*d*, 8)	48.16 (*d*)	2′	–	151.87 (*s*)
8	–	85.90 (*s*)	3′	7.96 (*dd*, 8.5, 1.5)	116.35 (*d*)
9	2.10 (*dd*, 10.4, 4.7)	46.43 (*d*)	4′	7.48 (*ddd*, 8.5, 7.5, 1.5)	135.83 (*d*)
10	1.94 (*m*)	44.28 (*d*)	5′	7.04 (*ddd*, 8.5, 7.5, 1.5)	116.88 (*d*)
11	–	49.17 (*s*)	6′	8.62 (*dd*, 7.5, 1.5)	130.62 (*d*)
12	2.05 (*m*)	27.76 (*t*)	1″	–	148.06 (*s*)
	1.62 (*m*)		2″	–	151.02 (*s*)
13	2.34 (*m*)	42.68 (*d*)	3″	7.17 (*bd*, 8.3)	114.21 (*d*)
14	4.14 (*t*, 5)	76.32 (*d*)	4″	7.45 (*td*, 8.3, 1.2)	121.30 (*d*)
15	2.15 (*dd*, 15, 5)	43.24 (*t*)	5″	6.75 (*td*, 8.3, 1.2)	118.63 (*d*)
	3.30 (*dd*, 15, 8.5)		6″	7.90 (*dd*, 8.3, 1.5)	114.26 (*d*)
16	3.25 (*brd*, 9)	82.63 (*d*)	OH	–	–
17	2.71 (*brs*)	65.46 (*d*)	OH	–	–
18	4.15 (*d*, 11)	68.74 (*t*)			
	4.22 (*d*, 11)				
19	2.70 (*d*, 13)	57.66 (*t*)			
	2.80 (*d*, 13)				
20	2.54 (*m*)	48.61 (*t*)			
	2.48 (*m*)				
21	1.32 (*t*, 4.5)	13.22 (*q*)			

Table 4.5 ^{1}H (500 MHz) and ^{13}C (125 MHz) NMR data of alkaloid **13** in $CDCl_3$

	δ_H (m, *J* Hz)	δ_C		δ_H (m, *J* Hz)	δ_C
1	3.24 (*dd*, 10.5, 6.8)	84.74 (*d*)	1-OMe	3.27 (*s*)	56.56 (*s*)
2	2.34 (*m*)	29.94 (*t*)	6-OMe	3.29 (*s*)	59.33 (*s*)
	1.88 (*m*)	–	14-OMe	3.29 (*s*)	57.94 (*s*)
3	1.92 (*m*)	37.74 (*t*)	16-OMe	3.35 (*s*)	57.59 (*s*)
	1.62 (*m*)	–	OH	3.57 (*brs*)	–
4	–	70.81 (*s*)	OH	3.94 (*brs*)	–
5	2.40 (*s*)	44.17 (*d*)			
6	3.97 (*s*)	90.63 (*d*)			
7	–	109.99 (*s*)			
8	–	78.79 (*t*)			
9	2.20 (*brt*, 6.3)	45.27 (*d*)			
10	1.85 (*m*)	37.93 (*d*)			
11	–	49.43 (*s*)			
12	1.95 (*m*)	30.77 (*t*)			
	1.65 (*m*)	–			
13	2.28 (*m*)	43.63 (*d*)			
14	3.56 (*t*, 4.8)	84.74 (*d*)			
15	2.54 (*m*)	33.76 (*t*)			
16	3.35 (*dd*, 10, 4.6)	83.08 (*d*)			
17	2.96 (*s*)	66.35 (*d*)			
18	–	–			
19	2.80 (*d*, 12)	57.53 (*t*)			
	3.50 (*d*, 12)				
20	2.88 (*m*)	49.62 (*t*)			
	2.60 (*m*)				
21	1.05 (*t*, 4.5)	14.22 (*q*)			

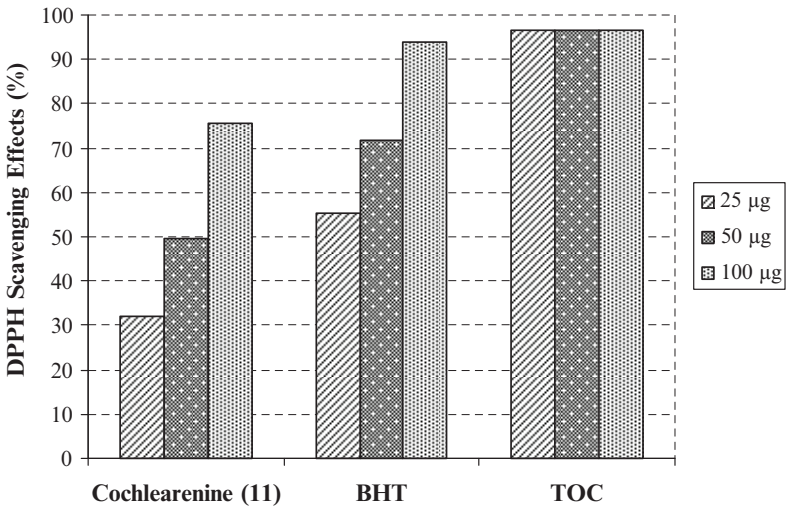

Fig. 4.3 Antioxidant activity by DPPH

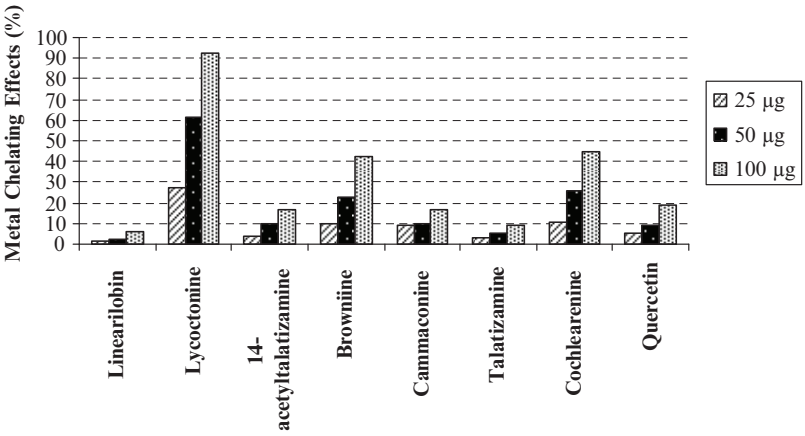

Fig. 4.4 Metal chelating activity test

The antioxidant activity of the alkaloids (linearilobin, lycoctonine, 14-acetyl-talatizamine, browniine, cammaconine, talatizamine and cochlearenine) of *D. linearilobum* was performed by DPPH [21] and by metal chelating activity [22] assays cochlearenine and lycoctonine showed high activity (Figs. 4.3 and 4.4).

Acknowledgements The author thanks Turkish Academy of Sciences (TUBA) for the support given to this paper.

References

1. Benn, M. H. and Jacyno, J. M., 1983, *Alkaloids* (S.W. Pelletier, ed.), Wiley, New York, vol. 1, pp 153–210.
2. Ulubelen, A., Meriçli, A. H. and Meriçli, F., 1998, *Advances in Natural Product Chemistry* (Ed. Atth-ur-Rahman, M. I. Choudhary, Harwood, Academic Publishers, USA, pp 247–260.
3. Tripp, E., 1970, *Crowell' Handbook of Classicals Mythology*, Crowell, New York.
4. Anonymous, 1958, *Encyclopedia Universal Ilustrado*, Espasa-Calpe S. A., Madrid, vol. 2, p 327.
5. Minton, F. and Minton, V., 1976, *Practical Modern Herbal*, W. Foulsham, London, p 102.
6. Woodward, M. (ed.), 1964, *Gerards Herbal*, Spring Books, London, pp 227, 249.
7. Hardwell, J. L., 1971, *Lloydia,* **34,** 103.
8. Emboden, W. A., 1979, *Narcotic Plants*, MacMillan, New York, pp 18, 127.
9. Jaretzsky, R. and Jaenececke, H., 1940, *Arch. Pharm.,* **278,** 156.
10. Swanson, E. E., Younken, H. W., Zufall, C.J., Husa, W.J., Munch, J.C. and Wolffe, J. B., 1938, Aconitum, American Pharmaceutical Association Monograph No 1, Washington, DC.
11. Pelletier, S. W. and Mody, N. V., 1979, *The Alkaloids: Chemistry and Physiology* (R. H. F. Manske and R. G. A. Rodrigo, eds.), Academic, New York, Vol.17, p 1.

12. Tulganov, N., Dzahakhangirov, F. N., Sadritdinov, F. S. and Khamdanov, I., 1976, *Farmacol. Rustit. Veshchestv* (M. B. Sultanov, ed.), Academy of Sciences Uzbek, SSR, Tashkent, USSR, p 76; CA, 1978, **89**, 140208.
13. Dzhakhangirov, F. N., Khamdamov, I. and Sadritdinov, F. S., 1976, *Dokl. Akad. Nauk. Uzb. SSR*, 32; CA, 1976, **85**, 103953.
14. Gubanow, I. A., 1965, *Planta Medica,* **13,** 200.
15. Beath, O. A., 1918, *Wyoming Agric. Exp. Stn. Bull.,* **120,** 53.
16. Jilani, G. Su, H. C. F., 1983, *J. Econ. Entomol.,* **76,** 154.
17. Ulubelen, A., 2006, *Essays on Science*, Felicitation Volume (Rashid, S. ed.), Hamdard Foundation Press, Karachi, Pakistan, pp 94–110.
18. Kolak, U., Türkekul, A., Özgökçe, F. and Ulubelen, A., 2005, *Pharmazie,* **60,** 953.
19. Shaheen, F., Zeeshan, M., Ahmad, M., Anjum, S., Ali, S., Siddique, H., Shah, A. J., Gilani, A. H., Ulubelen, A., Kolak, U., Özgökçe, F., Choudhary, M. I. and Atta-ur-Rahman, *Phytochemistry* (submitted).
20. Kolak, U., Öztürk, M., Özgökçe, F. and Ulubelen, A., 2006, *Phytochemistry,* **67,** 2170–2175.
21. Shaheen, F., Ahmad, M., Khan, M. T. H., Jalil, S., Ejaz, A., Sultankhodjaev, M. N., Arfan, M., Choudhary, M. I. and Atta-ur-Rahman, 2005, *Phytochemistry,* **66,** 935–940.
22. Gülçin, İ., Oktay, M., Kireçci, E. and Küfrevioğlu, Ö.İ., 2003, *Food Chemistry,* **83,** 371–382.

Chapter 5
Novel Bioactive Natural Products from Marine and Terrestrial Sources

Athar Ata

Abstract Recent chemical studies on the marine soft corals and terrestrial plants have resulted in the isolation of several novel compounds. The soft corals, *Pseudopterogorgia elisabethae* and *Cladiella* species yielded several novel terpenoids, exhibiting antimicrobial activities. New steroids were isolated from terrestrial fungi, *Mucor plumbeus* and *Coprinus micaceus*. Phytochemical studies on the *Buxus hyrcana*, collected from Iran, have yielded steroidal bases. This review describes the new natural products exhibiting different bioactivities from the aforementioned sources.

Keywords Acetylcholinesterase inhibitory, antimicrobial activity, bioactivity, *Buxus hyrcana*, *Cladiella*, *Coprinus micaceus*, coral, marine, *Mucor plumbeus*, *Pseudopterogorgia elisabethae*, steroids, terpenoids, terrestrial

Antibacterial Diterpenoids from *Pseudopterogorgia elisabethae*

Marine soft corals have provided several novel natural products exhibiting various promising bioactivities such as anti-inflammatory, anti-cancer, anti-tuberculosis, and anti-bacterial activities [1, 2]. This attracted organic chemist to explore these hidden resources. *Pseudopterogorgia elisabethae* is one of the soft corals. It is abundant in the Caribbean region and is a rich source of useful biomedical agents. For instance, most potent anti-inflammatory agents, pseudopterosins were purified from *P. elisabethae*, collected from the Bahamas [3–5]. Novel anti-mycobacterial diterpenes have also been isolated from this species [6–9]. A detailed chemical studies on the methanolic extract of *P. elisabethae* resulted in the isolation of two new anti-bacterial diterpenes, Pseudopterosin X and Y (**1**–**2**) along with known pseudopterosins A–D and E (**3**–**7**) [6–9].

Department of Chemistry, The University of Winnipeg, 515 Portage Avenue, Winnipeg, MB R3B 2E9, Canada

B. Sener (ed.), *Innovations in Chemical Biology*, doi: 10.1007/978-1-4020-69550

Pseudopterosin X (**1**) was isolated as a yellow colored gum. The UV spectrum of **1** showed maximum absorption at λ_{max} 280 nm due to the presence of a highly substituted benzene chromophore [10]. Its IR spectrum displayed intense absorption bands at 3,470 (OH), 2,904 (CH), 1,705 (C = O), 1,595 (C = C) and 1,100 (C-O) cm^{-1}. The high-resolution electron-impact mass spectrum (HREIMS) of **1** showed M^+ at *m/z* 474.2622, and this mass provided molecular formula $C_{27}H_{38}O_7$, indicating the presence of nine double bond equivalents in **1**. The ^{13}C-NMR chemical shift assignments of **1** are shown around structure **1**. On the basis of the detailed NMR studies and comparison with the reported pseudopterosins in the literature and L-xylose [3–5], structure **1** was proposed for this new natural product.

The second new compound, pseudopterosin Y (**2**) was also purified a yellow gum. Its UV and IR spectra were identical to those of compound **1**, indicating the presence of same π system and functional groups in **2**. The HREIMS of **2** showed the M^+ at *m/z* 516.2420 corresponding to the molecular formula $C_{29}H_{40}O_8$. A combination of ^{1}H-, ^{13}C-NMR, COSY, HSQC and HMBC spectral data revealed that compound **2** was C-3′ acetyl derivative of compound **1**. Based on these spectral data, structure **2** was assigned to this new compound.

Compounds **1** and **2** were tested for antibacterial activity against *Streptococcus pyogenes* (ATCC 19615), *Staphylococcus aureus* (ATCC 25923), *Enterococcus faecalis* (ATCC 19433), *Escherichia coli* (ATCC 25933) and *Pseudomonas aeruginosa* (ATCC 27853) at a concentration of 25 μg/ml by using Kirby-bauer method [11]. Compounds **1** and **2** exhibited a promising anti-bacterial activity against Gram-positive bacteria, *S. pyogenes*, *S. aureus* and *E. faecalis*. Both of these compounds were inactive against

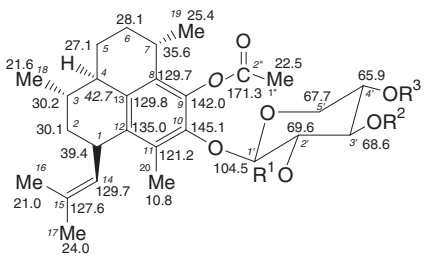

1 Ps P $R^1 = R^2 = R^3 = H$,C-3' δ 68.6
2 Ps Q $R^2 = Ac$, $R^1 = R^3 = H$,C-3' δ 74.1

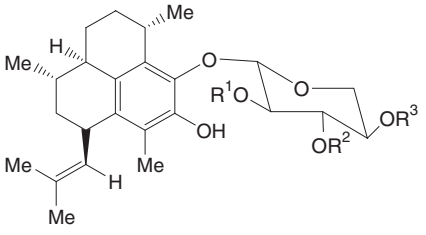

3 Ps A $R^1 = R^2 = R^3 = H$
4 Ps B $R^1 = Ac$, $R^2 = R^3 = H$
5 Ps C $R^2 = Ac$, $R^1 = R^3 = H$
6 Ps D $R^3 = Ac$, $R^1 = R^2 = H$

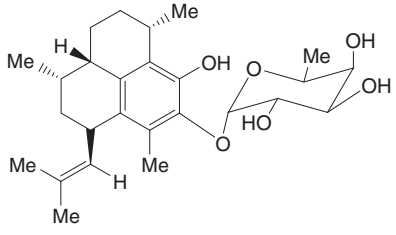

7 Ps E

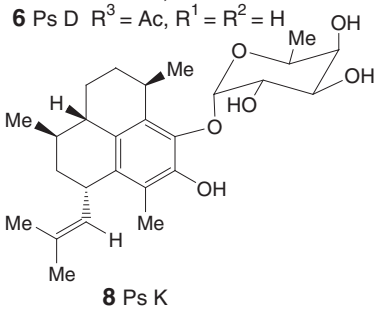

8 Ps K

Table 5.1 Antibacterial activity date of compounds **1–8**

	S. pyogenes		*Staph. aureus*		*Ent. faecalis*	
Compound	Diameter[a] of inhibition zone (mm)	MIC (μg/ml)	Diameter[a] of inhibition zone (mm)	MIC (μg/ml)	Diameter[a] of inhibition zone (mm)	MIC (μg/ml)
1	15	0.8	10	2.0	8	3.5
2	12	1.0	9	2.3	8	3.6.
3	15	0.8	11	2.1	9	3.4
4	13	1.0	10	2.3	8	3.2
5	16	1.0	11	2.0	8	3.7
6	17	1.0	9	2.3	9	3.8
7	12	1.0	8	2.3	8	3.6
8	14	1.0	9	2.1	8	3.4

[a] 25 μg/ml of test compounds were applied to 6 mm disc

Gram negative bacteria, *E. coli*, and *P. aeruginosa* at the same concentrations. To the best of my knowledge, pseudopterosins were reported to exhibit potent anti-inflammatory activity [3–5, 12] and did not find any report on anti-bacterial data for this class of compounds. Therefore, it was decided to isolate all of the previously reported pseudopterosins from this crude extract and to evaluate them for anti-bacterial activity. However, it could only be possible to isolate the known pseudopterosins A (**3**), B (**4**), C (**5**), D (**6**), E (**7**), and K (**8**) from this extract. Their structures were established by comparing their ^{1}H and ^{13}C-NMR data with those of previously reported in the literature [3–5]. Compounds **3–8** were found to be significantly active selectively against aforementioned Gram-positive bacteria at the same concentration and antibacterial data is summarized in Table 5.1. In summary, it was discovered that pseudopterosins exhibited strong anti-bacterial activity selectively against Gram positive bacteria. Previously, these compounds were known to exhibit anti-inflammatory activity only and our current studies resulted in the discovery of new bioactivity of pseudopterosins.

Bioactive Sesquiterpenoids from the Marine Soft Coral of Genus *Cladiella*

The marine soft corals of genus *Cladiella* have provided a number of bioactive eunicellane- and cembrane-type diterpenoids [13]. *Cladiella* species, collected from Andaman Island, India, was extracted with methanol. A detailed chemical analysis of this crude methanolic extract afforded two novel sesquiterpenoids, cladioxazole (**9**) and cladidol (**10**). Compound **9** showed positive test with Dragendroff's reagent indicating the presence of nitrogen in it. This was further confirmed from the HREIMS data, which showed the molecular ion peak at *m*/*z* 249.2089. This provided molecular formula $C_{16}H_{17}NO$ and indicated the presence of four degrees of unsaturation in **9**. The UV spectrum of **9** showed the terminal absorption suggesting the lack of π system in **9**. Its IR spectrum exhibited intense

absorption bands at 2,904 (CH) and 1,595 (C-N) cm^{-1}. The ^{1}H-NMR spectrum ($CDCl_3$, 500 MHz) of **9** showed two 3H doublets at δ 0.86 and 0.91 (J = 6.5 Hz) due to the C-13 and C-14 methyl protons. A 3H singlet at δ 1.36 was ascribed to the C-15 methyl protons. The C-3 methine protons resonated at δ 3.65 (ddd, J = 10.2, 9.8 and 0.3 Hz) while C-2 appeared at δ 3.02 (ddd, J = 9.8, 9.6 and 3.4 Hz). The downfield chemical shift values of H-3 and H-2 were due to the presence of geminal oxygen and nitrogen moieties, respectively. Another downfield signal at δ 7.69 was due to the C-1′ olefinic proton. The COSY-45° spectrum indicated the presence of two partial structures in **9**. The ^{13}C-NMR spectrum ($CDCl_3$, 125 MHz) of **9** showed the resonance of all sixteen carbon atom and DEPT spectrum revealed the presence of three methyl, six methylene and five methine carbon atoms. Subtraction of DEPT spectrum from the broadband ^{13}C NMR spectrum suggested the presence of one quaternary carbon atom in **9**. A combination of ^{1}H, ^{13}C-NMR, COSY, HSQC, HMBC, NOESY and mass spectral data led us to establish structure **9** for this novel sesquiterpene.

Compound **9** was tested for antibacterial activity and found to exhibit moderate antibacterial activity against *E. coli* at the does of 25 μg/ml.

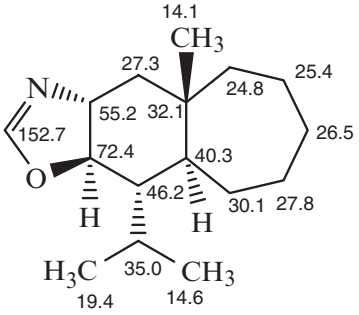

(**9**)

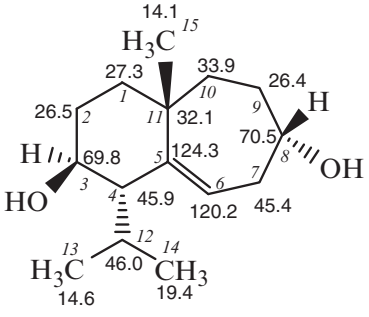

(**10**)

Cladidiol (**10**) was also isolated as colorless gum. Its UV spectrum also showed terminal absorption and IR spectrum showed the presence of a hydroxyl group (3,410 cm^{-1}) and carbon-carbon double bond (1,602 cm^{-1}). The ^{1}H- and ^{13}C-NMR spectra of compound **10** were nearly identical to those of compound **9** with an exception that the ^{1}H-NMR spectrum of **10** was lacking a signal at δ 7.69 (H-1′). This compound also showed negative Dragendroff test indicating the absence of nitrogen in **10**. A combination of mass, ^{1}H, ^{13}C-NMR and 2D-NMR (COSY, NOESY, HSQC and HMBC) spectral data led us to propose structure **10** for this new sesquiterpene.[13] The ^{13}C-NMR chemical shift assignments of **10** are shown around structure **10**.

Compound **10** was evaluated for anti-bacterial activity and acetylcholinesterase (AChE) inhibitory activities. This compound was found to be inactive in antibacterial assay and exhibited AChE inhibitory activity with an IC_{50} value of 67 μM. Acetylcholine serves as a neurotransmitter in the central and peripheral nervous system. Acetylcholinesterase (AChE) stops the function of acetylcholine by its

hydrolytic destruction [14]. Alzheimer's disease is a progressive degenerative neurologic disorder that results from the deficit of cholinergic function in brain [14]. Enhancement of acetylcholine level in the brain is considered one of the most promising approaches for treating Alzheimer's disease [15]. The use of potent inhibitors to inhibit AChE activity is one of the methods to enhance acetylcholine level in brain to cure Alzheimer's disease.

Bioactive Steroids from *Mucor plumbeus* and *Coprnusmicaceus*

Microbial natural product chemistry has generated a number of bioactive natural products. For instance cyclosporine A FK506 and rapamycin are used as immunosuppressants [16]. Other examples of microbial metabolites, having potential biomedical application include antihyperlipidemics, lovastatin and guggulsterone [17, 18]. The crude extracts of *Mucor plumbeus* exhibited acetylcholinesterase (AChE) enzyme inhibition activity. Our detailed chromatographic work on this crude extract resulted in the isolation of mucoralactone A (**11**), a novel steroid containing a lactone moeity incorporated in its structure.

Mucoralactone A (**11**) was purified as yellow colored gum. Its UV spectrum displayed maximum absorption at 241 nm indicating the presence of an α, β-unsaturated carbonyl group in **11** [19]. The IR spectrum displayed intense absorptions at 3,456 (OH), 2,900 (CH), 1,780 C = O) and 1,596 (C = C) cm^{-1}. Its high-resolution electron-impact mass spectrum (HREIMS) showed molecular ion peak at *m/z* 398.2798, which corresponded to the molecular formula $C_{26}H_{38}O_3$ (calcd 398.2821). The ^{1}H-NMR spectrum (acetone-d_6) of **11** displayed two 3H singlets at δ 0.73 and 1.07 due to the C-18 and C-19 methyl protons, respectively. A 3H doublet at δ 0.95 ($J_{21,20}$ = 6.5 Hz) was assigned to the C-21 methyl protons. The C-3 and C-16 methine protons appeared at δ 3.82 and 4.99, respectively. The downfield chemical shift values of C-3 and C-6 methine protons were indicative of the presence of geminal oxygen functionalities. The C-6 resonated at δ 5.36 while the sp^2 hybridized C-28 methylene protons resonated as two singlets, integrating for one proton each, at δ 5.56 and 6.06. A combination of ^{1}H and ^{13}C-NMR spectral data indicated to us that compound **11** has a steroidal skeleton. A detailed interpretation of broad ^{13}C-NMR and DEPT spectra revealed the presence of three methyl, ten methylene, eight methine and five quaternary carbon atoms in **11**. The stereochemistry at various chiral centers was established with the aid of NOESY spectrum.

Compound **11** showed AChE inhibitory activity with an IC_{50} 19 μM. and weak antifungal activity against *Candida albicans* with a minimum inhibitory concentration (MIC) value of 23 μg/ml.

Coprinus micaceus is abundant in the prairie region of Canada and is an edible mushroom. The methanolic extract of *C. micaceus* exhibited anti-bacterial activity against *E. faecalis*, *S. aureus*, *Corynebacterium xerosis* and *E. coli* at the concentration of 250 μg/ml in a preliminary anti-bacterial screening assay. A chromatographic fractionation of methanolic extract of this mushroom subsequently resulted in the isolation of a new bioactive sterol, micaceol (**12**).

Micaceol (**12**) was isolated as a light yellow amorphous solid. Its UV spectrum showed maximum absorption at 246 nm indicating the presence of a conjugated π system. The IR spectrum exhibited intense absorption bands at 3,425 (OH) and 1,601 (C = C) cm^{-1}. The Chemical Ionization Mass Spectrum (CI-MS) of **12** showed molecular ion peak at *m/z* 399 $[M-H]^+$. The HREIMS of this compound showed molecular ion peak at *m/z* 398.2392, which provided the molecular formula $C_{28}H_{46}O$ (calcd = 398.2360) and indicated the presence of six degrees of unsaturation in **12**. These six double bond equivalents were accounted for by the steroidal skeletons with two double bonds incorporated in its structure.

The ^{1}H NMR spectrum ($CDCl_3$, 500 MHz) of **12** showed two singlets (δ 0.83 and δ 0.95), each integrating for three protons due to the C-18 and C-19 methyl protons. Three 3H doublets at δ 0.78 (*J* = 6.5 Hz), δ 0.79 (*J* = 6.5 Hz) and δ 0.85 (*J* = 7.0 Hz) were due to the secondary C-26, C-27 and C-21 methyl protons, respectively. The C-3 methine proton resonated as a one-proton double doublet at δ 3.63 (*J1*= 10.5 Hz and *J2*= 3.5 Hz) and its downfield chemical shift value was indicative of the presence of a geminal hydroxyl functionality. A one-proton multiplet at δ 5.21 was ascribed to the C-6 olefinic proton. The C-28 exocyclic methylene protons appeared as two broad singlets at δ 5.40 and 5.58. The ^{13}C-NMR spectrum ($CDCl_3$, 125 MHz) showed the resonance of all 28 carbon atoms. The combination of ^{1}H and ^{13}C-NMR data suggested that compound **12** has a sterol like structure as most of the ^{1}H and ^{13}C-NMR chemical shift values of **12** were similar to those of sterols reported in the literature [19, 20]. The ^{1}H and ^{13}C-NMR chemical shift values were assigned with the aid of COSY-45^0, HSQC and HMBC spectral data. Compound **12** was found to have modest inhibitory activity against *C. xerosis* and *S. aureus* with minimal inhibitory concentration values of 82.35 and 146 μg/ml, respectively.

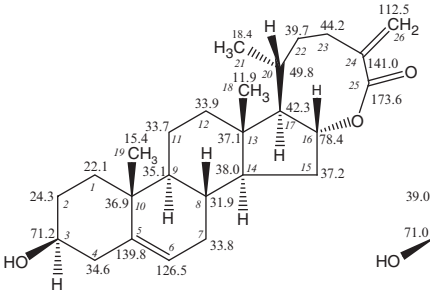

(**11**)

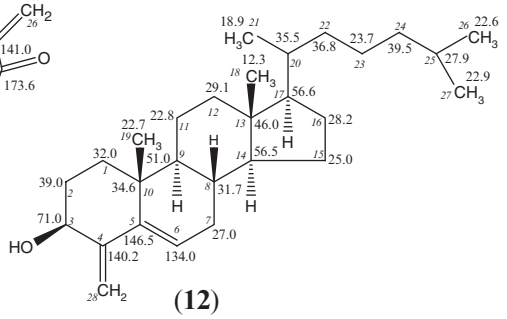

(**12**)

Bioactive Steroidal Alkaloids from *Buxus hyrcana*

Buxus alkaloids have a unique steroid-triterpenoid pregnane type skeleton with C-4 methyls, 9β, 10β cycloartenol system with a degraded C-20 side chain [21–33]. These alkaloids exhibit various biological activities including anti-HIV, anti-TB,

anti-malarial, and enzyme inhibitory activities, etc. [26–33]. In the last two decades over 90 steroidal alkaloids have been from different plants of genus *Buxus* [21]. The crude methanolic extract of *Buxus hyrcana*, collected from Iran, exhibited acetylcholinesterase inhibitory activity in our bioassay with an IC_{50} value of 45 μg/ml. Our detailed phytochemical studies on this plant resulted in the isolation of two new bioactive compounds, (+)-*O*^{6}-buxafurandiene (**13**) and (+)-7-deoxy-*O*^{6}-buxafurandiene (**14**). Compounds **13** and **14** belong to the rarely-occurring class of *Buxus* alkaloids having a tetrahydrofuran ring incorporated in their structures. To the best of my knowledge, only five compounds of this series have so far been reported in the literature [28, 29].

(+)-*O*^{6}-buxafurandiene (**13**) was isolated as a colorless amorphous solid. Its UV spectrum showed absorption maxima at 239 and 245 nm indicating the presence of an 9(10→19) *abeo* diene system [23]. The IR spectrum displayed intense absorption bands at 3,412 (OH), 1,710 (ester carbonyl), 1,644 (α,β-unsaturated amide carbonyl), 1,602 (C = C) and 1,100 (C-O) cm^{-1}. The Chemical Ionization Mass Spectrum (CIMS) of **13** showed $[M + H]^+$ ion at *m/z* 593. The HREIMS of **13** exhibited molecular ion peak at *m/z* 592.3519 corresponding to the molecular formula $C_{35}H_{48}N_2O_6$ (calcd 592.3512) and this indicated the presence of 13 degrees of unsaturation in compound **13**. The ion at *m/z* 577.3273 ($C_{34}H_{45}N_2O_6$, calcd 577.3278) was due to loss of a methyl group from the molecular ion. Another ion at *m/z* 105 was due to loss of a benzoyl group. The compound **13** showed a base peak at *m/z* 72 due to the loss of a trimethyl imminium cation and this indicated the presence of an *N*, *N*-dimethyl amino group at C-20 *[23]*.

The ^{1}H NMR spectrum of **13** showed the resonance of three 3H singlets at δ 0.92, 0.89 and 0.91 due to the tertiary C-18, C-30 and C-32 methyl protons, respectively. A 3H doublet at δ 1.03 (d, *J* = 6.5 Hz) was ascribed to the C-21 secondary methyl protons. The *N*, *N*-dimethyl protons, substituted at C-20, resonated as a six-proton broad singlet at δ 2.27. Four downfield signals at δ 3.54, 3.96, 4.08 and 5.00 were due to the C-7, C-6, C-2 and C-16 methine protons, respectively. Their downfield chemical shift values were indicative of the presence of geminal oxygen functionalities at C-2, C-6 and C-16, respectively. The C-3 methine proton, geminal to an amidic moiety, resonated at δ 4.01. Two AB doublets, integrating for one-proton each, at δ 3.86 and 4.06 (*J* = 11.0 Hz) were due to the C-31 methylene protons. The amidic NH appeared as a doublet at δ 5.99 (*J* = 9.5 Hz). Two olefinic signals at δ 5.33 and 5.85 in the ^{1}H NMR spectrum were assigned to the C-11 and C-19 methine protons, respectively. The aromatic protons appeared as two sets of two- and three-proton multiplets at δ 7.26–7.69.

The ^{13}C NMR spectrum of **13** showed the resonances of all 35 carbon atoms. A combination of broadband ^{13}C-NMR and DEPT spectra indicated the presence of 7 methyl, 4 methylene, 16 methine and 8 quaternary carbon atoms in compound **13**. Complete **13**C-NMR chemical shift assignments of **13** are shown around structure **13**. Based on these spectral data, structure **13** was established for this new compound.

7-dexoy-*O*^{6}-buxafurandiene (**14**) was also isolated as a colorless amorphous solid. A combination of mass, ^{1}H, ^{13}C-NMR, COSY, HSQC, HMBC and NOESY spectra suggested that compound **14** was 7-dexoyderivative of **13**.

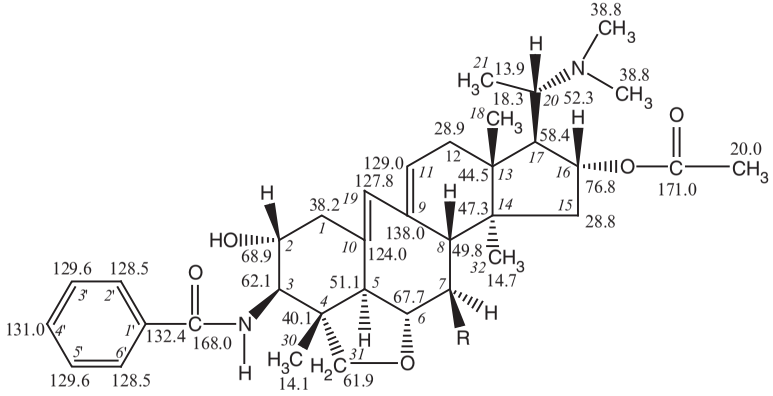

(**13**) R = OH, C-7 δ 70.1

(**14**) R = H, C-7 δ 27.2

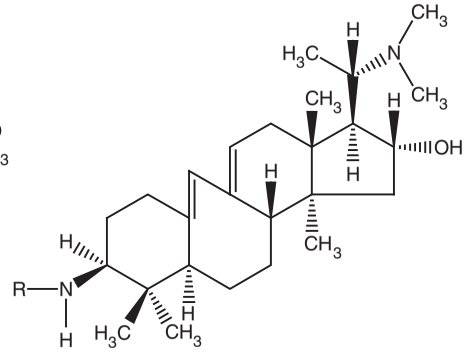

(**15**) R = PhCO

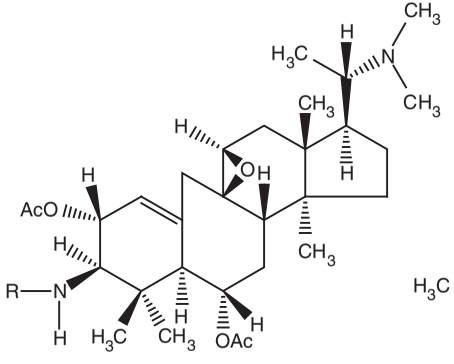

(**16**) R = PhCO

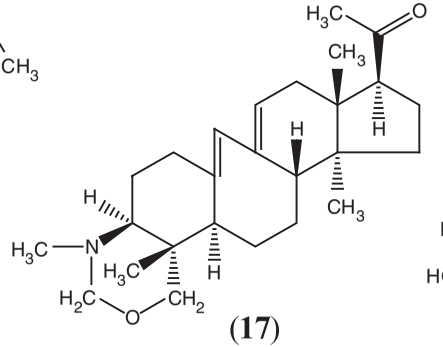

(**17**)

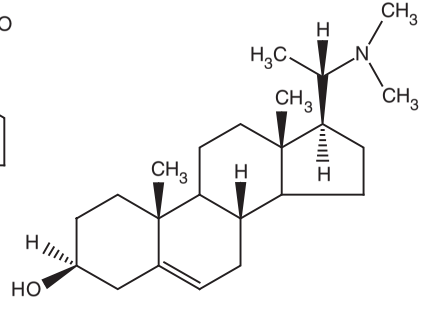

(**18**)

During this phytochemical studies we have also isolated four known compounds, benzoylbuxidienine (**15**), buxapapillinine (**16**), buxaquamarine (**17**) and irehine (**18**) for the first time from *B. hyrcana*. The UV, IR, ^{1}H NMR and mass spectra of compound **15**–**18** were identical with those of benzoylbuxidienine, buxapapillinine, buxaquamarine and irehine, respectively, as reported in the literature [29–32]. This helped us to characterize compounds **15**, **16**, **17** and **18** as benzoylbuxidienine, buxapapillinine, buxaquamarine and irehine, respectively. Previously, benzoylbuxidienine (**15**), buxapapillinine (**16**), and buxaquamarine (**17**) and irehine (**18**) were isolated from *B. sempervirens* and *B. papillosa* [29–33].

Compounds **13**–**18** were tested for acetylcholinesterase inhibition activity and it was found that compounds **13** and **14** exhibited acetylcholinesterase inhibition activity with IC_{50} values (inhibition of enzyme activity by 50%) of 17 and 13 μM, respectively. Compounds **15**–**18** showed moderate enzyme inhibition activity with IC_{50} values of 35, 80, 76, and 100 μM, respectively. This bioactivity data suggested that the higher enzyme inhibition potency of compounds **13** and **14** may hypothesized due to the presence of a tetrahydrofuran ring incorporated in their structures. Furthermore, compounds **1** and **2** exhibited nearly the same bioactivity and this indicated that C-7 hydroxyl group does not play any role in enzyme inhibition activity.

Acknowledgements Funding from Natural Science and Engineering Research Council (NSERC) Canada and Research Corporation, Tucson, Arizona, USA provided for these projects are gratefully acknowledged. I also wish to acknowledge a number of my co-workers (their names appear in the reference cited) and students including Dr. Ilkay Orhan, Ms. Leigha J. Conci, Ms. Hla Y Win, Mr. David Holt, Mr. Jordan Bettridge, Mr. Shamsulhaq Zahid, Mr. Chibuike C. Udenigwe and Ms. Kosmulalage S. Kalhari, who were involved on various aspects in the paper

References

1. Ata, A., Ackerman, and J. Radhika, P., 2003, *Tetrehedron Lett.,* **44,** 6951–6953.
2. Rodriguez, A.D. and Shi, Y.-P., 2000, *Tetrahedron,* **56,** 9015–9023.
3. Look, S.A., Fenical, W., Jacob, R.S. and Clardy, J., 1986, *Proc. Natl. Acad. Sci. USA,* **83,** 6238–6240.
4. Look, S.A., Fenical, W., Matsumoto, G.K. and Clardy, J., 1986, *J. Org. Chem.,* **51,** 5140–5145.
5. Roussis, V., Wu, Z. and Fenical, W., 1990, *J. org. Chem.,* **55,** 4916–4922.
6. Rodriguez, A.D., Ramierz, C., Rodriguez, I.I. and Gonzalez, E., 1999, *Org. Lett.,* **1,** 527–530.
7. Rodriguez, A.D. and Ramirez, C., 2001, *J. Nat. Prod.,* **64,** 100–102.
8. Rodriguez, A.D., Ramirez, C., Rodriguez, I.I. and Barnes, C.L., 2000, *J. Org. Chem.,* **65,** 1390–1398.
9. Rodriguez, A.D. and Ramirez, C., 2000, *Org. Lett.,* **2,** 507–510.
10. Scott, A.I., 1964, Interpretation of UV Spectral of Natural Products, Pergamon, Oxford.
11. National Committee for Clinical Laboratory Standards. 1995, *Performance Standards for Antimicrobial Disk Susceptibility*, 5th Edition, Approved standard. NCCLS Document M2-A5, Villanova, PA.
12. Ata, A., Kerr, R.G., Moya, C.E. and Jacobs, R.S., 2003, *Tetrahedron,* **59,** 4215–4222.
13. Ata, A., Ackerman, J., and Radhika, P., 2004, *Helv. Chim. Acta,* **87,** 592–597.
14. Rosenberry, T.L., 1975, *Adv. Enzymol. Relat. Areas Mol. Biol.,* **43,** 103–218.

15. Enz, A., Amstutz, R., Boddeke, H., Gmelin, G. and Malonowski, J., 1993, *Prog. Brain Res.,* **98,** 431–438.
16. Van Middlesworth, F. and Cannell, R. J. P., 1998, *Dereplication and Partial Identification of Natural Products: Methods in Biotechnology* (R. J. P Cannell Humana, ed.), Humana, Totowa, NJ, Vol. 4, pp 279–327.
17. Knight, V., Sanglier, J.-J., Ditullio, D., Braccili, S., Bonner, P., Waters, J., Hughes, D. and Zhang, L., 2003, *Appl. Microbiol. Biotechnol.,* **62,** 446–458.
18. Urizar, N.L., Liverman, A.B., Dodds, D.T., Silva, F.V., Ordentlich, P., Yan, Y., Gonzalez, F.J., Heyman, R.A., Mangelsdorf, D.J. and Moore, D.D., 2002, *Science,* **296,** 1703–1706.
19. Yamada, Y., Suzuki, S., Iguchi, K., Kikuchi, H., Tsakitani, Y., Horiai, H., and Nakanishi, H., 1980, *Chem. Pharm. Bull.,* **28,** 473–478.
20. Pettit, G.R., Numata, A., Cragg, G.M., Herald, D.L., Takada, T., Iwamoto, C., Riesen, R., Schmidt, J.M., Doubek, D.L. and Goswami, A., 2000, *J. Nat. Prod.,***63,** 72–78.
21. Ata, A., Naz, S., Choudhary, M.I., Atta-ur-Rahman, Sener, B. and Turkoz, S., 2002, *Z. Naturforsch,* **57c,** 21–28.
22. Atta-ur-Rahman, Ata, A., Naz, S., Choudhary, M.I., Sener, B. Turkoz, S., 1999, *J. Nat. Prod.,* **62,** 665–669.
23. Atta-ur-Rahman and Choudhary, M.I., 1988, Structural studies on new steroidal alkaloids of *Buxus papillosa.* In *Studies in Natural Products Chemistry* (Atta-ur-Rahman ed.), Elsevier Science, Amsterdam, Vol. 2, pp 175–189.
24. Atta-ur-Rahman, and Choudhary, M.I.,1999,*Nat. Prod. Rep.*,**71,**619–635.
25. Cordell, G.A., 1981, *Buxus*, Alkaloids: A Biogenetic Approach. In *Introduction to Alkaloids*Wiley Interscience, New York, pp 907–925.
26. Durant, J., Chantre, P., Gonzalez, G., Vandermander, J., Halfon, P., Rousse, B., Guedon, D., Rahelinirina, V., Chamaret, S., Montagnier, L. and Dellamonica, P., 1998, *Phytomedicine,* **5,** 1–10.
27. Wang, Y.X., Liu, J.W., Tan, Y.H. and Sheng, B.H., 1989, *Acta Pharmacol. Sin.,* **10,** 516–519.
28. Wang, Y.X., Tan, Y.H. and Sheng, B.H., 1992, *Acta Pharmacol. Sin.,* **13,** 226–230.
29. Atta-ur-Rahman, Choudhary, M.I. and Ata, A., 1992, *Heterocycles,* **34,** 157–171.
30. Atta-ur-Rahman, Iqbal, Z., Zaidi, R. and Choudhary, M.I., 1990, *J. Nat. Prod.,* **53,** 319–324.
31. Atta-ur-Rahman, Ahmed, D., Asif, E., Jamal, S.A., Choudhary, M.I., Sener, B. and Turkoz, S., 1991, *Phytochemistry,* **30,** 1295–1298.
32. Atta-ur-Rahman, Choudhary, M.I. and Nisa, M., 1985, *Heterocycles,* **23,** 1951–1954.
33. Kuchkova, K.I., Voticky, Z. and Paulik, V., 1976, *Chemicke Zvesti,* **30,** 174–178.

Chapter 6
Bioactive Turkish Plant Extracts and Their Constituents

Gülaçtı Topçu[1], Gülendam Tümen[2], Turgut Kılıç[2], Ahmet C. Gören[3], Aslı Barla[4], Zeynep Türkmen[4], and David G. I. Kingston[5]

Abstract Over 200 plant extracts were prepared from different family plants of rich flora of Turkey, in a frame of international collaborative project "Bioactive Turkish Plant Constituents". The plants were chosen randomly and/or partly based on their folkloric uses which belonged to 40 distinct families growing in Aegean and Marmara region, and their extracts were screened for their DNA damaging activity as well as for their human ovarian cytotoxic activity.

For this purpose, firstly, methanol extracts of the collected plants were prepared and tested for their DNA damaging activity. Active extracts were diluted with water and partitioned with hexane, dichloromethane and ethyl acetate, successively, and the extracts were then tested for their activity. For DNA damaging activity, the extracts were tested against three yeasts RS321NYCp50 grown on galactose, RS321NpRAD52 on galactose, and RS321NpRAD52 on glucose, while A2780 human ovarian cell lines were used for cytotoxic activity tests. Among the all tested extracts, four most active extracts were selected for further studies, which are *Ajuga postii, Laurus nobilis, Eucalyptus camaldulensis* and *Salvia hypargeia*.

In this presentation, bioactivity-directed isolation and structure elucidation of the active constituents will be given. Structures of the constituents, which form namely terpenoids (sesqui, di- and triterpenoids) were based on spectroscopic techniques, particularly intensive NMR and Mass spectroscopies.

[1] Istanbul Technical University, Faculty of Science and Letters, Department of Chemistry, Maslak, Istanbul, Turkey

[2] Balıkesir University, Faculty of Science and Letters, Department of Chemistry, 10100 Balıkesir, Turkey

[3] TUBITAK, Ulusal Metroloji Enstitüsü (UME), Group of Chemistry, P.O. Box 54, 41470, Gebze, Kocaeli, Turkey

[4] Istanbul University, Faculty of Pharmacy, 34116, Beyazıt, Istanbul Turkey

[5] Virginia Polytechnic Institute and State University, Department of Chemistry, M/C 0212, Blacksburg, VI 24061, USA

B. Sener (ed.), *Innovations in Chemical Biology*, doi: 10.1007/978-1-4020-6955-0

Keywords *Ajuga postii*, bioactive constituents, cytotoxic activity, DNA damaging activity, *Eucalyptus camaldulensis, Laurus nobilis, Salvia hypargeia*, spectroscopy, Turkish plants

Introduction

Contribution of higher plants to medicine and pharmaceutical industry due to nature's ability to present highly diverse chemicals [1] has prompted increasing interest of researchers in searching of natural product sources. For this purpose, various programs and methods have been developed to screen plants and/or other natural sources through bioactivity-guided fractionation, isolation and structure elucidation of active compounds [2]. Establishing a programme/method must have significant impact, not only in high-throughput screening, but also in alternative approaches to drug discovery. High-throughput screening is a way of innovation of lead structures for medicinal chemistry and pharmaceutical industry. The feasibility of a plant screening programme mainly depends on effective strategies. National and/or international collaborations are preferred to obtain more feeding, supportive and creative results with many benefits in different aspects of innovation of potential bioactive plants and their constituents.

Turkey is one of the unique countries in the world having three different climates, namely continental, mediterrenean and oceanic climates [3]. Turkey is also at the junction of three geographical regions for the plants, mainly Euro-Siberian in North Anatolia, Irano-Turanian in Central and East Anatolia, Mediterrenean in West and South Anatolia. All these properties contribute to the richness and diversity of the flora in Turkey with over 10,000 taxa in 173 families and 1,225 genera [4–7]. There are 15 endemic genera and over 2,650 endemic species. Endemism ratio is around 30%, however it is higher in certain families, such as Scrophulariaceae (52%), Campanulaceae (49%), Lamiaceae (=Labiatae) (44%), Asteraceae (=Compositae) (38%), and even in some particular species, the ratio reach 80–100%, such as *Ebenus* (100%), *Verbascum* (80%), *Sideritis* (78%) [7].

Mediterranean region is the richest in endemic plants with 633 species, followed by East Anatolia. Medicinal plants of Anatolia have been known since ancient times, the history can be traced to the Asyrians and Hittites. In immortal book of Dioscorides "Planta Medica", written in the 1st century, information, about over 500 medicinal plants growing in Mediterranean region and Anatolia, was presented. Now, over 1,000 plant drugs are found to be used in folk medicine. Since Mediterranean and Aegean regions of Turkey are rich in medicinal and aromatic plants, we aimed to investigate the plants growing in these area including Marmara region in the frame of an NSF-TUBİTAK supported Project (INT-0002071/TBAG-U53) on the basis of bio-assay directed isolation and structure elucidation.

Selection of Plants

About 200 plant species from 40 families were collected in small quantities, selection was made randomly as well as considering ethnobotanical information obtained from Marmara, Aegean and Mediterranean regions of Turkey. Random acquisition of available plant species is one approach. Maximum diversity in the botanical and geographical sources of the plant samples collected is preferred feature, and Turkey has an advantageous in this aspect [4–7].

Most of the plants, collected from Lamiaceae family, are aromatic and grown in Aegean-Mediterranean regions (West-South Anatolia). These are *Salvia, Sideritis, Thymus, Origanum, Satureja, Stachys, Micromeria, Nepeta etc.*

Mechanism-Based Isolation and Structures of Some Anticancer Active Natural Products

Except the last decade, in the previous years, the evolution of anticancer natural product drug discovery research is based on empirical searchs, in general for general cytotoxic agents to a more mechanism-based approach. Screening is a cursory look at many samples, not a in-depth investigation. An effective screening enables to choose the extracts containing selectively active potential lead compounds.

Our approach recently developed utilizes DNA repair- or recombination-deficient mutants of the yeast *Saccharomyces cerevisiae* [8]. An important feature of many tumor cells is that they have defects in their ability to repair damage to DNA as compared with normal cells, suggesting that agents with selective toxicity towards repair-deficient cells might be potential anticancer agents.

The mutant strain of *Saccharomyces cerevisiae* RS321NpRAD52, and deficient in recombination repair (RAD 52) and topoisomerase I was used in this assay [8]. But the strain carries a plasmid containing the RAD 52 repair pathway gene under the control of galactose promoter, will detect agents that specifically cause cytotoxicity by the way of DNA damage. Any agent that was cytotoxic to the yeasts in the RS321pRAD52 glucose and RS321NYCp50 galactose plates (>65% inhibition) but was not cytotoxic in the RS321pRAD52 galactose plate (<35% inhibition) will be considered a primary hit. Thus, an agent whose IC_{50} gives a threefold difference in the concentration response assay will be considered a lead [8, 9].

However, most of screens can show up false positives. False positives may arise from polyphenols, saponins, some pigments and fatty acids.

Results and Discussion

Over 170 Turkish plant extracts were screened for their DNA damaging activity (Table 6.1) using three yeasts, RS321NYCp50 grown on galactose (YCp50Gal), RS321NpRAD52 grown on galactose (RAD52Gal) and RS321NpRAD52 on glucose (RAD52Glu) [8, 9].

Table 6.1 DNA damaging assay against three yeasts[a] (dose 100 μg/mL)

No	**Plant family name** Plant genus and species name	YCp50 Galactose	RAD52 Galactose	RAD52 Glucose
	Anacardiaceae			
1	*Pistacia terebinthus* L. ssp. terebinthus L.	–16.5	–12.6	–23.0
2	*Pistacia lentiscus* L.	–6.3	–10.1	–11.7
	Apiaceae (Umbelliferae)			
3	*Angelica slyvestris* L. var. *slyvestris* Velen. (aerial parts)	27.5	54.3	49.9
4	*Angelica slyvestris* L. var. *slyvestris* Velen. (roots)	–13.4	–14.5	–9.3
5	*Coriandrum sativum* L.	5.2	41.9	25.6
6	*Echinophora tenufolia* L. ssp.*sibthorpiana* (Guss) Tutin	20.9	71.4	85.0
7	*Ferula* communis L. ssp. *communis* L.	1.7	26.7	25.5
	Apocynaceae			
8	*Vinca major* L. ssp. *major* L.	–5.0	–10.7	–9.1
9	*Amsonia orientalis Decne*	–13.7	–4.4	–17.6
10	**Araceae** *Arisarum vulgare* Targ.-Tozz ssp. Targ.-Tozz	–7.7	–2.3	–12.7
11	**Araliaceae** *Hedera helix*	–2.0	16.5	2.9
	Asteraceae (Compositae)			
12	*Anthemis aciphylla* Boiss. var. aciphylla Boiss.	–68.8	–37.0	–68.3
13	*Centaurea spinosa* L. var *spinosa* L.	–10.4	–9.7	–18.6
14	*Onopordum tauricum* Willd.	–9.9	–11.7	–14.8
15	*Pulicaria dysenterica* (L.) Bernh.	–3.3	1.9	–9.3
16	*Tanacetum cadmium* (Boiss.) Heywood ssp. *orientale* Grierson	11.1	8.2	0.7
17	*Tanacetum corymbosum* (L.) Schultz Bip. var. *cinereum* (Gris.) Hayek	17.1	0.0	–3.6
18	*Tanacetum parthenium* (L.) Schultz Bip.	43.3	38.6	8.3
19	**Boraginaceae** *Alkanna orientalis* (L.) Boiss. var. *orientalis* (L.) Boiss.	0.7	26.4	9.5
	Brassicaceae (Cruciferae)			
20	*Alyssum saxatile* L.	–6.0	–7.8	–6.6
21	*Cardaria draba* (L.) Desv. ssp. *draba* (L.) Desv.	–7.7	–12.8	–6.2
22	*Malcolmia flexuoso* (Sibth. & SM.) Sibth. & SM.	–2.7	–3.8	–6.6
23	*Matthiola fruticulosa* L. (Maire)	–5.7	–4.1	–7.3
24	*Raphanus raphanistrum* L.	–6.7	–9.6	–9.8

(continued)

Table 6.1 (continued)

No	**Plant family name** Plant genus and species name	YCp50 Galactose	RAD52 Galactose	RAD52 Glucose
	Buxaceae			
25	*Buxus sempervirens* L.	–4.0	5.2	–6.2
26	*Spiraea hypericifolia* L.	–4.7	4.3	–3.6
	Caprifoliaceae			
27	*Sambucus ebulus* L.	–3.3	–8.3	–12.1
	Caryophyllaceae			
28	*Gyposophila arrostii Guss*.	–20.0	–30.9	–17.7
	Chenopodiaceae			
29	*Ceratocarpus arenarius* L.	–1.5	–15.4	0.0
30	*Petrosimonia brachiata* (Pallas) Bunge	–16.3	–15.4	–8.0
31	*Chenopodium murale* L.	98.0	98.7	99.0
32	*Chenopodium vulvaria* L.	–3.0	–10.0	–1.3
33	*Cyathobasis fruticulosa* (Bunge) Aellen (Aqueous MeOH ext.)	–0.7	–7.8	–6.6
34	*Cyathobasis fruticulosa* (Bunge) Aellen ($CHCl_3$ soluble part)	1.7	–5.8	–7.3
35	**Cistaceae** *Cistus salviifolius* L.	–9.0	2.6	0.7
36	**Cucurbitaceae** *Ecballium elaterium* L. A. Rich	–1.6	–18.4	–20.3
	Cupressaceae			
37	*Juniperus excelsa* Bieb. berries	28.7	34.0	4.13
38	*Juniperus excelsa* Bieb. leaves	56.0	85.9	73.66
	Ericaceae			
39	*Arbutus unedo* L. fruits	6.7	8.6	10.3
40	*Arbutus unedo* L. leaves	–2.7	–4.6	–5.0
41	*Erica arborea* L.	–11.0	0.0	–17.0
42	*Rhododendron luteum* Sweet	–7.3	–12.5	–1.8
43	**Equisetaceae** *Equisetum arvense* L.	–1.3	–9.6	–1.3
44	**Euphorbiaceae** *Euphorbia platyphyllos* L.	–11.3	–1.7	–10.9
	Fabaceae			
45	*Anthyllis hermanniae* L.	–1.6	19.4	4.4
46	*Genista acanthoclada* DC.	12.7	26.4	11.3
47	*Lupinus micranthus* Guss.	1.7	2.9	–5.1
48	*Parkinsonia aculeate* L.	1.1	–2.4	–6.6
49	**Fagaceae** *Quercus cerris* L. *var. cerris* L.	–9.0	–7.5	–9.5
	Geraniaceae			
50	*Pelargonium odarassimum* Agnew	–4.0	0.3	–11.3
51	*Pelargonium zonale* (L.) L'herit	–2.0	0.9	–11.3
52	*Geranium lanuginosum* Lam.	–8.0	8.1	–7.6
53	**Guttiferae** *Hypericum retusum* Aucher	5.3	5.4	0.08

(continued)

Table 6.1 (continued)

No	**Plant family name** Plant genus and species name	YCp50 Galactose	RAD52 Galactose	RAD52 Glucose
	Iridaceae			
54	*Iris pallida* Lam.	−5.0	−8.7	−8.7
55	*Iris persica* L.	−4.4	34.0	35.1
56	**Juglandaceae** *Juglans regia* L.	0.0	24.1	9.0
	Lamiaceae (Labiatae)			
57	*Ajuga bombycina* Boiss.	−21.4	49.0	28.4
58	Ajuga postii Briq. (Methanol ext.)	69.1	7.5	30.5
59	*Ajuga postii* Briq. (Acetone ext.)	40.2	2.3	3.51
60	*Ajuga relicta* P.H.	−17.9	8.6	4.6
61	*Ajuga salicifolia* (L.) Schreber	7.4	10.5	15.9
62	*Ballota nigra* L. ssp. *nigra* L. (leaves)	3.0	2.4	5.0
63	*Ballota nigra* L. ssp. *nigra* L. (fruits)	−7.7	−17.0	−15.9
64	*Clinopodium vulgare* L. ssp. *vulgare* L.	−3.0	−10.0	−1.3
65	*Cyclotrichium origanifolium* (Labill.) Manden & Scheng	10.4	14.5	−2.2
66	*Lamium album* L.	18.6	65.8	46.8
67	*Lamium garganicum* L.	−17.6	−13.1	−23.6
68	*Lamium purpureum* L. ssp. *purpureum*	−25.0	−4.1	11.9
69	*Lavandula cariensis* Boiss.	−3.3	7.5	0.0
70	*Lavandula stoechas* L. ssp. *cariensis* (Boiss.) Rozeira	0.0	−9.5	−4.0
71	*Marrubium vulgare* L.	12.8	7.2	4.0
72	*Melissa officinalis* L. ssp. *officinalis* L.	−13.0	−9.7	−13.2
73	*Melissa officinalis* L. ssp. altissima (Sm.) Arcangeli	10.6	14.9	−3.9
74	*Mentha aquatica* L.	18.7	26.6	26.4
75	*Mentha longifolia* (L.) Hudson ssp. *longifolia* L.	1.7	5.3	7.9
76	*Mentha pulegium* L.	23.6	30.5	17.8
77	*Micromeria congesta* Boiss. & Hausskn. Ex Boiss.	31.9	9.5	57.9
78	*Micromeria fruticosa* (L.) Druce	23.0	10.5	17.2
79	*Micromeria juliana* (L.) Bentham ex Reichb.	−8.9	49.8	18.8
80	*Micromeria myrtifolia* Boiss. & Hohen.	15.4	11	3.1
81	*Nepeta fissa* C.A. Meyer	5.4	47.3	24.3
82	*Nepeta nuda* L. ssp. *glandulifera* Hub.-Mor. & Davis	−28.6	44.9	34.4
83	*Nepeta nuda* L. ssp. *albiflora* (Boiss.) Gams	−2.4	13.0	0
84	*Nepeta sulfuriflora* P.H. Davis	0.0	−27.2	−6.0
85	*Origanum hypericifolium* O. Schwarz & P.H. Davis	22.3	1.5	0.4
86	*Origanum majorana* L.	7.7	5.5	5.6
87	*Origanum onites* L.	8.9	24	14.0
88	*Origanum syriacum* L. var. *bevanii* (Holmes) Ietswaart	1.6	28.5	10.9
89	*Origanum vulgare* L. ssp. *gracile* (C. Koch) Ietswaart	22	14.3	23.3
90	*Origanum vulgare* L. ssp. *vulgare* L.	4.0	3.1	4.0

(continued)

Table 6.1 (continued)

No	**Plant family name** Plant genus and species name	YCp50 Galactose	RAD52 Galactose	RAD52 Glucose
91	*Origanum vulgare* L. ssp. *hirtum* (Link) Ietswaart	14.6	31.7	15.5
92	*Phlomis fruticosa* L.	−8.3	−7.2	−11.3
93	*Prunella laciniata* (L.) L.	−3.7	−3.5	−7.1
94	*Salvia amplexicaulis* Lam.	0	−20.1	−10.9
95	*Salvia blepharochlaena Hedge* & Hub.-Mor.	51.8	64.6	48.1
96	*Salvia cedronella* Boiss.	7.3	20.7	−1.6
97	*Salvia ceratophylla* L.	−18.6	−6.0	27.8
98	*Salvia cyanescens* Boiss. & Bal.	37.5	36.2	26.1
99	*Salvia eriophora* Boiss. & Kotschy (roots)	41.8	50.0	43.3
100	*Salvia eriophora* Boiss. & Kotschy (aerial parts)	−13.7	−16.5	−23.0
101	*Salvia kronenburgii* Rech. Fil.	−26.8	35.8	10.5
102	*Salvia limbata* C.A. Meyer	−7.3	0	−18.6
103	*Salvia staminea* Montbret & Aucher ex Bentham (Methanol extract)	10.7	47.3	11.0
104	*Salvia staminea* Montbret & Aucher ex Bentham (Acetone extract)	−41.8	−1.5	−17.6
105	*Salvia syriaca* L.	79.7	47.3	48.1
106	*Salvia tchihatcheffii* (Fisch. & Mey.)	5.4	35.8	16.9
107	*Salvia fruticosa* Miller, Gard (*syn*: S. *triloba* L.)	98.4	98.5	97.6
108	*Salvia yosgadensis* Freyn & Bornm.	−28.6	−39.1	−15.1
109	*Satureja cilicica* P.H. Davis	16.3	18.8	14.0
110	*Satureja cuneifolia* Ten.	35.7	7.0	−0.5
111	*Satureja hortensis* L.	7.0	2.4	7.3
112	*Satureja pilosa* Velen.	27.6	27.9	24.0
113	*Sideritis albiflora* Hub.-Mor.	−6.5	3.9	7.8
114	*Sideritis arguta* Boiss. & Heldr.	−8.9	0	22.5
115	*Sideritis athoa Papanikolaou* & Kokkini	−7.1	−4.9	−8.7
116	*Sideritis aytachii* H. Duman & P. Sahin	49.7	54.9	92.4
117	*Sideritis congesta* P.H. Davis & Hub.-Mor.	−3.7	−1.7	−1.3
118	*Sideritis dichotoma* Huter	−42.9	−11.1	−10.5
119	*Sideritis galatica* Bornm	−13.0	−11.0	0
120	*Sideritis leptoclada* O. Schwarz & P. H. Davis	−8.9	3.9	18.6
121	*Sideritis libanotica* Labill. ssp. *linearis* (Bentham) Bornm.	19.6	−4.1	0.9
122	*Sideritis lycia* Boiss. & Heldr.	9.1	7.0	10.6
123	*Sideritis lycia* Boiss. & Heldr. (Hexane ext.)	33.6	73.9	94.0
124	*Sideritis lycia* Boiss. & Heldr. (Acetone ext.)	−2.0	−3.1	0.0
125	*Sideritis perfoliata* L.	2.7	−1.2	1.7
126	*Sideritis pisidica* Boiss. & Heldr. Apud Bentham	−11.4	−3.9	−12.4
127	*Sideritis vuralii* H. Duman & Başer (Acetone ext)	−0.7	0.2	1.3
128	*Stachys annua* (L) L. ssp. *annua* L.	22.8	33.3	−2.3
129	*Stachys byzantina* C. Koch	3.3	−10.4	−6.2
130	*Stachys catonica* Bhattacharjee & Hub.-Mor.	−6.5	−11.0	-0.8
131	*Stachys cretica* L. ssp. *cretica* L.	−18.7	−5.2	14.0
132	*Stachys lavandufolia* Vahl var. *lavandulifolia* Gled.	26.5	22.1	16.6

(continued)

Table 6.1 (continued)

No	**Plant family name** Plant genus and species name	YCp50 Galactose	RAD52 Galactose	RAD52 Glucose
133	*Teucrium chamaedrys* L. ssp. *chamaedrys* Rech. Fil.	3.7	0.0	0.0
134	*Teucrium polium* L.	−15.4	−7.8	−3.1
135	*Teucrium polium* L.	11.7	10.3	8.9
136	*Thymbra spicata* L. var. spicata E. D. Clarke	39.8	56.4	67.4
137	*Thymus atticus* Celak	−82.1	−21.4	−6.9
138	*Thymus canoviridis* Jalas	34.1	37.6	43.4
139	*Thymus cariensis* Hub.-Mor. & Jalas	44.6	66.7	45.3
140	*Thymus fallax* Fisch. & Mey.	−5.5	−0.5	−7.1
141	*Thymus sipyleus* Boiss. ssp. *sipyleus* Boiss.	4.5	0.0	8.0
142	*Thymus pseudopulegioides* Klokov & Des.-Shost	−13.0	−2.6	−5.4
143	*Thymus pulvinatus* Celak	−6.5	4.5	−7.0
144	*Ziziphora clinopodioides* Lam.	7.0	0.2	6.0
145	**Lauraceae** *Laurus nobilis* L.	49.4	40.1	38.8
	Liliaceae			
146	*Allium subhirtum* L.	−7.0	−6.7	−9.8
147	*Asphodelus fistulous* L.	4.0	8.4	1.5
148	*Ruscus aculeatus* L. var. *aculeatus* L.	−1.0	−2.3	11.3
149	**Loranthaceae** *Viscum album* L. var. *album* L.	−1.7	1.2	2.3
150	**Malvaceae** *Malva neglecta* Wallr.	0.0	−1.7	4.6
151	**Meliaceae** *Melia azedarach* L.	−4.5	−22.9	−14.6
	Moraceae			
152	*Ficus carica* L. ssp. *carica* (All.) Schinz & Thell.	−3.3	−4.3	0.7
153	*Maclura pomifera* (Raf.) Schneid. (leaves)	3.0	−23.4	−13.7
154	*Maclura pomifera* (Raf.) Schneid. (fruits)	−5.9	−7.0	−18.1
155	**Myrtaceae** *Eucalyptus camaldulensis* Dehnh.	18.0	63.2	37.5
156	**Oleaceae** *Forsythia viridissima* Lindl.	1.3	5.5	−3.3
157	**Orobanchaceae** *Orobanche minor* SM.	−13.2	−10.2	−13.7
158	**Plantaginaceae** *Plantago major* L.	−4.4	−6.0	−2.6
159	**Platanaceae** *Platanus orientalis* L.	23.0	70.4	37.5
	Polygonaceae			
160	*Polygonum aviculare* L.	−5.2	−38.4	−20.3
161	*Rumex crispus* L. (seeds)	66.1	68.8	83.9
162	*Rumex dentatus* L.	8.9	2.0	−16.3
163	**Resedaceae** *Reseda lutea* L.	−14.8	−7.3	−15.9

(continued)

Table 6.1 (continued)

No	**Plant family name** Plant genus and species name	YCp50 Galactose	RAD52 Galactose	RAD52 Glucose
164	**Rosaceae**			
	Sanguisorba minor Scop.	−2.2	−15.4	−7.5
165	*Rosa canina* L. (leaves)	−5.0	2.0	−6.9
166	*Rosa canina* L. (fruits)	−5.7	−4.1	−8.7
	Rubiaceae			
167	*Galium spurium* L. ssp. *spurium* L.	−5.0	−3.8	0.0
	Scrophulariaceae			
168	*Bungea trifida* (Vahl) C.A. Meyer (roots)	−8.9	−17.4	−6.2
169	*Bungea trifida* (Vahl) C.A. Meyer (aerial parts)	3.7	4.0	−2.7
170	*Verbascum bithynicum* Boiss.	−1.6	−17.0	−0.5
171	*Verbascum speciosum* Schrader	−8.8	−15.0	−18.6
172	**Zygophyllaceae** *Peganum harmala* L.	28.2	27.1	15.2

[a] The studied extracts rather than MeOH extract or/and whole plant are shown in parenthesis

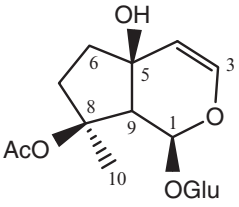

Fig. 6.1 Reptoside

The crude methanol extract of *Ajuga postii* Briq. showed the highest DNA damaging activity with IC_{50} values of 65.1 μg/mL against, >100 μg/mL against RAD52Gal, and 69.0 μg/mL against RAD52Glu. It was thus selected for isolation of its bioactive compounds. By bioassay-guided fractionation of the active methanol extract of *A. postii* afforded [10] an iridoid glucoside reptoside (Fig. 6.1) which was found to be responsible compound for the activity. Reptoside showed DNA damaging activity with IC_{50} values of 46.0 μg/mL against YCp50Gal, >100μg/mL against RAD52 on galactose and 30.4 μg/mL against RAD52Glu similar to the methanol extract of *A. postii* (Table 6.2). This result shows that reptoside has a DNA damaging activity but it has no cytotoxic activity. The other pure compounds, isolated from the direct acetone extract of *Ajuga postii* were two known triterpenic compounds ursolic acid, α-amyrin and two steroidal compounds (24*S*)-24-ethylcholesta-5,25-dien-3β-ol and β-sitosterol did not show any DNA damaging activity [10]. Although reptoside is a known iridoid glucoside, its structure was identified based on 1D- and 2D NMR techniques, mass and other spectral data as well as other known and new compounds isolated from other chemically investigated plant extracts.

Table 6.2 DNA damaging activity of reptoside and Ajuga postii Briq. (IC_{50} (μg/mL)

Sample	Ycp50Gal	pRAD52Gal	pRAD52Glu
MeOH extract	65.1	>100	69.0
CH_2Cl_2 fraction	47.6	>100	62.6
Reptoside	46.0	>100	30.4
Camptothecin (positive control)	–	100	0.6

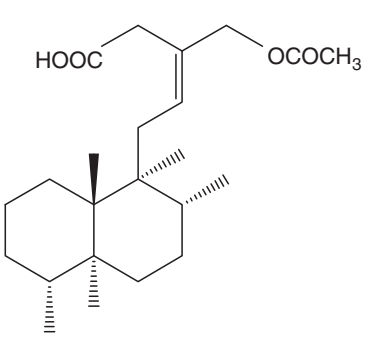

ajugalaevigatic acid
[IC_{50} = 17.7 μg/mL]

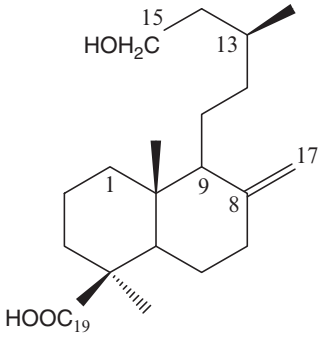

(13S)-15-hydroxylabd-8(17)-en-19-oic acid
[IC_{50} = 16.7 μg/mL]

Fig. 6.2 Diterpenes isolated from Ajuga chamaepytis ssp. laevigata

From another *Ajuga species*, *A. chamaepytis* ssp. *laevigata*, a new clerodane diterpene ajugalaevigatic acid, and (13S)-15-hydroxylabd-8(17)-en-19-oic acid (Fig. 6.2) which is the diastereomer of imbricatolic acid, and steroidal glucoside 3-O-β-D-glucopyranosylstigmasta-5,25 diene were evaluated in the yeast based assay (Table 6.3), but none of them showed activity while the new diterpene ajugalaevigatic acid showed only a weak A2780 ovarian cytotoxic activity [11] among against a panel of cancer cell line tested.

A monotypic "single species/single genus" *Cyathobasis fruticulosa* (Bunge) Aellen endemic plant for Turkey afforded a β-carboline, a tryptamine and two phenylethylamine derived alkaloids besides three simple aromatics [12]. Antifungal activity for hordenine, N-methyltetrahydro-*β*-carboline, and *N*-methyl,*N*-formyl-4-hydroxy-*β*-phenylethylamine (Fig. 6.3) was determined by a dose-dependent microtiter assay against the three yeast strains (Table 6.3). Among them, only the new alkaloid *N*-methyl, *N*-formyl-4-hydroxy-β-phenylethylamine showed marginal antifungal activity against two genetically modified yeasts RS321NYCp50 and RS321NpRAD52. Furthermore, the new alkaloid and hordenine were found to be weakly active against A2780 mammalian ovarian cell line exhibiting only 38% and 39 inhibition, respectively, at a dose 50 μg/mL dose.

Table 6.3 Inhibition (%) of the isolated compounds on the three yeasts (dose 100 μg/mL)

		YCp50gal	PRAD52gal	PRAD52glu
No	Compound name	Inhibition (%)	Inhibition (%)	Inhibition (%)
1	Oleanolic acid	0.0	1.4	4.18
2	Ursolic acid	4.0	23.1	0.0
3	Vergatic acid	0.0	0.0	0.0
4	2α,3β,11α-triacetoxy-urs-5,12-diene	56.0	68.9	51.0
5	1β,2α,3β,11α-tetrahydroxy-urs-12-ene	–28.6	–8.3	20.3
6	1β,2α,3β,11α-tetrahydroxy-olean-12-ene	5.5	–1.5	–1.6
7	1β,2α,11α-trihydroxy-3β-acetoxy-urs-12-ene	–8.2	–2.9	–3.3
8	Salvinemorol	–12.6	–18.0	3.8
9	*β*-Sitosterol	22.0	30.1	6.0
10	Stigmasta-5,25-diene-3*β*-D-glucoside	7.9	1.7	0.0
11	Microstegiol	0.0	0.0	4.18
12	Candidissiol	8.6	8.6	23.75
13	Cryptojaponol	16.5	0.0	0.0
14	Salvipisone	9.3	8.3	–7.7
15	6-Hydroxysalvipisone	11.5	–7.3	–4.9
16	Ferruginol	6.0	20.9	4.9
17	Acetylroyleanone	20.3	34.0	4.9
18	1-Oxo-salvibretol	–11.0	–4.4	0.5
19	Taxodione	39.6	66.5	62.5
20	3,12-Dihydroxysapriparaquinone	8.7	0.0	3.47
21	4,14-Dihydroxysapriparaquinone	20.5	12.5	10.05
22	Ajugalaevigatic acid	13.5	38.9	0.0
23	(13S)-15-hydroxylabd-8(17)-en-19-oic acid	15.7	15.5	0.0
24	Hordenin	6.0	0.0	4.16
25	N-methyl-tetrahydro *β*-carbolin	4.2	0.0	3.47
26	N-methyl,N-formyl-4-hydroxy-*β*-phenylethylamine	33.1	33.6	11.44
27	Khellin	39.0	15.4	12.48

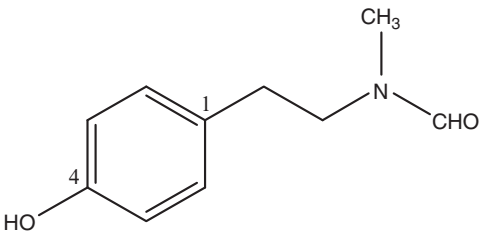

Fig. 6.3 N-methyl, N-formyl-4-hydroxy-β-phenylethylamine

Among Lamiaceae family plants, except *Ajuga postii*, none of the species gave hit in the yeast based assay. However, a few *Salvia* species (*S. triloba, S. blepharochlaena, S. syriaca*), and a few *Sideritis species* (*S. aytachii, S. lycia*) showed high inhibition against at least one or two tested yeasts among the three yeasts used in DNA damaging microtiter assay (Table 6.1).

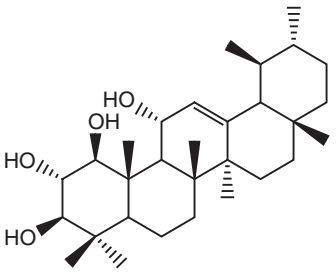

1β,2α,3β,11α-tetrahydroxy-urs-12-ene
[IC_{50} = 27.7 μg/mL]

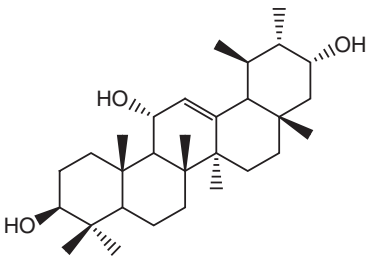

salvistamineol
[IC_{50} = 21.0 μg/mL]

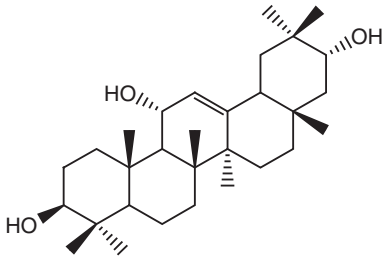

salvinemorol
[IC_{50} = 8.6 μg/mL]

Fig. 6.4 Triterpenoids isolated from Salvia kronenburgii Rech

In Lamiaceae family plants, particularly in *Salvia* species, oleanolic, ursolic and vergatic acids are common triterpenoids [13], however when they were evaluated in the yeast based DNA damaging activity assay, almost no inhibition was observed. A series highly hydroxylated terpenoids isolated from an endemic *Salvia* species *Salvia kronenburgii* [14, 15] were tested against the three yeasts, but, none of them showed higher inhibition than 50%, except diacetyl derivative of 3β,11α-dihydroxy,2α-acetoxyurs-5,12-diene (=2α,3β,11α-triacetoxy-urs-5,12-diene) (Table 6.3). Furthermore, the most abundant triterpenoid 1β,2α,3β,11α-tetrahydroxy-urs-12-ene (Fig. 6.4) of *S. kronenburgii* extract, required by NSF for 60 cell line screening, was found highly cytotoxic against non-small cell lung (EKVX), renal (RXF 393) and breast (BT-549) [15] cancer cell lines, while it was not active against A2780 ovarian cytotoxic cell lines.

On the other hand, salvinemorol showed highest A2780 activity (IC_{50} = 8.6 μg/mL) among a series triterpenes isolated from some *Salvia* species while the activity is highly decreased in its epimer salvistamineol [17] (Fig. 6.4).

From *Salvia staminea*, isolated abietane diterpenoids ferruginol, taxodione, cryptojaponol, microstegiol and 1-oxosalvibretol were tested against the three yeast through DNA damaging microtiter assay, and only taxodione showed relatively high inhibition, particularly against RAD52 galactose and glucose strains.

Since DNA damaging activity results didn't give almost no hit except a few extracts (*Ajuga and Juniperus*) (Table 6.4) we directed our bioactivity assay to ovarian cytotoxic activity search.

Among almost 70 plant extracts (Table 6.5), seven-eight plants were found potential cytotoxic active, and their extracts were subjected for fractionation and isolation of pure compounds, and then over 300 fractions and 35 pure compounds were searched for ovarian cytotoxic activity against A2780 human ovarian cell lines.

Table 6.4 Yeast based DNA damaging microtiter assay (% inhibition)

Dose (100 μg/mL)	YCp50Gal	pRAD52Gal	pRAD52Glu	IC50 Diff. GalGal	IC50 Diff. GalGlu
Ajuga postii Briq.	69.1	7.5	30.5	**2.99**	
Juniperus excelsa Bieb. M. (berries)	28.7	34.0	4.1	**1.0**	**1.0**
Juniperus excelsa Bieb. M. (leaves)	56.0	85.9	73.7	**2.1**	**0.6**

Table 6.5 Ovarian cytotoxic activity against A2780 human ovarian cell lines[a]

No	Plant name	Plant family	Inhibition (%)	IC_{50} (ug/mL)
1	*Pistacia lentiscus* L.	**Anacardiaceae**	–36	
2	*Ferula communis* L. ssp. *communis* L.	**Apiaceae = Umbelliferae**	–52	
3	*Conium maculatum* L.	**Apiaceae**	–17	
4	*Vinca major* L. ssp. *major* L.	**Apocynaceae**	46	
5	*Arisarum vulgare* Targ.-Tozz ssp. *vulgare* Targ.-Tozz	**Araceae**	35	
6	*Hedera helix* L.	**Araliaceae**	58	
7	*Anthemis aciphylla* Boiss. var. *aciphylla* Boiss.	**Asteraceae (Compositae)**	-35	
8	*Tanacetum balsamita* L. ssp. *balsamitoides* (Schultz Bip.) Grierson (aerial EtOAc)	**Asteraceae**	–34	
9	*Alkanna orientalis* (L.) Boiss. var. *orientalis* (L.) Boiss.	**Boraginaceae**	–59	
10	*Alyssum saxatile* L.	**Brassicaceae = Cruciferae**	42	
11	*Cardaria draba* (L.) Desv. ssp. *draba* (L.) Desv.	**Brassicaceae**	–45	
12	*Malcolmia flexuoso* (Sibth. & SM.) Sibth & SM.	**Brassicaceae**	46	
13	*Matthiola fruticulosa* L. (Maire)	**Brassicaceae**	–44	
14	*Raphanus raphanistrum* L.	**Brassicaceae**	–48	
15	*Buxus sempervirens* L.	**Buxaceae**	–48	

(continued)

Table 6.5 (continued)

No	Plant name	Plant family	Inhibition (%)	IC_{50} (ug/mL)
16	*Cyathobasis fruticulosa* (Bunge) Aellen (water ext.)	**Chenopodiaceae**	–47	
17	*Cyathobasis fruticulosa* (Bunge) Aellen ($CHCl_3$ ext)	**Chenopodiaceae**	–48	
18	*Cistus salviifolius* L.	**Cistaceae**	-48	
19	*Juniperus excelsa* Bieb. (leaves)	**Cupressaceae**	54	17.7
20	*Ephedra major* Host.	**Ephedraceae**		32.9
21	*Erica arborea* L.	**Ericaceae**	–39	
22	*Rhododendron luteum* Sweet	**Ericaceae**	35	
23	*Euphorbia platyphyllos*	**Euphorbiaceae**	–34	
24	*Genista acanthoclada* D.C.	**Fabaceae**	–42	
25	*Lupinus micranthus* Guss.	**Fabaceae**	–48	
26	*Quercus cerries* L. var. *cerries* L.	**Fagaceae**	–44	
27	*Geranium lanuginosum* Lam.	**Geraniaceae**	45	
28	*Pelargonium odarassimum* Agnew	**Geraniaceae**	34	
29	*Pelargonium zonale* (L.) L'herit	**Geraniaceae**	–53	
30	*Iris pallida* Lam.	**Iridaceae**	–50	
31	*Lavandula cariensis* Boiss.	**Lamiaceae**	–46	
32	*Melissa officinalis* L. ssp. *altissima* (SM.) Arcangeli	**Lamiaceae**	–49	
33	*Phlomis fruticosa* L.	**Lamiaceae**	–53	
34	*Salvia amplexicaulis* Lam. (roots)	**Lamiaceae**	59	21.0
35	*Salvia aucheri* Bentham var. *aucheri* Bentham (roots)	**Lamiaceae**	55	39.6
36	*Salvia bracteata* Banks & Sol. (roots)	**Lamiaceae**	58	38.2
37	*Salvia candidissima* Vahl ssp. *candidissima* Vahl. (roots)	**Lamiaceae**	63	31.9
38	*Salvia cassia* Samuelss. ex. Rech. Fil. (aerial parts)	**Lamiaceae**	64	29.4
39	*Salvia eriophora* Boiss. & Kotschy (aerial parts)	**Lamiaceae**	–	NA
40	*Salvia heldreichiana* Boiss. ex Bentham (roots)	**Lamiaceae**	64	36.0
41	*Salvia hypargeia* Fisch. & Mey. (Acetone root ext) (roots)	**Lamiaceae**	95	15.9
42	*Salvia napifolia* Jacq. (roots)	**Lamiaceae**	65	35.6
43	Salvia pilifera Montbret & Aucher ex Bentham (aerial parts)	**Lamiaceae**	62	33.3
44	*Salvia recognita* Fisch. & Mey.	**Lamiaceae**	85	29.7
45	*Salvia staminea* Montbret & Aucher ex Bentham (MeOH ext. roots)	**Lamiaceae**	–	36.2
46	*Salvia staminea* Montbret & Aucher ex Bentham (CH_2Cl_2 soluble part- roots)	**Lamiaceae**	–	38.8
47	*Salvia syriaca* L.	**Lamiaceae**	57	41.7
48	*Salvia tomentosa* Miller (roots)	**Lamiaceae**	61	36.3
49	*Salvia fruticosa* Miller (=*S. triloba*)	**Lamiaceae**	98	14.1
50	Salvia fruticosa Miller (=*S. triloba*) (CH_2Cl_2 soluble part)	**Lamiaceae**	63	17.2

(continued)

Table 6.5 (continued)

No	Plant name	Plant family	Inhibition (%)	IC_{50} (ug/mL)
51	*Salvia fruticosa* Miller (=*S. triloba*) (water soluble ext)	**Lamiaceae**	38	
52	*Sideritis lycia* L.	**Lamiaceae**	60	16.7
53	*Sideritis niveotomentosa* Hub.-Mor.	**Lamiaceae**	–23	
54	*Laurus nobilis* L. (fruits)	**Lauraceae**	98	17.3
55	*Laurus nobilis* L. (leaves)	**Lauraceae**	38	
56	*Laurus nobilis* L. (flowers)	**Lauraceae**	–41	
57	*Allium subhirsutum* L.	**Liliaceae**	–38	
58	*Asphodelus fistulosus* L.	**Liliaceae**	–43	
59	*Hyacinthus orientalis* L. ssp. *orientalis* L. (leaves)	**Liliaceae**	35	
60	*Ruscus aculeatus* L. var. *aculeatus* L.	**Liliaceae**	49	
61	*Ficus carica* L. ssp. *carica* (All.) Schinz & Thell.	**Moraceae**	28	
62	*Eucalyptus camaldulensis* Dehnh. (fruits)	**Myrtaceae**	91	17.5
63	*Eucalyptus camaldulensis* Dehnh. (fruits) (Hexane soluble part)	**Myrtaceae**	91	17.5
64	*Eucalyptus camaldulensis* Dehnh. (fruits) (CH_2Cl_2 soluble part)	**Myrtaceae**	97	17.2
65	*Eucalyptus camaldulensis* Dehnh. (Aqueous MeOH part) (leaves)	**Myrtaceae**	85	19.3
66	*Forsythia viridissima* Lindl.	**Oleaceae**	–42	
67	*Satureja cuneifolia* Ten.	**Oleaceae**	58	
68	*Olea europea* L.	**Oleaceae**	58	
69	*Passiflora incarnata* L.	**Passifloraceae**	–45	
70	*Platanus orientalis* L.	**Platanaceae**	–44	
71	*Laurencia obtusa* (Huds.) J.V. Lamour	**Rhodomelaceae**	42	
72	*Spireae hypericifolia* L.	**Rosaceae**	–51	
73	*Rosa canina* L. (leaves)	**Rosaceae**	–50	
74	*Rosa canina* L. (fruits)	**Rosaceae**	31	
75	*Galium spurium* L. ssp. spurium L.	**Rubiaceae**	–36	

[a] The studied extracts rather than MeOH extract or/and whole plant are shown in parenthesis

Salvia hypargeia was found to be the most ovarian cytotoxic active plant extract among the screened *Salvia* plants [18]. Isolated abietane diterpenoids have been previously tested against a panel of cancer cell line, through collaborative work with Professor Pezzuto's group [19]. Particularly demethylcryptojaponol, 6-hydroxysalvinolone and taxodione were found to be highly active against A2780 human ovarian cell lines, as observed in Fig. 6.5. It is noteworthy that cryptojaponol was inactive while its natural demethylated analogue demethylcryptojaponol showed the highest activity. In fact, 6-hydroxysalvinolone and taxodione have been previously found to be active against different cancer cell lines [19]. As a result, among investigated *Salvia* species, particularly the diterpenic constituents of *S. hypargeia, S. kronenburgii*, and *S. staminea* showed promising ovarian cytotoxic activity (Table 6.3).

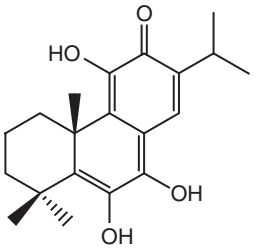

6,7,11-trihydroxy-12-oxo-abieta-5,7,9,13-tetraen
[IC_{50} = 18.8 μg/mL]

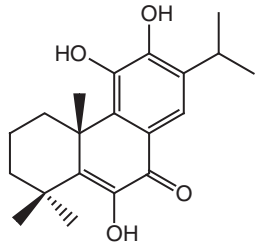

6-hydroxysalvinolone (14-deoxycoleon U)
[IC_{50} = 3.9 μg/mL]

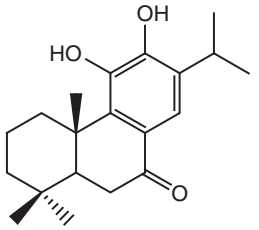

demethylcryptojaponol
[IC_{50} = 1.2 μg/mL]

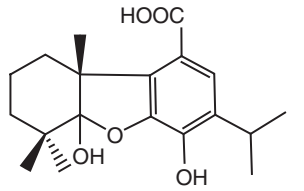

salvicanaric acid
[IC_{50} = 15.0 μg/mL]

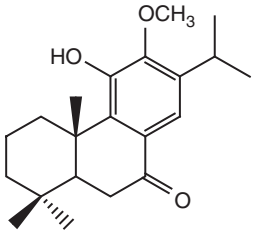

cryptojaponol (**5**)
[IC_{50} = 34.2 μg/mL]

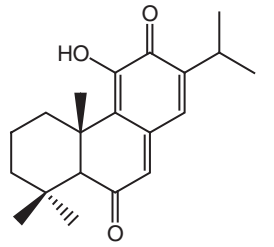

taxodione (**6**)
[IC_{50} = 9.0 μg/mL]

Fig. 6.5 Formulae of the isolated diterpenes from *S. hypargeia* and from some other Salvia species with cytotoxicity against the A2780 cell line

A series *ent*-kaurane diterpenoids isolated from *Sideritis* species were tested against A2780 ovarian cancer cell lines, and 7-*epi*candicandiol (Fig. 6.6) showed the highest cytotoxic potential with IC_{50} = 9.0 μg/mL, and sidol followed it (IC_{50} = 15.6 μg/mL).

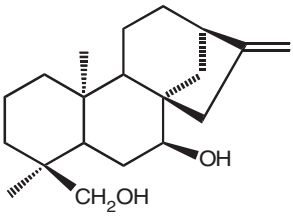

Fig. 6.6 7-Epicandicandiol (IC_{50} = 9.0 μg/Ml)

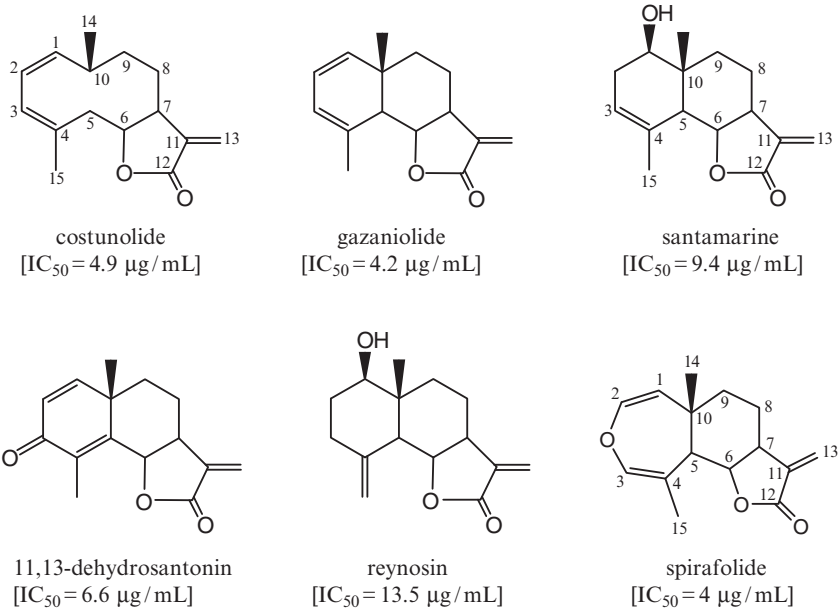

Fig. 6.7 Sesquiterpene lactones isolated from the fruits of *Laurus nobilis* L

Among all screened plant extracts against A2780 human ovarian cell lines, some *Salvia* extracts above mentioned, *Laurus nobilis* fruit extract [20] and *Eucalyptus camaldulensis* extracts showed meaningful activity (Table 6.5). Since the cytotoxicity of these extracts were found to be more active against human ovarian cell lines than the activity against the three yeasts through DNA damaging, the fractionation and then isolation of pure compounds of the extracts were directed to A2780 ovarian cytotoxic activity search [16].

From the fruits' extracts of *L. nobilis*, costunolide, santamarin, reynosin, gazaniolide, 11,13-dehydrosantonin and spirafolide were isolated as known sesquiterpene lactones (Fig. 6.7). The dichloromethane fraction also afforded a new sesquiterpene, named lauroxepine, which had oxepine type sesquiterpene structure as an derivative of spirafolide [20]. However, its activity was the least (IC_{50} = 34.6

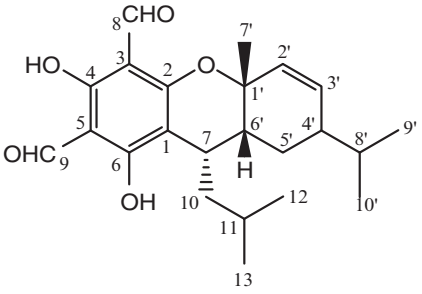

Fig. 6.8 Euglobal Ia_2 (IC_{50} = 11.0 μg/mL)

μg/mL) while its lactone analogue spirafolide (IC_{50} = 4 μg/mL) showed the highest activity. It should be considered that the lack of lactone moiety caused a decrease in the potential cytotoxic activity of the compound.

From *Eucalyptus camaldulensis* Dehnh. hexane and dichloromethane extracts, a series macrocarpals (phloroglucinol derivatives), several triterpenoids and a few sesquiterpenes have been isolated, they almost all showed moderate ovarian cytotoxic activity [21]. Structure elucidation studies on the isolated macrocarpals are going to be completed, Euglobal Ia_2 (Fig. 6.8) appeared as the most abundant macrocarpal in the extract. It has been previously isolated as one of granulation-inhibiting principles of *Eucalyptus globulus* Labill. [22].

Experimental

Bioactivity-Guided Fractionation, Isolation and Purification of the Compounds from Plants

Considering sustainability of the environment, only 100–200 g of each plant was collected in their flowering season, mostly in May–August, and they were dried. Their voucher specimen were deposited in either Herbarium of Faculty of Pharmacy, Anadolu University or deposited in special collection of Dr. Tuncay Dirmenci, Faculty of Art and Sciences, Balıkesir University, Turkey. In general, their direct methanol extracts were prepared by maceration. Occasionally, some plants are treated with dichloromethane or acetone, directly, instead of methanol. After preparation of the extracts, they were screened for their DNA damaging activity potential (Table 6.1). The assays were carried out against three yeasts, namely RS321NYCp50 grown on galactose (YCp50Gal), RS321NpRAD52 grown on galactose (RAD52Gal) and RS321NpRAD52 on glucose (RAD52Glu).

If the crude methanol extracts were found active, they immediately re-collected from the same location in larger amounts. Their methanol extracts were screened once again, and active ones were dissolved in a small volume of MeOH-H_2O (1:1) and partitioned against hexane and then dichloromethane (in some cases, final partition was carried out with either ethylacetate or buthanol).

Chromatographic and Instrumental Analyses

Optical rotations were determined on a Opt. Act. Ltd. AA-5 polarimeter. The IR spectra were recorded on Perkin Elmer 983 (in $CHCl_3$), and UV on a Varian DMS 90 or Shimadzu-1601 spectrophotometers (in MeOH or $CHCl_3$), in general. The NMR (^1H, ^{13}C BB, APT, DEPT, HETCOR, COLOC, HMQC, HMBC) spectra were recorded on either a Bruker 200 MHz or a Varian 400 MHz, or Jeol Eclipse 500 MHz NMR spectrometer and mostly in $CDCl_3$. In some cases, especially some 2D NMR experiments were carried out by using different NMR spectrometers in Turkey or USA (Virginia Polytechnic Institute and State University, Department of Chemistry, NMR Labs). TMS was used as an internal standard and chemical shifts were given as δ (ppm), and the coupling constants (J) were reported as Hz. The mass measurements were carried out either USA or Turkey by using different spectrometers, especially in MRC at TUBİTAK, Gebze. Column chromatography (CC) was carried out on Silica gel (Kieselgel 60, 0063–0.200 mm, Art. 7734, Merck) and Sephadex LH-20 (Pharmacia) filled columns, for flash chromatography Silica gel Merck 660 (230–400 mesh), for preparative TLC, Kieselgel 60 F_{254} (0.5 mm thickness, Art. 5554, Merck) plates were used, and visualized with UV light and sprayed with seric sulphate reagent [serium (IV) sulphate in aqueous methanol] and heated.

DNA Damaging Assay

The yeast based dose response microtiter assay, was carried out according to McBrien et al. [16]. The bioactivity of the samples was evaluated throughout the fractionation using RS321N, pRAD52 and RS321NYCp50 genetically engineered *Saccharomyces cerevisae* yeast strains. Growth inhibition was determined using a microplate assay in which the RS321NpRAD52 strain was seeded individually in minimal media (Difco) plus glucose and galactose (respectively), and RS321NYCp50 was seeded in minimal media plus galactose. Samples were dissolved in 10% DMSO and transferred to the seeded microtiter wells at a 1:10 dilution, for a final testing concentration of 100 μg/mL. Microtiter plates were incubated at 28°C for 48–72 hours, or until an optimum optical density of 0.15–0.25 was reached. Growth inhibition was elucidated using a linear regression analysis of the dose response scheme, and activity was reported in terms of an IC_{50} value, which is the concentration (μg/mL) necessary to produce 50% cell inhibition. Streptonigrin at 0.001 μg/mL and etoposide at 20 μg/mL were both used as positive controls for the RS321NpRAD52 and RS321NYCp50 strains.

A2780 Ovarian Cancer Cytotoxicity Assay

It was carried out according to Schwikkard et al. [9] and Actinomycin D was used as a positive control [16]. Cytotoxicity was determined against A2780 human ovarian cancer cells, using a microtiter plate assay. The plates were seeded with cells and

the compounds (dissolved in 1:1 DMSO:H_2O) were added to the cells at specific concentrations. The plates were incubated at 37°C and 5% CO_2 for 48 hours. Then Alamar Blue (Biosource International) was added to the cells and the plates were incubated for 3 hours. During this time the Alamar Blue is taken up by the live cells and reduced. The reduced form of Alamar Blue is stable and fluorescent. The fluorescence of each well in the plate was measured. The fluorescence is directly proportional to the percent inhibition of the growth of the cells. The IC_{50} value is determined by plotting the data on a dose response curve of percent inhibition versus concentration. The IC_{50} value is defined as the concentration of sample necessary to produce 50% inhibition of the growth of the cells. The smaller the IC_{50} value the more active the compound.

Conclusions

Application of a mechanism-based anticancer bioassay employing DNA repair- or recombination-deficient mutants of the yeast *Saccharomyces cerevisiae* for screening and subsequent bioassay-guided fractionation of bioactive higher plants led to the isolation of a variety of natural products with potential anticancer activity, but with a limited number extracts and compounds, namely *Ajuga postii* extract and its iridoid glycoside reptoside along with *Juniperus excelsa, Laurus nobilis* and *Eucalyptus camaldulensis* and a few *Salvia* extracts including *S. hypargeia, S. kronenburgii, S. staminea, S. triloba*. It can conclude that, this DNA damaging assay may need modification technically to be in place for following up primary screen hits and for selecting extracts as candidates for fractionation, isolation and structure elucidation of active compounds. Among the tested extracts, *Salvia triloba L.* and *Chenopodium murale* L. methanol extracts showed high inhibition percentages, almost 100% against all the three yeasts (over 98%) indicating that both plant extracts are promising antifungal agents, and additional tests are necessary to prove this action. Their fractionation and isolation studies are initiated, but have not been yet completed. Besides the DNA damaging microtiter assay, the extracts were subjected to screen of their ovarian cytotoxic activity. Interestingly, only several extracts were found to be active in both tests and most of them didn't showed any meaningful DNA damaging activity, therefore the phenomenone of this assay is reconsidered and might be modified. A2780 human ovarian cytotoxicity assays resulted in finding more than 15 active compounds, the most active ones being two abietane diterpenes demethylcryptojaponol and 6-hydroxysalvinolone (=14-deoxycoleon U) and a few sesquiterpene lactones spirafolide, costunolide and gazaniolide.

Acknowledgements This study was supported by the NSF/TUBITAK with a project "*Bioactive Turkish Plant Constituents*" (INT-002071/TBAG-U53) (Co-directors; DGI Kingston and G Topcu). The authors also thank to Mrs. Jeanine Hoch and Mrs. Jennifer K. Schilling for their technical assistance in bioassays.

References

1. Verpoorte, R., 1998, *Drug Discovery Today,* **3,** 232–238.
2. Kinghorn, A.D. and Balandrin, M.F. (eds), 1992, ACS Symposium Series 534, *Human Medicinal Agents from Plants*, San Franscisco, CA, American Chemical Society, Washington, DC, pp 191–204.
3. Akman, Y. and Ketenoğlu, O., 1986, The Climate and Vegetation of Turkey. In *Proceedings of the Royal Society of Edinburgh*, Section B, Biological Sciences, I.C. Hedge (ed), 89, pp 123–134.
4. Davis, P.H., 1965–1985, *Flora of Turkey and the East Aegean Islands*, University Press, Edinburgh, Vols 1–9.
5. Davis, P.H., Mill, R.R. and Tan, K. (eds), 1988, *Flora of Turkey and the East Aegean Islands*, (Supplement), University Press, Edinburgh, Vol 10.
6. Güner, A., Özhatay, N., Ekim, T. and Başer, K.H.C. (eds), 2001, *Flora of Turkey and the East Aegean Islands*, (Supplement 2), University Press, Edinburgh, Vol 11.
7. Baser, K.H.C., 2002, *Pure Appl. Chem.,* **74** (4), 527–545.
8. Johnson, R.K., Bartus, H.F., Hofmann, G.A., Bartus, J.O., Mong, S.-M., Faucette, L.F., McCabe, F.L., Chan, A. and Mirabelli, C.K., 1986, In Vitro and In Vivo Models for Detection of New Antitumor Drugs. In *Organizing Committee of the 14th International Congress of Chemotherapy*, L.J. Hanka, T.Kondo, and R. J. White (eds), Kyoto, Japan, pp 15–26.
9. Schwikkard, S., Zhou, B.N., Glass, T.E., Sharp, J.L., Mattern, M.R., Johnsson, R.K. and Kingston, D.G.I., 2000, *J. Nat. Prod.,* **63,** 457–460.
10. Gören, A.C., Zhou, B.N., Topcu, G., Kökdil, G. and Kingston, D.G.I. 2005, *Nat. Prod., Res.* **19,** 457–460.
11. Topçu, G., Kökdil, G., Türkmen, Z., Voelter, W., Adou, E. and Kingston, D.G.I., 2004, *Zeitschrift für Naturforschung,* **59b,** 584–588.
12. Bahçeevli, A.K., Kurucu, S., Kolak, U., Topçu, G., Adou, E. and Kingston, D.G.I., 2005, *J. Nat. Prod.,* **68,** 956–958.
13. Topçu, G., 2006, *J. Nat. Prod.,* **69,** 482–487.
14. Topçu, G. and Ulubelen, A., 1999, *J. Nat. Prod.,* **62,** 1605–1608.
15. Topcu, G.,Türkmen, Z., Schilling, J.K. and Kingston, D.G.I., 2004, *J. Nat. Prod.,* **67,** 118–121.
16. McBrien, K.D., Berry, R.L, Lowe, S.E., Neddermann, K.M., Bursuker, I., Huang, S., Klohr, S.E. and Leet, J.E., 1995, *J. Antibiot.,* **48,** 1446–1452.
17. Topcu, G., Altiner, E.A., Gozcü, S., Halfon, B., Pezzuto, J.M. and Kingston, D.G.I., 2003, *Planta Med.,* **69,** 464–467.
18. Ulubelen, A., Topçu, G., Chai, H.B. and Pezzuto, J.M., 1999, *Pharm. Biol.* **37,** 148–151.
19. Topcu, G., Türkmen, Z., Schilling, J.K., Kingston, D.G.I., Pezzuto, J.M. and Ulubelen, A., 2008. *Pharm. Biol.,* **46,** 180–184.
20. Barla, A., Topçu, G., Öksüz, S., Tümen, G. and Kingston, D.G.I., 2007, *Food Chem.,* **104,** 1478–1484.
21. Topcu, G., Turkmen, Z. Yapar, G. and Kingston, D.G.I., *J. Agric. Food Chem*. (submitted).
22. Kozuka, M., Sawada, T., Kasahara, F., Mizuta, E., Amano, T., Komiya, T. Goto, M., 1982, *Chem. Pharm. Bull.,* **30,** 1952–1963.

Chapter 7
Chamomile Biodiversity of the Essential Oil Qualitative-Quantitative Characteristics

Ivan Salamon

Abstract Biosynthesis of the special metabolite in ecological system is presented the unique and specific metabolite process, which is placed under general biomass production periodicity of plant. Each plant species has own specific limiting boundaries. There are presented its tolerance to influence of eco-physiological conditions. Extend of this tolerance is called the species ecological amplitude. Chamomile plants, *Matricaria recutita* L., have very wide ecological amplitude and this species geographical occurrence in practical all over the world. Plant habitat and the creation of secondary metabolites in plants are depended on the endogenous and exogenous factors, which can be divided in two groups: (a) morpho-ontogenetic variability, (b) genetic variability respectively genetic determination [1]. In chamomile plant habitat (diploid) is not possible to determinate any principal differences among plants. Impulse for the totally new valuation of the research and development has become if the identification of four chief chemical types of chamomile different by the qualitative – quantitative composition of chemical compounds (sesquiterpenes) in the essential oil was carried out [2]. This very important fact was referred to chamomile biodiversity. This biodiversity was created during long time process (evolution) in regard to influence of eco-physiological conditions (biotic- and abiotic- factors) on the concrete place of chamomile population growth. Contribution presents the results of the chamomile essential oil qualitative-quantitative characteristics of chemo types which are originated from various geographical parts of the world (Slovakia, Ukraine, Poland, Egypt, Malta and Crimea). Nowadays the centre of attention is being devoted to cultivation, breeding (tetraploid plants) and seed production of this special crop [3].

Keywords Biodiversity, **/-/-**α-bisabolol, **/-/-**α-bisabololoxide A and B, chamazulene, chamomile, chemo types, essential oil, sesquiterpenes

Department of Ecology, Faculty of Humanities and Natural Sciences, Presov University, 01, 17th November Street, 081 16 Presov, Slovakia

B. Sener (ed.), *Innovations in Chemical Biology*, doi: 10.1007/978-14020-69550

Introduction

Chamomile, *Matricaria recutita* L., is generally known as a weed – a weed with curative power. A medicinal plant, with a history going back to the time of Egyptian pharaohs, is used in phytotherapy today and unequivocally will be used tomorrow.

Chamomile is the most favorite and most used medicinal plant species in Slovakia. A very old folk saying in Slovakia says: "*An individual should always bow before the curative powers of the chamomile flower tea*". This respect resulted from hundreds of years experience in using it as a cure in folk medicine in this country.

About 120 chemical constituents have been identified in chamomile as secondary metabolites, including 28 terpenoids, 36 flavonoids and 52 additional compounds [4]. A substantial part of drug effects are determined by the essential oil content. Oil is collected from flower heads, either by steam distillation or solvent extraction, for yields of 0.24–1.90% of fresh or dry plant tissue. Among the essential oil constituents the most active are /-/-α-bisabolol and chamazulene. /-/-α-bisabolol has demonstrated anti-inflammatory, antispasmodic, antimicrobial, antiulcer, sedative and CNS activity. Chamazulene is also anti-inflammatory. Topical applications of chamomile preparation have shown benefit in the treatment of eczema, dermatitis and ulceration [5].

Material and Methods

Plants. Plant material, chamomile anthodia (42 different samples), was collected from natural sites (together 30 localities) in the East-Slovakian Lowland during four years (1995, 1996, 1997 and 1998). The dry flower heads were obtained from additional localities (Ukraine, Poland, Egypt, and Malta abroad Crimea) abroad in 1995, 1997, 1998, 2002, 2004 and 2005.

Flower chamomile drug (*Chamomilae Flos*) were dried in shielded room under laboratory standard temperature.

Steam distillation. Chamomile essential oil was isolated by steam distillation. Hydro distillation lasted for 2 h into n-hexane, sample weights were 2 g of dry drug matter. The modified distillation apparatus by Coocking and Middleton was used [6].

Chromatography. Compounds of essential oil were determined by the means HEWLETT –PACKARD 5890 Series II system, with capillary column HP–5, FID detector, Split-split less system for injection and automatic injector HP 7673.

The operating conditions were: injection temperature 150°C, detector temperature 250°C, carrier gas nitrogen. Sample sizes were used 1.0 μl and manual type of injection.

Composition of Chamomile essential oil was determined by capillary GC analysis: Hewlett-Packard 5890 Series II with FID and Split-split less system for injection. The column was used HP-5 (50 m long x 0.20 mm i.d.). The following temperature program was used: 90°C (0 min), then 10°C min^{-1}–150°C (5 min), then 5°C min^{-1}–180°C (3 min), then 7°C min^{-1} to finally isothermal 280°C for 25 min; nitrogen was

used as carrier gas. Detector temperature 250°C, carrier gas nitrogen (flow velocity 274 mm s^{-1}), auxiliary gases were nitrogen (30 ml min^{-1}), hydrogen (30 ml min^{-1}), air (400 ml min^{-1}).

Peak areas and retention times were measured by electronic integration with a Hewlett-Packard 3396 Series II integrator.

Compound identification. Determination of major components of essential oil was realized on the basis of use of standard compounds (/-/-α-bisabolol, chamazulene, cis-/trans-en-in-dicycloether and /-/-α-bisabololoxide A and B). Qualitative identification of selected components was carried out by the comparison the retention times of all detected components with retention time of standard compounds.

Results are presented in the percentage. Percentage of single chromatographic peak areas was measured on the basis of area of the single peaks to the total peak area ratio. Selected results were statistically evaluated using a t-test at the 0.05 level. The intervals of significance are presented in tables.

Results and Discussion

In a natural ecosystem, plant species separated on the basis of their secondary product contribute to the development or modification of the existing ecological balance. However, for a full understanding of their production processes, a detail analysis of the occurrences, and the possible exact circumscription of their role in the phytocenosis, as revealed by studies on geographical distribution of the secondary products, is required [7].

One part of production of the Slovak chamomile is collecting of the free growing plants originated approximately till the half of the 1950s, when large-scale cultivation began to be introduced. Chamomile can be found in the secondary plant communities in the East-Slovakian Lowland, such as trodden societies on dry and moist soils, weed and dump societies. There was large – scale monitoring of chamomile gene pool realized from the species identification of wild – grown population chemo types in 1995–1998 in the East Slovakian Lowland.

The percentage of essential oil content in dry chamomile flower-heads and its qualitative and quantitative characteristics, which were determined by the GC-analysis are presented in comprehensive Table 7.1. Percentage contents of the essential oil from chamomile flower anthodia were ranging 0.63 ± 0.19 over the whole examined samples.

Table 7.1 presents essential oil composition of dry chamomile flowers from individual natural sites and years of their collection in the East-Slovakian Lowland.

The highest contents of /-/-α-bisabololoxide A (39.9 ± 7.5%) and /-/-α-bisabololoxide B (9.75 ± 4.20%) are typical for chamomile plants, which flower anthodia were collected in various places in the East-Slovakian Lowland. In regard to following sesquiterpenes, the chamomile anthodia contain /-/-α-bisabolol (5.09 ± 1.55%) and chamazulene (7.65 ± 3.90%).

Chamomile widely spread in the Ukrainian Carpathians, is a popularly known medicinal herb. In nature, it is predominantly found in fields, meadows, gardens, along the roads growing as weeds, and sometimes forming dense stands. This

Table 7.1 Essential oil content and its composition of dry chamomile flowers from natural sites in the East-Slovakian Lowland

Localities on the East-Slovakian Lowland	Essential	Basic composition of essential oil (%)			
	Oil (%)	Fa	Bo	Ch	BoA
Michalovce (‘95,’96,’97,’98)	0.55–0.91	1.2–6.1	2.6–6.8	6.3–7.5	28.9–40.4
Vojany (‘95, ‘96, ‘97, ‘98)	0.40–0.71	5.3–10.5	3.4–6.1	5.0–9.1	39.8–48.4
Vysoká n/Uhom (‘95, ‘96, ‘97)	0.75–0.96	8.1–13.2	4.4–6.8	4.4–10.1	38.5–48.9
Vybuchanec (‘95, ‘96)	0.52–0.97	6.0–6.1	6,6–6,7	5.4–5.5	43.1–43.6
Trebišov (‘96,’97)	0.50–0.60	11.7–13.6	2.9–3.0	10.1–10.2	36.1–42.5
Veľké Raškovce (‘97,’98)	0.65–0.70	4.2–18.0	3.2–3.5	6.9–10.1	33.1–37.8
Krišovská Liesková (‘96,’98)	0.53–0.90	4.0–12.2	2.5–6.6	3.8–4.0	36.7–42.2
Bajany (‘95, ‘98)	0.60–0.74	1.5–3.2	3.8–5.1	4.7–7.4	32.8–52.9
Nižný Hrabovec (‘95)	0.61	3.8	4.9	10.8	34.6
Vranov nad Topľou (‘95)	0.82	4.1	5.2	7.6	48.3
Moravany (‘95)	0.93	4.6	9.6	9.9	37.9
Sírnik (‘95)	0.86	4.0	6.2	10.6	40.0
Malé Raškovce (‘96)	0.63	9.9	4.8	10.2	36.2
Rakovec nad Ondavou (‘96)	0.92	8.0	5.0	11.0	42.3
Čierne Pole (‘96)	0.72	8.3	4.5	9.8	43.8
Tibava (‘96)	0.85	12.6	5.1	9.0	36.8
Stretava (‘96)	0.60	2.9	7.7	10.8	45.6
Beša (‘96)	0.62	7.4	6.0	8.3	45.3
Veľké Kapušany (‘96)	0.55	7.9	6.9	6.9	48.7
Zálužice (‘97)	0.75	15.5	5.2	4.4	33.9
Pavlovce nad Uhom (‘97)	0.60	15.2	6.8	6.3	41.6
Pozdišovce (‘97)	0.30	17.2	6.8	5.8	26.6
Bracovce (‘97)	0.74	16.1	4.7	6.9	36.2
Malčice (‘97)	0.82	15.9	2.4	8.9	30.2
Trhovište (‘97)	0.90	15.7	5.1	6.2	38.6
Vojčice (‘98)	0.97	2.10	5,1	7.6	42.8
Novosad (‘98)	0.70	1.5	4.0	12.0	39.9
Hraň (‘98)	0.60	2.9	5.5	9.5	35.8
Zemplínska Branč (‘98)	0.50	0.4	3.2	7.7	49.2

Fa – farnesene, Bo – /-/-α-bisabolol, Ch – chamazulene, BoA – /-/-α-bisabololoxide A

plant species grows very frequently at abandoned disposal tips, from where the local population usually collects it for medicinal purposes. In Transcarpathia, it comes into flower in the 20th of May – beginning of June; mass flowering and, consequently, bulk collection takes place in the 1st half of June.

Flowers have a highest /-/-α-bisabololoxide A content, about 41% (Table 7.2). The pharmaceutically effective components (/-/-α-bisabolol and chamazulene) have a lower representation.

Chamomile has long been one of the very important medicinal plants collected and cultivated in Poland. A comparison of essential oil yields from the four Polish samples indicates the lowest essential oil content, about 0.3%, in the chamomile

Table 7.2 Quality of essential oil from the chamomile population in Transcarpathia region

Beregovo Rajon (locality, 2005)	Fa	BoB	BnA	Bo	Ch	BoA	Dc	
	% in essential oil						-cis	-trans
Velikaja Bakta	2.9	13.4	6.1	7.5	10.3	41.5	7.3	2.2

Fa – trans-β-farnesene, BoB – /-/-α-bisabololoxide B, BnA – /-/-α-bisabolonoxide A, Bo – /-/-α- bisabolol, Ch – chamazulene, BoA – /-/-α-bisabololoxide A, Dc – en-in-dicycloethers

Table 7.3 Contents (%) of main components in chamomile anthodia from Poland

Composition of essential oil (%)	Areas near Lublin (Poland, 2004)			
	Sample no. 1	Sample no. 2	Sample no. 3	Sample no. 4
/-/-α-bisabolol	17 ± 1	20 ± 2	17 ± 1	18 ± 1
Chamazulene	15 ± 1	16 ± 2	15 ± 1	17 ± 1
/-/-α-bisabololoxide A	15 ± 1	16 ± 2	15 ± 2	17 ± 1
/-/-α-bisabololoxide B	25 ± 2	28 ± 2	23 ± 2	27 ± 2
En-in-dicycloethers	3 ± 0.5	2 ± 0.5	2.5 ± 0.5	1,5 ± 0.5
β-farnesene	10 ± 1	10 ± 1	10 ± 1	10 ± 1

Table 7.4 Quality of essential oil from the Egyptian chamomile cultivation (1997/1998)

Egyptian localities	Fa	BoB	BnA	Bo	Ch	BoA	Dc	
	% in essential oil						-cis	-trans
El Fayoum	18.2	4.9	9.8	5.5	2.0	40.1	9.7	1.3
Beni Suef	5.1	2.7	8.7	2.4	1.7	50.7	8.7	1.5
El Tahrir Sahra	3.5	2.4	7.3	11.2	2.0	51.1	5.9	2.1
El Giza	2.4	1.6	2.7	3.6	2.6	68.2	7.6	1.8

Fa – trans-β-farnesene, BoB – /-/-α- bisabololoxide B, BnA – /-/-α-bisabolonoxide A, Bo – /-/-α- bisabolol, Ch – chamazulene, BoA – /-/-α-bisabololoxide A, Dc – en-in-dicycloethers

tubular flowers. One of the reasons is certainly ontogenetically stage of flower development. The flower heads were in full bloom with a beginning of seed creation. The high content of /-/- α-bisabololoxide B and A is characteristic to the Polish chamomile samples (Table 7.3). The higher part of chamazulene among other components is given a value for this raw material. The high content of chamazulene in the essential oil (15–20%) was presented by Seidler-Lozykowska [8].

One from very important exporter in the world of the chamomile flowers is Egypt. The possibility to visit some chamomile production areas in this African country occured several times in 1997 and 1998. Chamomile flowers from different Egyptian areas have a highest /-/-α-bisabololoxide content, from 40.1% to 68.2% (Table 7.4). The pharmaceutically effective components (/-/-α-bisabolol and

chamazulene) have very low representation. It is great pity that a cultivar or variety with the high content of bisabolol and chamazulene has not been yet introduced and a claim "for the future it is important to use selected seeds that yield flowers with a high percentage of azule" [9] remains in force a very long time.

In regard to the sesquiterpenes, original forms mostly show bisabololoxides. A form rich in /-/-α-bisabolol could be found in Spain /Catalonia/. The first time this proclamation was given was in 1973 [10], much earlier. Unfortunately the sufficient documentation material or scientific paper is not enduring. It is not suitable to comment at this time. The endemically, local and isolate chamomile population could be a type rich in /-/-α-bisabolol. The evidence is presented in Table 7.5. The chamomile genetically investigations are clear: /-/-α-bisabolol is inherited recessively and the formation of /-/-α-bisabololoxide A and B is dominant over one [11].

Impulse for the valuation of the chamomile collection has become if the identification of four chemical types of this plant species different by the qualitative – quantitative composition of chemical compounds in the essential oil was carried out by Schilcher in 1987 (Table 7.6). This very important fact was referred to chamomile biodiversity. This biodiversity was created during long time process (evolution) in regard to influence of eco-physiological conditions (biotic- and abiotic-factors) on the concrete place of chamomile population growth.

The results of qualitative-quantitative characteristics of chamomile essential oil from Slovakia, Ukraine and Egypt are showed there is the chemo type B of chamomile population. The results of two chamomile essential oil samples without any

Table 7.5 The /-/-α- bisabolol chamomile from two European Isles

	Fa	BoB	BnA	Bo	Ch	BoA	Dc	
	% in essential oil						-cis	-trans
Malta/1995/	6.3	1.1	Trace	67.3	0.9	1.1	8.8	1.3
Crimea/2002/	4.3	1.2	Trace	68.6	1.8	1.2	7.9	1.7

Fa – Trans-α-farnesene, BoB – /-/-α-bisabololoxide B, BnA – /-/-α-bisabolonoxide A, Bo – /-/- - bisabolol, Ch – chamazulene, BoA – /-/-α-bisabololoxide A, Dc – en-in-dicycloethers

Table 7.6 Four basic chemotypes of chamomile in regard to composition of main components (%) in essential oil [12]

	Type A	Type B	Type C	Type D
α-bisabololoxide A	4.74–15.68	31.07–52.25	2.13–18.50	9.62–25.83
α-bisabolol	4.37–15.41	8.81–12.92	24.18–77.21	8.49–19.58
α-bisabololoxide B	22.43–58.85	5.27–8.79	3.17–34.46	10.43–24.20
En-yn-dicycloethers	2.61–11.27	4.08–9.90	1.92–12.00	5.51–10.68
Chamazulene	2.70–17.69	5.40–7.95	1.45–14.90	1.91–7.89
Type A	α-bisabololoxide B	>α-bisabololoxide A	>α-bisabolol	
Type B	α-bisabololoxide A	>α-bisabololoxide B	>α-bisabolol	
Type C	α-bisabolol	>α-bisabololoxide B	>α-bisabololoxide A	
Type D	α-bisabololoxide B	≈α-bisabololoxide A	≈α-bisabolol	

color are determined the chemo type C on islands: Malta and Crimea. The Polish chamomile belongs to chemo type D.

The chemo type A is typical for chamomile with a high /-/-α-bisabololoxide B content of Argentine origin [13].

This fact was very important in these parts of the world where parts diploid chamomile population characterised by high content of bisabololoxide constituents occurred in large quantities. In regard to this observation began very intensive plant breeding program considering the flower anthodia yield, essential oil production and chamazulene and /-/-α-bisabolol content (an active components with the most precious pharmacological characteristics). Nowadays the centre of attention is being devoted to cultivation, breeding (tetraploid plants) and seed production of this special crop [3].

Chamomile is a very tolerant plant. It grows on areas with different soil and climate characteristics. The plants prefer a light and need intensive sunlight for their growth. They usually have a short vegetation period (90–100 days). Plant habitat is depended on the endogenous and exogenous factors, which can be divided in two groups: (a) morpho-ontogenetic variability, (b) genetic variability respectively genetic determination in order to diploid or tetraploid plants [1]. The evident range of ecological amplitude of chamomile species gives to the chamomile property to adapt to the less sufficient soil-climatic conditions [14]. Morphological variability is very extensive in the chamomile species. The morphological characteristics of chamomile plants are not stable and have direct connection to physio-ecological background of the plant grow. Therefore this plant represents suitable material for the study of variability and morphological variability of features such as plant highness, plant diversity, and biomass production of roots, stems, leaves, flower anthodia and number of the flower anthodia [15].

Conclusions

Chamomile plants, *Matricaria recutita* L., have very wide ecological amplitude. Plant habitat and the creation of secondary metabolites (natural products) in plants are depended on the endogenous and exogenous factors. Impulse for the totally new valuation of the chamomile research and development has become if the identification of four chief chemical types of chamomile differences by the qualitative – quantitative composition of chemical compounds in the essential oil was carried out in 1973. This very important fact is referred to chamomile biodiversity. This biodiversity was created during long time process (evolution) in regard to influence of eco-physiological conditions (biotic- and abiotic-factors) on the concrete place of chamomile population grows. Chamomile is a very tolerant plant. The exogenous morphological characteristics of chamomile plants are not stable and have direct connection to physio-ecological background of the plant growth.

References

1. Franz, C.H., 1982, Genetishe, ontogenetische und umweltbedingte Variabilität der Bestandteile des ätherishen Öls von Kamille, *Chamomilla recutita* (L.) Rauschert. In *Atherische Öle-Analytic. Physiologie und Zusammensetzung*, Georg Thieme Verlag, Stuttgart, Germany/New York, pp 214–224.
2. Schilcher, H., 1973, *Planta Medica,* **23,** 132–144.
3. Salamon, I., 2004, *Horticultural Science,* **31**(2), 70–75.
4. Mann, C. and Staba, E.J., 1986, The Chemistry, Pharmacology, and Commercial Formulations of Chamomile. In *Herbs, Spices, and Medicinal Plants: Recent Advances in Botany, Horticulture, and Pharmocology* (L. E. Craker, and J. E. Simon, eds.), Oryx, Phoenix, AZ, Vol. 1, pp 235–280.
5. Morgan, M., 1996, *Modern Phytotherapist,* **3,** 17–19.
6. Humphrey, A.M., 1992, Observation on Essential Oil Distillation in the Laboratory. In *The 23rd International Symposium on Essential Oils: Book of Abstracts*, Ayr, Scotland, OP IV-2.
7. Bernath, J., 1986, Production Ecology of Secondary Plant Products – Accumulation Level of Secondary Plant Products. In *Herbs, Spices, and Medicinal Plants: Recent Advances in Botany, Horticulture, and Pharmocology*, (L. E. Craker, and J. E. Simon, eds.), Oryx, Phoenix, AZ, Vol. 1, pp 180–234.
8. Seidler-Lozykowska, K., 2007, *Acta Horticulturae* **749**, 111–115.
9. Fahmi, T., 2005, Cultivation Experiences in Egypt. In *Chamomile – Industrial Profiles* (R. Franke and H. Schilcher, eds.), CRC Press, Taylor & Francis Group, Boca Raton, London, New York, Singapore, pp 156–162, ISBN 0-415-33463-2.
10. Karmazin, M. and Tyl, M., 1973, Breeding of Chamomile in Czechoslovakia. Proceedings of Chamomile Symposium, Lednice, Czechoslovakia, pp 23–27.
11. Horn, W., Franz, C.H., and Wickel, I., 1988, *Plant Breeding,* **101,** 307–312.
12. Lawrence, B.M., 1986, A Review of World Production of Essential Oils. In *Newsletter of Medicinal and Aromatic Plants* **2,** pp 66–69.
13. Honcariv, R. and Repcak, M., 1979, *Herba Polonica,* **25,** 261–267.
14. Doviak, V. and Andraščík, M., 1986, *Poľnohospodárstvo,* **32,** 330–342.
15. Salamon, I., 1998, *Acta Academiae Agriculturae Ac Technicae Olstenensis,* **66,** 273–278.

Chapter 8
Recent Progress on Bioactivity Studies on Turkish *Lycopodium clavatum L.*

Ilkay Orhan and Bilge Şener

Abstract In the current presentation, our latest results performed on *Lycopodium clavatum* L. the most common species in Turkey, are given in terms of biological activity, which include antibacterial, antifungal, antiviral, cytotoxic, antioxidant, anti-inflammatory and immunomodulatory activities of this fern. Antioxidant activity of the plant was assessed on the basis of the radical scavenging effect of the stable 1,1-diphenyl-2-picrylhydrazyl radical (DPPH) using ELISA microplate reader. However, all of the extracts had insignificant antiradical effect towards DPPH. For determination of antibacterial activity, standard and the isolated strains of a number of bacteria along with standard strains of *Candida albicans*, and *C. parapsilosis* for determination of antifungal activity were employed. All of the extracts possessed noteworthy activity against ATCC strain of *Streptomyces aureus* (4 μg/ml), while the LC extracts showed reasonable antifungal effect. In order to establish the antiviral activity, *Herpes simplex virus* (HSV) and *Parainfluenza*-3 *virus* (PI-3) were used and maximum cytopathogenic effect (CPE) concentrations as the indicator of antiviral activity of the LC extracts were determined. However, we found out that only the chloroform extract was active against HSV (16–8 μg/ml), while the petroleum ether and the alkaloid extracts inhibited potently PI-3 (16–4 μg/ml and 32–4 μg/ml, respectively). Moreover, anti-inflammatory potential of the plant was determined using acetic acid-induced increase in capillary permeability assessment in mice and the chloroform extract and the alkaloid fraction displayed marked anti-inflammatory effect at dose of 500 mg/kg. Gas chromatographic-mass spectrophotometric (GC-MS) analysis of the active fraction pointed out to lycopodine (84.5%) as the major component.

Keywords Biological activity, clubmoss, Lycopodiaceae, *Lycopodium clavatum*

Department of Pharmacognosy, Faculty of Pharmacy, Gazi University, 06330, Ankara, Turkey

B. Sener (ed.), *Innovations in Chemical Biology*, doi: 10.1007/978-1-4020-6955-0

Introduction

From ancient to modern history, traditional plant-based medicines have played an important role in health care. Traditional medicine has maintained its popularity in developing countries and has been becoming fashionable in industrialized countries as well. The *Lycopodium* genus (Lycopodiaceae) in Turkey is represented by five species, namely *L. alpinum* L., *L. annotinum* L., *L. clavatum* L., *L. complanatum* ssp. *chamaecyparissus* (A. Br.) Döll, and *L. selago* L. [1].

Among these species, *L. clavatum* L. is the most common one in Anatolia, which has been reported to have a healing effect on wounds and dermatological diseases including rush in babies in Anatolia and, therefore, called "belly powder" [2]. In fact, another species of *Lycopodium*, *L. serratum* (*syn. Huperzia serrata* (Thunb.) Trev.), has been quite reputed in the world for its promising effect against Alzheimer's Disease by inhibiting the enzyme called acetylcholinesterase [3, 4].

On this purpose, we aimed to investigate anti-inflammatory, antioxidant, antibacterial, antifungal, and antiviral properties of petroleum ether, chloroform, ethyl acetate and methanol extracts as well as the alkaloid fraction of *Lycopodium clavatum* L. (LC) from Lycopodiaceae growing in Turkey.

Materials and Methods

Plant Material

The plant material was collected from two different localities in northern Anatolia, firstly from the vicinity of Oymalitepe village, Yomra town, Trabzon at 600 m altitude (coded as LC-T) and secondly from Bagirankaya plataeu, Ikizdere town, Rize at 2,000 m altitude (coded as LC-R) in 2001. The identification of the plant samples was carried out by Dr. Salih Terzioglu from the Department of Forest Botany, Faculty of Forestry, Karadeniz Technical University, Trabzon, Turkey. The voucher specimen (GUE 2216) has been deposited at the Herbarium of the Faculty of Pharmacy of Gazi University, Ankara, Turkey.

Assessment of In Vivo Anti-inflammatory Activity

Effect of the extracts on the increased vascular permeability induced by acetic acid in mice was determined according to Whittle method with some modifications [5]. Each test sample was administered orally to a group of ten mice, which were male Swiss albino mice (20–25 g) were purchased from the animal breeding laboratories of Refik Saydam Central Institute of Health (Ankara, Turkey), in 0.2 ml/20 g body weight. Thirty minutes after the administration each mice was injected with 0.1 ml of 4% Evans blue (Sigma, St. Louis, Missouri, USA) in saline solution (*i.v.*) at the

tail. Then, 10 min after the *i.v.* injection of the dye solution, 0.4 ml of 0.5% (v/v) AcOH was injected *i.p.* After 20 min, the mice were killed by dislocation of the neck, and the viscera were exposed and irrigated with distilled water, which was then poured into 10 ml volumetric flasks through glass wool. Each flask was made up to 10 ml with distilled water, 0.1 ml of 0.1 N NaOH solution was added to the flask, and the absorption of the final solution was measured at 590 nm (Beckmann Dual Spectrometer). In control animals, a mixture of distilled water and 0.5% CMC were given orally, and they were treated in the same manner as described above. Indomethacin (CAS 53-86-1) was used as the reference drug.

Bioassay-Guided Fractionation of the Alkaloid Fraction of LC

The alkaloid extract of LC (LC-alk. – 10.7 g), which has been found to be active in the bioactivity experiment, was firstly applied to silica gel column chromatography eluting with chloroform (100%), followed by the gradient mixtures of chloroform/methanol (95:5, 85:15, 70:30, 60:40, 50:50), and chloroform/methanol/water mixture (50:50:10), which afforded 16 fractions in total and then, classified into 5 subfractions (SGa.1&2, SGa.3–11, SGa.12&13, SGa.14, and SGa.15&16). By Whittle method, SGa.14 and SGa.15&16 were found to be significantly effective (27.3% and 30.3% inhibition, respectively), which led to further fractionation. SGa.14 (0.5 g) was then submitted to Sephadex LH-20 column which yielded ten fractions and three subfractions (LHa.1–6, LHa.7–9, and LHa.10). Among them, LHa.7–9 was found to be active displaying 21.3% inhibition. Sequentially, SGa.15&16 (1.4 g) was also rechromatographied on Sephadex LH-20 which gave 13 fractions and later classified into 3 subfractions as LHb.1–5, LHb.6–8 and LHb.9–13. Out of them, LHb.6–8 (700 mg), which exhibited 27.5% inhibition, was applied on silica gel column eluting with chloroform (100%), followed by gradient mixtures of chloroform:methanol (90:10, 80:20, 75:25, 70:30, 60:40) and finally ethanol (100%). Forty-two fractions, which were later combined into 12 subfractions as SGb.1–4, SGb.5–7, SGb.8, SGb.9–14, SGb.15–23, SGb.24–29, and SGb.39–42, were collected. Among them, SGb.9–14 exerted significant anti-inflammatory activity with 29.7% inhibition. Consequently, LHa.7–9 obtained from SGa.14 and LHb.9–13 gathered from SGa.15&16 were checked by TLC using the solvent system consisting of chloroform/methanol/water (7:3:0.3) and similar components were identified in both subfractions.

Statistical Analysis

Data obtained from animal experiments were expressed as mean standard error (±SEM). Statistical differences between the treatments and the control were evaluated by ANOVA and Students-Newman-Keuls post-hoc tests. $p < 0.05$ was considered to be significant (* $p < 0.05$; ** $p < 0.01$; *** $p < 0.001$).

Conditions of Gas Chromatography-Mass Spectrometry (GC-MS) Analysis

Chromatographic analysis was carried out on Agilent 6890N Network GC system combined with Agilent 5973 Network Mass Selective Detector (GC-MS). The capillary column used was an Agilent 19091N-136 (HP Innowax Capillary; 60.0 m x 0.25 mm x 0.25 μm). Helium was used as carrier gas at a flow rate of 2.4 ml/min for MS and 2.3 ml/min for FID columns with 1 μl injection volume. Samples were analyzed with the column started initially 150°C, then increased to 250°C with 5°C/min heating ramp and kept at 250°C for 15 min. The injection was performed in split mode (20:1). Detector and injector temperatures were 250°C and 250°C, respectively. Run time was 35 min. MS interface temperature was 280°C. MS scan range was (m/z): 15–450 atomic mass units (AMU) under electron impact (EI) ionization (70 eV).

DPPH Free Radical-Scavenging Assay

Antiradical activity of the plant extracts and the reference were assessed on the basis of the radical scavenging effect of the stable 1,1-diphenyl-2-picrylhydrazyl radical (DPPH) free radical [6]. The concentration of DPPH was kept as 300 μM. The extracts and reference were dissolved in DMSO, while the DPPH solution was prepared in ethanol. Ten microliters of each extract and reference was allowed to react with 200 μl of stable free radical DPPH at 37°C for 30 min in a 96-well microtiter plate. After incubation, decrease in absorption for each solution was measured at 515 nm using ELISA microplate reader (Spectra MAX-340 Molecular Devices, USA). The corresponding blank readings were also taken and the remaining DPPH was calculated. Percent radical scavenging activity by samples was determined in comparison with a DMSO treated control group. BHA was used as reference. Inhibition of free radical DPPH in percent (I%) was calculated in following way:

$I\% = (1 - A_{sample}/A_{blank}) \times 100$, where A_{blank} is the absorbance of the control reaction (containing all reagents except the test sample), and A_{sample} is the absorbance of the extracts/reference.

Microbiological Studies

All of the LC extracts were dissolved in ethanol:hexane (1:1) by using 1% Tween 80 solution at a final concentration of 1,024 μg/ml and sterilized by filtration using 0.22 μm Millipore (MA 01730, USA) and used as the stock solutions. Standard antibacterial powders of ampicillin (AMP, Fako), ofloxacin (OFX, Hoechst Marion Roussel), and also standard antifungal powders of ketoconazole (KET, Bilim) and

fluconazole (FLU, Pfizer), were obtained from their respective manufacturers and dissolved in phosphate buffer solution (AMP, pH: 8.0, 0.1 mol/l), DMSO (KET), in water (FLU and OFX). The stock solutions of the agents were prepared in medium according to the NCCLS recommendations [7].

Microorganisms

Standard and the isolated strains of the following bacteria, namely *Escherichia coli* (ATCC 35218), *Pseudomonas aeruginosa* (ATCC 10145), *Proteus mirabilis* (ATCC 7002), *Klebsiella pneumoniae* (RSKK 574), *Acinetobacter baumannii* (RSKK 02026), *Staphylococcus aureus* (ATCC 25923), and *Enterococcus faecalis* (ATCC 29212) for determination of antibacterial activity, along with standard strains of *Candida albicans* (ATCC 10231) and *C. parapsilosis* (ATCC 22019) were used for determination of antifungal activity.

Inoculum Preparation

Mueller-Hinton Broth (Difco) and Mueller-Hinton Agar (Oxoid) were applied for growing and diluting of the bacteria. Sabouraud liquid medium (Oxoid) and Sabouraud dextrose agar (SDA) (Oxoid) were applied for growing and diluting of the fungi. The medium RPMI-1640 with L-glutamine was buffered pH: 7 with 3-[N-morpholino]-propansulfonic acid (MOPS). Prior to the tests, strains of bacteria and fungi were cultured on media and passaged at least twice to ensure purity and viability at 35°C for 24–48 h. Culture suspensions were prepared according to the NCCLS M27-A [11, 12] . The bacterial suspensions used for inoculation were prepared at 10^5 cfu/ml by diluting fresh cultures at McFarland 0.5 density (10^8 cfu/ml). The fungi suspension was prepared by the spectrophotometric method of inoculum preparation at a final culture suspension of 2.5 x 10^3 cfu/ml [8].

Antimicrobial Tests

The microdilution method was employed for antibacterial and antifungal activity tests. Media were placed into each well of the 96 well-microplate. Extract solutions at 1,024 μg/ml were added into first raw of microplates and twofold dilutions of the compounds (512–0.25 μg/ml) were made by dispensing the solutions to the remaining wells. Ten microliters of culture suspensions were inoculated into all the wells. The sealed microplates were incubated at 35°C for 24 and 48 h in humid chamber. The lowest concentration of the extracts that completely inhibit macroscopic growth was determined and minimum inhibitory concentrations (MICs) were

reported. Antimicrobial activity of the oils was tested against two Gram-positive, five Gram-negative bacteria and two yeast-like fungi, using AMP, OFX, KET, and FLU as the standards [8–10].

Cytotoxicity and Antiviral Tests

Cell Line and Growth Condition

African green monkey kidney (Vero cell line) and Madin-Darby bovine kidney (MDBK) used in this study were obtained from Department of Virology, Faculty of Veterinary, Ankara University (Turkey). The culture of the cells was grown in Eagle's Minimal Essential Medium (EMEM) enriched with 10% fetal calf serum (FCS) (Biochrom, Germany), 100 mg/ml of streptomycin and 100 IU/ml of penicillin in a humidified atmosphere of 5% CO_2 at 37°C. The cells were harvested using trypsin solution (Bipco Life Technologies, UK).

Test Viruses

In order to establish the antiviral activity, *Herpes simplex* virus (HSV) and *Parainfluenza*-3 virus (PI-3) were used. The test viruses were obtained from Department of Virology, Faculty of Veterinary, Ankara University (Turkey).

Antiviral Activity

Media (EMEM) were placed into each 96 wells of the microplates (Greiner^R, Germany). Stock solutions of the extracts were added into first raw of microplates and twofold dilutions of the extracts (512–0.25 μg/ml) were made by dispensing the solutions to the remaining wells. Twofold dilutions of each material were obtained according to Log_2 on the microplates. Acyclovir (Biofarma) and oseltamivir (Roche) were used as the references. Strains of HSV and PIV titers were calculated by the Frey and Liess method as $TCID_{50}$ [11]. They were inoculated into all the wells. The sealed microplates were incubated in 5% CO_2 at 37°C for 2 h to detect the possible antiviral activities of the samples. After incubation, 50 μl of the cell suspension of 300,000 cells/ml which were prepared in EMEM + 5% fetal bovine serum was put in each well and the plates were incubated in 5% CO_2 at 37°C for 48 h. After the end of this time, the cells were evaluated using cell culture microscope (X400), comparing with treated-untreated control cultures and with acyclovir and oseltamivir. Consequently, maximum cytopathogenic effect (CPE) concentrations as the indicator of antiviral activities of the extracts were determined [12].

Cytotoxicity

The maximum non-toxic concentration (MNTC) of each sample was determined according to the method described elsewhere based on cellular morphologic alteration [12]. Several concentrations of each sample were placed in contact with confluent cell monolayer and incubated in 5% CO_2 at 37°C for 48 h. MNTC values were determined by comparing treated and controlling untreated cultures.

Results and Discussion

Effects of different fractions obtained from LC after solvent partition of the crude extract on capillary permeability induced by acetic acid in mice are shown in Tables 8.1 and 8.2.

Among the extracts studied, the LC-$CHCl_3$ and LC-alk. (the alkaloid fraction) at 500 mg/kg dose provided 24.3% and 32.1% inhibition, respectively. Successive fractionation of the alkaloid fraction (LC-alk.) by silica gel and Sephadex columns, the best anti-inflammatory effect was observed in three subfractions as LHb.6–8

Table 8.1 Effect of extracts from LC on increased vascular permeability induced by acetic acid in mice

Material	Dose (mg/kg)	Evans blue concentration (μg/ml) ± SEM	Inhibition (%)
Control		9.0396 ± 0.48	
LC-PE	500	7.6667 ± 0.65	15.2
LC-$CHCl_3$	500	6.8445 ± 0.46	**24.3***
LC-$CHCl_3$ –alk.	500	6.1338 ± 0.34	**32.1***
LC-EtOAc	500	6.9618 ± 0.37	22.9
LC-MeOH	500	8.1046 ± 0.68	10.3
Indomethacin	10	5.0041 ± 0.29	**44.6*****

*p ; 0.05; **p ; 0.01; ***p ; 0.001 significant from control

Table 8.2 Effect of subfractions from LC-$CHCl_3$-alk. on increased vascular permeability induced by acetic acid in mice

Material	Dose (mg/kg)	Evans blue concentration (μg/ml) ± SEM	Inhibition (%)
Control		8.3519 ± 0.53	
SGa.14	55	6.0692 ± 0.48	27.3*
SGa.15&16	156.2	5.8217 ± 0.38	30.3*
LHa.7–9	44.78	6.5766 ± 0.04	21.3*
LHb.6–8	196.6	6.0526 ± 0.03	27.5*
SGb.9–14	84.88	5.9184 ± 0.28	29.2*

*p ; 0.05; **p ; 0.01; ***p ; 0.001 significant from control

and LHa.7–9 and the final one coded as SGb.9–14 were checked by TLC and analogous components were identified in these subfractions, which were considered probably to be in charge for the anti-inflammatory activity of the extract (Table 8.2). The prominent components were considered to be alkaloids as they were turned to orange-color on TLC analysis after being exposed to Dragendorff reagent, a specific revelator for alkaloids. GC-MS analysis of the active subfraction that we obtained from the alkaloid fraction of LC demonstrated that lycopodine, an alkaloid isolated from a few *Lycopodium* species, was the major alkaloid (84.5%).

Nevertheless, all of the extracts revealed to exhibit of no consequence antioxidant property against DPPH radical at 0.2 mg/ml with the highest inhibition of 44.1% from LC-$CHCl_3$-Alk, when compared to BHA, whose inhibition was 92.7% (Table 8.3).

Results of the antibacterial and antifungal tests are given in Table 8.4. According to data we obtained from the antibacterial assay, all of the extracts belonging to LC displayed inhibition against each bacterium used at the same MIC values ranging between 4–64 μg/ml, whereas to they were observed to be more susceptible against isolated bacterium strains. The extracts seemed to the most active towards the ATCC strain of *S. aureus* (4 μg/ml), while they showed inhibition against the standard strains of *P. mirabilis*, *K. pneumoniae*, *A. baumannii*, and *E. faecalis*, as well as the isolated strain of *S. aureus* (16 μg/ml).

As for the antifungal tests, LC-$CHCl_3$-Alk, LC-EtOAc, and LC-MeOH inhibited *C. albicans* and *C. parapsilosis* (16 μg/ml) moderately but better than LC-PE and LC-$CHCl_3$ (32 μg/ml) (Table 8.4). On the other hand, LC-$CHCl_3$ extract exerted good antiviral effect towards the DNA virus HSV (16–8 μg/ml) with the MNTC of 16 μg/ml, similar to that of acyclovir (16 to <0.25 μg/ml), except for its therapeutic range of LC-$CHCl_3$ was narrower (Table 8.5). As to PI-3, LC-PE and LC-alk exhibited some inhibition (16–4 and 32–4 μg/ml, respectively). In particular, the alkaloid fraction of LC showed quite similar anti-PI-3 effect and MNTC value to that of oseltamivir (32 to <0.25 μg/ml). Additionally, LC-PE and LC-$CHCl_3$ were more cytotoxic (32 and 16 μg/ml) as compared to the rest of the extracts. However, LC-$CHCl_3$ and LC-EtOAc were rather cytotoxic on Vero cells (8 μg/ml).

Table 8.3 Antioxidant activity of the LC extracts against DPPH radical at 0.2 mg/ml

Extracts	Inhibition (%)
LC-PE	11.3 ± 1.64***
LC-$CHCl_3$	–
LC-$CHCl_3$-Alk	44.1 ± 5.94***
LC-EtOAc	26.6 ± 0.70***
LC-MeOH	30.3 ± 0.15***
BHA	92.7 ± 0.21

–: No activity observed
*p 0.05; **p 0.01; ***p 0.001 Significant from control

Table 8.4 Antibacterial and antifungal activities of the LC extracts as minimum inhibitory concentrations (MICs) (μg/ml)

Microorganisms	*E. coli*		*P. aeruginosa*		*P. mirabilis*		*K. pneumoinae*		*A. baumannii*		*S. aureus*		*E. faecalis*		*C.*	*C.*
extracts	ATCC	Isol.	ATCC	Isol.	ATCC	Isol.	ATCC	Isol.	ATCC	Isol.	ATCC	Isol.	ATCC	Isol.	*albicans*	*parapsilosis*
LC-PE	32	64	32	64	16	32	16	32	16	64	4	16	16	32	32	32
LC-$CHCl_3$	32	64	32	64	16	32	16	32	16	64	4	16	16	32	32	32
LC-$CHCl_3$-Alk	32	64	32	64	16	32	16	32	16	64	4	16	16	32	16	16
LC-EtOAc	32	64	32	64	16	32	16	32	16	64	4	16	16	32	16	16
LC-MeOH	32	64	32	64	16	32	16	32	16	64	4	16	16	32	16	16
AMP[a]	2	64	–	–	2	4	2	4	2	4	<0.12	8	0.5	1	–	–
OFX[b]	0.12	1	1	4	<0.12	1	<0.12	1	0.12	2	0.5	4	1	2	–	–
LVX[c]	<0.12	0.25	1	2	<0.12	1	<0.12	1	0.12	2	0.5	4	0.5	2	–	–
KET[d]	–	–	–	–	–	–	–	–	–	–	–	–	–	–	1	1
FLU[e]	–	–	–	–	–	–	–	–	–	–	–	–	–	–	4	4

[a]AMP: Ampicilline, [b]OFX: Ofloxacine, [c]LVX: Levofloxacine, [d]KET: Ketoconazole, [e]FLU: Fluconazole

–: No activity observed

Table 8.5 Antiviral assessment of the LC extracts against MDBK and Vero cell lines

	MDBK[a] cells (μg/ml)			Vero[b] cells (μg/ml)		
		CPE inhibitory concentration			CPE inhibitory concentration	
		HSV			PI-3	
Extracts	MNTC (μg/ml)	Maximum	Minimum	MNTC (μg/ml)	Maximum	Minimum
LC-PE	32	–	–	16	16	4
LC-$CHCl_3$	16	16	8	8	–	–
LC-$CHCl_3$-Alk	64	–	–	32	32	4
LC-EtOAc	64	–	–	8	–	–
LC-MeOH	64	–	–	64	–	–
Acyclovir	16	16	<0.25	–	–	–
Oseltamivir	–	–	–	32	32	<0.25

[a]MNTC: maximum non-toxic concentration, [b]CPE: cytopathogenic effect

–: No activity observed

Fig. 8.1 Chemical structure of lycopodine

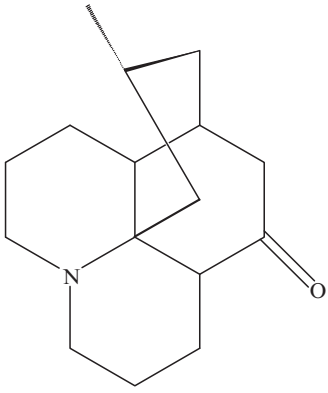

On the other hand, despite of the divergent bioactivities of plant medicines against various diseases, active component(s) of the most plant extracts have not been elucidated well, due to their complex mixtures containing up to hundreds of different ingredients. Amongst them, alkaloids in assorted skeletal types based on pyridine ring system have been presented with striking anti-inflammatory activity. As the *Lycopodium* genus, from which no anti-inflammatory effect have been beforehand reported, is known to contain a number of quinolizidine alkaloids, which have been shown to possess anti-inflammatory activity in several studies [13–15]. Accordingly, these experimental results point out that the anti-inflammatory activity of the alkaloid fraction of the aerial parts of LC are primarily due to the alkaloidal components, which might most probably be lycopodine as the responsible compound (Fig. 8.1).

L. clavatum was formerly reported to contain various phenolic acids such as dihydrocaffeic, vanillic, *p*-hydroxy-benzoic, syringic, *p*-coumaric, and ferulic acids [16] and phenolic acids are known to display antimicrobial activity against a variety of microorganisms [17, 18]. For that reason, the presence of these compounds in this plant may explain their antibacterial activity. In continuation of this study, we investigated the LC-alk extract by gas chromatography-mass spectrometry (GC-MS) in order to elucidate its main alkaloidal constituents of Turkish species of *L. clavatum*. Our GC-MS analysis demonstrated that LC-$CHCl_3$-Alk consisted of lycopodine (*m*/*z* 247, 89.7 ± 0.02%), as the major alkaloid, along with dihydrolycopodine (*m*/*z* 249, 7.6 ± 0.08%), and lycodine (*m*/*z* 242, 2.7 ± 0.09%). Existence of all the three alkaloids were previously reported from *L. clavatum* of different origins, which is in consistence with our data [19].

Conclusions

Plant extracts are known to have a quite complex mixture comprised of structurally diverse components and therefore, high probability of competing or synergistic interactions within the same extract may exist for any biological activity, which leads to a starting point for an activity-guided search for active metabolites. In this case, LC-$CHCl_3$-Alk extract might be considered worthy of advance phytochemical investigation to find out the active component(s) for its antiviral activity, although lycopodine, the major alkaloid, seems to be possibly responsible, which needs to be confirmed. To best of our knowledge, for the first time, we have reported anti-inflammatory, antioxidant, antibacterial, antifungal, and antiviral activities of *L. clavatum* L. and also explaining the alkaloidal content of the Turkish counterpart of the plant [20–21].

Acknowledgements Financial support for this work through the Scientific Research Projects Foundation of Gazi University, Ankara, Turkey is thankfully acknowledged (Project code no: 02/2005-12). Authors would also like to express their sincere thanks to their collaborators; Dr. S.Terzioglu from the Department of Forest Botany, Faculty of Forestry, Karadeniz Technical University, Trabzon, Turkey, Dr. M. Kartal and S. Aslan from Department of Pharmacognosy, Faculty of Pharmacy, Ankara University, Ankara, Turkey, Dr. T. Karaoğlu from Department of Virology, Faculty of Veterinary, Ankara University, Ankara, Turkey, Dr. B. Özçelik Department of Pharmaceutical Microbiology, Faculty of Pharmacy, Gazi University, Ankara, Turkey, Dr. E. Küpeli from Department of Pharmacognosy, Faculty of Pharmacy, Gazi University, Ankara, Turkey, Professor E. Ye ilada from Department of Pharmacognosy, Faculty of Pharmacy, Yeditepe University, Istanbul, Turkey, Professor M.I. Choudhary and Dr. A. Ejaz from H.E.J. Research Institute, University of Karachi, Karachi, Pakistan for the studies on *Lycopodium clavatum*.

References

1. Davis, P.H. and Cullen, J., 1984, *Lycopodium* L. In *Flora of Turkey and the East Aegean Islands* (P.H. Davis, ed), Edinburgh University Press, Edinburgh, volume 1, pp 88–90.

2. Baytop, T., 1999, *Therapy with Medicinal Plants in Turkey (Past and Present),* Nobel Tip Kitabevleri, Istanbul, 2nd edition, p 211.
3. Liu, J.S., Zhu, Y.L., Yu, C.M., Zhou, Y.Z., Han, Y.Y., Wu, F.W. and Qi, B.F., 1986, *Canadian Journal of Chemistry,* **64,** 837–839.
4. Cheng, D.H., Ren, H. and Tang, X.C., 1996, *Neuroreport,* **8,** 97–101.
5. Yeşilada, E., Tanaka, S., Sezik, E. and Tabata, M., 1988, *Journal of Natural Products,* **51,** 504–508.
6. Lee, S.K., Zakaria, H., Chung, H., Luyengi, L., Gamez, E.J.C., Mehta, R.J., Kinghorn, D. and Pezzuto, J.M., 1998, *Combinatorial Chemistry and High Throughput Screening,* **1,** 35–46.
7. National Committee for Clinical Laboratory Standards, 1996, Method for Broth Dilution Antifungal Susceptibility Testing Yeast; Approved Standard, M27-A, 15, 10, NCCLS, VA Medical Center, Tucson, AZ.
8. National Committee for Clinical Laboratory Standards, 2002, Methods for Dilution Antimicrobial Susceptibility Tests Bacteria that Grow Aerobically, 3rd edition, Approved Standard. NCCLS document M100-S12, NCCLS, Wayne, PA.
9. Özçelik, B., Küsmenoglu, Ş., Türköz, S. Abbasoglu, U., 2004a, *Pharmaceutical Biology,* **42,** 526–528.
10. Özçelik, B., Çitak, S., Cesur, S., Abbasoglu, U. and Içli, F., 2004b, *Drug Metabolism and Drug Interaction,* **20,** 1–2, 5–8.
11. Frey, H.R. and Liess, B., 1971, *Journal of Veterinary Medicine Series B,* **18,** 61–71.
12. Özçelik, B., Aslan, M., Orhan, I. and Karaoglu, T., 2005, *Microbiological Research,* **160,** 159–164.
13. Abdel-Halim, O.B., Abdel-Fattah, H., Halim, A.F. and Murakoshi, I., 1997, *Acta Pharmaceutica Hungaria,* **67,** 241–247.
14. Duan, H.Q., Takaishi, Y., Momota, H., Ohmoto, Y., Taki, T., Jia, Y.F. and Li, D., 2001, *Journal of Natural Products,* **64,** 582–587.
15. Lema, W.J., Blakenship, J.W. and Malone, M.H., 1986, *Journal of Ethnopharmacology,* **42,** 161–167.
16. Towers, G.H.N. and Maass, W.S.G., 1965, *Phytochemistry,* **4,** 57–66.
17. Herald, P.J. and Davidson, P.M., 1983, *Journal of Food Science,* **48,** 1378–1379.
18. Stead, D., 1993, *Journal of Applied Bacteriology,* **75,** 135–141.
19. Luan, X.H. and Xu, Z.L., 1986, *Acta Pharmaceutica Sinica,* **21,** 310–317.
20. Orhan, I., Küpeli, E., Şener, B. and Yeşilada, E., 2007, *Journal of Ethnopharmacology,* **109** (1), 146–150.
21. Orhan, I., Özçelik, B., Aslan, S., Kartal, M., Karaoğlu, T., Şener, B., Terzioğlu, S. and Choudhary, M.I., 2007, *Phytochemistry Reviews,* **6***, 189–196.*

Chapter 9
Separation and Characterization of the Vanillin Compound from Soda Lignin

Mohamad Nasir Mohamad Ibrahim[1], M. Y. Nor Nadiah[1], M. S. Norliyana[1], and S. Shuib[2]

Abstract The separation of vanillin from soda lignin that was extracted from black liquor of oil palm empty fruit bunches (EFB) using 20% sulfuric acid is presented in this paper. The degradation of soda lignin using alkaline nitrobenzene oxidation was carried out at 165°C for 3 hours in a 2 M NaOH and nitrobenzene solution. One of the major products obtained from the breakdown of lignin is vanillin. The crystallization process was used as a method to separate vanillin from other compounds. Based on the solubility of vanillin in acetone, 15 mL of acetone was added to the residue of the oxidized products. The mixture was slowly heated to 40–50°C for 15 minutes until the vanillin crystalline precipitated. A yield of about 1.6% vanillin was isolated from 50 mg sample of lignin. The isolated compound was analyzed utilizing high performance liquid chromatography, Fourier transform infrared spectrophotometry (FTIR) and nuclear magnetic resonance (^{1}H-NMR). The results of the characterization studies proved that the isolated compound was vanillin.

Keywords Black liquor, crystallization process, oil palm empty fruit bunches, soda lignin, vanillin

Introduction

The *Elaesis guineensis* or commonly known as the oil palm was introduced to various parts of the tropics for its oil producing fruit. It is estimated that 2.28 million hectares of land is being cultivated with oil palm trees in Malaysia [1]. Besides producing palm oil, the oil palm industry also generates massive amounts of lignocellulosic residues such as trunks, fronds and empty fruit bunches (EFB). EFB has been recognized as potentially being an alternative raw material for the paper and

[1] School of Chemical Sciences, Universiti Sains Malaysia, 11800 Minden, Pulau Pinang, Malaysia

[2] School of Mechanical Engineering USM Engineering Campus, Universiti Sains Malaysia 14300 Nibong Tebal, Pulau Pinang, Malaysia

B. Sener (ed.), *Innovations in Chemical Biology*, doi: 10.1007/978-1-4020-6955-0

pulp industry *[2–4]*. The general objective of this project is to identify a more efficient way of managing the disposal of lignocellulosic residue and at the same time transforming the residue into useful products such as lignin.

The main source of lignin in Malaysia is from abroad where it was originally extracted from pine and acacia trees as a byproduct of the wood and pulp industry. However, this method is less effective due to foreign currency exchange lost in importing foreign product [5]. There is a need to search for alternative sources of lignin that can be derived from waste material and at the same time help to preserve natural treasures for future generations. One such source is the oil palm empty fruit bunch (EFB). This is because large amounts of EFB are collected every day at more than the 300 palm oil processing mills scattered throughout Malaysia.

Lignin is an amorphous polyphenolic material arising from an enzyme-mediated dehydrogenates polymerization of three major phenylpropanoid monomers, which are coniferyl, sinapyl and p-coumaryl alcohol [6]. The lignin structural elements are linked by carbon-carbon and ether bonds to form tri-dimensional network associated with the hemicelluloses polysaccharides inside the cell wall [7]. Lignin is usually insoluble in all solvents and can only be degraded by physical or chemical pulping process at high-temperature and high pressure. The delignification reactions involved the cleavage of non-phenolic β-O-4 linkage, phenolic α-O-4 linkage and releasing from the associated by the polysaccharide *[8*, *9]*.

Due to the high macromolecular complexity of lignin, lignin need to be degraded via the oxidation process to monomers, which have lower molecular weight before they are analyzed. Nitrobenzene oxidation was used as a method to break down the lignin into monomers before identifying them using high performance liquid chromatography (HPLC) analysis.

A previous study [10] reported that eight components were found in degraded lignin. They are vanillin, syringaldehyde, 4-hydroxybenzaldehyde, syringic acid, 4-hydroxybenzoic acid, vanillic acid, p-coumaric acid and ferulic acid. Among these 8 compounds, vanillin was found to be the major component of soda lignin. Vanillin, a major component of vanilla, is widely used as an ingredient in food flavors, in pharmaceuticals and as a fragrance in perfumes and odor-masking products [11].

In this study the percentage of vanillin present in the soda lignin sample will be determined. Next, the vanillin compound will be separated from soda lignin via crystallization technique.

Experimental

Material

The oil palm empty fruit bunches (EFB) raw material in this study was supplied by Sabutek (M) Sdn. Bhd., Teluk Intan, Malaysia, a local company specializing in the recycling of EFB. The black liquor of EFB was supplied by the School of Technological Industry, Universiti Sains Malaysia (USM). This study was conducted

from May 2005 until March 2006 at the School of Chemical Sciences, Universiti Sains Malaysia (USM).

Extraction of Lignin

The pH of the obtained black liquor was 12.45 and its density 1.02 g/mL. The soda lignin was then precipitated from the concentrated black liquor by acidifying it to pH 2 using 20% concentrated sulfuric acid (H_2SO_4). The precipitated lignin was then filtered and washed with water adjusted to pH 2 using H_2SO_4. Then, the soda lignin was dried in a vacuum oven at 55°C for 24 hours prior to further analysis [12].

Nitrobenzene Oxidation

Nitrobenzene oxidation was carried out by adding 50 mg of dry soda lignin into a mixture of 7 mL of 2 M NaOH and 4 mL of nitrobenzene in a 15 mL steel autoclave. Then, the autoclave was heated to 165°C for 3 hours in a preheated thermostat oil bath. After the autoclave was cooled to room temperature, the mixture was then transferred to a liquid-liquid extractor for continuous extraction with chloroform (5 × 20 mL) in order to remove any nitrobenzene reduction product and excess nitrobenzene. The oxidation mixture was then acidified by concentrated HCl to pH 3–4 and further extracted with chloroform (5 × 15 mL). The solvent from the second chloroform solution was then removed using a rotary evaporator at 40°C under reduced pressure in order to obtain the nitrobenzene oxidation mixture. The mixture was then dissolved into dicloromethane and made up to 10 mL. This mixture was then used as a stock solution for high performance liquid chromatography (HPLC) analysis [6].

The nitrobenzene oxidation mixture was analyzed using the HPLC method. 0.2 mL of the stock solution was pipetted into a 25 mL volumetric flask and acetonitril-water (1:2 v/v) was added to it. About 20 µL of the sample solution was next injected into the HPLC system (Shimatzu) equipped with a Hypersil bond C_{18} column (particle size 5 µL, 25 × 4.6 mm i.d.) to quantitatively determine the vanillin component while another component was determined qualitatively. Acetonitril-water (1:8) containing 1% acetic acid was used as an eluent with a flow rate of 2 mL/min. The eluent was then monitored with an UV (ultraviolet) detector at 280 nm [6].

Crystallization Process

The nitrobenzene oxidation product was used in this process [13]. The mixture was dissolved into acetone and made up to 10 mL. Next, the mixture was heated to 60°C for 10 minutes using a hot plate. The precipitate was then filtered and washed using

acetone. Then, the precipitate was analyzed using Fourier transform infra-red (FT-IR), nucleus magnetic resonance (^{1}H-NMR) and high performance liquid chromatography (HPLC).

Results and Discussion

Percentage of Vanillin

The components of lignin obtained are listed in Table 9.1 and labeled alphabetically in Fig. 9.1. The standard solution for each expected component to be present in lignin was injected into three different concentrations, 10, 100 and 1,000 ppm. This was done to ensure that the solution for each similar component at different concentrations had the same retention time. From the HPLC chromatogram, six components were detected in the soda lignin. They are vanillin, syringaldehyde, 4-hydroxybenzaldehyde, 4-hydroxybenzoic acid, vanillic acid and syringic acid. From the analysis we found that the concentration of vanillin in 50 mg lignin is 0.8032 ppm or equivalent to 1.6%. Even though there is only a low percentage of vanillin present in lignin, it is adequate as the research utilize lignin samples from industrial waste, which is black liquor. Moreover, the research is aimed at producing new products from items which are commonly treated as a waste.

Separation process via crystallization technique was used to separate vanillin from other components present in the lignin. The precipitate obtained from this process

Table 9.1 Oxide peak identification in the lignin sample

Peak	Retention time (R_t)	Oxide component
A	≈ 8.750	4-Hydroxybenzoic
B	≈10.383	Vanillic acid
C	≈10.983	Syringic acid
D	≈13.192	4-Hydroxybenzaldehyde
E	≈16.592	Vanillin
F	≈19.883	Syringaldehyde

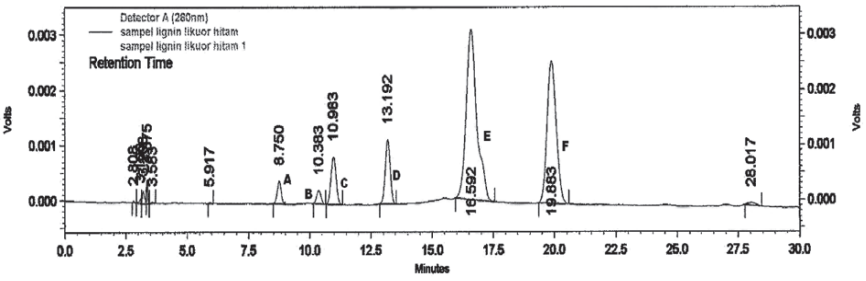

Fig. 9.1 Chromatogram sample of lignin sample

released an odor akin of the same kind to vanillin. Analysis was done in order to determine whether the precipitate obtained was vanillin. This involved the use of infra red (IR) spectrometry analysis in order to determine the functional groups present in the precipitate. This approach was selected as the precipitate easily formed pellets and was not destroyed when IR analysis was performed on it. The peaks formed from the IR analysis were also easier to be traced and observed. Characterization of the functional for the precipitate sample was performed on the 4,000–400 cm^{-1} frequency range.

The IR spectrum clearly shows the characterization of several main functioning groups in the vanillin structure. A typical IR spectrum of precipitate sample from the crystallization process is shown in Fig. 9.2. The strong and broad band at 3,471.25 cm^{-1} is the characteristic of the OH group or the phenolic compound. A part from this, C-H stretching of the aromatic ring was at the 3,230.12 cm^{-1} band. Yet, the frequency does not show a very obvious peak. The band at 1,636.19 cm^{-1} corresponds to that of the carbonyl group (C = O). Stretching bands at 1,399.83cm^{-1} and 1,338.6 cm^{-1} are characteristic of C-H vibration on the methyl group. While the vibration for C = C on the aromatic ring is at 692.77 cm^{-1} band [14]. Figure 9.3 depicts the structure of vanillin (4-hydroxy-3-methoxybenzaldehyde). Thus, the spectrum of precipitate

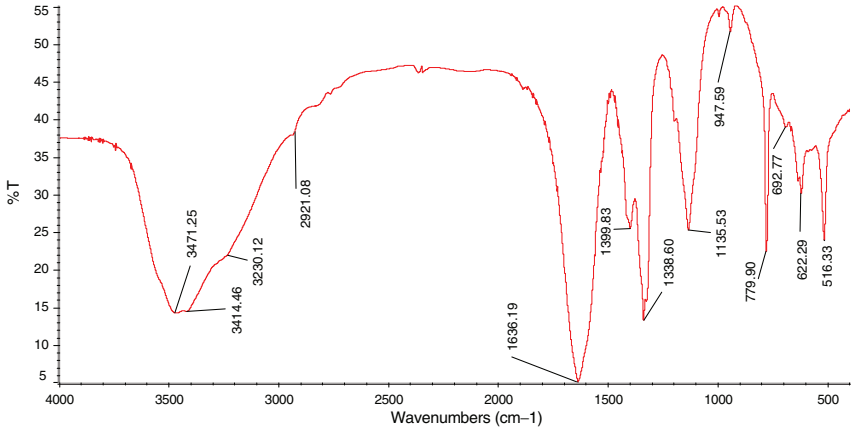

Fig. 9.2 IR spectrum of the precipitate sample (believe to be vanillin) from the crystallization process

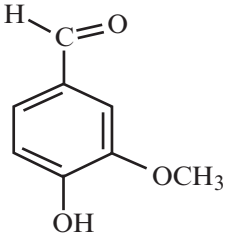

Fig. 9.3 Structure of vanillin

product from crystallization was identified as vanillin as the main functioning groups of the vanillin structure were revealed through the IR analysis.

The precipitate was then analyzed using high performance liquid chromatography (HPLC) to reaffirm the results as characterized by the IR analysis. The precipitate was collected and dissolved in an acetone solution with water (1:2 v/v) acting as the solvent before the analysis was done. Finally, the 1.0 ppm concentrated sample was injected into a HPLC machine. The chromatogram shows a peak at the retention time (R_t) which is almost the same as the retention time of standard vanillin with the same concentration. Figure 9.4 presents the HPLC chromatograms of the vanillin sample and the standard vanillin.

The ^{1}H-FT-NMR spectra were obtained from a Bruker Avance 300 operating in the FT mode at 400 MHz under total proton decoupled conditions. The spectra were recorded at 40°C from 200 mg sample vanillin dissolved in 1 mL $CDCl_3$ after 3,000 scans. A 90° pulse flipping angle, a 26.6 μs pulse width and a 1.74 s acquisition time were employed. There was no significant difference in the structure of vanillin precipitated from crystallization process and standard vanillin based on ^{1}H-NMR analysis (Fig. 9.5). Incomplete dissolution of the sample may because of the unexpected high signal/noise ratio. The peaks show that the chemical shifts for both of vanillins are very similar.

In conclusion, the HPLC, FT-IR and ^{1}H-FT-NMR analyses confirmed that the precipitate obtained via the crystallization process was vanillin.

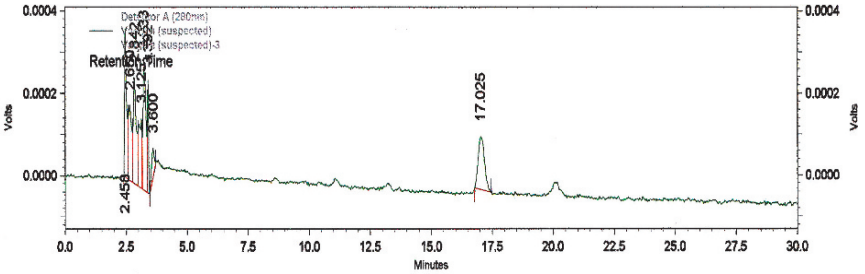

Precipitate from the crystallization process (1 ppm)

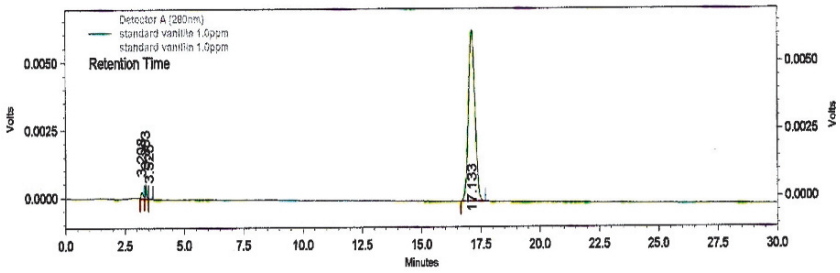

Standard vanillin (1ppm)

Fig. 9.4 The HPLC chromatograms of precipitate from the crystallization process and the standard vanillin (1 ppm)

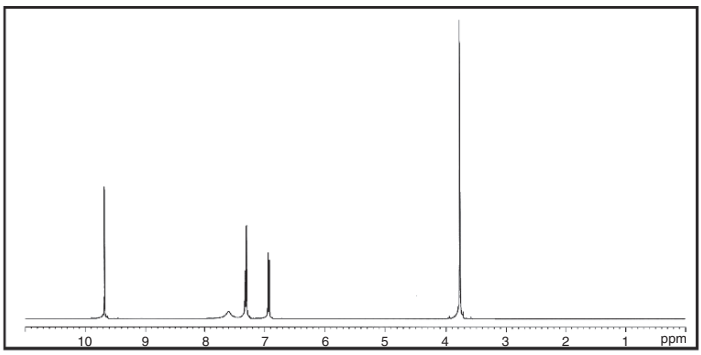

Standard vanillin

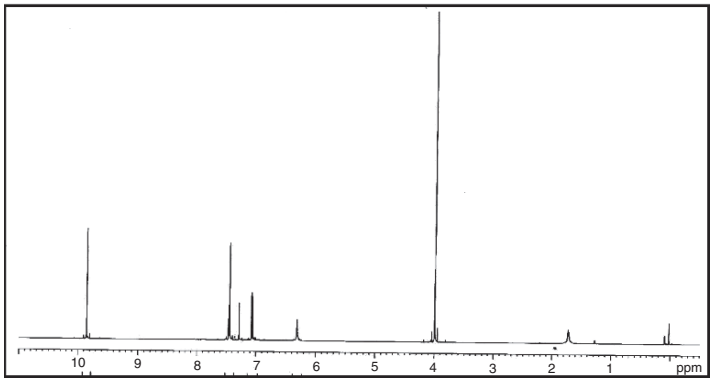

Precipitate from the crystallization process

Fig. 9.5 1H-NMR spectrums for standard vanillin and sample vanillin percipitate from crystallization process

Acknowledgements The authors would like to express their appreciations to Universiti Sains Malaysia and the Malaysian Ministry of Science, Technology and Innovations for providing the financial support for this project through a research grant. The authors would also like to thank Sabutek (M) Sdn. Bhd. for supplying the EFB long fibers.

References

1. Malaysian Palm Oil Board (MPOB), http://www.porim.gov.my (accessed on 24/04/2005).
2. Akamatsu, S., Kobayashi, Y., Kamishima, H., Hassan, K.B., Mohamad Yusof, M.N., Husin, M. and Hassan, A., 1987, *Cellulose Chemistry and Technology,* **21,** 191–197.
3. Khoo, K.C. and Lee, T.W., 1991, *Appita Journal,* **44** (6), 385–388.
4. Wan Rosli, W.D., Law, K.N. and Valade, J.J., 1998, *Cellulose Chemistry and Technology,* **32** (1), 133–143.
5. Mohamad Ibrahim, M.N., Azian, H. and Mohd Yusop, M.R., 2006, *Journal Technology* **44**, 83–94.
6. Stephen, Y.L. and Carlton, W.D., 1992, *Methods in Lignin Chemistry*, 1st Edition, Springer, Berlin/Heidelberg, Germany.

7. Sun, R.C., Thomkinson, J., and James, B., 1999, *Polymer Degradation and Stability,* **68,** 195–200.
8. Gellerstedt, G. and Lindfors, E.L., 1983, *Holzforchung,* **38** (3), 151–158.
9. Groot, B.D., Dam, J.E.G.V., Zwan, R.P.V.D. and Riet, K.V., 2000, *Holzforchung,* **48,** 207–214.
10. Mohamad Ibrahim, M.N., Nor Nadiah, M.Y. and Azian, H., 2006, *Journal of Applied Sciences,* **6** (2), 292–296.
11. Greener Industry, http://www.uyseg.org/greener_industry/pages/vanillin/1vanillin_AP.htm (accessed on 3/12/2005).
12. Mohamad Ibrahim, M.N., Chuah, S.B. and Wan Rosli, W.D., 2004, *AJSTD,* **21** (1), 57–61.
13. Crystallization Theory, http://www.chem.ualberta.ca/…/theory/theory2_02L.html (accessed on 28/02/2006).
14. Robert, M.S. and Francis, X.W., 1998, *Spectrometric Identification of Organic Compounds*, Wiley, New York.

Chapter 10
Recent Development of Ring Closing Metathesis Approach to Bioactive Heterocycles: Synthesis of Nakadomarin A, Quinolines, and Indoles

Masako Nakagawa[1], Mitsuhiro Arisawa[2], and Atsushi Nishida[3]

Abstract Asymmetric total synthesis of marine natural product, nakadomarin A, is described and as further extension, a novel synthesis of quinoline and indole ring system by ring closing metathesis is also described.

Keywords Bioactive heterocycles, indols, nakadomarin A, quinolines

Asymmetric Total Synthesis of (-)-Nakadomarin A Route A [1]

We have been interested in the synthesis of nakadomarin A 1 [2], which belongs to manzamine alkaloids [3] by two different routes (Routes A and B).

We envisioned that if functional group conversions of the key intermediate **1** for manzamine A to the new tricyclic system **2** followed by oxidative cleavage of the double bond could take place, then the resulting dialdehyde most probably undergoes aldol cyclization to form unsaturated aldehyde **3**. From **3** the furan ring could be constructed to give ABCD ring, an advanced key intermediate for nakadomarin A. Subsequent construction of both 8- and 15-membered azacycles could be performed by ring-closing metathesis (RCM) (Scheme 10.1).

The key chiral intermediate **4**, highly functionalized hydroisoquinoline, was obtained by a Diels-Alder reaction between siloxydiene **5** and chiral dienophile **6** which was prepared from *L*-serine [4]. Ruche reduction of enone **4** gave allyl alco-

[1] Department of Chemistry, Faculty of Science, Kanagawa University, Hiratsuka, Kanagawa, 259-1293, Japan

[2]Graduate School of Pharmaceutical Sciences, Hokkaido University, Kita 12, Nishi 6, Kita-ku, Sapporo, 060-0812, Japan

[3]Graduate School of Pharmaceutical Sciences, Chiba University, 1-33 Yayoi – cho, Inage-ku, Chiba, 263-8522, Japan

B. Sener (ed.), Innovations in Chemical Biology, doi: 10.1007/978-14020-69550

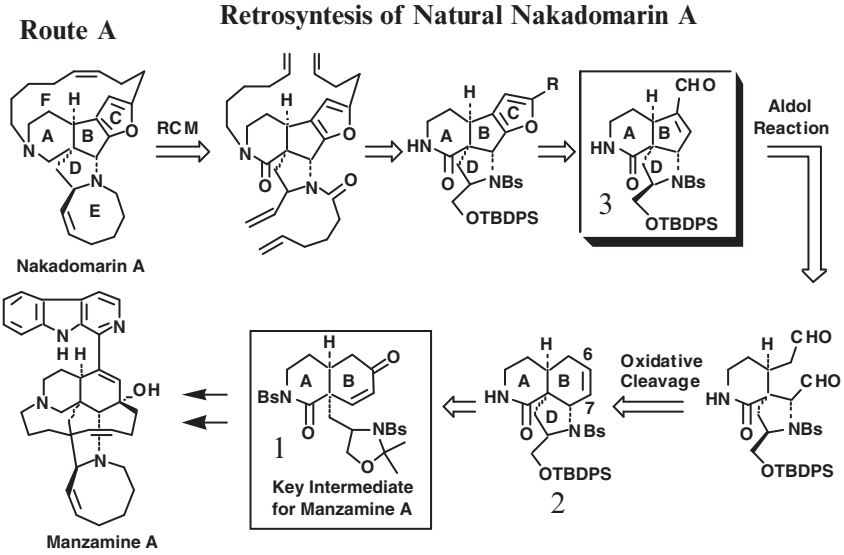

Scheme 10.1 Synthesis of nakadomarin A by Route A

hol **7**. When **7** was treated with 6N HCl, spontaneous cyclization took place to give the desired tricyclic alcohol **8**. The stereochemistry of **8** was unambiguously determined by X-ray crystallographic analysis. Deprotection and protection of **8** gave the key intermediate **9** for the ring cleavage.

Oxidative cleavage of the double bond of **9** with ozone provided the expected dialdehyde which was unstable and readily underwent expected aldol condensation to give the desired aldehyde **10** when treated with ***N***-methylanilinium trifluoroacetate [5].

Wittig reaction of **10** with pentyl phosphonium salt in the presence of NaH gave *Z*-olefin **11** selectively. Dye-sensitized photooxygenation of **11** proceeded exclusively to give the endoperoxides **12a** and **12b** in almost quantitative yield as a roughly 1:1 mixture of two diastereomers.

Both cyclic peroxides **12a** and **12b** transformed successfully into the furan derivative **13** in excellent yield when treated with *t*-BuOK followed by treatment with 6***N*** HCl [6]. Thus, stereoselective construction of chiral ABCD-ring system, the central core system of (-)-nakadomarin A was achieved.

Next step is the construction of 8- and 15-membered ring systems by sequential RCM [7]. Tetracyclic alcohol **13** was converted to **14** by sequential oxidation and Peterson olefination followed by deprotection of the TMS group. After protection of the amine with a Boc group, the imide carbonyl group was

reduced to give **15** by sequential reduction with DIBAH and St_3SiH/BF_3 Et_2O [8]. Deprotection of the benzenesulfonyl group of **15** followed by *N*-acylation with hexenoyl chloride gave dienyne **17**, a precursor for RCM to synthesize the azocine ring. The RCM of **17** was successfully carried out to give azocine lactam **18** when the acetylene group was protected as a Cobalt complex and the second generation Grubbs catalyst was used. On the other hand, the precursor for the final 15-membered azacycle **21** derived from **19** in three steps was subjected to the final RCM and the desired frame work was readily constructed to give dilactam (*Z*)-**21** in 26% yield, together with the (*E*)-isomer. Reduction of (*Z*)-**21** with Red-Al completed the first asymmetric synthesis of (-)-nakadomarin A [1] (Scheme 10.1).

The First Total Synthesis of Nakadomarin A Route B [9]

On the other hand, we also planned alternative completely new approach (Route B) to Nakadomarin A, which involves the spirolactam followed by coupling reaction with furan derivative and subsequent intramolecular electrophilic substitution reaction of an iminium cation generated from an aminal to give highly functionalized tetracyclic core system (Scheme 10.3).

For this purpose, the chiral acid (*R*)-(–)-**22** was chosen as the starting material and converted to the spirolactam **25**. Condensation with benzylamine followed by catalytic dihydroxylation and oxidation gave aldehyde **23**.

Wittig olefination of **23** followed by intramolecular Michael addition with DBU gave the desired spirolactam **25** which was reduced to the alcohol **26** in 54% yield in eight steps from (*R*)-**22**. Deprotection of the ketal **26** with 70% $HClO_4$, followed by protection of **27** with THP gave **28**, which was readily converted to the enol triflate **29**. Suzuki-Miyaura coupling reaction of the enol triflate **29** was carried out with substituted furan-3-boronic ester **30** to gave the highly functionalized spirolactam which was selectively hydrogenated to give **31** as expected from our previous model study [10].

To construct the ring B, **31** was converted to aminal **34** which was subjected to our previous model reaction conditions [11]. Thus, treatment of **34** with *p*-TsOH followed by deprotection of the THP group gave the expected tetracyclic core product **35**, a key intermediate having 3-acetoxypropyl group required for the construction of 15-membered ring and the hydroxyethyl group for the construction of 8-membered ring.

The alcohol **35** was converted to **36** by selenation and oxidation and the BOC group of **36** was in turn replaced with hexenoyl group to give the new diene **37**. Ring closing metathesis of **37** with the second generation Grubbs catalyst **38** provided the expected azocine lactam **39** in 70% yield. Sequential hydrolysis, oxidation, and Wittig reaction of **39** gave **40** whose structure was unambiguously confirmed by X-ray crystallography.

a
52%
b, c
69%
f, g
75%
h
76%
d, e
74%
i
quant.
(12a:12b, 1.2:1)
j
88% from 12a
69% from 12b
k-n
61%
o-q
78%
r, s
92%
t
91%
u
83%
v
75%
w, x
92%
y
72%
(Z:E= 1:1.8)
z
92%
6 (>99% ee)
4
8: R1 = Bs, R2 = H
9: R1 = H, R2 = TBDPS
10
11
12a: α-adduct
12b: β-adduct
13
14
15
16: R = ≡
17: R = ≡≡
18: R = ≡≡
19: R = ≡
20
21
(–)–1
A
B

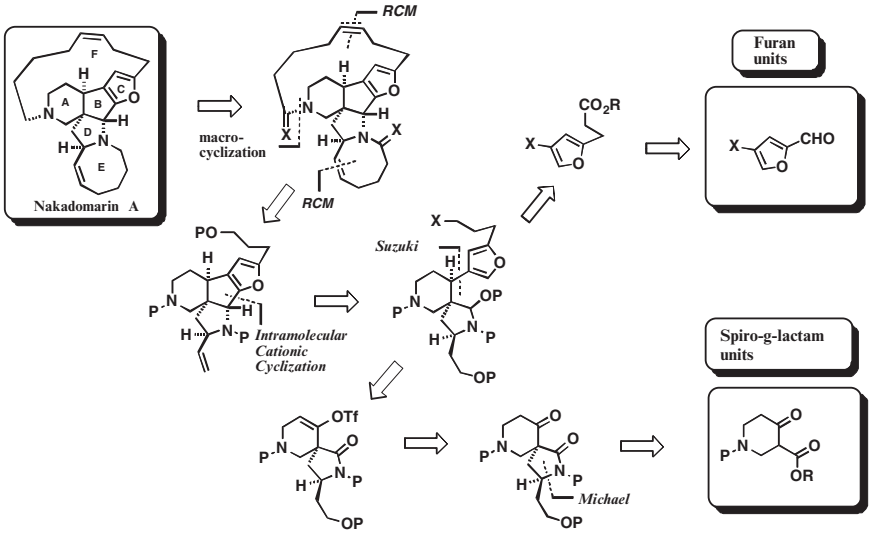

Scheme 10.3 Synthesis of nakadomarin A by Route B

Deprotection followed by *N*-acylation of **40** gave highly advanced diene **41** which was subjected to the final RCM with **42** and the desired dilactam (-)-(24*Z*)-**43** was isolated from the mixture of geometrical isomers (*Z*/*E* = ca. 2:3). Reduction of **43** with Red-Al resulted in the first total synthesis of *ent*-(+)-nakadomarin A from the readily available chiral acid **22**. The absolute configuration of natural nakadomarin A was assigned to be *R* (Scheme 10.4) [9].

Scheme 10.2 Asymmetric total synthesis of (–)-**1**.(a) **5** (3.0 eq) neat, 180°C, 1 h, then TFA, CH_2Cl_2, rt, 52% (diastereomer 35%); (b) $NaBH_4$, $CeCl_3$•$7H_2O$, CH_2Cl_2/MeOH, –78°C, 98% (*dr* = 2:1); (c) 6N HCl, benzene, reflux, 1 h, 70%; (d) TBDPSCl, imidazole; (e) Na/anthracene, DME, –65°C, 74% (two steps); (f) O_3, CH_2Cl_2, –78°C, then Me_2S, rt; (g) *N*-methylanilinium trifluoroacetate, THF, reflux, 75% (two steps); (h) $IPh_3PCH_2CH_2CH_2CCTMS$, NaH, THF, –78°C to rt, 76%; (i) O_2, halogen lamp, Rose Bengal, CH_2Cl_2/MeOH, 0°C, quant. (**12a**:**12b** = 1.2:1); (j) *t*BuOK, THF, –78°C, then 6N HCl, rt, 88% (from **12a**), *t*BuOK, THF, –30°C, then 6N HCl, rt, 69% (from **12b**); (k) Dess-Martin oxid., 90%; (l) $TMSCH_2MgCl$, Et_2O, rt, 83% (*dr* = 2:1); (m) BF_3•Et_2O, CH_2Cl_2, rt; (n) K_2CO_3, MeOH, 81% (two steps); (o) Boc_2O, DMAP, Et_3N, CH_2Cl_2, 93%; (p) DIBAH, toluene, –78°C; (q) Et_3SiH, BF_3•Et_2O, CH_2Cl_2, –78°C, 84% (two steps); (r) Na/naphthalene, DME, –65°C; (s) 5-hexenoyl chloride, Et_3N, CH_2Cl_2, 92% (two steps); (t) $Co_2(CO)_8$, CH_2Cl_2, 91%; (u) Grubbs catalyst **A** (25 mol%), 1.0 mM CH_2Cl_2, reflux, 1.5 h, 83%; (v) $n$$Bu_3SnH$, benzene, 65°C, 75%; (w) TFA, CH_2Cl_2; (x) 5-hexenoyl chloride, Et_3N, CH_2Cl_2, 92% (two steps); (y) Grubbs catalyst **B** (20 mol%), 0.5 mM CH_2Cl_2, reflux, 24 h, *Z* isomer 26%, *E* isomer 46%; (z) Red-Al®, toluene, reflux, 92%. TFA = trifluoroacetic acid, TBDPS = *tert*-butyldiphenylsilyl, DME = 1,2-dimethoxyethane, TMS = trimethylsilyl, Boc = *tert*-butoxycarbonyl, DMAP = 4-dimethylaminopyridine, DIBAH = diisobutylaluminium hydride, Red-Al® = sodium bis(2-methoxyethoxy)aluminium hydride

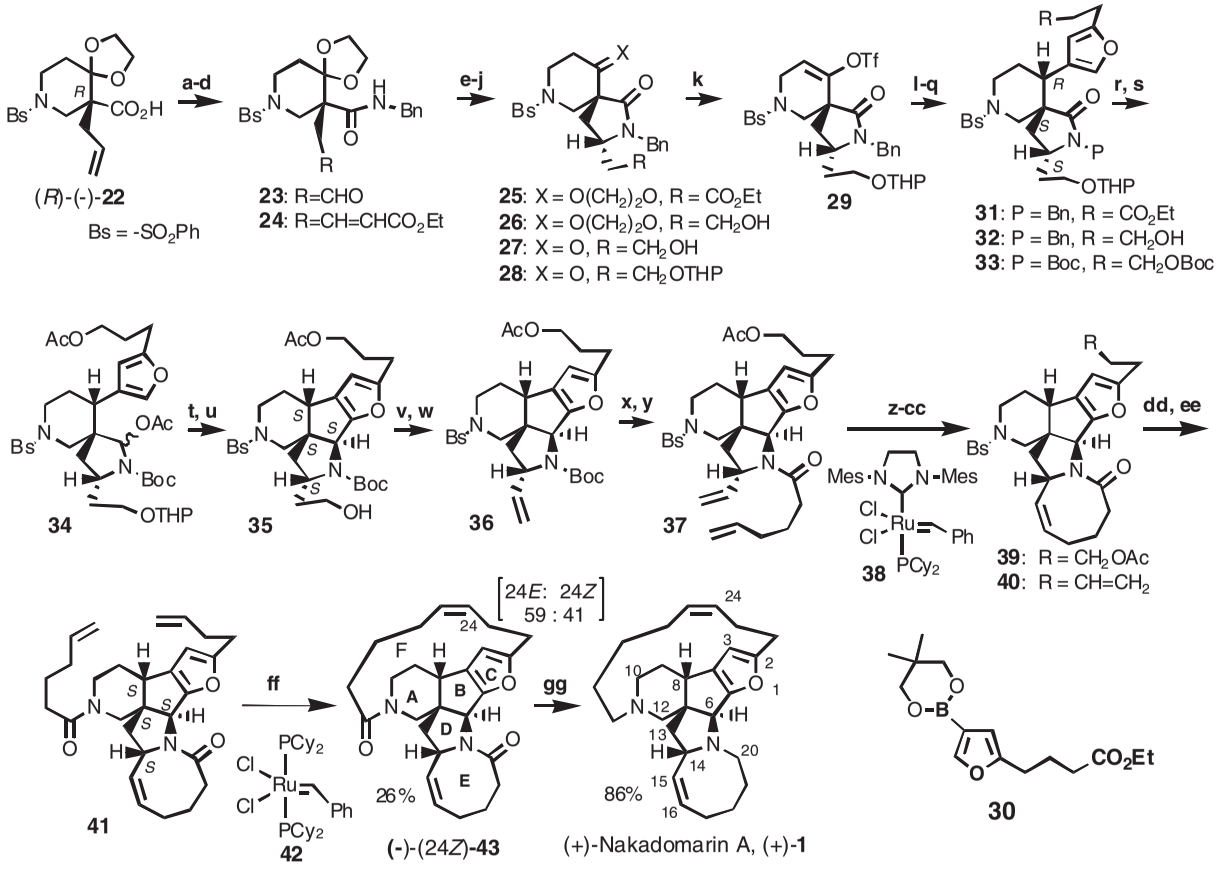

Scheme 10.4 The absolute configuration of natural nakadomarin A

Novel Synthesis of Quinolines and Indoles Using Ring Closing Metathesis

We have been investigating the feasibility of using metathesis to prepare heterocyclic compounds such as quinolines and indoles [12] (Scheme 10.5) and its application to the synthesis of bioactive natural products [13].

Recently, we found that *N*-allyl-o-vinylaniline **44** gave 1,2-dihydroquinoline **45** by normal RCM and developed silyl enol ether-ene metathesis for the novel synthesis of 4-siloxy-1,2-dihydroquinoline and demonstrated a convenient entry to quinolines and 1,2,3,4-tetrahydroquinoline [13]. We also have found a novel selective isomerization of terminal olefin to give the corresponding enamide **46** using ruthenium carbene catalyst [**Ru**] and silyl enol ether [14], which represented a new synthetic route to a series of substituted indoles **47** [12]. We also succeeded an unambiguous characterization of ruthenium hydride complex [**RuH**] with *N*-heterocyclic carbene

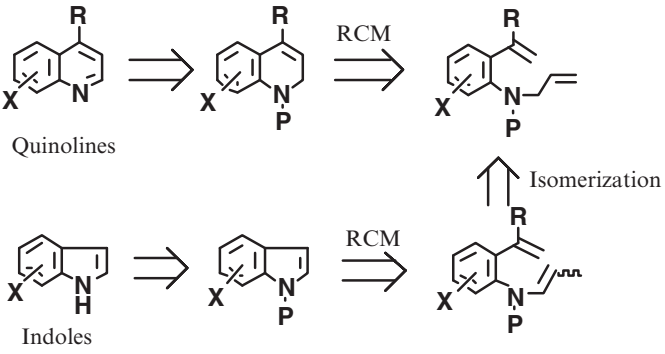

Scheme 10.5 Retrosynthesis of quinoline and indole

Scheme 10.4 (a) $BnNH_2$, 1-ethyl-3-(3-dimethylaminopropyl)carbodiimide (WSC)•HCl, HOBt, DMF, 91%; (b) cat. OsO_4, NMO, aq. THF, rt; (c) $NaIO_4$, CH_2Cl_2:H_2O (2:1), rt; (d) $Ph_3P{=}CHCO_2Et$, CH_2Cl_2, reflux; (e) DBU, EtOH; (f) 2 *N* NaOH, MeOH; (g) AcCl, EtOH, 54% (eight steps); (h) $LiBH_4$, MeOH, THF, 99%; (i) 70% $HClO_4$, CH_2Cl_2, rt, 91%; (j) DHP, cat. CSA, 91%; (k) (i) $LiN(TMS)_2$, THF, -78°C, (ii) $PhNTf_2$, 87%; (l) **30**, $PdCl_2$(dppf), K_3PO_4, 80°C, 3 h, 95%; (μ) (i) H_2, 10% Pd-C, MeOH, rt, 1.5 h, 71% (8a-H: 8b-H = 1:5.7), (ii) PPTS, EtOH, (iii) separation of diastereomers, (iv) DHP, cat. CSA, 69%; (n) $LiBH_4$, MeOH, THF, 99%; (o) Li, liq. NH_3; (p) $PhSO_2Cl$, aq. $NaHCO_3$, 80% (two steps); (q) $(Boc)_2O$, Et_3N, cat. DMAP, 98%; (r) DIBALH, CH_2Cl_2, toluene; (s) Ac_2O, pyridine, 80% (two steps); (t) *p*-TsOH, CH_2Cl_2; (u) 1 *N* HCl, THF, 87% (two steps); (v) 2-nitrophenylselenocyanate, *n*-Bu_3P; (w) *m*CPBA, aq. K_2HPO_4; (x) TFA, CH_2Cl_2; (y) 5-hexenoic acid, WSC•HCl, HOBt, 73% (four steps); (z) **38**(20 mol%), CH_2Cl_2, 2 mM, 50°C, 1.5 h; (aa) 2 *N* NaOH, MeOH, rt, 1.5 h, 64% (two steps); (bb) Dess-Martin periodinane, 80%; (cc) $Ph_3P{=}CH_2$, 72%; (dd) Na, naphthalene; (ee) 5-hexenoic acid, WSC•HCl, HOBt, 77% (two steps); (ff) **42**(15 mol%), CH_2Cl_2, 0.5 mM, 50°C, 24 h, 26% (24*Z*), 44% (24*E*); (gg) Red-Al, toluene, reflux

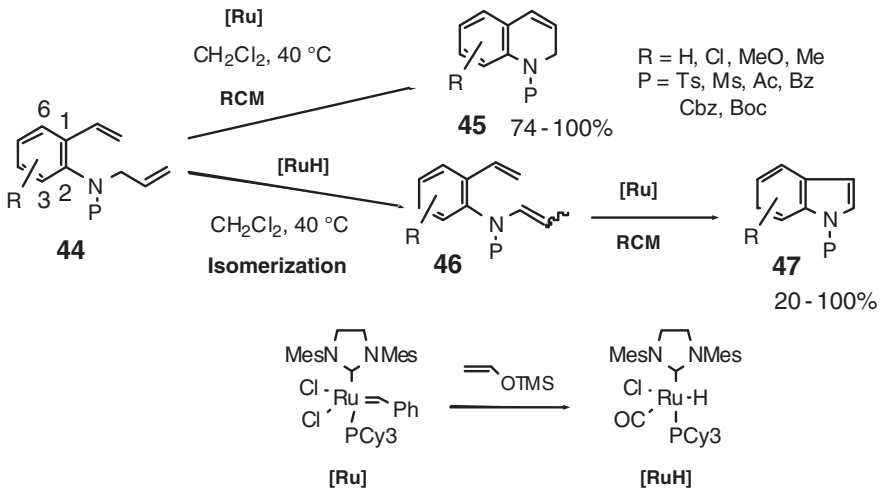

Scheme 10.6 New synthetic route to a series of substituted indoles

(NHC) ligand, which is generated from a second-generation Grubbs catalyst [**Ru**] and vinyloxytrimethylsilane and the actual active species for these nonmetathetic reactions, isomerization of a terminal olefin (Scheme 10.6) [15].

References

1. Ono, K., Nakagawa, M. and Nishida, A., 2004, *Angew. Chem. Int.Ed.,* **43,** 2020–2023.
2. Watanabe, D., Tsuda, M. and Kobayashi, J., 1998, *J. Nat. Prod.,* **61,** 689–692.
3. (a), Magnier, E. and Langlois, Y., 1998, *Tetrahedron,* **54,** 6201–6258.
   (b) Nishida, A., Nagata, T.and Nakagawa, M., 2006, *Top Heterocyl. Chem.,* **5,** 255–280.
4. Nakagawa, M., Uchida, H., Ono, K., Kimura, Y., Yamabe, M., Watanabe, R., Tsuji, R., Akiba, M., Terada, Y., Nagaki, D., Ban, S., Miyashita, N., Kano, T., Theeradanonm, C., Hatakeyama, K., Arisawa, M. and Nishida, A., 2003, *Heterocycles,* **59,** 721.
5. Gras, J.-L., 1978, *Tetrahedron Lett.,* **19,** 2111–2114.
6. Kondo, K. and Matsumoto, M., 1976, *Tetrahedron Lett.,* **17,** 4363–4366.
7. (a) Fürstner, A., 2000, *Angew. Chem. Int. Ed. Engl.,* **39,** 3012–3043.
   (b) Trunka, T. M. and Grubbs, R. H., 2001, *Acc. Chem. Res.,* **34,** 18.
   (c) Connon, S. J. and Blechert, S.,2003 , *Angew. Chem. Int. Ed. Engl.,* **42,** 1900–1923.
   (d) Deiters, A. and Martin, S. F., 2004, *Chem. Rev.,* **104,** 2199–2238.
   (e) Grubbs, R. H., 2004, *Tetrahedron,* **60,** 7117–7140.
   (f) Gradillas, A. and Perez-Castells, J., 2006, *Angew. Chem. Int. Ed. Engl.,* **45,** 6086–6101.
   (g) *Handbook of Metathesis* (Grubbs, R.H. ed.), 2003, Wily-VCH, Weinheim, Germany, Vols. 1–3.
8. (a) Hosaka, T., Torisawa, M. and Nakagawa, M. 1997, *Tetrahedron Lett.,* **38,** 3535–3538.
   (b) Pedregal, C., Ezquerra, J., Escribano, A., Carreno, M. C. and Ruano, J. L. G., 1994, *Tetrahedon Lett.,* **35,** 2053–2056.
9. Nagata, T., Nakagawa, M. and Nishida, A., 2003, *J. Am. Chem. Soc.,* **125,** 7484–7485.

10. Nagata, T., Nishida, A. and Nakagawa, M., 2001, *Tetrahedron Lett.,* **42,** 8345–8349.
11. (a) Miyaura, N. and Suzuki, A., 1995, *Chem. Rev.,* **95,** 2457–2483.
    (b) Suzuki, A., 1994, *Pure Appl. Chem.,* **66,** 213–222.
12. (a) Arisawa, M., Terada, Y., Nakagawa, M. and Nishida, A., 2002, *Angew. Chem. Int. Ed. Engl.,* **41,** 4732–4734.
    (b) Arisawa, M., Nishida, A. and Nakagawa, M., 2006, *J. Organomet. Chem.,* **691,** 5109–5121.
13. (a) Arisawa, M., Kato, C., Kaneko, H., Nishida, A. and Nakagawa, M., 2000, *J. Chem. Soc., Perkin Trans.,* **1,** 1873–1876.
    (b) Arisawa, M., Theeraladanon, C. H., Nishida, A. and Nakagawa, M., 2001, *Tetrahedron Lett.,* **42,** 8029–8033.
    (c) Arisawa, M., Kaneko, H., Nishida, A. and Nakagawa, M., 2002, *Perkin Trans.,* **1,** 959–964.
    (d) Theeraladanon, C., Arisawa, M., Nishida, A. and Nakagawa, M., 2004, *Tetrahedron,* **60,** 3017–3035.
    (e) Theeraladanon, C., Arisawa, M., Nakagawa, M. and Nishida, A., 2005, *Tetrahedron Asymm.,* **16,** 827–831.
14. Arisawa, M., Theeraladanon, C., Nishida, A. and Nakagawa, M., 2001, *Tetrahedron Lett.,* **42,** 8029–8033.
15. Arisawa, M., Terada, Y., Nakagawa, M. and Nishida, A., 2006, *J. Org. Chem.,* **71,** 4255–4261.

Chapter 11
Effect of Molecular Structure on Polymorphic Nucleation of BPT Derivatives

Mitsutaka Kitamura and Takayuki Hara

Abstract The effect of the molecular structure in the polymorphic crystallization was investigated by the rapid cooling method in ethanol solutions using BPT methyl ester (Me-est: Methyl 2-(3-Cyano-4-(2-methylpropoxy)-phenyl)-4-methyl-thiazole-5-carboxylate) and BPT propyl ester (Pr-est: Propyl 2-(3-Cyano-4-(2-methylpropoxy)-phenyl)-4-methyl-thiazole-5-carboxylate). The crystallization of Me-est resulted in only one crystal form at every initial concentration. On the other hand, in the crystallization of Pr-est at high initial concentrations, meta-stable A form first appeared, and after then, the stable B form nucleated and the solution-mediated transformation occurred. At low initial concentrations the stable form directly crystallized. Crystallographic analysis indicated that the Me-est crystal is constructed by stacking the flat sheet of the molecules that are formed by the two hydrogen bonding between a couple of molecules. Both of the stable and meta-stable forms of Pr-est are constructed also by stacking the sheet structures of the molecules. In the meta-stable form no hydrogen bonding was observed in the crystal, however, the structure of the stable form is stabilized by the hydrogen bonding through nitrile and carbonyl group. These results indicate that even the small change in molecular structure give rise to the large difference of the polymorphic nucleation behavior and crystal structure. The solvent effect on the polymorphic nucleation behavior of the Pr-est was also examined. From c-Hxn solution two polymorphs appeared and the same transformation was observed as that in EtOH. However, from MeCN solution the stable form directly crystallized.

Keywords BPT derivatives, crystallization, crystallographic analysis, molecular structure, polymorphic nucleation

Department of Mechanical and System Engineering,
University of Hyogo, 2167 Shosha, Himeji, 671-2201, Japan

B. Sener (ed.), *Innovations in Chemical Biology*, doi: 10.1007/978-1-4020-6955-0

Introduction

Polymorphs and solvated crystals is generally observed in pharmaceutical industry [1]. The bioavailability, stability, solubility, and morphology of the pharmaceutical products are very influenced by polymorphs [2–7], therefore the control of the polymorphic crystallization is very important. The crystallization process of polymorphs and solvated crystals is composed of competitive nucleation, growth, and transformation from a meta-stable form to a stable form [4]. Furthermore, the crystallization behavior is influenced by various controlling factors such as temperature, supersaturation, additives and solvents [8]. In order to perform the selective crystallization of the polymorphs, the mechanism of each elementary step in the crystallization process and the key controlling factor needs to be elucidated [8]. On the other hand, we reported for L-Glutamic acid and L-Histidine system previously [4] that the nucleation and transformation behaviors of polymorphs depend on the molecular structures. If the relationship between molecular structure and polymorphic crystallization behavior is known, the prediction of the polymorphism may become to be possible for the related compound. However, detail in such relationship is not clearly understood.

We reported in the previous papers [8, 9] that the effect of the operational factors such as temperature and solvents on the polymorphic crystallization of a thiazole derivative – 2-(3-Cyano-4-(2-methylpropoxy)-phenyl)-4-methyl-thiazole-5-carboxylic acid (BPT) – which is an enzyme inhibitor. In this paper, we synthesized the esters of BPT and studied the effect of the molecular structure on polymorphic nucleation systemically, and at the same time we also examined the solvent effect on the polymorphic nucleation of the ester.

Experimental

Methyl ester (Me-est: Methyl 2-(3-Cyano-4-(2-metylpropoxy)-phenyl)- 4-methyl-thiazole-5-carboxylate) and propyl ester (Pr-est; Propyl 2-(3-Cyano-4-(2-methyl-propoxy)-phenyl)-4-methyl-thiazole-5-carboxylate) were synthesized (Fig. 11.1)

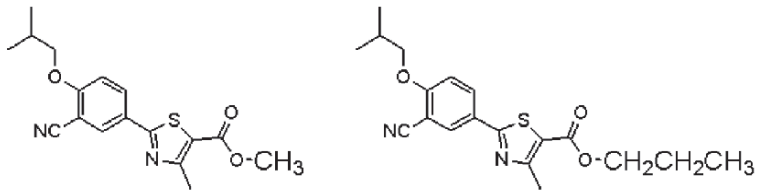

BPT-methyl ester (Me-est) BPT-propyl ester (Pr-est)

Fig. 11.1 Structure of BPT esters

and the influence of molecular structure on polymorphic crystallization behaviors was investigated.

Crystallization was carried out by the rapid cooling method in ethanol (EtOH) solutions. Various amounts of Me-est and Pr-est crystals were dissolved in ethanol at 323 K. After the crystals completely dissolved, the solution was rapidly cooled to 298 K to perform the crystallization. The slurry was sampled at constant intervals and filtered to separate the crystals from the solution. The concentration of the solution was measured by a UV spectroscopic method. After drying the separated crystal, the crystal structure was examined by powder X-ray diffraction (XRD) using the RINT2200 (Rigaku). The crystal structures were analyzed with a single crystal, by a Rigaku R-AXIS with Cu-Kα radiation.

The solvent effect was also investigated by the same method using cyclohexane (c-Hxn) and acetonitrile (MeCN) as solvents.

Results and Discussion

Crystallization Behavior of Me-est from EtOH Solutions

Rapid cooling crystallization of Me-est from ethanol solutions was carried out at the various initial concentrations. Figure 11.2 shows the changes in the concentration of the solution during each run. After a decrease in the concentration due to the crystallization, the concentration attained a constant value. In the case of crystallization at low initial concentrations, the concentration change was gentler than that

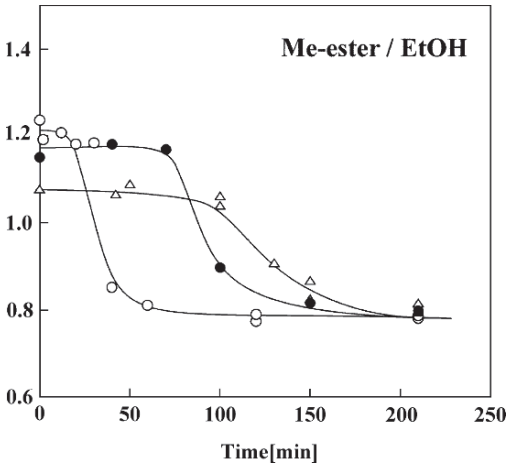

Fig. 11.2 Changes in the concentration of Me-est from ethanol solutions using the rapid cooling crystallization method

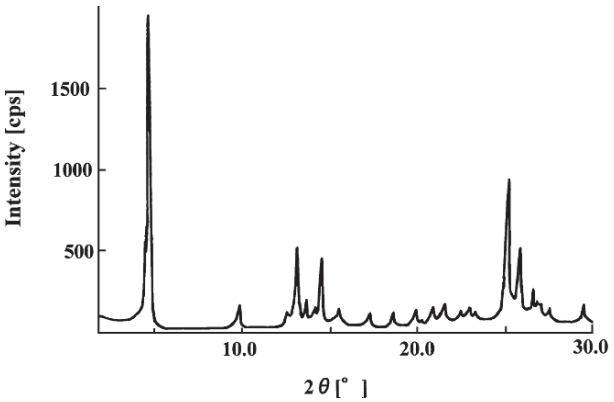

Fig. 11.3 XRD pattern of a Me-est crystal

in the case of high initial concentrations. This result indicates that the crystallization rate at low initial concentrations is lower than that at high initial concentrations. The crystals were analyzed by XRD measurement (Fig. 11.3) and it indicated that the XRD patterns of the crystals obtained in different initial concentrations are identical. Thus, no polymorphs were formed in the crystallization of Me-est from ethanol solutions at every initial concentration.

Crystal Structure of Me-est

The X-ray analysis of a single crystal obtained from an ethanol solution was performed.

The following data were obtained: space group is triclinic (P-1); a, 6.959(14) Å; b, 7.253(12) Å; c, 17.90(3) Å; α, 81.96(11)°, β, 82.81(7)°; and γ, 72.86(9)°. Figure 11.4 shows molecular arrangement (a) and crystal structure (b) of the Me-est. It was found that the crystal is constructed by stacking sheets of molecules (phenyl and thiazole rings, and the ester group lie on the same plane). With regard to a couple of molecules, two hydrogen bondings were observed in the same plane between an oxygen atom of the carbonyl group and a hydrogen atom in the phenyl ring of another molecule as shown in Fig. 11.4a (the distance between the two atoms was observed to be 2.45 Å). On this account, nitrile group in the phenyl ring and methyl groups of the ester and thiazole ring are oriented to outside from a couple of molecules to avoid the repulsion of the groups in each molecules. This results in the cis position of the methyl groups of the ester and thiazole ring. This hydrogen bond appears to stabilize the conformation that the methyl group of the ester and the thiazole ring are located on the same side. Therefore, the crystal is constructed by stacking a pair of molecules; further, the phenyl and thiazole rings were stacked between the sheet structures due to the π-π interaction.

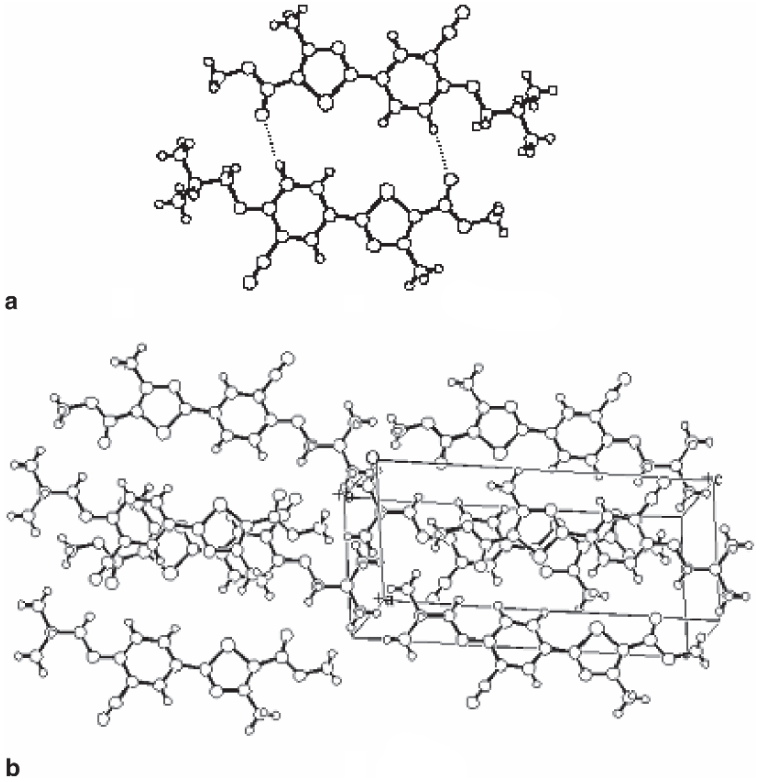

Fig. 11.4 Crystal structure of a Me-est: (a) a coupled molecules; (b) crystal structure

Crystallization Behavior of Pr-est from EtOH Solutions

The crystallization was carried out in EtOH solutions at various initial concentrations. Figure 11.5 shows the changes in the concentration of the solution during each run. With regard to the crystallization at initial concentrations of 23.3 and 26.0 mmol/l, the two staged concentration decrease was observed. The XRD measurement was done for the crystals sampled at 180 min and 1,250 min (Fig. 11.6a and b). These results indicate that two polymorphs were crystallized from the EtOH solution. The two stages in the concentration changes are considered to be due to the solution-mediated transformation from the meta-stable to the stable form. Thus, the crystals obtained at 180 min is the meta-stable form, while the crystals obtained at 1,250 min is a stable form. We refer to the meta-stable form as the A form and the stable one as the B form. At these conditions only the meta-stable A form crystallizes initially, and after then the stable B form nucleates and the solution-mediated transformation proceeds, i.e. the Ostwald step rule is established. It can be observed that the A form has the needle-like morphology and the B form has the prismatic

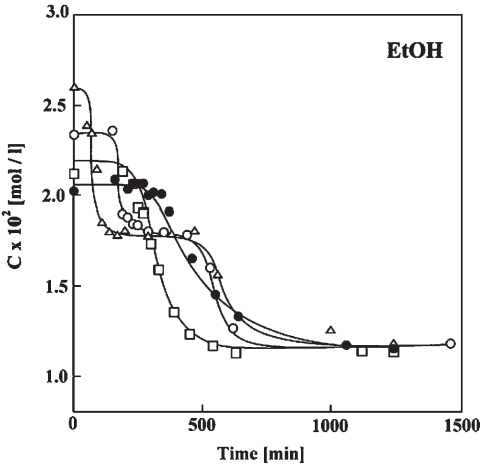

Fig. 11.5 Changes in the concentration of Pr-est from ethanol solutions using the rapid cooling crystallization method

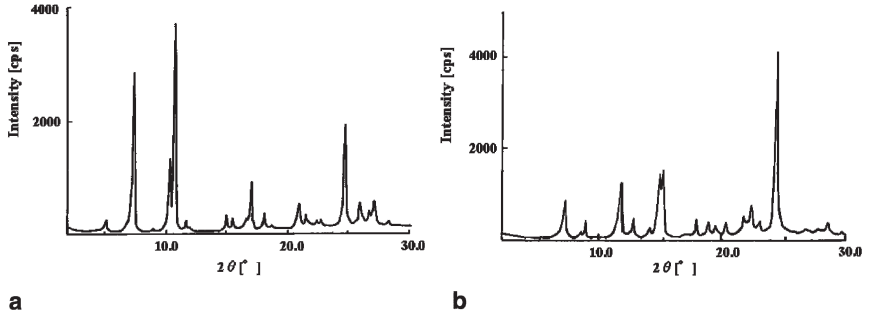

Fig. 11.6 XRD pattern of Pr-est crystal: (a) sampled for 180 min (b) sampled for 1,250 min; (at initial concentrations of 23.3 and 26.0 mmol/l)

shape. Furthermore, the constant concentration value at 18.1 mmol/l shows that the dissolving rate of the A form is faster than the precipitation rate of the B form. Therefore, the concentration attained after the first decrease in the concentration change (18.1 mmol/l) is considered as the solubility of the A form. On the other hand, the concentration finally attained is the solubility of the B form in EtOH at 298 K (11.6 mmol/l). In the case of crystallization at initial concentrations of 20.2 and 21.2 mmol/l, only the stable form is directly crystallized. This may indicate that the supersaturation is very influential on the polymorphic crystallization in EtOH solutions.

Crystal Structure of Pr-est (A form)

The X-ray analysis of a single crystal with the A form was performed. The following data was obtained: space group is Cmca; a, 7.1146(8) Å; b, 33.901(13) Å; and c, 16.253(3) Å. Figure 11.7 shows the molecular conformation (a) and crystal structure (b) of the A form. In this crystal, the molecules line up on the same plane to form a sheet structure in the bc face, and the crystal is constructed by stacking the sheet structures as well as the B form. In the sheet structure, there is no hydrogen bonding. With regard to the interaction of the inter-sheet structures, the π-π interaction seems to exist. However, hydrogen bonding for inter-sheet structures is not observed. From these results, the A form is formed mainly by the π-π interaction between the sheet structures.

Crystal Structure of Pr-est (B form)

The X-ray analysis of a single crystal of B form was performed. The following data was obtained: space group is $P2_1/a$; a, 8.1526(9) Å; b, 19.637(3) Å; c, 12.2979(17) Å; and β, 100.117(5)°.

Figure 11.8 shows the molecular conformation (a) crystal structure (b) of Pr-est (B form). It is found that the crystal is constructed by stacking the sheets of molecules. In the same plane, two hydrogen bondings are formed between a couple of

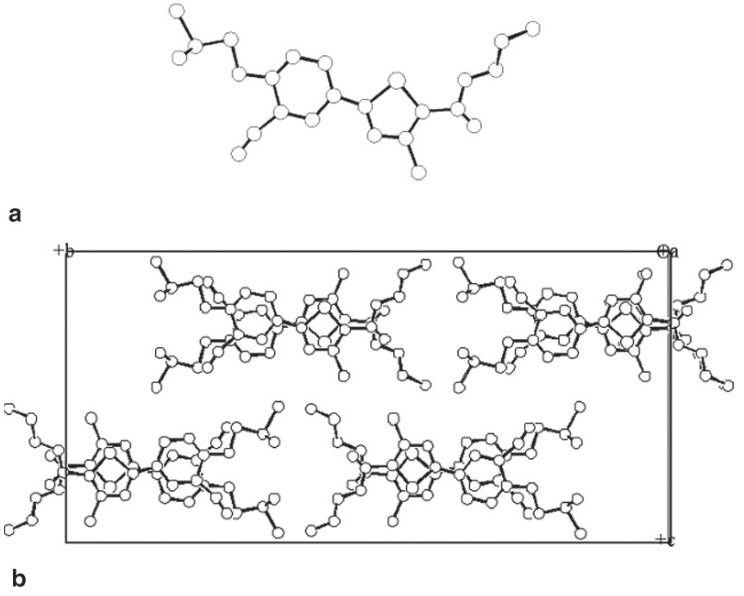

Fig. 11.7 Crystal structure of Pr-est (A form): (a) molecular conformation; (b) crystal structure

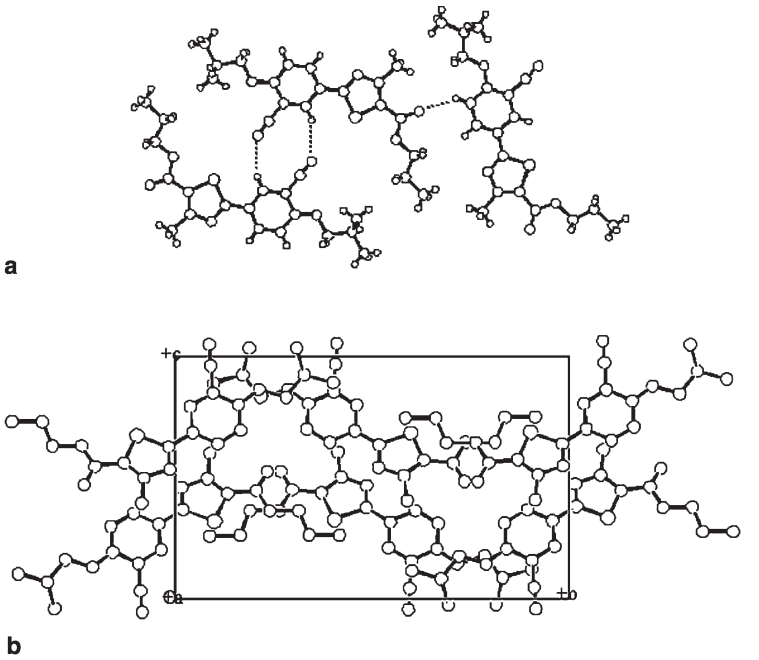

Fig. 11.8 Crystal structure of Pr-est (B form): (a) molecules in sheet structure; (b) crystal structure

molecules through the nitrogen atom of the nitrile group and a hydrogen atom in the phenyl ring of another molecule. In addition, hydrogen bonding between an oxygen atom of the carbonyl group and a hydrogen atom of the phenyl ring is also observed in the same plane. Hence, the pairs of molecules are connected with each other to form the sheet structure. These sheet structures stack due to the π-π interaction. Thus, this crystal is constructed by the hydrogen bonding in the sheet structure and the π-π interaction between the sheet structures.

Solvent Effect on the Nucleation Behavior of Pr-est

As described previously in the crystallization from ethanol (EtOH) solutions A and B polymorphs appeared. However, with kinds of the solvent the polymorphic nucleation behavior may change. In this section the solvent effect in the nucleation behavior of Pr-est is shown.

Crystallization of Pr-est from c-Hxn Solutions

Crystallization was carried out from cyclohexane (c-Hxn) solutions. Figure 11.9 shows the concentration changes of the solution during each run. With regard to the

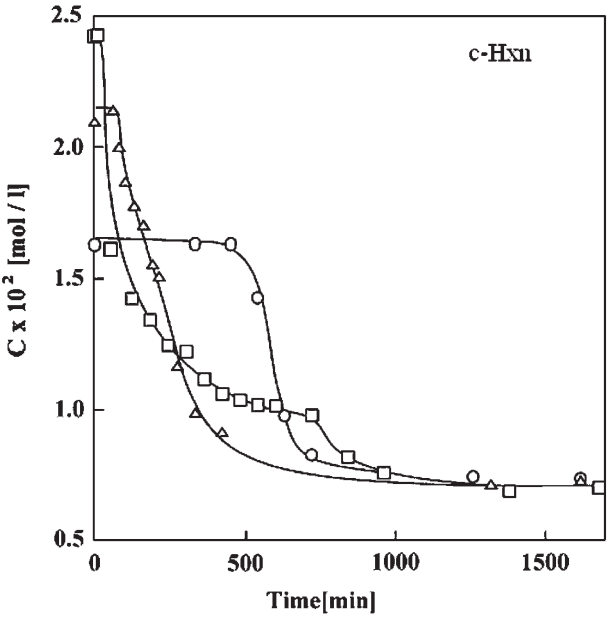

Fig. 11.9 Change in concentration of Pr-est in the crystallization from c-Hxn solutions

crystallization at high initial concentration (24.3 mmol/l), the two staged concentration decrease was observed. On the other hand, in the case of crystallization at lower initial concentrations, the concentration decreased simply. This behavior is similar to that in EtOH solutions. The XRD measurements of the crystals obtained at the initial concentration of 24.3 mmol/l indicated that the crystals crystallized at 500 min corresponds to the A form, and that at 1,300 min corresponds to the B form. This result also indicates that the solution-mediated transformation from A to B form occurs during the crystallization in the same manner with that in EtOH solutions. On the other hand, in the case of crystallization at low initial concentrations only the stable form crystallized directly.

Crystallization of Pr-est from MeCN Solutions

Figure 11.10 shows the changes of the Pr-est concentration in acetonitrile (MeCN) solutions during each run. In this case the simple decrease was observed in the concentration change and it reached constant values. It was found that the diffraction patterns of the crystals obtained in all conditions were the same with that of the stable B form (Fig. 11.6b). Thus, the crystallizations of Pr-est from MeCN solutions resulted in the same crystal form at every initial concentration.

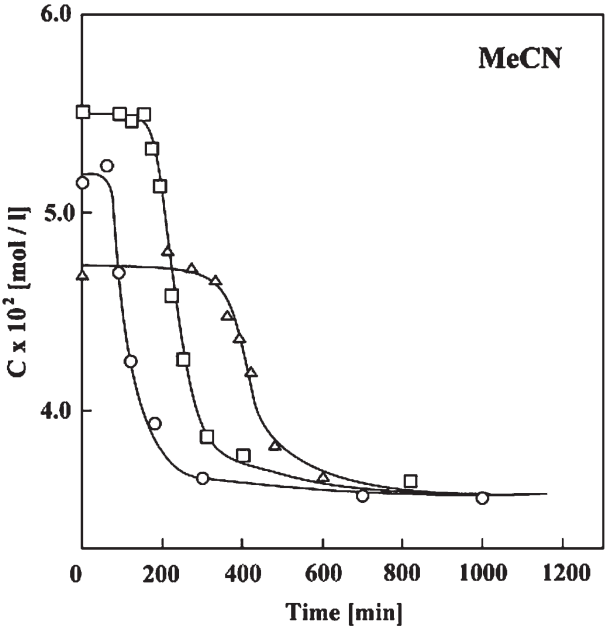

Fig. 11.10 Change in concentration of Pr-est in the crystallization from MeCN solutions

Discussion

In the crystallization of Me-est, only one crystal form crystallized at every initial condition, while the two forms appeared in the case of Pr-est dependently on the initial super saturations. The appearance of the two polymorphs in the Pr-est may be due to the greater conformational flexibility of the propyl group as compared to the methyl group. In the case of Me-est, strong hydrogen bonding between the carbonyl group and hydrogen atom in phenyl ring results in a pair molecule. The nitrile group in the phenyl ring, methyl group in the thiazole ring, and the methyl group in ester take the positions outside of the pair molecules to avoid the contact. In the case of Pr-est, the steric hindrance due to the propyl group of ester becomes larger than Me-est, this may result the trans geometry between the methyl group in the thiazole ring and the alkyl group in the ester. In the meta-stable form, a nitrile group and a methyl group on the thiazole ring are located in the cis-position. On the other hand, in the stable form, these groups are in the trans-position. The structure of the stable form is stabilized by the hydrogen bonding through nitrile and carbonyl group.

In c-Hxn solutions the nucleation behavior is similar to that in EtOH solutions. It is presumed that the concentrations of conformer regarding to the A and B form are competitive and the nucleation process of the polymorph is determined by the supersaturation and the kinetic process. On the other hand in MeCN solutions only the stable form nucleates. In MeCN solution it is considered that the thermodynamic stability of the meta-stable form is extremely low due to the large solvent-solute

interaction. This may correspond to the low concentration of the conformer regarding to the meta-stable form. Even if the meta-stable form nucleates, it should quickly transform to the stable form by the solution-mediated mechanism.

Conclusion

In the crystallization of Me-est, only one crystal form appeared at every initial concentration. The crystal is constructed by stacking the flat sheet of the molecules that are formed by the two hydrogen bonding between a couple of molecules. In the crystallization of Pr-est at high initial concentrations, two polymorphs appeared, and the solution-mediated transformation occurred. At low initial concentrations, the B form was obtained directly. Both of the stable and meta-stable forms of Pr-est are constructed also by stacking the sheet structures of the molecules. In the meta-stable form no hydrogen bonding was observed in the crystal, however, the structure of the stable form is stabilized by the hydrogen bonding through nitrile and carbonyl group. These results indicate that even the small change in molecular structure give rise to the large difference of the polymorphic nucleation behavior and crystal structure. The solvent effect on the polymorphic nucleation behavior of the Pr-est was also examined. From c-Hxn solution two polymorphs appeared and the same transformation was observed as that in EtOH. However, from MeCN solution the stable form directly crystallized.

References

1. Henck, J.O., Griesser, U.J. and Burger, A., 1997, *Pharm. Ind.,* **59,** 165–169.
2. Giron, D., 1995, *Thermochim. Acta,* **248,** 1–59.
3. Sanjay, R., Chemburkar, J.B., Deming, K., Spiwek, H., Patel, K., Morris, J., Henry, R., Spanton, S., Dziki, W., Porter, W., Quick, J., Bauer, P., Donaubauer, J., Narayanan, B.A., Soldani, M., Riley, D. and McFarland, K., 2000, *Org. Proc. Res. Dev.,* **4,** 413–417.
4. Kitamura, M., 2002, *J. Crystal Growth,* **237**–**239**2205–2214.
5. Byrn, S., Pfeiffer, R., Ganey, M., Hoiberg, C. and Poochikian, G., 1995, *Pharm. Res.,* **12,** 945–954.
6. Rollinger, J.M., Gstrein, E.M. and Burger, A., 2002, *Eur. J. Pharm. Biopharm.,* **53,** 75–86.
7. Gavezzotti, A. and Filippini, G., 1995, *J. Am. Chem. Soc.,* **117,** 12299–12305.
8. Kitamura, M., 2004, *Cryst. Growth Des.,* **4,** 1153–1159.
9. Kitamura, M. Sugimoto, M., 2003, *J. Crystal Growth,* **257,** 177–184.
10. Kitamura, M., Hara, T. and Takimoto-Kamimura, M., 2006, *Cryst. Growth Des.,* **6,** 1945–1950.

Chapter 12
The Golden Ratio in the Creations of Nature Arises in the Architecture of Atoms and Ions

Raji Heyrovská

Abstract The Golden ratio, $\phi = a/b = (a + b)/a$, where a and b are the Golden sections of their sum, has long been known to operate in a variety of the creations of Nature, ranging from the mollusks in the oceans to the spiral galaxies in the Universe. Recently, while researching for the exact values of ionic radii and for the significance of the ionization potential ($I_H = e/2\kappa a_B$) of hydrogen, it was found that a_B, the Bohr radius has two Golden sections pertaining to the electron and proton. Further, ϕ was also found to be the ratio of the anionic to cationic radii of an atom (A), their sum being the covalent bond length, d(AA). With these radii many bond lengths were shown to be sums of the covalent and or ionic radii, whether partially or fully ionic or covalent. For example, the crystal ionic distances of all alkali halides were shown to be sums of the ϕ-based ionic radii. When the ion-water distances were plotted against the above ϕ-based ionic radii, linear relations were found. This enabled the assignment of exact ionic radii in water, and to show that the hydration bond lengths of O (oxygen coordination bond) with cations and of H (hydrogen bond) with anions are constants. Simple integral multiples of the cationic radius, $d(H^+) = d(HH)/\phi^2$, and the covalent radius of H, were found to *quantitatively* account for the lengths of the hydrogen bonds in many inorganic and biochemical groups.

Keywords Covalent and ionic radii, Golden ratio, hydrogen bond length

Introduction

A proper understanding of the properties of solutions of electrolytes begins with that of sodium chloride, the common salt. It is a typical example of a strong electrolyte and its characteristics in the solid state and in the dissolved state in aqueous

Institute of Biophysics, Academy of Sciences of the Czech Republic, Královopolská 135, 612 65 Brno, Czech Republic

B. Sener (ed.), *Innovations in Chemical Biology*, doi: 10.1007/978-1-4020-6955-0

solutions are explained here from a new point of view developed recently for atoms and ions [1]. The crystal ionic radii of Na^+ and Cl^- and ions of other alkali halides (MX) are found to be [1] the Golden sections, $d(MM)/\phi^2$ and $d(XX)/\phi$, of the metal-metal and halogen-halogen inter-atomic distances, respectively, where $\phi = (1 + 5^{1/2})/2 = 1.618$, is the Golden ratio. The latter is a mathematical constant, which operates in the geometry of many inorganic, organic and biological creations of Nature, and hence is also called the Divine ratio [2a, b]. The ϕ-based ionic radii show that the bond lengths d(AB) between many atoms or ions are sums of the atomic/ionic radii [1, 3] and that the partial/complete ionic character is due to either/both A and B being ionic.

More recently, the ion-water distances, d(i…w) [4–6] of various ions in solutions were found to increase linearly [7] with the covalent radii [8] d(A) of the corresponding atoms, taken as half the inter-atomic distances [8, 9], d(AA). The ionic radii in aqueous solutions were calculated as $d(i)_{aq} = kd(A)$ using the slopes (k) of these lines. It was found [7] that k is a function of ϕ and that it depends on the valencies of the ions. The intercepts gave the hydration lengths, d(--O) for cations and anions. The halide ions were found to form a hydrogen bond of constant length, $d(–H) = d(H) + d(H^+) = 0.65$ Å, where $d(H)$ is the covalent radius of H and $d(H^+) = d(HH)/\phi^2$ is the radius of the proton taken as the cationic radius of H (italics denotes that it is a vacant distance). To ascertain whether the result is meaningful, the lengths of the hydrogen bonds in many other inorganic and biochemical groups were analyzed and it was found [10] that, in general, $d(–H) = nd(H^+) + md(H)$, where n = 1 or 2 and m = 0, 1, 2 or 3, depending on the chemical context of the hydrogen bond.

This paper starts with a brief description of the Golden ratio and the ϕ-based crystal ionic radii and is then followed by the ϕ-based aqueous ionic radii and hydration lengths. The role of ϕ in the sizes of the ions in the crystal and in aqueous solutions and their hydration bonds with water can be seen in Fig. 12.3 for Na^+ and Cl^- ions (used as the examples).

The Golden Ratio, Golden Point and Golden Sections

The Golden Ratio, $\phi = (1 + 5^{1/2})/2 = 1.618…$, is the positive root of the quadratic equation, $\phi^2 – \phi – 1 = 0$. It is also the ratio of two quantities (e.g., segments of a circle or of a line) a and b, which are such that

$$a/b = (a + b)/a = b/(a – b) = \phi;\ 1(a + b) = (1/b) – (1/a) \qquad (12.1a, b)$$

ϕ has the unique property of forming a power series,…, $1/\phi^3$, $1/\phi^2$, $1/\phi$, 1, ϕ, ϕ^2, ϕ^3,…, which is also a Fibonacci series (0, 1, 1, 2, 3, 5, 8, 13,…, where every number is the sum of the previous two). The ratio of any Fibonacci number to its previous one oscillates around ϕ as the numbers increase and becomes closer to ϕ as the numbers become large. Many growth processes in Nature which originate as Fibonacci series also ultimately reach the Golden ratio.

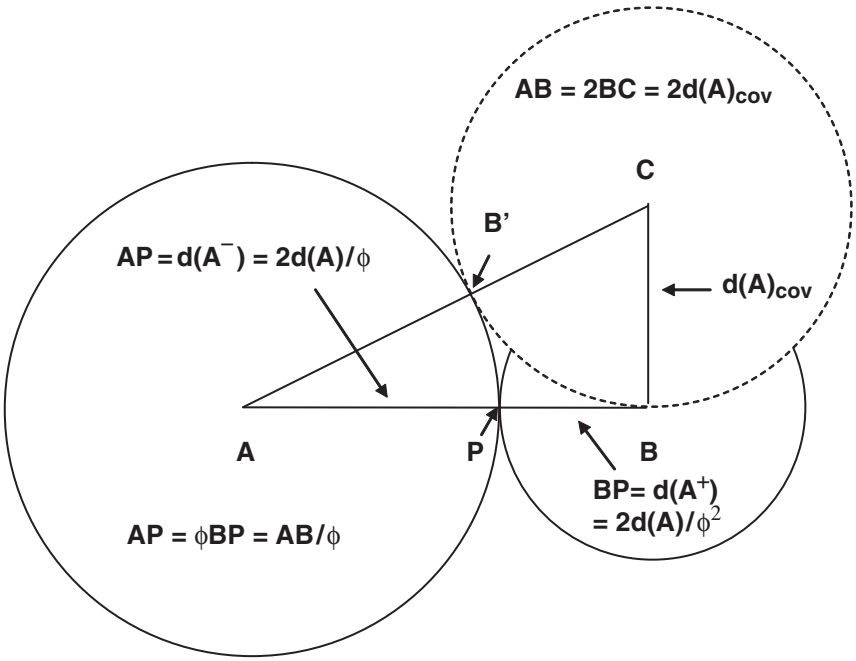

Fig. 12.1 The Golden point (P) on a line (AB). For any atom A, if AB = 2BC = d(AA), then AP = $d(A^-)$ and BP = $d(A^+)$ are the Golden sections denoting the anionic and cationic radii of A

A fascinating account of the occurrence of the Golden ratio in the various creations of Nature can be found in [2a–c]. Geometrically, ϕ is the ratio of a diagonal to a side in a regular pentagon (e.g., in the 12 pentagons in fullerenes [2b]). The ratio $\phi/2 = \cos 36^0$, where 36^0 is the central angle in a regular decagon (e.g., cross section of the DNA double helix [2b]). The number $1 = \phi - (1/\phi) = \phi^2 - \phi = (1/\phi) + (1/\phi^2)$, where the last two terms are the Golden sections of 1. Note: $\phi + (1/\phi) = 5^{1/2}$, $(1/\phi) - (1/\phi^2) = (1/\phi^3) = 5^{1/2} - 2 = 0.236$ and that $\pi \sim (6/5)\phi^2$ (area of five circles of radii r ~ area of six squares of sides rϕ!).

Any line AB can be divided at the Golden point P (see Fig. 12.1) by erecting a perpendicular BC = AB/2 at B, marking the distance CB' = CB on the hypotenuse AC and locating P on AB such that AB' = AP. The Golden sections, $AP = AB/\phi = (AB/2)(1 + \phi^{-3})$ and $BP = AB/\phi^2 = (AB/2)(1 - \phi^{-3})$.

The Golden Sections of the Ground State Bohr Radius for Hydrogen

For a hydrogen atom, the ionization potential, $I_H = e/(2\kappa a_B) = (I_p + I_e)/2 = (e/2\kappa)[(1/a_p) - (1/a_e)]$, where $I_p = e/\kappa a_p$ and $I_e = -e/\kappa a_e$ pertain to the proton (p^+) and electron (e^-), respectively [1], and $a_B = a_p + a_e$ is the Bohr radius. Therefore, relations similar to Eqs. 12.1a, b are valid:

$$(1/a_B) = (1/a_p) - (1/a_e);\ (a_e a_p)^2 - (a_e/a_p) - 1 = 0;\ \phi = (a_e/a_p) \qquad (12.2a, b, c)$$

where, $a_p = a_B/\phi^2$ and $a_e = a_B/\phi$, respectively, are the distances of p^+ and e^- from the Golden point P of electrical neutrality, and are the Golden sections of a_B. In Fig. 12.1, if $AB = a_B$, then $BP = a_p = a_B/\phi^2$, $AP = a_e = a_B/\phi$ and $(a_e - a_p) = AP - BP = a_B/\phi^3 = 0.236a_B$. Thus, an atom is a unique construction of Nature!

For hydrogen, it was shown [11] that $(g_p - g_e)/(g_p + g_e) = 2/\phi^3 = (360/\phi^2) - \alpha^{-1}$, where g_p and g_e are the g-factors (arising from the magnetic moment anomalies) for the proton and electron, respectively, α is the fine structure constant and $(360/\phi^2)$ is a Golden section of a circle. Since λ_{dB}, the de Broglie wavelength, is the circumference $(2\pi a_B)$ of the circle with the Bohr radius, λ_{dB} also has two Golden sections proportional to $(360/\phi^2)$ and $(360/\phi)$, see Fig. 1 in [11].

Ionic Radii as the Golden Sections of Inter-Atomic Distances

The inter-atomic distance in a molecule of hydrogen [8], $d(HH) = 2^{1/2}a_B = 0.74$ Å is also divided into the two Golden sections [1], $d(HH) = d(HH)/\phi^2 + d(HH)/\phi = d(H^+) + d(H^-)$, since a_B is divided into the Golden sections. In this case, P is the Golden point if $AB = d(HH)$ in Fig. 12.1. The Golden section, $BP = d(H^+) = 0.28$ Å is the radius of the cation of hydrogen, see [1, 3].

On looking into the literature to see whether this value of $d(H^+) = 0.28$ Å is meaningful, it was found [1] that this is the value suggested by Pauling [8] to account for the radius of H in the partially ionic bonds in hydrogen halides and in alkali metal hydrides! The author then used this value of $d(H^+) = 0.28$ Å to estimate the radii of alkali metal ions from the observed bond distances $d(MH)_{obs}$ in the metal hydrides, MH. It was a pleasant surprise to find that,

$$d(MH)_{obs} - d(H^+) = L(MM)/\phi^2 = d(MM)\phi^2 = d(M^+) \qquad (12.3)$$

$$d(MX)_{obs} - d(M^+) = d(X^-) = d(XX)/\phi \qquad (12.4)$$

where L(MM) in Eq. 12.3 is the lattice edge length equal to the inter-atomic distance d(MM) in alkali metals. The cationic radius $d(M^+)$ is thus a Golden section of d(MM). Eq. 12.4 shows that on subtracting the value of $d(M^+)$ obtained in Eq. 12.3 from the observed inter-ionic distances $d(MX)_{obs}$ in alkali halide crystals, one obtains the anionic radii, $d(X^-)$ as the Golden section of d(XX). Thus, the calculated sum, $d(MX)_{cal}$ (based on ϕ)

$$d(MX)_{cal} = d(M^+) + d(X^-) = d(MM)/\phi^2 + d(XX)/\phi \qquad (12.5)$$

was found to reproduce the observed sum, $d(MX)_{obs}$, for all the alkali halides [1], without the use of the suggested radius ratio corrections in [8].

This showed that, in general, for any atom (A) the inter-atomic distance d(AA) can be divided into two Golden sections, which give the anionic and cationic radii,

$d(A^-) = d(AA)/\phi$ and $d(A^+) = d(AA)/\phi^2$ respectively. In Fig. 12.1, if AB = d(AA) then BC = d(A) and AP = $d(A^-)$ > BP = $d(A^+)$. Thus, the anionic radius of any atom is greater than its cationic radius, as is known [8].

The Golden Ratio, Aqueous Ionic Radii and the Hydration Bonds

The dissolved state of the electrolytes in water has long been of great interest. More than a century ago, Mendelejew [12] suggested that sulphuric acid forms hydrates, and Arrhenius [13] put forward the theory of partial dissociation of electrolytes, both in the same Journal. These pioneering ideas have eventually proved to be correct [14] for electrolyte solutions from zero to saturation.

Another important topic of interest has been the interpretation of the observed ion-water distances $d(i\ldots w)_{obs}$ [4–6] in terms of the ionic radii in solutions and the radii of water molecules. The present author made the surprising observation recently [7] that $d(i\ldots w)_{obs}$ increases linearly with the covalent radius d(A) of the atom [9], for many ions according to the equation,

$$d(i\ldots w)_{obs} = kd(A) + d(-O);\ d(i)_{aq} = kd(A) \qquad (12a, b)$$

where k is the slope, d(–O) is the intercept and $d(i)_{aq}$ is the ionic radius in water. The values of k for alkali metal and halogen ions were found to be $0.81 = \phi/2$ and $1.57 = 2/\phi^{1/2}$, respectively. These values of k are geometrically described by the triangle in Fig. 12.2 and compared with the crystal ionic radii in Fig. 12.3.

The hydration bond length d(–O) = 0.64 Å for the cations [7] is the distance between the point of contact P(i/w) at the periphery of the cations and the center of the oxygen of water (see Fig. 12.3). For anions, this distance was found to be larger since d(–O) = d(–H) + d(OH) = 1.60 Å (+/– 0.04), where d(OH) = 0.97 Å

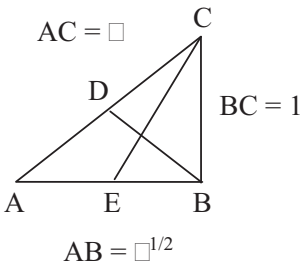

$$k_{cat} = d(M^+)_{aq}/d(M) = DC/BC = \square/2;\ k_{an} = d(X^-)_{aq}/d(X) = BC/BE = 2/\square^{1/2}$$

Fig. 12.2 The ratio of radii, k (=ionic radius/covalent radius), for alkali metal cations (M^+) and halide anions (X^-) in aqueous solutions (Eqs. 12.6a, b). In the right angled triangle, ABC, E and D are the mid points of AB and AC

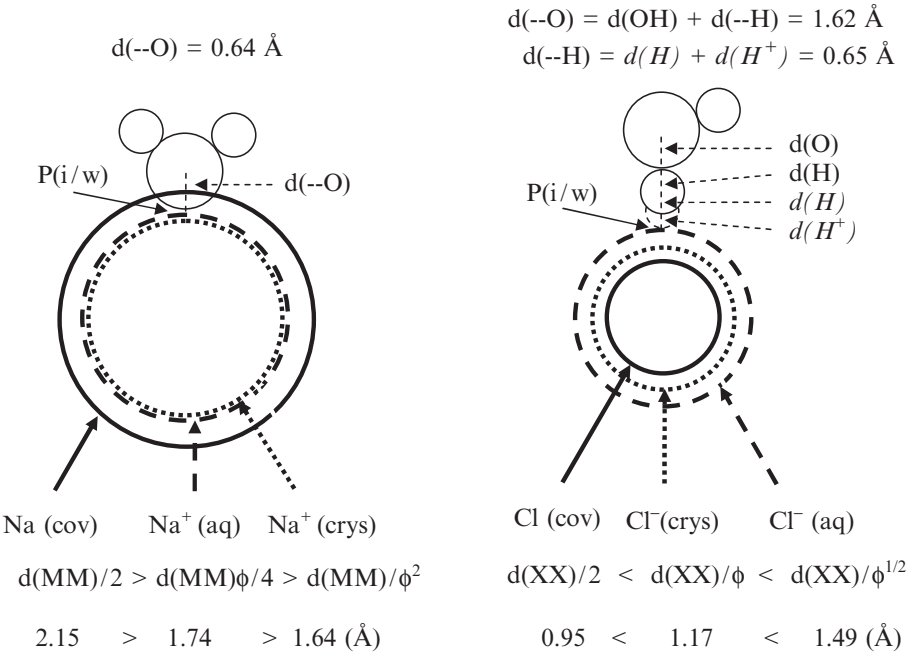

Fig. 12.3 The covalent radii and ionic radii in NaCl crystals and in aqueous solutions, the hydration bond lengths, d(-O) from the ion/water point of contact, P(i/w) to the center of O of water and the length of the hydrogen bon, d(-–H) with Cl^-

is the covalent bond length of the OH bond in water and d(--H) = $d(H) + d(H^+)$ = 0.65 Å is the length of the hydrogen bond. Note that $d(H^+) = d(HH)/\phi^2 = 0.28$ Å, the radius of the proton, is the cationic radius of H. Fig. 12.3 for Na^+ and Cl^- ions shows a comparison of the covalent radii with the ionic radii in the crystal and in aqueous solutions. The results for many other ions (including Lanthanides) can be found in [7].

The Golden Ratio and the Length of the Hydrogen Bond: in General

In general, in a group XH…Y, where X and Y are the H-donor and H-acceptor respectively, it was found [10] that the length of the hydrogen bond, d(--H) = $md(H) + nd(H^+)$, where $d(H)$ is the covalent radius of H, $d(H^+) = d(HH)/\phi^2 = 0.28$ Å, n = 1 or 2 and m = 0, 1, 2 or 3. Six values were found [11] for d(–H) (in Å): 0.28 (FH…F in KHF_2), 0.65 (FH…F in aqueous solutions, HF solid and gas), 1.02 (OH…O, in ice and NH…O in DNA), 1.30 (CH…O, PH…P), 1.39 (OH…O in water and NH…N, DNA) and 1.67 (NH…N in ammonia crystal).

Acknowledgements This research was supported by grants of the Academy of Sciences of the Czech Republic AVOZ50040507 and of the Ministry of Education, Youth and Sports of the Czech Republic, LC06035. I am indebted to the Organizers of the *9th Eurasia Conference in Chemical Sciences*, Antalya, Turkey, September 2006, for inviting me to give the above talk and for the financial support

References

1. Heyrovská, R., 2005, *Mol. Phys.,* **103,** 877–882.
2. (a) Livio, M., 2003, The Golden Ratio, the Story of Phi, the World's most Astonishing Number, Broadway Books, New York.
   (b) http://www.goldennumber.net
   (c) http://en.wikipedia.org/wiki/Golden_ratio
3. Heyrovská, R., 2004, *Intl. Joint Meeting of ECS, USA and Japanese, Korean and Australian Societies*, Honolulu, HI, Extended Abs., 2004, Vol. 2, Abs. C2-0551; http://www.electrochem.org/dl/ma/206/pdfs/0551.pdf
4. Marcus, Y., 1988, *Chem. Rev.,* **88,** 1475–1498.
5. Ohtaki, H. and Radnai, T., 1993, *Chem. Rev.,* **93,** 1157–1204.
6. David, F., Volkhmin, Y. and Ionova, G., 2001, *J. Mol. Liquids,* **90,** 45–62.
7. Heyrovská, R., 2006, *Chem. Phys. Letts.,* **429,** 600–605.
8. Pauling, L., 1960, The Nature of the Chemical Bond, Cornell University Press, Ithaca, NY.
9. http://www.webelements.com
10. Heyrovská, R., 2006, *Chem. Phys. Letts.,* **432,** 348–351.
11. Heyrovská, R. and Narayan, S., http://arxiv.org/ftp/physics/papers/0509/0509207.pdf
12. Mendelejew, D., 1887, *Z. Phys. Chem.,* **1,** 273–284.
13. Arrhenius, S., 1887, *Z. Phys. Chem.,* **1,** 285–298.
14. Heyrovská, R., 2006, *Electroanalysis,* **18,** 351–361.

Chapter 13
Interaction of Thioamides, Selenoamides and Amides with Di-iodine: A Study of the Mechanism of Action of Anti-thyroid Drugs

Sotiris K. Hadjikakou and Nick Hadjiliadis

Abstract This presentation is a brief review on the results of our work on iodine interaction with thioamides, selenoamides and amides. The thioamides, benzothiazole-2-thione (**BZT**) (**1**), 6-*n*-propyl-2-thiouracil (**PTU**) (**2**), 5-chloro-2-mercaptobenzothiazole (**CMBZT**) (**3**), N-methyl-benzothiazole-2-thione (**NMBZT**) (**4**), benzimidazole-2-thione (**BZIM**) (**5**), thiazolidine-2-thione (**TZD**) (**6**), 2-mercaptopyridine (**PYSH**) (**7**), 2-mercapto-nicotinic acid (**MNA**) (**8**), 2-mercapto-benzoic acid (**MBA**) (**9**) and 2-mercapto-pyrimidine (**PMT**) (**10**) react with I_2 producing three type of complexes of formulae: $\{[(HL)I_2](I_2)_n\}$ (HL= thioamide and n= 0, 1), $\{[(HL)_2I^+][I_3^-]\}$ and $\{[(HL\text{-}L)]^+[I_3^-]\}$. The interaction of seleno-amides, derived from, 6-*n*-propyl-2-thiouracil (**RSeU**) (R= Me- (**11**), Et- (**12**), *n*-Pr- (**13**) and *i*-Pr- (**14**)) with I_2, have also been studied and produced the complexes $[(RSeU)I_2]$ of "spoke" structure. These complexes are stable in non-polar solvents, but they decompose in polar solvents, producing dimeric diselenide compounds or undertake deselenation.

All these results are well correlated with the mechanism of action of anti-thyroid drugs.

Finally the amides pyridone-2-one (**PYOH**) (**15**) and 2-hydroxy-pyrimidine (**$PMOH_2^+$ Cl^-**) (**16**) react with I_2 and produce the complexes $\{[(PYOH)_3[(PYOH)]^+\cdot I_3^-\}$, $\{(PYOH)_6\cdot[(PYOH)_2]^{2+}\cdot ((1/2)I^-)\cdot((3/2)I_7^-)\cdot(I_2)\}$ and $\{[PMOH_2]^+Cl^-I_2\}$. The structures of all these compounds are discussed.

Keywords Anti-thyroid drugs, amides, iodine interaction, selenoamides, thioamides

Section of Inorganic and Analytical Chemistry, Department of Chemistry, University of Ioannina, 45110, Ioannina, Greece

B. Sener (ed.), *Innovations in Chemical Biology*, doi: 10.1007/978-1-4020-6955-0

Introduction

When di-iodine reacts with heterocycles like thioamides or selonoamides new "charge transfer" complexes containing iodine are obtained [1–10]. Various types of such complexes have been obtained thus far, including so called "spoke" or "extended spoke" structures ($DS{\cdot}I_2$ or $DS{\cdot}I_2{\cdots}I_2$) (D is the ligand donor) *[1]*. Also iodine coordinated to two thioamides to form "iodonium salts" ($[DS\text{-}I\text{-}DS]^{+}{\cdot}(I_3)^{-}$) [6] and monocations of formulae ($[DS\text{-}SDH]_2(I_3)^{-}$) *[4]* (DS or D=S, a thioamide ligand donor).

The interest in studying I_2 interaction with thioamides and selenoamides arise from their application in both biological chemistry and material sciences. Thus:

(i) Thioamides, like 6-*n*-propyl-thiouracil (**PTU**), N-methyl-imidazoline-2-thione (methimazole, **MMI**), 3-methyl-2-thioxo-4-imidazoline-1-carboxylate (carbimazole) (**CBZ**), are known anti-thyroid drugs [11] against hyperthyroidism (Grave's disease), a disease characterized by the overproduction of T4 and T3 hormones.

(ii) Iodine chemistry is recently proving to be of considerable interest, also in material sciences because of the discovery of low-temperature, semi- and superconducting polyiodides [12]. The ability of iodine to catenate, leads to the formation of polyiodides of various structures reviewed recently by P.D. Boyle et al., P. Deplano et al. and P. Svensson et al. [12–14].

In this paper, we briefly review the results of our work on the iodine interaction with the thioamides: benzothiazole-2-thione (**BZT**) (**1**), 6-*n*-propyl-2-thiouracil (**PTU**) (**2**), 5-chloro-2-mercaptobenzothiazole (**CMBZT**) (**3**), N-methyl-benzothiazole-2-thione (**NMBZT**) (**4**), benzimidazole-2-thione (**BZIM**) (**5**), thiazolidine-2-thione (**TZD**) (**6**), 2-mercapto-pyridine (**PYSH**) (**7**), 2-mercapto-nicotinic acid (**MNA**) (8), 2-mercapto-benzoic acid (**MBA**) (**9**) and 2-mercapto-pyrimidine (**PMT**) (**10**), selenoamides, derived from 6-*n*-propyl-2-thiouracil (**RSeU**) (R= Me- (**11**), Et- (12), *n*-Pr- (**13**) and *i*-Pr- (**14**)) and amides 2-hydroxy-pyridine (**PYOH**) (**15**) and 2-hydroxy-pyrimidine ($\mathbf{PMOH_2^{+}\ Cl^{-}}$) (**16**).

Synthesis of Thioamide-Diiodine Complexes

Charge Transfer Complexes with "Spoke" or "Extended Spoke" Structures

Reactions between di-iodine and the thioamides (**1**)–(**5**) lead to the formation of charge transfer (c.t.) complexes with the so called "spoke" or "extended spoke" structures ($DS{\cdot}I_2$ or $DS{\cdot}I_2{\cdots}I_2$) according to the general reaction shown in Scheme 13.1 [10].

Thus, reaction of di-iodine with (**1**), (**2**), (**3**) or (**4**) in a molar ratio 1:1 (I_2:L) results to the formation of c.t. complexes of formulae $[(BZT)I_2]$ (**17**) [1], $[(PTU)I_2]$ (**18**) [3], $[(CBZT)I_2]$ (**19**) [3] and $[(NMBZT)I_2]$ (**20**) [6] with spoke structures.

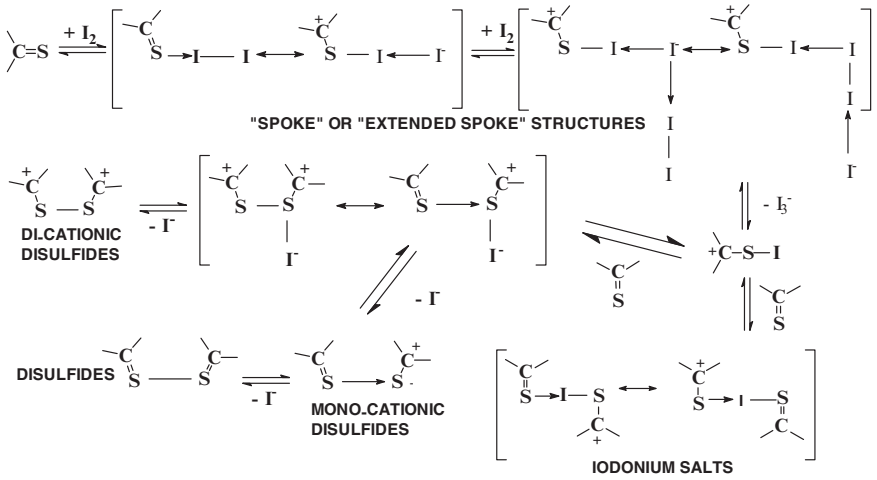

Scheme 13.1 Synthesis of thioamide-diiodine complexes **[14]**

Reactions of di-iodine with (**1**) or (**5**) in 2:1 (I_2:L) molar ratio form c.t. complexes of extended spoke structures with formulae [(BZT)I_2 I_2] (**21**) [1] and [(BZIM)I_2 I_2 H_2O] (**22**) [1].

The I-I bond distances are varying from 2.79 Å, in case of complexes with weak I–S interaction, to 3.08 Å, as a result of a strong I-S interaction. The corresponding I-I bond is subsequently elongated with respect to the corresponding distance in free I-I in the solid state (2.717 Å at 110 K). Bigoli et al. [10] has classified iodine adducts of sulfur donors into three classes, depending on I-I bond order (n). When $n \geq 0.6$ and d(I-I) < 2.85 Å the adduct is type **A** and when $n \leq 0.4$ and d(I-I) > 3.01 Å it is type **C**. Compounds with intermediate values were classified as type **B**. Thus, compounds (**18**) and (**20**) are classified to **A** type, compounds (**19**), (**21**) and (**22**) to **B** type, whereas compound (**17**) is of **C** type.

The S-I-I group has a linear structure with an angle of almost 180°. The N-C-S-I torsion angle is also found almost equal to 180° indicating an almost co-planar arrangement of the I_2 towards >C=S bond except the case of [(PTU)I_2] complex, where it is found to be –95.93°. In fact [(PTU)I_2] complex is the first c.t. complex with perpendicular arrangement of I_2 towards >C=S characterized by X-ray crystallography [3].

Iodonium Salt Complexes

Reaction between di-iodine and thioamides such as BZIM (**5**) **or** TZD (**6**) leads to the formation of iodonium salt complexes of [{$(TZD)_2I^+$}·I_3^-·$2I_2$] (**23**) and {[$(BZIM)_2I^+$}·I_3^-·{·[(BZIM)I_2]} (**24**) formulae according to the reaction in Scheme 13.1 [10].

The two I-S bond distances are 2.654(6) Å in (**23**) and in case of (**24**) they are 2.597(4) and 2.702(4) Å respectively. The I-I bond distance in I_3^- counter anions are found to be equal (I-I= 2.9195(14) Å) in case of (**23**). In case of (**24**) two types of I_3^- counter anions are observed, one is symmetric with I(1)-I(2)= 2.9300(12) Å while the other is not since it participates in hydrogen bonding (I(1A)-I(2A)= 2.880(6) and I(1A)-I(3A)= 3.058(5) Å respectively) and better described as I^-, interacting with I_2 ($I^-\ldots I_2$) [10]. The two hydrogen bonding interactions taking place between the I^+ and the hydrogen atoms of the amide nitrogen atoms (H[N]···I= 2.9336(6) Å) in case of (**23**) and I(11)…H-N(11) ″ of 3.20 Å in case of (**24**). *Ab initio* quantum mechanical methods and Density Functional Theory (DFT) techniques applied on the iodonium part of (**24**) suggested that the conformations obtained in the crystalline state result from an intermolecular electrostatic interaction between the positively charged iodine and the negatively charged NH group (total group (NH) charges calculated -0.005 e for N(11)″, -0.014 e for N(21)″, -0.004 e for N(13)″ and -0.012e for N(23)″ [6].

When (NMBZT) (**4**), reacts with di-iodine in the presence of $FeCl_3$ in a molar ratio of 3:6:1 (NMBZT: I_2: $FeCl_3$), complex $\{[(NMBZT)_2I]^+\}\cdot[FeCl_4]^-\}$ (**25**) together with $\{[(NMBZT)_2I^+\}\cdot[I_7]^-$ were formed [6]. The I-S bond distances are I-S= 2.5961(15) and 2.6596(14) Å, respectively, with an almost linear S-I^+-S arrangement (S-I-S= 177.77(5)^o)

Monocationic and Neutral Disulfides

The reaction of 2-mercaptopyridine (PYSH) (**7**), with di-iodine in a molar ratio of 1:2 led to the oxidation and dimerization of the ligand and produced $\{(PYS\text{-}PYSH)^+\cdot I_3^-\}$ (**26**). The structure of the compound consists of two residues, one cationic $(PYS\text{-}PYSH)^+$, containing the S-S bond linking the two 2-mercapto-pyridine molecules one of which is protonated and I_3^- as a counter anion. In the crystal lattice there are four symmetry-independent cation-anion pairs. There are only a few crystal structures reported in the literature containing open chain stable cations of DS-SD dimers, such as the monocationic: $\{[(C_4H_6N_2S\text{-}SN_2C_4H_5)_2\}^{2+}\cdot(I_3^-)\cdot(I_5^-)\}$ [15]. The two I-I bond distances of the I_3^- in the four components of complex (**26**) are 2.887(4) and 2.944(3) Å in component **a**, 2.874(4) and 2.957(3) Å in **b**, 2.968(3) and 2.862(3) Å in **c** and 2.855(4) and 2.927(3) Å in **d,** respectively, indicating a slight asymmetry of I_3^- in this complex (covalent linear asymmetric).

Moreover, when MNA (**8**), MBA (**9**) or PMT (**10**) react with di-iodine under the same experimental conditions as in the case of the preparation of complex (**7**) (see above), neutral disulfides were produced with formulae $[(MNA)_2]$ (**27**), $[(MBA)_2]$ (**28**) and $[(PMT)_2]$ (**29**) according to the reaction shown in Scheme 13.1.

Complex (**24**) isolated from the reaction of (**5**) and I_2, reveals the co-crystallization of both a “spoke” structure and an iodonium salt structure. This leads to the conclusion that an equilibrium as shown in Scheme 13.2, is established in solution.

Scheme 13.2 Equilibrium between "Spoke" strucutre and iodonium salt in solution

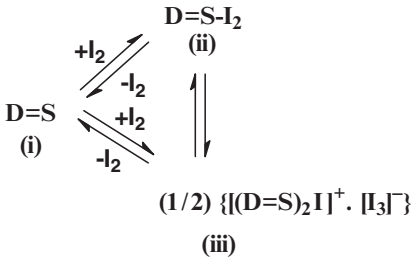

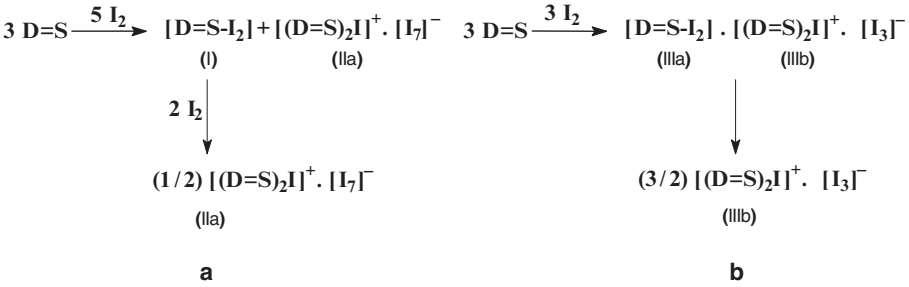

Scheme 13.3 Di-iodine - thione interactions detected by conductivity titrations

It has also been shown that the disproportionation reaction, with the generation of the ionic compound from thioamide-iodine complexes, exhibits pressure dependence [2]. A pressure increase, leads to the ionic iodonium salt (iii) from (ii) (Scheme 13.2). The favouring of $\{[MBZIM)_2I]^+ [I_3]^-\}$ (**24a**) formation, is also proven by computational studies, based on energetic grounds [6].

The conductivity measurements indicate that when di-iodine is added to a solution of BZIM (**5**) (D=S), initially both the neutral (**I**) and the ionic (**IIa**) compounds are formed as it is shown in Scheme 13.3A. Further addition of di-iodine results to the ionic complex (**IIa**). In the case of NMBZT (Scheme 13.3B) a cocrystallization of both the spoke and iodonium complexes takes place producing only the iodonium complex, in excess of I_2.

For the mechanism of action of anti-thyroid drugs the reaction scheme shown in Scheme 13.4 is followed.

Our results strongly indicate that the antithyroid drugs PTU (**2**) and N-Methyl-2-mercapto-imidazoline (MMI) have a different way of action. Thus, (**2**) together with NMBZT (**4**) forming weak S-I c.t. complexes (Table 13.1) may interfere either by inhibiting TPO activity or by inhibiting Deiodinase (ID-1) enzyme which is responsible for the formation of T3 from T4 hormone.

MMI, TZD (**6**), PYSH (**7**), PMT (**10**), MNA (**8**) and MBA (**9**) on the other hand that strongly bind to I_2 or are oxidized to disulfides [15] most probably interfere in the formation of mono-iodotyrosine (MIT), di-iodotyrosine (DIT) by the tyrosine residues of thyroglobuline Tyr(TG), competing with active iodine.

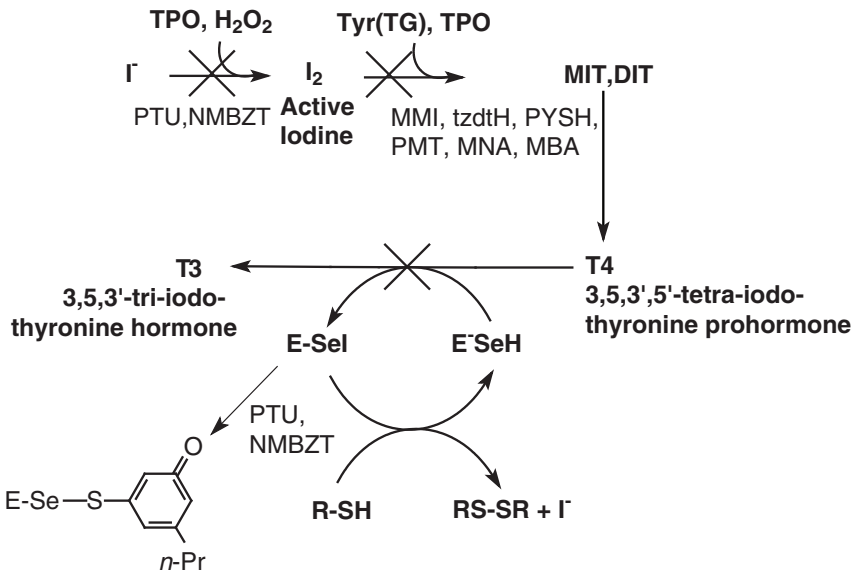

Scheme 13.4 General reaction scheme for the mechanism of action of anti-thyroid drugs

Table 13.1 d(S-I) vs d(I-I) data of some D-I2 "spoke" or D-I2-I2 "extended spoke" complexes.

Thioamide (D)	d(S-I)	d(I-I)	Bond order (n)	type
BZT	2.5870	2.9690	0.4449	B
BZT	2.7280	3.0770	0.3320	C
BZIM	2.5710	2.9890	0.4214	B
BZIM	2.6700	2.8869	0.5557	B
PTU	2.7805	2.8264	0.6546	A
CBZT	2.6337	2.9205	0.5073	B
NMBZT	2.8080	2.7912	0.7201	A

Synthesis of Selenoamide-Diiodine Complexes

Since thyroid de-iodinase contains selenocysteine [16], the seleno-analog of PTU (PSeU) is expected to exhibit a higher antithyroid activity than PTU, because of the easier formation of the Enzyme-Se-Se-PSeU species, than Enzyme-Se-S-PTU due to the higher nucleophilicity of Se. To examine this possibility we have extended our studies to the interaction of I_2 with selenoamides.

Reactions of alkyl-selenoamides with diiodine in a 1:1 molar ratio in dichloromethane solutions result in the formation of [(RSeU)I_2] [R= methyl-, ethyl-, *n*-propyl- and *i*-propyl-]. Complex [(*n*-PrSeU)I_2] (**30**) was found to be a charge transfer complex with a Se-I bond. The I-I interatomic distance of 2.8928(10) Å is longer than that in either the gas phase (2.677 Å) or crystalline diiodine (2.717 Å

at 110 K) presumably owing to the Se···I interaction. It is, however, the shortest such distance measured for a diiodine-selenoamide complexes suggesting a minimal perturbation resulting from the Se···I contact, which is the longest measured thus far [7].

The diselenides [*N*-(6-Et-4-pyrimidone)(6-Et-SeU)$_2$] (**31**) and [*N*-(6-*n*-Pr-4-pyrimidone)(6-*n*-Pr-SeU)$_2$] (**32**) were produced upon re-crystallization of [(*n*-PrSeU)I$_2$] (**30**) and [(n-EtSeU)I$_2$] (**33**) from acetone, as oxidation products. On the other hand deselenation with the formation of 6-*n*-propyl-2-uracil (n-Pr-U) (**34**) was observed when (**30**) was re-crystallized from methanol/acetonitrile solutions [7].

In conclusion, while 6-alkyl-2-selenouracil compounds (RSeU) are stable in various solvents, including water and other polar or non-polar solvents, "spoke" c.t. complexes of formulae [(RSeU)I$_2$] are formed in dichloromethane solutions, but are unstable in methanol/acetonitrile and/or acetone solutions. [(RSeU)I$_2$] is transformed to 6-alkyl-2-uracil in methanolic/acetonitrile solutions. Upon re-crystallization in acetone the diselenides are formed possibly through the formation of a substituted selenouracil as indicated by ^{1}H, ^{13}C NMR spectra and ESI-MS spectra. The whole process may be hydrolytic (Scheme 13.5).

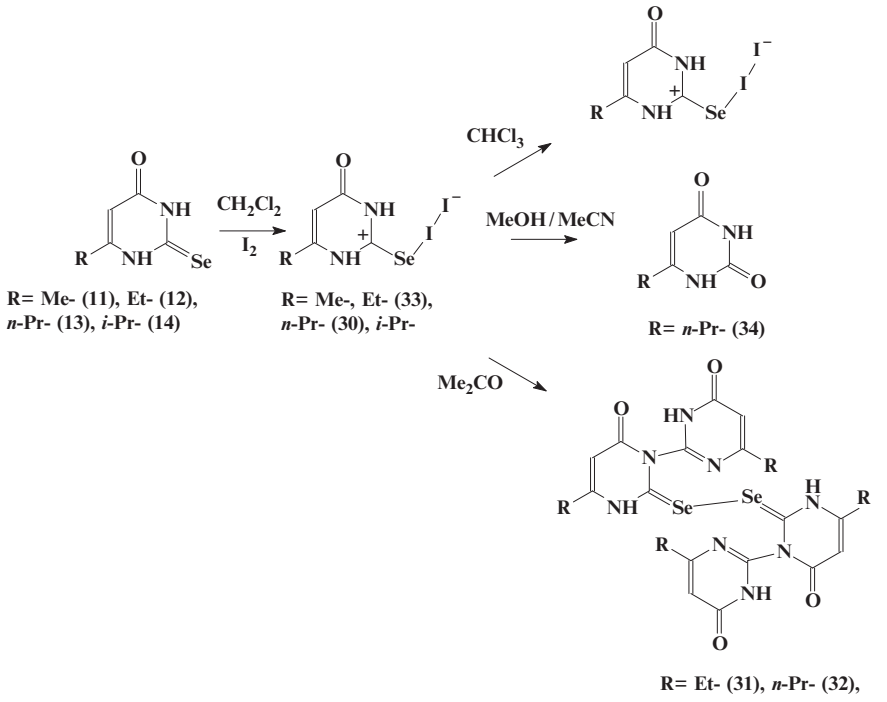

Scheme 13.5 Reactions of alkyl-selenoamides with diiodine

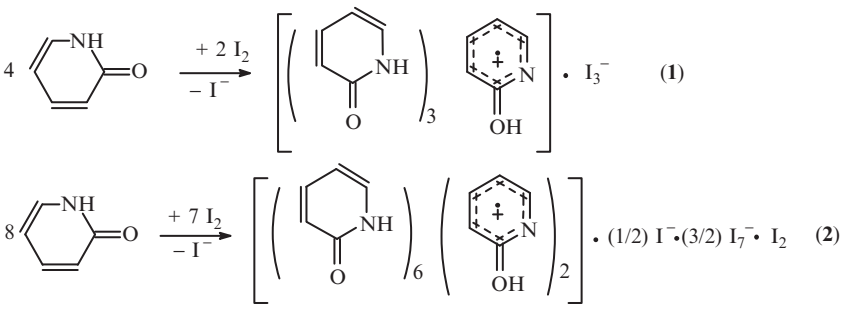

Scheme 13.6 Reactions of 2-pyridone (PYOH) with di-iodine

Synthesis of Amide-Diiodine Complexes

The reaction of 2-pyridone (PYOH) (**15**) with di-iodine in a molar ratio of 2:1 and 1:2 respectively resulted to the formation of $\{[(PYOH)_3[(PYOH)]^+ \cdot I_3^-\}$ (**35**) and $\{(PYOH)_6 \cdot [(PYOH)_2]^{2+} \cdot ((1/2)I^-) \cdot ((3/2)I_7^-) \cdot (I_2)\}$ (**36**) complexes (Scheme 13.6). In case of complex (**36**) the counter anions form a poly-iodine network.

The reaction of 2-pyrimidone ($PMOH_2^+ Cl^-$) (**15**) with di-iodine in a molar ratio of 1:1 resulted to the formation of $\{[LOH]^+Cl^-I_2\}$ (**37**) complex.

In conclusion, structures containing polyiodide anions, with cationic aromatic ligands as counter parts of formulae $\{[(L)(HL^+)] \cdot (I_n^-)\}$ are known to be synthesized by the treatment of the appropriate amide with HI [26–28]. In contrast, the complexes with PYOH, in the present case, were formed by the direct reaction of 2-hydroxypyridine with di-iodine in a molar ratio of 2:1 and 1:2. This is a redox reaction, where 2-hydroxy-pyridine firstly is oxidized to pyridinone-2 radical cation. In the case of 2-hydroxy-pyridine however, peroxide structures are not formed like disulphides in the case of PYSH. Polyiodide anions are simultaneously produced in this case This should be a consequence of redox differences between –SH and OH groups and may be proven a useful pathway for the synthesis of polyiodide materials.

References

1. Daga, V., Hadjikakou, S.K., Hadjiliadis, N., Kubicki, M., dos Santos, J.H.Z. and Butler, I.S., 2002, *Eur. J. Inorg. Chem.*, 1718–1728.
2. dos Santos, J.H.Z., Butler, I.S., Daga, V., Hadjikakou, S.K. and Hadjiliadis, N., 2002, *Spectrochim. Acta Part A,* **58,** 2725–2735.
3. Antoniadis, C.D., Corban, G., Hadjikakou, S.K., Hadjiliadis, N., Kubicki, M., Warner, S. and Butler, I.S., 2003, *Eur. J. Inorg. Chem.*, 1635–1640.
4. Antoniadis, C.D., Hadjikakou, S.K., Hadjiliadis, N., Kubicki, M. and Butler, I.S., 2004, *Eur. J. Inorg. Chem.*, 4324–4329.

5. Antoniadis, C.D., Hadjikakou, S.K., Hadjiliadis, N., Kubicki, M. and Butler, I.S., 2005, *New J. Chem.,* **29,** 714–720.
6. Corban, G.J., Hadjikakou, S.K., Hadjiliadis, N., Kubicki, M., Tiekink, E.R.T., Butler, I.S., Drougas, E. Kosmas, A.M., 2005, *Inorg. Chem.,* **44,** 8617–8627.
7. Antoniadis, C.D., Hadjikakou, S.K., Hadjiliadis, N., Papakyriakou, A., Baril, M. Butler, and I.S., 2006, *Chem. A Eur. J.,* **12,** 6888–6897.
8. Antoniadis, C.D., Blake, A.J., Hadjikakou, S.K., Hadjiliadis, N., Hubberstey, P., Schröder, M. and Wilson, C., 2006, *Acta Cryst. B.,* **B62,** 580–591.
9. Corban, G.J., Antoniadis, C., Hadjikakou, S.K., Hadjiliadis, N., Meng, J-F. and Butler, I.S., 2006, *Bioinorg. Chem. Appl., Article ID* **68542,** 1–5.
10. Hadjikakou, S.K. and Hadjiliadis, N., 2006, *Article ID* **60291,** 1–10.
11. Martindale, The Extra Pharmacopoeia, 28th edition, 1982 The Pharmaceutical Press, London.
12. Svensson, P.H. and Kloo, L., 2003, *Chem. Rev.,* **103,** 1649–1684.
13. Boyle, P.D. and Godfrey, S.M., 2001, *Coord. Chem. Rev.,* **223,** 265–299.
14. Deplano, P., Ferraro, J.R., Mercuri, M.L. and Trogu, E.F., 1999, *Coord. Chem. Rev.,* **188,** 71–95.
15. Aragoni, M.C., Arca, M., Demartin, F., Devillanova, F.A., Garau, A., Isaia, F., Lippolis, V. and Verani, G., 2002, *J. Am. Chem. Soc.,* **124,** 4538–4539.
16. Berry, M.J., Banu, L. and Larsen, P.R., 1991, *Nature,* **349,** 438–440.

Chapter 14
Catalytic Properties of Polyamido Dendrimers

Metin Tülü and Mehmet Şenel

Abstract PAMAM types polyether based dendrimers were synthesized from three branched Jeffamines®. Synthesized compounds bears metylester/*tert*-butylester, carboxylic acid or amine groups. In the synthesis iterative Micheal type of reaction paths were followed. Catalytic properties of the molecules were studied in homogenous phase.

Keywords Catalysis, dendrimer, dendritic Jeffamines, Micheal addition, PAMAM

Introduction

The Jeffamines® brand polyoxyalkyleneamines are a part of an ever-expanding family of Industrial chemistry. They contain primary amino groups attached to the terminus of a polyether backbone. They are thus "polyether amines." The polyether backbone is based either on propylene oxide (PO), ethylene oxide (EO), or mixed EO/PO. The Jeffamines® product family consists of monoamines, diamines, and triamines, which are available in a variety of molecular weights, ranging up to 5,000 g\mol. The wide range of molecular weights, amine functionality, oxide type and distribution provides flexibility in synthetic design of compounds made from Jeffamines® products. They are generally low viscos liquids, exhibiting low vapor pressure [1]. It is well known that poly(oxyethylene) POE or poly(oxypropylene) (POP) backbone incorporates with different materials so that new structure can change their properties [2] such as solubility, biocompatibility and kinetics. Moreover, polyethers having different molecular weight and bearing different functional groups such as amine or metal coordinated carboxylic groups can improve their conductivity and thermal stability [3]. Jeffamine® undergoes reactions [4] typical of primary amines. For example epoxy reactions occur by the non-catalyzed

Fatih University, Department of Chemistry, 34500 B. Çekmece, Istanbul, Turkey

B. Sener (ed.), *Innovations in Chemical Biology*, doi: 10.1007/978-1-4020-6955-0

Table 14.1 Catalytic activities of synthesized products

Products	Mw	Press. (H2, psi)	Free NH2	Iodine number	Cat. eff. (%)
SFO	0	0	0	154.82	0.00
SFO	0	2	0	154.82	0.00
SFO + 0	**3,000**	2	**0.25**	**144.67**	**6.56**
SFO + 1	3,606	2	0.00	152.28	1.64
SFO + 2	3,522	2	0.00	152.28	1.64
SFO + 3	**3,774**	**2**	**0.40**	**142.13**	**8.20**
SFO + 4	4,986	2	0.00	150.34	2.89
SFO + 5	4,818	2	0.00	150.35	2.89
SFO + 6	**5,322**	**2**	**0.56**	**139.22**	**10.07**
SFO + 7	7,768	2	0.00	148.64	3.99
SFO + 8	7,432	2	0.00	148.64	3.99
SFO + 9	**8,440**	**2**	**0.71**	**137.10**	**11.44**

addition of epoxides to Jeffamines® amines so that it alkoxylates each NH functionality to produce aminoalcohols, one another example is polyurea [5] linkages which are formed from the rapid uncatalyzed reaction of Jeffamines® amines with polyisocyanates. Substituted ureas are formed by heating Jeffamines® amines with urea at temperatures of 125–175C. while removing ammonia. Dendritic effects of Jeffamines® was also be studied [6]. The T-series products are propylene oxide based tri-amines which are prepared [7] by reaction of PO with a triol initiator, followed by amination of the terminal hydroxyl groups. This character is appropriate for the dendritic construction as a core.

In this work as a starting material, Jeffamine® which bears three terminal amino groups were selected, since it has great interior void and flexible terminal group with hydrophilic character. This group could be modified with methylacrylate and then hydrolyzed from the esteric groups so that it was aimed to coordinate with metals. By using excess amount of ethylene diamine esteric hyperbranched molecules converted again to amine terminated dendrimer. This step was repeated several times to obtain up to third generation esteric, acidic and amine functionalized dendrimer. After purification and characterizations of new macromolecules via NMR and FT-IR catalytically studies were performed (Table 14.1).

Experimental

Methylacrylate and ethylenediamine were obtained from the Merck. Jeffamine® T-3000 was purchased from Texaco Chemical Company. Other chemicals were used as obtained from the Fluka without further purification unless otherwise noted. Solvents were dried and distilled according to literature procedures prior to use. Reactions were controlled by thin layer chromatography (TLC) on silica gel 60 F254 and spots were detected either by UV-visible light or by charging with I_2 vapor.

Instrumentations

^{1}H NMR and ^{13}C NMR spectra were recorded on a NMR using an Inova 500 MHz Varian system spectrometer for solutions in $CDCl_3$. Multiplicities are described using the following abbreviations: s = singlet, d = doublet, t = triplet, q = quartet, m = multiplet, br = broad and bs = broad singlet. FT-IR spectra were recorded on Mattson Satellite spectrophotometer in the range of 400–4,000 cm^{-1} (abbreviations: m, s, br and w). Some of the important spectra were given behind the procedure as a numeric value and full spectrum were given at appendices.

Synthesis of Jeff-Hexacarboxylate 1

The way for the synthesis of dendritic product **1** from Jeffamine® was outlined in Scheme 14.1 and abbreviated as Jeff-$(CO_2Me)_6$. It was synthesized by Micheal addition reaction under mild condition [8] modified from [9] (Scheme 14.1). After the purification it was hydrolyzed in the presence of formic acid to generate the jellowish oil Jeff-hexacarboxylic acid [10] Jeff-$(CO_2H)_6$ with a yield of 98%, confirmed by the appearance of the typical IR band of hydroxyl group at 3,480 cm^{-1} and disappearance of ^{13}C NMR resonance methyl peaks at δ 55.2. Jeff-hexamine Jeff-$(CONH(CH_2)_2NH_2)_6$ [11] **3** was synthesized from the **1** by using tenfold excess amount of ethylene diamine under mild conditions at relative high yield (93%). Formation of first generation pamam dendrimers (Scheme 14.2) was confirmed with the appearance of new broad amine peak at 3,347 cm^{-1} in the FT-IR spectra. This result was also correlated with ^{13}C NMR by again appearance of methyl amine at 41.0 ppm.

By applying general procedure A. B and C three class nine different dendrimers (1, 2, 3, 4 [12], 5 [13], 6 [14], 7 [15], 8 [16], 9 [17]) were synthesized. Each class of molecules we came up to third generation (Scheme 14.3) and characterized.

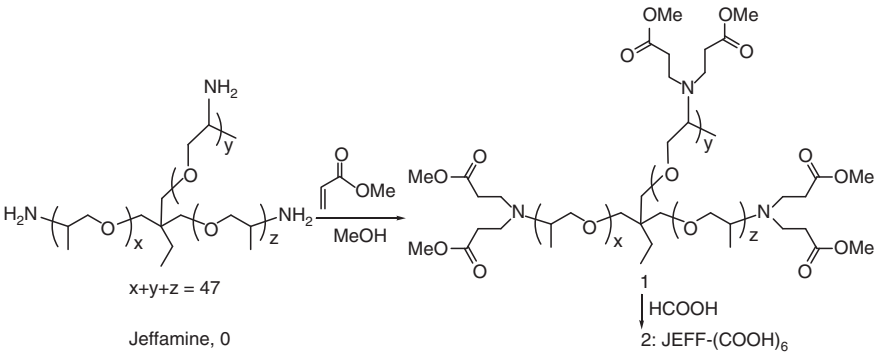

Scheme 14.1 Acrylation of Jeffamine and corresponding acid (Jeff-$(CO_2Me)_6$ and Jeff-$(CO_2H)_6$)

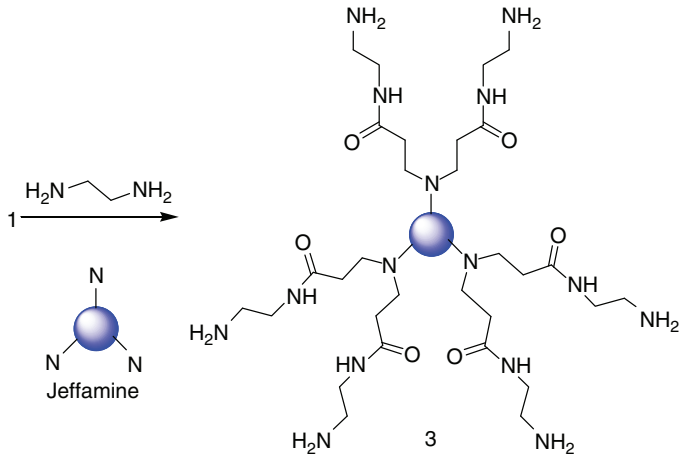

Scheme 14.2 Synthesis of first generation PAMAM **3** from the **1**

Yield optimization of the all kinds of products through from 1 to 9 required high temperatures and long reaction times. Naturally with increasing the generation the nucleophilicity of amines or acrylic groups were decreased, this could be explained according to three main reasons: (i) effect of steric hindrance, (ii) the presence of methyl substitution next to the amine in PPO might have negative effect on reactivity comparative to simple aliphatic amines, and finally (iii) intra and intermolecules interactions caused by hydrogen bond formation. Since all the chains contain ether group, namely strong H-acceptor could be also responsible for the decrease of the amine nucleophilicity.

Catalytical Studies

Catalytical studies of synthesized products were tested according to the Hanus Method [18]. Since Triglycerides (fats and oils) are esters of glycerol with three fatty acids. These long chain fatty acids may contain one or more double bonds. With no double bonds, the fatty acid is termed saturated (with hydrogen), and with double bonds, it is termed unsaturated. The iodine number is an indication of the degree of unsaturation of the oil (Scheme 14.4).

In this work, halogens were added across the double bonds of unsaturated fatty acids (commercial available sunflower oil) to form addition compounds and the degree of uptake was measured. A measured excess of iodine monobromide (IBr) was allowed to react with the oil in the dark. At the end of a timed period, an excess of KI was added to convert the remaining IBr to I_2. The I_2 formed was then titrated with standard thiosulfate. This was a back-titration method. A back-titration blank was also required, where the sample was omitted. The uptake of iodine was calculated

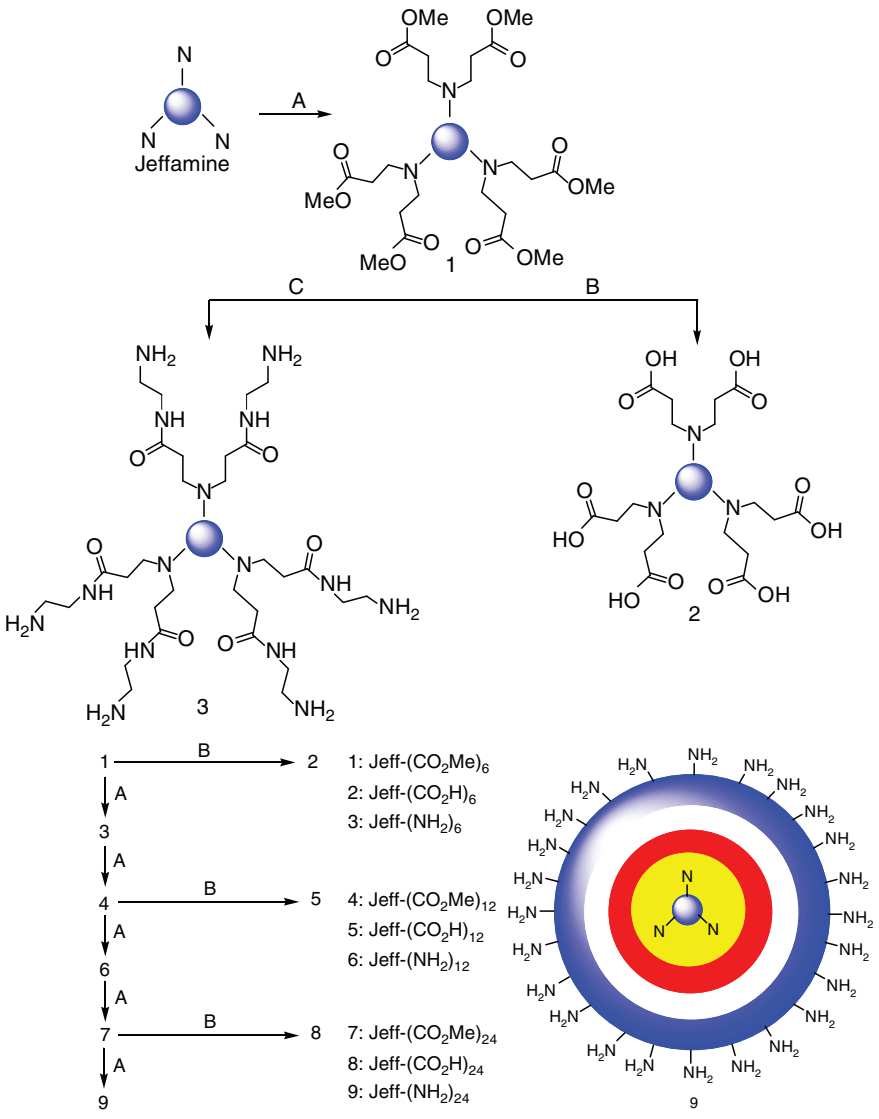

Scheme 14.3 Compounds derived from the Jeffamine® T-3000

from the difference between the blank and the back-titration volumes. We have noted that the titrant did not react directly with the analyte. This was an indirect Iodine method. I_2 was generated from excess reagent in the second step and this I_2 was titrated by the standard thiosulfate solution in the third step. The Iodine number is defined as the number of grams of iodine taken up by 100 g oil (g I/100 g oil).

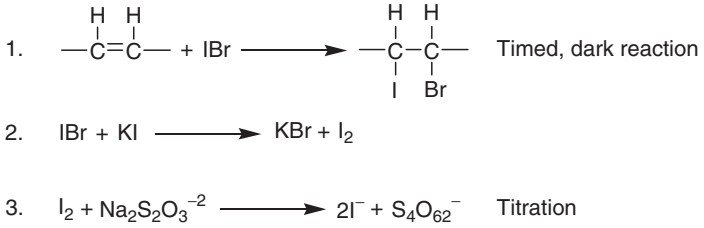

Scheme 14.4 Halogenation of double bonds

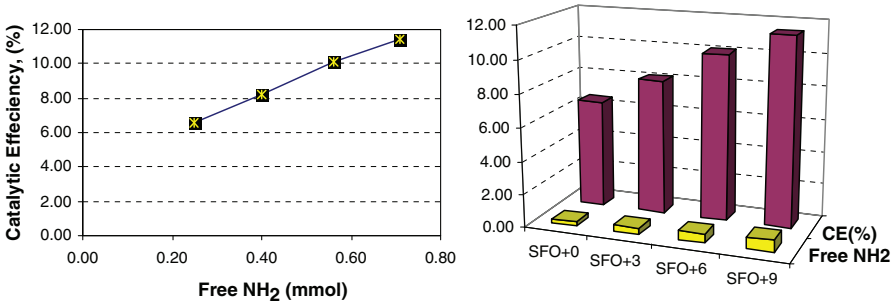

Fig. 14.1 The relationship between free amines and catalytical efficiency

Application

In order to prepare Hanus-iodine solution, 13.2 g of iodine was dissolved in 1,000 ml of glacial acetic acid the solution was gently heated to dissolve completely, then cooled to room temperature. To determine the iodine content 25,00 ml portion of solution was titrated with 0.1 N sodiumthiosulfate, later added to the remainder of the solution a quantity of bromine equivalent to that of iodine present, and entire solution was kept in dark. According to procedure [11] described above the iodine number of oil solution was determined before and after using polyamido dendrimers as catalysts. In order to test the catalytic effect of dendrimers, equal amount of Jeffamine® and the products **1, 2, 3, 4, 5, 6**, **7, 8, 9** were used separately. Two hundred and fifty milligrams of each products were mixed with 5 g of sun flower oil in DCM, then under 2 psi of H_2 atmosphere the solution was stirred in rector for 2 h. The degree of unsaturation results were listed in Table 14.1 and figured out in Fig. 14.1

Conclusion

We have described a straightforward method for the synthesis of three directional ester, carboxylic acid and amine terminated Dendritic molecules from Jeffamine® all of the products were soluble in most of the organic solvents, In addition,

carboxylic acid and amine terminated products were water soluble. This physical property has provided a great advantage in the purification. All the products and sunflower oil were soluble in dichloromethane that's why catalytical studies were quite facile in homogenous phase. The progress of hydrogenation process was strongly dependent on the number of free amines. From Table 14.1 it was clearly seen that only the free primary amine groups has been involved into catalytic activities, and there is a liner relationship between increasing the free amino groups and catalytical efficiency up to third generation. However, there was a slight deviation from linear curve after the second generation (Fig. 14.1), it was expected that this deviation would be greater with increasing the generations, it could be explained with respect to the steric hindrance.

Acknowledgements This work was financially supported by Fatih University Scientific Research Projects Coordination Department, Istanbul Turkey and Turkish Prime Ministry State Planing Organization (DPT), we thank Professor Peter Eilbracht, Dortmund University for the helpful discussion and Dr. Bayram Cakir, Bochum University, Germany for providing NMR opportunities.

References

1. Froimowicz, P., Gandini, A. and Strumina, M., 2005, *Tetrahedron Lett.,* **46,** 2653–2657.
2. Meador, M., Cubon, V., Scheiman, D. and Bennet, W., 2003, *Chem. Matter.,* **15,** 3018–3025.
3. Sung-Tso, L. 2006, *Nanotechnology,* **17,** 3197–3203.
4. http://www.huntsman.com
5. Perez, Jr., A. and Johnston, J. A., Performance and processing enhancements of aromatic polyurea elastomer systems prepared from high 2,4'-MDI isocyanates, presented at *Polyurethanes Conference*, 2000, October 8–11.
6. Chow, H., Leung, C. H., Wang, G. and Yang, Y. C. R., *Chimine,* 2003, **6,** 735–745.
7. Nithianandam, V. S. *J.* and Erhan, S., *Appl. Polym. Sci.,* 2003, **42,** 2385–2389.
8. **General Procedure A (esterification of amine) 1:** A 50 wt% methanol solution of methyl acrylate (17 g, 0.2 mol) was added to the methanolic solution of Jeffamine® T-3000 (100 g, 0.033 mol). This reaction was allowed to stir at room temperature under a nitrogen atmosphere for 48 h. The reaction was then heated to 50°C for 1 h. methanol and excess methyl acrylate were removed by rotary evaporator. After the dialysis using membrane filter with a MWCO of 3 D in methanol, the product was obtained as a yellow viscous oil (6 g, 98%). ^{1}H NMR ($CDCl_3$, δ), 1.11 (q, OCH_2CH_2O), 2.39 (t, NCH_2CH_2COO, 6H), 2.76 (m, NCH_2CH_2COO, 6H), 3.63 (s, OCH_3, 18H). ^{13}C NMR ($CDCl_3$, δ), 17.2, 17.40 (OCH_2CH_2O), 34.50 (NCH_2CH_2COO), 51.40 (NCH_2CH_2COO), 55.20 (OCH_3), 173.00 ($COCH_3$). IR (neat) cm^{-1}: 1736 (ester C=O), 1107 (ester C–O).
9. Beezer, A. E., King, A. S. H., Martin, I. K., Mitchel, J. C., Twyman, L. J. and Wain, C. F., *Tetrahedron,* 2003, **59,** 3873–3880.
10. **General Procedure B (converting the ester to the acid) 2:** A solution of **1** (3.5 g, 0.1 mmol) in formic acid (20 ml) was stirred for 12 h. The formic acid and hydrolyzed esteric groups were removed by rotary evaporator; The aqueous solution of **2** was dialysed (3 D, MWCO membrane). The oily product was obtained quantitatively (3.45 g, 98%). ^{1}H NMR ($CDCl_3$, δ), 1.11 (q, OCH_2CH_2O), 2.65 (m, NCH_2CH_2COO, 6H and NCH_2CH_2COO, 6H), 8.18 (s, CO_2H, 6H). ^{13}C NMR ($CDCl_3$, δ), 17.11 (OCH_2CH_2O), 31.30 (NCH_2CH_2COO), 50.40 (NCH_2CH_2COO), 171.00 ($COOH$). IR (neat) cm^{-1}: 3,480 (br, OH), 1,730 (acid C=O).

11. **General Procedure C (PAMAM formation) 3:** Ethylenediamine (1 g, 18 mmol) was mixed with 20 ml of methanol and a 50% (w/w) methanol solution of **1** (1 g, 0.3 mmol) was added with stirring. The reaction was allowed to proceed under a nitrogen atmosphere at room temperature for 5 days, followed by heating at 50°C for 5 h. Excess ethylenediamine and methanol were removed by rotary evaporation. The remaining ethylenediamine was removed by azeotroping mixture using a 3/1 toluene/methanol. The product **3** as a viscous yellow oil was obtained after removing volatiles by high vacuum and dialyzing with membrane filter, MWCO of 3.0 D in water (13 g, 93% yield). ^{1}H NMR ($CDCl_3$, δ), 1.09 (q, OCH_2CH_2O), 2.31 (m, NCH_2CH_2CO, 12H), 2.63 (m, $NHCH_2CH_2N$, 12H), 2.76 (t, NCH_2CH_2CO, 12H), 3.23 (t, $NHCH_2CH_2N$, 12H), 4.79 (bs, NH_2, 12H), 7.02 (bs, $CONHCH_2$, 6H). ^{13}C NMR ($CDCl_3$, δ), 17.30 (OCH_2CH_2O), 35.00 (NCH_2CH_2CO), 41.00 ($NHCH_2CH_2N$), 44.00 (NCH_2CH_2CO), 46.00 (NCH_2CH_2CO), 173.00 ($CONH$). IR (neat) cm^{-1}: 3,347 (br, NH), 1,571 (amide C=O).
12. *The product* **4** *was synthesized according to General Procedure A except reactiontime:* A 50 wt% methanol solution of methyl acrylate (34 g, 0.4 mol) was added to the methanolic solution of **3** (92.5 g, 0.025 mol). This reaction was allowed to stir at room temperature under a nitrogen atmosphere for 5 days. The reaction was then heated to 50°C for 1 more day. Rotary evaporator was used to remove methanol and excess methyl acrylate. The product was obtained as a yellow viscous oil after removing volatiles by high vacuum and dialyzing with molecular weight cutoff, 3,500 (MWCO=3.5 D) in methanol, the purity of product was correlated via TLC (6 g, 88% yield). ^{1}H NMR ($CDCl_3$, δ): 1.09 (q, OCH_2CH_2O), 2.40 (t, NCH_2CH_2CO. 30H), 2.50 (t, $NHCH_2CH_2N$ 12H), 2.72 (μ, NCH_2CH_2CO, 30H), 3.23 (t, $NHCH_2CH_2N$, 12H), 3.63 (s, OCH_3, 36H), 7.15 (bs, $CONHCH_2$ 6H). ^{13}C NMR ($CDCl_3$, δ): 17.4 (OCH_2CH_2O), 32.6 (NCH_2CH_2CO), 49 ($NHCH_2CH_2N$), 51.5 (NCH_2CH_2CO), 52.2 (OCH_3), 172.9 ($COCH_3$). IR (neat) cm^{-1}: 3,440 (NH), 1,728 (ester C=O), 1,663 (amide C=O), 1,102 (ester C–O).
13. *The product* **5** *was synthesized according to General Procedure B*. A solution of **4** (4.7 g, 0.1 mmol) in formic acid (30 ml) was stirred for 12 h. After removing formic acid and methanol by rotary evaporator oily product was dialyzed with MWCO of 3.5 D in water and obtained quantitatively (4.4 g, 100%). ^{1}H NMR ($CDCl_3$, δ): 1.05 (q, OCH_2CH_2O), 2.6 (m, NCH_2CH_2CO, 30H and $NHCH_2CH_2N$, 12H), 2.75 (μ, NCH_2CH_2CO, 30H). 3.10 (t, $NHCH_2CH_2N$, 12H), 8.16 (bs, $CONHCH_2$, 6H), 9.97 (s, CO_2H, 12H). ^{13}C NMR ($CDCl_3$, δ): 16.95 (OCH_2CH_2O), 29.55 (NCH_2CH_2CO), 49.00 ($NHCH_2CH_2N$), 52.00 (NCH_2CH_2CO), 172.00 ($COOH$). IR (neat) cm^{-1}: 3,438 (br, NH and OH), 1,731 (acid C=O), 1,664 (amide C=O).
14. *The product* **6** *was synthesized according to General Procedure C:* Ethylenediamine (1 g, 18 mmol) was mixed with 20 ml of methanol and a 50% (w/w) methanol solution of **4** (2 g, 0.04 mmol). The reaction was allowed to proceed under a nitrogen atmosphere at room temperature for 10 days, followed by heating at 50°C for 2 days. Excess ethylenediamine and methanol were removed by rotary evaporator. The remaining ethylenediamine was removed by azeotrping using a 3/1 toluene/methanol mixture. The oily product was dialyzed with membrane filter of MWCO of 5 D in water (1.8 g, 84%). ^{1}H NMR ($CDCl_3$, δ): 1.11 (q, OCH_2CH_2O), 2.34 (m, NCH_2CH_2CO, 36H), 2.64 (m, $NHCH_2CH_2N$. 36H), 2.78 (t, NCH_2CH_2CO, 36H), 3.26 (t, $NHCH_2CH_2N$, 36H), 4.87 (bs, NH_2 24H), 7.02 (bs, $CONHCH_2$, 18H). ^{13}C NMR ($CDCl_3$, δ): 17.30 (OCH_2CH_2O), 34.30 (NCH_2CH_2CO), 44.00 ($NHCH_2CH_2N$), 45.00 (NCH_2CH_2CO), 46.30 (NCH_2CH_2CO), 173.00 ($CONH$). IR (neat) cm^{-1}: 3,360 (NH), 1,644, 1,559 (amide C=O).
15. *The product* **7** *was synthesized according to General Procedure A except reaction time:* A 50% (wt/w) methanol solution of methyl acrylate (17 g, 0.2 mol) was added to the methanolic solution of **6** (21 g, 42 mmol). This reaction was allowed to stir at room temperature under a nitrogen atmosphere for 2 weeks. The reaction was then heated to 50°C for 2 days. Rotary evaporation under vacuum was used to remove methanol and excess methyl acrylate. The oily product was dialyzed with membrane filter of MWCO of 5 D in water (8 g, 88%). ^{1}H NMR ($CDCl_3$, δ): 1.11 (q, OCH_2CH_2O), 2.42 (t, NCH_2CH_2CO, 84H), 2.52 (t, $NHCH_2CH_2N$. 36H), 2.74 (m, NCH_2CH_2CO, 84H), 3.26 (m, $NHCH_2CH_2N$, 36H). 3.65 (s, OCH_3. 72H), 7.15 (bs, $CONHCH_2$, 18H). ^{13}C NMR ($CDCl_3$, δ): 17.20 (OCH_2CH_2O), 32.50 (NCH_2CH_2CO), 49.00 ($NHCH_2CH_2N$),

51.00 (N*C*H_2CH$_2$CO), 52.00 (OCH$_3$), 172.00 (*C*OCH$_3$), 174.00 (*C*ONH). IR (neat) cm^{-1}: 3,308 (NH), 1,735 (ester C=O), 1,653 and 1,543 (for two amides C=O), 1,045 (ester C-O).

16. *The product* **8** *was synthesized according to general procedure B:* A solution of **6** (7.1 g, 0.1 mmol) in formic acid (20 ml) was stirred for 12 h. After removing formic acid and methanol by rotary evaporator The oily product was dialyzed with membrane filter of MWCO of 5 D in water (6.8 g, 95%). ^{1}H NMR (CDCl$_3$, δ): 1.11 (q, OC*H*$_2$C*H*$_2$O), 2.50 (t, NCH$_2$C*H*$_2$CO, 84H), 2.66 (t, NHCH$_2$C*H*$_2$N, 36H), 2.85 (m, NC*H*$_2$CH$_2$CO, 84H), 3.33 (m, NHC*H*$_2$CH$_2$N, 36H), 8.23 (bs, CON*H*CH$_2$, 18H), 8.31 (s, CO$_2$*H*, 24H). ^{13}C NMR (CDCl$_3$, δ): 17.00 (O*C*H$_2$*C*H$_2$O), 31.50 (NCH$_2$*C*H$_2$CO), 49.00 (NH*C*H$_2$*C*H$_2$N), 51.00 (N*C*H$_2$CH$_2$CO), 172.00 (*C*OOH), 173.00 (*C*ONH). IR (neat) cm^{-1}: 3,426 (br, NH and OH), 1,726 (acid C=O), 1,660 and 1,588 (for two amide C=O).
17. *The product* **9** *was synthesized according to General Procedure C:* Ethylenediamine (1 g, 18 mmol) was mixed with 20 ml of methanol and a 50% (w/w) methanol solution of ***7*** (2 g, 0.03 mmol). The reaction was allowed to proceed under a nitrogen atmosphere at room temperature for 14 days, followed by heating at 50°C for 2 days. Excess ethylenediamine and methanol were removed by rotary evaporation under vacuum. The remaining ethylenediamine was removed by dialysis (Spectra/Por MWCO of 5D) and The product was a viscous yellow oil (1.5 g, 70% yield). ^{1}H NMR (CDCl$_3$, δ): 1.11 (q, OC*H*$_2$C*H*$_2$O), 2.33 (m, NCH$_2$C*H*$_2$CO, 84H), 2.63 (m, NHCH$_2$C*H*$_2$N, 84H), 2.78 (t, NC*H*$_2$CH$_2$CO, 84H). 3.25 (t, NHC*H*$_2$CH$_2$N, 84H), 7.02 (bs, CON*H*CH$_2$, 18H), ^{13}C NMR (CDCl$_3$, δ): 17.30 (O*C*H$_2$*C*H$_2$O), 34.00 (NCH$_2$*C*H$_2$CO), 41.00 (NH*C*H$_2$*C*H$_2$N), 44.00 (N*C*H$_2$CH$_2$CO), 49.00 (N*C*H$_2$CH$_2$CO), 173.00 (*C*ONH). IR (neat) cm^{-1}: 3,347 (NH$_2$), 1,643 and 1,566 (for two amides C=O).
18. M.,Yasuda J. Bio. Chem., 1931, 401–409.

Chapter 15
Swell Ratio Parameter for Prediction of Chemically Crosslinked Low Density Polyethylene Foam Expansion Characteristics

Coswald Stephan Sipaut [1] and Geoff L. A. Sims [2]

Abstract Chemically crosslinked Low Density Polyethylene (LDPE) foam formation with traditional crosslinking system using Dicumyl Peroxide (DCP) alone and with the introduction of polyfunctional monomer, triallycynurate (TAC) is investigated. Samples were characterized as a function of relative concentration of DCP and DCP with TAC in solid and foamed states. It is shown that the introduction of TAC monomer in the crosslinking system provides higher crosslinking level than DCP alone. The addition of TAC monomer also showed significant reduction in DCP concentration to obtain similar crosslinking level. Foam density indicates that traditional parameter i.e. gel content to predict foam expansion is not suitable parameter when polyfunctional monomer is introduced into the system. Swell ratio which is crosslink density dependent is more suitable parameter to predict LDPE foam expansion characteristics. The results also showed that at a similar value of swell ratio either using DCP alone or with the addition of TAC into the system, give similar foam expansion characteristics i.e. similar foam density, cell size and foam mechanical properties.

Keywords Crosslinked, foam formation, low density polyethylene, swell ratio parameter

Introduction

In the manufacturing of crosslinked polyolefin foam, the foam expansion and cell stabilization highly dependent on the degree of crosslinking. It has been reported that at higher crosslinking level the foam produce have higher density [1, 2].

[1] School of Chemical Sciences, Universiti Sains Malaysia, 11800, Penang, Malaysia
[2] Manchester Materials Science Centre, UMIST and University of Manchester, Grosvenor Street, Manchester M1 7HS, UK

B. Sener (ed.), *Innovations in Chemical Biology*, doi: 10.1007/978-1-4020-6955-0

Mechanical properties of the based polymer and cell structure which includes cell size, cell shape also play a significantly roles in foam properties [3–5]. The properties of crosslinked material can be varied with the degree of crosslinking [1–4, 6]. The assessment of the degree of crosslinking formed in the polymeric system is important to predict or correlate with the foam properties (i.e. foam density). There are a few methods to assess the crosslinking level in the polymer depending on the type of the polymer. For polyolefin base materials, the measurement of gel content and melt modulus are often employed to predict the foam density [1, 7, 8]. The principle of determination of degree of crosslinking involves of controlling the process and rating the quality of final product. Gel content determination is the one of the normally used method for measuring the content of gel (insoluble fraction) produced in crosslinked ethylene plastic after extracting with solvent [6, 8]. Another method to determine the degree of crosslinking in a polymer (i.e. composite) is swell ratio measurements. In this method, the correlation between gel content and network density can be predicted with the determination of swell ratio of the crosslinked composite in hot p-xylene [9]. So far the correlation between swell ratio and foam expansion characteristic is not yet been conducted. It has been reported that triallylcyanurate (TAC), have the propensity to promote crosslinking. However, the foam produced using TAC system compared to traditional system i.e. using peroxide alone did not give similar foam density at similar gel content [6]. Therefore this paper investigates the effect of incorporating TAC in DCP-based crosslinking system over a broader range of formulations as a function gel content melt modulus and swell ratio in an attempt to find a suitable physical parameter to better judge foam density and correlate with foaming behaviour.

Experimental

Materials

Base polymer used was LDPE Stamylan 1808 supplied by DSM with a density of 918 kg m^{-3} and melt flow index of 8 dg min^{-1}. Dicumyl peroxide (DCP) was selected as crosslinking agent. Formulations were investigated using a range of DCP concentrations up to 1.0 phr (parts per hundred resin). Polyfunctional monomers used was triallyl cyanurate (TAC) supplied by Degussa. Concentrations in the range 0.025–5.0 phr were used. The chemical blowing agent used was DP45/1, manufactured by Bayer AG at a fixed concentration of 8.0 phr.

Sample Preparation

Mixing was conducted on a thermostatically controlled, electrically heated two-roll mill. Compounding temperature and time mixing of component of LDPE, DCP,

TAC and DP45/1 as detailed in previous paper [6]. Crosslinked matrix samples were prepared by compression moulded of 45 g of compounded samples in a square plate with a thickness of 1.5 mm for 20 min. The mould was then water-cooled to 30°C under pressure. Foaming was carried out by a two stage heat and chill process using pre-heated 10 mm deep mould. After compounding, the foamable samples were compression moulded at 14 MPa for 20 min at 165°C and cooled under pressure to 30°C. The partially expanded moulding was then immediately transferred to a circulating hot air oven at 130°C for 20 min to gradually complete the expansion.

Solid Matrix Characterisations

Gel content was determined by refluxing in a stainless-steel mesh cage in boiling xylene for 24 h according to ASTM D2765-01. Melt tensile behaviour of the solid crosslinked matrix was performed in an Instron tensile testing machine fitted with an environmental chamber at 130°C (the final expansion temperature in the heat and chill process) to assess expansion resistance. The gauge length was set at 30 mm and the crosshead speed at 20 mm min^{-1} where sample were conditioned for 10 min before commencing the test. Swell ratios were determined in accordance with standard procedure detailed in ASTM D2765-01.

Foam Characterisations

Foam density was determined from the weight and volume of regular parallelepiped samples (50 x 50 x 20 mm) free of skin, voids or other irregularities. Cell size determination was conducted using Scanning Electron Microscope (SEM) images. The mean apparent cell size was obtained from SEM images by a modified cell count per unit length method described elsewhere [3]. Foam compression properties were performed using Instron Universal Testing Machine fitted with a compression cage at a crosshead speed of 20 mm min^{-1} and compressing the samples to 80% of their original thickness. Parallelepiped specimens (free of defects and skins) 50 x 50 mm with an average thickness of 20 mm were cut from bulk foamed samples.

Results and Discussion

Various workers [2, 7] suggested that increasing either gel content (above 50%, which is typical for foam manufactures) or melt modulus results in increased in foam density. Figures 15.1 and 15.2 for systems containing DCP alone and in the

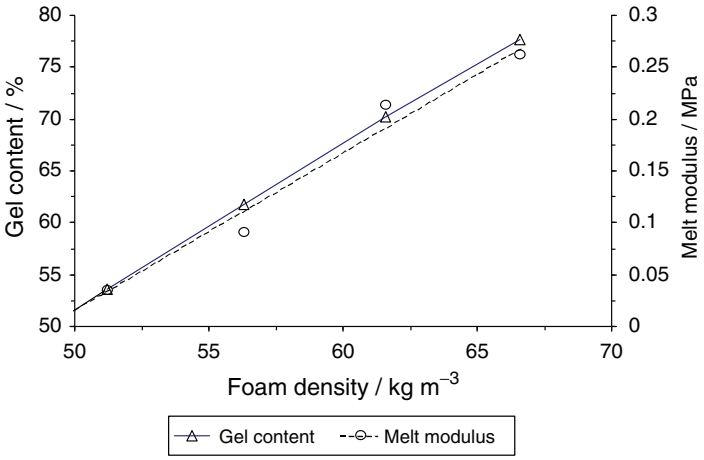

Fig. 15.1 Effect of gel content and melt modulus on foam density (1808)

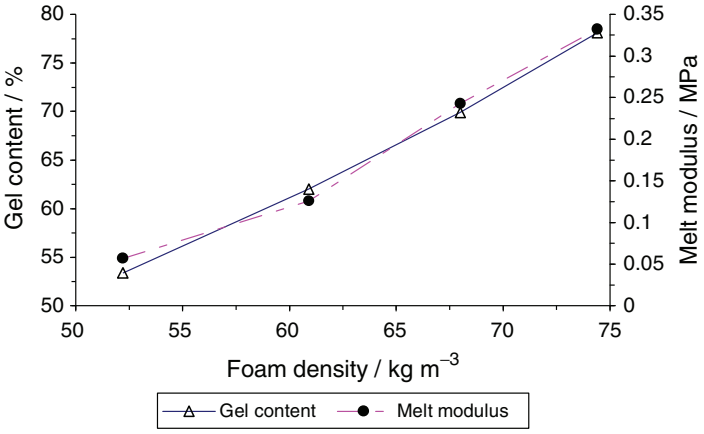

Fig. 15.2 Dependence of foam density on gel content and melt modulus for samples containing varying concentrations of DCP and a TAC concentration fixed at 0.5 phr

presence of a fixed 0.5 phr TAC (i.e. increasing DCP concentration) respectively. The results indicated that foam density have an approximately linear relationship with gel content and melt modulus. Increasing gel content or melt modulus resulted in increased in foam density. This suggested that increasing degree of crosslinking resulted in increased resistance to expansion by increase in melt strength of the polymer matrix, which is line with the work by other researcher [4, 7]. However, they also claimed that either gel content or melt modulus could be used to defined foam density using system containing LDPE crosslinked with DCP. Both this parameters were investigated separately.

Foam Density of Similar Gel Content

Foam densities in a range of formulations (with and without polyfunctional monomer, TAC) giving gel contents of approximately 62%, 70% and 77.5% is shown in Fig. 15.3. Generally, within the limits of experimental error, at any specific gel content, the higher the TAC concentration, the higher the foam density. The results also showed that when using DCP alone or with 0.5 phr TAC, an approximately linear response was observed between foam density and gel content. In the presence of 2.0 phr TAC, the slope of the curve up to approximately 70% gel content is similar to DCP alone. However, at higher gel contents, the slope appears to divergently increase (compared with DCP alone).

This suggested that gel content is not a suitable parameter to define foam behaviour when TAC is introduced into the system. The foam density increases with increasing TAC tends to suggest increasing TAC at any specific DCP concentration seemed to give higher crosslink density. This in turn would explain the increases in melt modulus (restricting cell expansion and limiting foam density reduction) with increasing TAC concentration as indicated in Fig. 15.4.

Foam Density Against Melt Modulus

Figure 15.5 gives a wealth of information. It is important to understand that each series of three separate results at each nominal gel content represents an adjustment in DCP concentration to give the nominal gel content in the presence of 0, 0.5 and 2.0 phr TAC (increasing TAC concentration produces progressive increase in melt modulus and foam density). Result positively indicates that gel content is not a suitable indicator to predict foam density (as previously suggested). However, if all

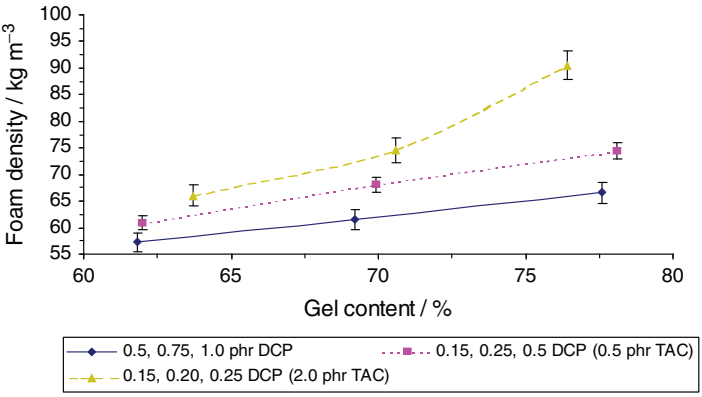

Fig. 15.3 The effect of formulation on foam density at similar gel content

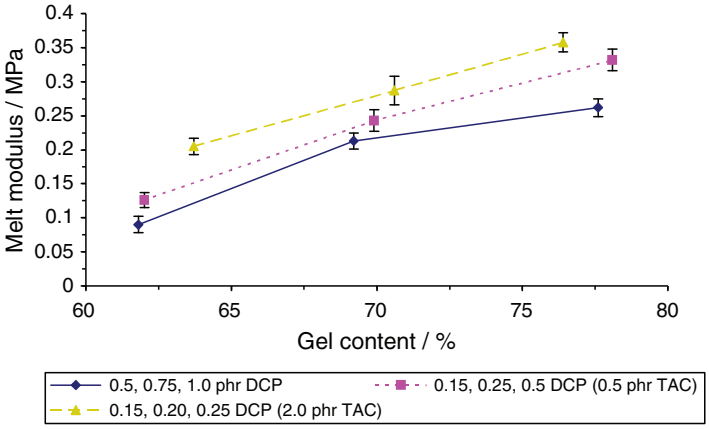

Fig. 15.4 The effect of formulation on melt modulus at similar gel content

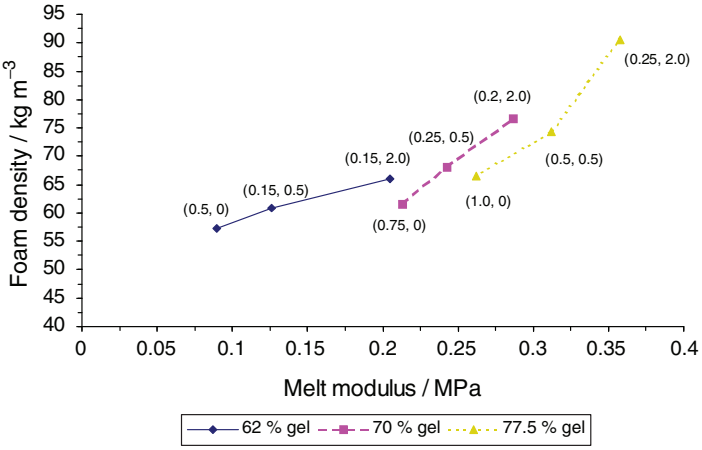

Fig. 15.5 The dependence of foam density on melt modulus at specific gel contents (DCP, TAC ratios [phr] shown in parentheses)

data points could be considered as part of a mastercurve then the Mahapatro theory [7] appears to hold some validity.

However, when experimental errors are taken into account, three separate curves are strongly suggested. It appears that the Mahapatro theory may be valid in the presence of TAC but only at a specific gel content. Overall, however, the incorporation of TAC in the crosslinking system seems to invalidate general application of the Mahapatro theory. In order to explain these phenomena, an attempt was made to estimate crosslink density using the standard characterisation technique of equilibrium swelling i.e. swell ratio. It is reported elsewhere that higher swell ratios indicate lower crosslink density and the lower the swell ratio the higher the crosslink density [9].

The Effect of Gel Content on Swell Ratio

The effects of formulations containing similar gel content on swell ratio are shown in Fig. 15.6. The results show that at any specific gel content, the swell ratio reduces with increasing TAC concentration. This confirms the earlier hypothesis that higher TAC concentrations in the crosslinking system produce higher crosslink density. The results are also in accordance with melt properties where the higher the TAC concentration, the higher the melt modulus.

Moreover, the curves of 2.0 and 5.0 phr TAC, have a more linear relationship compared with those crosslinked with DCP alone or in the presence of 0.5 phr TAC. This strongly suggested that at higher TAC concentrations, a more rigid network was present which restricted the ability of samples to swell. The results also give further evidence that gel content is not really a suitable parameter to evaluate solid properties when using TAC in the crosslinking system.

Effect of Swell Ratio on Foaming Behaviour

The relationship between swell ratio and foam properties was initially established for LDPE crosslinked by DCP alone. Figure 15.7 shows that an increase in swell ratio is accompanied by a decrease in foam density and an increase in mean cell size. The higher swell ratios are associated with a more loosely crosslinked network (i.e. lower crosslink density) that has a greater ability to expand and hence lowers the foam density.

Of considerable interest, is foam density dependence on swell ratio of various crosslinking system formulations including those containing up to 2.0 phr TAC

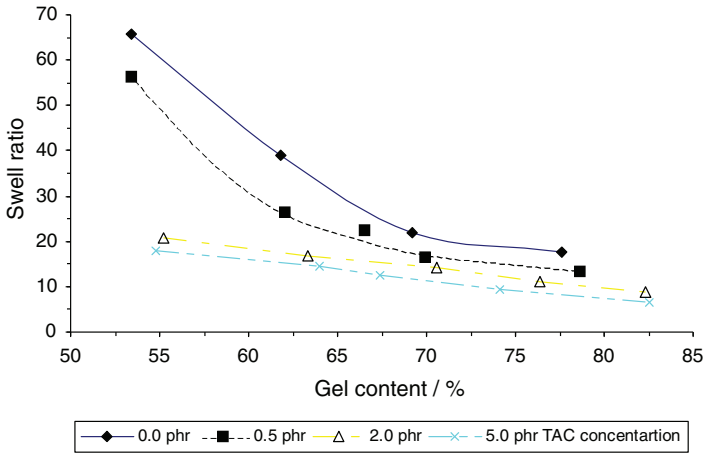

Fig. 15.6 Effect of gel content on swell ratio

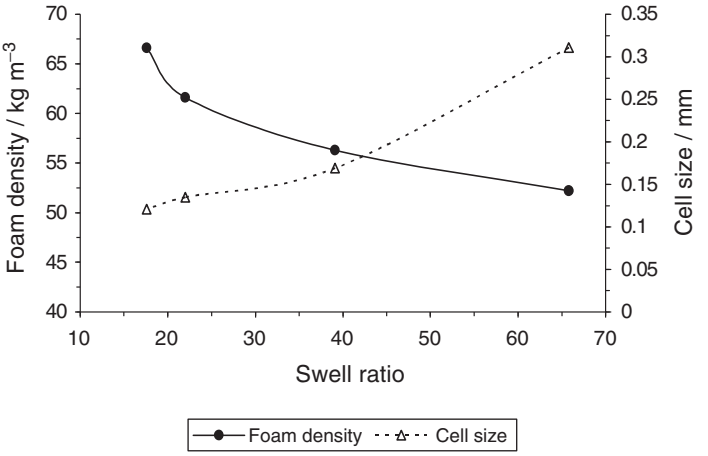

Fig. 15.7 The effect of swell ratio on foam density and mean cell size for DCP crosslinked LDPE foam

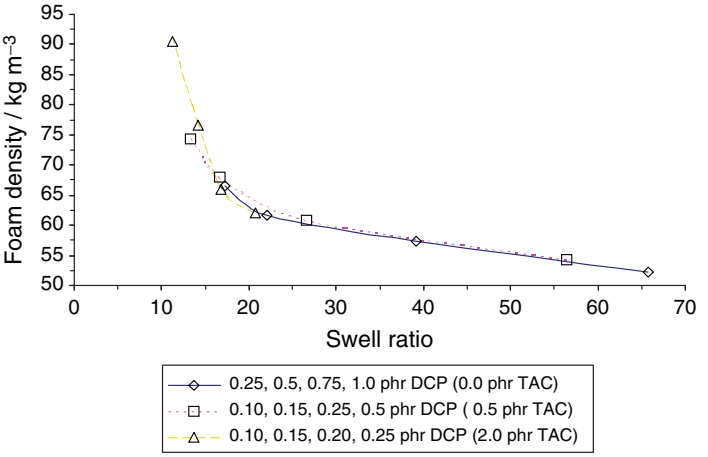

Fig. 15.8 The dependence of foam density on swell ratio as a function of crosslinking system formulation

(Fig. 15.8). There is a positive indication that all data points may approximate to a mastercurve more conclusively than those seen with melt modulus results (Fig. 15.5). The results suggested that swell ratio (itself related to crosslink density) might be a useful parameter upon which to base prediction of foaming behaviour.

Therefore an attempt was made to investigate similar swell ratios of approximately 39, 22 and 17 (equivalent to crosslinking with DCP alone at concentrations of 0.5, 0.75 and 1.0 phr respectively) independent of formulations. Table 15.1 indicates that formulations of similar swell ratio give approximately similar foam

Table 15.1 Effect of formulation on foam properties at similar swell ratios

DCP (phr)	TAC (phr)	Swell ratio	Foam density (kg m^{-3})	Compression modulus (MPa)	Average cell size (mm)
0.500	None	39.1 ± 1.1	56.3 ± 1.2	1.17 ± 0.06	0.169 ± 0.012
0.125	0.5	38.0 ± 1.4	57.3 ± 0.9	1.19 ± 0.05	0.157 ± 0.010
0.750	None	22.0 ± 0.5	61.6 ± 1.7	1.52 ± 0.07	0.135 ± 0.010
0.200	0.5	22.0 ± 0.8	62.2 ± 0.9	1.60 ± 0.06	0.126 ± 0.009
0.100	2.0	20.8 ± 0.9	62.0 ± 1.4	1.55 ± 0.04	0.130 ± 0.011
1.000	None	17.2 ± 0.6	66.6 ± 1.6	1.81 ± 0.08	0.115 ± 0.009
0.250	0.5	16.6 ± 0.8	68.0 ± 1.1	1.95 ± 0.09	0.108 ± 0.011
0.150	2.0	17.2 ± 0.5	66.0 ± 1.2	1.90 ± 0.08	0.102 ± 0.012

density, compression modulus and mean cell size. This suggested that all selected formulations of similar swell ratio had similar expansion characteristics and presumably, similar matrix properties. A further consideration is that swell ratio is based on volume whereas melt modulus measurements consider only uniaxial stress which may explain why swell ratio has a more universal applicability.

The most important finding is, however, that swell ratio appeared to be able to define expansion characteristics not only of traditional crosslinking systems but also those containing crosslinking promoter.

Conclusions

When foaming traditional DCP/LDPE systems, the foam density appeared to be controlled by gel content and/or the melt modulus (above 50% gel fraction). It was concluded that either gel content or melt modulus was inadequate to define foaming behaviour when TAC is included in the crosslinking system. Moreover, that swell ratio (crosslink density related) was a more universal parameter to predict foaming behaviour than either gel content or melt modulus independent of formulation.

References

1. Sims, G.L.A. and Khunniteekool, C., 1994, *Cell. Polym.,* **13,** 137–146.
2. Sims, G.L.A. and Khunniteekool, C., 1996, *Cell. Polym.,* **15,** 14–29.
3. Sims, G.L.A. and Khunniteekool, C., 1996, *Cell. Polym.,* **15,** 1–13.
4. Klempner, D. and Frisch, K.C., 2001, Handbook of Polymeric Foams and Foam Technology, Hanser, New York.
5. Gosselin, R. and Rodrigue, D., 2005, *Polym. Test.,* **24,** 1027–1035.
6. Sims, G.L.A. and Sipaut, C.S., 2001, *Cell. Polym.,* **20,** 255–277.
7. Mahapatro, A., Mills, N.J. and Sims, G.L.A., 1998, *Cell. Polym.,* **19,** 252–270.
8. Sirisinha, K. and Chimdist, S., 2006, *Polym. Test.,* **25,** 518–526.
9. Baba, M., Gardette, J-L. and Lacoste, J., 1999, *Polym. Degrad. Stab.,* **63,** 121–126.

Chapter 16
Ruthenium Tris-bypyridine/Zeolite-Y/Titanium Dioxide Nano-Assembly: 'Ship-in-a-Bottle' Synthesis and Application in Heterogeneous Photodegradation of 2,4-xylidine

Leon M. Jr. Payawan[1], Eva Marie Ratilla[1], and Stefan Bossmann[2]

Abstract The synthetic route followed in the encapsulation of $[Ru(bpy)_3]^{2+}$ in ZeoliteY is referred to as "ship-in-a-bottle" synthesis due to non-extractability of the $[Ru(bpy)_3]^{2+}$ complex, once encapsulation has taken place within the cages of the zeolite Y. Nanoparticles of TiO_2 was then introduced through $TiCl_3$ in ethylene glycol mixture under argon, with sintering at 200°C. Spectroscopic, surface, and electrochemical characterization confirmed the presence of $[Ru(bpy)_3]^{2+}$ complex within the cages of zeolite Y, and nanoparticles of TiO_2 in its cages.

The amount of TiO_2 was varied, and the assembly was tested for its photocatalytic activity using degradation of 2,4-xylidine as test reaction probe. The decrease in the concentration of xylidine and the corresponding increase in oxalate concentration were monitored through HPLC. A pseudo-first order kinetics was observed in the photodegradation process based on the Langmuir-Hinshelwood mechanism. An inverse correlation was observed between the kinetic rate constant and the obtained Light-Induced Optoacoustic Spectroscopy (LIOAS) frequency maxima.

Enhanced rate of photodegradation observed with the use of new and efficient photocatalyst such as $[Ru(bpy)_3]^{2+}$/TiO2 co-doped Zeolite Y may pave the way for development of large-scale advanced oxidation processes for other pollutant system.

Keywords Photodegradation, Ruthenium tris-bypyridine, Synthesis, Titanium Dioxide, 2,4-xylidine, Zeolite-Y

[1] Institute of Chemistry, University of the Philippines, Diliman, 1101 Q.C., Philippines

[2] Lehrstuhl für Umweltmesstechnik, Universität Karlsruhe, 76128, Karlsruhe, Germany

B. Sener (ed.), *Innovations in Chemical Biology,* doi: 10.1007/978-1-4020-6955-0

Ship-in-a-Bottle Synthesis

The synthetic route followed in the encapsulation of $[Ru(bpy)_3]^{2+}$ in ZeoliteY is referred as "ship-in-a-bottle" synthesis due to non-extractability of the $[Ru(bpy)_3]^{2+}$ complex, once encapsulation has taken place within the cages of the zeolite Y. Nanoparticles of TiO_2 was then introduced through $TiCl_3$ in ethylene glycol mixture under argon, with sintering at 200°C. A schematic diagram of the synthesis is shown in Fig. 16.1 [1].

The amount of TiO_2 was varied, and the assembly was tested for its photocatalytic activity using degradation of 2,4-xylidine as test reaction probe. Results show that the maximum catalytic efficiency was obtained at 52% TiO_2 loading. The material's experimentally determined kinetic rate constant was correlated with the obtained Light–Induced Optoacoustic Spectroscopy (LIOAS) frequency at different $\%TiO_2$ loading in the figure below Fig. 16.1 superimposed with the measured kinetic rate constant plot at various TiO_2 loading. It may be surmised that the molecular non-radiative relaxation of the material may be directly correlated with its catalytic efficiency as measured by the first-order rate constant.

The photodegradation mechanism of 2,4-xylidine to a mineralized form, oxalate was deduced from GC-MS trace detection of reaction intermediates. A summary of the proposed degradation path is shown in Fig. 16.2. The presence of some of these intermediates are supported by GC and HPLC data [2].

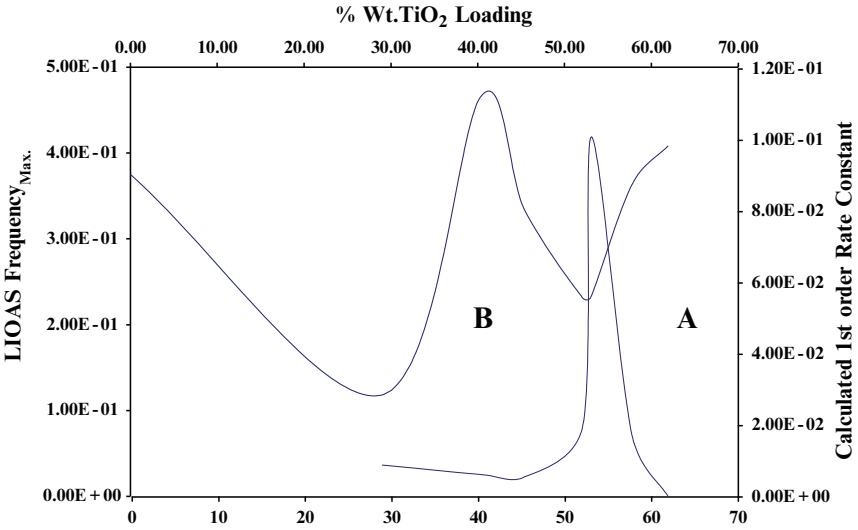

Fig. 16.1 (A) Calculated 1st order rate constant, and (B) LIOAS frequency in relation to $\%TiO_2$ loaded in the zeoliteY/$[Ru(bpy)_3]^{2+}$/TiO_2

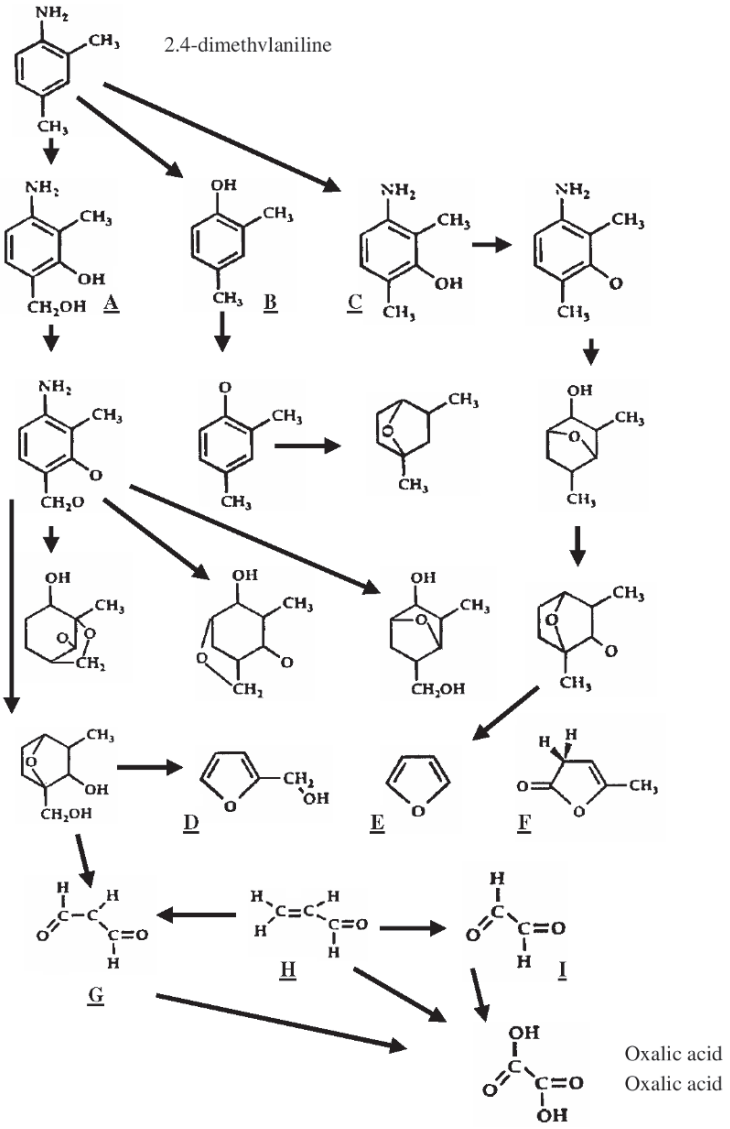

Fig. 16.2 Proposed degradation pathway of 2,4-xylidine to oxalic acid. Intermediates A to I have been identified through GC-MS analysis

References

1. Bossmann, S.H., Turro, C., Schnabel, C., Pokhrel, M.R., Payawan, L.M. Jr.Baumeister, B. and Woerner, M., 2001, *J. Phys. Chem. B.,* **105,** 5374–5382.
2. Bossmann, S.H., Jockusch, S., Schwarz, P., Baumeisters, B., Gob, S., Schnabel, C., Payawan, L.M. Jr.Pokhrel, M.R., Worner, M., Baraun, A.M. and Turro, N.J., 2003, *Photochem. Photobiol. Sci.,* **2,** 477.

Chapter 17
Infrared Spectroelectrochemical Analysis of the Binuclear Rhenium Complex of the Form, $[Re(CO)_3Cl]_2(tpbq)$

Arnie R. de Leon[1], Girlie Naomi N. Sison[2], and Stacey J. Borg[3]

Abstract A number of transition metal complexes have been investigated as potential electrocatalysts for CO_2 reduction, including rhenium monometallic complexes, which exhibited unique activity towards CO_2 reduction. Further development of multimetallic systems is also gaining interest, attributed to its likelihood in increasing the selectivity of converting CO_2 into highly reduced products. In this study, the binuclear rhenium complex of the form $[Re(CO)_3Cl]_2(tpbq)$, where tpbq = 2,2',3,3'-tetra-2-pyridyl-6,6'-biquinoxaline, has been synthesized and characterized in our laboratory. Typical yield for the synthesis is about 45%. Characterization was done using UV-Vis spectroscopy, FTIR spectroscopy, and cyclic voltammetry. The results of the characterization procedure have been compared and found very similar to analogous complexes of rhenium such as the monometallic $Re(bpy)(CO)_3Cl$ where bpy = 2,2'-bipyridine. Tandem infrared spectroelectrochemical analysis confirmed the reversibility of the reduction processes at –0.50 V and at –0.90 V versus SCE.

Keywords CO_2 reduction, cyclic voltammetry, polymetallic complexes, rhenium polypyridyl, spectroelectrochemical analysis

Introduction

The conversion of carbon dioxide into carbon feedstock for the manufacture of fuels and chemicals is an important area of research. It has the advantage of lower cost, due to the abundant supply of CO_2, and has the environmental benefit of

[1] Natural Sciences Research Institute, University of the Philippines, Diliman, Quezon City, 1101, Philippines

[2] Institute of Chemistry, University of the Philippines, Diliman, Quezon City, 1101, Philippines

[3] School of Chemistry, Faculty of Science, University of Melbourne, Australia

B. Sener (ed.), *Innovations in Chemical Biology*, doi: 10.1007/978-1-4020-6955-0

aiding in the reduction of CO_2 levels in the atmosphere believed to cause the 'greenhouse effect'. The continued search for energy efficient electrocatalysts has been the focus of this research field in which inorganic complexes have played a major role. Rhenium monometallic complexes, among others, had shown unique activity towards CO_2 reduction. The development of multimetallic systems in their capability to store multiple equivalents of electrons is showing great promise in increasing the selectivity of the CO_2 conversion processes toward highly reduced products.

Infrared spectroelectrochemical technique proved to be an excellent method to look at time and potential dependent changes of various types of chemical species. The employment of this technique will surely be significant on the mechanistic study of electron-transfer reactions of rhenium complexes.

The main goals of this research are: (1) to characterize polynuclear rhenium complexes which are capable of multielectron transfer reactions (2) to come up with appropriate conclusions on the redox-initiated transformations of this synthetic analog through the use of a new design of spectroelectrochemical cell; and (3) propose possible systems or investigations where infrared spectroelectrochemistry can be very useful.

Background

Investigations concerning the development of carbon dioxide as a potential alternate carbon source for commercial fuels have grown enormously with time. One reason is its potential for use in reversing the "greenhouse effect" attributed to CO_2 accumulation in the atmosphere. Several transition metal complexes have been investigated as electrocatalysts for CO_2 reduction [1]. Unique properties of metal polypyridyl complexes, such as the ability of the polypyridyl ligands to act as "electron reservoirs" by utilizing vacant π^* orbitals and to stabilize metals in a large number of oxidation states, lead to several investigations on these systems as electrocatalysts for CO_2 reduction [2–7]. In addition, these complexes can also be used as light absorbing moieties for photoinitiated processes [8–16].

fac-[Re(bpy)$(CO)_3$Cl] and related complexes had been found to be highly selective for the conversion of CO_2 to CO (98% current efficiency) in aprotic solvents both photochemically and electrochemically (–1.25 V vs. NHE) [5–7]. Its reactivity was associated with the rapid reaction of the complex with CO_2 followed by the dissociation of the chloride ligand. The chloride ligand was labilized upon initial one-electron reduction of the complex [3, 4]. Similar reactivity was also observed with [Re$(CO)_3$(dmbpy)Cl] [8]. The catalytic activity of the complex was found to involve a *sesqui*-coordinated bipyridine intermediate which allowed coordination of CO_2 to the empty coordination site generated on the rhenium.

Spectroelectrochemical methods refer to spectroscopically probing unique chemical species that are generated *in situ* during redox reactions at or near electrode

surfaces [17]. Spectroelectrochemical techniques present a significant extension to electrochemical studies, providing detailed insights into the chemical and structural changes following electron transfer reactions. A wide range of spectroscopic techniques has been interfaced with electrochemical techniques to generate varieties of hybrid techniques [18]. Infrared spectroscopy is well suited to spectroelectrochemical experiments because they provide results that are sensitive to the molecular structure of the compound under study. The high sensitivity and specificity obtained from IR-spectroelectrochemical measurements make it particularly valuable for the study of electrogenerated chemical species near the electrode surface and in the bulk solution [18]. Consequentially, the sample size and electrode geometry needed for such measurements are compatible with that required for electrochemical investigation [19].

Various designs of spectroelectrochemical cell have been developed that use optically transparent or perforated electrodes for transmission measurements and reflective electrodes for use in reflection/absorption experiments [20–25]. Transmission electrochemical cells, using perforated and minigrid electrodes, measure the IR features of the electrochemical species in the bulk solution. In contrast, most reflectance methods measure the IR features of electrochemical species near or on the electrode surface, with either totally reflective or transparent electrodes [20]. Borg et al. designed a reflection/absorption spectroelectrochemical cell capable of operation at gas pressures 0–1 Mpa [19]. It can also operate at low solution volumes (~100 μL) and collect good-quality electrochemical results from the solution under spectroscopic study due to the multi-electrode assembly. This advancement in spectroelectrochemical design greatly facilitates the study of highly air-sensitive samples particularly in cases where sample quantity is a limiting factor [19].

Experimental

Materials and Reagents

All reagents (analytical grade) were used without further purification, unless otherwise specified. The transition metal precursor, $Re(CO)_5Cl$ and the ligand precursors 1,2,4,5-benzenetetraamine tetrahydrochloride, 3,3'-diaminobenzidine, and 2,2'-pyirdyl were all purchased from Aldrich Chemical Company. Absolute ethanol, diethyl ether, n-pentane and dichloromethane were all purchased from Merck. Triethylamine and acetonitrile (both AR and HPLC grades) were acquired from J.T. Baker. The supporting electrolyte, tetrabutylammonium hexafluorophosphate (TBAHP), used for the electrochemical experiments was prepared by the metathesis of tetrabutylammonium bromide (SIGMA) with potassium hexafluorophosphate (SIGMA), recrystallized several times from hot ethanol and vacuum dried.

Syntheses

Synthesis of the Bridging Ligand 2,2',3,3'-tetra-2-pyridyl-6,6'-biquinoxaline, tpbq

The synthesis of tpbq was adopted from the procedure published by Rillema et al. [26]. 3,3'-diaminobenzidine (0.5 g, 2.34 mmol) and 2,2'-pyridyl (1.0 g, 4.67 mmol) were placed in a round bottom flask. Then 50 mL of absolute ethanol was added into the flask, stirred, and heated under reflux for 5 hours, where a brownish-yellow precipitate formed. The product was filtered, washed with small portions of cold ethanol, followed by ether, then vacuum-dried, and stored in a desiccator. A typical yield is ~45%; m/z 567.8; UV-Vis (nm): 367.5, 281; FTIR (cm^{-1}): 3,060.5, 3,010.4, 1,999.2, 1,613.2–1,570.8, 1,474, 1,281–999.61, 891.54–710.15, 663.

Synthesis of $[Re(CO)_3Cl]_2$(tpbq)

The binuclear rhenium(I) complex was synthesized according to the procedure by Wrighton and Morse [27] but with some modifications. Stoichiometric amounts of $Re(CO)_5Cl$ and tpbq (in 1:2 mmol ratios BL:metal salt) were mixed in 50 mL benzene. The resulting mixture was stirred and heated under reflux for 5 hours at 60^0C. The product was filtered under vacuum then recrystallized by dissolving in dicholoromethane and recrystallizing in n-pentane. The purified complex was filtered again under vacuum and air-dried. The brownish precipitate was obtained with a typical yield of ~78%. UV-Vis (nm): 383.8 and 292.6; FTIR (cm^{-1}): 3,087.6 (broad), 999.61 – 1,092.2, 1,196.1 – 1,130.8, 717.86 – 833.65, 1,532.2 – 1,613.2, 1,474.3, 1,358.5, 532.8 – 609.8; CV data in $E_{1/2}$ (V vs. Ag/AgCl): + 1.49, –0.565, –1.051.

Characterization

Infrared Spectroscopy

The infrared spectra of the bridging ligands and the complexes were obtained in peak view mode using a Bio-Rad FTS-40A FTIR Spectrophotometer using a tungsten halogen lamp as light source and a cryogenic MCT as detector. Samples were oven-dried and kept in a vacuum desiccator prior to analyses. These were prepared as pellets in KBr matrix.

Electronic Absorption Spectroscopy

The electronic absorption spectra of the complexes were obtained at room temperature using a Shimadzu UV-3101PC UV-VIS-NIR Scanning Spectrophotometer with 2 nm resolution. The wavelength range is between 200 and 900 nm.

Electrochemistry

Cyclic voltammetry was conducted using a Powerlab ADI Potentiostat interfaced to a computer. A typical three electrode system was used for the analysis: Ag/AgCl electrode (2.0 mm) as reference electrode; Pt disc (2.0 mm) as working electrode; and Pt rod (2.0 mm) as auxiliary electrode. The supporting electrolyte used was a TBAHP/acetonitrile electrolyte-solvent system. The instrument was preset using a Metrohm 693 VA Processor. Potential sweep rate was 200 mV/s using a scan range of –1,800 to ±1,800 mV.

Infrared-Spectroelectrochemical Analysis of $[Re(CO)_3Cl]_2(tpbq)$

The synthesized complex was sent to the Department of Chemistry at University of Melbourne in Australia and the infrared-spectroelectrochemical (IR-SEC) experiments were done at Dr. Stephen Best's laboratory. The following procedure was conducted.

Solvents were purified and dried by standard methods [28] and distilled under an atmosphere of nitrogen immediately prior to use. Solutions used for electrochemical or spectroscopic analyses were prepared under an atmosphere of nitrogen or argon using either standard Schlenk techniques or with the aid of a vacuum atmospheres glovebox. High purity Ar, N_2, and CO were obtained from BOC gases. The tetra-n-butylammonium perchlorate (TBA[ClO_4]) or tetra-n-butylammonium hexafluorophosphate (TBA[PF_6]), used as supporting electrolyte, were prepared and purified using standard procedures [29]. *CAUTION! Perchlorate salts are potentially explosive. Solutions containing TBA[ClO_4] as a supporting electrolyte should not be allowed to evaporate to dryness.*

Cyclic voltammetry experiments were controlled using a Powerlab 4/20 interface and PAR model 362 scanning potentiostat with EChem software (v1.5.2, ADInstruments) and were carried out using a 1 mm diameter vitreous carbon working electrode, platinum counter electrode, and 2 mm silver wire reference electrode. The potential of the reference electrode was determined using the ferrocenium/ferrocene (Fc^+/Fc) couple, and all potentials are quoted relative to the SCE reference electrode. Against this reference, the Fc^+/Fc couple occurs at +0.38 V in acetonitrile and +0.53 V in THF [30, 31].

A PAR model 362 scanning potentiostat was used for the SEC experiments, and these were conducted using a purpose-built reflection/absorption cell capable of operating at moderate gas pressures (1 MPa). The design and operation of the high-pressure SEC cell has been previously described [32]. The current response of the SEC cell was monitored using a Powerlab 4/20 interface and recorded with Chart 4 software (AD Instruments). The solution under spectroscopic investigation is comprised of a 10–30 μm layer of solution trapped between the multielectrode and a CaF_2 window. The thickness of the layer was adjusted under micrometer control and its value estimated using the extinction coefficients of absorptions due to the solvent [33, 34].

Infrared spectra were collected using a Biorad FT175C FTIR spectrometer utilizing a Ge/KBr beam splitter and a narrow-band MCT detector. The IR-SEC spectra were collected in single beam mode, and differential absorbance spectra were calculated from these using the spectrum recorded immediately prior to the application of the potential step as the reference. Spectra for the individual reduced species were obtained by spectral subtraction using Grams/32 AI software (Galactic).

Results and Discussion

The binuclear rhenium(I) complex was obtained at very reasonable yield (Fig. 17.1). The metal salt [$Re(CO)_5$ Cl] incorporated with the bridging ligand was added in slight excess to ensure the attachment to the BL. The chelating nature of the tpbq, which has four bidentate sites allows them to form stable polymetallic complexes with rhenium(I) (Fig. 17.2). The two nitrogen (N) atoms in the pyridyl and pyrazyl groups of the BL's allow for the attachment of one rhenium(I) center. The number of coordinated metal centers formed actually depends on the molar ratio of the starting materials.

The basic features of the electronic absorption spectra of the synthesized rhenium(I) complex which were also found in analogous complexes, such as

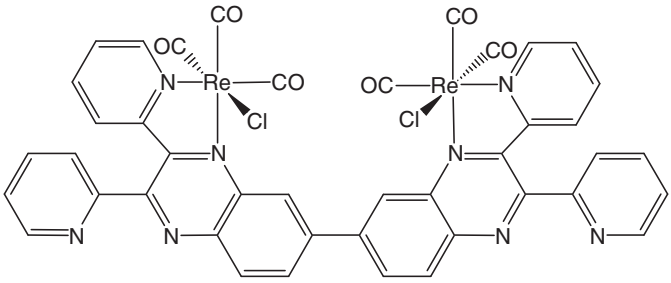

Fig. 17.1 Possible structure of $[Re(CO)_3Cl]_2$tpbq

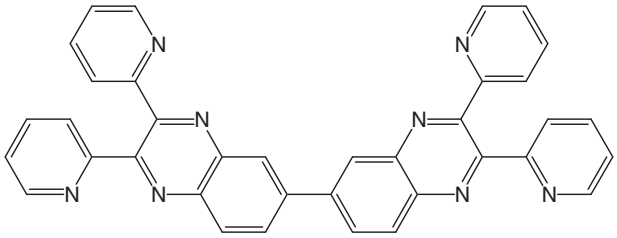

Fig. 17.2 Structure of tpbq

$Re(CO)_3XCl$ [X = 5-Y-1,10-phenanthroline (Y = H, CH_3, Cl, Br, NO_2), 4,7-diphenyl-1, 10-phenanthroline-5,6-dione, and 2,2'-biquinoline] [35] include the appearance of low energy absorption bands between 352–416 nm arising from metal-to-ligand charge transfer (MLCT) transitions from the dπ orbitals of Re(I) to the π* orbitals of the BL's, and that of a higher energy absorption band at around ~275 nm arising from a ligand-localized $\pi \rightarrow \pi^*$ transition in the BL's. The molar absorptivity (ε) of the complex confirm the occurrence of a MLCT transition, which has ε values 10^3–10^6 while ligand based transitions have magnitudes greater than 10^3.

The complex exhibited characteristic group absorptions corresponding to C–H, C–N, and C–C stretching vibrations. The metal salt precursor, $Re(CO)_5Cl$ exhibited characteristic group vibrations attributed to Re–Cl and C–O stretching vibrations. The characteristic group absorptions are similar, but not identical to those of the precursors, $Re(CO)_5Cl$ and the BL tpbq. The peaks alone corresponding to the C–O stretch immediately confirms the attachment of Re(I) metal center. The C–O stretching frequencies are a bit lower compared to that of their precursor metal complex, largely due to the presence of strongly π-accepting bridging ligand. Broad bands in the C–O region of the spectra may indicate the overlap of numerous peaks, another indication of binding of more than one Re(I) metal centers to the tpbq (Fig. 17.3).

Distinct peaks at the positive (+) and negative (–) regions of the voltammogram (Fig. 17.4), are observed. The cyclic voltammogram of $[Re(CO)_3Cl]_2$tpbq is dominated by metal-localized oxidation and ligand-localized reductions, as observed in analogous complexes. Reduction in the complexes may be attributed to the BL/BL^-

Fig. 17.3 FTIR spectrum of $[Re(CO)_3Cl]_2$tpbq in KBr matrix

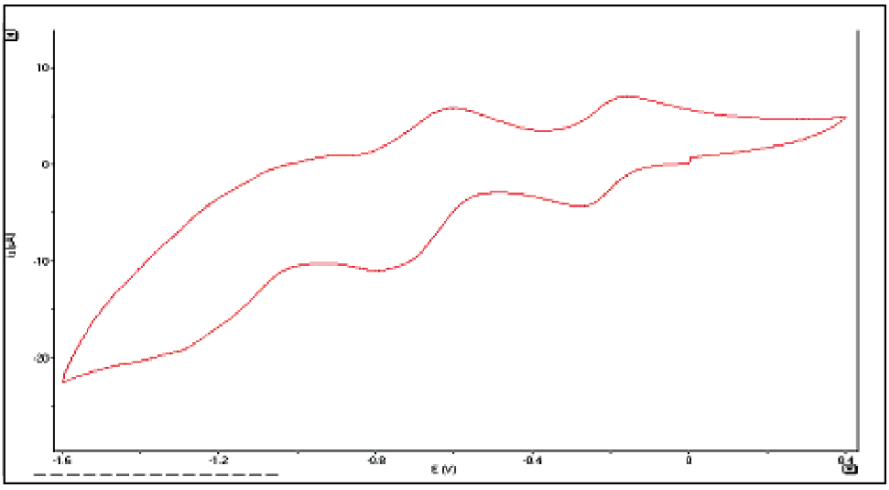

Fig. 17.4 Cyclic Voltammogram of 5 mM solution of $[Re(CO)_3Cl]_2$tbpq on 1 mm Pt wire, in SEC cell (0.2 M $TBAPF_6/CH_3CN$)

and BL^-/BL^{2-}, i.e. tpbq/tpbq$^-$ and tbpq$^-$/tpbq^{2-} reductive couples. The oxidation is attributed to Re(I)/Re(II) couple. A more positive value for oxidation and reduction generally implies greater ease of oxidation of the Re(I) metal centers and easier reduction of the BL's. It can be observed experimentally that as more metal centers are bound to the BL's, the more difficult it is to reduce the BL's, meaning the more Re(I) metal is attached to the BL, the more "localized" the electrons become, thus hindering the oxidative ability of the BL.

Figure 17.5 shows the IR-SEC spectra of $[Re(CO)_3Cl]_2$tbpq complex: the first oxidized species (at 600 mV), neutral, first reduced species (at –500 mV), second reduced species (at –900 mV). The IR-SEC measurements of $[Re(CO)_3Cl]_2$tpbq were done at potentials referring to the peaks of its cyclic voltammogram. The first oxidized species (taken at 600 mV) showed an IR spectrum with the C-O stretching bands occurring at higher frequency compared with that of the neutral species. As the complex is reduced, the C-O stretching frequency is lowered which is consistent with the increased electron density in the CO π^* orbitals. All of these species are fairly stable and exist in the solution even in the absence of applied potential. Figure 17.6 and the cyclic voltammogram (Fig. 17.4) show that the first reduction is reversible, recovering almost all the neutral species upon reoxidation at +100mV. On the other hand, the second reduction is quasi-reversible in the CV, but has reasonable chemical reversibility, recovering about 80–90% of the neutal species upon reoxidation.

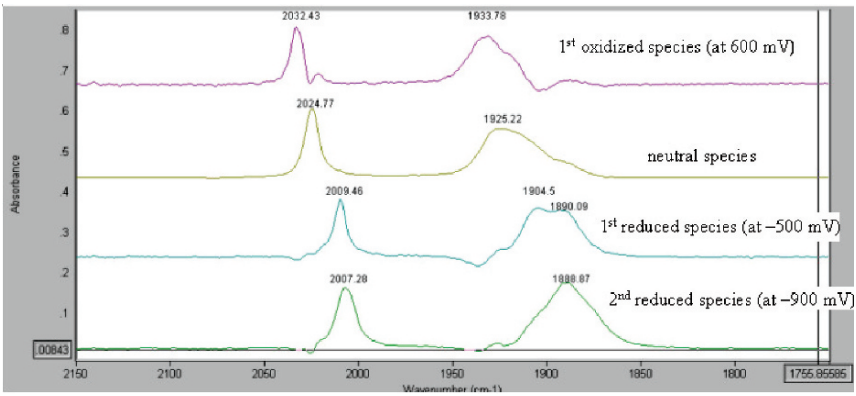

Fig. 17.5 IR-SEC spectra of $[Re(CO)_3Cl]_2$tbpq under 40 psi Ar. All potentials are versus the bare Ag wire in our system

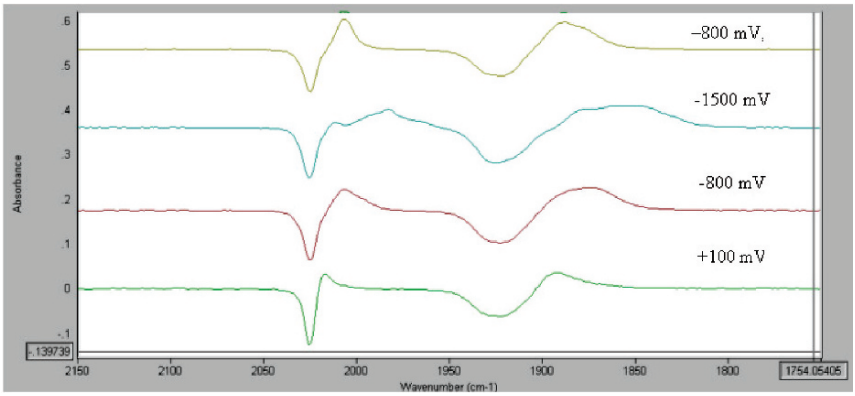

Fig. 17.6 IR-SEC spectra of $[Re(CO)_3Cl]_2$tbpq under 40 psi Ar. All potentials are versus the bare Ag wire in our system

Conclusion

The bimetallic complex $[Re(CO)_3Cl]_2$tbpq synthesized in this work showed the typical spectroscopic and electrochemical behavior based on analogous polypyridyl complexes of rhenium(I). Re(I) $d\pi \rightarrow$ tpbq π^* charge transfer transition and ligand-field $\pi \rightarrow \pi^*$ transitions are observed. Typical redox behavior of this system consists of Re^{I}/Re^{II} oxidation and tpbq/tpbq$^-$ reduction. Such electrochemical activity, particularly in the reductive region, is found ideal for catalytic processes such as CO_2 reduction. IR-SEC studies have shown that the reduction process occurring at –0.50

V is reversible where the complex is recovered completely after re-oxidation. The second reduction at –0.90 V has relatively good chemical reversibility. In this region, the complex is expected to undergo some chemical transformations such as a probable loss of Cl ligand which subsequently opens up a coordination site for any substrate molecule.

Further studies on this system will include IR-SEC experiments under an atmosphere of CO_2 to verify its catalytic activity for CO_2 reduction and to aid in formulating a mechanism for the reaction. Other multimetallic systems used as CO_2 reduction catalysts such as ruthenium-, iridium-, and cobalt-based complexes, or metal clusters used as models in the active sites of biological systems, many of which have complex redox behavior can also be investigated using the IR-SEC technique.

References

1. (a) Kubiak, C.P., Woodcock, C. and Eisenberg, R., 1982, *Inorg. Chem.,* **21,** 2119–2129.
   (b) Calabrese, J.C., Herskovitz, T. and Kinney, J.B., 1983, *J. Am. Chem. Soc.,* **105,** 5914–5915.
   (c) Lundquist, E.G., Folting, K., Huffman, J.C. and Caulton, K.G., 1987, *Inorg. Chem.,* **26,** 205–208.
   (d) Szymaszek, A. and Pruchnik, F.P., 1989, *J. Organomet. Chem.,* **376,** 133–140.
   (e) Palmer, D.A. and Eldik, R.V., 1983, *Chem. Rev.,* **83,** 651–731.
   (f) Sakaki, S., Aizawa, T., Koga, N., Morokuma, K. and Ohkubo, K., 1989, *Inorg. Chem.,* **28,** 103–109.
2. Hamnett, A., Muir, A.V.G. and Timney, J.A., 1992, *J. Chem. Soc., Dalton Trans,* **4,** 337–341.
3. Vlcek, A. Jr. 1992, *Chemtracts - Inorg. Chem.,* **4,** 337–341.
4. Hawecker, J., Lehn, J.M. and Ziessel, R., 1984, *J. Chem. Soc.*, *Chem. Commun.*, 328–330.
5. Hawecker, J., Lehn, J.M. and Ziessel, R., 1986, *Helv. Chim. Acta,* **69,** 198–201.
6. Hawecker, J., Lehn, J.M. and Ziessel, R., 1983, *J. Chem. Soc.*, *Chem. Commun.*, 536–538.
7. Breikss, A.I. and Abruna, H.D., 1986, *J. Electroanal. Chem.,* **201,** 347–358.
8. Molnar, S.M., Jensen, G.E., Vogler, L.M., Jones, S.W., Laverman, L., Bridgewater, J.S., Richter, M.M. Brewer, K.J., 1994, *J. Photochem. Photobiol. A: Chem.,* **80,** 315–322.
9. Berger, R.M., 1990, *Inorg. Chem.,* **29,** 1920–1924.
10. Bridgewater, J.S., Vogler, L.M., Molnar, S.M. and Brewer, K.J., 1993, *Inorg. Chim. Acta,* **208,** 179–188.
11. Vogler, L.M., Franco, C., Jones, S.W. and Brewer, K.J., 1994, *Inorg. Chim. Acta,* **221,** 55–59.
12. Vogler, L.M., Scott, B. and Brewer, K.J., 1993, *Inorg. Chem.,* **32,** 898–903.
13. Richter, M.M. and Brewer, K.J., 1993, *Inorg. Chem.,* **32,** 2827–2834.
14. Molnar, S.M., Nallas, G., Bridgewater, J.S. and Brewer, K.J., 1994, *J. Am. Chem. Soc.,* **116,** 5206–5210.
15. Kalyanasundaram, K., Gratzel, M. and Nazeeruddin, Md.K., 1992, *J. Phys. Chem.,* **96,** 5865–5872.
16. MacQueen, D.B. and Petersen, J.D., 1990, *Inorg. Chem.,* **29,** 2313–2320.
17. Kirchoff, J.R., 1997, *Curr. Sep.,* **16,** 11–14.
18. Truccolo, D. and Best, S.P., 1998, Druskovich D.M. (ed), In Electrochemistry: Crossing the Boundaries, RACI, Australia, pp 15–24.
19. Borg, S.J. and Best, S.P., 2002, *J. Electronal. Chem.*, **535**(1–2), 57–64.
20. Visser, H., Curtright, A.E., McCusker, J.K. and Sauer, K., 2001, *Anal. Chem.,* **73,** 4374–4378.
21. Simmons, N.J. and Porter, M.D., 1997, *Anal. Chem.,* **69,** 2866–2869.
22. Mosier-Boss, P.A., Newbery, R., Szpak, S. and Lieberman, S.H., 1996, *Anal. Chem.,* **68,** 3277–3282.

23. Flowers, P.A. and Callendar, S.A., 1996, *Anal. Chem.,* **68,** 199–202.
24. Flowers, P.A., and Maynor, M.A. and Owens, D.E., 2002, *Anal. Chem.,* **74,** 720–723.
25. Paulson, S.C. and Elliott, M., 1996, *Anal. Chem.,* **68,** 1711–1716.
26. Rillema, D.P., Callahan, R.W. and Mack, K.B., 1982, *Inorg. Chem.,* **21(7),** 2589–2596.
27. Wrighton, M. and Morse, D.L., 1974, *J. Am. Chem. Soc.,* **96(4),** 998–1002.
28. Errington, R.J., 1997, *Guide to Practical Inorganic and Organo-Metallic Chemistry*, Blackie Academic & Professional, London.
29. Sawyer, D.T., Sobkowiak, A. and Roberts, J.J.L., 1995, Electrochemistry for Chemists, 2nd ed. Wiley-Interscience, New York, p 336.
30. Chang, D., Malinski, T., Ulman, A. and Kadish, K.M., 1984, *Inorg. Chem.,* **23,** 817–824.
31. Connelly, N.G. and Geiger, W.E., 1996, *Chem. Rev.,* **96,** 877–910.
32. Borg, S.J. and Best, S.P.J., 2002, *Electroanal. Chem.,* **535,** 57–64.
33. Christensen, P.A., Hamnett, A., Higgins, S.J. and Timney, J.A., 1995, *J. Electroanal. Chem.,* **395,** 195–209.
34. Goplen, T.G., Cameron, D.G. and Jones, R.N., 1980, *Appl. Spectrosc.,* **34,** 657–691.
35. Nallas, G.N.A. and Brewer, K.J., 1996, *Inorg. Chim. Acta,* **253,** 7–13.

Chapter 18
Microbial Synthesis of Poly (3-Hydroxybutyrate-*co*-4-Hydroxybutyrate) by *Cupriavidus* sp. USMAA1020 Isolated from Malaysian Environment

Amirul A. Abdullah[1], Ahmad R. M. Yahya[1], Kumar Sudesh[1], Mohd N. M. Azizan[1], and Mohd I. A. Majid[2]

Abstract A locally isolated Gram negative bacterium designated as USMAA1020 was able to produce poly(3-hydroxybutyrate-*co*-4-hydroxybutyrate) [P(3HB-*co*-4HB)] when grown on γ-butyrolactone as the sole carbon source. The polyester was purified from freeze-dried cells and analyzed by nuclear magnetic resonance (NMR) spectroscopy. ^{1}H and ^{13}C NMR results confirmed the presence of 3HB and 4HB monomers. USMAA1020 are able to grow and produce 67 wt% P(3HB-*co*-8mol%4HB) of the dry cell weight in a one-step cultivation process using γ-butyrolactone as the sole carbon source. It accumulated P(3HB-*co*-4HB) copolyesters with higher 4HB fraction in nitrogen-free mineral medium containing various carbon sources such as γ-butyrolactone, 1,4-butanediol and 4-hydroxybutyric acid through a two-step cultivation process. The two-step cultivation process produced significantly higher 4HB fraction in the copolyester and the composition of copolyesters varied from 19 to 43 mol% 4HB, depending on the carbon sources supplied. Biochemical characterization, 16S rRNA sequence analysis, cellular fatty acids analysis and DNA base ratio determination revealed that strain USMAA1020 may represent a strain of a new species within the genus *Cupriavidus*.

Keywords Bacteria, biosynthesis, copolyesters, *Cupriavidus*, Malaysian environment

Introduction

Polyhydroxyalkanoate (PHA) is a biodegradable and biocompatible thermoplastic that can be synthesized in many microorganisms from almost all genera of the microbial kingdom. Many microorganisms synthesize polyhydroxyalkanoates (PHAs) as intracellular carbon and energy reserve materials [1]. These microbial polyesters materials are thermoplastics with biodegradable properties [2]. PHAs are usually accumulated

[1] School of Biological Sciences, Universiti Sains Malaysia,11800 Penang, Malaysia

[2] Malaysian Institute of Pharmaceuticals and Nutraceuticals, MOSTI, Malaysia

B. Sener (ed.), *Innovations in Chemical Biology*, doi: 10.1007/978-1-4020-6955-0

within cells when growth is limited by the depletion of nutrients such as nitrogen, oxygen, and other essential elements but have an excess of carbon source. Microorganisms are able to accumulate various types of PHAs in the form of homopolyesters, copolyesters, or polyester blends [3]. More than 150 different monomer units are known to be incorporated into the polyester chain [4]. Accordingly, various kinds of copolyesters are expected when a bacterium is grown on mixtures of different precursors [5]. One of these polyesters, poly(3-hydroxybutyrate-*co*-4-hydroxybutyrate) [P(3HB-*co*-4HB)] has been found to exhibit particular useful material properties relative to other PHAs. Generally, P(3HB-*co*-4HB) is produced by feeding precursor carbon sources such as 4-hydroxybutyric acid, 1,4-butanediol and γ-butyrolactone. Doi and coworkers were the first to report that *Ralstonia eutropha* and *Alcaligenes latus* can produce PHA containing 4HB monomers [6–8]. In 1994, they described another bacteria, *Comamonas acidovarans* which is a wild type microorganism with suitable metabolic pathways for the production of P(3HB-*co*-4HB) [9]. Among the various monomer constituents, the incorporation of 4HB has resulted in PHAs with a wide range of physical properties [2]. With an increase in the 4HB fraction, this copolyester shows properties that range from being highly crystalline thermoplastic to strong elastomeric rubber-like material [9]. Among these microorganisms, *R. eutropha* has been reported to produce P(3HB-*co*-4HB) with various 4HB fractions (0–100 mol%) and has been studied most extensively due to its easy growth and ability to accumulate large amount of polymers from simple carbon sources [10].

Poly(4-hydroxybutyrate) [P(4HB)] is a highly ductile, flexible polymer withstanding an extension of around 1,000% before breaking, compared to P(3HB), which can only extend to less than 10% before breaking. Combining these different monomers to form copolymers, as in P(3HB-*co*-4HB), been described as one of the most useful PHAs by Sudesh et al. [5], produces a family of materials with mechanical properties that can be tailored to specific needs. P(3HB-*co*-4HB) has been found to have desirable mechanical properties for applications in the medical and pharmaceutical field [11]. The biocompatibility and bioabsorbable nature of P(3HB-*co*-4HB) makes it the most valuable type of biopolymer among the vast number of different PHAs synthesized by microorganisms. To date, five wild-type bacteria, which can produce P(3HB-*co*-4HB), i.e. *R. eutropha* [7], *Alcaligenes latus* [8, 12], *Comamonas acidovorans* [9, 13], *Comamonas testosteronii* [14] and *Hydrogenphaga pseudoflava* [15] have been reported. In the present study, we report the biosynthesis of P(3HB-*co*-4HB) by *Cupriavidus* sp. USMAA1020 that was isolated from Malaysian environment.

Materials and Methods

Isolation and Identification of P(3HB-co-4HB) Producer

Samples from environments such as soil, sludge and water in Peninsular Malaysia were screened for PHA producers. Samples were enriched with mineral salts medium (MSM) containing γ-butyrolactone as the sole carbon source (0.7% v/v)

but with limited nitrogen source to maintain the C/N ratio at 20. After overnight incubating, cultures then diluted in sterile distilled water and plated on solid mineral salts medium containing γ-butyrolactone and Nile red stain (5 μg/mL) [16]. Colonies that formed following incubation were replicated onto a fresh medium. The original plate then exposed to ultraviolet (320 nm) illumination to identify PHA producers. In addition, biochemical characterization, 16 S rRNA sequencing, DNA base composition and fatty acids analysis were performed to determine the identity of the isolate, USMAA1020.

P(3HB-co-4HB) Accumulation

P(3HB-*co*-4HB) accumulation was carried out in a two-step batch cultivation process. The microorganisms were grown in 150 mL of nutrient broth (NB) for 20 to 22 hours. The cells were then harvested by centrifugation (10,000 g), washed with sterile distilled water, and transferred (1 g/L) into nitrogen-free MSM. The second-step culture medium consists of 3.70 g/L KH_2PO_4, 5.80 g/L K_2HPO_4, 0.2 g/L $MgSO_4.7H_2O$ and 1.0 mL/L microelements solution (2.78 g/L $FeSO_4.7H_2O$, 1.98 g/L $MnCl_2.4H_2O$, and 2.81 g/L $CoSO_4.7H_2O$, 1.67 g/L $CaCl_2.2H_2O$, 0.17 g/L $CuCl_2.2H_2O$ and 0.29 g/L $ZnSO_4.7H_2O$/L of 0.1 M HCl). The medium was added with filter-sterilized γ-butyrolactone, 1,4-butanediol and 4-hydroxybutyric acid at a concentration 0.56% (wt) carbon as the sole carbon source to promote PHA synthesis.

Observation of PHA Granules

Intracellular PHA granules in the microbial cells were observed using phase contrast light microscopy. The granules appeared distinct and light refractive inclusion bodies in the cell cytoplasm. These granules can also be stained by the oxazine dye, Nile red which results in pink or orange fluorescence when exposed to UV light [16]. In addition, morphology of the isolate was examined by transmission electron microscopy (TEM) according to standard methods.

Gas Chromatography and Nuclear Magnetic Resonance Analysis of PHA

PHA content and composition in the lyophilized cell material were determined using gas chromatography (GC) and nuclear magnetic resonance (NMR) analyses. For GC analysis [17], approximately 15 mg of lyophilized cell was subjected to methanolysis in the presence of methanol and sulfuric acid [85%:15% (v/v)]. The reaction mixture was incubated at 100°C for 3 hours. The organic layer containing the reaction products was separated, dried over Na_2SO_4, and analyzed by GC. For

NMR analysis, the PHA was extracted from freeze-dried cells. For this purpose, 1.0 g freeze-dried cells were stirred in 200 mL of chloroform for 24 hours at 30°C. The extract was filtered to remove cells debris, and the chloroform was concentrated to a volume of about 15 mL using rotary evaporator. The concentrated solution was then added drop-wise to 150 mL of rapidly stirred methanol to precipitate the dissolved PHA.The precipitated PHA was then recovered by filtration using a 0.45 μm PTFE membrane and dried overnight at room temperature. The purified PHA was dissolved in deuterated chloroform ($CDCl_3$) and subjected to ^{1}H and ^{13}C NMR analyses.

Results and Discussion

Isolation of P(3HB-co-4HB) Producer

In total of 663 isolates were isolated from various samples from Peninsular Malaysia. One hundred nineteen out of the 663 isolates were identified as possible PHA producers based on Nile red staining methods. All the 119 PHA producers emitted pink fluorescence when grown on solid MSM containing Nile red and exposed to UV light. The isolates obtained in this study were cultivated in MSM containing γ-butyrolactone as carbon source. GC analysis confirmed that 95 out of the 119 isolates were PHA producers. Among the 95 positive isolates, 77 isolates produced only P(3HB) homopolymer and 18 isolates produced PHA containing 3-hydroxybutyrate (3HB) and 4-hydroxybutyrate (4HB) monomers. Among these 18 isolates, USMAA1020 was screened as the best P(3HB-*co*-4HB) producer. For further confirmation, PHA was extracted from the latter isolate and analyzed by GC as well as NMR. Results from both analyses confirmed that the isolate USMAA1020 was capable of producing PHA containing (3HB) and (4HB). Figure 18.1 shows the ^{13}C-NMR spectra of P(3HB-*co*-4HB) copolymer sample purified from USMAA1020 in chloroform together with the ^{13}C chemical assignments. The six ^{13}C resonances at 15–70 ppm could be assigned to specific carbon species in the 3HB and 4HB units [18].

Identification of Isolate USMAA1020

Morphological and biochemical tests were performed on USMAA1020. The following characteristics were present: cells are Gram-negative, aerobic, non-spore forming, motile, and rod-shaped (0.7–0.9 × 1.5–3.0 μm). Colonies on NB agar are circular, convex, opaque, and creamy. Growth is observed at 30°C and 37°C but not at 42°C. No indole production or production of acid from glucose occurs. Gelatin, aesculin and arginine are not hydrolysed. Nitrate is not reduced to nitrite. Assimilates p-hydroxy-benzoate, mesaconate, trans-aconitate, D/L-tartrate, citrate, malate, adipate, caprate and gluconate but not D-galactose, D-fucose, D-xylose, glucose, arabinose, mannose, mannit and maltose. The DNA G + C content is 62.3%. The

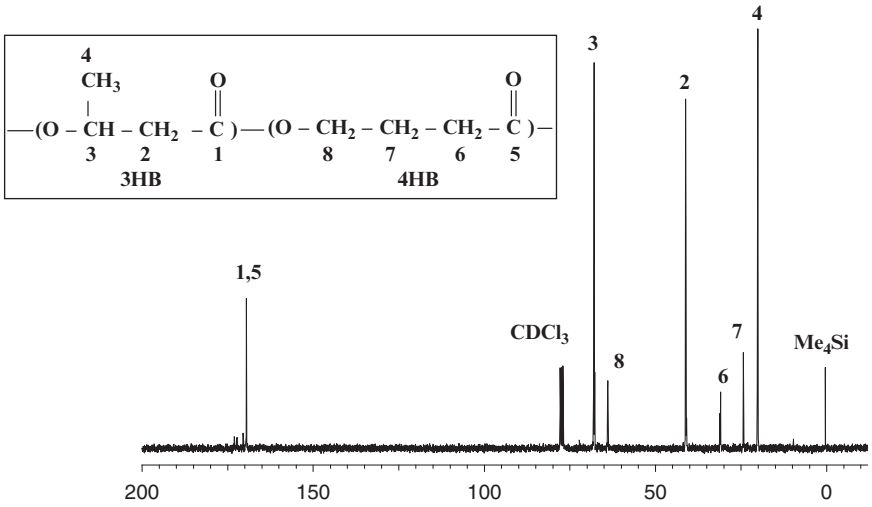

Fig. 18.1 ^{13}C-NMR spectrum of PHA purified from USMAA1020. Inset shows the chemical structure of P(3HB-*co*-4HB) copolyester. Numbers 1 to 8 refer to the peak assignments in the NMR spectrum

profile of the cellular fatty acids is typical for the genus *Cupriavidus*. These results suggested that USMAA1020 belong to the genus *Cupriavidus* [19]. This was further supported by the 16S rRNA sequence analysis (results not shown). The complete 16S rRNA gene sequence of strain USMAA1020 (GenBank accession no. DQ351699) shows highest similarity of 98.4% with *Cupriavidus pauculus*. Based on these results, strongly suggested that the isolate USMA1020 may represent a strain of a new species within the genus *Cupriavidus*.

Growth Characteristics and P(3HB-co-4HB) Accumulation of Cupriavidus sp. USMAA1020 Using γ-Butyrolactone

Figure 18.2 shows that the growth profile and PHA content of *Cupriavidus* sp. USMAA1020 on MSM containing γ-butyrolactone [0.74% (v/v)] as the sole carbon source. A period of 72 hours was required for maximum growth of the strain and P(3HB-*co*-4HB) copolymer was produced at maximally 67 wt% of dry cell weight using γ-butyrolactone as the sole carbon source. The molar carbon to nitrogen (C/N) ratio of 20 in the medium led to higher accumulation of PHA during the steady-state growth. GC analysis shows that *Cupriavidus* sp. USMAA1020 is capable of producing P(3HB-*co*-4HB) using single-stage cultivation process and the 4HB content was 8 mol%. Cells that were grown in conditions that do not promote PHA biosynthesis and do promote PHA biosynthesis were subjected to morphological examination using transmission electron microscopy (TEM). Transmission electron micrograph of *Cupriavidus* sp. USMAA1020 are shown in Fig. 18.3a and b.

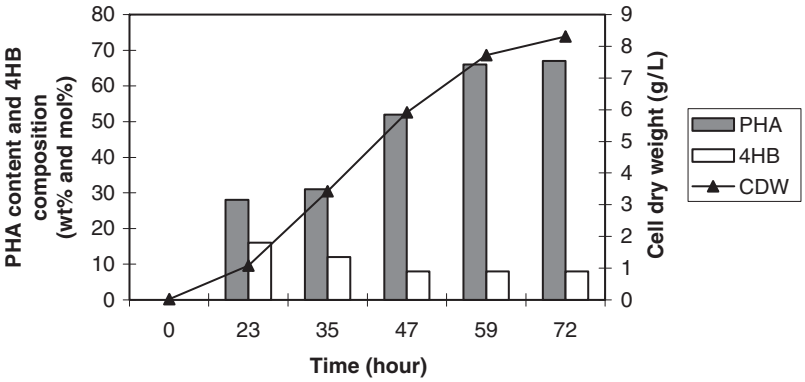

Fig. 18.2 Growth and P(3HB-*co*-4HB) accumulation of *Cupriavidus* sp. USMAA1020 on MSM containing γ-butyrolactone as the sole carbon source in a one-step cultivation process. The one-step culture medium is same as two-step culture medium but contains 1.1 g/L $(NH_4)_2SO_4$ as nitrogen source

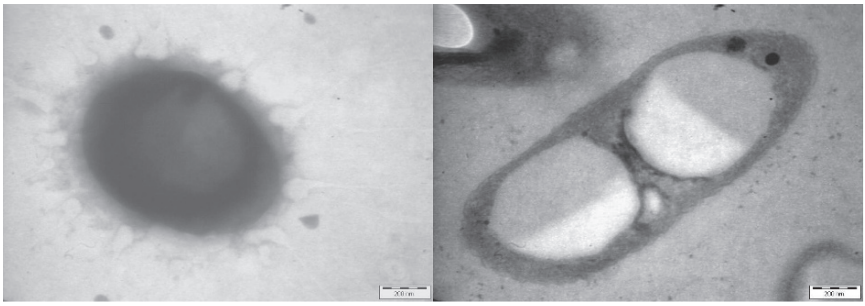

Fig. 18.3 Transmission electron micrograph of USMAA1020. (a) Morphology of cell with no PHA accumulation. (b) Morphology of cell with PHA granules in the cell cytoplasm. PHA granules appear as translucent bodies

The presence of translucent bodies in cell cytoplasm is a clear indication of PHA accumulation. It can be seen that the accumulated PHA occupies a very significant portion of the cell volume. The number of PHA granules in the cells ranged from one to two and their sizes ranged from 300 to 500 nm.

Biosynthesis of P(3HB-co-4HB) in a Two-Step Cultivation

PHAs are usually accumulated within microbial cells when growth is limited by the depletion of nutrients such as nitrogen, oxygen, and other essential elements but have an excess of carbon source. Therefore, two-step cultivation is applied, whereby

cell biomass from the nutrient broth is transferred to a second-step in which the medium is usually nitrogen-limited or nitrogen-free [21]. This medium is added with suitable carbon sources to promote the biosynthesis of a particular type of PHA. In this study, we have tested γ-butyrolactone, 1,4-butanediol and 4-hydroxybutyric acid that are known to promote the biosynthesis of PHAs containing 4HB monomers. Table 18.1 summarizes the results obtained when different carbon sources were added to the second-step cultivation. All carbon sources resulted in the accumulation of P(3HB-*co*-4HB) with 4HB content ranged from 19 to 43 mol% when a two-step cultivation used. The molar fraction of 4HB was highest (43 mol%) when 4-hydroxybutyric acid used as the carbon source. γ-butyrolactone resulted in the accumulation of 45 wt% of the dry cell weight P(3HB-*co*-4HB) and also resulted in fairly high contents of 4HB in the copolymer (37 mol%). A random copolymer of 3HB and 4HB was produced even when 4-hydroxybutyric acid was used as sole carbon source for *Cupriavidus* sp. USMAA1020. According to Doi [2], 4-hydroxybutyryl-CoA is first formed from these carbon sources in the cells. A portion of the 4-hydroxybutyryl-CoA is then metabolized into D(-)-3-hydroxybutyryl-CoA via a complex metabolic pathway. A random copolyester of 3HB and 4HB units is then produced by the copolymerization of D(-)-3-hydroxybutyryl-CoA with 4-hydroxybutyryl-CoA under the action of PHA synthase. The expanded spectra of carbonyl carbon resonances at 163–173 ppm are shown in Fig. 18.4. The carbonyl resonances are resolved into four groups of peaks that arise from the different dyad sequences of connected 3HB and 4HB units. The dyad 3*3 (3HB-3HB), 3*4 (3HB-4HB), 4*3 (4HB-3HB), 4*4 (4HB-4HB) fractions are determined from the well-resolved peaks of carbonyl resonance. Assuming that these are statistically random copolymers that can be described by Bernoullian statistics, the dyad fractions, F_{33}, F_{34}, F_{43}, F_{44} can be expressed with mole fraction of the 4HB unit in the polymer, F_4, as follows [20]:

$$F_{33} = (1-F_4)^2 \; F_{34} = F_{43} = F_4\,(1\text{-}F_4)\; F_{44} = F_4^{\,2}$$

The expression of randomness in sequence distribution is as follows:

$$D = F_{33}\,F_{44}/F_{34}\,F_{43}$$

Table 18.1 Polyester accumulation by *Cupriavidus* sp. USMAA 1020 on nitrogen-free MSM containing various carbon sources in a two-step cultivation[a]

Carbon source (0.56% (wt) carbon)	Cell dry weight (g/L)	PHA content (wt %)[b]	PHA composition (mol%)[c]		D[d]
			3HB	4HB	
γ-Butyrolactone	2.63 ± 0.10	45 ± 1	63 ± 1	37 ± 1	1.6
4-Hydroxybutyric acid	2.10 ± 0.08	31 ± 1	57 ± 2	43 ± 2	1.8
1,4-Butanediol	2.92 ± 0.12	49 ± 2	81 ± 1	19 ± 1	1.3

[a] The cells were harvested after 48 hours [b] Calculated from GC analysis [c] Calculated from GC analysis and ^{1}H-NMR spectra [d] $D = F_{33}F_{44}/F_{34}F_{43}$

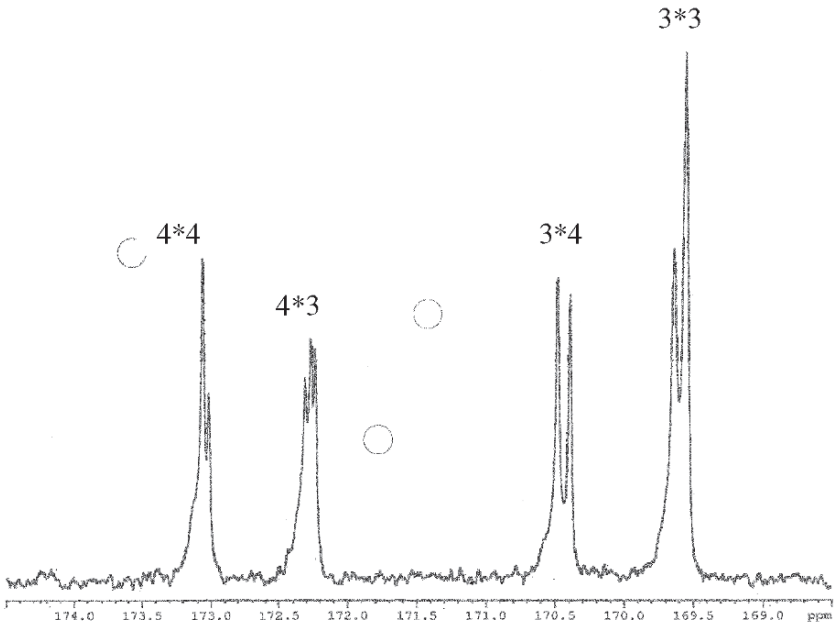

Fig. 18.4 Expanded ^{13}C-NMR spectrum of carbonyl carbon resonances in P(3HB-*co*-38mol%4HB) sample

where if *D* is nearly equal to 1, then the copolymer is a typical copolymer and if *D* is too larger than 1, then the copolymer is a block or blend. As shown in Table 18.1, the *D* values of the samples were close to 1.0, suggesting that the samples had a random distribution of 3HB and 4HB units.

Conclusion

In this study, we have isolated a bacterium belongs to genus *Cupriavidus* from Peninsular Malaysia that is capable of growing and accumulating P(3HB-*co*-4HB) copolyesters using γ–butyrolactone as the sole carbon source. This isolate was able synthesized random copolyesters with 19–43 mol% 4HB when cultured in nitrogen-free MSM containing various carbon sources such as γ-butyrolactone, 1,4-butanediol and 4-hydroxybutyric acid. P(3HB-*co*-4HB) is a biodegradable and biocompatible copolyester with great potential in the medical and pharmaceutical fields. The ability to produce these copolyesters from γ-butyrolactone is an added advantage because this carbon source is cheaper and more readily available. Further studies are ongoing to produce P(3HB-*co*-4HB) with various 4HB contents.

Acknowledgement The authors acknowledge the research grant provided by Universiti Sains Malaysia, Penang that has resulted in this article.

References

1. Anderson, A.J. and Dawes, E.A., 1990, *Microbiol. Rev.,* **54,** 450–472.
2. Doi, Y., 1990, Microbial Polyesters, VCH, New York.
3. Steinbüchel, A., 2001, *Macromol. Biosci.,* **1,** 1–24.
4. Steinbüchel, A., and Valentin, H.E., 1995, *FEMS Microbiol. Lett.,* **128,** 219–228.
5. Sudesh, K., Abe, H. and Doi, Y., 2000, *Prog. Polym. Sci.,* **25,** 1503–1555.
6. Kunioka, M., Kawaguchi, Y. and Doi, Y., 1989, *Appl. Microbiol. Biotechnol.,* **30,** 569–573.
7. Nakamura, S., Doi, Y. and Scandola, M., 1992, *Macromolecules,* **25,** 4237–4241.
8. Hiramitsu, M. and Doi, Y., 1993, *Biotechnol. Lett.,* **15,** 461–464.
9. Saito, Y. and Doi, Y., 1994, *Int. J. Biol. Macromol.,* **16,** 99–104.
10. Kim, J.S., Lee, B.H. and Kim, B.S., 2005, *Biochem. Eng. J.,* **23,** 169–174.
11. Williams, S.F. and Martin, D.P., 2002, Applications of PHAs in medicine and pharmacy. In *Biopolymers: Polyesters* (Y. Doi and Steinbüchel (eds.), A. Vol. III, 4, Wiley-VCH, Weinhem, Germany, p 91.
12. Kang, C.K., Kusaka, S. and Doi, Y., 1995, *Biotechnol. Lett.,* **17,** 583–588.
13. Lee, W.H., Azizan, M.N.M. and Sudesh, K., 2004, *Polym. Deg. Stab.,* **84,** 129–134.
14. Renner, G., Pongratz, K. and Braunegg, G., 1996, *Food Technol. Biotechnol.,* **34,** 91–95.
15. Choi, M.H., Yoon, S.C. and Lenz, R.W., 1999, *Appl. Environ. Microbiol.,* **65,** 1570–1577.
16. Spiekermann, P., Rehm, B.H.A., Kalscheuer, R., Baumeister, D. and Steinbüchel, A., 1999, *Arch. Microbiol.,* **171,** 73–80.
17. Braunegg, G., Sonnleitner, B. and Laffer, R.M., 1978, *Eur. J. Appl. Microbiol. Biotechnol.,* **6,** 29–37.
18. Doi, Y., Kunioka, M., Nakamura, Y. and Soga, K., 1988, *Macromolecules,* **21,** 2722–2727.
19. Vandamme, P. and Coenye, T., 2004, *Int. J. Syst. Evol. Microbiol.,* **54,** 2285–2289.
20. Kamiya, N., Yamamoto, Y., Inoue, Y., Chujo, R. and Doi, Y., 1989, *Macromolecules,* **22,** 1676–1682.
21. Sudesh, K. and Doi, Y., 2000, *Polym. Adv. Technol.,* **11,** 865–872.

Chapter 19
Rust Phase Transformation in the Presence of Mangrove Tannins

Afidah A. Rahim[1], Noor Hamdah Musa[1], Rohana Adnan[1], M. Jain Kassim[1], E. Rocca[2], and J. Steinmetz[2]

Abstract The transformation of rust in the presence of 5 g L^{-1} tannins extracted from mangrove barks was studied. Pre-rusted samples prepared resulted in the formation of predominantly lepidocrocite and magnetite. Partial transformation of rust components, particularly lepidocrocite in the presence of mangrove tannins was found to occur when observed via infrared spectroscopy, X-ray diffraction and SEM analysis. The anti-corrosive properties of the mangrove bark extracts seem to be related to the tannins which are capable of chelating with Fe^{3+} giving a highly stable, and insoluble ferric-tannate complexes. A molecular modeling study of the reaction of catechin, a flavanoid of mangrove tannins with Fe^{3+} to form a ferric-tannate complex was performed to explain the adsorption mechanism of tannins on iron. The correlation between the electronic density of the catechin molecule and the inhibiting properties is reported.

Keywords Mangrove barks, molecular modeling, phase transformation, rust, spectroscopy, tannin, transformation.

Introduction

The known hazardous effects of most synthetic corrosion inhibitors are the reasons for the search of safer and environmentally friendly natural products. Plant extracts are viewed as an incredibly rich source of naturally synthesized chemical compounds that can be extracted at low costs. Naturally occurring substances such as vanillin [1], *Opuntia* extracts [2], lawsonia extract [3], natural honey [4] and extracts of chamomile, halfabar, black cumin and kidney bean [5] are some

[1]School of Chemical Sciences, Universiti Sains Malaysia, 11800 Penang, Malaysia
[2]Laboratoire de Chimie du Solide Mineral-Universite Henri Poincare-Nancy I BP239-54506 Vandoeuvre Les Nancy, France

B. Sener (ed.), *Innovations in Chemical Biology*, doi: 10.1007/978-1-4020-6955-0

of the recent studies on corrosion inhibition for different metals in various environments.

Tannins are polyphenols that occur only in vascular plants such as leaves, needles, barks heartwood, seeds and flowers. Tannins exist primarily in condensed and hydrolysable forms. Natural tannin extracts have been employed since the turn of the last century in leather industry. Recent development of their industrial uses as adhesives, flocculants, depressants, viscosity modifier agents and more recently as corrosion inhibitors reflects their importance as industrial raw materials. Electrochemical studies have shown that tannins extracted from the barks of mangrove trees are excellent corrosion inhibitors of steel at very low pH. The mechanism of inhibition at this pH was due to the chemisorption of tannin molecules while at higher pH, inhibition was achieved via formation of ferric-tannates [6].

Contradictory opinions have been referred to in the literature particularly on the nature of the iron-tannate and its interaction with the rusted steel due to the diversity of the material used in different studies. Studies have included the use of tannic acid [7–10], gallic acid [11], oak tannin [12, 13], pine tannin [14] and mimosa tannin [15]. In order to establish the correlation between the ferric-tannate formation and the low inhibition efficiency observed at high pH from the electrochemical studies, phase transformations of pre-rusted steels in the presence of tannins were evaluated. In this work the quantum chemical calculations are conducted to analyse the relationship between the molecular structure and properties of ferric-tannate complex and its inhibitory mechanism.

Experimental

Phase Transformation Studies

Mild steel plates obtained from ARCELOR, France were washed with distilled water and ethanol prior to sample treatments. Pre-rusted samples were prepared by subjecting the mild steel plates to the salt spray chamber according to the ASTM B 117 [16] standard procedure (6 hours exposure in 5% (w/v) NaCl at 98% humidity, 1.0 mL $hour^{-1}$ spray rate, 1.0 kg cm^{-3} of pressure and followed by drying in an oven at 40°C)

The pre-rusted plates were immersed in 5 g L^{-1} mangrove tannin solution at pH 4.0 for 24 hours. The changes in the rust structures were observed via X-ray diffractions, SEM and FTIR analyses. The SEM analysis was carried out using SEM S-2500 Hitachi Thermo NORAN equipped with an energy-dispersive X-ray spectrometer and prior to the SEM studies the surface was gold or carbon-coated using a vacuum evaporator Edwards Auto 306. A Perkin Elmer System One spectrometer was used to obtain the FTIR spectrums while a Goniometre C diffractometer, incorporating a cobalt radiation (λ = 1.78892 Å) was used to obtain the X-ray diffraction patterns.

Computational Details

For calibration purposes, computations were performed in two steps. Initial calculation was performed using MOPAC available in CAChe version 5.0 program. The semi empirical AM1 [17] method was first used to generate various stable structures of lowest energy conformations. This is represented as a function of three dihedral angles: ∠FeOCC (+90.0, 180.0, −90.0) at A, B and C rings. These binding sites are denoted as A_1, A_2, B_1, B_2, C_1 and B_1B_2 (between two phenolics) and the atomic numbering for catechin molecule are as shown in Fig. 19.1. PRECISE keyword was used to ensure stable geometry.

In the second step, single point energy calculations were performed on each of the optimized structures derived from the semi empirical calculation using the hybrid Becke3 exchange functional and Perdew and Wang correlation functional (B3PW91 method) [18] using 6-31G** basis set, available in Gaussian03, to compute more accurate energy values and other quantum properties. The verification of the structures as a minimum on the potential energy surface, PES was carried out using FREQ that yielded all positive frequencies.

Results and Discussion

Transformation Studies

From the X-ray diffraction, XRD pattern in Fig. 19.2, the pre-rusted sample was found to consist of mainly lepidocrocite and magnetite and traces of geothite. The XRD pattern indicated the reduction of several lepidocrocite peaks in favour of ferric-tannate formation after the addition of mangrove tannins.

Similarly the FTIR spectrum in Fig. 19.3 exhibited the presence of lepidocrocite (1,022, 891 and 474 cm^{-1}), goethite (800 cm^{-1}) and magnetite (571 cm^{-1}) in the

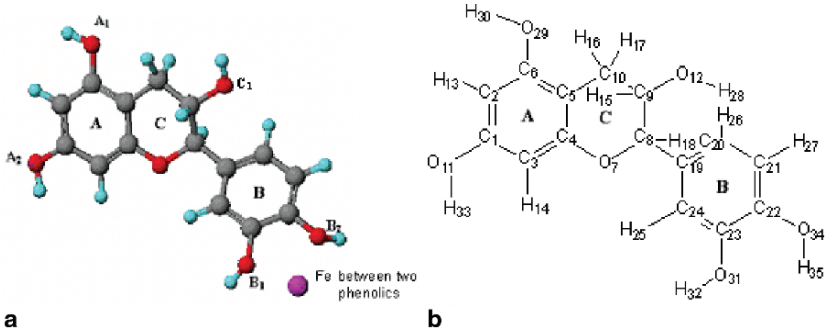

Fig. 19.1 (a) The labeling of phenolic positions. (b) Atomic numbering for catechin molecule

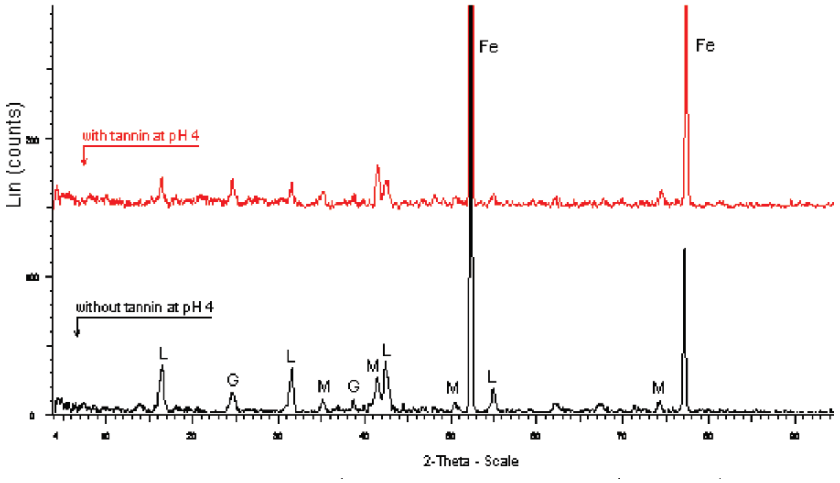

Fig. 19.2 Phase transformation of bare rust surface when treated with 0.5% mangrove tannins

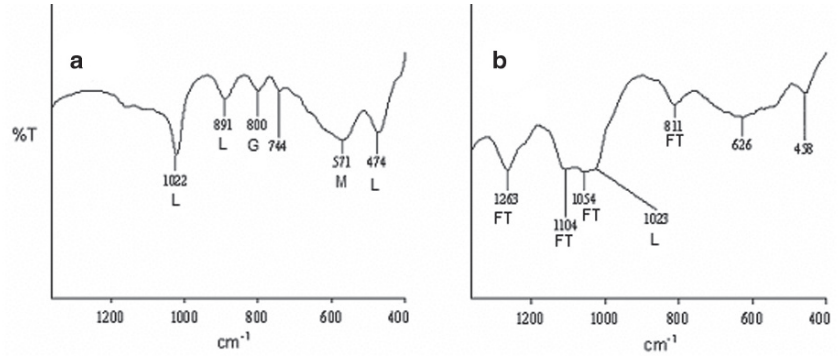

Fig. 19.3 FTIR spectrum of (a) bare rust and (b) converted rust samples: FT-ferric-tannate, G-geothite, L-lepidocrocite, M-magnetite

untreated pre-rusted sample. Upon treatment of tannins, ferric-tannate peaks at 1,163, 1,104, 1,054 and 811 cm^{-1} were evident. A reduction in the intensity of the lepidocrocite peak was also observed. The principal magnetite peak at 571 cm^{-1} may have been superimposed by the broad 626 cm^{-1} peak.

Figure 19.4 shows the SEM micrographs of the rust surfaces before and after immersion in the mangrove tannin solution at pH 4.0. The pre-rusted sample shows basically coral-like structures distributed in a random manner. This structure disappeared with the tannin treated samples and was replaced by a coarse layer with cracks of irregular shapes. A closer inspection of the surface of each crack revealed tiny flowered-like structures stacked on top of one another. Unconverted rust structures were observed underneath the transformed tannins.

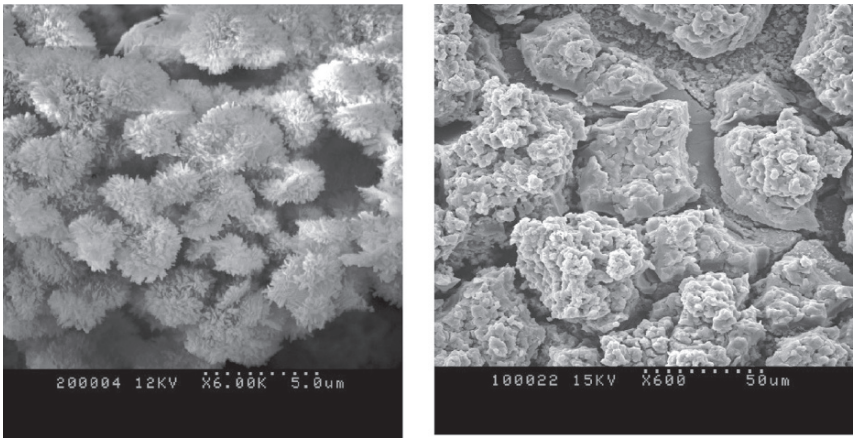

Fig. 19.4 SEM micrographs of pre-rusted steel surface (a) before tannin immersion and (b) after tannin immersion

The above results indicated that partial transformations of rust into ferric-tannates without other oxide or oxyhydroxides as reaction products. Depolymerisation of mangrove tannins in the presence of phloroglucinol nucleophiles in acidic ethanol followed by the separation of flavan-3-ols and their phloroglucinol adducts using reversed phase high performance liquid chromatography resulted in the identification of four major flavanoids namely catechin, epicatechin, epicatechin gallate and epigallocatechin [19]. The proximity of hydroxyl groups on the aromatic rings of the flavanoid monomers enables the mangrove tannin to chelate the iron (II) and iron (III) ions forming iron-tannates. In the presence of oxygen, Fe (II) tannate is oxidized to the Fe (III) form, a blue-black insoluble complex, which impedes steel corrosion. However the lack of adhesion of tannates as shown from SEM micrographs inferred a physical adsorption of deposits and the cracked morphology of deposits provided easy penetration of moisture into the cracks leading to the formation of new rust. This resulted in a low protective behaviour. Hence the correlation between ferric-tannate formation and the low inhibition efficiency observed at high pH from the electrochemical studies was established.

Molecular Modeling

The energy calculated using both the AM1 semi empirical method and B3PW91/6–31G** calculations of the optimized complexes for each phenolic position indicated that position C_1 with Fe-O-C-C dihedral angle of +90° has the lowest total energy, followed by binding at position B_1B_2 ($\angle$FeOCC −90°). At C_1 ($\angle$FeOCC + 90°) position, the breaking of two bonds was observed, namely between C_9 and C_{10} as well as

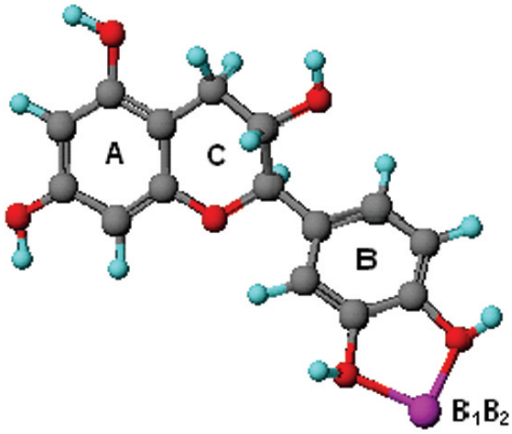

Fig. 19.5 The most stable ferric-tannate complex with B_1B_2 conformation

between O_{12} and H_{28} which was confirmed by bond order calculations. Whilst, a new bond between Fe^{3+} and H_{28} (1.56 Å) was formed (bond order of 0.983).

At B_1B_2 position and dihedral angle of −90°, Fe^{3+} forms bonds with two oxygen atoms i.e. O_{31} and O_{34}. The bond length of $Fe_{36}O_{31}$ and $Fe_{36}O_{34}$ are 1.965 and 1.958 Å respectively, both within the normal experimental Fe-O distance (1.875–2.042 Å). Apparently, binding at this site is due to the electron-donating properties of the phenolic oxygen and the electron-deficient Fe^{3+}. The lengthening and shortening of bonds are also observed, and are consistent with the electron transfer from catechin to the metal ion. Bond order calculations showed that the interaction between Fe^{3+} with O_{31} and O_{34} resulted in a value of 0.653 and 0.650 each, indicating a weak single bond being formed.

The HOMO-LUMO energy gap, $\Delta E_{HOMO\text{-}LUMO}$ of Fe^{3+}-tannate shows that the binding at B_1B_2 has the largest energy gap indicating the stability of the complex. The structure of this stable complex is as shown in Fig. 19.5. Conversely, the HOMO-LUMO smaller energy gap value for C_1 ring signifies a less stable complex. The results from the energy calculations and $\Delta E_{HOMO\text{-}LUMO}$ values show that this B_1B_2 conformation is the most stable form of ferric-tannate compared to the other OH positions while binding at position C_1 is unlikely to form a ferric-tannate complex.

Conclusion

Partial transformation of rust into ferric-tannates was found to occur with the addition of mangrove tannins leading to a low inhibitive behaviour. The mechanism of adsorption of catechin onto the iron surface has been established via theoretical

calculation using both semi empirical and density functional theory. The most probable position of adsorption occurs on the B ring of the two phenolic positions following the electron donating properties of the phenolic OH groups in catechin.

References

1. El-Etre, A.Y., 2001, *Corrosion Science,* **43,** 1031–1039.
2. El-Etre, A.Y., 2003, *Corrosion Science,* **45,** 2485–2495.
3. El-Etre, A.Y., Abdullah, M. and El-Tantawy, Z.E., 2005, *Corrosion Science,* **47,** 385–395.
4. El-Etre, A.Y. and Abdullah, M., 2000, *Corrosion Science,* **42,** 731–738.
5. Abdel-Gaber, A.M., Abd-El-Nabey, B.A., Sidahmed, I.M., El-Zayady, A.M. and Saadawy, M., 2006, *Corrosion Science*, **48**(9), 2765.
6. Rahim, A.A., Rocca, E., Steinmetz, J., Kassim, M.J., Adnan, R. and Sani Ibrahim, M., 2007, *Corrosion Science*, **49**, 402.
7. Morcillo, M., Feliu, S., Simancas, J., Bastidas, J.M., Galvan, J.C., Feliu, S. Jr.Almeida, E.M., 1992, *Corrosion NACE,* **48** (12), 1032.
8. Barrero, C.A., Ocampo, L.M. and Arroyave, C.E., 2001, *Corrosion Science,* **43,** 1003.
9. Deslauriers, P.J., 1987, *Material Performance*, 35.
10. Nasrazadani, S., 1997, *Corrosion Science,* **39** (10–11), 1845.
11. Favre, M. Landolt, D., 1993, *Corrosion Science,* **34** (9), 1481.
12. Gust, J., 1991, *Corrosion NACE,* **47** (6), 453.
13. Gust, J. Bobrowicz, J., 1993, *Corrosion NACE,* **49** (1), 24.
14. Ocampo, L.M., Margarit, I.C.P., Mattos, O.R., Cordoba-de-Torresi, S.I. and Fragata, F.L., 2004, *Corrosion Science,* **46,** 1515–1525.
15. Ross, T.K. and Francis, R.A., 1978, *Corrosion Science,* **18,** 351.
16. ASTM B 117, 1973, *Salt Spray Resistance Test*, American Society for Testing and Materials, Philadelphia, PA.
17. Öğretir, C., Mihci, B. Bereket, G., 1999, *Journal of Molecular Structure (THEOCHEM),***488,** 223.
18. (a) Becke, A.D., 1993, *Journal of Chemical Physics,* **98,** 5648.
    (b) Perdew, J.P., Burke, K. Wang, Y., 1996, *Physical Review B,* **54,** 16533.
19. Rahim, A.A., Rocca, E., Steinmetz, J., Adnan, R. and Kassim, M.J., 2004, Mangrove tannins as corrosion inhibitors in acidic medium-Study of flavanoid monomers. In *Proceedings of the European Corrosion Conference (EUROCORR 2004)*, 12–16 September, Nice, Paper No. 41.

Chapter 20
Treatment of Oil-Water Mixture Using Illite Clay Mineral

Fatma Turak and Hüseyin Afşar

Abstract The aim of this work was to study the simultaneous effect of amount of clay, activation temperature, contact time, pH, and size of the adsorbent on the retention of oil-grease thermally activated illite by adsorption. The values obtained for the percentage of oil-grease removed ranged from 93.87% for 110°C up to 66.73% for 900°C. The adsorption experiment showed surface that the stronger heat treatment the most effective adsorption of oil-grease.

Keywords Adsorption, clay, illite, x-ray diffraction

Introduction

Oil-grease effluent is produced in municipal sewer, petroleum refineries, petrochemical plants, steel mills workshops, food-processing plants, and in the textile industry.

Oil-grease must be removed from wastewater since these materials interfere with other processes (particularly gravity settling) and may accumulate in unwanted areas of the treatment system causing a performance problem. Furthermore, if oil-grease will pass through to a receiving body of water, it composes a oil layer and this layer causes a significant pollution problem in the form of reduced light penetration and photosynthesis. In addition, it hinders oxygen transfer from atmosphere to water medium. Consequently, amount of dissolved oxygen in the bottom layer of water will be decreased. This situation affects survival of aquatic life in water. The removal of oil-grease from wastewater can be accomplished by the use of several well-known and widely accepted techniques. Conventionally, gravity separation, dissolved air flotation, chemical coagulation, filtration, membrane processes, biological processes, adsorption are used for the removal of oil-grease.

Yıldız Technical University, Faculty of Science and Art, Department of Chemistry, Davutpasa, 34220 İstanbul, Turkey

B. Sener (ed.), *Innovations in Chemical Biology*, doi: 10.1007/978-1-4020-6955-0

Adsorption techniques have been successful in removing oil-grease. Clay minerals have been the most widely used absorbent because its cost is low and they can be reached easily. Oil-grease adsorption on various sorbents has been studied by many researchers [1–6].

Materials and Methods

The illite sample was supplied from Marmara region (Çanakkale, Çan) in Turkey for ceramic industries. The clay samples air dried and sieved from 425 μm sieve. Chemical composition of the clay samples were determined by X-ray diffraction. The results are given in Table 20.1.

Surface area measurements of natural and thermal activated clay minerals were made and the results are given Table 20.2.

Figure 20.1 show as an example the thermogravimetric curve (TG) obtained for the natural illite. A continuous weight loss can be seen between 150°C and 980°C the differential thermogravimetric curve (DTG) showing two endothermic effects. The first one is centered at 150°C which corresponds to loss of illite water. The second one is centered about 580°C and is mainly associated to the loss of structural water.

Experimental

Natural clay samples were heated from 110°C to 900°C for 1 hour to obtain thermal activated clay samples. Then samples put in a desiccator containing dried silica gel. Adsorption experiments were carried out in a cylindrical vessel (2.4 L). The constant initial concentrations of 800–920 mg/L of engine oil (SAE 40) were dispersed in 250 mL drinking water by stirring for 5 minutes (synthetically wastewater). Mixing

Table 20.1 Chemical composition of clay sample

Moisture (%)	Weight of loss (%)	Constituent and percentage present								
2.29	10.07	SiO_2	Al_2O_3	Fe_2O_3	TiO_2	CaO	MgO	K_2O	Ma_2O	SO_3
		57.13	23.61	4.02	1.04	0.14	0.60	2.74	0.04	0.10

Table 20.2 Surface areas of clay sample

Type of clay minerals	Surface area (m^2/g)
N	30.0
TA (110°C)	24.5
TA (900°C)	21.0

N: natural clay sample; TA: thermal activated clay sample

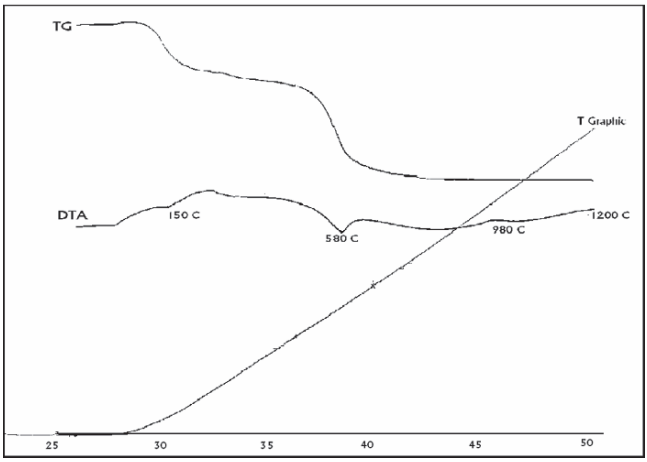

Fig. 20.1 TG and DTG curves obtained for the illite clay sample

was provided by a stainless-steel stirrer while maintaining the stirring speed at round 1,400 rpm. Then the clay sample of 5 g (optimum amount of clay) was added into this mixture and stirred again for 12 minutes (optimum contact time). At the end of adsorption period, the supernatant was centrifuged for 10 minutes at 2,000 rpm. The concentration of oil-grease in the supernatant solution was determined by using UV spectrophotometer. The supernatant solution (acidify with HCl to pH 1) was extracted with 30 mL (three times) of trichloroethylene (Merck 958) separatory funnel. The oil content of investigated oil-in water dispersions were completely removed by using trichloroethylene extractions. Residual concentration of engine oil was calculated with the help of a calibration plot obtained by measuring the absorbance at 274 nm. The amount of adsorbed oil was calculated with the help of the following mass balance equation:

Amount of adsorbed oil (mg g^{-1}) = [(Co-Ce)/μ].V

Where Co and Ce are the initial and equilibrium concentrations (mg mL^{-1}) of oil solution, respectively, V is volume of oil-in water dispersions (mL) and m the amount of adsorbent in gram.

Results and Discussion

Effect of Temperature

The studies relating the effect of temperature on adsorption was carried out at eight different temperatures (natural illite clay, 110°C, 200°C, 350°C, 450°C, 550°C, 750°C, 900°C) with a oil-grease concentration of 1,000 mg L^{-1} and 5 g of illite clay sample, keeping the other parameters constants. Figure 20.2 shows oil-grease adsorption as a function of temperature.

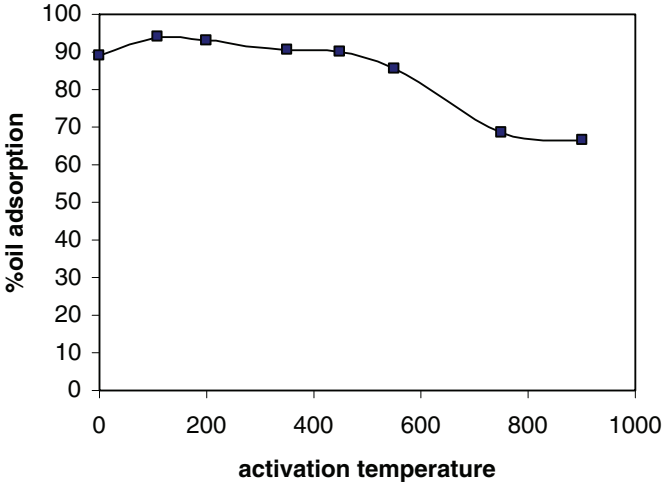

Fig. 20.2 Effect of temperature on percentage adsorption of oil at natural and thermal activate illite clay minerals

Table 20.3 Effect of particle size on adsorption of oil thermal activated illite mineral

Particle size	Oil adsorption (%)
710–600	88.97
600–425	88.61
425–355	88.67
355–150	87.76
150–75	87.34
<75	88.46

Effect of Particle Size

Adsorption of oil- grease for seven different particle sizes on thermally activated illite clay (>710 μm; 710–600 μm; 600–425 μm; 425–355 μm; 355–150 μm; 150–75 μm; <75 μm) was studied keeping the other parameters as constant. The result of variation of this particle sizes on oil-grease adsorption show in Table 20.3.

Effect of pH

pH is one of the important parameters controlling of pH on the adsorption capacity of thermally activated illite, experiments were carried out using various pH

solutions starting from 2 to 11 for the 250 mL volume of oil-grease concentration 1,000 mg L^{-1} and 5 g adsorbent. The result is shown in Fig. 20.3.

Effect of Adsorbent Mass

Figure 20.4 shows the removal of oil-grease by thermally activated illite at different adsorbent doses (0.3–6 g) for the volume of 250 mL at the oil concentration 1,000 mg mL^{-1}. To study the effect of an increase in the adsorbent dose on removal of oil-grease, experiments were conducted employing adsorbent doses ranging from 0.3 to 6 g/250 mL. The results are presented in Fig. 20.4, where it can be seen that oil-grease adsorption is high for higher dosages.

Effect of Contact Time

Figure 20.5 shows the effect of contact time and percentage adsorption oil-grease on the removal by thermally activated illite.

Conclusion

The adsorption capacity of thermal activated illite is increased as 5.5% according to natural illite mineral. It has seen that there is on significant loss of adsorption capacity of illite at about 550°C. The capacity of oil – grease adsorption is

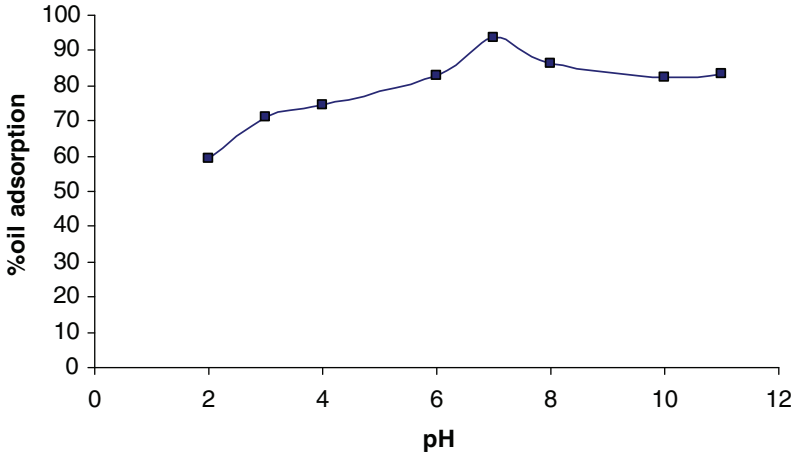

Fig. 20.3 Effect of adsorption on adsorption of oil

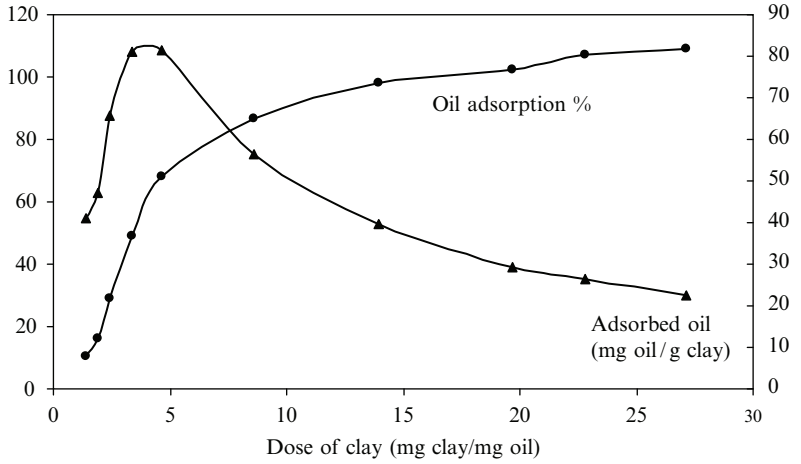

Fig. 20.4 Effect of thermal activated illite clay mineral dose on adsorption of oil grease

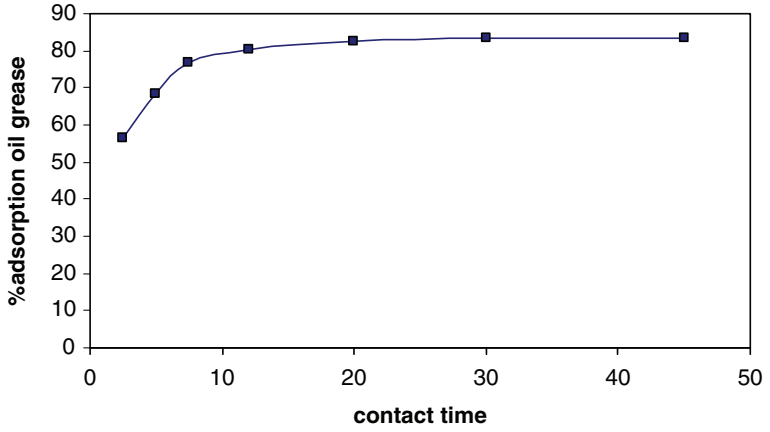

Fig. 20.5 Effect of contact time on adsorption of oil grease

decreased with the temperatures more than 600°C. It can be observed that as the particle size decreases and increases, the adsorption of the oil-grease not effected. The uptake of oil-grease at pH 2 was minimum and the maximum observed at pH 7. It is evident from the Fig. 20.4 that as the mass of the adsorbent dosage increases, the percentage of oil-grease removal also increases. Complete removal of oil-grease was observed at a particular mass in the case, this is due to the increase in surface area with a high dosage of the adsorbent. The adsorption oil-grease at 5 g was the maximum. The adsorption of oil-grease occurred quickly from the beginning of the experiment and as the time progresses the adsorption was not drastically

increased. It can be seen from the graph that maximum adsorption took place at 12 minutes for thermally activated illite. After this time; percentage adsorption was slow leading to a single, smooth and continuous saturation curve. The values obtained for the percentage of oil-grease removed ranged from 93.87% for 110°C up to 66.73% for 900°C. The adsorption experiment showed surface that the stronger heat treatment the most effective adsorption of oil-grease.

References

1. Mohammadi, T. and Esmaelifar, A., 2005, *Journal of Membrane Science,* **254,** 129–137.
2. Alther, G.R., 2002, *Waste Management,* **22,** 507–513.
3. Alther, G.R., 1995, *Waste Management,* **15** (8), 623–628.
4. Almalah, K., Azzam, M.O.J. and Abu-Lail, N.I., 2000, *Separation and Purification Technology,* **20,** 225–234.
5. Chou, K.-S., Tsai, J.-C. and Lo, C.-T., 2001, *Bioresource Technology,* **78** (2), 217–219.
6. Tryba, B., Morawski, A.W., Kalenczuk, R.J. and Inagak, M., 2003, *Spill Science of Technology Bulletin,* **8** (5–6), 569–571.

Chapter 21
Removal of Catechol and Resorcinol from Aqueous Solution by Adsorption onto High Area Activated Carbon Cloth

Numan Hoda*, Edip Bayram, and Erol Ayrancı

Abstract Removal of catechol and resorcinol from aqueous solutions by adsorption onto high area activated carbon cloth (ACC) was investigated. Kinetics of adsorption was followed by in-situ uv-spectroscopy and the data were treated according to pseudo-first-order, pseudo-second-order and intraparticle diffusion models. It was found that the adsorption process of these compounds onto ACC follows pseudo-second-order model. Furthermore, intraparticle diffusion is effective in rate of adsorption processes of these compounds. Adsorption isotherms were derived at 25°C on the basis of batch analysis. Isotherm data were treated according to Langmuir and Freundlich models. The fits of experimental data to these equations were examined.

Keywords Activated carbon cloth, adsorption isotherm, adsorption kinetic, catechol, resorcinol

Introduction

Phenolic compounds and their derivatives are major pollutants for environment because of being widely used in pharmaceutical, plastics, steel, paint, leather industries and oil refineries. Most of these compounds are recognized as toxic and carcinogens. There are some proposed methods to remove phenols from waste effluents such as chemical oxidation, coagulation, solvent extraction, liquid membrane permeation and adsorption [1]. Among these methods, adsorption is an effective method to remove relatively low molecular weight organic compounds with moderate and low concentrations. Activated carbon is the most widely used adsorbent material for adsorption because of its efficiency [1]. Utilization of activated carbon can be in the form of powder, granular and fiber or cloth form. Activated carbon cloth (ACC)

Akdeniz University, Faculty of Arts and Sciences, Department of Chemistry, 07058 Antalya, Turkey
*Corresponding author

B. Sener (ed.), Innovations in Chemical Biology, doi: 10.1007/978-14020-6955-0

having very high specific surface area, adsorption capacity, uniform pore size and mechanical strength has attracted more attention in recent years.

The aims of this study are to investigate the removability of resorcinol and catechol from aqueous solutions by adsorption onto ACC in relation to waste water purification and to determine kinetic and equilibrium adsorption models.

Materials and Methods

Materials

ACC used in the present work was provided by Spectra Corp. (MA, USA) coded as Spectracarb 2225. The chemicals studied catechol and resorcinol were purchased from Sigma and Merck respectively. The chemical structures of these compounds are given in Fig. 21.1. Deionized water was used in adsorption experiments.

Treatment of ACC

It was found by Ayranci and Conway that ACC material provides spontaneously a small but significant quantity of ions into the conductivity water, probably due to its complex structure originating from its somewhat unknown proprietary preparation procedure [2]. A deionization cleaning procedure was therefore applied, as described previously [2, 3] to avoid desorption of ions during the adsorption measurements. In this procedure, ACC sample was placed in a flow-through washing cup and eluted with 5 L of warm (60°C) conductivity water in a kind of successive batch operations for 2 days with N_2 bubbling in order to avoid possible adsorption of CO_2 that might have been dissolved in water. The out-flow water from each batch was tested conductometrically for completeness of the washing procedure. The washed ACC modules were then dried under vacuum at 120°C, cut to desired dimensions (about 1.0 × 1.5 cm), weighed accurately and kept in a desiccator for further use.

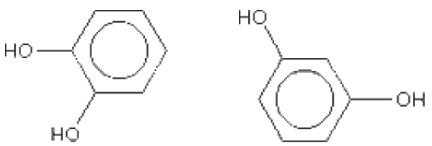

Fig. 21.1 The chemical structures of catechol and resorcinol

Characterization of ACC

Prior to nitrogen adsorption experiment to determine surface properties, ACC sample was degassed at 130°C under vacuum (up to 10^{-6} torr) for 12 h. The N_2 adsorption data were obtained at the Central Laboratory of Middle East Technical University (METU) with a Quantachrome Autosorb-1-C/MS apparatus over a relative pressure ranging from 10^{-6} to 1. The BET specific surface area, S_{BET}, total pore volume, V_{tot}, micropore volume, V_{micro}, mesopore volume, V_{meso}, and pore size distribution, PSD, of ACC were yielded by using the software of the apparatus.

The pH_{pzc} value of washed ACC which is the pH of the solution when the net charge on ACC piece dipped into it is zero, was determined in our previous work [4] using batch equilibrium method described by Babič et al. [5].

Adsorption Cell

A specially designed cell was used to carry out the adsorption studies and simultaneously to perform in situ concentration measurements by means of UV absorption spectrophotometry. This cell, described in detail including a diagram in our previous works [2, 3], was V-shaped with one arm containing ACC attached to a short Pt wire sealed to a glass rod and the other arm containing a thin glass tube through which N_2 gas was passed for the purposes of mixing and eliminating any dissolved CO_2. The two arms were connected to a glass joint leading to a vacuum pump at the upper part of the V-shaped cell in order to provide the opportunity for initial outgassing of the carbon adsorbent. A quartz spectrophotometer cuvette was sealed to the bottom of the adsorption cell.

Optical Absorbance Measurements

A Varian Cary 100 model Uv/vis spectrophotometer was used for optical absorbance measurements. The absorbance measurements were conducted in situ for the study of the kinetics of adsorption process. In all experiments, the size and mass of ACC was kept as constant as possible (about 18.0 ± 0.1 mg). Weighed ACC pieces were pre-wetted by leaving in water for 24 h before use. The idea of using pre-wetted ACC originates from previous findings that pre-wetting enhances the adsorption process [2, 6]. A pre-wetted ACC piece was dipped into the adsorption cell initially containing only water and vacuum was applied to remove all air in the pores of ACC. Then wetted and degassed ACC piece was removed from the cell for a short time and water in the cell was replaced with a known volume of sample solution (20 mL). The sliding door of the sample compartment of the spectrophotometer was left half-open and the quartz cuvette fixed at the bottom of the adsorption cell (which now contained the sample solution) was inserted into the front sample compartment. A teflon tube connected to the tip of a thin N_2-bubbling glass tube

was lowered from one arm of the adsorption cell down the UV cell to a level just above the light path to provide effective mixing. Finally, the ACC piece which was removed temporarily after wetting and degassing was inserted from the other arm of the adsorption cell into the solution. Then, quickly, an opaque curtain was spread above the sample compartment of the spectrophotometer, over the cell, to prevent interference from external light. The temperature of the adsorbate solution was kept constant at 25 ± 1°C during the adsorption process using a termostated cell holder in the sample compartment of the spectrophotometer.

The program for monitoring the absorbance at a specific wavelength of maximum absorbance pre-determined by taking the whole spectrum of each adsorbate was then run on the software of the spectrophotometer. Absorbance data were recorded in programmed time intervals of 2 min until the equilibrium is reached. Then these data were converted into concentration data using calibration relations pre-determined at the wavelength of interest for each adsorbate.

Determination of Adsorption Isotherms

The adsorption isotherms of catechol and resorcinol onto ACC were determined on the basis of batch analysis. ACC pieces of varying weights were allowed to equilibrate with adsorbate solutions of constant initial concentration at 25°C for 48 h. The initial concentration was 7.5 x 10^{-4} M for catechol 7.6 x 10^{-4} M for resorcinol. Preliminary tests showed that the concentration of adsorbates solutions remained unchanged after 18–24 contact with ACC depending on the type of adsorbate. So, the allowed contact time of 48 h ensures the equilibration for two adsorbates. The equilibrium concentrations of adsorbate solutions were measured spectrophotometrically. The amount of adsorbate adsorbed per unit mass of ACC at equilibrium, q_e, was calculated by Eq. 21.1,

$$q_e \frac{V.(c_0 - c_e)}{m} \tag{21.1}$$

where V is the volume of adsorbate solution in liter, c_0 and c_e are the initial and equilibrium concentrations, respectively, of the adsorbate solutions in moles per liter and μ is the mass of ACC in grams. Eq. 21.1 gives q_e as mole adsorbate adsorbed per gram of ACC.

Results and Discussion

Characteristics of ACC

The specific surface area of ACC (S_{BET}) was calculated according to Brunauer, Emmet, Teller method using the linear part of the nitrogen adsorption isotherm shown in Fig. 21.2. S_{BET} was determined as 1,870 $m^2\ g^{-1}$. The total volume of pores,

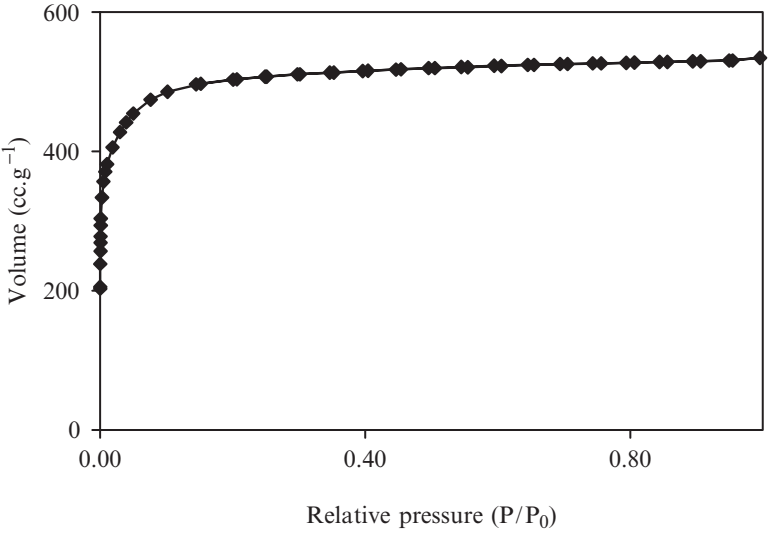

Fig. 21.2 Nitrogen adsorption isotherm at 77.4 K for ACC studied

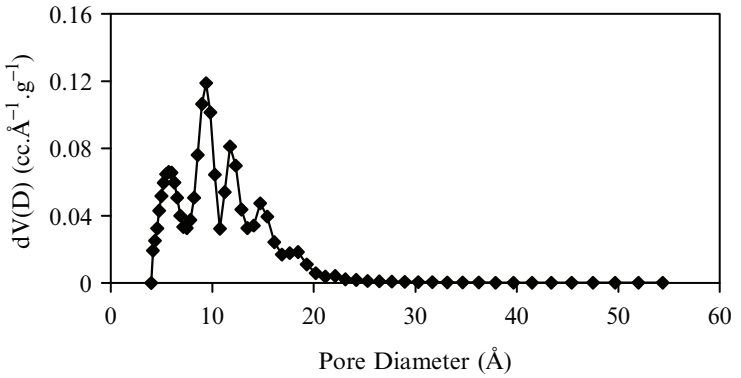

Fig. 21.3 Pore size distribution of ACC according to DFT theory

V_{tot}, was calculated as 0.827 cm^3 g^{-1} using the volume value at the relative pressure of 0.995 from Fig. 21.2.

The pore size distribution (PSD) for mesopores and micropores were calculated using DFT (Density Functional Theory) method and the resulting distribution curves are given in Fig. 21.3. Total mesopore volume (V_{meso}) was determined as 0.022 cm^3 g^{-1} and total micropore volume (V_{micro}) was determined as 0.709 cm^3 g^{-1} from the corresponding method. The ACC consists of pores mainly in micro character (<20 Å) as seen both from Fig. 21.3. The pH_{pzc} value of ACC used in this study had been previously found to be 7.4 [4].

Adsorption Kinetics

Absorption properties and calibration data were studied and the calibration curves of each adsorbate were obtained. Adsorption of adsorbates onto ACC was monitored spectrophotometrically by the procedure described above. Absorbance data, obtained in 2-min intervals until equilibrium, were converted into concentration data using the corresponding calibration relations which were evaluated for catechol at 275 nm and for resorcinol at 274 nm, and then plotted as a function of time in Fig. 21.4 for each adsorbate. Adsorption process of resorcinol was followed during the period of 850 min and of catechol was followed during the time period of 1,042 min which were the times considered the equilibrium reached or near equilibrium. In order to compare adsorption behaviors of adsorbates, the initial concentrations (5.7×10^{-5} M), volumes (20 mL) of adsorbate solutions and the mass of ACC (18.0 ± 0.1 mg) were taken to be the same during the whole adsorption studies. As seen in Fig. 21.4, concentration vs time curves of adsorbates catechol and resorcinol, at the initial stages of adsorption processes, resorcinol is more adsorbed than catechol. At the later stages their adsorption rate almost overlapped. Concentrations of adsorbates catechol and resorcinol in solution decreased to 4.4×10^{-5} and 4.2×10^{-5}, respectively, all from the same initial concentration of 5.7×10^{-5} M, by adsorption onto ACC during the course of adsorption. In other words, concentrations of adsorbates in aqueous solution were reduced by a factor of approximately 13 for catechol, 13.5 for resorcinol over the periods of their adsorption.

Three kinetic models were applied to adsorption kinetic data in order to investigate the behavior of adsorption process of adsorbates catechol and resorcinol onto ACC. These models are the pseudo-first-order, the pseudo-second-order and the intraparticle diffusion models. Linear form of pseudo-first-order model can be formulated as

$$\ln(q_e - q_t) = \ln(q_e) - k_1 t \tag{21.2}$$

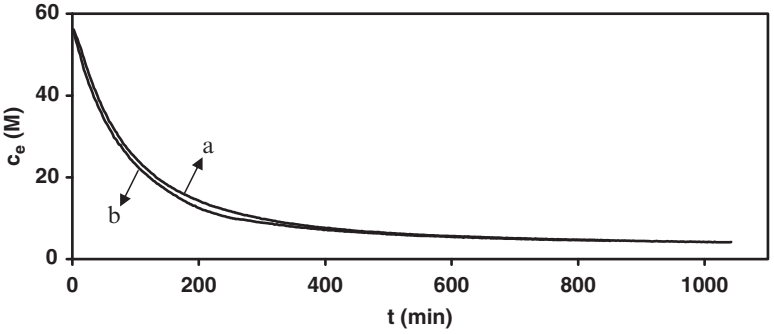

Fig. 21.4 Adsorption behaviors of catechol (a) and resorcinol (b) from aqueous solutions onto ACC

where q_e (mol g^{-1}) and q_t (mol g^{-1}) are the amount of adsorbate adsorbed at equilibrium and at time t, respectively, and k_1 (min^{-1}) is the rate constant. k_1 values were evaluated from the linear regression of ln (q_e-q_t) vs t data for each adsorbate and are tabulated in Table 21.1. In this table the experimental q_e values calculated using initial and equilibrium concentrations (Fig. 21.4) of each adsorbate according to Eq. 21.1 and q_e values from the intercept of linear regression analysis according to the model (Eq. 21.2) are also given.

The linear form of pseudo-second-order equation can be formulated as

$$\frac{t}{q_t} = \frac{1}{k_2 q_e^2} + \frac{1}{q_e} t \tag{21.3}$$

where k_2 (g mol^{-1} min^{-1}) is the second-order rate constant. The linear plot of t/qt as a function of t provided not only the rate constant k_2, but also an independent evaluation of q_e. The results are given in Table 21.1. The fit of experimental data to the pseudo-first-order and the pseudo-second-order equations seemed to be quite good when correlation coefficients (r) obtained from linear regression analysis were examined (r values are not given but all are greater than 0.9). However, it is very difficult to decide which model represents the experimental data best just on the basis of regression coefficients. A better criterion to find the best model for the experimental data is a parameter known as normalized percent deviation [1] or in some literature percent relative deviation modulus, P, defined by the following equation [7]

$$p = (100 / N) \sum (| q_{t(\text{expt})} - q_{t(\text{pred})} | / q_{t(\text{expt})}) \tag{21.4}$$

where $q_{t(\text{expt})}$ is the experimental q_t at any t, $q_{t(\text{pred})}$ is the corresponding predicted q_t according to the equation under study with best fitted parameters, N is the number of data points. It is clear that the lower the P value, the better is the fit. When the P values given in Table 21.1 are examined, it can be seen that they are much smaller for the second-order model than for the first-order model leading to a conclusion that the kinetic data of adsorption of catechol and resorcinol onto ACC fit to the second-order model better than the first-order model. This is also evident that in differences in experimental (q_e(expt)) and calculated (q_e(cal)) values which are given in Table 21.1. Calculated q_e values are much closer for second-order model than that for first-order model. Other researchers have investigated the kinetics of adsorption of catechol and resorcinol onto different polymers within first 80 min. They applied their experimental

Table 21.1 Experimental and calculated q_e values, rate constants of pseudo-first-order, pseudo-second-order and intraparticle diffusion models

	q_e	k	P	q_e	k_2	P	q_e	k_i	P
Adsorbate	(Experimental)			(Calculated)			(Calculated)		
Resorcinol	6.1×10^{-4}	2.28×10^{-3}	23.75	2.6×10^{-4}	25.54	2.49	6.3×10^{-4}	4.50×10^{-5}	1.29
Catechol	5.9×10^{-4}	5.60×10^{-3}	10.69	4.2×10^{-4}	22.07	2.88	6.4×10^{-4}	4.79×10^{-5}	1.17

data first-order kinetic model and found that k_1 values of resorcinol were higher than that of catechol. At the early stages of adsorption process, generally, adsorption data fit to first-order kinetic model as can be concluded from literature; Adsorption of inorganic S-containing anions [2], ethyl xanthate and thiocyanate [6, 8], phenol, phenoxide and chlorophenols [9], some aromatic heterocyclic compounds [10] pyridine, aniline and bipyridyls [11, 12] metribuzin, bromacil, 2,4-D, atrazine, bentazon and propanil [3, 13]. In our work, if the adsorption kinetic data of adsorbates were fitted to first-order kinetic model at the initial stages of adsorption, it could be obtained that adsorption processes of these adsorbates fit to first-order model well and resorcinol has higher k_1 value that that of catechol (Fig. 21.4).

Kinetic data of adsorption of catechol and resorcinol were also tested according to intraparticle diffusion model which can be formulated as

$$q_t = k_i t^{1/2} + I \tag{21.5}$$

where k_i (mol g^{-1} $min^{-1/2}$) is the intraparticle diffusion rate constant and I (mol g^{-1}) is a constant. q_t vs $t^{1/2}$ plots may present multi-linearity indicating that two or more stages occur. The first linear portion is the instantaneous adsorption stage or external surface adsorption while second portion is the gradual adsorption stage where intraparticle diffusion is rate limiting and third one is the final equilibrium stage where the intraparticle starts to slow down due to extremely low adsorbate concentrations left in the solution. The value of I provides information about the thickness of the boundary layer, i.e. the larger intercept is the higher external resistance [14]. From Figs. 21.5 and 21.6, it can be observed that the

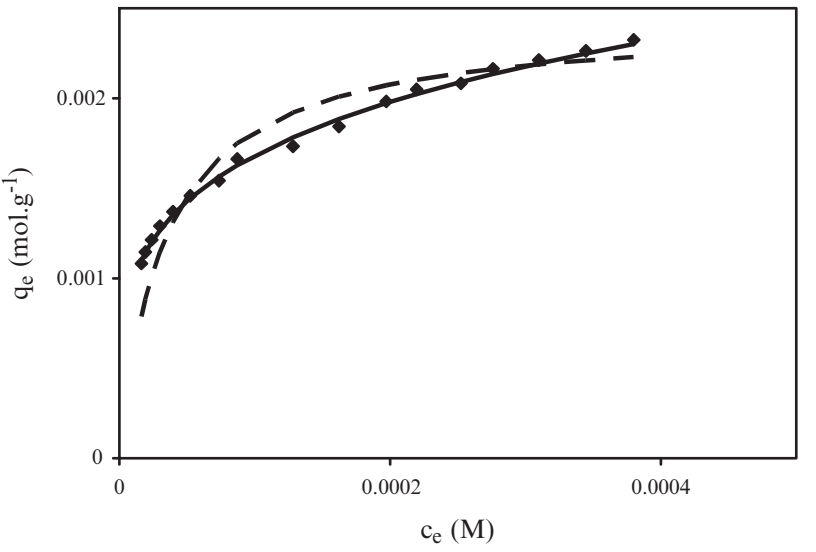

Fig. 21.5 The fit of experimental adsorption data (▲) to Freundlich (—) and Langmuir (---) models for catechol

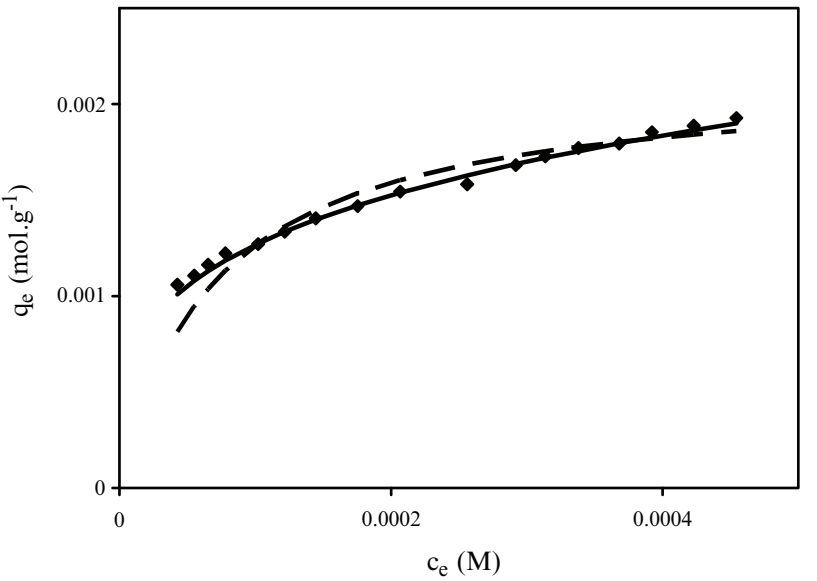

Fig. 21.6 The fit of experimental adsorption data (▲) to Freundlich (—) and Langmuir (---) models for resorcinol

straight line does not pass through the origin indicating that the intraparticle diffusion is not only the rate controlling step [15–17]. As can be seen in Table 21.1 the second portion shows a well linearity with high P values and also there can seen that k_i value of catechol is higher than that of resorcinol. Therefore, it can be concluded that intraparticle diffusion appears to be rate limiting step in the adsorption of catechol and resorcinol onto ACC from aqueous solutions.

Adsorption Isotherms

Adsorption isotherms of catechol and resorcinol were determined on the basis of batch analysis at 25°C using a series of adsorbate solutions at fixed concentration and volume in contact with ACC pieces of varying masses. Adsorption isotherm data of catechol and resorcinol were fitted to well-known and widely applied isotherm models of Langmuir and Freundlich. The Langmuir isotherm is based on the assumption that adsorption takes place at specific homogeneous sites within the adsorbent and there is no significant interaction among adsorbed species and that the adsorbent is saturated after one layer of adsorbate molecules formed on the adsorbent surface. The linearized Langmuir isotherm equation can be written as follows

$$\frac{c_e}{q_e} = \frac{1}{bq_m} + \frac{c_e}{q_m} \tag{21.6}$$

Table 21.2 The parameters of Langmuir and Freundlich isotherm equations for the adsorption of catechol and resorcinol

	Langmuir			Freundlich		
Adsorbate	q_m(mol g^{-1})	b (L mol^{-1})	P	K (mol$^{1-(1/n)}$ L$^{1/n}$ g^{-1})	1/n	P
Resorcinol	2.11 x 10^{-3}	15,728	5.25	1.35 x 10^{-2}	0.25	1.37
Catechol	2.24 x 10^{-3}	29,686	7.93	1.47 x 10^{-2}	0.23	1.25

where q_e (mol g^{-1}) is the amount of solute adsorbed per unit mass of adsorbent, c_e (mol L^{-1}) is the equilibrium concentration of solute, q_m (mol g^{-1}) is the maximum amount of adsorbent to form a complete monolayer on the surface, b (L mol^{-1}) is a constant related to the heat of adsorption. When c_e/q_e is plotted against c_e and the data are regressed linearly, q_m and b constants can be calculated from the slope and the intercept.

The Freundlich isotherm model takes the multilayer and heterogeneous adsorption into account. Its linearized form can be given as follows

$$\ln q_e = \ln K + \frac{1}{n}\ln c_e \tag{21.7}$$

where q_e and c_e have the same definitions as in Langmuir equation above. Freundlich constant, K (mol$^{1-(1/n)}$ L$^{1/n}$ g^{-1}) is related to the adsorption capacity of ACC and 1/n is another constant related to the surface heterogeneity. When lnq_e is plotted against lnc_e and the data are treated by linear regression analysis, 1/n and K constants are determined from the slope and intercept. The value of 1/n is known as the heterogeneity factor and ranges between 0 and 1; the more heterogeneous the surface, the closer 1/n value is to 0 [18].

The Langmuir and Freundlich isotherm parameters for the adsorption of catechol and resorcinol onto ACC are given in Table 21.2. Experimental isotherm data for these adsorbates are given in Figs. 21.5 and 21.6 where the fitted Langmuir and Freundlich isotherm curves are also shown. As in the case of examining the goodness of fit of kinetic models to experimental data, the regression coefficients alone were insufficient in determining the best isotherm model to represent the experimental data because they were mostly greater than 0.9 for both models. So, again a P parameter defined by an equation similar to Eq. 21.4 with q_t terms replaced by q_e terms was used as a criterion in finding the best isotherm model to fit the experimental data. These P values are included in Table 21.2. In general, it is accepted that when the P value is less than 5, the fit of data to the model is considered to be excellent. The P values for Freundlich model are much less than 5 for catechol and resorcinol. So, it can be concluded that Freundlich model is good for representing the adsorption isotherm data of the adsorbates studied.

Acknowledgements Authors thank to the Scientific Research Projects Unit of Akdeniz University for the support of this work through the project 2003.01.0300.009, to the Spectra Corp. (MA., USA) for providing the ACC and to METU for carrying out measurements to determine the surface properties of the ACC.

References

1. Juang, R.-S., Tseng, R-L., Wu, F-C. and Lee, S-H., 1996, *Separ. Sci. Technol.,* **31,** 1915–1931.
2. Ayranci, E. and Conway, B.E., 2001a, *J., Appl. Electrochem.,* **31,**257–266.
3. Ayranci, E. and Hoda, N., 2004a, *J. Hazard. Mater.,* **B112,** 163–168.
4. Duman, O. and Ayranci, E., 2005, *J. Hazard. Mater.,* **B120,** 173–181.
5. Babić, B.M., Milonjić, S.K., Polovina, M.J. and Kaludierovi , B.V., 1999, *Carbon,* **37,** 477–481.
6. Ayranci, E. and Conway, B.E., 2001b, *Anal. Chem.,* **73,** 1181–1189.
7. Ayranci, E. and Dalgıç, A.C., 1992, *Lebensm-Wiss. Technol.,* **25,** 482–483.
8. Conway, B.E., Ayranci, E. and Al-Maznai, H., 2001, *Electrochim. Acta,* **47,** 705–718.
9. Ayranci, E. and Conway, B.E., 2001c, *J. Electroanal. Chem.,* **513,** 100–110.
10. Conway, B.E., Ayranci, G. and Ayranci, E., 2003, *Z. Phys. Chem.,* **217,** 315–331.
11. Niu, J. and Conway, B.E., 2002a, *J. Electroanal. Chem.,* **521,** 16–28.
12. Niu, J. and Conway, B.E., 2002b, *J. Electroanal. Chem.,* **536,** 83–92.
13. Ayranci, E. and Hoda, N., 2004b, *Chemosphere,* **57,** 755–762.
14. Kannan, N. and Sundaram, M.M., 2001, *Dyes Pigments,* **51,** 25–40.
15. Mohan, S.V. and Karthikeyan, J., 1997, *Environ. Pollut.,* **97,** 183–187.
16. Sankar, M., Sekoron, G., Sadulla, S. and Ramasami, T., 1999, *J. Chem. Technol. Biot.,* **74,** 337–344.
17. Gupta, G.S., Prasad, G. and Singh, V.N., 1988, *J. Environ. Sci. Heal. A.,* **23,** 205–217.
18. Al Duri, B. and McKay, G. (eds), 1995, *Adsorption Modeling and Mass Transfer*, CRC, Boca Raton, FL, pp 133–173.

Chapter 22
Removal of Metobromuron Pesticide from Aqueous Solutions by Adsorption at High Area Activated Carbon Cloth

Numan Hoda*, Edip Bayram, and Erol Ayrancı

Abstract Removal of the pesticide metobromuron from aqueous solutions by adsorption at the high area activated carbon cloth was investigated. Kinetics of adsorption was followed and adsorption isotherms of the pesticide was also be determined. In kinetic studies a special V-shaped cell with an UV cuvette attached to it was used for adsorption processes. With this cell it was possible to follow the concentration of pesticide molecule by in situ UV spectroscopy as it is adsorbed at the activated carbon cloth. The obtained absorbance vs time data were converted into concentration vs time data and these data were treated according to pseudo-first-order and pseudo-second-order kinetic models. Adsorption of that pesticide was found to follow second-order kinetic model with k_2 87.35 g mol^{-1} min^{-1}. Adsorption isotherms were derived at 25°C on the basis of batch analysis. Isotherm data were treated according to Langmuir and Freundlich models. The fits of experimental data to these equations were examined and founded that the adsorption isotherm was well represented by Freundlich model.

Keywords Activated carbon, isotherm, kinetics, metobromuron, pesticide

Introduction

Pesticides are chemicals, which are commonly used in agriculture to protect crops from pest organisms including insects, plants, fungi, rodents and nematodes. Pollution of surface and ground waters because of extensive application of pesticides causes risk to human health during their cycles. Before offering drinking waters to public use they should be treated to remove such pollutants. Adsorption is one of the most frequently applied methods. The most commonly used adsorbent in adsorption processes is activated carbon [1–5]. Utilization of activated carbon can be in the form of powder, granular and fiber or cloth. Activated carbon cloth

Akdeniz University, Faculty of Arts and Sciences, Department of Chemistry, 07058 Antalya, Turkey
*Corresponding author

B. Sener (ed.), *Innovations in Chemical Biology*, doi: 10.1007/978-1-4020-6955-0

(ACC) having very high specific surface area, adsorption capacity and mechanical strength, has gained increasing in studies of the removal of many pollutants from waste water by adsorption in recent years [5, 6–13].

The purpose of the present study was to investigate the adsorption behavior of the metobromuron (3-(4-bromophenyl)-1-methoxy-1-methylurea) at the high area ACC from aqueous solutions and thus the possibility of removal of that pesticide from waters.

Materials and Methods

Materials

Activated carbon cloth ACC used in the present work was provided by Spectra Corp. (MA, USA) coded as Spectracarb 2225. The pesticide metobromuron was obtained from Riedel de Häen. The chemical structure of that pesticide is given in Fig. 22.1. Deionized water was used in adsorption experiments.

Methods

The commercial ACC was washed by the procedure, especially ions, described in our previous works [6, 14] to remove impurities remaining in its structure from the activation process. In this procedure, ACC sample was placed in a flow-through washing cup and eluted with 5 L of warm (60°C) conductivity water in a kind of successive batch operations for 2 days with N_2 bubbling in order to avoid possible adsorption of CO_2 that might have been dissolved in water. The out-flow water from each batch was tested conductometrically for completeness of the washing procedure. The washed ACC modules were then dried under vacuum at 120°C, cut to desired dimensions (about 1.0 × 1.5 cm), weighed accurately and kept in a desiccator for further use.

Surface characterization of washed ACC was already described in our previous works [15, 16]. The results of chemical and physical characteristics of ACC are summarized in Table 22.1.

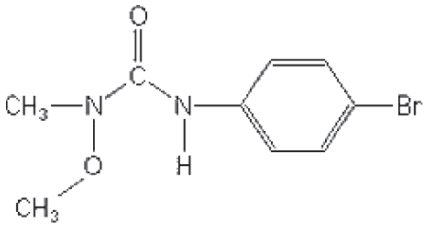

Fig. 22.1 Chemical structure of metobromuron

Table 22.1 Chemical, physical and surface properties of washed ACC

Specific surface area	1,870 m^2 g^{-1}
Total pore volume	0.827 cm^3 g^{-1}
Micropore volume	0.709 cm^3 g^{-1}
Mesopore volume	0.082 cm^3 g^{-1}
Average fiber diameter	17 μm
Carbon content	95.14%
Hydrogen content	0.37%
Oxygen content	4.49%
Nitrogen and Sulfur content	0%
pH_{pzc}	7.4
Total acidic group content	0.25 meq g^{-1}
Total basic group content	0.28 meq g^{-1}

A specially designed cell was used to carry out the adsorption studies and simultaneously to perform in situ concentration measurements by means of UV absorption spectrophotometry. This cell, described in detail, including a diagram, in our previous works [6, 9] was V-shaped with one arm containing ACC attached to a short Pt wire sealed to a glass rod and the other arm containing a thin glass tube through which N_2 gas was passed for the purposes of mixing and eliminating any dissolved CO_2. The two arms were connected to a glass joint leading to a vacuum pump at the upper part of the V-shaped cell in order to provide the opportunity for initial outgassing of the carbon adsorbent. A quartz spectrophotometer cuvette was sealed to the bottom of the adsorption cell.

A Varian Cary 100 model UV/vis spectrophotometer was used for optical absorbance measurements. The absorbance measurements were conducted in situ for the study of the kinetics of adsorption process. In all experiments, the size and mass of ACC was kept as constant as possible (about 18.0 ± 0.1 mg). Weighed ACC pieces were pre-wetted by leaving in water for 24 h before use. The idea of using pre-wetted ACC originates from previous findings that pre-wetting enhances the adsorption process [9, 11].

A pre-wetted ACC piece was dipped into the adsorption cell initially containing only water and vacuum was applied to remove all air in the pores of ACC. Then wetted and degassed ACC piece was removed from the cell for a short time and water in the cell was replaced with a known volume of sample solution (20 mL). The sliding door of the sample compartment of the spectrophotometer was left half-open and the quartz cuvette fixed at the bottom of the adsorption cell (which now contained the sample solution) was inserted into the front sample compartment. A Teflon tube connected to the tip of a thin N_2-bubbling glass tube was lowered from one arm of the adsorption cell down the UV cell to a level just above the light path to provide effective mixing. Finally, the ACC piece removed temporarily after wetting and degassing was reinserted from the other arm of the adsorption cell into the solution. Then, quickly, an opaque curtain was spread above the sample compartment of the spectrophotometer, over the cell, to prevent interference from external light. The temperature of the adsorbate solution was kept constant at 25 ±

1°C during the adsorption process using a termostated cell holder in the sample compartment of the spectrophotometer.

The program for monitoring the absorbance at a specific wavelength of maximum absorbance (244 nm) pre-determined by taking the whole spectrum of metobromuron was then run on the software of the spectrophotometer. Absorbance data were recorded in programmed time intervals of 1 min until the equilibrium is reached. Absorbance data were converted into concentration data using calibration relations pre-determined at the wavelength of interest for pesticide metobromuron.

The adsorption isotherms of metobromuron onto ACC were determined on the basis of batch analysis. ACC pieces of varying weights were allowed to equilibrate with metobromuron solutions each having the same initial concentration of 1.05×10^{-4} M at 25°C for 48 h. Preliminary tests showed that the concentration of pesticide solution remained unchanged after about 19 h contact with ACC. So, the allowed contact time of 48 h ensures the equilibration for metobromuron. The equilibrium concentrations of pesticide solutions were measured spectrophotometrically. The amount of pesticide adsorbed per unit mass of ACC at equilibrium, q_e, was calculated by Eq. 22.1,

$$q_e \frac{V.(c_0 - c_e)}{m} \tag{22.1}$$

where V is the volume of pesticide solution in liter, c_0 and c_e are the initial and equilibrium concentrations, respectively, of the pesticide solution in moles per liter and μ is the mass of ACC in grams. Eq. 22.1 gives q_e as mole pesticide adsorbed per gram of ACC.

Results and Discussion

In order to obtain the calibration curve of pesticide metobromuron, absorbances were measured at the corresponding λ_{max} as a function of concentration and the data were fitted to Lambert–Beer law by the method of least square analysis. The resulting correlation coefficient (R^2: 1.0000) show that the fit to Lambert–Beer law is excellent. The obtained calibration equation was used to convert absorbances into concentrations in kinetic and equilibrium studies.

Adsorption of metobromuron onto ACC was monitored spectrophotometrically at 244 nm by the procedure described above. Absorbance data, obtained in 1-min intervals until equilibrium, were converted into concentration data using the corresponding calibration relation and then plotted as a function of time in Fig. 22.2. Initial concentration of pesticide in the solution was 7.64×10^{-5} M and adsorption equilibrium time using 18 mg ACC, determined as the time after which the concentration of the pesticide solution remained unchanged during the course of adsorption process, was 1,156 min. The decrease in concentration of pesticide is fast at the early stages, while it slows down toward the end of adsorption period. Concentration

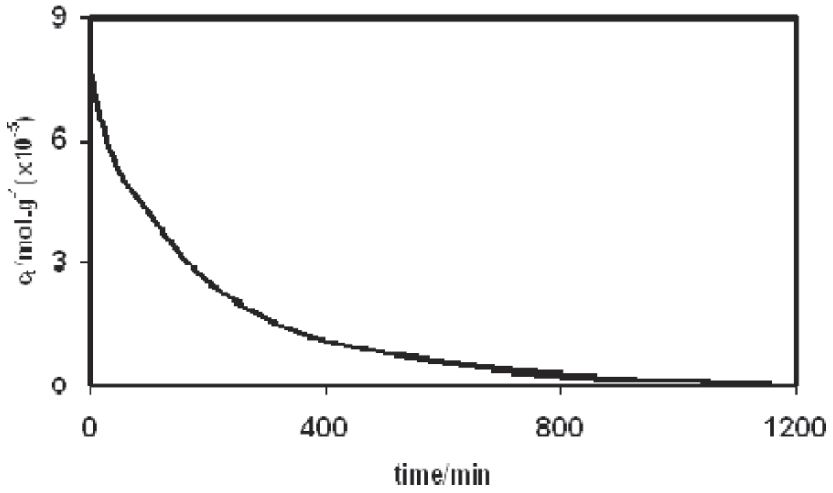

Fig. 22.2 Adsorption behaviors of pesticide metobromuron from aqueous solutions onto ACC

of pesticide solution decreased to 1.35 x 10^{-6} M from the initial concentration of 7.64 x 10^{-5} M, by adsorption onto ACC until its equilibrium time. In other words, concentrations of pesticide in aqueous solution were reduced by a factor of approximately 57 over the course of adsorption.

Kinetic data presented in Fig. 22.2 for the adsorption of metobromuron were fitted to the pseudo-first-order and the pseudo-second-order rate laws. Linear form of pseudo-first-order model can be formulated as

$$\ln(q_e - q_t) = \ln(q_e) - k_1 t \tag{22.2}$$

where q_e (mol g^{-1}) and q_t (mol g^{-1}) are the amount of pesticide adsorbed at equilibrium and at time t, respectively, and k_1 (min^{-1}) is the rate constant. k_1 value was evaluated from the linear regression of ln (q_e–q_t) vs t data for pesticide.

The linear form of pseudo-second-order equation can be formulated as

$$\frac{t}{q_t} = \frac{1}{k_2 q_e^2} + \frac{1}{q_e} t \tag{22.3}$$

where k_2 (g mol^{-1} min^{-1}) is the second-order rate constant. The linear plot of t/q_t vs t provided not only the rate constant k_2, but also an independent evaluation of q_e.

The results of applied kinetics model are given in Table 22.2. In this table the experimental q_e values calculated using initial and equilibrium concentrations (Fig. 22.1) of the pesticide according to Eq. 22.1 and q_e values from the intercept of linear regression analysis according to the model (Eq. 22.2) are also given. The fit of experimental data to the pseudo-first-order and the pseudo-second-order equations seem to be quite good when correlation coefficients (R^2) obtained from linear regression analysis are examined. However when the experimental and calculated

Table 22.2 Rate constants and correlation coefficients obtained from treatment of adsorption data according to the two kinetic models

First-order		
q_e (mol g^{-1}) (calculated)	k_1 (min^{-1})	R^2
1.50 x 10^{-2}	1.77 x 10^{-3}	0.9980
Second-order		
q_e (mol g^{-1}) (calculated)	k_{29} (g mol^{-1} min^{-1})	R^2
9.35 x 10^{-6}	87.35	0.9992

q_e values obtained from these models are compared, it can be seen that q_e value calculated from second-order model is closer to the experimental q_e value of 8.4 x 10^{-5} than that calculated from the first order model. So, it can be concluded that adsorption of metobromuron onto ACC follows pseudo-second-order kinetics.

Adsorption isotherm of metobromuron was determined on the basis of batch analysis at 25°C using a series of pesticide solutions at a fixed concentration of 1.05 × 10^{-4} M and a volume of 50 mL in contact with ACC pieces of varying masses covering the range from 6.0 to 34.0 mg. Adsorption isotherm data of pesticide were fitted to well-known isotherm models of Langmuir and Freundlich. The Langmuir isotherm is based on the assumption that adsorption takes place at specific homogeneous sites within the adsorbent and there is no significant interaction among adsorbed species and that the adsorbent is saturated after one layer of adsorbate molecules formed on the adsorbent surface. The linearized Langmuir isotherm equation can be written as follows

$$\frac{c_e}{q_e} = \frac{1}{bq_m} + \frac{c_e}{q_m} \tag{22.4}$$

where q_e (mol g^{-1}) is the amount of solute adsorbed per unit mass of adsorbent, c_e (mol L^{-1}) is the equilibrium concentration of solute, q_m (mol g^{-1}) is the maximum amount of adsorbent to form a complete monolayer on the surface, b (L mol^{-1}) is a constant related to the heat of adsorption. When c_e/q_e is plotted against c_e and the data are regressed linearly, q_m and b constants can be calculated from the slope and the intercept.

The Freundlich isotherm model takes the multilayer and heterogeneous adsorption into account. Its linearized form can be given as follows

$$\ln q_e = \ln K + \frac{1}{n} \ln c_e \tag{22.5}$$

where q_e and c_e have the same definitions as in Langmuir equation above. Freundlich constant, K ($mol^{1-(1/n)}$ $L^{1/n}$ g^{-1}) is related to the adsorption capacity of ACC and 1/n is another constant related to the surface heterogeneity. When $\ln q_e$ is plotted against $\ln c_e$ and the data are treated by linear regression analysis, 1/n and K constants are determined from the slope and intercept. The value of 1/n is known as the heterogeneity

factor and ranges between 0 and 1; the more heterogeneous the surface, the closer 1/n value is to 0 [17].

The Langmuir and Freundlich isotherm parameters for the adsorption of pesticide studied onto ACC are given in Table 22.3. Experimental isotherm data for the pesticide are given in Fig. 22.3 where the fitted Langmuir and Freundlich isotherm curves are also shown. The correlation coefficients, R^2, given in Table 22.3 for fitting the experimental data points to the linear forms of the two equations can be considered as a measure of goodness of fit. It is seen that Freundlich model having R^2 greater than that of Langmuir model, is successful in representing experimental isotherm data. According to the IUPAC classification metobromuron adsorption isotherm exhibits a type I isotherm which is for microporous adsorbents. Furthermore, the S_{BET} and PSD data of this adsorbent described above also support this suggestion.

According to another system of classification of solution adsorption isotherms by Giles et al. [18] the main classes are S, L, H and C isotherms. These workers indicated that L curves occur in probably the majority of cases of adsorption from

Table 22.3 The parameters of Langmuir and Freundlich isotherm equations for the adsorption of metobromuron

Langmuir parameters	
q_m (mol g^{-1})	1.01 x 10^{-3}
b (L mol^{-1})	298,900
R^2	0.9219
Freundlich parameters	
K ($mol^{1-(1/n)}$ $L^{1/n}$ g^{-1})	0.426
1/n	0.542
R^2	0.9901

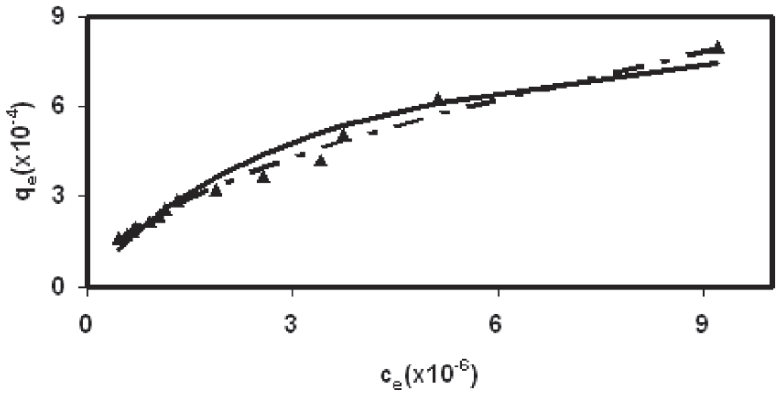

Fig. 22.3 The fit of experimental adsorption data (▲) to Langmuir (—) and Freundlich (---) models for metobromuron

dilute solutions. Indeed, the shape of isotherm of metobromuron obtained in the present work fall into L class isotherm. In this type of isotherm the initial curvature shows that as more sites on the surface are filled it becomes increasingly difficult for a bombarding of solute molecule to find a vacant site available. One more implication of this is that there is no strong competition from the solvent [18].

Conclusions

Adsorption kinetic and adsorption isotherm of pesticide metobromuron at the high area ACC were investigated in relation to water treatment. The ACC used in this study seems to be quite effective in adsorption of metobromuron from aqueous solutions. Adsorption of that pesticide was found to follow second-order kinetic model and the adsorption isotherm is well represented by Freundlich model.

Acknowledgements Authors thank to the Scientific Research Projects Unit of Akdeniz University for the support of this work through the project 2003.01.0300.009.

References

1. Yang, M., Hubble, J., Lockett, A.D. and Rathbone, R.R., 1997, *Water Research,* **31,** 2356–2362.
2. Kouras, A., Zouboulis, C. and Kouimtzis, Th., 1998, *Environmental Pollution,* **109,** 193–202.
3. Baup, S., Jaffree, D., Wolbert, D. and Laphanche, A., 2000, *Adsorption,* **6,** 219–228.
4. Campos, C., Snoeyink, V.L., Marinas, B., Baudin, I. and Laine, J.M., 2000, *Water Research,* **34,** 4070–4080.
5. Martín-Gullón, I. and Font, R., 2000, *Water Research,* **35,** 516–520.
6. Ayranci, A. and Hoda, N., 2004, *Journal Hazardous Materials,* **B112,** 163–168.
7. Brasquet, C. and Le Cloirec, P., 1997, *Carbon,* **35,** 1307–1313.
8. Faur-Brasquet, C., Kadirvelu, K. and Le Cloirec, P., 2002, *Carbon,* **40,** 2387–2392.
9. Ayranci, E. and Conway, B.E., 2001, *Journal of Applied Electrochemistry,* **31,** 257–266.
10. Conway, B.E., Ayranci, G. and Ayranci, E., 2003, *Zeitschrift für Physikalische Chemie,* **217,** 315–331.
11. Ayranci, E. and Conway, B.E., 2001, *Analytical Chemistry,* **73,** 1181–1189.
12. Ayranci, E. and Conway, B.E., 2001, *Journal of Electroanalytical Chemistry,* **513,** 100–110.
13. Niu, J. and Conway, B.E., 2002, *Journal of Electroanalytical Chemistry,* **551,** 16–28.
14. Ayranci, E. and Hoda, N., 2004, *Chemosphere,* **57,** 755–762.
15. Hoda, N., Bayram, E. and Ayranci, E., 2006, *Journal of Hazardous Materials,* **137,** 344–351.
16. Duman, O. and Ayranci, E., 2005, *Journal of, Hazardous Materials,* **B120,** 173–181.
17. Al Duri, B., 1995, Adsorption Modeling and Mass Transfer. In *Use of Adsorbents for the Removal of Pollutants from Wastewaters,* G. McKay (ed.), CRC, Boca Raton, Florida, pp 133–173.
18. Giles, C.H., MacEwan, T.H., Nakhwa, S.N. and Smith, D., 1960, *Journal of Chemical Society,* 3973–3993.

Chapter 23
Effects of Thermal Treatment and Storage on Hydroxymethylfurfural (HMF) Content and Diastase Activity of Honeys Collected from Middle Anatolia in Turkey

Kadir Turhan

Abstracts The composition and properties of honey are dependent on floral origins utilized by the bees and the climatic conditions of the area from which honey is harvested. Honey is a complex mixture, mainly composed of water, sugars (glucose, fructose, sucrose, maltose, and higher sugars), gluconic acid, lactone, nitrogenous compounds, minerals, and some vitamins. Novel studies on physical and chemical properties of the types of honey produced in different countries have been reported by many scientists. Hydroxymethylfurfural (HMF) is a cyclic aldehyde that is produced by degradation of sugars.

Several factors influence the formation of HMF in honey: temperature and time of heating; storage conditions; use of metallic containers and the chemical properties of honey, which are related to the floral source from which the honey has been extracted, these indicate pH, total acidity, mineral content; however, no information on the correlation between chemical characteristics and HMF level of the honey is available.

This study has two goals: The first one is to investigate the effects of storage on HMF formation and diastase activity of honey. Second one is to determine HMF level and formation kinetics of honey after heating process. For this purpose 40 samples of honey were collected from Middle Anatolia and surrounding areas. The physicochemical properties of honey collected were determined. The obtained data were compared with results of other researchers.

Keywords Anatolia, diastase activity, honey, hydroxymethylfurfural

Introduction

The composition and properties of honey are dependent on floral origins utilized by the bees and the climatic conditions of the area from which honey is harvested *[1, 2]*. Honey is a complex mixture, mainly composed of water, sugars (glucose, fructose,

Yıldız Technical University, Department of Chemistry, Davutpasa Campus, 34220 Esenler-Istanbul, Turkey

B. Sener (ed.), *Innovations in Chemical Biology*, doi: 10.1007/ 978-1-4020-6955-0

sucrose, maltose, and higher sugars), gluconic acid, lactone, nitrogenous compounds, minerals, and some vitamins [3]. Novel studies on physical and chemical properties of the types of honey produced in different countries have been reported by many scientists [4]. Hydroxymethyl-furfural (HMF) is a cyclic aldehyde that is produced by degradation of sugars [3].

HMF levels and diastase testing, for measuring honey quality have been in use for over 75 years. A detailed description of the step-by-step process in using these tests, as well as a criticism of diastase as a quality index, has been reported [5]. Based on the assumption that an index for excessive storage and/or heat exposure should be: (1) easily measurable, (2) virtually absent in the fresh honey, (3) responsive in a predictable way to heating and storage, (4) independent of honey type or composition in its response, White proposed the HMF level as the only reliable heating/storage index in honey.

It is well known that heating of honey results in HMF, which is formed during acid-catalysed dehydration of hexoses [6]. The presence in honey of simple sugars (glucose and fructose) and many acids is a favourable condition for the production of this substance.

Several factors influence the formation of HMF in honey: temperature and time of heating [7]; storage conditions; use of metallic containers [8] and the chemical properties of honey, which are related to the floral source from which the honey has been extracted, these indicate pH, total acidity, mineral content [9]; however, no information on the correlation between chemical characteristics and HMF level of the honey is available.

This study has two goals: The first one is to investigate the effects of storage on HMF formation and diastase activity of honey. Second one is to determine HMF level and formation kinetics of honey after heating process. For this purpose 40 samples of honey were collected from Middle Anatolia and surrounding areas. The physicochemical properties of honey collected were determined. The obtained data were compared with results of other researchers.

Materials and Methods

Honey Samples

Forty natural liquid honey samples from Middle Anatolia and surrounding areas, marked as a red circle in the map of Turkey (Fig. 23.1), were collected directly from different beekeepers during the months of January and February in 2003. The honey samples, stored in glass jars, were kept in the dark at room temperature until analyzed. Moisture was determined by measuring the refractive indices at 200°C with a refractometer (Abbe Refractometer NAR2T) and the corresponding moisture content (%) was calculated according to AOAC method [10].

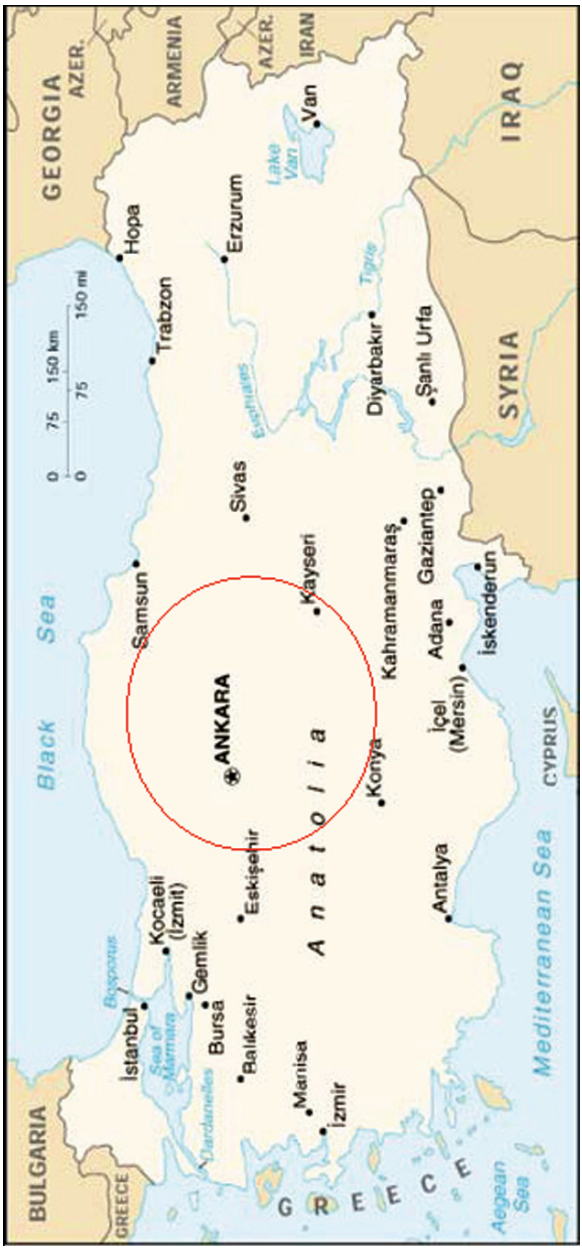

Fig. 23.1 Sampling area: Middle Anatolia and surrounding area of Turkey

Physicochemical Analysis

5-hydroxymethylfurfural (HMF) and diastase activity were determined according to Standard Methods of the Association of Official Analytical Chemists (AOAC) [10, 11].

Diastase number was measured using a buffered solution of starch according to AOAC [10]. HMF was determined colorimetrically after dilution with distilled water and addition of p-toluidine solution. Absorbance of the solution was determined at 550 nm using a spectrophotometer (HP 8450A UV/VIS). Three replicate analyzes were performed from each sample for data reliability.

Thermal treatment, applied to honey, may destroy vitamins and bionutrients, and produce a simultaneous decrease in diastase activity and an increase in HMF content. Honey treatment temperature and time must be limited when pasteurising and stabilising it; both diastase activity and HMF content are national and international parameters used as controls so as to limit thermal treatment application. HMF can be formed by hexose dehydration in acid media or by the Maillard reaction [11, 12]. According to Ibarz et al., HMF formation can be described by a second order kinetics (auto-catalytic), with the following equation as expression model [13]:

$$\left[\mathrm{HMF}\right]_t = \frac{1}{\frac{1}{\left[\mathrm{H}\right]_0 + \left[\mathrm{HMF}\right]_0} + \left(\frac{\left[\mathrm{H}\right]_0 + \left[\mathrm{HMF}\right]_0 - \left[\mathrm{HMF}\right]_0}{\left(\left[\mathrm{H}\right]_0 + \left[\mathrm{HMF}\right]_0\right)\left[\mathrm{HMF}\right]_0}\right) e^{\left[-k_2 t\right]}}$$

where:

$[\mathrm{HMF}]_t$ = HMF final concentration at time t
$[\mathrm{HMF}]_0$ = HMF initial concentration
$[\mathrm{H}]_0$ = Hexose initial concentration
t = Thermal treatment time
k_2 = Velocity constant for autocatalytic kinetics of second order (s^{-1})

Considering that the total hexose concentration in honey is higher than the HMF concentration normally present in honey, HMF0, the HMF formation could follow a first order kinetics, the expression of which is:

$$\left[\mathrm{HMF}\right]_t = \left[HMF\right]_0 e^{(k_1 t)}$$

where:

k_1 = Reaction rate constant of first order kinetics (s^{-1})

On the other hand, as the reaction rate constant k1 is a temperature (T) function, it is feasible to correlate it with T by means of an Arrhenius from equation:

$$k_1 = K_f.e^{-\left(\frac{E_q}{R\left(T+273^\circ C\right)}\right)}$$

where

T = Honey temperature (°C)
t = Honey treatment time
K_f = Frequency constant (s^{-1})
E_a = Activation energy (kJ/mol)
R = Gas constant (kJ/mol K)

During heating, two stages can be identified: the transitory or transient stage, which corresponds to an increase in temperature, starting from its initial value and reaching the treatment temperature, followed by the isothermal stage, in which temperature remains constant at the obtained value. There exists a definite time for each of these stages. In the transient stage, time is characteristic and depends on the system properties and heat flow. In the isothermal stage, time is generally fixed according to test targets [14].

Results and Discussion

Figure 23.2 shows the experimental values, expressed as HMF_r and the adjustment exponential curves corresponding to the isothermal heating stage. The resulting HMF values are due to the isothermal treatment effect only. The HMF formed as consequence of the transient stage, was discounted from the values obtained at the end of the complete transient-isothermal treatment. Table 23.1 shows the origin ordinates, first order reaction pseudo rate constant and the regression coefficients. The use of thermal treatments for technological purposes, such as the elimination of

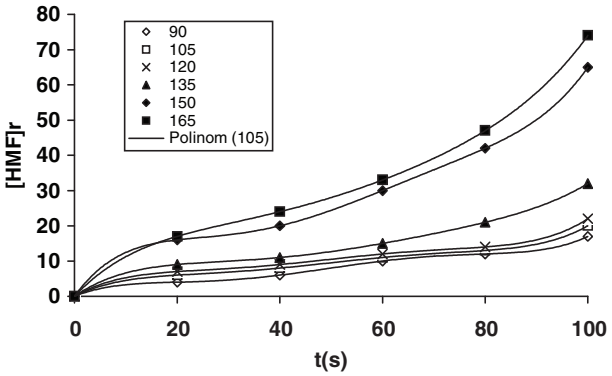

Fig. 23.2 HMF relative concentration variation as function of time and temperature of the isothermal heating stage is constant and equal to 15 s

Table 23.1 HMF formation kinetics in isothermal heating as a function of treatment temperature, first order reaction pseudo rate constant and regression coefficients

T (°C)	k_1 10^2 (s^{-1})	r^2
90	1.84	0.98
105	2.06	0.98
120	2.24	0.97
135	2.87	0.99
150	3.38	0.97
165	3.95	0.98

HMF, hydroxymethylfurfural content

crystallization or pasteurization, can increase the HMF content. Therefore, treatment time at a given temperature must be as short as possible. If temperatures are higher that 135°C, even for short times, HMF increase reaches values above these accepted by international standards. Figure 23.2 shows that a 100 s at 135°C treatment produces approximately the same HMF increase as a 40 s at 150°C. The HMF contents and diastase activity of fresh and stored honey samples are shown in Table 23.1. The mean diastase numbers in the honey samples following one year storage (20 ± 5°C) decreased from 14.6 to 10.7. Thrasyvoulou found that the average decrease in diastase number for 20 samples stored for one year at 25 ± 4^{0}C was 40%, while Sancho et al. reported [15] a decrease of 33% in 115 samples after one year storage at 15–25°C. Yılmaz and Küfrevioğlu [16] found that the average decrease in diastase number for 45 samples stored for one year at 20 ± 5°C was 27%. In the present study, the 30% average decrease in diastase number found after storage was lower than those found for other honeys in the research above (Table 23.2).

Upon storage for up to 12 months at 25 ± 1°C, the HMF in all honey samples increased progressively with four samples showing the least HMF level. With the exception of two samples, all other honey samples were either very close or have exceeded the maximum allowed level of HMF of 40 mg/kg in the Turkish Alimentarus Codex [17]. This is a clear indication that at such a high storage temperature, honey should not be kept for more than eight months.

The storage temperature of honey should be carefully controlled to preserve its quality. At its best, honey should be consumed within six months following its harvesting.

The initial HMF content in all honey samples was lower than the allowed maximum limit of 40 mg/kg as recommended by Turkish Alimentarus Codex [17], for honey in general. These results contradict the observation made by some authors that the types of honey produced in subtropical climates have high HMF exceeding 40 mg/kg [18]. However, the European Union council directive also allows for a maximum of 80 mg/kg for honey from tropical climates. The HMF level in honey is said to depend on the type of sugar present in honey and the fructose: glucose ratio [19]. The HMF formation results from the acid catalyzed dehydration of hexose

Table 23.2 Diastase number and HMF content of fresh and stored honey samples collected in Middle Anatolia and surrounding areas

Analytical values	Number of samples	Mean	Min.	Max.
HMF[a] (mg kg^{-1})	40	4.5	0.0	19.4
HMF[b](mg kg^{-1})		25.6	9.3	39.5
Diastase number[a]		16.3	10.4	29.1
Diastase number[b]		11.4	7.7	19.8

[a] Fresh honey [b] Stored honey

sugars with fructose being particularly susceptible. Fructose has been reported to be unstable at pH 4.6 and is five times more reactive than glucose [20]. Low levels of initial HMF observed in all honey samples may also be attributed to low pH values, ranging from 3.70–4.60.

References

1. Anass, T., Diez, M.J. and Heredia, J.F., 2003, *International Journal of Food Sciences and Technology,* **38**(4),395–402.
2. Perez-Arquillue, C., Concello, P., Arino, A., Juan, J. and Herresa, A., 1994, *Food Chemistry,* **51,** 207–210.
3. Ramirez, C.M.A., González, N.S.A. and Sauri, D.E., 2000, *Apiacta,* **35** (4),162–170.
4. Singh, and N. Bath, P.K., 1997, *Food Chemistry,* **58** (1),129–133.
5. White, J.W., 1994, *Bee World,* **75** (3),104–117.
6. Belitz, H.D. and Grosch, W., 1999, Food Chemistry, Springer, New York. CAC, (2001, July). *Draft Report of 24th Session*, Geneva.
7. Bath, P.K. and Singh, N., 1999, *Food Chemistry,* **67,** 389–397.
8. White, J.W., 1978, *Advances in Food Research,* **24,** 287–374.
9. Anam, O.O. and Dart, R.K., 1995, *Analytical Proceedings Including Analytical Communications,* **32,** 515–517.
10. AOAC, 1995, Official Methods of Analysis, Arlington,VA, Association of Official Analytical Chemists, 16th edn.
11. Hoseney, R.C., 1984, *Journal of Chemical Education,* **61,** 308–312.
12. Feather, M.S., Harris, D.W. and Nichols, S.B., 1982, *Journal of Organic Chemistry,* **37,** 1600–1606.
13. Ibarz, A., Casero, T., Miguelsanz, R. and Pagon, J., 1989, *Alimentaria,* **199,** 81–84.
14. Tosi, E., Ciappini, M., Re, E. and Lucero, H., 2002, *Food Chemistry,* **77,** 71–74.
15. Sancho, M.T., Muniategui, S., Huidobro, J., and Lozano, J.S., 1992, *Journal of Agricultural and Food Chemistry,* **4,** 134–138.
16. Yılmaz, H. and Küfrevioğlu, İ., 2001, *Turkish Journal of Agriculture Forestry,* **25**(5), 347–349.
17. Anonymous, 2003, Honey Rescript, Turkish Alimentarus Codex, The official gazette of the Republic of Turkey, 25180 (in Turkish).
18. Lagrange, V. and Sanders, S.W., 1988, *Cereal Foods World,* **33,** 833–838.
19. Doner, L.W., 1977, *Journal of the Science of Food and Agriculture,* **28,** 443–456.
20. Lee, H.S. and Nagy, S., 1990, *Journal of Food Processing and Preservation,* **14,** 121–178.

Chapter 24
The Degradation Kinetics of Phenol Solutions with Ozone

Kadir Turhan and Süheyla Uzman

Abstract Aromatic compounds are extensively used in several of industries and can cause pollution in water sources. This work aims are to examine the degradability by cleavage of phenol in aqueous solutions using ozone, and to determine the kinetics of those cleavage reactions. Phenol has been prepared in four different concentrations and the flow rate of ozone supplied for each solution has been selected. The reaction of ozone with phenol was investigated at several conditions, such as different phenol and ozone concentrations, and contact times. Total Organic Carbon (TOC) and UV analysis of the aromatic by-products formed during and after the ozonation reaction were employed. The reaction rates calculated from TOC analysis were investigated.

Keywords Degradation kinetics, ozone, phenol, pollution

Introduction

Many industries use phenolic materials in their manufacturing processes. Phenol is also used in the production of drugs, weed killers, and synthetic resins. Phenol and its derivatives are present in the wastewaters of industries such as cooking, pulp mills, paint and dyes, wine distilleries, oil and gasoline, synthetic rubber, textiles, pharmaceuticals, solvent, manufacture of pesticides, paper, and wood etc. [1].

With the rapid increase in the number of chemical industries, a great deal of wastewater is produced, which causes pollution and degrades the environment. Many of these industrial wastewaters, particularly the ones, containing phenolic compounds, are well known to be characterized by higher salinity, acidity, chemical oxygen demand (COD) value and low biodegradability, which means that the effluent cannot be treated by the conventional process [2, 3]. An alternative method of treating such

Yıldız Technical University, Department of Chemistry, Davutpaşa Campus, 34220 Esenler-Istanbul, Turkey

B. Sener (ed.), *Innovations in Chemical Biology*, doi: 10.1007/978-1-4020-6955-0

wastewater is Advanced Oxidation Processes (AOPs), where highly reactive free radicals, especially hydroxyl radicals, are mostly utilized to destroy the pollutants in wastewater. These processes involve the following main sub-processes: Direct ozonation, Wet Air Oxidation (WAO), Hydrogen peroxide oxidation, UV photolysis etc. [4]. Ozonation is widely employed in water treatment for disinfection.

In this study, synthetic aqueous solutions of phenol were treated with ozone. The reaction of ozone with phenol was investigated at several conditions, such as different phenol and ozone concentrations, and contact times. Total Organic Carbon (TOC) and UV analysis of the aromatic by-products formed during and after the ozonation reaction were employed. The reaction rates calculated from TOC analysis were investigated.

Materials and Methods

Phenol solution was prepared from pure standard (Merck, 99.9% of purity) with distilled water. The concentrations of phenol solutions were 25, 50, 75 and 100 mg/L, respectively. The ozonization reaction was carried out in the system which was shown in Fig. 24.1. The reactor capacity was 3,000 mL. Ozonation experiments were performed in a 2,000 mL capacity ozone bubble column between 0 and 2 h in semi-batch supplied with counter current recirculation of the liquid to the gas flow. Fischer 502 model ozone generator was used for the production of ozone from dry oxygen (99.9% of purity). The oxygen flow rate to the generator was adjusted at 120 L/h and monitored with a rotameter incorporated into the ozone generator. The ozone stream was continuously introduced in the sample through a porous sparger as microbubbles at the bottom of the ozone contactor. The diffusion rates of the ozone/oxygen mixture, introduced from the bottom of the reactor through a

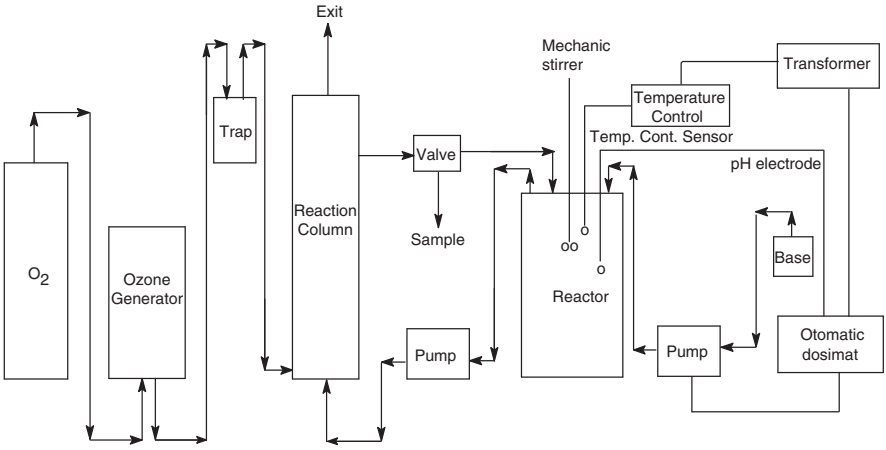

Fig. 24.1 Scheme of ozonization

sintered glass diffusing plate, were 2, 4 and 6 g/L h. Excess ozone was passed into gas absorption bottle containing KI solution (2% wt). The excess amount of ozone was determined by titration of the solutions in the bubblers using sodium thiosulphate and starch as indicator, and calibration curve was established [5]. All tubing and the fittings from the ozone generator to the reactor and the gas absorption bottles were made of glass and teflone. The dosages of ozone consumed in medium were calculated for all the experiments, which were performed at ambient temperature at 20 ± 10°C. Rate of mechanical stirrer was adjusted to 2,100 rpm, and circulation rate of pump between reactor and reaction column adjusted 1,875 mL/min.

Seventy-five milliliters of samples were collected from reaction column upper end at different time intervals during the ozonation reaction for the determination of the by products. Ozonation of phenol was carried out at four different initial concentrations, 25, 50, 75 and 100 mg/L, with three different ozone concentrations 2, 4 and 6 g/L h.

Results and Discussion

In this study, the degradability of phenol in aqueous solutions was investigated with using ozone. Additionally, decomposition kinetic of phenol in the presence of ozone was calculated using maximum rate constants, from graphics of concentration versus time.

The UV absorbance is used for the preliminary control of the degree of decomposition. The GC/MS and HPLC analysis are used to identify intermediate and final products formed during ozonation. It was found that reaction of ozone with phenol at pH 9, in addition to catechol (C) and hydroquinone (HQ) are likely primary oxidation products, p-benzoquinone (PBQ) and o-benzoquinone (OBQ), the others are more oxidized species, and CO_2 and water the final oxidation products. The detected degradation products are shown in Scheme 24.1.

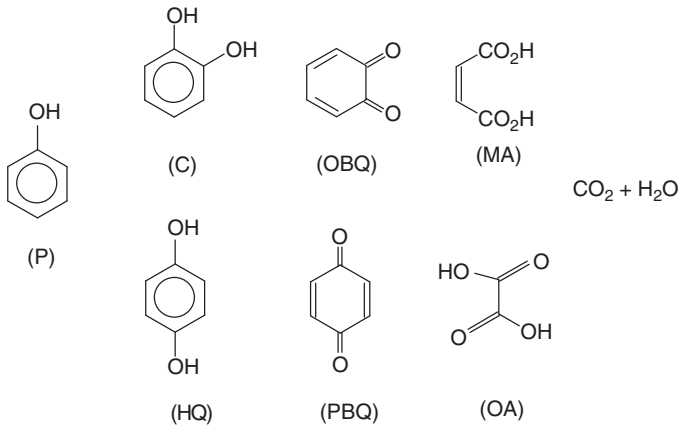

Scheme 24.1 Reaction pathway in the phenol degradation

This initial attack of the ozone molecule leads first to the formation of ortho- and para-hydroxylated by-products. These hydroxylated compounds are highly susceptible to further ozonation. The compounds lead to the formation of quinoid and, due to the opening of the aromatic cycle, to the formation of aliphatic products with carbonyl and carboxyl functions. The nucleophilic reaction is found locally on molecular sites showing an electronic deficit and, more frequently, on carbons carrying electron acceptor groups. In summary, the molecular ozone reactions are extremely selective and limited to unsaturated aromatic and aliphatic compounds as well as to specific functional groups.

TOC and phenol concentration decreased same trend and the forming of by product was determined by mass spectrum. It was shown that formed by product was not stabile, whereas it immediately decomposes to different products. It was also determined that the amounts of ozone were sufficient for phenol decomposing. As a result of kinetic investigation of phenol, decomposition reaction was found first order because of obtaining almost constant k values (Fig. 24.2a–f). As expected

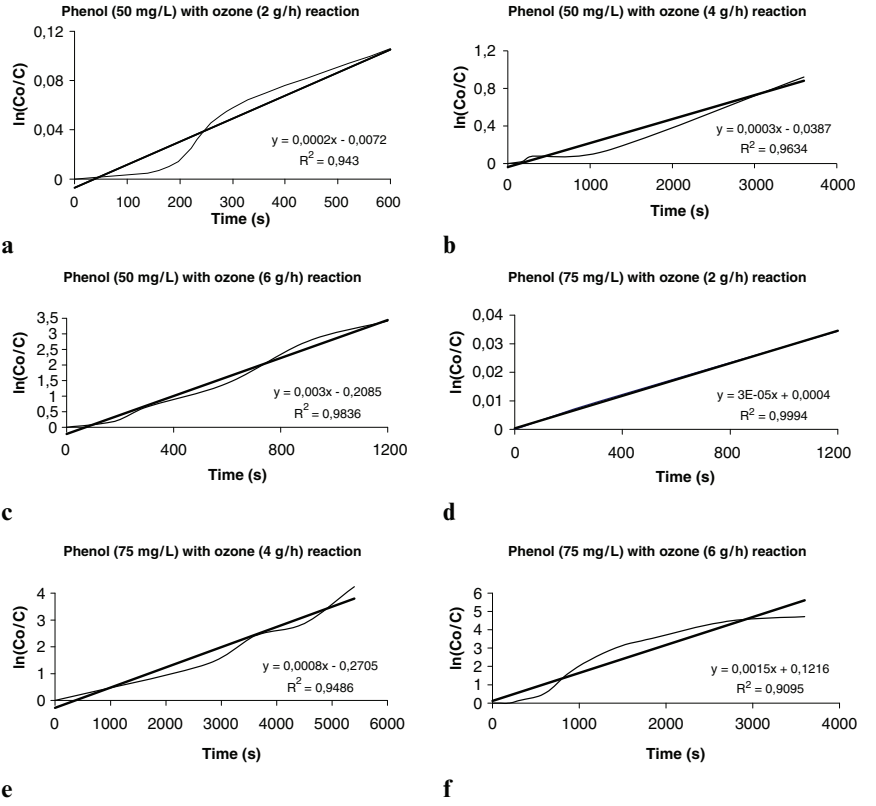

Fig. 24.2(a–f) Changing of phenol concentration (A) with ozone concentration (O) versus time A: 50 mg/L, O: 2 g/h L (a), O: 4 g/h L (b), O: 6 g/h L (c), respectively. A: 75 mg/L, O: 2 g/h L (a), O: 4 g/h L (b), O: 6 g/h L (c), respectively.

that, R_{max} values increased with the increasing O_3 concentration especially for two phenol concentrations (50 and 75 mg/L). Decomposition kinetic of phenol in the presence of ozone was calculated using maximum rate constants, from graphics of concentration versus time. Maximum R value was found as 409.55 mg/L h for phenol. According to all obtained results, it was found that phenol decomposition occurs in the using of enough ozone, and the decomposition reaction follows first order reaction kinetics [6].

Acknowledgement Financial support of this research by TUBITAK (the Scientific and Technological Research Council of Turkey) [Project Number: KTCAG-71] is gratefully acknowledged.

References

1. Abdo, M.S.E., Nosier, S.A., El-Tawil, Y.A., Fadi, S.M. and El-Khairy, M.I., 1997, *Journal of Environmental Science and Health* A, **32** (4), 1159–1169.
2. Miller, J.S. and Olejnik, D., 2004, *Ozone Science and Engineering,* **26**(5), 453–464.
3. Poznyak, T. and Arazia, B.G., 2005, *Ozone Science and Engineering,* **27**(6), 351–357.
4. Esplugas, S., Gimenez, J., Contreras, S., Pascual, E. and Rodrguez, M., 2002, *Water Research,* **36**(4), 1034–1042.
5. APHA-AWWA-WPCF, 1995, *Standard Methods for the Examination of Water and Wastewater*, 19th ed., A.D. Eaton, L.S. Clesceri and A.E. Greenberg (eds.), Washington, DC.
6. Turhan, K., 2001, *Investigation of Decomposition Kinetics of Aromatic Compounds with Ozone in Aqueous Solutions,* Ph.D. dissertation, Yıldız Technical University, Istanbul, Turkey.

Chapter 25
Determination of Some Trace Metals in Edible Mushrooms Samples Using Atomic Absorption Spectrometry

Kadir Turhan

Abstract Trace metal levels in ten different mushroom species, *Lactarius decipiens Quel.*, *Lactarius piperatus*, *Lactarius resimus Fr.*, *Lactarius valemus Fr.*, *Lactarius vietus (Fr.) Fr.*, *Laccaria lacceta*, *Agaricus bisporus*, *Agaricus silvicola*, *Lentinula edodes* and *Morchella deliciosa* obtained from different areas of the middle Black Sea region of Turkey were determined by flame and graphite furnace atomic adsorption spectrometry after microwave digestion. The contents of trace metals in the mushroom samples were found in the ranges 74.21–127.70, 23,444–49,880, 69.51–99.93, 46.23–129.38, 3.69–27.51, 0.71–3.11, 0.41–1.57, 16.35–27.92, 3.54–29.87, 759–1,200, 0.24–1.41, 8.69–22.41and 0.13–0.54 μg/g for Na, K, Ca, Fe, Cu, Pb, Cd, Zn, Mn, Mg, Cr, Ni, and Co, respectively. Results obtained are in agreement with trace data reported in the literature.

Keywords Atomic absorption, Black Sea, mushrooms, trace metals

Introduction

Mushrooms are important in the ecosystem because they are able to biodegrade the substrate and therefore use the wastes of agricultural production [1]. Mushrooms have also been reported as therapeutic foods, useful in preventing diseases such as hypertension, hypercholesterolemia, and cancer. These functional characteristics are mainly due to their chemical composition [2]. Heavy metal concentrations in mushroom are considerably higher than those in agricultural crop plants, vegetables and fruit. This suggests that mushrooms possess a very effective mechanism that enables them readily to take up some heavy metals from the ecosystem.

The concentrations of trace elements in the fruiting bodies of fungi are primarily species-dependent. The concentrations were found to depend on the physiology of

Yıldız Technical University, Department of Chemistry, Davutpasa Campus, 34220 Esenler-Istanbul, Turkey

B. Sener (ed.), *Innovations in Chemical Biology*, doi: 10.1007/978-1-4020-6955-0

the species and particularly on its ecosystem pattern. It has proven rather difficult to determine the effects of environmental factors on the heavy metals [3].

Mushrooms are valuable health foods, low in calories, high in vegetable proteins, iron, zinc, chitin, vitamins and minerals. In general, their fruiting bodies, on a dry weight basis, contain about 39.9% carbohydrate, 17.5% protein and 2.9% fats with the rest constituting the minerals [4, 5]. Wild-growing macrofungus have been a favorite delicacy in many countries. Some people collect macrofungus to make a substantial contribution to food intake. Therefore, it is necessary to know the levels of toxic and essential elements in edible mushrooms [6].

Turkey has a large edible mushroom potential and is becoming an important exporter of wild mushrooms. However, qualified studies have not been carried out on this subject in Turkey [7]. Turkey is located in southeastern Europe and Asia. It is bordered in the north by the Black Sea, the south by Iraq, Syria, and the Mediterranean, in the west by the Aegean Sea, in the northeast by Georgia and Armenia, in the northwest by Bulgaria and Greece. Turkey can be separated into seven geographic regions. One of them is the Black Sea region. The Black Sea region can be separated into three smaller geographic regions. The middle Black Sea region is one of them. In this region, the climate is mild and rainy. The seasons are normally wet with mild temperatures. The climate during the year, especially, in spring and autumn, is ideal for fungal growth [4].

Wild edible mushrooms in the middle Black Sea region of Turkey (Sinop) are widely consumed because of their delicacy and abundance. Sinop is located in the middle Black Sea region of Turkey (41.480 N, 34.700 E). Sinop is an industrial agricultural city in the central Black Sea-Turkey and has a population of a quarter million. The temperature ranges between -10.5 and 410°C, average values being 200°C during summer and 70°C during winter in Sinop. Many studies have been carried out on the metal contents of macrofungus in Turkey [7–11]. However, qualified studies have not been carried out in this area of Turkey, especially in Sinop (Scheme 25.1).

In this study, the levels of trace metals in ten different species mushroom samples collected from Sinop, Turkey were determined by flame and graphite furnace AAS after microwave digestion methods. The purpose of the present study was the determination of Ca, Fe, Cu, Pb, Cd, Zn, Mn, Mg, Cr, Ni and Co contents, by using an AAS method, in the fruiting bodies of macrofungus specimens collected from the middle Black Sea region of Turkey.

Materials and Methods

In this study, 96 samples of wild edible mushrooms, corresponding to 10 different, were used in autumn and spring 2003. The samples of mushroom were collected from Sinop in Turkey. Species include *Lactarius decipiens Quel.*, *Lactarius piperatus*, *Lactarius resimus Fr.*, *Lactarius valemus Fr.*, *Lactarius vietus (Fr.) Fr.*, *Laccaria lacceta*, *Agaricus bisporus*, *Agaricus silvicola*, *Lentinula edodes*, *Morchella deliciosa*. Collected mushrooms were cleaned, cut into slices and the samples were washed with demineralized water. Each sample was dried at 105°C for 24 h. Dried samples

Scheme 25.1 Sampling area: Middle Anatolia and surrounding area of Turkey

Table 25.1 Digestion conditions for mushroom samples in the microwave digestion system

Steps	Time (min)	Power (W)
1	3	600
2	3	0
3	5	600
4	3	900
5	3	1,200

were homogenized using an agate homogenizer and stored in polyethylene bottles prior to analysis.

For digestion, CEM Mars 5 microwave closed system was used in this study. 0.5 g of samples was digested with 5 mL of HNO_3 (65%) and 2 mL of H_2O_2 (30%) in a microwave digestion system for 17 min and final diluted to 25 mL with deionized water. A blank digest was carried out in the same way. Digestion conditions are given in Table 25.1.

This procedure was preferred because it is more accurate with respect to both time and recovery values.

Sodium and potassium were determined using Jenway PFP-7 model flame photometer and sodium or potassium chloride to prepare the standards. Calcium, iron,

copper, magnesium, zinc, manganese, chromium, nickel and cobalt were determined with a Varian FS 220S model atomic absorption spectrophotometry (AAS) using flame atomization. Lead and cadmium levels in the mushroom samples were determined using Varian GTA 110 model graphite furnace atomic absorption spectrophotometry (GFAAS) (Table 25.2.)

Results and Discussion

Trace metal levels in the analyzed samples are listed in Table 25.3. All metal concentrations were determined on a dry weight basis. The content of trace metals in the samples were found to be in the ranges 74.21–127.70, 23,444–49,880,

Table 25.2 The wavelengths for AAS and flame photometer analyzes

Elements	Na	K	Ca	Fe	Cu	Pb	Cd
Wavelength (nm)	589.0	766.5	393.4	248.3	324.8	283.3	228.8
Elements	**Zn**	**Mn**	**Mg**	**Cr**	**Ni**	**Co**	
Wavelength (nm)	213.9	279.5	285.2	357.9	232.0	230.8	

Table 25.3 Trace metal levels in the analyzed samples

Mushroom species	Na	K	Ca	Fe	Cu	Pb	Cd
Lactarius decipiens Quel.	114.03 ± 2.92	26,070 ± 1,233	72.78 ± 2.31	66.95 ± 0.94	6.61 ± 0.31	1.30 ± 0.06	0.41 ± 0.12
Lactarius piperatus	80.72 ± 9.86	28,720 ± 2,655	72.53 ± 7.68	129.38 ± 18.44	16.81 ± 1.41	3.11 ± 0.51	0.83 ± 0.08
Lactarius resimus Fr.	91.66 ± 1.16	38,380 ± 862	84.15 ± 1.72	89.02 ± 1.55	7.55 ± 0.45	1.42 ± 0.06	0.98 ± 0.12
Lactarius valemus Fr.	92.72± 7.33	39,600± 1,059	74.55± 7.55	58.16± 5.41	18.68± 0.88	1.45± 0.08	1.22± 0.08
Lactarius vietus (Fr.) Fr.	91.79 ± 1.59	24,940 ± 353	75.63 ± 1.04	73.00 ± 1.69	6.54 ± 0.35	1.30 ± 0.08	1.13 ± 0.12
Laccaria lacceta	127.70 ± 7.23	49,880 ± 3,666	99.71 ± 6.37	120.82 ± 5.57	27.51 ± 2.08	1.39 ± 0.04	1.57 ± 0.06
Agaricus bisporus	97.44 ± 1.39	27,233 ± 577	89.08 ± 1.39	87.86 ± 2.10	10.90 ± 0.71	1.17 ± 0.08	0.76 ± 0.14
Agaricus silvicola	74.21 ± 1.35	23,444 ± 414	69.51 ± 0.86	79.53 ± 1.33	7.47 ± 0.39	1.00 ± 0.10	0.71 ± 0.14
Lentinula edodes	110.93 ± 1.65	37,033 ± 506	99.93 ± 1.80	88.66 ± 1.16	7.34 ± 0.27	1.48 ± 0.12	1.32 ± 0.12
Morchella deliciosa	81.10 ± 1.63	32,789 ± 252	71.69 ± 0.82	46.23 ± 1.08	3.69 ± 0.20	0.71 ± 0.14	0.45 ± 0.06
	Zn	**Mn**	**Mg**	**Cr**	**Ni**	**Co**	
Lactarius decipiens Quel.	25.98 ± 0.80	4.87 ± 0.43	1,153 ± 43.86	1.00 ± 0.05	13.60 ± 0.55	0.54 ± 0.05	

(continued)

Table 25.3 (continued)

Mushroom species	Na	K	Ca	Fe	Cu	Pb	Cd
Lactarius piperatus	25.52 ± 2.43	7.39 ± 1.06	821 ± 76.12	1.04 ± 0.20	8.69 ± 1.45	0.47 ± 0.10	
Lactarius resimus Fr.	27.92 ± 0.71	3.65 ± 0.49	1,051 ± 30.93	0.85 ± 0.06	12.54 ± 0.57	0.49 ± 0.07	
Lactarius valemus Fr.	24.52 ± 3.04	5.45 ± 0.55	969 ± 37.65	0.91 ± 0.14	22.41 ± 1.04	0.38 ± 0.05	
Lactarius vietus (Fr.) Fr.	24.95 ± 0.73	4.64 ± 0.35	834 ± 39.40	0.52 ± 0.04	10.41 ± 0.47	0.42 ± 0.07	
Laccaria lacceta	26.99 ± 1.88	29.87 ± 2.55	891 ± 35.53	1.41 ± 0.08	15.58 ± 0.65	0.16 ± 0.04	
Agaricus bisporus	18.68 ± 0.55	19.20 ± 1.12	1,200 ± 86.18	0.64 ± 0.08	9.77 ± 0.27	0.18 ± 0.05	
Agaricus silvicola	17.89 ± 0.55	8.59 ± 0.45	1,144 ± 82.69	0.82 ± 0.11	10.21 ± 0.53	0.25 ± 0.04	
Lentinulaedodes	27.73 ± 0.55	8.74 ± 0.65	759 ± 47.51	0.48 ± 0.06	13.08 ± 0.69	0.29 ± 0.06	
Morchella deliciosa	16.35 ± 0.37	3.54 ± 0.41	941 ± 35.12	0.24 ± 0.05	9.10 ± 0.55	0.13 ± 0.03	

69.51–99.93, 46.23–129.38, 3.69–27.51, 0.71–3.11, 0.41–1.57, 16.35–27.92, 3.54–29.87, 759–1,200, 0.24–1.41, 8.69–22.41and 0.13–0.54 μg/g for Na, K, Ca, Fe, Cu, Pb, Cd, Zn, Mn, Mg, Cr, Ni, and Co, respectively.

References

1. Manzi, P., Aguzzi, A., Vivanti, V., Paci, M. and Pizzoferrato, L., 1999, Mushrooms as a source of functional ingredients. In *Euro Food Chem* X *European Conference on: Functional Foods. A New Challange for the Food Chemist*, 22–24 September, Budapest, Hungary, 1, pp 86–93.
2. Manzi, P., Aguzzi, A. Pizzoferrato, L., 2001, *Food Chemistry,* **73,** 321–325.
3. Lepšová, A. and Mejstřík, V., 1998, *The Science of the Total Environment,* **76,** 117–128.
4. Demirbaş, A., 2001, *Food Chemistry,* **75,** 473–457.
5. Latiff, L.A., Daran, A.B.M. and Mohamed, A.B., 1996, *Food Chemistry,* **56** (2), 115–121.
6. Işıloğlu, M., Yılmaz, F. and Merdivan, M., 2001, *Food Chemistry,* **73,** 169–175.
7. Demirbaş, A., 2000, *Food Chemistry,* **68,** 415–419.
8. Tüzen, M., Özdemir, M. Demirbaş, A., 1998, *Food Chemistry,* **63** (2), 247–251.
9. Yıldız, A., Karakaplan, M. and Aydın, F., 1998, *Food Chemistry,* **61,** 127–130.
10. Sesli, E. and Tüzen, M., 1999, *Food Chemistry,* **65,** 453–460.
11. Sivrikaya, H., Bacak, L., Saraçbaşi, A., Toroğlu, I. Eroğlu, H., 2002, *Food Chemistry,* **79** (2), 173–176.

Chapter 26
Sorption of Zn(II) and Pb(II) Ions by a New Resin Synthesized from Sumac Tannin and Gelatin

Kadir Turhan, Fatma Turak, and Mahmure Üstün Özgür

Abstract Recently, the interest on biomaterials and especially in tannins was growing and some attractive results were obtained in the adsorption of some metals by tannin adsorbents. Tannins are widely distributed in nature and have multiple adjacent polyhydroxyphenyl groups in their chemical structure which have extremely high affinity for heavy metal ions. This study will describe how tannin can be used as an effective zinc and lead sorbent by the use of tannin resins. Batch method was used in the experiments in which pH profile, adsorption time, adsorbent/liquid ratios, initial concentration of metal ions, adsorbent amount and temperature were investigated to determine binding properties of adsorbent for the Zn(II) and Pb(II) ions.

Keywords Biomaterials, gelatin, lead, resin, sorption, sumac, tannin, zinc

Introduction

Lead pollution has been recognized as a potential threat to air, water and soil. Lead is known to damage the kidney, liver and reproductive system, basic cellular processes and brain function [1]. Lead has been found to be acute toxic to human beings when present in high amount [2]. The toxic symptoms are anemia, insomnia, headache, dizziness, and irritability, weakness of muscles, hallucination and renal damage. The main sources of human exposure to lead include the use of leaded, gasoline, industrial sources such as lead mining, smelting and coal combustion, the use of lead-based paint and lead-containing pipes in water supply systems. Additional sources may be food can solders, ceramic glazes, lead containing batteries and cosmetics.

Yıldız Technical University, Department of Chemistry, Davutpaşa Campus, 34220 Esenler, İstanbul,Turkey

B. Sener (ed.), *Innovations in Chemical Biology*, doi: 10.1007/978-1-4020-6955-0

Heavy metals are introduced into the soil mainly by the application of fertilizers, sewage sludge, liming materials, and other industrial and urban waste materials. In recent years, increased anthropogenic inputs of heavy metals in terrestrial environments have caused considerable concern relative to their impact on groundwater contamination. Zinc is a key element in plant growth and human health. It has been used by human beings since immemorial time and is still widely applied in our industrialized society. Zinc is an essential element for the normal activity of DNA polymerase and protein synthesis. Its deficiency in human body can cause many diseases, such as liver disease, gastrointestinal disorders, renal diseases, neoplastic diseases, burns, skin disorders, etc. So, it plays a vital role in the healthy development of many life forms. Excessive amounts of Zn, however, may be toxic, especially to the aquatic biota. The EPA recommends that drinking water should contain no more than 5 milligrams per liter of water (5 mg/L) because of taste [3, 4].

Much work has been done on the removal of Pb and Zn from aqueous solution. Removal of these ions has been attempted by several researches employing a wide variety of techniques. Adsorption of removal of Pb and Zn from solution agricultural waste [5], three fern [6], tannin gel [7], removal of Pb sea module [8], tannin gel adsorbent synthesized from condensed tannin [8] and removal of Zn green macro alga [9], soil [3] have been extensively studied for this purpose.

Biomass materials, potentially serve as remediation factors in contaminated areas for preventing environmental pollution because of possible waste water treatment. During the last years, the interest on biomaterials and especially in tannins was growing. Tannins are an important class of secondary plant metabolites, water soluble polyphenolic compounds of molecular weight range between 500 and some thousands Daltons [10]. There are three kinds: hydrolizable, condensed and complex tannins [11]. Tannins have multiple adjacent phenolic hydroxyl groups and exhibit specific chelation ability toward metal ions. However, tannins are sparingly water soluble compounds. When they are used directly as adsorbent for metal ions in aqueous system, they have the disadvantage of being leaked by water. To overcome this disadvantage, attempts were made to immobilize tannins onto various water-insoluble matrices. The immobilization of tannin on to agarose [12], cellulose powder rayon fibre [13] matrices with have amino groups such as albumin, gelatin, aminopolystyrene and 2-vinly-4,6-diamino-S-triazine [14] and collagen fibres [15] and animal fibrous proteins [16] were also reported. However, no data have been reported for the adsorption of Pb^{2+} and Zn^{2+} on the resin synthesized from sumac leaves (contain hydrolysable tannin) and gelatin.

Taking into account all the above, we have considered it of great interest to assess the ability of locally available sumac leaves and for the removal of Pb(II) and Zn(II) from aqueous solution and optimization of conditions for theirs adsorption. Firstly, a new resin was synthesized from sumac leaves and animal gelatin.

Experimental

Adsorbent Synthesis

For synthesized Gelatin (G)/Tannin (T) resins, gelatin powder was purchased from Ülker Food Company-İstanbul, Turkey. Hydrolyzable tannins were obtained from the sumac leaves which were collected from Siirt, Turkey. The raw leaves were dried at room temperature in dark and then ground 500 μm particle sizes. For the total tannin determination Folin-Ciocalteu method was used and tannin content found 27%. Tannins are extracted from sumac leaves with 1:1 (v/v) acetone/water solution [15]. Tannic acid (TA) powder, which was extracted from sumac leaves (30 g) was dissolved in distilled waster at 95–98°C, then solution cooled at room temperature and 37% formaldehyde solution added to the solution. G powder was dissolved distilled water at 95–98°C and then added to the TA/formaldehyde solution. Concentrated hydrochloric acid was added to the mixture and heated 95–98°C for 12 h with a reflux condenser. G/TA resin was washed distilled water, dried at 110°C. Dried resin was crushed into small particles, <500 μm [16].

Reagents and Chemicals

Chemicals used were of analytical/laboratory grade procured either from Merck or Aldrich. Stock lead and zinc solutions 1,000 mg/L for adsorption study were prepared from AR grade lead nitrate [$Pb(NO_3)_2$] and from zinc chloride [$ZnCl_2$]. Different concentrations of Pb and Zn solutions were prepared from the stock solutions. All working solutions were prepared by diluting the stock solutions with distilled water.

Instruments

The values of solutions were adjusted with 0.1 mol/L NH_4OH or HNO_3 and measured with Metrohm Herisau E510 pH meter. A magnetic stirrer model Arex was used for stirring the adsorption batches. The concentration of solution before and after adsorption was measured by using Atomic Absorption Spectrometer (AAS) Analytika Jena. All the measurements were made under optimization of the below mentioned parameters.

Metal ion	Band width	Flame	Detection limit	Concentration range (μg/mL)
Pb(II)	1.2	C_2H_2/air	1.00	0.1–30
Zn(II)	0.5	C_2H_2/air	0.01	0.01–2

Adsorption Experiments

Method

Adsorption measurements were made by batch technique at room temperature (25 ± 3°C). Known amounts of tannin resin were placed in 250 mL erlenmeyer flasks containing 100 mL of metal ion solution of known concentration and were stirred for a given time period. The solutions were then filtered, centrifuged and the concentrations of metal ions were measured by AAS. The difference in the metal ion (Pb^{2+} and Zn^{2+}) content before and after adsorption represented the amount of Pb and Zn adsorbed by new resin.

The Effect of Stirring Time

The time-dependent behaviors of metal ions adsorption were measured by varying the equilibrium time between the adsorbate and adsorbent in the range of 30–300 min. The concentration of Pb(II) and Zn(II) were kept as 50 μg/mL while the amount of resin added was 0.5 g. The experiments were performed at pH 4 for Pb^{2+}.

The Effect of pH on Adsorption Equilibrium

Effect of initial pH on adsorption of Pb^{2+} ions were investigated as follows: 0.5 g of the resin was weighed and 100 mL of a heavy metal ion solution was added. The pH of each solution was adjusted to desired values. After stirring 5 h the reaction mixture was filtered through membrane filter to remove particulates and analyzed with an AAS.

The Effect of the Ratio of Solution Volume to Mass of Resin (V/m, mL/g)

To investigate the effect of ratio of solution volume to mass of solid and adsorption of metal ions; 0.5 g resin samples were mixed 25–75 mL of aqueous solution of the constant initial concentration of metal ions (50 μg/mL Pb^{2+}). The pH was adjusted to 4 for adsorption of Pb^{2+}. The flasks with their contents were stirred for 4 h.

The Effect of Adsorbent Amount

The concentration of Pb^{2+} and stirring time were fixed at 50 μg/mL and 4 h, respectively, while amount of resin was varied from 0.1–0.5 g.

Results and Discussion

Recently, the interest on biomaterials and especially in tannins was growing and some attract results were obtained in the adsorption of some metals by tannin adsorbents [17]. Tannins are widely distributed in nature and have multiple adjacent polyhydroxyphenyl groups in their chemical structure which have extremely high affinity for heavy metal ions [18, 19].

Sumac tannins is illustrated in Fig. 26.1 whose basic structure is of flavon-3-ols [20].

Various adsorption parameters for the effective removal of Pb^{2+} and Zn^{2+} ions by using new synthesized resin as an adsorbent from aqueous solutions were studied and optimized. Time-dependent behavior of Pb^{2+} and Zn^{2+} ions adsorption was measured by varying the equilibrium time between in the range of 30–300 min. The percentage adsorption of Pb^{2+} plotted in Fig. 26.2 as a function of contact time

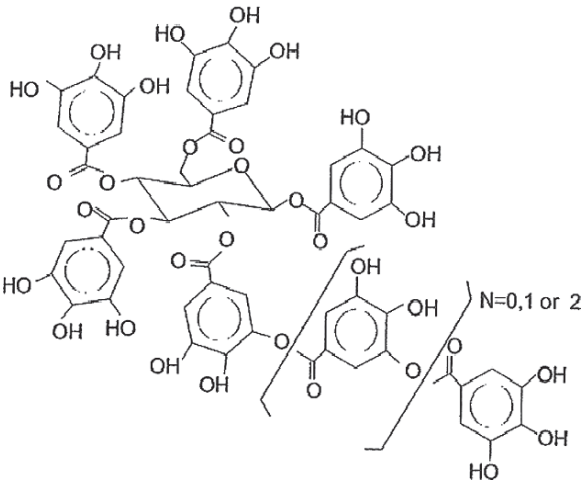

Fig. 26.1 Chemical structure of sumac tannin

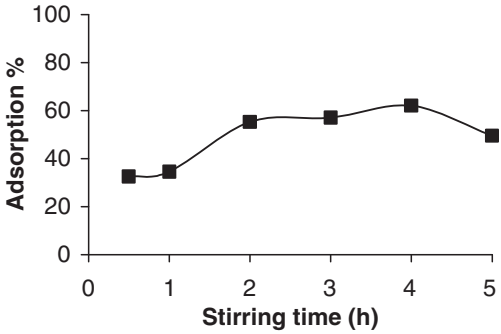

Fig. 26.2 Effect of stirring time on the adsorption of lead $c^0_{Pb^{2+}}$: 50 μg/mL, amount of resin: 0.5 g, pH 4

indicates that the equilibrium between to Pb^{2+} and new resin was attained within 4 h. Therefore, a 4 h stirring time was found to be appropriate for maximum adsorption and was used in all subsequent measurements.

The pH of the aqueous solution is an important variable which controls the adsorption of the metal at the resin-water interfaces. Hence, the influence of pH on the adsorption Pb^{2+} on resin was also examined in the pH range of 2–6. The results of studied elements are given in Fig. 26.3. As seen both metal cations have a pH dependent adsorption behavior. Adsorption of lead was about maximum values (49.46%) at pH 4.0, then decreases to 16.02% at pH 2.

Figure 26.4 shows the sorption of Pb^{2+} ions by resin (0.5 g) as a function of V/m. The results indicate that adsorption percentage did not change much with increasing V/m values. Therefore 50 of the V/m m rate were selected as the optimum value.

The amount of adsorption on the resin was determined from the difference in concentration before and after, the adsorption experiment as the following equation.

$$q^* = V\left(C^0 - C^*\right) / m$$

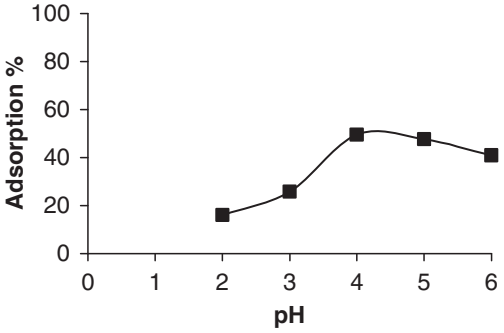

Fig. 26.3 Effect of pH on the adsorption of lead
$c^0_{Pb^{2+}}$: 50 µg/mL, stirring time 4 h, amount of adsorbent 0.5 g

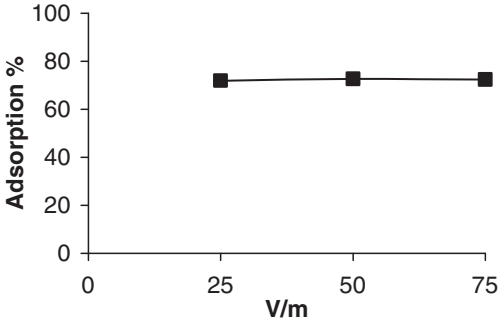

Fig. 26.4 Effect of V/m on the adsorption of lead
$c^0_{Pb^{2+}}$: 50 µg/mL, stirring time 4 h, pH 4, amount of adsorbent 0.5 g

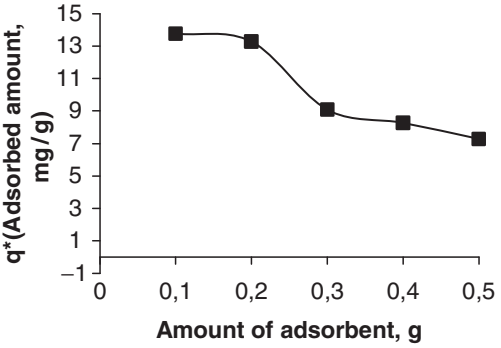

Fig. 26.5 Effect of q* on the adsorption of lead
$c^0_{Pb^{2+}}$: 50 µg/mL, stirring time 4 h, pH 4

where q* is the metal adsorption in milligram per gram at equilibrium, C^0 and C* are the concentration of the element in the initial and final solution in milligram per liter, V is the volume of supernatant solution in liter and m is the resin mass in gram.

The dependence of Pb^{2+} ion sorption on resin amount was studied by varying the sorbent amount from 0.1–0.5 g while keeping the volume 50 mL, concentration of Pb^{2+} 50 mg/L, pH 4 and stirring time 4 h. The results indicated that adsorbed amount of Pb^{2+}, q*, was high and remained almost constant up to 0.2 g then slowly decreased with increasing resin mass from 0.2 to 0.5 (Fig. 26.5).

Adsorption of Zn^{2+} ions was studied at the same conditions which studied for Pb^{2+} ions. The results showed that the resin couldn't adsorbed at these conditions. We decided that to study other conditions at the future program.

Acknowledgement The research was supported by Scientific Research Project Coordination Center of YTÜ (project no. 2004-01-02-19).

References

1. US EPA, US EPA 230-03-84-005, Washington, DC.
2. Tackett, S.L., 1987, *J. Chem. Educ.,* **64,** 14–19.
3. Covelo, E.F., Alvarez, N., Andrade Couce, M.L., Vega, F.A. and Marcet, P., 2004, *J. Colloid Interface Sci.,* **280,** 343–349.
4. Wang, Y., Zhou, D., Sun, R., Cang, L. and Hao, X., 2006, *J. Hazard. Mater.,* **A137,** 76–82.
5. Ji-Yuan, L., Hong-Chi, L., Nongye, Z. and Huizhi, H., 1999, **37** (3), 412–419.
6. Ho, Y.S. and Huang, H.W., 2002, *Process Biochem.,* **37,** 1421–1430.
7. Suziki, Y., Sawada, K. and Chihara, K., 2004, Fundamentals of Adsorption and Ion Exchange, November 7–14. AICHE 2003 Annual Meeting, Session (265), Austin Convention Center, Austin, TX.
8. Bhattacharjee, S., Chakrabarty, S., S-Kar, S., Thakur, P. and Bhattacharyya, G., 2003, *Water Res.,* **37,** 3954–3966.
9. Aparittukul, R., Marhaba, T.F., Wattanachira, S. and Pavasant, P., 2004, *Songklanakarin J. Sci. Technol.,* **26,** 199–207.
10. Koshiwada, Y., 1992, *J. Nat. Prod.,* **55,** 1003.

11. Okuda, T., Yoshida, T. and Hatano, T., 1990, *Heterocycles,* **30,** 202.
12. Nakajima, A. and Sakaguchi, T., 1987, *J. Chem. Tech. Biotechnol.,* **40,** 223.
13. Sakaguchi, T. and Nakajima, A., 1987, *Separ. Sci. Technol.,* **22,** 1609.
14. Nakajima, A. and Sakaguchi, T., 1990, *J. Chem. Tech. Biotechnol.,* **47,** 31.
15. Xuepin, L., Li, L. and Bi, S., 2004, *J. Radioanal. Nucl. Chem.,* **260** (3), 619–625.
16. Nakano, Y., Tanaka, M., Nakamura, Y. and Konno, M., 2000, *J. Chem. Eng. Japan,* **33** (5), 747–752.
17. Santana, J.L., Lima, L., Torres, J., Martinez, F. and Olivares, S., 2003, *J. Radioanal. Nucl. Chem.,* **251,** 467.
18. Yamguchi, H., Higasida, R., Higuchi, M. and Sakata, I., 1992, *J. Appl. Polym. Sci.,* **45,** 1463.
19. Masatoshi, G. and Kyozo, S., 2000, *Appl. Biochem. Biotech.,* **84–86,** 1021–1038.
20. Zalacain, A., Carmona, M., Lorenzo, C., Blazouez, I. and Alonso, G.L., 2002, *JALCA,* **97,** 137–142.

Chapter 27
In Quest of Friendly Free Radicals: Reactions of Iodine Atom Free Radicals with Some Biologically Important Compounds

M. Mohammad[1], A. Dar[1], Sajid Jahangir[1,3], I. A. Tahiri[2,3], M. S. Subhani[2], and K. M. Khan[1]

Abstract Free radicals are generally considered as villain. Thus the image of free radicals emerges as a dangerous entity which is perhaps always injurious to health. One could, however, ask if there is any beneficial effect of free radicals. A series of studies has been embarked upon this idea: *"in quest of friendly free radicals"* in this concept the possible use of iodine free radicals was explored initially through their reaction with various biologically important compounds including components of DNA/RNA/PROTEIN.

Cyclic voltammetry technique was used for generation, characterization and monitoring reactions of free radicals with above mentioned compounds. Results of these studies are presented.

Keywords Bioactive compounds, cyclic voltammetry, free radicals, iodine, villain

Introduction

Free radicals are generally considered as villain. The most familiar being superoxide O_2^- and hydroxyl radical $OH^{\bullet}$. Every now and then it is proposed that free radicals are involved in various ailments. Thus the image of a free radical emerges as a dangerous entity which is perhaps always injurious to health.

One could, however, ask if there is any beneficial effect of free radicals. In other word is there any "friendly" free radical. A series of studies has been embarked

[1] International Center for Chemical Sciences, H.E.J. Research Institute of Chemistry, University of Karachi, Karachi-75270, Pakistan

[2] Department of Chemistry, Quaid-i-Azam University, Islamabad, Pakistan

[3] Department of Chemistry, Federal Urdu University of Arts Science and Technology, Gulshan- i-Iqbal Campus Karachi, Pakistan

B. Sener (ed.), *Innovations in Chemical Biology*, doi: 10.1007/978-1-4020-6955-0

upon this idea: “In quest of friendly free radicals”. One of the worst modern scourges is cancer. Free radicals have been claimed to be involved in cancer cell productions [1]. However, not much attention has been paid to explore possibility of using a free radical which can attack cancer cells. If such a possibility is to be explored, it is necessary to consider that the free radical be discriminatory – discriminating a normal cell from a cancer cell. A highly reactive free radical is indiscriminate while a “stable” free radical would be discriminating. A free radical attack on a cell C (normal/cancer) can be depicted as

$$C + A \rightarrow CA \rightarrow \text{products} \tag{27.1}$$

where A is a stable free radical.

There are stable organic free radicals, most familiar DPPH (diphenyl picryl hydrazyl) which is rather unstable (in open atmosphere) in solution phase. There are other “stable” (organic) free radicals but mostly stable under vacuum or inert atmosphere [2]. Thus these organic free radicals are not good candidates for studying their reaction with (living) cells. In situ generation of free radicals: e.g. superoxide O_2^-, hydroxyl OH^-, can be achieved but these free radicals are themselves suspected villains-suspected to play role in the generation of cancer cells. Halogen atoms $F^\bullet$ (fluorine), $Cl^{1\bullet}$ (chlorine), $Br^\bullet$ (bromine) and $I^\bullet$ (iodine) are free radicals [3]. These free radicals can be investigated: their generation, characterization and reaction with normal blood cells and/ or cancer cells. Of these halogen free radicals $I^\bullet$ is the least reactive while $F^\bullet$, the most. $F^\bullet$ and $Cl^\bullet$ free radicals are undesirable in the sense that being extensively reactive, they can be indiscriminate in attacking both – the normal blood as well as cancer cells. “Stable” free radicals are discriminating.

While elements in their atomic state are highly reactive, atomic iodine is not as reactive. This could be advantageous as well as disadvantageous. Disadvantageous: when the reaction of $I^\bullet$ (with a substrate) is slow then a recombination (of $I^\bullet$ atoms to form I_2) is more likely. The question arises as how to generate $I^\bullet$ and study its kinetics which ultimately lead us to investigate its reaction with cancer and normal cells. Iodine atom-free radicals $I^\bullet$ can be produced, and is generally thought to be produced photochemically. The reaction of a halogen with on alkane is a case in point [3]. Zawail and coworkers [4], found the rate constant for the decay of I_2^- into $I^\bullet$ and I^- as 7.1×10^{11} s^{-1} and recombination rate constant for $I^\bullet$ to I_2 as [O] 10^9 M^{-1} s^{-1} {[O] means order of}. For the reaction of $I^\bullet$ with a free radical [5], 1-ethyl-4-carbomethoxy pyridinyl the rate constant is 10^7–10^8 M^{-1} s^{-1} [5]. All these reactions, however, are in gaseous phase. Also since the recombination of $I^\bullet$ atoms is bimolecular, at low concentration of $I^\bullet$ the rate of recombination would be low. Electrochemically one can generate $I^\bullet$ by reduction of I_2 [6]

$$I_2 + \bar{e} \rightleftharpoons I_2^- \rightarrow I + I^- \tag{27.2}$$

or oxidation *[6–8]*

$$I^- - \bar{e} \rightarrow I \tag{27.3}$$

Both reactions depicted in Eqs. 27.2 and 27.3 involve follow-up chemical reactions. Popov and Geske *[7]* claimed that the recombination of **I.**, in solution, is slow compared to its reaction with pyridine:

$$I^{+} 2Py - \bar{e} \rightarrow \left[I(Py)_2 \right]^{+} \tag{27.4}$$

The formation of $I^{\bullet}$ from I^{-} had been postulated by Vetter [8a]. From the above information we can make the following conclusions: (a) $I^{\bullet}$ (atom-free radical) can be produced electrochemically, (b) $I^{\bullet}$ does react with pyridine and may react with similar compounds and (c) recombination of $I^{\bullet}$ may be slow in solution phase. Molecular iodine (di-iodine) I_2, the radio-isotope, is being used in the treatment of thyroid disorder. One can ask the question: is there any biologically beneficial or toxic effect of iodine atom. There has been no study [8b].

Cyclic voltammetry is a powerful technique to generate and characterize the oxidation/reduction product(s) and also to study the follow up chemical reaction of charge (electron) transfer products [9]. In the present study, cyclic voltammetry has been used to carry out such investigation on I^{-} ion: the electro-oxidation of I^{-}, the reaction of $I^{\bullet}$ with some familiar biologically important compounds and raw human blood samples.

Experimental

Material

All the chemicals were reagent grade or of higher purity and were used as received. Blood sample 250 ml blood sample bag was obtained from Liaquat National Hospital, Karachi, Pakistan. It was kept in the refrigerator and was utilized within a couple of days. The deterioration of blood sample was monitored and no significant deterioration was found. The composition of blood is well known [11]. The type of anticoagulant with PBS buffer contained 3.8% by weight citrate. The one in the blood sample, called drip anticoagulant, contain (per 100 ml blood): sodium citrate 2.63 g; citric acid anhydrous 3.30 g; sodium biphosphate monohydrate 0.22 g; dextrose monohydrate 3.19 g.

Procedure

Cyclic voltammetry was carried out on the Sycopel Work Station AEW 2, a three electrode assembly: glassy carbon electrode as working, graphite rod as counter and an Hg-pool as reference electrode were used. The stability and drift of Hg-pool was checked from time to time and found satisfactory. The scan rate was either 50 or 100 mV/s.

Results and Discussion

Results of the present studies can be categorized as follow: (i) identification of the electro-oxidation product of I– as I**.**, (ii) reaction of iodine free radical with various substrates, (iii) reaction of iodine free radical with raw human blood samples.

Identifying the electro-oxidation product At higher concentration $[I^-] \geq 1$ mM $[I^-] \leq 5$ mM (Fig. 27.1), there are two anodic and corresponding two cathodic peaks. Processes may be, suggested to be

$$I^- - \bar{e} \rightleftharpoons I^{\bullet}E_1 \tag{27.5}$$

$$\text{And } I - \bar{e} \rightleftharpoons I^{+}E_2 \tag{27.6}$$

Simulation through DigiSim software was used to help in elucidating mechanism.

To further identify the electro-oxidation products of I^-, the C.V. of I_2 and I_3^- were also recorded. There are similarities and dissimilarities in the cyclic voltamogram. While $(Ep)_a = 0.690$ V is same in both the C.V.'s, there is another anodic peak at 1,054 mV (absent in the $I^- - \bar{e} \rightarrow I^{\bullet}$ case) for the same concentration of I–and two corresponding cathodic peaks at 787 and 406 mV as compared to that of I^-. It was also noted that the anodic peak in the case of $[I^-] = 0.5$ mM was quite sharp manifesting a two-electron oxidation. It is not so in the case of I_3^-. Thus recombination I**.**to form I_2, followed by the reaction of I_2 with (excess) I^- in solution to form I_3^- and oxidation of I_3^- is not involved in the electro-oxidation of I^-.

A cyclic voltamogram of a saturated solution of I_2 shows an anodic peak at 637 mV (scanning upto 1,000 mV) and two cathodic peaks at 615 and 316 mV. None of them at the position of the anodic/cathodic peak in C.V. of oxidation of I^-. To further identify the electro-oxidation product of I^- Eq. 27.5, cyclic voltammogram of I^- at low concentration of I^- was rerecorded. For $[I^-] \leq 0.5$ mM there is only one

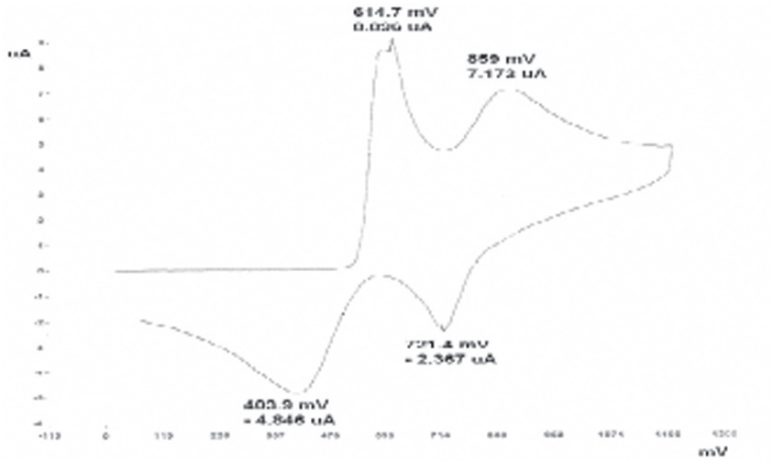

Fig. 27.1 Cyclic voltammogram of 5 mM Kl (0.1 M NaCl, aqueous system)

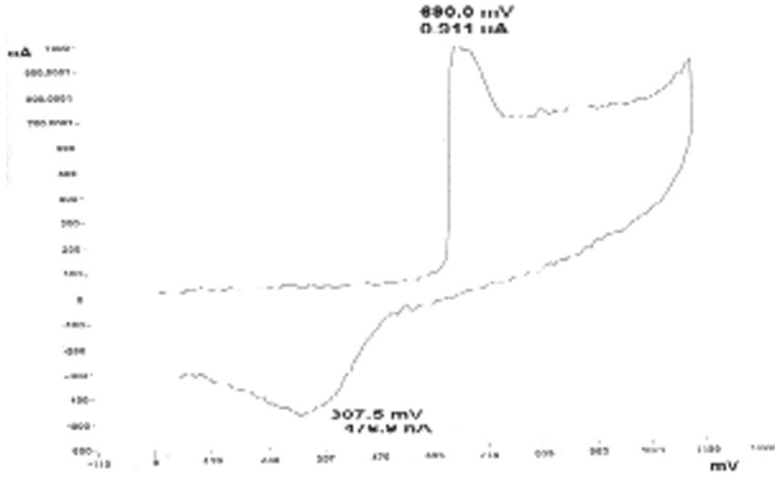

Fig. 27.2 Cyclic voltammogram of 0.5 mM Kl (0.1 M NaCl, aqueous system)

anodic and corresponding one cathodic peak (Fig. 27.2). It may be concluded that only one electro-oxidation process is taking place. This, however, does not mean that no subsequent chemical reaction (e.g. e-c-e) is taking place. As it is noticed, at higher concentration a second peak at more anodic position emerges. Since for [I^-] ≤ 0.5 mM there is no second anodic wave hence process in Eq. 27.6 may be ruled out for this concentration. The recombination of $I^\bullet$ would give I_2 Eq. 27.3 but no second oxidation wave of I_2 was found either. Thus at least on the C.V. time scale (100 mV/s) and at such concentration of I^- (≤0.5 mM), the formation of I_2 from $I^\bullet$ is slow as proposed by Popov and Geske [7].

From these data one can infer that the electro-oxidation of I^- proceeds with the formation of $I^\bullet$ without the complication from the formation and hence the oxidation of I_3^- and /or I_2, at least at 100 mV/s time scale. The reaction of **I.** with a substrate A is given as,

$$I + A \xrightarrow{k_2} \text{Product} \tag{27.7}$$

Where k_2 is the bimolecular rate constant between $I^\bullet$ and A. Results of our kinetic studies of $I^\bullet$with components of DNA/RNA/protein and others are collected in Table 27.1.

Reaction of $I^\bullet$ with raw human blood samples Since blood samples contained anticoagulant, buffer and blood (itself a composite of various chemicals) hence C.V. studies of $I^\bullet$ were also carried out on blood sample in the absence and the presence of buffer and anticoagulant. PBS (buffer) + anticoagulant showed the presence of an electroactive moiety which could undergo electro-oxidation in the range 0.000–1.000 V. However, addition of 1 ml of this buffer + anticoagulant solution to 9 ml of 0.5 mM I^- solution moved the anodic peak cathodically from 456 to 170 mV.

Table 27.1 Reactions of I˙with various compounds (0.1 M (aqueous) KCl/NaCl)

Compounds	k_2 (M^{-1} s^{-1})	Compounds	k_2 (M^{-1} s^{-1})
Cytosine	2 x 10^{8b}	Citric acid	$\geq 10^{3b}$
2-Picoline	1.6 x 10^{6c}	Acetic acid	[d]
Nicotine	[d]	Glycine	[e]
Acetaldehyde	[d]	Glucose	[e]
Fructose	[e]	Acetone	[e]
Uracil	10^{10b} 10^{2f}	Ethanol	[e]
Nicotinic acid	[e]	Buffer media	[e]

[a]Working electrode: glassy carbon, Ref. electrode: Hg-pool; counter: graphite; scan rate: 0.1 V/s [b]Simulation [c]Estimated [d]Reaction but k_2 not determined [e]No reaction [f]From (ip)c/(ip)a and switching time

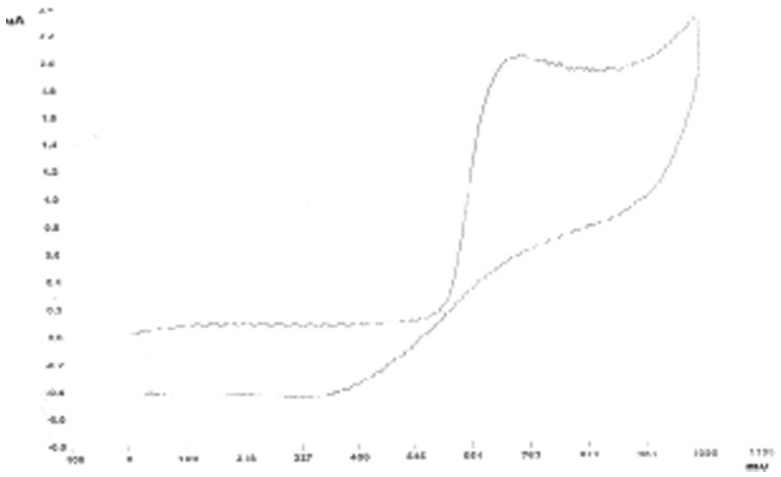

Fig. 27.3 Cyclic voltammogram of effect of blood (containing anticoagulant + buffer) on 5 mM Kl (0.1m NaCl, aqueous system)

The effect of the addition of anticoagulant containing buffer, and blood (containing anticoagulant and buffer) on the C.V of I^- is rather ambivalent: The C.V. of I^- was affected but since on the addition of large excess of these substrates, the C.V of I^- was obliterated, it could be inferred that the anticoagulant and/or blood complexes with I^-itself [10]. However, this (complexion) does not explain the initial shifting of the anodic peak to more cathodic peak from 456 to 170 mV as mentioned above. The cathodic peak, on the addition of this substrate, becomes well defined. The effect of addition of blood sample (containing anticoagulant + buffer) in 1 ml aliquots to a 5 mM I^- solution in such a way to keep the total volume constant was also studied (Fig. 27.3). From the cyclic voltamograms one concludes that blood sample may be reacting with I^- itself but also with the first oxidation product of I^- i.e. $I^{\bullet}$ atom-free-radical.

Conclusion

From the table it can be concluded that (a) $I^{\bullet}$ reacts with pyridine and pyrimidine bases. Then If $I^{\bullet}$ reacts with DNA, it will preferably react at purine and pyrimidine sites and (b) $I^{\bullet}$ and I^{-} both react with blood sample. It is however not clear why I^{-}should react with blood sample or its components.

Acknowledgements The work is supported by Pakistan Science Foundation through project no. S-KU/CHEM (367).

References

1. Fridovich, I., 1982, In Pathology of Oxygen, A.P. Autor (ed.), Academic, New York, pp 1–20.
2. Mohammed, M. and Kosower, E.M., 1971, *J. Am. Chem. Soc.,* **93,** 2709–2713.
3. Morrison, R.T. and Boyd, R.N., 1992. 6th ed. *Org. Chem.*, Allyn & Bacon, Boston, MA.
4. Su, J.T. and Zewail, A.H., 1998, *J. Phys. Chem. A,* **102,** 4082–4099.
5. Kosower, E.M., 1968, An introduction to Physical Organic Chemistry, Wiley, New York.
6. Mohammad, M., Shaheen, R., Khan, A.Y., Iqbal, R. and Subhani, M.S., 1989, *Pak. J. Sci., Ind. Res.,* **32,** 447–452.
7. Popov, A.I. and Geske, D.H., 1958, *J. Am. Chem. Soc.,* **80,** 1340–1352.
8. (a) Vetter, K.J., 1951, *Z. Electrochem. C,* **55 ,**121.
   (b) Bard, A.J. and Faulkner, L.R., 1980, Electrochemical Methods, Wiley, New York.
9. Bard, A.J. and Faulkner L.R., 2001, Electrochemical Methods: Fundamental and Applications, 2nd ed. John Wiley & Sons, New York, pp 471.
10. Blood Composition: Hole's Human Anatomy & Physiology by David Shier, 2002, 9th ed. McGraw-Hill, Boston, MA.

Chapter 28
Adsorption of Cu (II) from Aqueous Solutions by Sumac (*Rhus coriaria* L.) Tannins

Ahmet Lütfi Uğur, Mahmure Üstün Özgür, and Gülşah Gümrükçü

Abstract In this study, a new natural adsorbent (sumac leaves) for removing Cu (II) ion from the aqueous solutions has been investigated. Leaves of sumac were obtained from Siirt, Turkey. The tannins were extracted with acetone:water (70:30, v/v) mixture from the leaves of sumac. For the total tannin determination Folin-Ciocalteu method was used and tannin content was found 27%. In batch experiments, pH profile, adsorption time, adsorbent/liquid ratio, initial concentration of metal ions, adsorbent amount, particle size of adsorbent and temperature were performed to determine binding properties of adsorbent for the Cu(II) ions. The concentrations of the metal ions in solutions before and after adsorption were measured with an atomic absorption spectrophotometer.

Keywords Cu(II) adsorption, *Rhus coriaria* L., sumac leaves, tannins

Introduction

Environmental pollution caused by toxic heavy metals occurs globally through industrial, military and agricultural processes as well as waste disposal. The discharge of heavy metals into the environment is a major concern because of their toxicity and threat to human life and to the environment. Strict environmental regulations on the discharge of heavy metals make it necessary to develop efficient technologies for their removal. Removing and collecting heavy and rare metal ions from industrial effluents and waste aqueous solutions are important problems.

The main techniques that have been used to dispose of industrial effluents include chemical precipitation, ion exchange, electrochemical processes, and adsorption onto various adsorbents and/or membrane filtration. Although all of these techniques are capable of removing heavy metals to some extent, adsorption by solid substrates is preferred because of its high efficiency, easy handling and cost as well as the availability of adsorbent.

Yildiz Technical University, Faculty of Arts and Sciences, Departmant of Chemistry, 34210, Davutpasa, İstanbul Turkey

B. Sener (ed.), *Innovations in Chemical Biology*, doi: 10.1007/978-1-4020-6955-0

The removal of metal ions from waste aqueous solutions is of importance to many countries of the world both environmentally and for water re-use. The application of low-cost sorbents including carbonacceous materials, agricultural products and waste by-products has been investigated [1]. Several researchers employing wide variety techniques have attempted removal of metal ions from contaminated water bodies. Majorities of these are adsorption on various surfaces. In recent years, agricultured by products have been widely studied for metal removal from water. These include peat [2], pine bark [3], banana peat [4], peanut shells [5], sawdust [6] and leaves [7].

Tannins are important commercial products of complex and diverse chemistry. During the last years, the interest of biomaterials and specifically in tannins was growing. The ability of tannins to precipitate metal ions is due to their multiple adjacent phenolic hydroxyl groups, which can form stable complexes with many metal ions [8, 9].

Rhus coriaria L. is a shrub, which reaches 3–4 μ in high in the wild. Its powdered leaves were used as a tanning agent for its high tannin content [10]. Tannins are found in the leaves, fruit, barks, roots and wood of trees. They can be classified into two groups; condensed tannins and hydrolysable tannins [11]. The co-occurrence of both kinds of tannins in the same plant or plant tissue is often observed [12]. The main compounds present in *Rhus coriaria* L. are hydrolysable gallatonnins.

In this work, sumac leaves will use to remove Cu^{2+} ions in aqueous solutions. Firstly the tannins will extract from leaves and determine tannin contents. Then, binding properties of leaves for the Cu^{2+} ions will be investigated.

Experimental

Chemicals and Solutions

Tannic acid (TA) was obtained from Merck [K30231073-212]. Stock TA solution (100 μg mL^{-1}), was prepared freshly with doubly distilled water.

All the reagents used were of analytical reagent grade. The stock solution of Cu^{2+} (1,000 μg mL^{-1}) was prepared in distilled water using $Cu(CH_3COO)_2.H_2O$. All working solutions were prepared by diluting the stock solutions with distilled water.

Folin-Ciocalteu reagent was obtained from Merck (Darmtstad, Germany).

Material

Leaves of Sumac were collected from Siirt in Turkey. They were dried at room temperature and darkness. Leaves were ground with hand and screened through a set of sieves to get different geometrical size such as 300, 425, 600, 710, 850 μm. Samples were stored in an air-tight plastic container and in dark conditions until extraction time.

Rhus Coriariaria L.

Instruments

The pH values of the solutions were adjusted with 0.1 mol/L NH_4OH or HCl and measured with Metrohm Herisau E510 pH meter. A magnetic stirrer was used for stirring the adsorption batches. The concentration of the Cu^{2+} solution before and after adsorption was measured by using Analytika Jena Atomic Absorption Spectrometer (AAS). All the measurements were made under optimization of the below mentioned parameters: Band witdh: 1.2, flame: C_2H_2/Air, detection limit: 0.70 ppm, concentration range: 1–10 μg mL^{-1}.

Extraction

Tannins were extracted from ground samples (300–850 μm) with aqueous acetone [13]. The ground leaves (0.01 g) were extracted with 2 mL of acetone–water (70:30, v/v) in a water bath at 30–35°C for 30 min, shaking every 5 min. The sample was centrifuged and supernatant collected. Extraction repeated three times, the combined supernatants were filtered, evaporated to dryness and taken up in 2–5 mL methanol [14].

Determination of TA in Sumac Sample Solutions by Folin-Ciocalteu (FC) Method

To 0.2 mL of FC reagent, 1 mL of Na_2CO_3 (75 g/L) and 0.1–0.5 mL of sumac extract was added and the mixture was rinsed to 10 mL with distilled water and kept at room temperature for 60 min. The absorbance of this solution was measured at 760 nm on an Agillant spectrophotometer [15].

Calibration Graph

A calibration graph 3–15 ppm TA concentration range was constructed and the content of tannins in sumac leaves was determined by the Folin-Ciocalteu method.

Adsorption Experiments

Batch adsorption experiments were performed at a constant temperature (20 ± 2°C) on a magnetic stirrer using 100 mL erlenmayer flasks. In bath experiments, adsorption time, particle size of adsorbent, adsorbent amount, pH profile, and adsorbent/liquid ratio were performed to determine binding properties of adsorbent for the Cu^{2+} ions. The concentration of the metal ions in solutions before and after adsorption was measured with an AAS.

Effect of Particle Size

Batch adsorption tests were done at five different particle sizes 300, 425, 600, 710 and 850 μm. 0.1 g of the sumac leaves was weighed and 8 mL of Cu^{2+} ion solution was added. The volume was completed 50 mL. After stirring 2 h, the reaction mixtures were filtered through a filter paper to remove particulates and the filtrate was analyzed with an AAS.

Effect of Stirring Time

The time-dependent behavior of Cu^{2+} ions adsorption was measured by varying the equilibrium time between the adsorbent (ground sumac leaves) and adsorbent (Cu^{2+} ions) in the range of 30 min and 24 h. The concentration of Cu^{2+} was kept 40 μg mL^{-1}, particle size 710 μm, and amount of adsorbent 0.1 g.

Effect of Temperature and pH

Batch adsorption experiments were carried out at the desired temperature (20°C, 30°C and 40°C) and each used a range of pH from 6 to 10. The concentration of Cu^{2+} was kept 10 μg mL^{-1} particle sizes < 300 μm and amount of adsorbent 0.2 g, stirring time 4 h.

Effect of the Amount of Sumac Leaves

The dependence of Cu^{2+} ion sorption on sumac leaves amount was studied by varying the sorbent amount from 0.1 to 1.0 g while keeping constant Cu^{2+} ion concentration 20 μg mL^{-1}, stirring time 90 min for 710 μm particle size.

Effect of the Amount of Cu^{2+} Concentration

The adsorption of Cu^{2+} ion sumac leaves as a function of its concentration was studied by varying the metal ion concentration from 10 to 100 μg mL^{-1}, while keep all other parameters constant.

Results and Discussion

In the adsorption of some metal ion by tannin adsorbents [16], tannins are widely distributed in nature and have multiple adjacent phenolic hydroxyl groups and exhibit specific chelation ability toward metal ions [17]. According to the chemical structures of tannins, they can usually be classified into hydrolyzable tannins, condensed tannins and complex tannins. Hydrolyzed tannins yield gallic acid or ellagic acid when hydrolyzed by acid, base or some enzymes [18]. Turkish sumac tannin (hydrolyzable tannin) is illustrated in Fig. 28.1 whose basic structure is of flavan-3-ols.

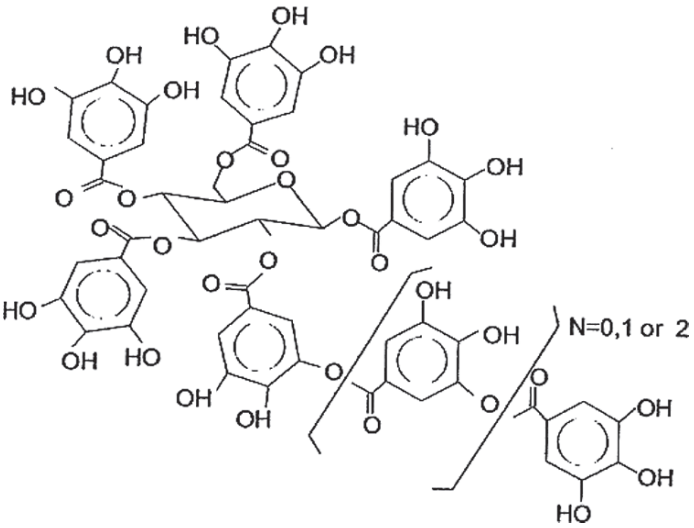

Fig. 28.1 Chemical structure of Turkish Sumac, tannin

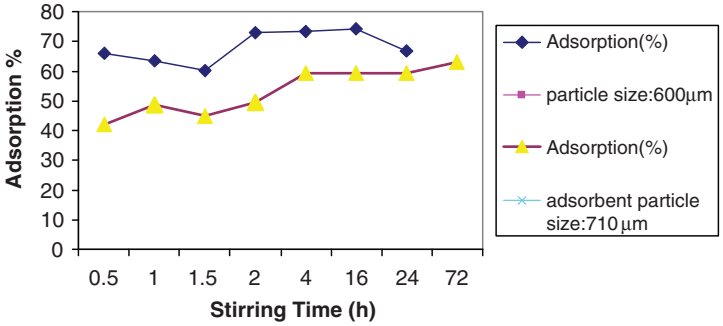

Fig. 28.2 Effect of stirring time on the adsorption of Cu^{2+} ions Amount adsorbent = 0.1 g, $C_{Cu(II)0}$ = 16 µg mL^{-1} for 710 µm, $C_{Cu(II)0}$ = 32 µg mL^{-1} for 600 µm

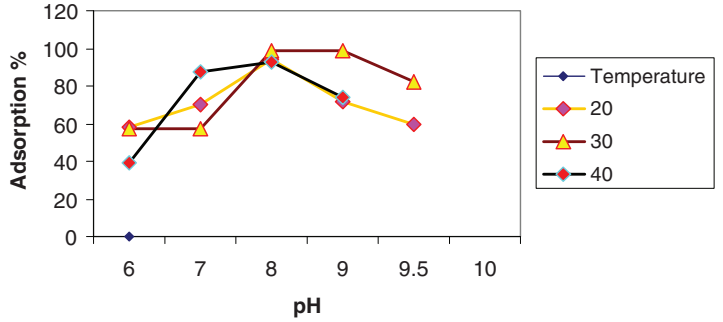

Fig. 28.3 Effect of temperature and pH on the adsorption of Cu^{2+} ions $C_{Cu(II)0}$ = 10 µg mL^{-1}, adsorbent amount = 0.2 g, stirring time = 4 h, particle size < 300 µm

Leaves of Sumac were used for removal of Cu^{2+} ions in aqueous solution. Tannins were extracted from the leaves of sumac by extracting with 70% (v/v) acetone-water solution. For the total tannin determination Folin-Ciocalteu method was used and tannin content was found 27%. Various adsorption parameters for the effective removal of Cu^{2+} ions by using sumac leaves as an adsorbent from aqueous solutions were studied and optimized.

Time-depended behavior of Cu^{2+} ion adsorption was measured by varying the equilibrium time between in the range of 0.5–72 h. The percentage adsorption of Cu^{2+} ions plotted in Fig. 28.2 as a function of contact time. The percentage adsorption of Cu^{2+} indicates that the equilibrium between the Cu^{2+} ions and sumac leaves was attained 4 h. Therefore, 4 h stirring time was found to be appropriate for maximum adsorption and was used in all subsequent measurement. The effect of temperature and pH the adsorption equilibrium of Cu^{2+} on sumac leaves was investigated by varying the solution temperature from 283 to 303 and pH from 6 to 10. The results are presented in Fig. 28.3. The results indicated that the best adsorption results were obtained at pH 8 at 293 K.

Table 28.1 Effect of particle size on the adsorption of Cu^{2+}

Particle size (μm)	300	425	600	710	850
Adsorption (%)	67.7	63.1	61.2	62.5	59.8

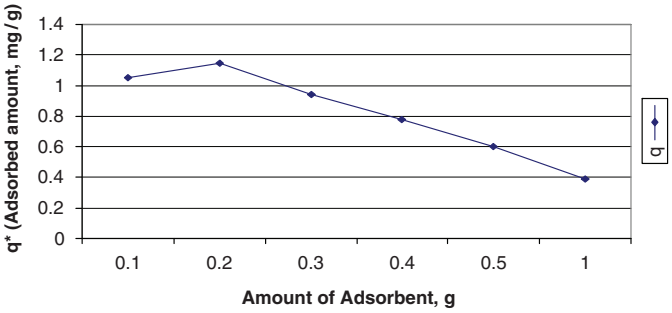

Fig. 28.4 Effect of the amount of sumac leaves on the adsorption of Cu^{2+} ions $C_{Cu(II)0}$ = 20 μg mL^{-1}, stirring time = 90 min, particle size = 710 μm

Dissociation of the phenolic hydroxyl groups of tannin, resulting in stronger complexing ability with metal ions. However at higher pH values, Cu^{2+} would be precipitated and the phenolichydroxyl groups of the tannin would more readily be oxidized. So making it impractical to apply this approach above pH 8 [19].

To investigate of the effect of particle size on the adsorption of Cu^{2+} ions, batch adsorption tests were done at five particle size. The percentage of adsorption of Cu^{2+} indicates that increasing particle size was decreased the percentage adsorption (Table 28.1). Therefore <300 μm was found to be appropriate for maximum adsorption and was used in all subsequent measurement.

The concentration of Cu^{2+} and stirring time were fixed at 20 μg mL^{-1} and 90 min, respectively while amount of sumac leaves varied from 0.1 to 1.0 g. Figure 28.4 displays the effect of changing of sumac leaves on Cu^{2+} uptake. Increasing sumac leaves mass from 0.1 to 1.0.

The amount of adsorption on the sumac leaves (*Rhus coriaria* L.) was determined from the difference in concentration before and after the adsorption experiment as the following equation.

$$q^* = V(C^0 - C^*)/m$$

Where q* is the metal adsorption in milligram per gram at equilibrium, C^0 and C* are the concentration of the element in the initial and final solution in milligram per liter, V is the volume of supernatant solution in liter and μ is the sumac leaves mass in gram.

Figure 28.5 displays the effect of changing initial concentration of Cu^{2+} from 10 to 100 μg mL^{-1} on the rate of adsorption. Increasing the initial concentration increases the competition of Cu^{2+} ions molecules at the active site of the adsorbent and as a result more Cu^{2+} adsorbed per gram of leaves.

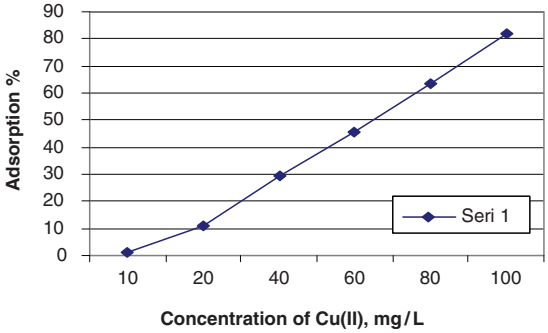

Fig. 28.5 Effect of initial concentration of Cu^{2+} Particle size < 300 μm, amount adsorbent = 0.2 g, pH = 8, temperature = 30 ^{0}C, stirring time = 4 h

References

1. Nguyen, C. and Do, D.D., 2001, *Carbon,* **39,** 1327–1336.
2. Ho, Y.S. and Mc Kay, G., 2000, *Water Research,* **34,** 735–742.
3. Al-Asheh, S. and Duvnjak, Z., 1997, *Journal of Hazardous Materials,* **56,** 35–51.
4. Low, K.S., Lee, C.K. and Leo, A.C., 1995, *Bioresource Technology,* **51,** 227–231.
5. Wafwoyo, W., Seo, C.W. and Marshail, W.E., 1999, *Journal of Chemical Technology and Biotechnology,* **74,** 1117–1121.
6. Yu, B., Zhang, Y., Shukla, A., Shukla, S.S. and Dorris, K.L., 2001, *Journal of Hazardous Materials,* **84,** 83–94.
7. Taggout, F.R., 2001, *Asian Journal of Chemistry,* **13,** 639–650.
8. Krisper, P., Tisler, V., Skubic, V., Rupnik, I. and Kobal, S., 1992, *Basic Life Sciences,* **59,** 1013–1019.
9. Yamaguchi, H., Higasida, R., Higuchi, M., and Sakata, I.,1992, *Journal of Applied Polymer Science,* **45,** 1463.
10. Howes, E., 1953, Sumac. In Vegetable Tanning Materials, Butterworths Scientific Publications, London, pp 209–218.
11. Haslam, E., 1998, Practical Polyphenolics. From Structure to Molecular Recognition and Physiological Action, Cambridge University Press, Cambridge.
12. Scalbert, A., Monties, B., and Janin, G., 1989, *Journal of Agricultural Food Chemistry,* **37**(5), 1324–1329.
13. Haslam, E., 1966, Chemistry of Vegetable Tannins, Academic, London.
14. Morrison, I.M., Asiedu, E.A., Stuckbury, T. and Powell, A.A., 1995, *Annals of Botany,* **76,** 287–290.
15. Zalacain, A., Prodanov, M., Carmona, M. Alonso, P.L., 2003, *Biosystems Engineering,* **84**(2) 211–216.
16. Khoo, K.M. and Ting, Y.P., 2001, *Biochemical Engineering Journal,* **8,** 51.
17. Xuepin, L., Li, L. and Shi, B., 2004, *Journal of Radioanalytical and Nuclear Chemistry,* **260**(3), 619–625.
18. Shi, B. and Di, Y., 2000, Plant Polyphenols, Science Press, Beijing.
19. Xuepin, L., Zhonbing, L., Zhang, M., Xin, L. and Shi, B., 2004, *Journal of Chemical Technology and Biotechnology,* **79,** 335–342.

Chapter 29
Sorption of Pb(II) and Zn(II) Ions from Aqueous Solution by Tannin Resins

Fatma Turak, Kadir Turhan, and Mahmure Üstün Özgür

Abstract Recently, the interest on biomaterials and especially in tannins was growing and some attractive results were obtained in the adsorption of some metals by tannin adsorbents. Tannins are widely distributed in nature and have multiple adjacent polyhydroxyphenyl groups in their chemical structure which have extremely high affinity for heavy metal ions. This study will describe how tannin can be used as an effective zinc and lead sorbent by the use of tannin resins. Batch method was used in the experiments in which pH profile, adsorption time, adsorbent/liquid ratios, initial concentration of metal ions, adsorbent amount and temperature were investigated to determine binding properties of adsorbent for the Zn(II) and Pb(II) ions.

Keywords Biomaterial, heavy metals, lead, resin, tannin, zinc

Introduction

Lead pollution has been recognized as a potential threat to air, water and soil. Lead is known to damage the kidney, liver and reproductive system, basic cellular processes and brain function [1]. Lead has been found to be acute toxic to human beings when present in high amount [2]. The toxic symptoms are anemia, insomnia, headache, dizziness, and irritability, weakness of muscles, hallucination and renal damage. The main sources of human exposure to lead include the use of leaded, gasoline, industrial sources such as lead mining, smelting and coal combustion, the use of lead-based paint and lead-containing pipes in water supply systems. Additional sources may be food can solders, ceramic glazes, lead containing batteries and cosmetics.

Heavy metals are introduced into the soil mainly by the application of fertilizers, sewage sludge, liming materials, and other industrial and urban waste materials. In recent years, increased anthropogenic inputs of heavy metals in terrestrial environments have caused considerable concern relative to their impact on groundwater

Yıldız Technical University, Chemistry Department, Davutpaşa Campus, 34220, Esenler, İstanbul, Turkey

B. Sener (ed.), *Innovations in Chemical Biology*, doi: 10.1007/978-1-4020-6955-0

contamination. Zinc is a key element in plant growth and human health. It has been used by human beings since immemorial time and is still widely applied in our industrialized society. Zinc is an essential element for the normal activity of DNA polymerase and protein synthesis. Its deficiency in human body can cause many diseases, such as liver disease, gastrointestinal disorders, renal diseases, neoplastic diseases, burns, skin disorders, etc. So, it plays a vital role in the healthy development of many life forms. Excessive amounts of Zn, however, may be toxic, especially to the aquatic biota. The EPA recommends that drinking water should contain no more than 5 milligrams per liter of water (5 mg/L) because of taste [3, 4].

Much work has been done on the removal of Pb and Zn from aqueous solution. Removal of these ions has been attempted by several researches employing a wide variety of techniques. Adsorption of removal of Pb and Zn from solution agricultural waste [5], three fern [6], tannin gel [7], removal of Pb sea module [8], tannin gel adsorbent synthesized from condensed tannin [8] and removal of Zn green macro elga [9], soil [3] have been extensively studied for this purpose.

Biomass materials, potentially serve as remediation factors in contaminated areas for preventing environmental pollution because of possible waste water treatment. During the last years, the interest on biomaterials and especially in tannins was growing. Tannins are an important class of secondary plant metabolites, water soluble polyphenolic compounds of molecular weight range between 500 and some thousands Daltons [10]. There are three kinds: hydrolizable, condensed and complex tannins [11]. Tannins have multiple adjacent phenolic hydroxyl groups and exhibit specific chelation ability toward metal ions. However, tannins are sparingly water soluble compounds. When they are used directly as adsorbent for metal ions in aqueous system, they have the disadvantage of being leaked by water. To overcome this disadvantage, attempts were made to immobilize tannins onto various water-insoluble matrices. The immobilization of tannin on to agarose [12], cellulose powder rayon fibre [13] matrices with have amino groups such as albumin, gelatin, aminopolystyrene and 2-vinly-4,6-diamino-S-triazine [14] and collagen fibres [15] and animal fibrous proteins [16] were also reported. However, no data have been reported for the adsorption of Pb^{2+} and Zn^{2+} on the resin synthesized from sumac leaves (contain hydrolysable tannin) and gelatin.

Taking into account all the above, we have considered it of great interest to assess the ability of locally available sumac leaves and for the removal of Pb(II) and Zn(II) from aqueous solution and optimization of conditions for theirs adsorption. Firstly, a new resin was synthesized from sumac leaves and animal gelatin.

Experimental

Adsorbent Synthesis

For synthesized the gelatin (G)/tannic acid (TA) resin, gelatin powder was purchased from Ülker Company-İstanbul, Turkey and tannic acid (TA) purchased from E. Merck. TA powder was dissolved in distilled water at 95–98°C, then solution

cooled at room temperature and 37% formaldehyde solution added to the solution. G powder was dissolved distilled water at 95–98°C and then added to the TA/formaldehyde solution. Concentrated hydrochloric acid was added to the mixture and heated 95–98°C for 12 h with a reflux condenser. G/TA resin was washed distilled water, dried at 110°C. Dried resin was crushed into small particles, <500 μm [17].

Reagents and Chemicals

Chemicals used were of analytical/laboratory grade procured either from Merck or Aldrich. Stock lead and zinc solutions 1,000 mg/L for adsorption study were prepared from AR grade lead nitrate [$Pb(NO_3)_2$] and from zinc chloride [$ZnCl_2$]. Different concentrations of Pb and Zn solutions were prepared from the stock solutions. All working solutions were prepared by diluting the stock solutions with distilled water.

Instruments

The values of solutions were adjusted with 0.1 mol/L NH_4OH or HNO_3 and measured with Metrohm Herisau E510 pH meter. A magnetic stirrer model Arex was used for stirring the adsorption batches. The concentration of solution before and after adsorption was measured by using Atomic Absorption Spectrometer (AAS) Analytika Jena. All the measurements were made under optimization of the below mentioned parameters.

Metal ion	Band width	Flame	Detection limit	Concentration range (μg/mL)
Pb(II)	1.2	C_2H_2/air	1.00	0.1–30
Zn(II)	0.5	C_2H_2/air	0.01	0.01–2

Adsorption Experiments

Method

Adsorption measurements were made by batch technique at room temperature (25 ± 3°C). Known amounts of tannin resin were placed in 250 mL erlenmeyer flasks containing 100 mL of metal ion solution of known concentration and were stirred for a given time period. The solutions were then filtered, centrifuged and the concentrations of metal ions were measured by AAS. The difference in the metal ion (Pb^{2+} and Zn^{2+}) content before and after adsorption represented the amount of Pb and Zn adsorbed by new resin.

The Effect of Stirring Time

The time-dependent behaviors of metal ions adsorption were measured by varying the equilibrium time between the adsorbate and adsorbent in the range of 30–300 min. The concentration of Pb(II) and Zn(II) were kept as 50 μg/mL while the amount of resin added was 0.5 g. The experiments were performed at pH 4 for Pb^{2+}.

The Effect of pH on Adsorption Equilibrium

Effect of initial pH on adsorption of Pb^{2+} ions were investigated as follows: 0.5 g of the resin was weighed and 100 mL of a heavy metal ion solution was added. The pH of each solution was adjusted to desired values. After stirring 5 h the reaction mixture was filtered through membrane filter to remove particulates and analyzed with an AAS.

The Effect of the Ratio of Solution Volume to Mass of Resin (V/m, mL/g)

To investigate the effect of ratio of solution volume to mass of solid and adsorption of metal ions; 0.5 g resin samples were mixed 25–75 mL of aqueous solution of the constant initial concentration of metal ions (50 μg/mL Pb^{2+}). The pH was adjusted to 4 for adsorption of Pb^{2+}. The flasks with their contents were stirred for 4 h.

The Effect of Adsorbent Amount

The concentration of Pb^{2+} and stirring time were fixed at 50 μg/mL and 4 h, respectively, while amount of resin was varied from 0.1–0.5 g.

Results and Discussion

Recently, the interest on biomaterials and especially in tannins was growing and some attract results were obtained in the adsorption of some metals by tannin adsorbents [18]. Tannins are widely distributed in nature and have multiple adjacent polyhydroxyphenyl groups in their chemical structure which have extremely high affinity for heavy metal ions [16, 19].

Various adsorption parameters for the effective removal of Pb^{2+} and Zn^{2+} ions by using new synthesized resin as an adsorbent from aqueous solutions were studied and optimized. Time-dependent behavior of Pb^{2+} and Zn^{2+} ions adsorption was measured by varying the equilibrium time between in the range of 30–300 min. The percentage adsorption of Pb^{2+} plotted in Fig. 29.1 as a function of contact time indicates that the equilibrium between to Pb^{2+} and new resin was attained within 4 h.

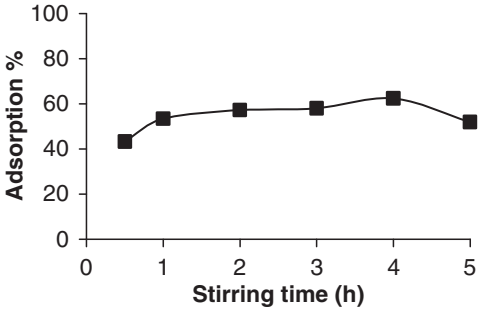

Fig. 29.1 Effect of stirring time on the adsorption of lead
$C^0_{Pb^{2+}}$: 50 µg/mL, amount of resin: 0.5 g, pH 4

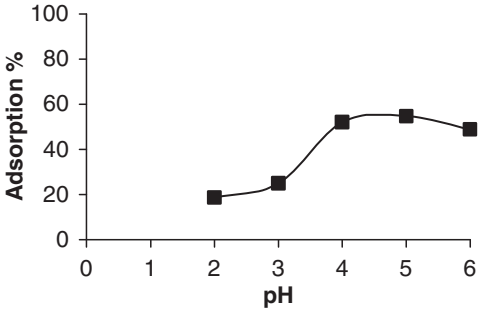

Fig. 29.2 Effect of pH on the adsorption of lead
$C^0_{Pb^{2+}}$: 50 µg/mL, stirring time: 4 h, amount of adsorbent 0.5 g

Therefore, a 4 h stirring time was found to be appropriate for maximum adsorption and was used in all subsequent measurements.

The pH of the aqueous solution is an important variable which controls the adsorption of the metal at the resin-water interfaces. Hence, the influence of pH on the adsorption Pb^{2+} on resin was also examined in the pH range of 2–6. The results of studied elements are given in Fig. 29.2. As seen both metal cations have a pH dependent adsorption behavior. Adsorption of lead was about maximum values (52.00%) at pH 4, then decreases to 18.74% at pH 2.

Figure 29.3 shows the sorption of Pb^{2+} ions by resin (0.5 g) as a function of V/m. The results indicate that adsorption percentage did not change much with increasing V/m values. Therefore 50 of the V/m rate were selected as the optimum value.

The amount of adsorption on the resin was determined from the difference in concentration before and after, the adsorption experiment as the following equation.

$$q^* = V\left(C^0 - C^*\right)/m$$

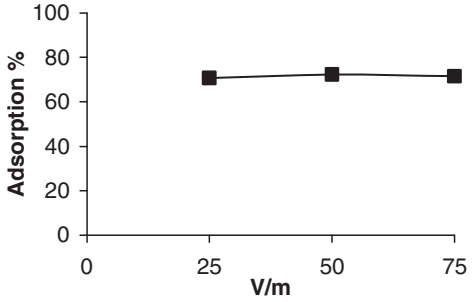

Fig. 29.3 Effect of V/m on the adsorption of lead
$C^{0}_{Pb^{2+}}$: 50 µg/mL, stirring time: 4 h, pH 4, amount of adsorbent 0.5 g

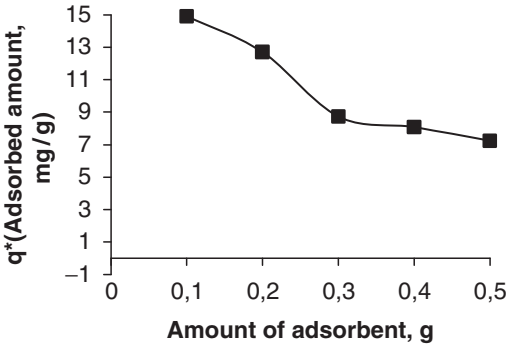

Fig. 29.4 Effect of q* on the adsorption of lead
q* = : 50 µg/mL, stirring time: 4 h, pH 4

where q* is the metal adsorption in milligram per gram at equilibrium, C^{o} and C* are the concentration of the element in the initial and final solution in milligram per liter, V is the volume of supernatant solution in liter and µ is the resin mass in gram.

The dependence of Pb^{2+} ion sorption on resin amount was studied by varying the sorbent amount from 0.1–0.5 g while keeping the volume 50 mL, concentration of Pb^{2+} 50 mg/L, pH: 4 and stirring time 4 h. The results indicated that adsorbed amount of Pb^{2+}, q*, was high and remained almost constant up to 0.2 g then slowly decreased with increasing resin mass from 0.2 to 0.5 (Fig. 29.4).

Adsorption of Zn^{2+} ions was studied at the same conditions which studied for Pb^{2+} ions. The results showed that the resin couldn't adsorbed at these conditions. We decided that to study other conditions at the future program.

Acknowledgement The research was supported by Scientific Research Project Coordination Center of YTÜ (project no. 2004-01-02-19).

References

1. US EPA, US EPA 230-03-84-005, Washington, DC.
2. Tackett, S.L., 1987, *J. Chem. Educ.,* **64,** 14–19.
3. Covelo, E.F., Alvarez, N., Andrade Couce, M.L., Vega, F.A. and Marcet, P., 2004, *J. Colloid Interface Sci,* **280,** 343–349.
4. Wang, Y., Zhou, D., Sun, R., Cang, L. and Hao, X., 2006, *J. Hazard Mater.,* **A137,** 76–82.
5. Ji-Yuan, L., Hong-Chi, L., Nongye, Z and Huizhi, H., 1999, **37**(3), 412–419.
6. Ho, Y.S. and Huang, H.W., 2002, *Process Biochem.,* **37,** 1421–1430.
7. Suziki, Y., Sawada, K. and Chihara, K., 2004, AICHE 2003 Annual Meeting, Austin Convention Center, Austin, TX, Session (265) Fundamentals of Adsorption and Ion Exchange, November 7–14.
8. Bhattacharjee, S., Chakrabarty, S., S-Kar, S., Thakur, P. and Bhattacharyya, G., 2003, *Water Res.,* **37,** 3954–3966.
9. Aparittukul, R., Marhaba, T.F., Wattanachira, S. and Pavasant, P., 2004, *Songklanakarin J. Sci. Technol.,* **26,** 199–207.
10. Koshiwada, Y., 1992, *J. Nat. Prod.,* **55,** 1003.
11. Okuda, T., Yoshida, T. and Hatano, T., 1990, *Heterocycles,* **30,** 202.
12. Nakajima, A. and Sakaguchi, andT., 1987, *J. Chem. Tech. Biotechnol.,* **40,** 223.
13. Sakaguchi, T. and Nakajima, A., 1987, *Separ. Sci. Technol.,* **22,** 1609.
14. Nakajima, A. and Sakaguchi, T., 1990, *J. Chem. Tech. Biotechnol.,* **47,** 31.
15. Xuepin, L., Li, L. and Bi, S., 2004, *J. Radioanal. Nucl. Chem.,* **260**(3),619–625.
16. Masatoshi, G. and Kyozo, S., 2000, *Appl. Biochem. Biotech.* **84–86,** 1021–1038.
17. Nakano, Y., Tanaka, M., Nakamura, Y. and Konno, M., 2000, *J. Chem. Eng. Japan,* **33** (5),747–752.
18. Santana, J.L., Lima, L., Torres, J., Martinez, F. and Olivares, S., 2003, *J., Radioanal. Nucl. Chem.* **251,** 467.
19. Yamguchi, H., Higasida, R., Higuchi, M. and Sakata, I., 1992, *J. Appl. Polym. Sci.,* **45,** 1463.

Chapter 30
Determination of Ibuprofen, Pseudoephedrine HCl, Chlorpheniramine Maleate and Nipagen by Liquid Chromatography and Fractional Factorial Design

Bürge Aşçı, Özlem Aksu Dönmez, Abdürrezzak Bozdoğan, and Sıdıka Sungur

Abstract In the present work, a rapid and sensitive gradient HPLC method was developed for the analysis of a new syrup preparation containing ibuprofen, pseudoephedrine HCl, chlorpheniramine maleate and nipagen. The optimization process was carried out using 2^{5-1} fractional factorial design. Five variables pH, flow rate and solvent ratios for three steps of gradient profile were regarded as factors in the optimisation. The resolution was used as analytical response. Using the optimised experimental conditions, the limits of quantitations (10σ/s) determined as 0.09, 0.01, 0.04 and 0.01 ppm for ibuprofen, pseudoephedrine HCl, chlorpheniramine maleate and nipagen, respectively.

The obtained results indicated that this procedure could be applied for the determination of ibuprofen, pseudoephedrine hydrochloride, chlorpheniramine maleate and nipagen in syrup preparations.

Keywords Chlorpheniramine, fractional factorial design, RP-HPLC, ibuprofen, nipagen, pseudoephedrine

Introduction

Chemometric techniques have been frequently used for optimization of analytical methods, as they are faster, more economical and effective and allow more than one variable to be optimized simultaneously. Among these, two level fractional factorial design (2^{k-1}) is used mainly for preliminary evaluation of the significance of the variables and its interactions [1].

Ibuprofen, pseudoephedrine and chlorpheniramine are the drug substances have an effect as antihistaminic, nasal decongestant and antiinflammatory, respectively. The combination of these drugs, is effective in cold, sinus and flu symptoms and used for upper respiratory infections. Nipagen (methylparaben) is widely used as

Yildiz Technical University, Department of Chemistry, 34210 Davutpasa, İstanbul, Turkey

B. Sener (ed.), *Innovations in Chemical Biology*, doi: 10.1007/978-1-4020-6955-0

an antimicrobial preservative in pharmaceutical formulations. Numerous methods have been proposed for the determination of these drugs in various dosage forms containing different combinations, but there was no report about the analysis of this quaternary combination [2–4].

The aim of this work, to develop a RP-HPLC method for the determination of four components given above in a new syrup preparation by optimizing the experimental conditions using two level fractional factorial design.

Experimental

Chemicals and Solutions

Pharmaceutical grade ibuprofen, pseudoephedrine HCl, chlorpheniramine maleate, nipagen and syrup preparation were kindly supplied by Berko İlaç Sanayi A.Ş, İstanbul. 0.03 M H_3PO_4 and KH_2PO_4 solutions were prepared with analytical grade chemicals and milliQ water. HPLC grade acetonitrile was used.

Standard drug stock solutions (5,000 ppm for ibuprofen and 1,000 ppm for other drugs) were prepared in water-acetonitrile (50:50).

Standard Preparation

Appropriate amount of stock solutions were mixed and diluted with water-acetonitrile (50:50) to obtain the final concentration of 1,000, 150, 10 and 50 ppm for ibuprofen, pseudoephedrine HCl, chlorpheniramine maleate and nipagen.

Sample Preparation

0.5 mL of the syrup was transferred into a 10 mL volumetric flask and diluted to its volume with water-acetonitrile (50:50). Ten microliters of this solutions was injected for HPLC.

Apparatus

HPLC system consisting of a model LC-20 AT pump unit SPD-20A uv-vis detector, 7,725 20 µL sample injection, a computer and a 10 µm alphabond C_{18} (300 x 3.9 mm) RP column was used. Elution was obtained by using the following gradient steps of acetonitrile and 0.03 M pH 3 phosphate buffer. Acetonitrile:Buffer (15:85)

for 5.5 min (45:55) for 5.5–12 min and (60:40) for 12–17 min. The flow rate was 1.5 mL min $^{-1}$. UV detector was used at 220 nm.

Results and Discussion

Factorial Design

Ph, flow rate and solvent ratios for three steps of gradient profile were chosen as factors for the optimization. Two level fractional factorial 2^{5-1} design for 16 runs was carried out in order to determine the effect of factors and their interactions on the results. Low and high levels of each factor which is given in Table 30.1 were chosen according to the data from previous experiments. The fractional factorial design was evaluated using as response the analytical signal "resolution". The defining relation for this design is I = ABCDE and resolution is V. Table 30.2 shows the experimental design matrix and analytical signal. Table 30.3 shows the effect estimates and model regression coefficients for 15 main and interaction effects. Normal probability plot of effects is shown in Fig. 30.1. From normal probability plot and Table 30.3, the order of significant of factors was found to be A (–635.28), C (–158.62), D (–120.55) and B (83.25) and the factor E (–17.69) is not significant.

Correlation between the observed experimental and the predicted resolutions by using the regression coefficients given in Table 30.3 was shown in Fig. 30.2 and demonstrated that the model obtained is well fitted. The determination coefficient was found as $R^2 = 0.9997$

Analysis of the Syrup

Various reversed phase HPLC systems were studied for the separation of ibuprofen, pseudoephedrine HCl, chlorpheniramine maleate and nipagen at various flow rates under both isocratic and gradient conditions. The best separation was accomplished using three steps gradient elution with acetonitrile/pH = 3 phosphate buffer. Figures 30.3 and 30.4 show the scheme of the gradient profile and the obtained chromatogram

Table 30.1 The levels of the factors in the design

	Factor				
Level	A	B (mL min^{-1})	C (%)	D (%)	E (%)
–	3	1.2	85	55	40
+	4	1.5	90	60	45

A: pH, B: flow rate, C, D, and E: buffer composition of first, second and third step of gradient profile

Table 30.2 2^{5-1} fractional factorial design for factors

Run no	A	B	C	D	E	$R^{1,2}$	$R^{2,3}$	$R^{3,4}$	$R^{4,5}$	$R^{5,6}$	R*
1	–	–	–	–	+	6.63	1.88	8.14	2.21	8.44	1,887.50
2	+	–	–	–	–	5.08	0.63	6.94	0.99	5.75	126.74
3	–	+	–	–	–	4.20	1.18	13.30	2.23	9.15	1,340.95
4	+	+	–	–	+	3.61	1.19	12.48	1.10	6.94	372.82
5	–	–	+	–	–	6.67	1.72	4.86	2.18	7.53	915.25
6	+	–	+	–	+	5.82	1.43	3.53	1.08	6.27	198.62
7	–	+	+	–	+	6.07	1.16	4.76	1.73	7.54	438.68
8	+	+	+	–	–	6.09	1.34	4.69	0.86	6.23	206.45
9	–	–	–	+	–	3.25	1.08	9.67	2.24	6.48	495.25
10	+	–	–	+	+	3.75	1.25	9.97	1.12	6.28	328.56
11	–	+	–	+	+	3.57	1.06	11.99	2.05	7.90	731.67
12	+	+	–	+	–	2.99	1.06	13.81	1.08	7.52	356.18
13	–	–	+	+	+	5.67	1.26	3.74	2.12	7.26	410.77
14	+	–	+	+	–	5.49	1.66	6.60	1.00	515	308.90
15	–	+	+	+	–	6.38	1.61	6.90	2.21	8.44	1,325.87
16	+	+	+	+	+	5.70	1.59	9.24	1.03	6.60	565.42

$R^{n,n+1}$, the resolution between the two near peaks, such as $R^{1,2}$, $R^{2,3}$, $R^{3,4}$, $R^{4,5}$ and $R^{5,6}$ in which resolution between maleic acid: pseudoephedrine hydrochloride, pseudoephedrine hydrochloride: aroma, aroma: nipagen, nipagen: chlorpheniramine and chlorpheniramine: ibuprofen respectively. $R^* = (R^{1,2})(R^{2,3})(R^{3,4})(R^{4,5})(R^{5,6})$

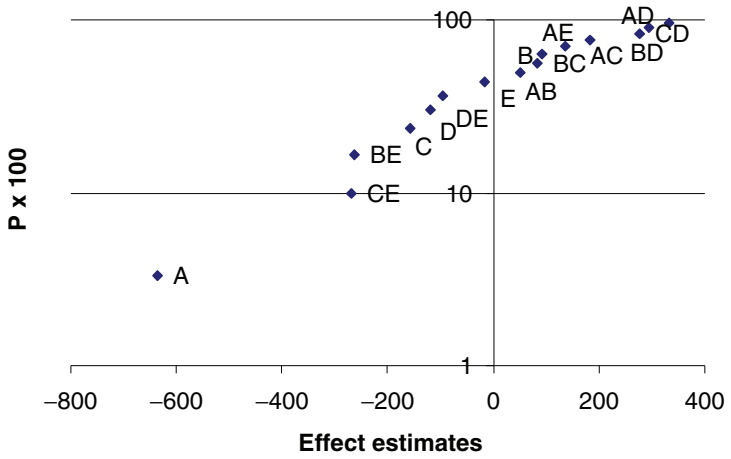

Fig. 30.1 Normal probability plot of effect estimates

under these conditions at 220 nm. The retention times of pseudoephedrine HCl, nipagen, chlorpheniramine and ibuprofen are 4.80, 8.70, 10.21 and 14.38 min, respectively. The limits of quantitations (10σ/s) determined as 0.09, 0.01, 0.04 and 0.01 ppm for ibuprofen, pseudoephedrine HCl, chlorpheniramine maleate and nipagen, respectively. In Table 30.4 the results of the analysis of the syrup are shown.

Table 30.3 Main and interaction effect estimates and regression coefficients for design

Variable	Regression coefficients	Estimated effects
Overall average	625.60	
A	–317.64	–635.28
B	41.62	83.25
C	–79.31	–158.62
D	–60.27	–120.55
E	–8.84	–17.69
AB	25.60	51.21
AC	91.25	182.49
AD	147.07	294.15
AE	67.24	134.48
BC	46.20	92.41
BD	137.80	275.61
BE	–131.25	–262.50
CD	166.76	333.52
CE	–134.02	–268.05
DE	–47.37	–94.75

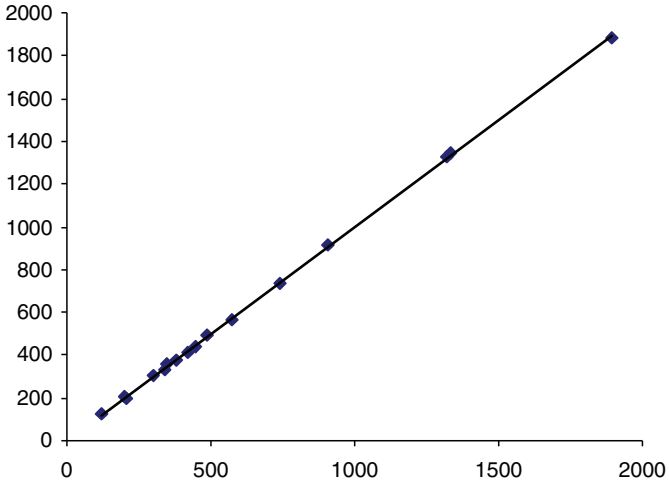

Fig. 30.2 Plot of predicted (R^*) versus experimental resolutions (*R**)

Conclusions

Application of 2^{5-1} fractional factorial design allowed the optimization of the gradient HPLC procedure for the determination of ibuprofen, pseudoephedrine HCl, chlorpheniramine maleate and nipagen in syrup preparation. The optimum conditions for this determination were found to be 3 of pH, 1.5 mL/min of flow rate, 85%, 55% and 40% of buffer compositions of steps of gradient profile.

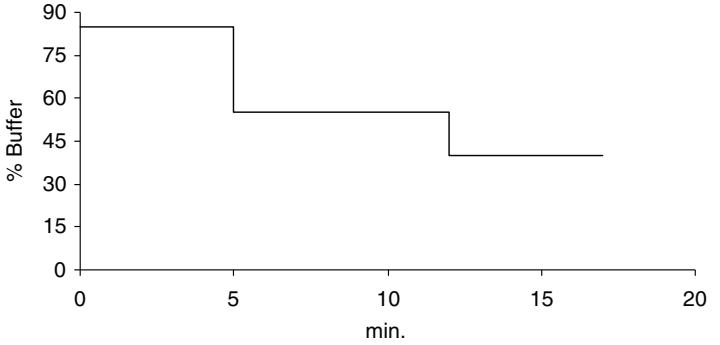

Fig. 30.3 The scheme of step gradient profile

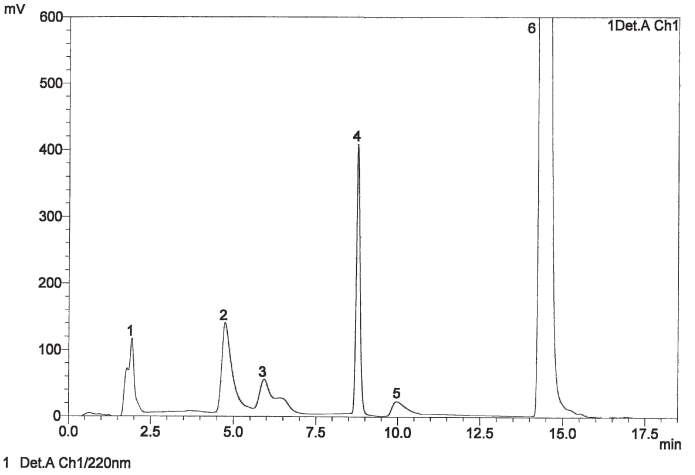

Fig. 30.4 UV-detected chromatogram of the syrup1: maleic acid, 2: pseudoephedrine hydrochloride, 3: aroma, 4: nipagen, 5: chlorpheniramine, and 6: ibuprofen under optimal conditions described in the text

Table 30.4 Results obtained in the HPLC analysis of the syrup samples (n = 5)

	Label (mg/mL)	Found (mg/mL)	Recovery (%)
Ibuprofen	20.0	20.47 ± 0.180	102.3
Pseudoephedrine HCI	3.0	2.99 ± 0.030	99.6
Chlorpheniramine maleate	0.2	0.20 ± 0.001	100.0
Nipagen	1.0	1.01 ± 0.006	101.0

References

1. Montgomery, D.C., 1997, Design and Analysis of Experiments, 4th ed., Wiley, New York.
2. Supelco, Chromatograpy, Products for Analysis and Purification, 2003–2004.
3. Dong, Y.M., Chen, X.F. and Chen, Y.L., 2005, *J. Pharm. Biomed. Anal.,* **39,** 285–289.
4. Palabıyık, I.M., Dinç, E. and Onur, F., 2004, *J. Pharm. Biomed. Anal.,* **34,** 473–483.

Chapter 31
Comparison of Derivative Spectrophotometry and Partial Least Square (PLS-1) Calibration for the Determination of Caffeine in Energy Drinks

Özlem Aksu Dönmez, Mahmure Üstün Özgür, and Abdürrezzak Bozdoğan

Abstract Caffeine, a xanthine alkaloid, occurs in teaplants, coffee, mate leaves and cola nuts. It is also commonly found beverages, such as cola drinks, tea and energy drinks.

In this work, two methods for the determination of caffeine in energy drinks by derivative spectrophotometry and by partial least–squares multivariate spectrophotometric calibration (PLS-1) are described. Proposed methods involve background correction methods that interferences from vitamins, taurin and food colours were minimized by treating the sample with basic lead acetate and $NaHCO_3$ for the analysis of caffeine in energy drinks.

In the first method, derivative spectrophotometry, the amplitudes in the first derivative spectra at 287 and 260 nm were selected to determine caffeine. The concentration range of application is 3–15 μg mL^{-1} for caffeine.

In the other method, PLS-1, the absorption spectra of caffeine solutions were recorded between 240–320 nm and the absorbance values recorded every 5 nm.

The methods were applied to determine caffeine in commercial energy drinks and the results obtained are compared. It was found that these methods don't require expensive solvents and can confidently be used for rapid, precise and sensitive quantitation of caffeine in energy drinks, especially for routine quality control analyses.

Keywords Alkaloid, caffeine, energy drinks, spectrophotometry,

Introduction

Caffeine, 1,3,7-trimethylxanthine, is the major alkaloid, occurs in teaplants, coffee, guarana, cola nuts, cocoa beans, mate and other plants. It is a powerful stimulant of the central nervous system and also stimulates the cardiac muscle. However, high

Yildiz Technical University, Department of Chemistry, 34210 Davutpasa, İstanbul Turkey

B. Sener (ed.), *Innovations in Chemical Biology*, doi: 10.1007/978-1-4020-6955-0

amounts of this alkaloid have noticeable irritation of gastrointestinal tract as well causes many unwanted effects [1].

Caffeine containing beverages, known as power or energy drinks, are popular in part due to effects of decreasing fatigue, increasing mental activity and improving cognitive functioning following the intake of moderate doses [2]. The levels of caffeine in drinks has been determined by different analytical techniques, such as UV-Vis spectrophotometry [3, 4], potentiometry [5], chromatography [6, 7], capillary electrophoresis [8], solid-phase FT-Raman spectrophotometry [9] and continuous flow system [10].

The application of derivative techniques to spectroscopy is very useful when signal overlap or interference exits and it offers a powerful tool for both qualitative and quantitative analysis of components in pharmaceutical [11, 12], biomedical [13, 14] and food analysis [15, 16].

Partial least-squares (PLS) is the most widely used chemometric technique employed to solve data-analysis problems [17–19]. This method has the advantage of using full spectral information, and allow for a rapid determination of mixture components, often with no need or prior separation or sample pre-treatment [20–22].

The popularity of energy drinks has risen considerably over the past few years, especially for younger adults, and thus there is interest in monitoring levels in beverages and in ensuring intakes do not exceed recommended levels. The aim of this paper was to investigate the possibility of using derivative spectrophotometry and PLS-1 procedure for the simple, fast and cheap caffeine determination in energy drinks.

Experimental

Apparatus

The absorbance measurements were performed with an Agilent 8453 UV-Vis Spectrophotometer, using 1.00 cm quartz cells. PLS-1 was applied with an in-house program written according to the algorithm given by Martens and Naes [23].

Reagents and Samples

All chemicals and solvents used were of analytical and spectroscopic grades. Caffeine was obtained from Bilim Pharm. Ind., Turkey. Stock solutions of 100 μg mL^{-1} of caffeine was prepared in distilled water.

Solution of basic lead acetate: An amount of 23 g of neutral lead acetate, Pb $(CH_3COO)_2.3H_2O$, was mixed with 70 mL of water and then boiled. Twelve grams of lead oxide, PbO, was added to this solution. The precipitate was filtered off

and the solution was then transferred to a 100 mL volumetric flask and diluted to the volume with distilled water (1.25 mg/mL).

Energy drinks, Red Devil and Tiger Shot, containing 150 mg/L caffeine were acquired from Turkey supermarkets.

Calibration for the Derivative Spectrophotometric Method

The calibration samples were prepared in 10 mL calibrated flasks containing 3–15 μg mL^{-1} of caffeine and were diluted with distilled water. The peak amplitudes of the first-derivative spectra was measured at 287 and 260 nm.

Calibration Set for the PLS-1 Method

The same calibration samples were used for PLS-1 calibration. The absorbances were recorded in 1.00 cm cuvettes between 240–320 nm every 5 nm.

Application of the Proposed Procedures for the Determination of Caffeine in Energy Drinks

In analysing the caffeine of energy drinks, an accurately weighed amount of 15 mL of sample to 50 mL volumetric flask containing 25 mL water. Two milliliters of basic lead acetate solution was added to this solution and diluted the mark with distilled water. After filtering, 25 mL of filtrate was taken and 0.25 g of $NaHCO_3$ was added to this solution. Then, the solution was filtered. Five milliliters of filtrate was transferred to a 25 mL volumetric flask and adjusted to volume with distilled water. The peak amplitudes of the first-derivative spectra was measured at 287 and 260 nm. The sample preparation procedure was also used for PLS-1 method and the absorbances of this solution were recorded between 240–320 nm.

Results and Discussion

Many food additives and naturally occurring admixed ingredients interfere with the direct UV determination of caffeine in coffee, tea and beverages. Energy drinks also include some ingredients that have adverse effects on spectrophotometric measurement of caffeine (Table 31.1). In this study, basic lead acetate was used as a clarifying agent for removing interfering substances and $NaHCO_3$ was used to remove unreacted lead ions [24].

Table 31.1 Some ingredients in energy drinks

Red Devil	Tiger Shot
Vitamin C	Colorant Red
Vitamin B_2	Ponceu E 124
Niacin	Niacin
Vitamin B_5	Taurine
Vitamin B_6	Vitamin B_6
E 163	Vitamin B_2
E 104	E 330
E 150	Calcium pantothenate
Taurine	

The absorption spectra and first derivative spectra of 9 μg mL^{-1} solution of caffeine and energy drinks samples are given in Figs. 31.1 and 31.2. Upon examining the first spectra of two samples, it can be noticed that caffeine can be determined 287 and 260 nm.

The calibration curves was constructed by plotting $d_A/d\lambda$ values at selected wavelength against corresponding caffeine concentrations. The regression equation of the calibration graphs were calculated as follows:

$$^1D_{287} = 3.13 \times 10^{-3}C + 836 \times 10^{-4} \text{ (r = 0.9990) and}$$
$$^1D_{260} = 2.01 \times 10^{-3}C - 6.8 \times 10^{-4} \text{ (r = 0.9996) respectively.}$$

Although good linearity was observed at 260 nm, the obtained recoveries were too high (150–175%) for reasonable analysis. So, this method was more suitable at 287 nm.

With the aim of improving the analysis of caffeine in energy drinks, the multivariate calibration method PLS-1 was tested. The method was evaluated by using the absorption spectra for the analysis. The absorption spectra of caffeine standards and samples were recorded in the 240–320 nm range, digitized every 5 nm.

The suggested derivative spectrophotometric method and PLS-1 were applied to determination of caffeine in energy drinks (Table 31.2). The assay results obtained by both methods were statistically compared at the 5% level. As shown in Table 31.2 there was no significant differences between the mean values and precisions of two methods.

Conclusions

The determination of caffeine has always been problematic with specific methods or modifications being required for specific foodstuffs. The proposed derivative spectrophotometry and PLS-1 involve sample pretreatment with basic lead acetate.

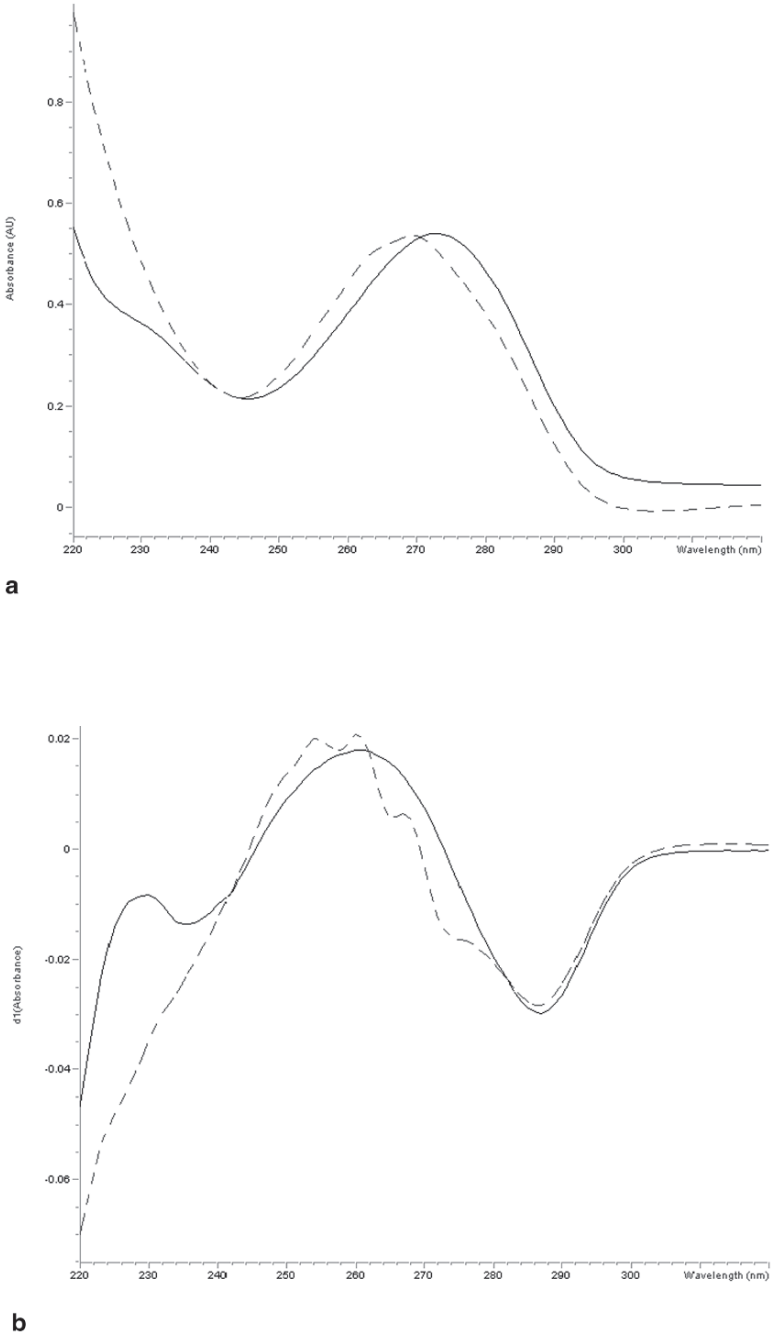

Fig. 31.1 (a) Absorption and (b) first derivative spectra of caffeine (———) (9 μg mL^{-1}) and Tiger Shot sample solution (--------) (prepared as under experimental) in distilled water

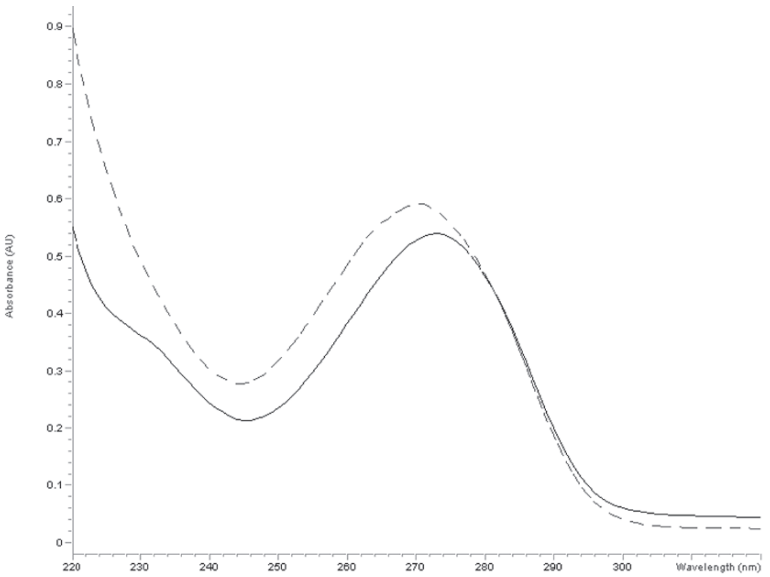

a

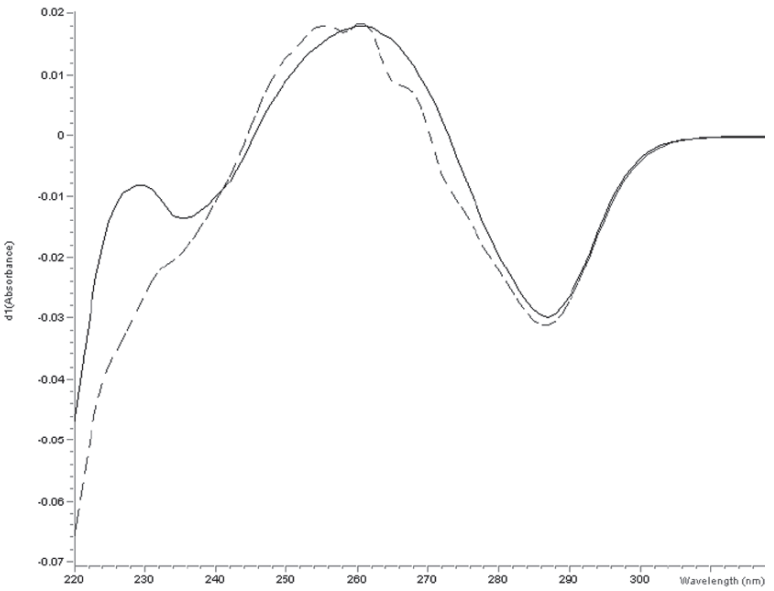

b

Fig. 31.2 (a) Absorption and (b) first derivative spectra of caffeine (———) (9 μg mL^{-1}) and Red Devil sample solution (--------) (prepared as under experimental) in distilled water

Table 31.2 Results obtained in the analysis of commercial samples of energy drinks

Sample	Caffeine (mg L^{-1})		$t_4^{0.05} = 2.77$	$F_{2,2}^{0.05} = 19$
Red Devil	Derivative spectrophotometry	PLS-1	t_{exp}	F_{exp}
1	160.96	156.5		
2	159.89	161.66		
3	160.96	158.00		
Mean ± SD	160.60 ± 0.62	158.71 ± 2.65	1.2	18.26
Recovery (%)	107	105.8		
Tiger Shot				
1	144.83	145.33		
2	144.83	143.5		
3	143.76	140.66		
Mean ± SD	144.47 ± 0.62	143.16 ± 2.35	1.72	14.36
Recovery (%)	96.31	95.44		

However, only common and inexpensive reagents are used. They are rapid and do not require any expensive or sophisticated apparatus, in contrast with chromatographic methods. So, the proposed methods can be used for the routine analysis of caffeine in energy drinks.

References

1. Ashihara, H. and Crozier, A., 2001, *Trends Plant Sci.,* **6,** 407–413.
2. Tanda, G. and Goldberg, S., 2000, *Pharmacol. Biochem. Behav.,* **66,** 47–64.
3. Lau, O., Luk, S., Cheng, and O. Chiu, T., 1992, *Analyst,* **117,** 777–783.
4. Lima, J.L.F.C., Delerue-Matos, C., Nows, H.P.A. and Vaz, M.C.V.F., 1998, *Food Addit. Comtam.,* **15,** 265–269.
5. Abdennabi, A.M.S. and Sultan, S.M., 1993, *Electroanalysis,* **5,** 709–712.
6. Chen, O.C., Mou, S.F., Hou, X.P. and Ni, Z.M., 1998, *Anal. Chim. Acta,* **371,** 287–296.
7. Abourashed, E.A. and Mossa, J.S., 2004, *J. Pharm. Biomed. Anal.,* **36,** 617–620.
8. Okamoto, H., Nakajima, T. and Ho, Y., 2002, *J. Pharm. Biomed. Anal.,* **30,** 815–822.
9. Armenta, S., Garrigues, S. and Guardia, M., 2005, *Anal. Chim. Acta,* **547,** 197–203.
10. Lucena, R., Cardenas, S., Gallego, M. and Valcarcel, M., 2005, *Anal. Chim. Acta,* **530,** 283–289.
11. Ivanoviç, D., Medenica, M., Kojic-Marinkoviç, S. and Raduloviç, D., 2000, *J. Pharm. Biomed. Anal.,* **23,** 965–971.
12. Özgür, M.Ü., Alpdogan, G. and Asci, B., 2002, *Monatshefte für Chemie,* **133,** 219–223.
13. Boutolleau, D., Lefrune, G. and Etienne, J., 1997, *Ann. Biol. Clin.,* **55,** 592–596.
14. Grau, A., Guardida, F., Boatella, J., Baucalls, M.D. and Codony, R., 2000, *J. Agric. Food. Chem.,* **48,** 4128–4135.
15. Özgür, M.Ü., Alpdogan, G. and Koyuncu, I., 2002, *Anal. Lett.,* **35,** 721–732.
16. Bosch Ojeda, C. and Sannchez Rojas, F., 2004, *Anal. Chim. Acta,* **518,** 1–24.
17. Geladi, P. and Kowalski, B., 1986, *Anal. Chim. Acta,* **185,** 19–32.
18. Otto, M. and Wegscheider, W., 1985, *Anal. Chem.,* **57,** 63–69.
19. Haaland, D. and Thomas, E., 1998, *Anal. Chem.,* **60,** 1193–1202.

20. Aksu, Ö., Bozdogan, A. and Kunt, G., 1998, *Anal. Lett.,* **31** (5), 859–866.
21. Lopez-Martinez, L., Lopez-de-Alba, P.L., Garcia-Campos, R. and Leoan- Rodriguez, L.M., 2003, *Anal. Chim. Acta,* **493,** 83–94.
22. Aksu, Ö., Bozdogan, A. and Kunt, G., 2006, *Anal. Lett.,* **39** (4), 751–761.
23. Martens, H. and Naes, T., 1989, Multivariate Calibration, Wiley, New York.
24. Li, S., Berger, J. and Hartland, S., 1990, *Anal. Chim. Acta,* **232,** 409–412.

Chapter 32
Simultaneous Spectrophotometric Determination of Food Additives (Benzoic Acid, Caffeine, Aspartame and Acesulfame-K) in Cola Drinks by PLS Multivariate Calibration Method

Fatma Turak, Mahmure Üstün Özgür, and Abdürrezzak Bozdoğan

Abstract Aspartame (Apt), Acesulfame-K (Ace-K) low-calorie, high-potency artificial sweeteners are currently used in beverages and dietary food and drinks. Their increased application in food and drink products has given a new impetus to develop fast and accurate methods for their determination. Absorption spectra of Asp, Caf, Ace-K and BA strongly overlap. Therefore a direct determination of these analytes in quaternary mixture is impossible without a separation step. In order to overcome this difficulty partial least squares (PLS) method has been proposed.

A spectrophotometric method for the routine, rapid end simultaneous determination of Ace-K, Caf, Aspt and BA in cola drinks was investigated. A calibration set containing between 3–5 μg mL^{-1} of Ace-K, Caf, and BA, 5–7 μg mL^{-1} of Aspt was used.

The method involves the use of 27 standard mixtures of the four compounds assayed, considered at three concentration levels and measured of samples in a 0.1 N H_3PO_4. The designed and optimized training set of calibration was applied to the determination of four food additives in several synthetic mixtures. Three commercial cola drinks (coca-cola, pepsi-cola, cola-turka) that contained the four additives were also satisfactorily analyzed without separation step.

Keywords Cola drinks, food additives, spectrophotometry, sweeteners

Introduction

Sweeteners have a great impact on the acceptance of beverages, affecting not only the taste but also their texture. Beverage blends instead of single sweeteners in reduced-calorie beverages for some time now, with many successful products well established in the market place Aspartame (Aspt) and Acesulfame-K (Ace-K) low-calorie high potency artificial sweeteners are currently used in beverages, and dietary food and drinks. Structures and names of sweeteners (Aspt, Ace-K), preservative (Na-Benz) and caffeine (Caf) used are shown in Fig. 32.1.

Yıldız Technical University, Department of Chemistry, Davutpasa Campus, 34220, Esenler, İstanbul,Turkey

B. Sener (ed.), *Innovations in Chemical Biology*, doi: 10.1007/978-1-4020-6955-0

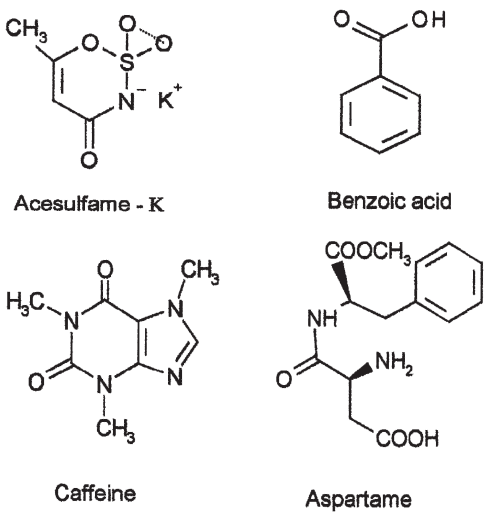

Fig. 32.1 Structural formulas of studied food additives

In 1977, The Food and Drug Administration initiated a warning label policy in light of inconclusive evidence that the sweetener might cause cancer in high doses. Their increased application in food and drink products has given a new impetus to develop fast and accurate methods for their determination.

Caffeine is a powerful stimulant of central nervous system and also stimulates the cardiac muscle. However, high amounts of the alkaloid have noticeable irritation of gastrointestinal tract as well causes many unwanted effects [1].

Fort he determination of preservatives and sweeteners in soft drinks or fruit juices LC analysis with UV detection is widely used. The sample pretreatment, prior to LC analysis, often consists only of degassing, filtration and dilution of the liquid [2]. Sometimes a liquid-liquid extraction, suitable not only for soft drinks but also for more complex matrices, is applied [3]. Chemometric methods applied to overlapped spectra offer the advantage of minimizing or eliminating sample preparation by allowing to simultaneously determining one or more analytes in relatively complex matrices.

In this present work, an alternative PLS-2 method was investigated and applied to the determination of sodium benzoate (used for preservatives) artificial sweeteners Aspartame, Acesulfame-K and caffeine in diet cola drinks.

Experimental

Apparatus

The absorbance measurements were performed with an Agillant 8453 UV-Vis Spectrophotometer using 1.00 quartz cells. Computations were run on Pentium-100 computer. A computer program for PLS-2 was written according to the algorithm

given by Maren and Naes [4]. Bandelin Storex ultrasonic water bath was employed to degassing the samples previously to their analyses.

Reagents and Samples

All chemicals and solvents used were analytical and spectroscopic grade. The sweeteners (aspartme, acesulfame-K), caffeine and sodium benzoate were obtained from Ülker Food Company, Turkey. Cola drinks were purchased from local markets. Stock solutions of 100 mL^{-1} of Aspt, Ace-K, Caf and Na-Benz were prepared in 0.1 N H_3PO_4. 0.1 N H_3PO_4 solution was prepared by diluting 9.09 mL orthophosphoric acid (85%) to 1,000 mL.

Some cola drinks containing Aspt, Ace-K, Caf and Na-Benz were analyzed: Coco-Cola (light) Pepsi (light) and Cola-Turka (light).The amount of Aspt in these samples ranged between 0.2 g/L and 0.35 g/kg, Ace-K 0.2 g/L and 0.09 g/kg and Caf 0.15–0.1 g/L and 0.12 g/kg Sodium benzoate, orthophosphoric acid, and citric acid were also present in the samples.

Method

Sample Pretreatment

The diet cola drinks were degassed 10 min in an ultrasonic bath and diluted 60-fold in 0.1 N H_3PO_4. In 10 mL volumetric flasks, an aliquot (0.35–0.4 mL) of the pre-treated sample of cola drink was introduced, and then diluted to the mark with 0.1 N H_3PO_4. The electronic absorption spectrum was recorded from 190–300 nm against a blank of 0.1 N H_3PO_4.

Procedure for Analyzing Cola-Drinks

The Aspt, Ace-K, Caf and Na-Benz contents were determined by using spectra fort he mixtures studied above were registered in the spectral range 190–300 nm using 0.1 N H_3PO_4 solution as a reference and the absorbance values were recorded every 5 nm from these spectra. By application of the PLS-2 algorithm a model was optimized using three factors for Aspt, Ace-K, Caf and Na-Benz calculated by analysis of the optimized PLS-2 model.

Procedure for Calibration Set

The PLS method requires a carefully experimental design the standard composition of the calibration set in order to provide good predictions. In this study a calibration

set was prepared of the quaternary standard mixtures summarized in Table 32.1. The method involves the use of 27 standard mixture of four compounds assayed, considered at three concentration levels and the measurement of the absorbance values every 5 nm of samples in 0.1 N H_3PO_4.

The absorption spectra of Aspt, Ace-K, Caf and Na-Benz were recorded from 190 to 300 nm. The calibration set was generated by a three-level full factorial design (4).The absorbance values were recorded every 5 nm. The calibration samples were measured in random order, so that experimental errors due to drift were not introduced.

Results and Discussion

The absorption spectra of Aspt, Ace-K, Caf and Na-Benz solutions were recorded between 190 and 300 nm in Fig. 32.2. The absorption spectra for the four component are shown.

Table 32.1 Composition of the calibration training set

Analyte solutions	Ace[a]	Apt[a]	Caf[a]	BA[a]
1	4	6	3	3
2	5	7	4	2
3	4	5	4	3
4	4	6	3	1
5	3	7	4	2
6	4	5	4	1
7	5	6	5	2
8	3	5	4	2
9	5	6	4	3
10	4	5	5	2
11	4	7	3	2
12	4	6	5	1
13	5	6	3	2
14	5	6	4	1
15	5	5	4	2
16	4	6	5	3
17	3	6	4	3
18	4	6	4	2
19	4	7	5	2
20	4	7	4	1
21	3	6	3	2
22	4	7	4	3
23	3	6	4	1
24	4	6	4	2
25	4	6	4	2
26	4	5	3	2
27	3	6	5	2

[a]Concentration in microgram per milliliter

For wavelengths shorter than 250 nm, a very high overlapping is observed between Aspt, Ace-K and Na-Benz. As can be observed absorption spectra resolution of ternary mixtures using conventional methods is impossible. Caf can be determined. In order to resolve this quaternary mixture we applied partial least square method (PLS-2). The PLS-2 technique is a typical full spectrum method where the data are fitted to many data points, thereby improving the precision and requires a carefully experimental design of the Standard composition of the calibration set in order to provide good predictions. In this study a training set of 27 representative quaternary mixtures was constructed and the absorption spectra were recorded. In Table 32.1 the compositions of the quaternary mixtures employed are summarized. PLS calibrations were performed on 27 calibration spectra and, with the use of the calibration, the concentration of the samples left out during calibration was predicted.

The absorption spectra of solutions Coco-Cola(light), Pepsi(light), Cola-Turka (light) in 0.1 N H_3PO_4 were recorded between 190 and 300 nm. Figure 32.3 the absorption spectra for the three components are shown.

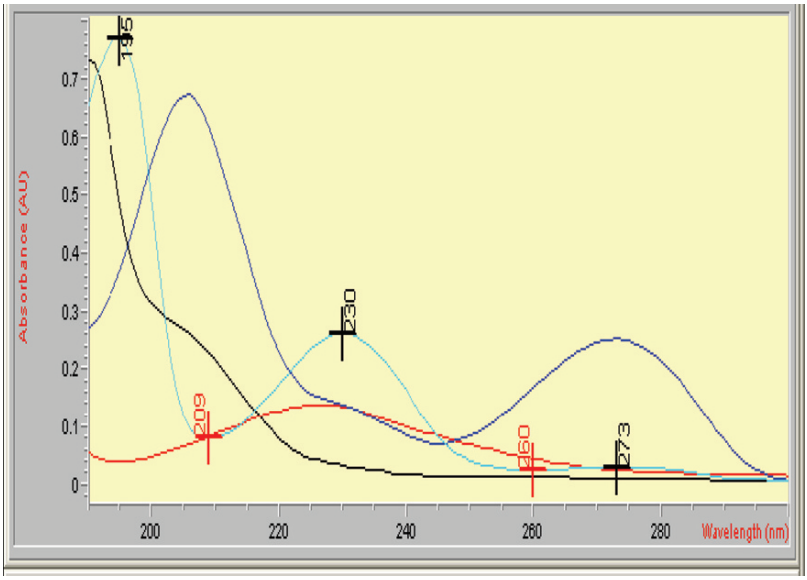

Fig. 32.2 Absorption spectra of (a) Aspt (b) Ace-K (c) Caf and (d) Na-Benz in 0.1 N H_3PO_4

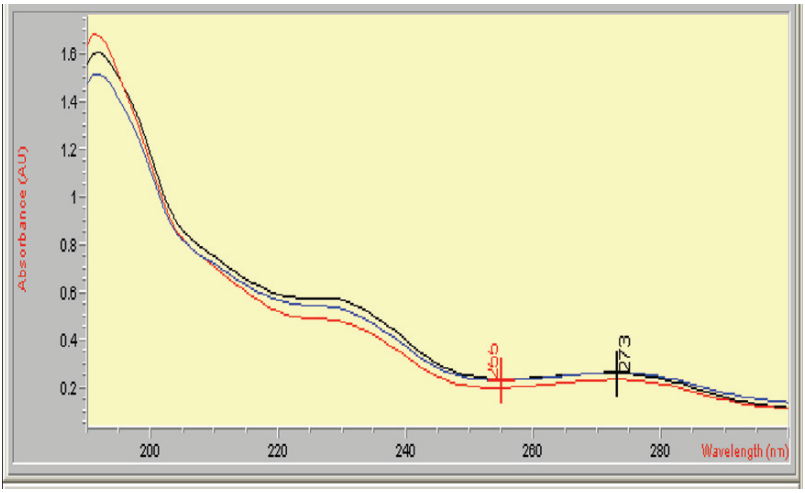

Fig. 32.3 Absorption spectra of sample solutions (a) Coco-cola (light) (b) Pepsi (light) (c) Cola-Turka (light) in 0.1 N H_3PO_4

References

1. Ashihard, H. and Crozier, A., 2001, *Trends Plant Sci.,* **6,** 407.
2. Mors, M. and Massart, D.L., 1990, *Trends Anal. Chem.,* **9,** 164.
3. Sher Ali, M., 1985, *J. Assoc. Anal. Chem.,* **68,** 488.
4. Martens, H. and Naes, T., 1993, *Multivariate Calibration,* Willey, New York, pp 77–354.

Chapter 33
PLS-UV Spectrophotometric Method for the Simultaneous Determination of Ternary Mixture of Sweeteners (Aspartame, Acesulfame-K and Saccharin) in Commercial Products

Fatma Turak, Mahmure Üstün Özgür, and Abdürrezzak Bozdoğan

Abstract Aspartame (Apt), Acesulfame-K (Ace-K) and Saccharin (Sac), low-calorie, high-potency artificial sweeteners are currently used in carbonated beverages, dietary food and drinks. Their increased application in food and drink products has given a new impetus to develop fast and accurate methods for their determination. Absorption spectra of Apt, Ace-K and Sac strongly overlap. Therefore a direct determination of these analytes in ternary mixture is impossible without a separation step. In order to overcome this difficulty partial least squares (PLS) method has been proposed.

In this work, a simple and fast analytical procedure is proposed for the simultaneous determination of Apt, Ace-K and Sac in commercial products (powder drinks and colored beverages). The sweeteners were extracted n-butanol solution and the absorption spectra were recorded between 190–300 nm against blanc solution and the absorbance values were taken 5 nm interval. The method involves the use of 27 standard mixtures of the three compounds assayed, considered at three concentration levels and measured of samples in 0.1 N H_3PO_4 solution.

A calibration set containing between 7–9 μg mL^{-1} of Apt, 1–3 μg mL^{-1} of Ace-K, and 2–4 μg mL^{-1} of Sac was used. The designed and optimized training set of calibration was applied to the determination of three sweeteners of several synthetic mixtures. The method was also applied to commercial drinks and satisfactorily results were obtained. The procedures do not require any separation step for colorless sample (powder drink), but only an extraction step for colored beverages (powder and liquid) was used. The effect of cyclamate (CA) and ascorbic acid (AA) was also investigated.

Keywords Commercial products, spectrophotometry, sweeteners

Yıldız Technical University Department of Chemistry, Davutpasa Campus, 34220 Esenler, İstanbul, Turkey

B. Sener (ed.), *Innovations in Chemical Biology*, doi: 10.1007/978-1-4020-6955-0

Introduction

Aspartame (Apt), Acesulfame-K (Ace-K) and Saccharin (Sac) are low-calorie, high potency artificial sweeteners. They are currently used in carbonated beverages, dietary food and drinks. The oldest artificial sweeter is saccharin, 300–500 times sweeter than sugar. Because it is relatively stable at high temperature, and inexpensive to manufacture, saccharin has been widely used as a sugar substitute since in the 1950s. In1977, the Food and Drug Administration initiated a warning label policy in light of inconclusive evidence that the sweetener might cause cancer in high doses. The labeling requirement was rescinded in 2000 when the U.S. Department of Health and Human Services released its National Toxicology Report on Carcinogens, which removed saccharin from its list of cancer-causing substances.

The only knock against saccharin presently is its bitter metallic aftertaste. This property was the reason for aspartme's quick ascendancy as the number-one-selling low-calorie sweetener soon after its approval in 1981. It is 180 times sweeter than sugar, but breaks down under high temperatures. For that reason, aspartame is most widely used in beverages and tabletop packets. The market again expanded in 1988 with the approval of Nutrinova, Inc.'s Acesulfame-K which is 200 times sweeter than sugar. It is holds up to heat, but has some bitterness. It is used in foods such as gum, powdered drink mixes, table top packets, pudding and bake mixes, and yogurt [1].

Their increased application in light food and drink products has given a new impetus to develop fast and accurate method for their determination. Among computer-controlled instruments multivariate calibration methods and derivative techniques are playing very important role in the multicomponent analysis of mixtures by UV-VIS molecular absorption spectrophotometry [2]. Both approaches are useful in the resolution of overlapping band in quantitative analysis [3, 4].

In this paper, for the first time a chemometric model based on the application of a partial-least-squares (PLS-2) method is proposed fort he resolution of a complex artificial sweetener mixture(Ace-K, Sac, Apt) and Vit C have been tested to check to abilities of PLS optimized model. Also the possibility of analyzing powdered drinks (Sahlep and Tang) are shown (Fig. 33.1).

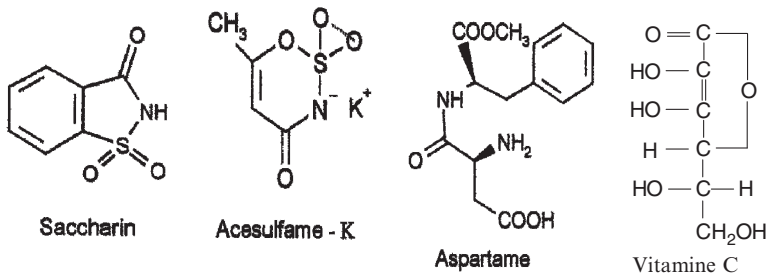

Fig. 33.1 Structures and names of the artificial sweeteners and Vitamin C

Experimental

Reagents and Samples

All reagents were of analytical grade or better. Ace-K, Apt, Sac, Cyclamate-Na (Cyc-Na) and Vit C were kindly supplied from Ülker Gıda Company, Turkey. H_3PO_4 (85%), n-butyl alcohol were supplied from Merck (Darmstadt, Germany).

Stock Standard solutions of the analytes (100 μg L^{-1}) were prepared separately by dissolving appropriate amount of these compounds in 0.1 H_3PO_4.Working solutions were prepared separately by dissolving appropriate amount of these compounds in 0.1 N H_3PO_4. Working solutions were prepared on a daily bases by rigorous dilution of the stocks.

Powdered drinks (Sahlep and Tang) samples were purchased from local markets.

Apparatus

The absorbance measurements were performed with an Agillant 8453 UV-Vis Spectrophotometer using 1.00 quartz cells. Computations were run on Pentium-100 computer. A computer program for PLS-2 was written according to the algorithm given by Maren and Naes [5]. A Bandelin Storex ultrasonic water bath was employed to degassing the samples previously to their analyses.

Sample Preparation

Powdered drink sample (*Sahlep*) It contains three artificial sweeteners: Apt, Ace-K, Sac. An accurately weighted amount of 0.05 g powdered drink (Sahlep) was transferred to 100 mL volumetric flask. The flask was filled up 0.1 N H_3PO_4 and agitated 5 min. The solution was diluted 100 mL with 0.1 N H_3PO_4.

The absorbance values of this solution was recorded between 190 and 300 nm spectral range every 5 nm for PLS analysis of sweeteners (Apt, Ace-K, Sac).

Powdered drink sample (*Tang*): It contains three artificial sweeteners, Apt, Ace-K, Sac, Vit C, and food colors (allura red, titanium dioxide, brilliant blue, tartrazine).

For extraction of synthetic food colors from sample; 0.1 g powdered drink sample was dissolved in 20 mL 0.1 N H_3PO_4 solution.

The color solution was poured into a 100 mL separatory funnel supported on a ring support. Ten milliliters of n-butyl alcohol was added and shaked gently until the color is transferred to the upper layer. The lower layer was drawn off and discarded. The extraction procedure was repeated two times with 5 mL n- butyl

alcohol. Twenty milliliters of colorless solution was transferred into a 50 mL volumetric flask and diluted to volume with 0.1 N H_3PO_4 solutions. From this solution 10 mL was transferred into 25 mL volumetric flask and diluted to volume with 0.1 N H_3PO_4 solutions. The absorbance values of this solution was recorded between 190–300 nm spectral range every 5 nm for PLS analysis of sweeteners (Apt, Ace-K, Sac) and Vit C.

Results and Discussion

The absorption spectra Apt, Ace-K and Sac solutions were recorded between 190 and 300 nm. In Fig. 33.2, the three components are shown. For wavelengths shorter 235 nm, a very high overlapping is observed between Apt, Ace-K, Sac.

The absorption spectra of Apt, Ace-K, Sac and Vit C solutions were also recorded between 190 and 300nm. In Fig. 33.3, the absorption spectra for the four components are shown. For wavelengths shorter 240 nm, a very high overlapping is observed between Apt, Ace-K, Sac and Vit C.

As can be observed absorption spectra resolution of ternary and quaternary mixture, conventional methods is impossible.

PLS is a factor analysis-based method that has recently demonstrated to have a high capacity to resolve complex mixtures of components with similar spectral

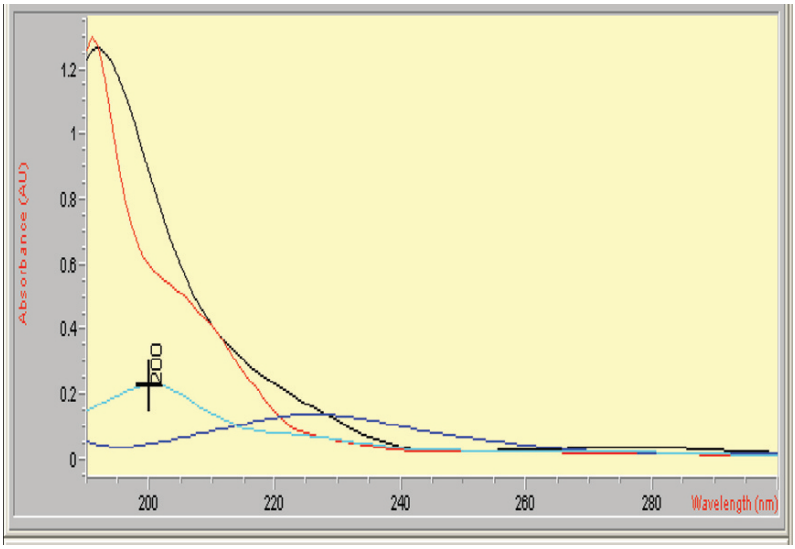

Fig. 33.2 Absorption spectra of (a) Apt, (b) Ace-K, (c) Sac, and (d) Salep sample in 0.1 N H_3PO_4

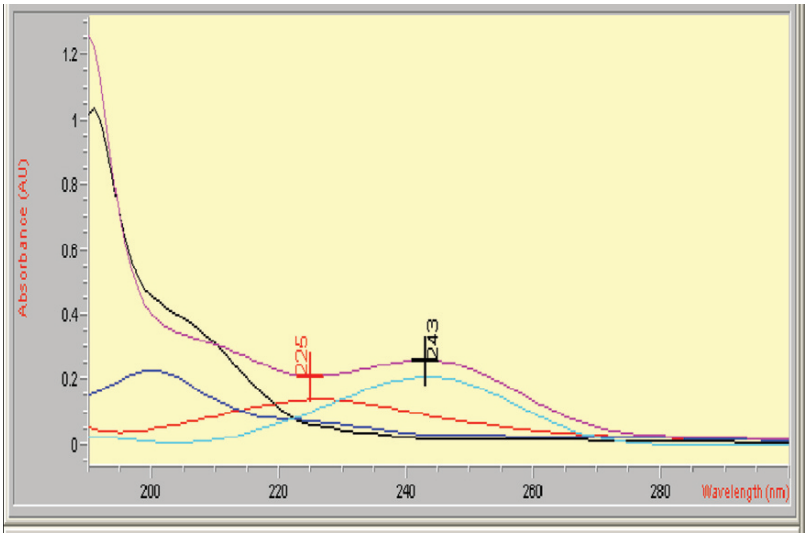

Fig. 33.3 Absorption spectra of (a) Apt, (b) Ace-K, (c) Sac, and (d) Vit C and powder drink (Tang) sample in 0.1 N H_3PO_4

characteristics. PLS performs the spectral factoring by trying to account fort he spectral variation while assuming that the new basis vectors relate to the calibration [6] concentrations.

The PLS-2 technique is a typical full spectrum method where the data are fitted to many data points, thereby improving the precision and requires a carefully experimental design of the Standard composition of the calibration set order the provide good predictions. In this study training set of 27 representative ternary mixtures was constructed and the absorption spectra were recorded. In Table 33.1, the compositions of the ternary mixtures employed are summarized.

These standards (Apt, Ace-K and Sac) were used for analysis Sahlep sample we also constructed another training set of 27 standard samples from different quaternary mixtures (Apt, Ace-K and Sac and Vit C). These standards were used for analysis of colored beverages (powdered and liquid).

The effect of sodium cyclamate (Cyc-Na) was also investigated. It was seen that there is no effect of Cyc-Na for the determination of Apt, Ace-K and Sac and Vit C to 40 ppm concentration level. So 5 ppm Cyc-Na was added to Standard sample solutions. The spectral region between 190 and 300 nm which implies working with 22 experimental points per spectrum was selected for analysis. In Table 33.2 the compositions of the quaternary mixtures employed are summarized. PLS calibrations were performed on 27 calibration spectra and, with the use of the calibration, the concentration of the samples left out during calibration was predicted.

Table 33.1 Composition of the calibration training set

Standard	Ace-K[a]	Sac[a]	Apt[a]
S1	0.5	0.4	5.0
S2	0.5	0.4	9.0
S3	0.5	0.4	13.0
S4	0.5	1.0	5.0
S5	0.5	1.0	9.0
S6	0.5	1.0	13.0
S7	0.5	1.6	5.0
S8	0.5	1.6	9.0
S9	0.5	1.6	13.0
S10	1.5	0.4	5.0
S11	1.5	0.4	9.0
S12	1.5	0.4	13.0
S13	1.5	1.0	5.0
S14	1.5	1.0	9.0
S15	1.5	1.0	13.0
S16	1.5	1.6	5.0
S17	1.5	1.6	9.0
S18	1.5	1.6	13.0
S19	3.0	0.4	5.0
S20	3.0	0.4	9.0
S21	3.0	0.4	13.0
S22	3.0	1.0	5.0
S23	3.0	1.0	9.0
S24	3.0	1.0	13.0
S25	3.0	1.6	5.0
S26	3.0	1.6	9.0
S27	3.0	1.6	13.0

[a]Concentration in microgram per liter

Table 33.2 Composition of the calibration training set

Standard	Ace-K	Sac	Apt	Cvit
S1	2	0.4	10	3
S2	3	0.6	8	4
S3	2	0.6	10	2
S4	2	0.4	5	3
S5	1	0.6	8	4
S6	2	0.6	5	2
S7	3	0.8	8	3
S8	1	0.6	8	2
S9	3	0.6	10	3
S10	2	0.8	8	2
S11	2	0.4	8	4
S12	2	0.8	5	3
S13	3	0.4	8	3

(continued)

Table 33.2 (continued)

Standard	Ace-K	Sac	Apt	Cvit
S14	3	0.6	5	3
S15	3	0.6	8	2
S16	2	0.8	10	3
S17	1	0.6	10	3
S18	2	0.6	8	3
S19	2	0.8	8	4
S20	2	0.6	5	4
S21	1	0.4	8	3
S22	2	0.6	10	4
S23	1	0.6	5	3
S24	1	0.6	8	3
S25	2	0.6	8	3
S26	2	0.4	8	2
S27	2	0.8	8	3

[a] Concentration in microgram per liter

References

1. Lyn O'Brien, N., 2002, *Food Technology,* **56,** (7)28–45.
2. Berzas, J.J., Rodriguez, J. Penalvo, G.C., 1997, *Analytica Chimica Acta,* **340,** 257.
3. Üstün Özgür, M., Alpdoğan, G. Koyuncu, I., 2002, *Analytical Letters,* **35,** (4)721–732.
4. Üstün Özgür, M., Bozdoğan, A., Ercağ, A. Koyuncu, I., 2001, *Monotshefte für Chemie,* **132,** 669–673.
5. Martens, H. Naes, T., 1993, *Multivariate Calibration*, Willey, New York, pp 77–354.
6. Espinose-Maansilla, A., Duran-Meras, I. Salinas, F., 1998, *Journal of Pharmaceutical and Biomedical. Analysis,* **17,** 1325–1334.

Chapter 34
Factorial Design in the Optimization of Preconcentration Procedure for Aluminum Determination by AAS

Şule Dinç, Abdürrezzak Bozdoğan, Güzin Alpdoğan, Bürge Aşçı, and Sıdıka Sungur

Abstract A preconcentration method using Amberlite XAD-16 column for the enrichment of aluminum was proposed. The optimization process was carried out using fractional factorial design. The factors involved were: pH, resin amount, reagent/metal mole ratio, elution volume and sampling flow rate. The absorbance was used as analytical response. Using the optimised experimental conditions, the proposed procedure allowed determination of aluminum with a detection limit ($3\sigma/s$) of 6.1 μg L^{-1} and a quantification limit ($10\sigma/s$) of 20.2 μg L^{-1}, and a precision which was calculated as relative standard deviation (RSD) of 2.4% for aluminum concentration of 30 μg L^{-1}. The preconcentration factor of 100 was obtained. These results demonstrated that this procedure could be applied for separation and preconcentration of aluminum in the presence of several matrix.

In this work, a procedure for the preconcentration and determination of aluminum was proposed. The experimental conditions of the procedure were obtained by using two level fractional factorial design.

Keywords Fractional factorial design, aluminum, morin, preconcentration, XAD-16, AAS.

Introduction

The use of multivariate experimental design techniques in analytical chemistry is increased. Multivariate designs allow the simultaneous optimization of several control variables. These design are faster to implement and more cost-effective than univariate approaches [1]. The most popular multivariate design is the two-level full factorial design (2^k). In this design, every factor is experimentally studied at two levels. Due to its simplicity and relatively low cost, two level full factorial design is very useful for optimization. However, as the number of factors in 2^k design

Yildiz Technical University, Faculty of Arts and Sciences, Department of Chemistry, 34210 Davutpaşa-Istanbul, Turkey

B. Sener (ed.), *Innovations in Chemical Biology*, doi: 10.1007/978-1-4020-6955-0

increases, the number of experiments required increases exponentially. If the problem involves a large number of factors, fractional factorial design (2^{k-1}) is preferred for optimization procedure.

Aluminum is a metal which exists abundantly and widely in the earth and is commonly used in food packaging, antiperspirants, antiacid in digestion remedies, cosmetics and in beverages industries [2]. Aluminum sulfate is the most common aluminum-based coagulant used in purify water in many countries and it is found in most drinking water. WHO guidelines set its permissible level in drinking water at 200 ppb [3]. Upper levels can lead to serious problems such as Alzeheimer's disease. So, optimized preconcentration methods are required for the determination of trace amounts aluminum.

Experimental

Chemicals and Solutions

All chemicals were of analytical reagent grade. MilliQ water was used throughout the experimental work. Al(III) working solution (15 μg mL^{-1}) was prepared daily by diluting standard Al solution (1,000 μg mL^{-1}, Fluka, 06155). Amberlite XAD-16 resin (20–50 mesh, Fluka, 06442) was used. Buffer solution of pH 4 was prepared by mixing appropriate amounts of 0.1 mol L^{-1} solutions of acetic acid and sodium acetate. 5.55 x 10^{-3} mol L^{-1} solution of Morin (Fluka, 69870) in methanol was used as complexing reagent.

Apparatus

A glass column with 10 cm length and 1 cm i.d. was filled with 500 mg of resin. The ends of the column were sealed with small glass wool beds. The resin was conditioned with 10–15 mL of pH 4 buffer solution before using.

Analytikjena Atomic Absorption Spectrometer equipped with an aluminum hollow cathode lamp was used to measure aluminum concentrations. The wavelength and spectral bandpass were set at 309.3 and 1.2 nm, respectively. Gas/Oxidant ratio was 0.553. A digital pH meter model Metrohm was used for pH measurements.

General Procedure

In the experiments for testing the preconcentration method and factorial design, aluminum working solution (15 μg mL^{-1}) was used. One milliliter of this solution

was transferred into a 50 mL of volumetric flask, 1 mL of Morin solution (5.55 x 10^{-3} mol L^{-1}) was added. The mixture was diluted to its volume with pH 4 buffer solution and mixed. The solution was passed through the column at 1 mL min^{-1} flow rate. The adsorbed metal chelate on the column was eluated with 15 mL of 1 mol L^{-1} HNO_3 in acetone. The eluate was evaporated to near dryness over a hot plate. The residue was dissolved in 5 mL of 0.1 mol L^{-1} HNO_3 and Al (III) concentration in this solution was measured by flame AAS and recovery was calculated from this result.

Results and Discussion

Factorial Design

pH, resin amount, reagent/metal mole ratio, elution volume and sampling flow rate were chosen as factors for the optimization of preconcentration. Two level fractional factorial design 2^{5-1} for 16 runs was carried out in order to determine the effect of factors and its interactions on the results. Low and high levels of each factor which is given in Table 34.1 were chosen according to the data from previous experiments. The fractional factorial design was evaluated using as response the analytical signal absorbance. The defining relation for this design is I = ABCDE and the resolution is V. Table 34.2 shows the experimental design matrix Table 34.3 shows the effect estimates and model regression coefficients for the 15 main and interaction effects. Normal probability plot of the effect estimates is shown in Fig. 34.1. It was found from normal probability plot and Table 34.3 that the factors pH (+27.545) and reagent/metal mole ratio (+14.27) are the most significant, elution volume and flow rate are the relatively significant, and resin amount is not significant.

Analytical Performance of the Method

The precision of the method calculated as the relative standard deviation (RSD) for five replicates was 2.4% for the level of 30 μg L^{-1} of aluminum in water.

Table 34.1 Factors and levels used in 2^{5-1} design

Factor	Low (−)	High (+)
pH (A)	3	4
Resin amount (B) (mg)	200	500
Reagent /metal mole ratio (C)	5	10
Elution volume (D) (mL)	10	15
Flow rate (E) (mL min^{-1})	1	2

Table 34.2 Design matrix and results

Run no	A	B	C	D	E	Recovery (%)
1	–	–	–	–	+	42.31
2	+	–	–	–	–	66.92
3	–	+	–	–	–	34.62
4	+	+	–	–	+	65.38
5	–	–	+	–	–	40.00
6	+	–	+	–	+	76.92
7	–	+	+	–	+	56.15
8	+	+	+	–	–	98.70
9	–	–	–	+	–	47.69
10	+	–	–	+	+	69.23
11	–	+	–	+	+	45.38
12	+	+	–	+	–	70.77
13	–	–	+	+	+	59.20
14	+	–	+	+	–	100.1
15	–	+	+	+	–	63.85
16	+	+	+	+	+	61.54

Table 34.3 Main and interaction effect estimates and regression coefficients for design

Variable	Regression coefficients	Estimated effects
Overall average	62.422	
A	13.78	27.55
B	−0.37	−0.75
C	7.14	14.27
D	2.30	4.60
E	−2.91	−5.82
AB	1.72	−3.45
AC	0.99	1.97
AD	−3.08	−6.17
AE	−5.02	−10.04
BC	0.88	1.75
BD	−3.96	−7.92
BE	−2.03	−4.06
CD	−0.68	−1.37
CE	−3.20	−6.39
DE	−2.97	−.95

The preconcentration factor was 100, considering the aqueous sample volume of 500 mL and the final volume of analysis of 5 mL. The limits of detection (LOD) and determination (LOQ) defined as 3σ basis were 6.1 and 20.2 μg L^{-1}, respectively.

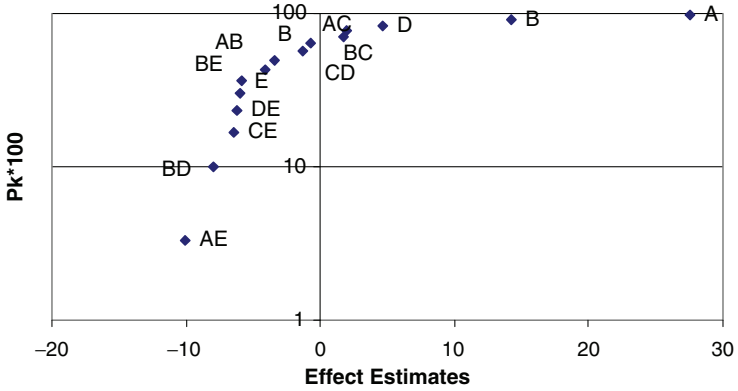

Fig. 34.1 Normal probability plot of effect estimates

Conclusion

Application of 2^{5-1} fractional factorial design allowed the optimization of the enrichment procedure for the determination of aluminum by AAS. The optimum conditions were found to be 4 of pH, 10 of reagent/metal mole ratio, 15 mL of elution volume and 1 mL min^{-1} of flow rate.

References

1. Montgomery, D.C., 1997, Design and Analysis of Experiments, 4th ed., Wiley, New York.
2. Hoch, R.L., 1999, *Analyst,* **124,** 793–796.
3. Dillen, J.W., Birch, B.J. and Hagget, B.G.D., 1999, Anal. Commun., 36.

Chapter 35
Oxidation of L-Ascorbic Acid in Copper(II) Ion – Catalyzed Polyvinylpyrrolidone Solutions

Serkan Angı[1], Hasan Kılıç[2], and Filiz İmer[3]

Abstract The effects of Cu (II) ion and polyvinylpyrrolidone (PVP) (K-30) concentrations on the oxidation kinetics of ascorbic acid (Vitamin C: H_2A) in aerated and acetate buffered solution (pH = 4.5) have been investigated at 25°C. The study was carried out in the concentration range of PVP between 0.2% and 0.6%, and in the concentration range of Cu (II) between 0.785 and 3.14 x 10^{-7} M. The initial concentrations of H_2A were 2.8–11.3 x 10^{-5} M. The changes in H_2A concentrations during the reactions were determined from absorbance measurements at a wavelength of 264.0 nm, using direct UV spectrophotometric method. Molecular weight (MW) of the PVP has been redetermined as a mean MW, using viscosimetric method.

The rate equation of the Cu (II) ion – catalyzed reaction was found to be first order with respect to H_2A. The oxidation rate constant decreased with increasing PVP amount for a fixed Cu (II) ion concentration, whereas it increased with increasing Cu (II) ion concentration for a fixed PVP level. It also increased with increasing concentration of H_2A for a fixed Cu (II) ion concentration.

Keywords Ascorbic acid, copper (II)-catalyzed oxidation, kinetic-spectrophotometric method, polyvinylpyrrolidone

Introduction

Ascorbic acid (Vitamin C: H_2A) has been widely used in pharmaceutical, chemical, cosmetic and food industry because of its bioactive and antioxidant properties [1]. Cu (II) ion is important nutrients found in many food and pharmaceutical products. Traces of transition metal ions like as Cu(II) ion also acts as catalyst in the oxidation

[1]Esenler Primary School, Esenler, İstanbul Turkey

[2]Marmara University, Department of Chemistry, 34722 Ziverbey, İstanbul Turkey

[3]Yıldız Technical University, Department of Chemistry, 34220 Davutpasa, İstanbul Turkey

B. Sener (ed.), *Innovations in Chemical Biology*, doi: 10.1007/978-1-4020-6955-0

of H_2A. Because of its biochemical importance in the food and pharmaceutical industries, Cu (II) ion-catalyzed oxidation of H_2A by molecular oxygen has been extensively studied [2–7]. The role of buffers on the kinetics of L-ascorbic acid oxidation catalyzed by copper(II) ions has been also studied [8]. Polyvinylpyrrolidone (PVP) is very useful in pharmacy and medicine due to its important absorptive and complexing properties and, physiological inertness as well [9]. Weak complexes of PVP with L-ascorbic acid [10] and with Fe(III), Co(II) and Ni(II) have been reported [11]. In previous part of this study the effects of pH and molecular weight (MW) of PVP on the kinetics of Cu(II) ion-catalyzed and uncatalyzed oxidation of H_2A were reported. The rates of oxidation reaction have been found to increase in both the catalyzed and uncatalyzed reactions containing PVP, in the pH range from 4.5 to 6.0 [12, 13].

The aim of this study to investigate the effects of Cu(II) ion and PVP concentrations on the oxidation kinetics of H_2A in aerated and acetate buffered solution, at 25°C, using direct UV spectrophotometric method [14, 15].

Experimental

Materials and Methods

All chemicals were of analytical reagent grade and were supplied by E. Merck (AG, Darmstadt, Germany). L–ascorbic acid (mentioned as ascorbic acid in the text) was used without purification. Acetate buffer solutions at pH 4.50 were prepared according to Hsieh and Harris [16]. PVP (K-30) was purchased from BASF and its molecular weight was redetermined as a mean molecular weight, M_v (23458) by using Mark-Houwink equation from viscosimetric measurements by using Ubbelohde viscosimeter. Deionized distilled water was used to prepare and dilute all solutions.

The absorbances were measured and spectra taken with a SCHIMADZU UV-1601 Spectrophotometer using a pair of matched quartz cuvettes of 1.0 cm thickness. The pH measurements were made using a SCHOTT CG 841 type pH- meter with N2042 combined glass electrode system. The ionic strength of the medium was maintained at I = 0.10 M (KNO_3) in order to keep the activity coefficients of the relevant species constant during the kinetic process. All the experiments were carried out at 25°C by means of a thermostated system (±0.5°C) which contained an immersion circulator (Thermomix 1419 B. Braun model, AG Melsungen, Germany).

Sample Preparation and Kinetic Measurements

A stock of copper(II) nitrate solution with a Cu(II) ion concentration of 1.57×10^{-5} M, PVP solution of 2%, H_2A solution of 5.67×10^{-3} M, and acetate buffer solution of 0.5 M were prepared. A sample solution containing 0.10 M KNO_3, 0.5 M acetate

buffer, PVP in the concentration range from 0.2% to 0.6%, Cu(II) ion in the concentration range from 0.785 to 3.14 x 10^{-7} M was prepared in a 100 ml volumetric flask. H_2A solution, in the range 2.8–11.3 x 10^{-5}M was added immediately to that solution and the reaction was timed. Sample solution was placed in a 250-ml Erlenmeyer flask in contact with a water bath thermostated at 25°C. During this time a stream of air (flow rate = 60 $L.h^{-1}$) was passed through the Erlenmeyer flask and the solution was saturated with oxygen. The air was presaturated with water vapor passed through a wash-bottle. Since the rate of reaction is slow compared to the rate of dissolution of oxygen, the reacting solution was considered to be saturated with oxygen at all times. Two milliliters aliquots were taken at regular time intervals for absorbance measurements and the change in the concentration of H_2A was measured by direct UV spectrophotometry [14, 15], by quantifying the residual H_2A during the course of oxidation. The pH of the worked solution was rechecked. All tests were made in triplicate, and the results were presented as means.

Theoretical Considerations

The pK_a values of ascorbic acid are 4.1 and 11.79 [17]. Basically, the undissociated (H_2A) and monoanionic (HA^-) forms of ascorbic acid predominate in solutions at pH 3.2 and 5.6, respectively. Copper (II) nitrate was used as the catalyst because of that it forms the least stable complex with nitrate ions among the inorganic anions. Sulfate and chloride ions form more stable complexes with copper, though all of them are relatively weak.

The oxidation of ascorbic acid in the presence of an excess of oxygen (saturation) was assumed to follow a first order reaction [2, 3, 5]. The reaction rate can be expressed as:

$$-d[H_2A]/dt = k[H_2A] \ldots \text{(Proportional to } A_{264})$$

where $[H_2A]$ is the concentration of remaining ascorbic acid during the course of autoxidation, t is the time and k is the first order rate constant which can be calculated from a plot of $\log[H_2A]$ *vs* time. It gives a straight line with a slope –k/2.303.

Results and Discussion

First, in order to follow the uncatalyzed and Cu(II) ion catalyzed oxidation of ascorbic acid at 2.85, 5.67, 8.50 and 11.35 x 10^{-5} M concentrations, solutions with Cu(II) ion levels of 0, 0.785, 1.570, 3.140 x 10^{-7} M were studied, in the absence of PVP at 25°C and an ionic strength of I = 0.10M (KNO_3). Further, the same experiments were performed in the presence of PVP, ranging from 0.2% to 0.6%. Each of the reaction was followed for 60 min at a pH value of 4.50. In these experiments,

the plot of the logarithm of absorbance values *versus* time yielded a straight line, which indicated a first order reaction. Absorbance values are directly proportional with H_2A concentrations. The related plots were given in Figs. 35.1–35.6. The first-order rate constants were calculated by linear regression analysis and presented in Table 35.1.

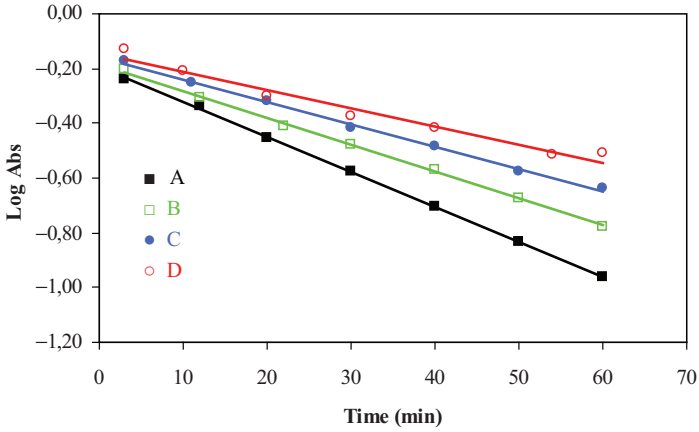

Fig. 35.1 Kinetic data for Cu(II) ion-catalyzed (0.785 x 10^{-7} M) oxidation of ascorbic acid (5.67 x 10^{-5} M) in acetate buffered PVP solutions at pH = 4.5 [PVP concentrations A: Absence, B: 0.2%, C: 0.4%, D: 0.6%]

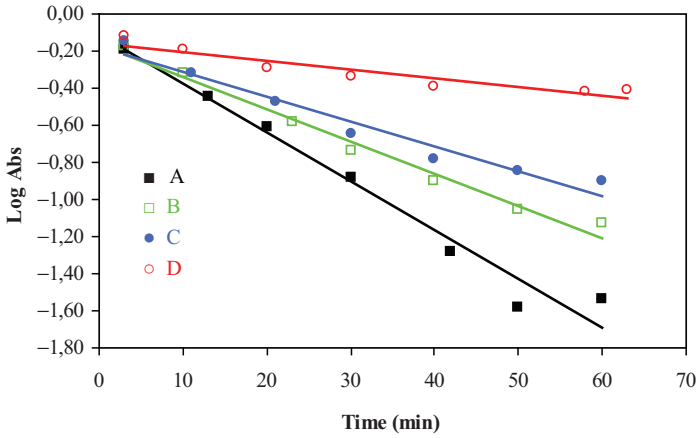

Fig. 35.2 Kinetic data for Cu(II) ion-catalyzed (1.57 x 10^{-7} M) oxidation of ascorbic acid (5.67 x 10^{-5} M) in acetate buffered PVP solutions at pH = 4.5 [PVP concentrations A: Absence, B: 0.2%, C: 0.4%, D: 0.6%]

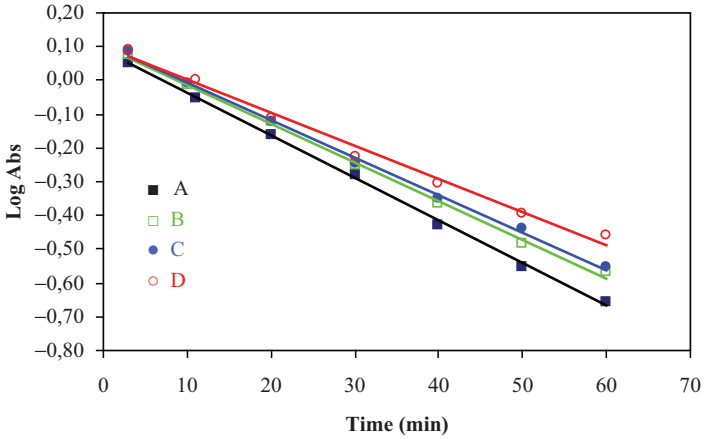

Fig. 35.3 Kinetic data for Cu(II) ion-catalyzed (0.785 x 10^{-7} M) oxidation of ascorbic acid (11.35 x 10^{-5} M) in acetate buffered PVP solutions at pH = 4.5 [PVP concentrations A: Absence, B: 0.2%, C: 0.4%, D: 0.6%]

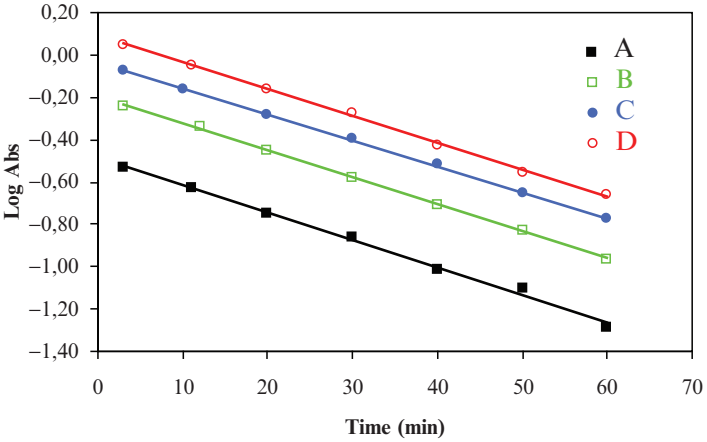

Fig. 35.4 Kinetic data for Cu(II) ion-catalyzed (0.785 x 10^{-7} M) oxidation of ascorbic acid in absence of PVP in acetate buffered solutions at pH = 4.5 [Ascorbic acid concentrations (A: 2.85, B: 5.67, C: 8.50, D: 11.35) x 10^{-5} M]

The results obtained from aforementioned experimental study can be summarized as follows:

1. In the absence and presence of PVP, on increasing concentration of the ascorbic acid, the reaction rate was found to increase in all experiments. Moreover, it was also found to increase on increasing concentration of ascorbic acid for a fixed copper (II) ion concentration (Figs. 35.4 and 35.5).

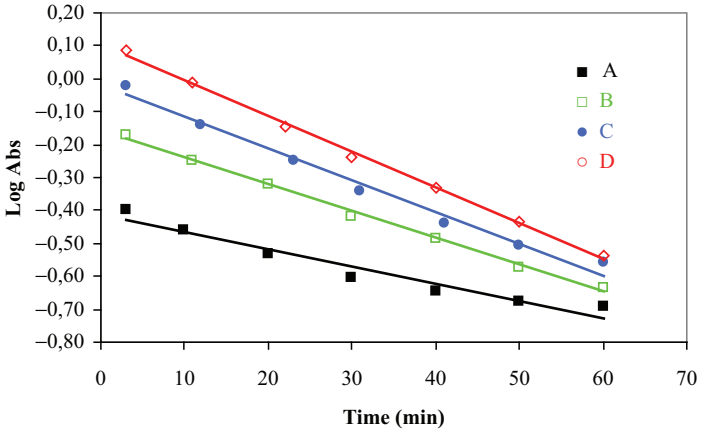

Fig. 35.5 Kinetic data for Cu(II) ion-catalyzed (0.785 x 10^{-7} M) oxidation of ascorbic acid in acetate buffered PVP solution (0.4%) at pH = 4.5 [Ascorbic acid concentrations (A: 2.85, B: 5.67, C: 8.50, D: 11.35) x 10^{-5} M]

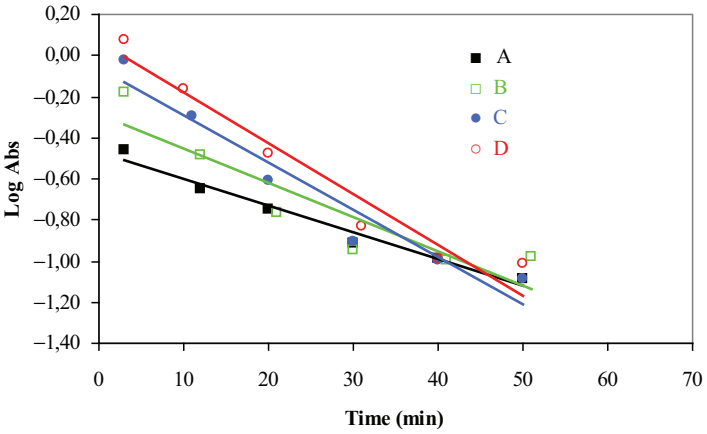

Fig. 35.6 Kinetic data for Cu(II) ion-catalyzed (3.14 x 10^{-7} M) oxidation of ascorbic acid in acetate buffered PVP solution (0.2%) at pH = 4.5 [Ascorbic acid concentrations (A: 2.85, B: 5.67, C: 8.50, D: 11.35) x 10^{-5} M]

2. In the absence of PVP, the rate constant was found to increase on increasing copper (II) ion concentration. However, it was found to decrease in the presence of PVP (Table 35.1).
3. On increasing concentration of PVP, the rate constant was found to decrease at a fixed copper (II) ion concentration. Similar result was obtained at each copper (II) ion concentration studied (Figs. 35.1 and 35.2). On contrary, the rate constant was found to increase on increasing copper (II) ion concentration for a fixed PVP level (Table 35.1).

Table 35.1 The rate constants of Cu(II)ion-catalysed oxidation of ascorbic acid at different PVP, Cu(II) and ascorbic acid concentrations at pH = 4.5

	k (min^{-1})											
	0.785 x 10^{-7} M Cu^{++}				1.57 x 10^{-7} M Cu^{++}				3.14 x 10^{-7} M Cu^{++}			
Ascorbic acid alone	PVP absence	+PVP (0.2%)	+PVP (0.4%)	+PVP (0.6%)	PVP absence	+PVP (0.2%)	+PVP (0.4%)	+PVP (0.6%)	PVP absence	+PVP (0.2%)	+PVP (0.4%)	+PVP (0.6%)
2.85 x 10^{-5} M H_2A	29.3 x 10^{-3}	18.9 x 10^{-3}	12.0 x 10^{-3}	8.59 x 10^{-3}	51.2 x 10^{-3}	25.9 x 10^{-3}	16.4 x 10^{-3}	7.11 x 10^{-3}	52.2 x 10^{-3}	25.3 x 10^{-3}	5.23 x 10^{-3}	5.05 x 10^{-3}
k = 1.50 x 10^{-3} min^{-1}	r^2 = 0.9954	r^2 = 0.9861	r^2 = 0.9439	r^2 = 0.9580	r^2 = 0.9866	r^2 = 0.9083	r^2 = 0.9092	r^2 = 0.8393	r^2 = 0.9007	r^2 = 0.9257	r^2 = 0.7310	r^2 = 0.6195
5.67 x 10^{-5} M H_2A	29.4 x 10^{-3}	22.7 x 10^{-3}	18.8 x 10^{-3}	15.3 x 10^{-3}	47.3 x 10^{-3}	40.0 x 10^{-3}	31.0 x 10^{-3}	10.7 x 10^{-3}	55.5 x 10^{-3}	30.5 x 10^{-3}	20.8 x 10^{-3}	10.8 x 10^{-3}
k = 1.77 x 10^{-3} min^{-1}	r^2 = 0.9997	r^2 = 0.9986	r^2 = 0.9967	r^2 = 0.9705	r^2 = 0.9965	r^2 = 0.9828	r^2 = 0.9570	r^2 = 0.8771	r^2 = 0.9777	r^2 = 0.7602	r^2 = 0..7130	r^2 = 0..7483
8.50 x 10^{-5} M H_2A	28.3 x 10^{-3}	26.1 x 10^{-3}	23.4 x 10^{-3}	19.2 x 10^{-3}	59.6 x 10^{-3}	45.1 x 10^{-3}	35.6 x 10^{-3}	24.1 x 10^{-3}	61.1 x 10^{-3}	40.2 x 10^{-3}	31.8 x 10^{-3}	20.0 x 10^{-3}
k = 1.64 x 10^{-3} min^{-1}	r^2 = 0.9994	r^2 = 0.9257	r^2 = 0.9950	r^2 = 0.9744	r^2 = 0.9632	r^2 = 0.9659	r^2 = 0.9669	r^2 = 0.9691	r^2 = 0.9685	r^2 = 0.8307	r^2 = 0.9800	r^2 = 0.8024
11.35 x 10^{-5} M H_2A	29.1 x 10^{-3}	26.5 x 10^{-3}	25.6 x 10^{-3}	22.5 x 10^{-3}	56.5 x 10^{-3}	49.2 x 10^{-3}	40.4 x 10^{-3}	29.2 x 10^{-3}	63.9 x 10^{-3}	56.7 x 10^{-3}	35.2 x 10^{-3}	27.5 x 10^{-3}
k = 0.97 x 10^{-3} min^{-1}	r^2 = 0.9984	r^2 = 0.9980	r^2 = 0.9973	r^2 = 0.9887	r^2 = 0.9949	r^2 = 0.9994	r^2 = 0.9704	r^2 = 0.9891	r^2= 0.9567	r^2 = 0.9452	r^2 = 0.81088	r^2 = 0.8305

From these results it can be said that presence of PVP in pH 4.50 solution definitely causes to decrease in the copper (II) ion catalyzed oxidation reaction rate of ascorbic acid.

Conclusion

One of the reasons for the decrease in the oxidation reaction rate can be considered a complexation reaction between PVP molecules and copper (II) ions, and further study is needed to clarify it.

Acknowledgement We thank the Yıldız Technical University Scientific Research Projects Coordination Department, Istanbul, Turkey for supporting this program.

References

1. Martell, A.E., 1989, Ascorbic Acid: And Its Chemistry, Metabolism Uses. In: P.A., Seib B.M.Tolbert (eds.), *Advances in Chemistry Series 200*, Am. Chem. Soc. Publishing, Washington, DC, p 153.
2. Khan, M.M.T. and Martel, A.E., 1967a, *J. Am. Chem. Soc.,* **89,** 4176–4185.
3. Ogata, Y., Kasugi, Y. and Morimoto, T., 1968, *Tetrahedron,* **24** (1968), 4057–4066.
4. Eison-Perchonok, M.H. and Downes, T.W., 1982, *J. Food Sci.,* **47** (1982), 765–773.
5. Khan, M.M.T. and Martel, A.E., 1967b, *J. Am. Chem. Soc.,* **89,** 7104–7110.
6. Ohta, Y., Shiraishi, N., Nishikawa, T. and Nishikimi, M., 2000, *Biochim. Biophys. Acta,* **1474,** 378–382.
7. Imer, F., Koseoglu, A. and Sefer, T., 1989, *J. Sci. Tech., Univ Marmara,* **6,** 119–129.
8. Imer, F., Sönmezoğlu, I.C. and Kozcaz, M., 2003, *Ital. J. Food Sci.,* **15** (4), 521–529.
9. Blecher, L., Lorenz, D.H., Lowd, H.L., Wood, A.S. Wyman, D.P., 1980. R.L. Davidson (ed.), *Handbook of Water Soluble Gums and Resins,* Chapter 21, Polyvinylpyrrolidone, McGraw-Hill, New York.
10. Melent'eva, T.A., Verenikina, S.G., Dolgushina, N.N., Bolyakina, M.V., Gunar, V.L. and Taber, A.M., 1993, *Khim-Farm. Zh.,* **27** (8), 60–63.
11. Liu, M., Yan, X., Liu, H. and Yu, W., 2000, *React. Funct. Polym.,* **44** (1), 55–64.
12. Angi, S., 2005, *MSc. thesis*, Yıldız Technical University, Istanbul, Turkey.
13. Imer, F. and Kılıç, H., 2004, *Proceedings of the 4th Aegean Analytical Chemistry Days*, pp 599–601.
14. Fung, Y.-S. and Luk, S.-F., 1985, *Analyst,* **110,** 201–204.
15. Lau, O.-W., Luk, S.-F. and Wong, K.-S., 1986, *Analyst,* **111,** 665–670.
16. Hsieh, Y.-H.P. and Harris, N.D., 1993, *J. Agric. Food Chem.,* **41,** 259–262.
17. Weast, R.C., 1982, *CRC Handbook of Chemistry and Physics*, 62nd ed., CRC, Boca Raton, FL.

Chapter 36
A Potentiometric Investigation of Primary Amines in Non-aqueous Media

Feray Aydogan, Sevgi Kocaoba, and Huseyin Afsar

Abstract Titration of weak bases in non-aqueous solvents can provide valuable information about these weak bases. Some primary amines; 1-aminobutane, 1-aminopropane, 2-aminoheptane, aminocyclohexane, 3-amino-1-phenylbutane were titrated with hydrochloric acid in toluene solvent. All the primary amines gave very well-shaped potentiometric titration curves. The same titrations were done with hydrochloric acid in methanol solvent to show the effect of amphiprotic solvent in the titrations with hydrochloric acid.

As a result, toluene is a suitable solvent for titrating some of the primary amines potentiometrically with hydrochloric acid.

Keywords Amphiprotic solvent, potentiometric titration, primary amines

Introduction

Titrations in non-aqueous solvents have been traditionally an important tool for the accurate determination of various pharmaceuticals, some acids in foods, use of some acids or bases in detergents, cosmetics and textile auxiliaries, in the analysis of industrial process streams, the analysis of polymers [1–7]. The determination of the pK_a or pK_b values of organic compounds with acidity or basicity constant less than 10^{-8} can only be realised in non-aqueous media. Although water has excellent solvent properties, it is not suitable for such organic compounds since the pH jump at the equivalence point in aqueous solution cannot be evaluated with reasonable accuracy, with this result, the end point cannot be found. Moreover, most of this compounds are not soluble in water. For these reasons, titration in non-aqueous media has recently acquired great importance. It is now well known that non-aqueous titrations greatly depend on the solvents used [4, 8–13].

Yildiz Technical University, Faculty of Arts and Sciences, Department of Chemistry, 34210 Esenler, Istanbul, Turkey

B. Sener (ed.), *Innovations in Chemical Biology*, doi: 10.1007/978-1-4020-6955-0

Many weak bases can be determined titrimetrically. However, titration of this weak bases in aqueous solution will be neither accurate nor precise because the end-points generated from weak bases are not significant [14]. Generally, $HClO_4$ is used as a titrant for determination of weak bases in non-aqueous media. However, commercial $HClO_4$ contains 28–30% water corresponding to approximately $HClO_4.2H_2O$. Anhydrous $HClO_4$ titrant is prepared by dissolving the aqueous $HClO_4$ in acetic acid or in sulfolane and then adding enough acetic anhydride to react with all the water. When combined with $HClO_4$, weak acid, acetic acid shows strong acid effect at the end point of the titration. Furthermore, acetic anhydride contained in titrant may interfere by reacting with some amines to generate corresponding acetylated product, which do not consume acid. To eliminate the problems mentioned above with $HClO_4$, we used HCl as a strong acidic titrant in non-aqueous titration of some primary amines which are weak bases. Although, very weak bases can not be quantitatively determined, when amphiprotic solvents used in neutralisation titrations, there are very limited numbers of research and published papers focusing on titration in aprotic solvents. These are mainly on titrations having benzene, which is highly carcinogenic, as solvent. So, toluene which is an aprotic inert solvent, was chosen in non-aqueous titration with HCl. The major advantage of inert solvents is that they do not compete for protons with the reactant in a titration; that is, these solvents have autoprotolysis constants approaching zero. Thus, neutralisation reactions should be more nearly complete when carried out in solvents of this type. Primary disadvantage of these solvents is that most acids and bases tend to be sparingly soluble in them but this disadvantage can be eliminated by using a small volumes of amphiprotic solvents together with inert solvents. The small amounts of amphiprotic solvents do not effect the competition of weak bases with solvent in proton transfer. Because the amount of aprotic solvents is very less competition between weak bases and amphiprotic solvents in proton transfer can be done easily.

Experimental

Chemicals

1-Aminobutane, 1-aminopropane, 3-amino-1-phenylbutane, 2-aminoheptane, aminocyclohexane, toluene, methanol, calcium chloride, potassium chloride, calcium oxide were purchased from Merck, sulphuric acid and sodium chloride were technical grade. Toluene was dried by distillation from metallic sodium. Methanol was dried on calcium oxide. Standard hydrochloric acid solution was prepared by passing of hydrogen chloride gas evolved from concentrated sulphuric acid and solid sodium chloride through dry toluene. 0.1 M HCl solution was used as titrant for each titration. The hydrochloric acid solution in methanol was prepared same way using water free methanol instead of toluene. Standard 0.02 M amine solutions were

prepared by dissolving of corresponding amounts (2 mmol) of amines in water free toluene containing 5% dry methanol (100 ml). Methanol was used for development solubility of amines in toluene.

Apparatus

Metrohm Herisau Prazisions-pH meter E 510 and combined electrode were used for the potentiometric titrations and electrode was filled with saturated solution of potassium chloride in water free methanol instead of aqueous potassium chloride.

The potentiometric titrations were performed in a three necked vessel equipped with electrode, drying tube filled with calcium chloride, semi-microburette and a magnetic stirrer. Burette had an adaptor which connected with a drying tube and the 0.12 M HCl solution bottle, and filled with the solution by means of nitrogen gas flow dried over calcium chloride.

Titrations were carried out at room temperature. The volume of amine solution titrated was 50 ml and this was magnetically stirred during the addition of titrant. The titrant was added in 0.5 ml quantities. After each addition of titrant, approximately one minute was allowed before measurement were made to reach ionic equilibrium.

Results and Discussion

Titration curves of the weak bases with HCl in toluene (0.12 M) solvent are given in Fig. 36.1. The shapes of the titration curves indicate that toluene is an excellent solvent for these weak bases.

The same titrations were done with hydrochloric acid in methanol solvent to show the effect of amphiprotic solvent in the titrations with hydrochloric acid. But, some of the compounds did not show expected results, while most of them gave well shaped curves.

As a result, inert and aprotic solvent toluene is suitable for the titration of weak bases in non-aqueous media as solvent, although benzene which is more carcinogenic aromatic hydrocarbon used widely in literature for non-aqueous titrations. The major advantage of toluene is that it does not compete for protons with the reactant in the titrations because of its autoprotolysis constant approaching zero. The major disadvantages of solubility can be removed by using small amount of amphiprotic solvents.

HCl is also good titrant for weak bases because of its great solubility in most solvent; i.e. 0.58 N in toluene and 0.86 N in MeOH at saturation point and availability from the cheap compounds such as NaCl and H_2SO_4. The method used for non-aqueous titrations of weak bases is also easily applicable and convenient method in every laboratory.

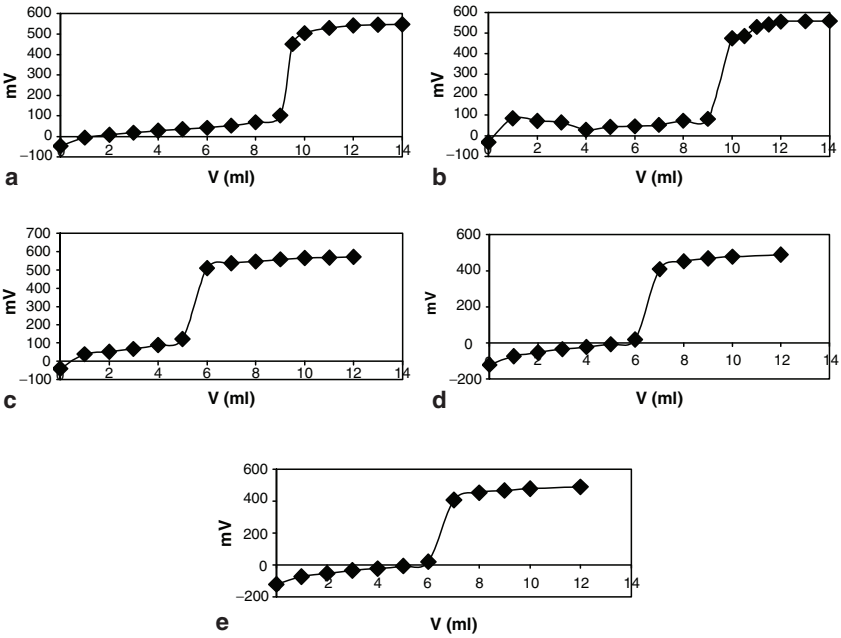

Fig. 36.1 Titration curves of the weak bases with HCl in toluene (a: Butylamine, b: Propylamine, c: 3-Amino-1-phenylbutane, d: 2-Aminoheptane, e: Cyclohexylamine)

References

1. Bos, M. and Linden, W.E., 1996, *Anal. Chim. Acta,* **332,** 201–211.
2. Kılıc, E., Köseoğlu, F., Kenar, A. and Akay, M.A., 1995, *J. Pharm. Biomed. Anal.,* **13,** 1453–1458.
3. Aktaş, A.H., Yasar, G., Alsancak, G.O. and Demirci, S., 2001, *Turk. J. Chem.,* **25,** 501–507.
4. Yalçın, M., Tanyolaç, S., Kızılcıklı, I. and Tavman, A., 1998, *Turk. J. Chem.,* **22,** 155–160.
5. Vyas, R.H.Q. and Kharat, R.B., 1988, *Ind. J. Pharm. Sci.,* **50**(5), 279.
6. Urbanski, J., Czerwinski, K., Janicka, F., Majewska, H. and Zowall, H., 1977, Handbook of Analysis of Synthetic Polymers and Plastics, Ellis Horwoord, Chichester, UK.
7. Gündüz, T., Ozkan, G. and Gündüz, B., 1997, *Microchim. Acta,* **126**(3–4), 227–230.
8. Gündüz, T., Gündüz, N. and Hayvalı, M., 1993, *Anal. Chim. Acta,* **78**(2), 243–247.
9. Gündüz, T., Kılıç, E., Özkan, G., Awaad, M. and Taştekin, M., 1990, *Anal. Chim. Acta,* **234**(2), 339–344.
10. Gündüz, T., Kılıç, E. and Çakırer, O., 1996, *Talanta,* **43**(5), 771–776.
11. Çakırer, O., Gündüz, T. and Kılıç, E., 1998, *Ind. J. Chem. A.,* **37**(11), 1032.
12. Glinski, J., Chavepeyer, G. and Platten, J.K., 2001, *Chem. Phys.,* **272,** 119–126.
13. Kaczmarczyk, E. and Chmurzynski, L., 2000, *J. Mol. Struct.,* **526,** 41–47.
14. Qui, X.S., Miller, R.B., Namiki, Y., Zhang, Z. and Jacobus, R., 1997, *J. Pharm. Biomed. Anal.,* **16,** 413.

Chapter 37
Domino-Heck Type Reactions of N-Benzoyl-2-Azabicyclo [2.2.1]Hept-5-ene-3-one

Cigdem Yolacan[1], Nuket Ocal[1], and Dieter E. Kaufmann[2]

Abstract The coupling of 2-azabicyclo[2.2.1]hept-5-en-3-one and trimethylsilylacetylene or phenylacetylene under Domino Heck conditions gives compounds **2a-c** and **4a-c** in moderate yields and cyclopentene derivatives, **3a-c** in low yields. The procedure can be of use for the synthesis of alkynyl bicyclic lactams.

Keywords Alkynyl lactams, Heck reaction, Domino-Heck type reaction, rearrangement

Introduction

In the last decade, organopalladium-catalysist C-C bond formation has become one of the most efficient approaches to synthesize organic molecules. The Heck reaction, in particular, is widely used as an important method to build biologically active compounds in synthetic chemistry and the pharmaceutical industry.

As an extension of the Heck reaction, Pd-catalyzed hydroarylation of alkynes and alkenes continues to attract high level of research interest in simple coupling processes and in cyclization reactions. The use of this type of transformation as part of a domino reaction will be of increasing interest. The research in the field of domino reactions is attracting considerable attention in synthetic organic chemistry since it enables the rapid assembly of complex molecules in one-pot processes. Very elegant examples of palladium-catalyzed cascade processes where a single catalytic cycle entails several sequential bond transformations have been recently reported [**1a, b, 2a, b, c**].

We recently focused on processes involving the reductive Heck and Domino-Heck reactions [3] in a single synthetic operation by treating aryl iodides in conjunction with this work.

[1] Yildiz Technical University, Department of Chemistry, Davutpasa Campus, 34210, Esenler-Istanbul, Turkey

[2]Clausthal Technical University, Institute of Organic Chemistry, Leibnizstr 6, D-38678, Clausthal-Zellerfeld, Germany

B. Sener (ed.), *Innovations in Chemical Biology*, doi: 10.1007/978-1-4020-6955-0

Results and Discussions

We showed that compound **1** converted cyclic alkynic lactams (**2a-c** and **4a-c**) which can be used in the synthesis of natural products [4] by treating alkynes such as trimethylsilylacetylene (Scheme 37.1) and phenylacetylene (Scheme 37.2) using Heck

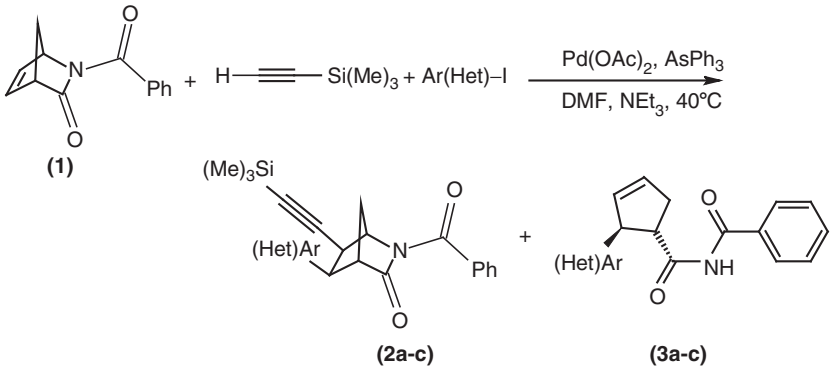

Scheme 37.1 Domino-Heck reactions of compound 1 with trimethylsilylacetylene and aromatic iodides

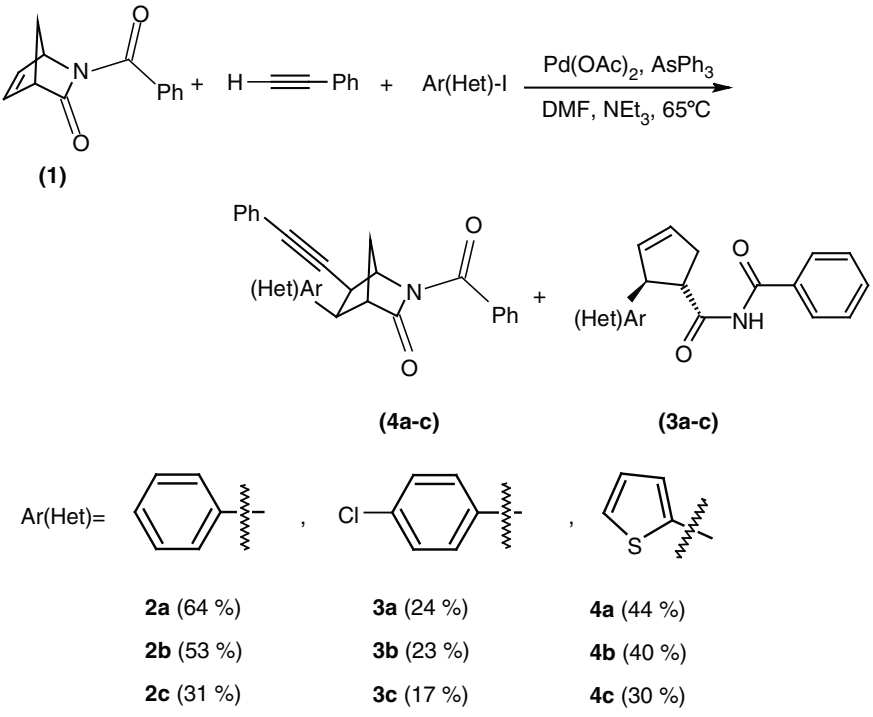

2a (64 %)	**3a** (24 %)	**4a** (44 %)
2b (53 %)	**3b** (23 %)	**4b** (40 %)
2c (31 %)	**3c** (17 %)	**4c** (30 %)

Scheme 37.2 Domino-Heck reaction of compound 1 with phenylacetylene and aromatic iodides

reaction conditions in the presence of palladium(II) acetate. The desired products, **2a-c** and **4a-c** were obtained in 30–64% yields after chromatographic separations. We also observed rearrangement products **(3a-c)** as expected [5, 6] in 17–24% yields.

All compounds were determined by NMR spectroscopy (Table 37.1) and diagnostic spin-spin interactions were identified with the aid of HH COSY experiments (Fig. 37.1). The *exo*-location of the substituent on C_6 was confirmed by the fact that H_6 showed no significant interaction with H_1 also showed a cross-peak as a result of W-coupling to H_{7syn}.

Examining the coupling pattern of H_5 in the compounds sufficient to distinguish *exo*-position of the 5-alkynyl groups. As the dihedral angle between H_4 and H_5 is close to 90°, the coupling constant between H_4 and H_5 is near to 0 Hz. H_{5endo} was

Table 37.1 Selected ^{1}H NMR data for compounds **2a-c** and **4a-c**

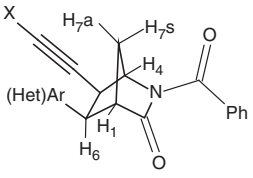

	2a (ppm)	**2b** (ppm)	**2c** (ppm)	**4a** (ppm)	**4b** (ppm)	**4c** (ppm)
H_1	5.04 bs	4.99 bs	4.86 bs	5.11 bs	4.93 bs	4.82 bs
H_4	3.16 bs	3.15 bs	3.15 bs	3.26 bs	3.15 bs	3.14 bs
H_5	3.46 dd	3.44 dd	3.40 d	3.69 d	3.55 d	3.65 d
H_6	3.75 d	3.71 d	4.02 d	3.87 d	3.70 d	4.02 d

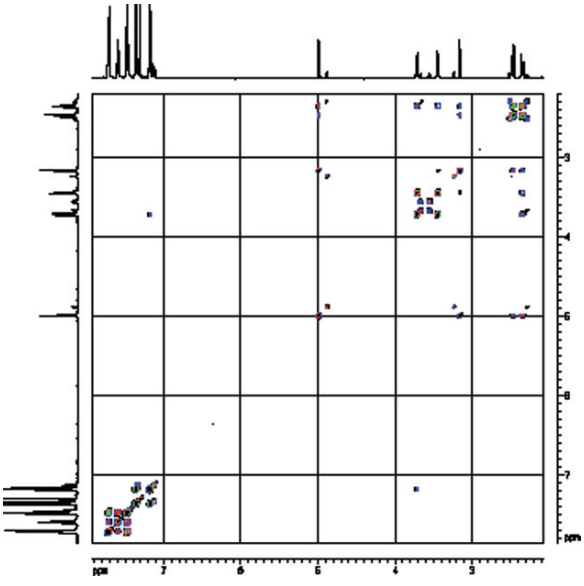

Fig. 37.1 HH-COSY spectra of compound **2b**

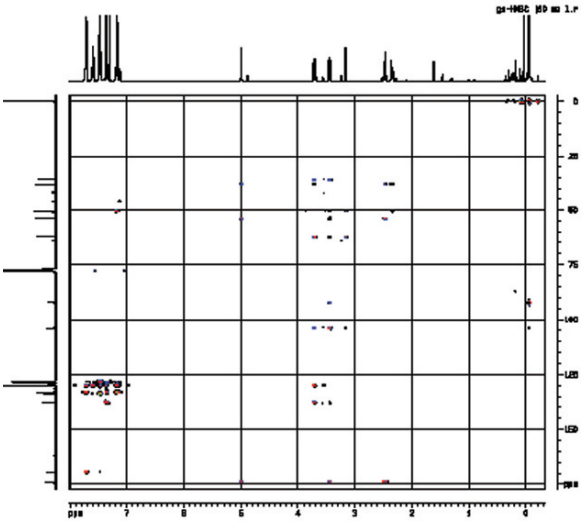

Fig. 37.2 HMBC spectra of compound **2b**

Table 37.2 Selected ^{1}H NMR and FTIR data for compounds 3a-c

Compound	**3a**	**3b**	**3c**
FTIR (cm-1)	3304 (N-H), 1720 (C = O), 1681 (C = O)	3250 (N-H), 1725 (C = O), 1681 (C = O)	3277 (N-H), 1731 (C = O), 1681 (C = O)
^{1}H NMR (ppm)	2.67–2.75 and 3.15–3.25 (m, CH_2), 3.94–4.00 (m, 4-H), 4.55–4.59 (m, 3-H), 5.80 and 5.90 (d, = CH), 7.25–7.77 (m, aromatic), 8.56 (bs, NH)	2.58–2.66 and 3.13–3.21 (m, CH_2), 3.93–3.99 (m, 4-H), 4.51–4.56 (m, 3-H), 5.70 and 5.90 (d, = CH), 7.16–7.75 (m, aromatic), 8.55 (bs, NH)	2.65–2.69 and 2.86–2.92 (m, CH_2), 3.92–3.96 (m, 4-H), 4.22–4.24 (m, 3-H), 5.90 and 6.10 (d, = CH), 6.92–7.65 (m, aromatic), 8.38 (bs, NH)

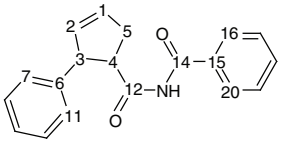

identified by vicinal coupling to H_{6endo} ($J_{5,6endo}$ = 9.0 Hz). Comparison of the 5_{endo} and 6_{endo} protons resulted in that 6_{endo} protons also did show interaction with phenyl group (o-position) in HMBC spectra (Fig. 37.2). Investigation of the ^{13}C NMR spectra supported this reassignment. The shifts for C_1, C_3, C_5 and C_6 were diagnostic and the agreement within each family is reassuring.

Cyclopentene derivatives (**3a-c**) were also characterized by FTIR and various NMR techniques. N-H, C = O and C = C peaks were identified in expected fields (Table 37.2).

Experimental

NMR spectra were recorded on Bruker Digital FT-NMR 'Avance 400' spectrometer ($CDCl_3$ solvent) with TMS as internal reference. In the ^{13}C spectra quaternary, methylene and methyl carbons were identified using DEPT experiments. IR spectra were recorded on Perkin Elmer FT-IR spectrometer (KBr). Reactions were performed under dry nitrogen. Melting points were measured on a Gallenkamp melting point apparatus. Silica gel 60 (Merck) was used for column separations. TLC was conducted on standart conversion aluminium sheets pre-coated with a 0.2 mm layer of silica gel.

Domino-Heck Reactions – General Procedure: 5.6 mg (25 μmol) of palladium(II) acetate and 55 μmol of the arsine ligand were dissolved in 3 ml of dry dimethyl formamide and the solution was stirred at 65°C (40°C for trimethylsilylacetylene) for 15 min. Then, 127 mg (1.35 mmol) N-Benzoyl-2-azabicyclo[2.2.1]hept-5-en-3-one, 1 mmol of the aryl compound. Four hundred and eighty-eight microliters (3.50 mmol) of triethylamine, and 3.00 mmol of the phenylacetylene (or silylmethylacetylene) were added rapidly in one portion. The mixture was heated at the same temperature for 24 h. After cooling down to room temperature 50 ml of brine were added, the reaction mixture was extracted with ethyl acetate and dried over $MgSO_4$. The solvent was evaporated, the residue purified by column chromatography (n-Hexan-Ethyl acetate 4:1).

Acknowledgments We would like to thank Yıldız Technical University Research Foundation (24-01-02-14) for financial support, to Dr. Jan C. Namyslo from Clausthal Technical University-Germany for NMR and GC-MS measurements and fruitful discussions, to Bayer AG for providing the starting material.

References

1. (a) Negishi, E. and Meijere, A., 2002, *Handbook of Organopalladium Chemistry for Organic Synthesis.* Wiley-Interscience, New York, p 1133.
   (b) Beletskaya, I.P. and Cheprakov, A.V., 2000, *Chem. Rev.,* **100,** 3009–3066.
2. (a) Tietze, L.F., 1996, *Chem. Rev.,* **96,** 115–136.
   (b) Zhang, Y., Wu, G., Agnel, G. and Negishi, E., 1990, *J. Am. Chem. Soc.,* **112,** 8590–8592.
   (c) Poli, G., Giambastiani, G. and Pacini, B., 2001, *Tetrahedron Lett.,* **42,** 5179–5182.
3. Yolacan, C., Bagdatlı, E., Ocal, N. and Kaufmann, D.E., 2006, *Molecules,* **11,** 603–614.
4. Daluge, S.M., Martin, M.T., Sickles, B.R. and Livingston, D.A., 2000, *Nucleos. Nucleot. Nucleic Acids,* **19,** 297.
5. Yao, M.L., Adiwidjaja, G. and Kaufmann, D.E., 2002, *Angew. Chem. Int. Ed.,* **41,** 3375–3378.
6. Storsberg, J., Yao, M.L., Ocal, N., Meijere, A., Adam, A.E.W. and Kaufmann, D.E., 2005, *Chem. Commun.,* **45,** 5665–5666.

Chapter 38
Synthesis of Different Epibatidine Analogues with Domino- and Reductive Heck Reactions

Emine Bağdatlı and Nüket Öcal

Abstract New epibatidine analogues were synthesized by palladium catalyzed reductive Heck and Domino-Heck reactions and regioselective results were obtained.

Keywords Epibatidine analogues, *Epipedobates tricolor*, Domino Heck reaction, frog, synthesis

Introduction

For thousands of years, nature, especially plant life, was the 'pharmacy' from which people obtained their medicines. Even today it is estimated that 40% of all drugs contain at least one plant-derived ingredient [1, 2].

One of these natural products, epibatidine (**1**) was isolated from the skin of the *Ecuadorian* frog, *Epipedobates tricolor*, by Daly and coworkers in 1992 and found to have powerful analgesic activity and high binding affinity to nicotinic acetylcholine receptors (nAChRs). This is reminiscent of a classical application of nicotine (**2**), being structurally related to **1** [3].

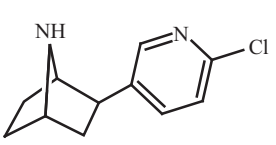

1

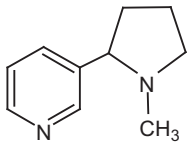

2

Epibatidine provides an attractive lead for the treatment of mainly central nervous system disorders such as Alzheimer's and Parkinson's diseases, dyskinesias,

Yıldız Technical University, Department of Chemistry, Davutpaşa Campus, 34210, Esenler-İstanbul, Turkey

B. Sener (ed.), *Innovations in Chemical Biology*, doi: 10.1007/978-1-4020-6955-0

Tourette's syndrome, schizophrenia, attention deficit disorder, anxiety, pain and for the many other diseases [1].

Toxic effects of epibatidine and the fact that the amount of this compound had been isolated from some 750 *Ecuadorian* frogs less than one milligram [4], causes the need of synthesizing new analogues which are not toxic but have the same biological properties. We, therefore become interested in synthesizing of the new epibatidine analogues.

Materials and Methods

All reactions were conducted under an atmosphere of dry nitrogen at Schlenk system. NMR spectra ($CDCl_3$ solvent) were recorded on Bruker Digital FT-NMR Avance 400 and Varian Inova 500 MHz NMR spectrometers, with TMS as internal reference. FTIR spectra (KBr) were recorded on a Perkin Elmer FT-IR spectrometer. GC-EIMS spectra were measured on a Varian SAT2100T/GC3900 spectrometer using ionisation by FAB. Melting points were measured on a Gallenkamp melting point apparatus. Silica gel 60 (Merck) was used for column chromatography separations. TLC was conducted on standard aluminium sheets pre-coated with a 0.2 mm layer of silica gel.

Results and Discussion

The starting material was prepared with the modification on the epibatidine bicyclic ring system by repositioning the nitrogen atom to a methylene group. We carried out the Hetero-Diels Alder reaction of cyclopentadiene and iminium ion generated from ammonium chloride and formaldehyde in the aqueous medium and protected resulted unstable secondary amine with benzoyl chloride to provide (**3**) in good yields [5] (Scheme 38.1).

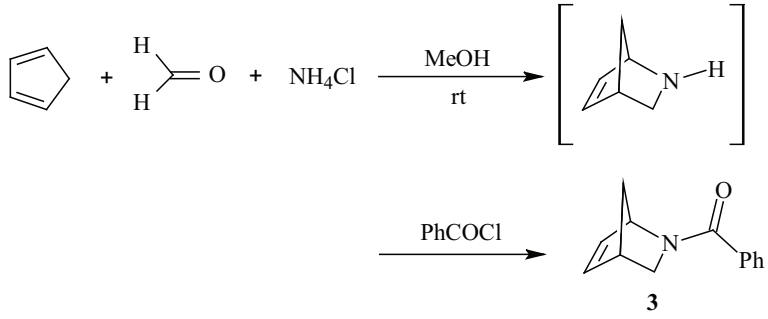

3

Scheme 38.1

Heck reactions, the hydroarylation methodology, has been a key tool in the synthesis of various epibatidine analogues, due to the ability of this approach to address regio- and stereochemistry in substituted azabicyclo ring systems [6].

We continued our work with the reductive Heck and Domino-Heck reactions *[1, 7]* of new bicyclic compound (**3**) by treating it with different aryl- and hetaryl-iodides, as a result a series of new epibatidine analogues were synthesized, continuously separated and purificated by column chromatography on silica gel. Treatment of **3** with iodobenzene, 2-iodothiophene, 1-iodonapthalene and 2-chloro-5-iodopyridine under reductive Heck conditions gave new compounds **4a–d** and **5b**, **5d** as *exo*-regioisomers after chromatographic separations. The reactions with iodobenzene and 1-iodonapthalene gave only 5-*exo*- products. The use of trimethylsilylacetylene under Domino-Heck conditions provided alkynic bicyclic systems **6e** and **f**.

New epibatidine analogues were characterized with the aid of one and two dimensional NMR techniques and IR, GC-MS spectroscopies (Fig. 38.1). All signals in the NMR spectra appeared in pairs due to the presence of rotamers that are resulted from the rotation between the unpaired electrons and benzoyl substituent on the nitrogen atom (Scheme 38.2).

The regioisomers of **4b** and **5b** can be identified obviously from their ^{1}H NMR spectra. For compound **4b** (the red spectrum in Fig. 38.2) the multiplet signal between 3.13–3.19 ppm which is belong to $H5^{n}$ can be seen at 2.08–2.14, in a higher field, as a multiplet again for compound **5b** (the blue spectrum in Fig. 38.2).

For the *exo*-regioisomers of **6e** and **f** resulting from the Domino-Heck reaction were also identified from the HMBC spectra. In the spectrum of **6f**, the interaction of the acetylene carbon (at 103.5 ppm) with the H_1 proton (at 4.24 ppm) was obvious; in the isomer **6e**, an interaction between the phenyl group quaternary carbon (at 139.0 ppm) with the H_1 proton (at 4.40 ppm) was apparent, but in both cases similar effects were not seen in the other isomers.

Conclusions

It has been proven that palladium catalyzed reductive Heck reactions are versatile and high-yield approach for preparing of new bioactive alkaloid epibatidine (**1**) analogues from N-benzoylated 2-aza-bicyclo[2.2.1]hept-5-ene (**3**) and it has been shown that in case of aryl- groups reaction progresses regioselectively. All Heck type reactions proceed *exo*-selectively, leading to the same stereochemistry as found in **1**.

Acknowledgement This research has been supported by the Yıldız Technical University Scientific Research Projects Coordination Department; Project Number: 26-01-02-04.

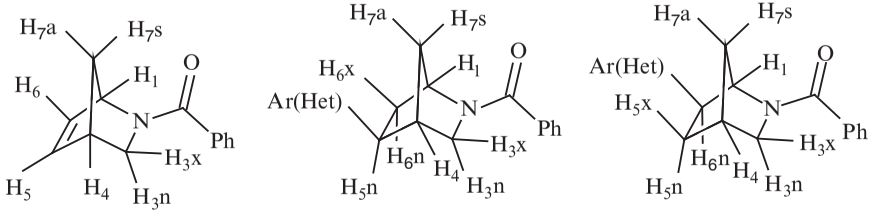

^{1}H NMR data	3	4a	4b	4c	4d	5b	5d	6e	6f
H1	4.46, bs	4.08, bs	4.15, bs	4.55, bs	4.14, bs	4.04, bs	4.16, bs	4.40, bs	4.40, bs
$H3^n$	3.49–3.55, m	3.54–3.64, m	3.59–3.62, dd	3.76–3.82, m	3.52–3.62, m	3.49–3.52, m	3.48–3.52, tt	3.69–3.72, dd	3.69–3.72, dd
$H3^n$	2.90–2.92, dd	3.32–3.36, m	3.23–3.34, m	3.56–3.60, dd	3.33–3.38, m	3.20–3.23, dd	3.19–3.24, dd	3.55–3.57, d	3.55–3.57, d
H4	3.24, bs	2.74, bs	2.72, bs	2.90, bs	2.74, bs	2.72, bs	2.74, bs	2.89, bs	2.89, bs
$H5^n$	6.34–6.36, dd	3.06–3.14, m	3.13- 3.19, m	3.34–3.38, d	3.06–3.15, m	2.08–2.14, m	2.02–2.12, m	3.24–3.31, m	3.24–3.31, m
$H5^x$		–	–	–	–	1.92–1.98, m	1.92–2.00, m	–	–
$H6^x$	6.20–6.22, dd	1.76-1.86, m	1.80–1.89, m	1.93–2.01, m	1.78–2.20, m	–	–	—	–
H6		2.26–2.32, ddt	2.30–2.36, ddt	2.29–2.35, dddd	2.38–2.44, dddd	3.54–3.60, m	3.54–3.58, m	2.19–2.22, d	2.19–2.22, d
$H7^n$	1.56–1.62, dd	1.51–1.70, m	1.58–1.74, m	1.71–1.92, m	1.52–1.70, m	1.52–1.66, m	1.52–1.68, m	1.81–1.89, m	1.81–1.89, m
$H7^s$	1.56–1.62, dd	1.51–1.70, m	1.58–1.74, m	1.71–1.92, m	1.52–1.70, m	1.52–1.66, m	1.52–1.68, m	1.81–1.89, m	1.81–1.89, m
Aromatic protons	7.30–7.45, m	7.08–7.51, m	6.72–7.08, m 7.30–7.46, m	7.11–8.08, md	7.26–7.28, d 7.30–7.49, m 8.22–8.24, d	6.82–7.10, dd 7.28–7.52, m	720–7.40, m 7.41–7.50, dd 8.16–8.18, d	7.06–7.54, m	7.06–7.54, m

Fig. 38.1 ^{1}H NMR Data (δ: ppm) of new epibatidine analogues

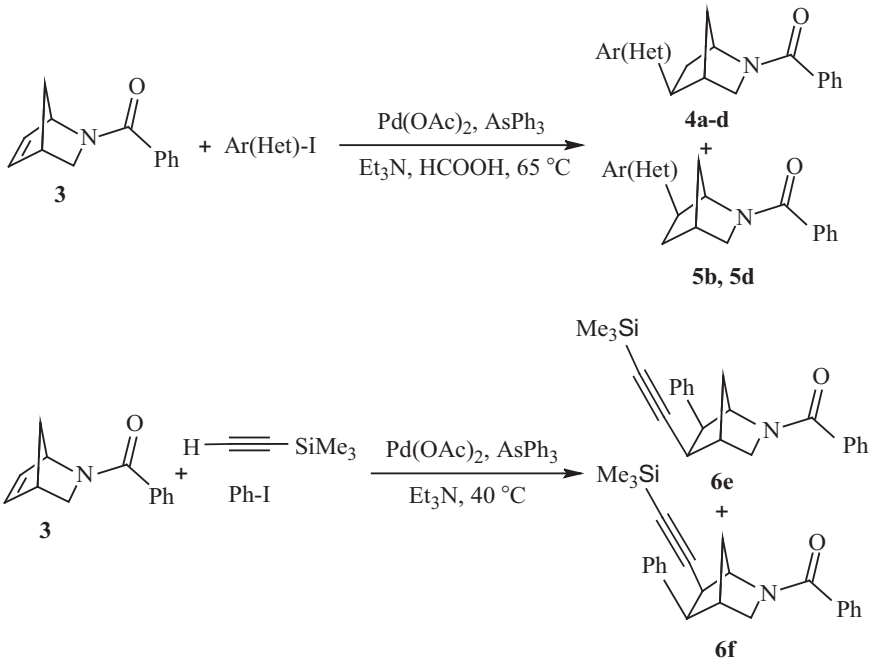

	Ar(Het)-
a	-Phenyl
b	2-Thienyl
c	1-Napthyl
d	6-Chloro-3-pyridyl

Scheme 38.2

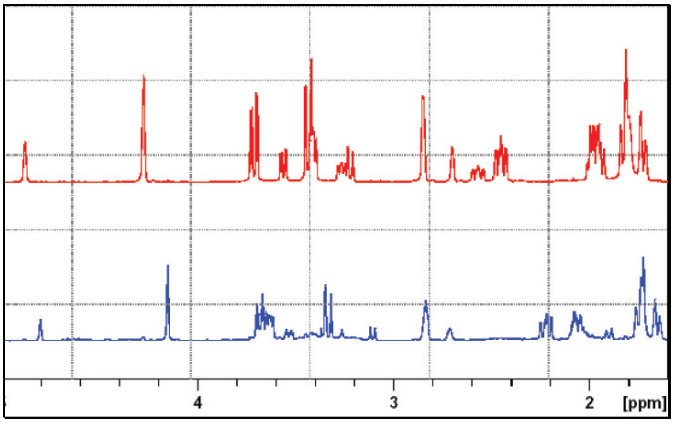

Fig. 38.2 Separation of the isomers (**4b** and **5b**)

References

1. Wei, Z.-L., George, C. and Kozikowski, A.P., 2003, *Tetrahedron Lett.,* **44,** 3847–3850.
2. Spande, T.F., Garraffo, H.M., Edwards, M.W., Yeh, H.J.C., Pannell, L. and Daly, J.W., 1992, *J. Am. Chem. Soc.,* **114,** 3475–3478.
3. Stuhlmann, F. and Kaufmann, D.E., 1999, *J. Prakt. Chem.,* **341,** (5)455–460.
4. Evans, D.A., Scheidt, K.A. and Downey, C.W., 2001, *Org. Lett.,* **3,** 3009–3012.
5. Kasyan, A., Wagner, C. and Maier, M.E., 1998, *Tetrahedron*, 8047–8054.
6. Mitchell, D. and You, H., 2003, *Curr. Opin. Drug Discov. Dev.,* **6** (6),876–883.
7. Krow, G.R., Yuan, J., Huang, Q., Meyer, M.D., Anderson, D.J., Campell, J.E. and Caroll, P.J., 2000, Tetrahedron, 9233–9239.

Chapter 39
Synthesis of 2,4-Disubstituted-3,4-Dihydro-2*H*-Naphth[2,1-e][1,3]Oxazines

Zuhal Turgut, Emel Pelit, and Kadir Turhan

Abstract 2,4-Disubstituted-3,4-dihydro-2*H*-naphth[2,1-e][1,3]oxazines were prepared through the ring-closure reactions of the starting aminonaphthols with substituted aromatic and hetaryl aldehydes.

Keywords Aminonaphthol, biological activity, naphth-1,3-oxazines, ring-closure reactions

Introduction

Developments of synthetic methods for construction of new analogs of bioactive heterocyclic compounds represent a major challenge in synthetic organic and medicinal chemistry. Due to their broad spectrum of biological activities, including analgesic, anticonvulsants, antitubercular, antibacterial and anticancer 1,3-oxazines are an interesting class of compounds for further structural modifications [1–4]. In addition, they can be used as intermediates in the synthesis of N-substituted amino alcohols nitrogen-bridged heterocyclic systems and in enantioselective syntheses of chiral amines. The tautomeric character of the 1,3-O,N-heterocycles offers a great number of synthetic possibilities [5–7].

Cyclization reactions have been realized by using 2-naphthol and various substituted aromatic and hetarylaldehydes in the presence of dry methanolic ammonia and napth-1,3-oxazine derivatives have been obtained [8–10].

Results and Discussion

Condensation of 1-naphthol and hetaryl- or substituted-benzaldehydes in the presence of ammonia, and subsequent acidic hydrolysis, gave **2** in moderate yields. Reactions of amino naphthols with equivalent amounts of aldehydes resulted in

Yıldız Technical University, Faculty of Arts and Sciences, Department of Chemistry, Davutpasa Campus, 34210, Esenler-Istanbul, Turkey

B. Sener (ed.), *Innovations in Chemical Biology*, doi: 10.1007/978-1-4020-6955-0

2,4-disubstituted-3,4-dihydro-2*H*-naphth[*2*,*1*-e][*1*,*3*]oxazines, **3**. In consequence of the close analogy to 1-(α-aminobenzyl)-2-naphthtols, which are known as "Betti Bases", the regiosomeric compounds, **2,** can be referred as to "reverse Betti bases".

The potential utility of the Mannich-type phenolic bases makes the aminoalkylation reaction of naphthol derivatives a subject of current chemical interest. But, because of the relatively low reactivity of 1-naphthol, the reaction gave only a moderate yield and displayed moderate diastereoselectivity [*5*].

The structures of the new compounds were assigned by elemental analysis and FTIR, NMR and MS spectroscopic data (Scheme 39.1).

The ^{1}H NMR spectra of **1a–f** and **3d–c**, **3d–a**, **3d–b**, **3e–b**, **3e–f** proved that, in DMSO solution. Each set of compounds formed three-component ring-chain tautomeric mixtures, containing epimeric naphthoxazines together with the open-chain tautomer. Compounds displayed singlets at δ 5.40–6.32 due to NphCHArNH; 8.41–8.73 due to NH = CHAr.

In the IR spectra of 1,3-oxazines, the characteristic C = O bands of aldehydes disappeared and NH bands appeared in the region of 3,320–3,600 cm^{-1}.

The structures of the obtained new compounds have been confirmed with elemental analysis results.

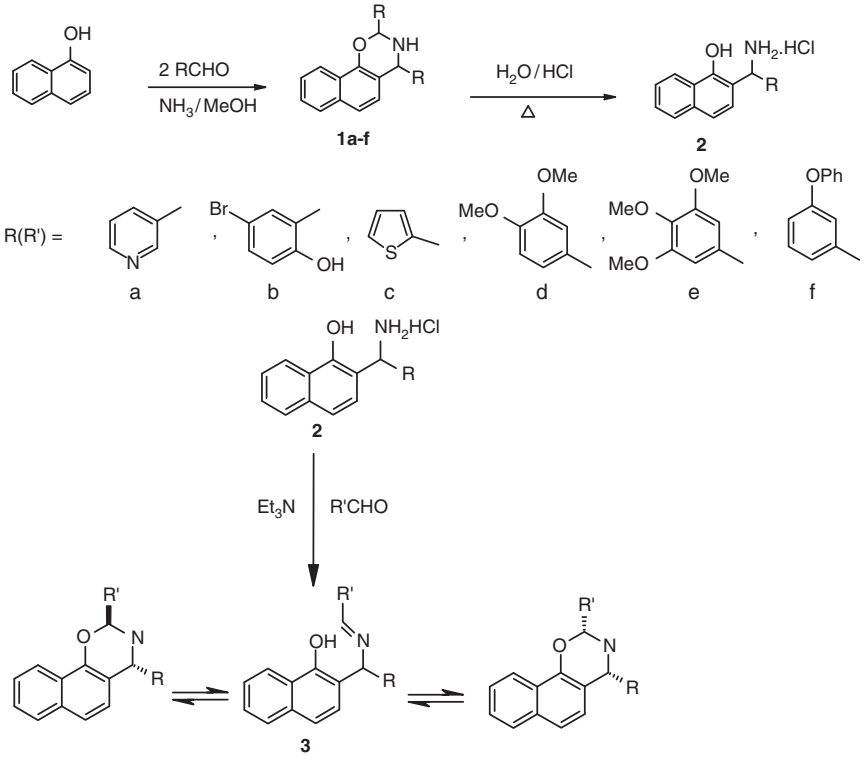

Scheme 39.1 General method for the synthesis of 1,3-oxazines

Conclusion

Substituted amino naphthols were synthesized with reactions of 1-naphthols and the appropriate aldehydes. Some new 2,4-disubstituted-3,4-dihydro-*2H*-naphth [*1,2-e*][*1,3*]oxazines that are expected to show biological activities were obtained by the ring-closure reactions with these aminonaphthols and various aldehydes. In addition, substituted-1,3-amino-hydroxy compounds, **2**, can be used in chiral ligands synthesis.

Experimental

NMR spectra were recorded on Bruker Digital FT-NMR 'Avance 400' spectrometer ($CDCl_3$ solvent) with TMS as internal reference. IR spectra were recorded on Perkin Elmer FT-IR spectrometer (KBr). GC-EIMS spectra were measured on a Varian SAT2100T mit GC3900 spectrometer using ionization by FAB. Melting points were measured on a gallenkamp melting point apparatus. Silica gel 60 (Merck) was used for column separations. TLC was conducted on standard conversion aluminium sheets precoated with a 0.2 mm layer of silica gel. Elemental analyses were performed using Flash EA 1112 series apparatus.

General Method for the Synthesis of 2,4-Disubstituted-3,4-Dihydro-2H-Naphth[2,1e][1,3]Oxazines, 1 a–f

The appropriate aromatic or heteryl- aldehyde (2 mmol; freshly distilled if liquid) and 25% methanolic ammonia solution (5 mL) were added to a solution of 1-naphthol (1 mmol) in absolute MeOH (5 mL).The mixture was left to stand at ambient temperature for 2 days, during which oily products separated. The solvent was evaporated and the crude oily products were purified by column chromatography. The physical data for the compounds **1a–f** are listed Table 39.1.

General Method for the Synthesis of 2,4-Disubstituted-3,4-Dihydro-2H-Naphth[2,1e][1,3]Oxazines, 3

To the oily or crystalline naphthoxazines, **1a–f** (1 mmol) and 20% HCl (20 mL) were stirred and refluxed for 3 hours. The solvent was evaporated and the oily residue was crystallized from EtOAc (10 mL), and the obtained products, **2**, recrystallized from a mixture of MeOH (1 mL) and Et_2O (10 mL).

Table 39.1 Physical data of naphth[2,1-e][1,3]oxazines, **1** and **3**

Compound	Conditions (h, rt)	Product	Yield (%)	Empirical formula
R,' = a	24	1a	63	$C_{22}H_{17}N_3O$
R,' = b	48	1b	51	$C_{26}H_{17}Br_2NO_3$
R,' = c	48	1c	49	$C_{20}H_{15}NOS_2$
R,' = d	48	1d	52	$C_{28}H_{27}NO_5$
R,' = e	48	1e	59	$C_{30}H_{31}NO_7$
R,' = f	48	1f	69	$C_{36}H_{27}NO_3$
2d	48	3d–c	46	$C_{24}H_{21}NO_3S$
2d	48	3d–a	43	$C_{25}H_{22}N_2O_3$
2d	48	3d–b	51	$C_{26}H_{22}BrNO_4$
2e	48	3e–b	49	$C_{27}H_{23}$ $BrNO_5$
2e	48	3e–f	41	$C_{39}H_{22}NO_5$

Et_3N (1.1 mmol) and an equivalent amount of aromatic aldehyde (freshly distilled if liquid) were added to solution of the appropriate aminonaphthol hydrochloride (1 mmol) in absolute MeOH (20 mL). The mixture was left to stand at ambient temperature for 2 days. Oily crude products were purified by column chromatography. The physical data for some of the compounds, **3**, are listed Table 39.1.

Acknowledgement The authors would like to express their gratitude to the Research Foundation of Yıldız Technical University (BAPK. no. 26-01-02-02) for financial support.

References

1. Adib, M., Sheibani, E., Mostofi, M., Ghanbary, K. and Bijanzadeh, H.R., 2006, *Tetrahedron,* **62**(14), 3435–3438.
2. Kurz, T., 2005, *Tetrahedron,* **61,** 3091–3096.
3. Zhang, P., Terefenko, E.A., Fensome, A., Wrobel, J., Winneker, R. and Zhang, Z., 2003, *Bioorg. Med. Chem. Lett.,* **13,** 1313–1316.
4. Poel, H., Guilaumet, G. and Viaud-Massuard, M., 2002, *Tetrohedron Lett.,* **43,** 1205–1208.
5. Cimarelli, C., Mazzanti, A., Palmieri, G. and Volpini, E., 2001, *J. Org. Chem.,* **66,** 4759–4765.
6. Cimarelli, C., Palmieri, G. and Volpini, E., 2001, *Tetrahedron,* **57,** 6089–6096.
7. Dong, Y., Sun, J., Wang, X., Xu, X., Cao, L. and Hu, Y., 2004, *Tetrahedron Asymm.,* **15,** 1667–1672.
8. Smith, H.E. and Cooper, N.E., 1970, *J. Org. Chem.,* **35,** 2212–2215.
9. Szatmari, I., Martinek, T.A., Lazar, L. and Fülop, F., 2003, *Tetrahedron,* **59,** 2877–2879.
10. Szatmari, I., Martinek, T.A., Lazar, L. and Fülop, F., 2004, *Eur. J. Org. Chem.*, 2231–2238.

Chapter 40
Chemical Constituents of *Salvia frigida* Boiss.

Mehmet Dişbudak[1] and Ümit Salan[2]

Abstract The genus *Salvia* L. belongs to the Lamiaceae family, which had 87 species in Turkey, most of which are endemic. Some of these species have been used for a long time in folk medicine. Previous studies on the biological activities of some species showed that some of the chemical constituents possessed antimicrobial, antioxidant, antitumour and antibacterial activities. In our study, we report here the isolation and structure elucidation of chemical compounds of *Salvia frigida* Boiss. through spectral analyses. Plant samples were collected in June 2005 at Keltepe-Turkey. The extracts of *Salvia frigida* Boiss. yielded two oleanane type and two cycloartane type triterpenoids and one royleanone type diterpenoids together with the compounds α-amyrin and β-sitoserol. The structure of the isolated compounds were characterized by UV-vis, IR, 1H NMR, 13C NMR and MS spectroscopy. The structure of the known compounds were also established by comparing their spectral data to those of authentic samples as well as by TLC comparison.

Keywords α-amyrin, diterpenoids, *Salvia frigida*, β-sitoserol, triterpenoids.

Introduction

One of the most interesting genera of shrubs in the mint family (Lamiaceae) is *Salvia*. Worldwide, there are over 700 species in the genus *Salvia*, including the garden sage (*S. officinalis*) native to Europe and Asia Minor. The latter species has been used in medicines from classical Greek times through the Middle Ages. To this day, the dried leaves are a popular cooking herb in the world. Volatile essential oils responsible for the pungent odor of sages include several monoterpenes (pinene, salvene and camphor) and some phenolic compounds.

[1]Istanbul University, Department of Forensic Medicine, İstanbul, Turkey
Marmara University, Faculty of Arts and Sciences, Department of Chemistry, 81040,
[2]Göztepe-İstanbul, Turkey

B. Sener (ed.), *Innovations in Chemical Biology*, doi: 10:1007/978-1-4020-6955-0

Although the genus *Salvia* is placed in the mint family (Lamiaceae), it is listed under Labiatae in older references. The family is typically characterized by flowers with bilabiate (two-lipped corollas), aromatic (mint-like) foliage, opposite leaves and square stems. The flowers typically occur in dense clusters (glomerules) along the main stem axis. By contrast, the sagebrushes (*Artemisia*) have small, rayless heads typical of the sunflower family (Asteraceae). Flowering times vary from cultivar to cultivar, but the best displays are from the second half of summer through to autumn.

Salvia (Labiatae) is a genus which has 87 genus in Turkey, most of which are endemic. *Salvia* species are used as *anipyretic*, *cytotoxic*, *antifungal*, *antibacterial*, *diuretic*, *menstuating*, *stomachic in traditional medicine* in the world [1–3].

Salviafrigida Boiss., perennial herb with a thick woody rootstock. Stems solitary or several, erect, 10–30 (-50) cm, below pilose to villous with sessile glands, densely glandular above with capitate glands. Leaves mostly basal, variable, ovate to narrowly oblong, 2–12 x 1.2–5 cm.

In our study on the chemical constituents of *Salvia frigida* Boiss., we report here the isolation and identification of two oleanane type (compound **1**, **2**) and two cycloartane type triterpenoids (compound **3**, **4**) with the compounds α-amyrin **5** and β-sitoserol **6**. The compounds have been characterized by UV/*vis*, IR, ^{1}H NMR, ^{13}C NMR and MS spectroscopy.

Materials and Methods

General

^{1}H NMR (400 MHz), ^{13}C NMR spectra were recorded on a Varian Mercury-Vx (3000Mx) ve Brucker AC-400L spectrometer using deuterated chloroform solvents and TMS as internal standard. IR spectra were recorded on a Schimadzu Fourier Transform FTIR-8300 instrument. Mass spectra were recorded on a VG Zap spec instrument (1,000 resolution) (the Chemistry of the Turkish Scientific and Research Institue-Gebze).

For the isolation and purification of the compounds TLC: Kieselgel 60F254 (E. Merck) precoated plates. CC: Silicagel 60 and Sephadex LH-20 were used.

Plant Material

Salvia frigida Boiss. is a perennial plant, growing to height of 10–30 (-50) cm with pink flowers. *Salvia frigida* Boiss. was collected in June 2005 from Keltepe-Kocaeli-Turkey. A voucher specimen is deposited in the Herbarium of the Biology Department, University of Marmara.

Extraction and Fractionation

Dried and powdered aerial parts of the plant (500 g) were extracted with actone at room temperature for 24 h. After filtration, the extract was evaporated in vacuo to a small volume. The extract was concentrated by distillation and evaporated to dryness. The residue (16 g) was chromatographed over a silica gel column eluting with on petroleum ether, a gradient of petroleum ether-chloroform, up to chloroform, followed by chloroform-ethylacetate, up to ethylacetate and finally with methanol.

Isolation of the Compounds

The similar fractions were combined and further chromatographed on small columns when necessary. The relevant fractions were further separated and cleaned by preparative TLC. Compounds **1**, **2**, **3**, **4**, **5**, **6** were isolated. They were identified on the basis of ^{1}H NMR, ^{13}C NMR, IR and Mass spectral analysis.

Results and Discussion

Isolated Compounds

I. **Olean-12-ene-3β-28-diol (Erythrodiol)**

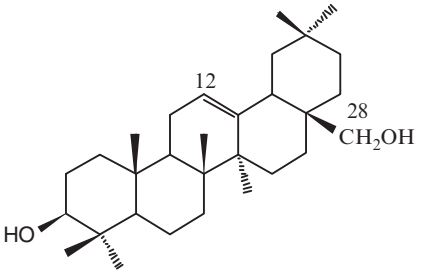

IUPAC name Olean-12-ene-3β-28diol
Molecular formula $C_{30}H_{50}O_2$
Molecular weight 442
Melting point 231–232°C
IR (KBr pellet) $\nu_{max/cm\text{-}1}$ 3,440, 2,933, 2,850, 1,650, 1,639, 1,506, 1,461, 1,382, 1,249, 15, 1,037, 997, 663.

^{1}H NMR ($CDCl_3$) δ 0.80 (3H, s), 0.88 (3H, s), 0.89 (3H, s), 0.94 (3H, s), 0.95 (3H, s), 1.00 (3H, s), 1.18 (3H, s), 3.24 (1H, d, *J* = 11 Hz, H-28a), 3.56 (1H, d, *J* = 11 Hz, H-28b), 5.19 (1H, t, *J* = 3.5 Hz, H-12).

^{13}C NMR ($CDCl_3$) δ 38.5 (C-1), 27.1 (C-2), 78.9 (C-3), 38.7 (C-4), 55.0 (C-5), 18.27 (C-6), 32.4 (C-7), 39.2 (C-8), 47.5 (C-9), 36.8 (C-10), 23.4 (C-11), 122.2 (C-12), 144.0 (C-13), 39.2 (C-14), 25.8 (C-15), 21.9 (C-16), 36.8 (C-17), 42.2 (C-18), 46.3 (C-19), 30.9 (C-20), 34.0 (C-21), 30.8 (C-22), 27.1 (C-23), 15.4 (C-24), 15.5 (C-25), 16.6 (C-26), 25.9 (C-27), 69.6 (C-28), 33.1 (C-29), 23.5 (C-30).

EI MS m/z 442 [M+] $C_{30}H_{50}O_2$

The structure of the compound **1** was also established by comparing their spectral data [4] to those of authentic samples as well as by TLC comparison.

II. **Olean-12-ene-3β-ol**

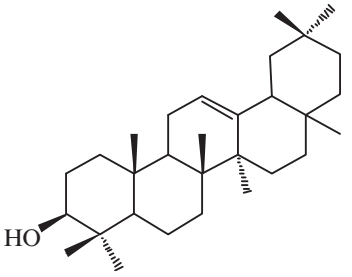

IUPAC name Olean-12-ene-3β-ol

Molecular formula $C_{30}H_{50}O$

Molecular weight 426

Melting point 226–227°C

IR (KBr pellet) $\nu_{max/cm-1}$ 3,433, 2,933, 2,842, 1,647, 1,506, 1,465, 1,377, 1,334, 280, 1,186, 1,097, 1,049, 1,024, 989, 912, 731, 644.

^{1}H NMR ($CDCl_3$) δ 0.78 (3H, s), 0.88 (3H, s), 0.89 (3H, s), 0.94 (3H, s), 0.95 (3H, s), 1.00 (3H, s), 1.28 (3H, s), 3.22 (1H, dd, *J* = 4.5 ve 11 Hz, H-3a), 5.19 (1H, t, *J* = 3.5 Hz, H-3).

III. **24-Methylenecycloartanol**

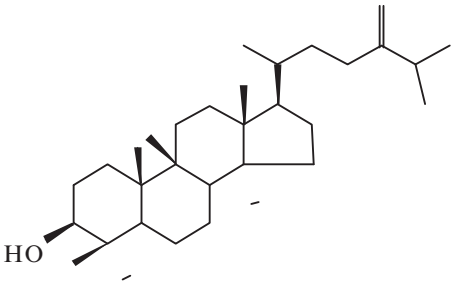

IUPAC name 24-Methylenecycloartanol
Molecular formula $C_{31}H_{52}O$
Molecular weight 440
Melting point 95°C
IR (KBr pellet) $\nu_{max/cm-1}$ 3,388, 2,933, 2,866, 1,679, 1,461, 1,373, 1,282, 1,089, 1,035, 889, 723, 551.
^{1}H NMR ($CDCl_3$) δ 0.35 (1H, d, *J* = 5 Hz, H-19a), 0.55 (1H, d, *J* = 5 Hz, H-19b), 0.89–1.10 (21H, μ, CH3 proton), 3.29 (1H, dd, *J* = 4.5 ve 11 Hz, H-3a), 4.63 (1H, bs, H-31a), 4.70 (1H, bs, H-31b).
^{13}C NMR ($CDCl_3$) δ 34.9 (C-1), 30.4 (C-2), 78.9 (C-3), 40.5 (C-4), 47.2 (C-5), 21.2 (C-6), 28.2 (C-7), 48.0 (C-8), 49.4 (C-9), 26.5 (C-10), 26.0 (C-11), 32.9 (C-12), 45.4 (C-13), 48.0 (C-14), 29.7 (C-15), 26.6 (C-16), 52.3 (C-17), 18.1 (C-18), 29.7 (C-19), 32.9 (C-20), 18.4 (C-21), 35.5 (C-22), 31.4 (C-23), 159.8 (C-24), 33.9 (C-25), 21.4 (C-26), 19.4 (C-27), 18.1 (C-28), 14.1 (C-29), 25.5 (C-30), 106.1 (C-31).

The structure of the compound **3** was also established by comparing their spectral data [5–7] to those of authentic samples as well as by TLC comparison.

IV. **Cycloartanol**

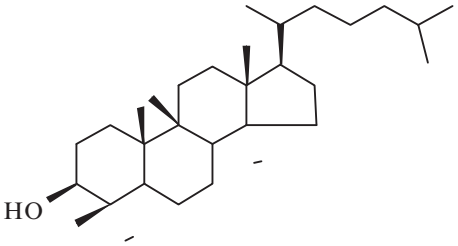

IUPAC name Cycloartanol
Molecular formula $C_{30}H_{52}O$
Molecular weight 428
Melting point 95°C
IR (KBr pellet) $\nu_{max/cm-1}$ 3,387, 2,933, 2,866, 1,679, 1,461, 1,373, 1,282, 1,089, 1,035, 889, 723, 551
^{1}H NMR ($CDCl_3$) δ 0.33 (1H, d, *J* = 5 Hz, H-19a), 0.55 (1H, d, *J* = 5 Hz, H-19b), 0.80 (3H, s, H-29), 0.87 (3H, d, *J* = 6Hz, H-21), 0.88 (3H, s, H-30), 0.89 (3H, s, H-18), 0.98 (3H, s, H-28), 1.01 (6H, d, *J* = 6Hz, H-26 ve H-27), 3.29 (1H, dd, *J* = 4.4 ve 11 Hz, H-3a).
^{13}C NMR ($CDCl_3$) δ 32.18 (C-1), 30.8 (C-2), 79 (C-3), 45.51 (C-4), 52.46 (C-5), 22.40 (C-6), 26.32 (C-7), 48.16 (C-8), 21.31 (C-9), 26.68 (C-10), 27.40 (C-11), 30.60 (C-12), 47.32 (C-13), 49.05 (C-14), 33.12 (C-15), 28.40 (C-16), 52.65 (C-17), 18.25 (C-18), 29.20 (C-19), 35.75 (C-20), 19.52 (C-21), 37.25 (C-22), 25.64 (C-23), 40.70 (C-24), 28.25 (C-25), 22.85 (C-26), 23.10 (C-27), 26.20 (C-28), 14.20 (C-29), 20.20 (C-30).

The structure of the compound **4** was also established by comparing their spectral data [8] to those of authentic samples as well as by TLC comparison.

References

1. Davis, P.H., 1975, *Flora of Turkey and the East Aegean Islands,* Vol. 5, Edinburgh University Press, London.
2. Lin, L-Z., Wang, X-M, Huang, X-L, Huang, Y. and Cordell, G.A., 1989, *Photochemistry,* **28,** 3542–3543.
3. Dobrynin, V.N., Kolosov, M.N., Chernov, B.K. and Derbentseva, N.A., 1976, *Khim. Prir. Soedin.,* **5,** 686–687.
4. Mahato, S.B. and Kundu, A.P., 1994, *Phytochemistry,* **37,** 1517–1575.
5. Teresa, J.D., Urones, J.G., Mrcos, I.S., Basabe, P., Cuadrado, M.J.S., and Fernandez, R., 1987, *Phytochemistry,* **26,** 1767–1776.
6. Kikuchi, T., Kadota, S. and Tsubano, K., 1986, *Chem. Pharm. Bull.,* **34,** 2479–2486.
7. Kolak, U., Topçu, G., Birteksöz, S., Ötük, G. and Ulubelen, A., 2005, *Turk. J. Chem.,* **29,** 177–186.
8. Akihisa, T., Hideshima, R., Koike, K., Kimura, Y. and Nikaido, T., 2000, *Chem. Pharm. Bull.,* **47,** 1157–1160.

Chapter 41
Protease Inhibition and Antioxidant Actions of Some Aqueous *Allium* Extracts

Eugenia Teodor, Wanda Buzgariu, Alexandrina Rugina, Mirela Diaconu, and G.L. Radu

Abstract Garlic and onion (*Allium* sp.*)* have attracted particular attention of modern medicine because of its widespread health use around the world, and the cherished belief that it helps in maintaining good health warding off illnesses and providing more vigor. To date, many favorable experimental and clinical effects of garlic and onion preparations have been reported. These biological responses have been largely attributed to (i) reduction of risk factors for cardiovascular diseases and cancer, (ii) stimulation of immune function, (iii) enhanced detoxification of foreign compound, (iv) hepatoprotection, (v) antimicrobial effect, and (vi) antioxidant effect [1–7]. Beside these, recently was reported the sperm immobilization activity of the aqueous homogenate of garlic and onion extracts [8].

The aim of our work is to evaluate the inhibition effect of some *Allium* extracts on acrosin and trypsin, comparatively with antioxidant effect and cytotoxicity of extracts.

The methods used were acrosin proteolytic activity (APA) assay (with gelatin) and acrosin activity assay with N-α-benzoyl-DL-arginine-p-nitroanilide (BAPNA)-Triton X 100, and BAPNA assay for trypsin activity [9–11]. The antioxidant activity was tested spectrometrical with $ABTS^{+}$ [12]. Cytotoxicity of extracts was determined by MTT Cell Proliferation Assay [13].

The experiment with 0.5 g/mL of crude extracts of different parts of *Allium* plants (bulb, green leaf, white stalk) showed the inhibition of acrosin and trypsin activities, mostly the red onion and garlic extracts. These results demonstrated that spermicidal effect of *Allium* extracts is determined also by their capacity of protease inhibition. The red onion extract shows the higher antioxidant capacity and a very low cytotoxicity.

Keywords *Allium* extracts, antioxidant capacity, cytotoxicity, garlic, protease inhibition

National Institute of Research and Development for Biological Sciences, Center for Bioanalysis, 296, Spl. Independentei Bucharest, Romania

B. Sener (ed.), *Innovations in Chemical Biology*, doi: 10.1007/978-1-4020-6955-0

Introduction

The *Allium* genus includes approximately 500 species, the most widely used of which are onions (*Allium cepa*), garlic (*Allium sativum*), leeks (*Allium porrum*), chives (*Allium schoenoprasum*), and shallots (*Allium ascalonicum*). Garlic and onion (*Allium* sp.*)* have attracted particular attention in modern medicine because of their widespread use around the world and the cherished belief that it helps in maintaining good health, warding off illnesses, and providing more vigor. To date, many favorable experimental and clinical effects of garlic and onion preparations have been reported. These biological responses have been largely attributed to (i) reduction of risk factors for cardiovascular diseases and cancer, (ii) stimulation of immune function, (iii) enhanced detoxification of foreign compound, (iv) hepatoprotection, (v) antimicrobial effect, and (vi) antioxidant effect [1–7]. Beside these the sperm immobilization activity of an aqueous homogenate of garlic and onion extracts was reported recently [8].

Organosulfur compounds present in *Allium* vegetables, which are either lipid or water soluble, are considered responsible for the beneficial effects of these herbs. Garlic derivatives generally have a thioallyl moiety, whereas onion extracts contain a thiopropyl group with somewhat different chemical properties [14].

Acrosin is present in mammalian spermatozoa [15], and has been identified as a serine proteinase with substrate specificity and inhibitor sensitivity similar to that of trypsin [16]. It is an important proteolytic enzyme capable of hydrolyzing the zona pellucida (ZP) in oocytes, and plays a vital role in the process of fertilization. Inhibition of proteolytic activity is generally employed for two purposes: (i) for the prevention of unwanted degradation of proteins during their isolation and characterization, and (ii) to study regulatory aspects of specific proteolytic events as they relate to cellular processes. Some of the most studied proteolytic-related processes include the blood coagulation and complement cascades, hormonal regulation, apoptosis, extracellular matrix degradation, proteasome and lysosomal regulation, and disease states such as Alzheimer's and viral replication [17–20].

The aim of this work was to evaluate the inhibition effect of some *Allium* aqueous extracts on acrosin and trypsin activities, a new aspect in the wide spectrum of *Allium* compound activities. The antioxidant capacity, probably responsible for antithrombosis and antitumoral effects, was determined for different parts of *Allium* plants (bulb, green leaf, white stalk). The toxicity of crude extracts was also determined.

Materials and Methods

Fresh plant materials, *Allium sativum* (bulb and green), *Allium cepa rubra* (bulb) and *Allium cepa* (bulb and green), were homogenized separately in physiological saline (pH 7.4). Homogenates were centrifuged at 10,000 *g* at 4°C for 30 min.

Boar semen was kindly supplied by ROMSUIN Peris. All other chemicals and reagents were of the highest quality commercially available.

Acrosin Assay

The methods used were acrosin proteolytic activity (APA) assay (with gelatin) and acrosin activity assay with *N*-α-benzoyl-DL-arginine-*p*-nitroanilide (BAPNA)-Triton X 100. The method based on *Kennedy assay* [10, 21] has been developed to assess total acrosin activity (acrosin and activable proacrosin). To perform the test, liquefied semen is centrifuged over Ficoll, the washed sperm pellet is suspended in a detergent (Triton X-100)-substrate (BAPNA) buffer, pH. 8.0, and the amidase activity is determined spectrometrically (410 nm) after a 3 h incubation period. Amidase activity can be inhibited with benzamidine, indicating that the activity is primarily or entirely due to acrosin. One IU of acrosin activity was defined as the substrate amount that hydrolyzed 1.0 μmol/min of BAPNA at 24°C according to the formula: acrosin activity (μIU)/10^6 sperm) = (OD_{obs} – $OD_{control}$) x 10^6/(1,485 x spermatozoa number)

Acrosin proteolytic activity Proteolytic activity of individual spermatozoa was determined using a gelatin substrate film assay following the procedure described by Liu and Baker [9]. Gelatin substrate film slides were prepared on one side of glass slides with a 5% gelatin solution. Boar spermatozoa treated with or without *Allium* extracts for 1 h were spread on the surface of gelatin-coated slides and incubated at 37°C to allow proteolysis of the gelatin by acrosin. At intervals, the slides were observed by phase contrast microscopy. Formation of a clear halo around the sperm head indicated acrosin proteolytic activity.

Trypsin inhibition The ability of the various trypsin inhibitors (*Allium* extracts) to prevent trypsin hydrolysis of BAPNA is measured spectrophotometrically (405 nm, ε = 9.96 cm^2 μmol^{-1}) [11] at 25°C, with a Jasco UV-Vis spectrometer by time course measurement of ΔAbs. One trypsin unit hydrolyzes 1.0 μmol of *N*-*α*-benzoyl-DL-arginine *p*-nitroanilide (BAPNA) per minute at pH 7.8 and 25°C and one Trypsin Inhibitor Unit (TIU) will decrease the activity of 2 trypsin units by 50%.

In vitro *Antioxidant capacity* was measured by the method of Trolox equivalent antioxidative capacity (TEAC) [12]. The TEAC assay used 20 μL of the extract sample mixed with a 980 μL solution of $ABTS^{*+}$ [2.2′-azobis-(3-ethylenebenzothiazoline-6-sulfonic) acid], the decolorization of $ABTS^{*+}$, which is a long-life radical cation and blue-green chromophore, measured at 734 nm. Results are expressed as millimoles of Trolox equivalent per kilograms of fresh weight.

Cytotoxicity of extracts was determined by MTT Cell Proliferation Assay [13], a quantitative, convenient method for evaluating a cell population's response to external factors, whether it be an increase in cell growth, no effect, or a decrease in growth due to necrosis or apoptosis.

The MTT method is simple, accurate and yields reproducible results. The key component is (3-[4,5-dimethylthiazol-2-yl]-2,5-diphenyltetrazolium bromide) or MTT. Mitochondrial dehydrogenases of viable cells cleave the tetrazolium ring, yielding purple formazan crystals insoluble in aqueous solutions. The crystals are dissolved in acidified isopropanol. The resulting purple solution is measured spectrophotometrically. An increase or decrease in cell number results in a concomitant

change in the amount of formazan produced, indicating the degree of cytotoxicity caused by the test material.

MTT test was done after 3 days on tumor cells (cell line established from a glioblastoma multiform grade IV in our laboratory and named T11, 20–25 passage) and Vero cells (from the *Vero* lineage derived from epithelial cells of kidney from African green monkey, 20–25 passage), cultured with different concentrations of 0.5 g/mL *Allium* extracts (0.1–10%). Cell suspension was obtained by subconfluent culture trypsinization and was seeded into 24-well plates; each well was seeded with 3 x 10^4 cells /mL. Cells were cultured 24 h in Dulbecco's modified Eagles medium/10% FBS (DMEM) and after standing overnight the culture medium was replaced with plant extract medium.

The supernatant was replaced after 3 days of exposure of cells (tumor and normal) to plant extracts and the cells were washed with PBS, then 500 μL MTT solution (0.25 mg/mL) was added to each well. The cells were washed after 3 h of incubation at 37^0C, the formazan crystals formed in living cells solubilized with 1 mL isopropanol, and the absorbance measured at 570 nm with a Jasco UV-Vis spectrometer. Cell viability was expressed as a percentage of control treated with different concentrations of plant extracts.

Results

The values of *acrosin activity* obtained by the method based on the *Kennedy* et al. *assay* are summarized in Table 41.1. The boar semen (~6.5 x 10^6 spermatozoa/mL) was treated, or not, with plant extract (0.5 g/mL) and the inhibition of acrosin activity indicates the spermicidal effect of plant extracts, about 50% for red onion extract and 25% for garlic extract, for instance.

The micrographs obtained with *APA assay* show that treated spermatozoa with *Allium* extracts had low acrosin activity, especially the slides treated with garlic (Fig. 41.1a) and red onion extracts (data not shown). The untreated spermatozoa had protein-digested halos generated by acrosin activity on the gelatin substrate films (Fig. 41.1b).

Table 41.1 Values of acrosin activity for untreated semen and *Allium* extracts treated semen

	Untreated semen	Treated semen		
Acrosin activity (μ Ul/10^6 spermatozoa)	Sperm/PBS (1:0.1)	Sperm/red onion extract (1:0.1)	Sperm/onion extract (1:0.1)	Sperm/garlic extract (1:0.1)
	257.60 ± 23/10^6 sperm	134.75 ± 16/10^6 sperm	206.35 ± 19/10^6 sperm	199.30 ± 34/10^6 sperm

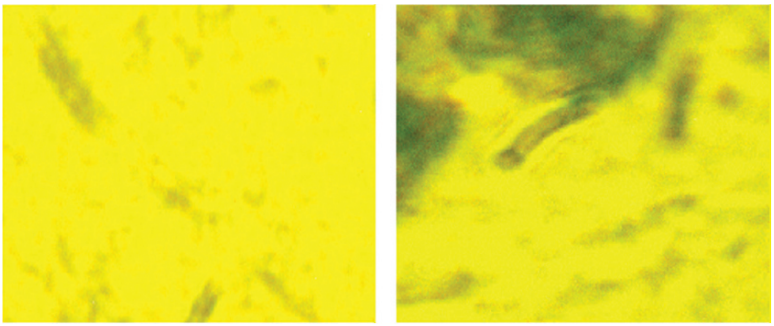

Fig. 41.1 Micrographs of boar spermatozoa treated with *Allium* extracts (0.5 g/mL): (a) garlic bulb extract, (b) untreated spermatozoa. Formation of a clear halo around the sperm head indicated acrosin proteolytic activity

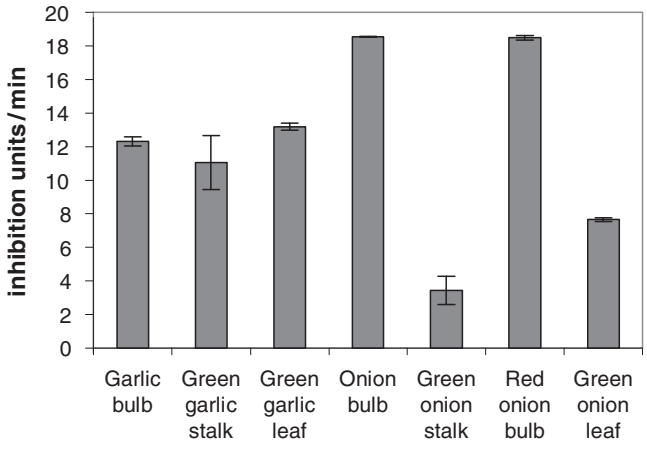

Fig. 41.2 Inhibition activities of plant extracts on trypsin activity (mean value ± SD)

Trypsin inhibition activity was determined by measuring the decrease of trypsin activity in the presence of *Allium* extracts. The results obtained with different types of extracts (bulb, stalk, green leaf – 0.5 g/mL) are presented in Fig. 41.2. All determinations were carried out in triplicate. The higher inhibition activity was obtained with red onion bulb extract (18.55 ± 0.14 UI/min or 27.94 ± 0.21 U/g fresh plants). Onion bulb extract shows also a high trypsin inhibition (18.48 ± 0.035 UI/min, 27.83 ± 0.053U/g), and all extracts of garlic (bulb, leaf and stalk) show activities between 11.05 ± 1.615 – 13.185 ± 0.205 UI/min (16.64 ± 2.42 – 19.86 ± 0.31 U/g).

The *in vitro antioxidant capacity* was measured at 2, 4 and 6 min in duplicate. The results presented in Fig. 41.3 are obtained at 4 min (the best correlation coefficient for △Abs calculation, data not shown) and Trolox equivalents were calculated

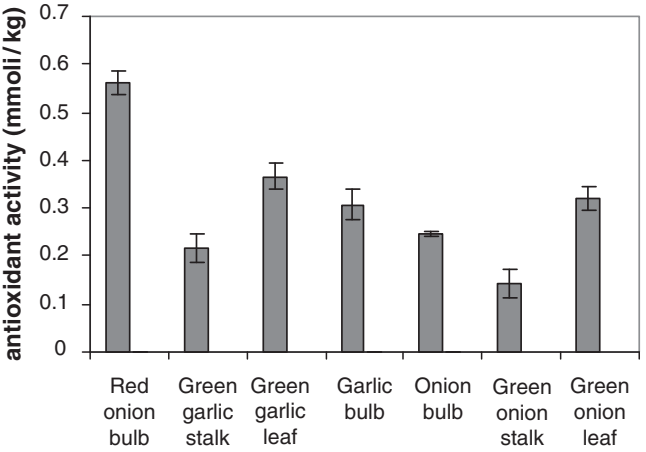

Fig. 41.3 Antioxidant activities of plant extract (mean value ± SD)

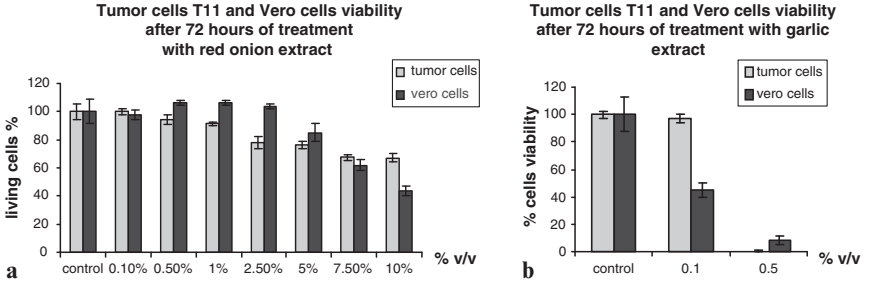

Fig. 41.4 Cytotoxicity induced by different concentrations of 0.5 g/mL: (a) red onion and (b) garlic bulb extract (0.1–10%) (v/v) from the initial 0.5 g/mL culture medium; mean value ± SD). The absorbance at 570 obtained for control was considered 100%. The results for the treated cells were expressed as percentage from the control, untreated culture

using formula y = 0.0067 x + 0.004. The red onion extract showed the higher antioxidant capacity, 0.562 ± 0.025 mmol TE/kg fresh weight while the green leaves from garlic and onion showed a good antioxidant capacity, of 0.367 ± 0.028 mmol/kg and 0.322 ± 0.025 mmol/kg, respectively.

The tests for *in vitro* biocompatibility were performed on normal cells (Vero) and tumor cells (glioblastoma). No cytotoxicity was detected in cells (normal or tumor) cultured with red and white onion extracts at low concentrations (between 0% and 1%), the cell viability being around 90%. At higher concentration, the viability decrease slowly at 80% (Fig. 41.4a). On the other hand, garlic extracts induce toxicity both on normal and tumor cells at very low concentrations (Fig. 41.4b).

Discussion

The majority of the studies about the benefits of *Allium* components have been done with nonaqueous extracts. In our study, only water-soluble components are responsible for the biological effects observed. On the other hand, garlic extracts are considered the most efficient for biomedical effects. In our experiments with 0.5 g/mL of crude aqueous extracts of different parts of *Allium* plants (bulb, green leaf, white stalk), the red onion bulb extract showed the highest inhibition of acrosin and especially trypsin activity. The acrosin inhibition was reported regarding with spermicidal effect of garlic [8], but the protease inhibition has not been reported before in relation to the clinical effects of these plants.

These results demonstrate that the spermicidal effect of *Allium* extracts is determined by their capacity to inhibit proteases, *and these plants actually contain a protease inhibitor*. The clear inhibition of trypsin should encourage the use of these extracts to investigate others known effects of great importance in medicine (treatment HIV infections, hepatitis, pancreas illness, lunge affections, sterility) and in biotechnology (purification of protease by affinity chromatography) as well as leading to potent new sperm immobilizing agents as possible male oral contraceptives.

The red onion extract show the highest antioxidant effect. There have been reports on the distribution of antioxidant components, including sulfur compounds and flavonoids, in *Allium* vegetables [22, 23]. In aqueous extracts, sulfur compounds are mostly responsible for antioxidant activity. The green part of plants showed a good antioxidant activity while the bulbs had a good protease inhibition activity. All the onion extracts were devoid of toxicity, but garlic extracts are very toxic for cells, even tumor cells or normal cells, a fact which might explain the highest spermicidal effect of garlic extracts.

Organosulfur compounds have been shown to modulate the activity of glutathione *S*-transferases (GST), a family of enzymes important in detoxification of carcinogens [24], and cytochromes P450 (CYP), a family of enzymes that activate many chemical carcinogens in experimental animals [25]. The effect of proteases inhibition is a new aspect of the biological activity of these plants and further research should be carried out to identify the specific compounds from *Allium* or *Allium* products that are responsible for this biochemical effect.

Acknowledgement The research was supported by Biostar Grant no. PN 06-400106/2006

References

1. Banerjee, S.K. Maulik, S.K., 2002, *Nutr. J.,* **1,** 4.
2. Fleishchauer, A.T. Arab, L., 2001, *J. Nutr.,* **131,** 1032S–1040S.
3. Yu-Yan, Yeh and Liu, L., 2001, *J. Nutr.,* **131,** 989S–993S.
4. Makheja, A.N. Bailey, J.M., 1990, *Agents Actions,* **29,** 360–363.
5. Sheen, L.Y., Li, C.K., Sheu, S.F., Meng, R.H.C. and Tsai, S.J., 1996, *Food Chem. Toxicol.,* **34,** 971–978.

6. Barnett, K.S., Bolduc, E.D. and Klein, G.R., 1993, *Pediatr. Infect. Dis., J.,* **12**(7), 613–614.
7. Imai, J., Ide, N., Nagae, S., Moriguchi, T., Matsuura, H., Itakura, Y., 1994, *Planta Med.,* **60,** 417–420.
8. Chakrabarti, K., Pal, S. and Bhattacharyya, A.K., 2003, *Asian J. Androl.,* **5,** 131–135.
9. Liu, D.Y. and Baker, G., 1993, *Biol. Reprod.,* **48,** 340–348.
10. Kennedy, W.P., Kaminski, J.M., Van der Ven, H.H., Jeyendran, R.S., Reid, D.S., Blackwell, J., Bielfeld, P. and Zaneveld, L.J., 1989, *J. Androl.,* **10**(3), 221–231.
11. Kassell, B., 1970, *Methods Enzymol.,* **XIX,** 844–852.
12. Pellegrini, R. et al., 1999, *Methods Enzymol.,* **299,** 379–389.
13. Mosmann, T., 1983, *J. Immunol. Methods,* **65,** 55–63.
14. Block, E., 1985, *Sci. Am.,* **252,** 94–99.
15. Morton, D.B., 1977, (Barrett, A.J., ed.), Amsterdam, In *Proteinases in Mammalian Cells and Tissues* North-Holland, pp 445–500.
16. Schleuning, W-D., Hell, R. and Fritz, H., 1976, *Z. Physiol. Chem.,* **357,** 207–212.
17. Buhling, F., Groneberg, D. and Welte, T., 2006, *Curr. Drug Targets,* **7**(6), 751–759.
18. Walli, R., Herfort, O., Michl, G.M., Demant, T., Jager, H., Dieterle, C., Bogner, J.R., Landgraf, R. and Goebel, F.D., 1998, *AIDS,* **12,** F167–F173.
19. Grigem, S., Fischer-Posovszky, P., Debatin, K.M., Loizon, E., Vidal, H. and Wabitsch, M., 2005, *Horm Metab Res.,* **37**(10), 602–609.
20. Beher, D. and Graham, S.L., 2005, *Expert. Opin. Investig. Drugs,* **14**(11), 1385–1409.
21. Cui, Y-H., Zhao, R-L., Wang, Q. and Zhang, Z-Y., 2000, *Asian J. Androl.,* **2,** 229–232.
22. Sakakibara, H., Honda, Y., Nakagawa, S., Ashida, H. and Kanazawa, K., 2003, *J. Agric. Food Chem.,* **51,** 571–581.
23. Higuchi, O., Tateshita, K. and Nishimura, H., 2003, *J. Agric. Food Chem.,* **51,** 7208–7214.
24. Sparnins, V.L., Mott, A.W., Barany, G. and Wattenberg, L.W., 1986, *Nutr. Cancer,* **8,** 211–215.
25. Reicks, M.M. and Crankshaw, D.L., 1996, *Nutr. Cancer,* **25,** 241–248.

Chapter 42
Synthesis and Characterization of Novel Zn(II) Dimeric Phthalocyanines

Şaziye Abdurrahmanoğlu, Mustafa Bulut, and Özer Bekaroğlu

Abstract Starting with tetracyanodibenzo(1,4,7,10-tetrathia-(12-crown-4)) **(1)** and 4-nitro-1,2-dicyanobenzene **(2)**, nitro-substituted dimeric phthalocyanine **(3)** was synthesized. In the second step, using hydrazine hydrate as a reductant, amine-substituted dimeric phthalocyanine **(4)** was synthesized from nitro-substituted dimeric phthalocyanine. Structrures of all synthesized compounds were determined by elemental analyses, UV/vis, ^{1}H-NMR and IR spectroscopy.

Keywords Amine, dimeric, nitro, phthalocyanine

Introductıon

The design of novel substituted phthalocyanines closely follows the requirements of their intended applications. Phthalocyanines, in particular their readily soluble peripherally substituted derivatives, possess a wide range of chemical and physical properties that make them interesting building blocks for a number of applications and new materials [1]. Among these properties are the presence of highly conjugated π-electron systems, high absorptivity in the near-IR region, the ability to exhibit varying conductivity upon doping, and photocatalitic effects [2]. The importance of phthalocyanines in many fields including chemical sensors, solar cells, electrochromism, batteries, photodynamic therapy, semiconductive materials and liquid crystals is increasing rapidly as a result of newly-synthesized compounds. Various strategies have been promulgated in efforts to achieve products with different substituents on each of the benzo units. Although at first glance it appears possible to obtain asymmetrically substituted phthalocyanines by cyclotetramerization of a mixture of two or more phthalonitrile derivatives with different substituents, isolation of each isomer is hardly possible, and the yield of the desired product

Marmara University, Department of Chemistry, 34722 Göztepe-İstanbul, Turkey

B. Sener (ed.), *Innovations in Chemical Biology*, doi: 10.1007/978-1-4020-6955-0

could be very low. Some unsymmetrical structures have been acquired by making use of the boron subphtalocyanines *[3a, b]*. Many binuclear phthalocyanine have been synthesized and various properties have been reported in last decade [4]. In the our previous study, starting from a tetracyano compound with 12-membered dioxa-dithia macrocycles in which oxygen and sulphur atoms are diagonally positioned, it has been possible prepared either polymeric or dimeric pthalocyanines over iminoisoindoline compounds with subphthalocyanine *[5a, b]* and statistically mixed method *[6a, b]*.

The aim of this study is to synthesize of binuclear octaphthalocyanine and dimeric phthalocyanines. For this purpose, nitro-substituted dimeric phthalocyanine **3** using **1** and **2**. In the second step, using hydrazine hydrate as a reductant, amine-substituted dimeric phthalocyanine **4** was synthesized from nitro-substituted dimeric phthalocyanine **3**.

Experimental

All chemicals used were of reagent grade. All solvents were dried and purified as described by Perrin and Armarego [7]. The solvents were stored over molecular sieves. Soluble derivatives with eight alkylthio substituents have been synthesized through cyclotetramerization of 4,5-bis(hexylthio)phththalonitrile which has been prepared directly from the 4,5-dichloro compound with hexanethiol [8]. 4-nitrophthalonitrile **2** was synthesized by the method described previously in literature [9]. The progress of the reactions was monitored by thin layer chromatography (TLC).

Elemental analyses were performed on a LECO CHNS 932 instrument. ^{1}H-NMR spectra were determined with a Varian UNITY INOVA 500 MHz NMR spectrometer. IR spectra were recorded as KBr disks in the range of 400–4000 cm^{-1} on a SHIMADZU FTIR-8300 spectrometer. The electronic absorptions spectra were measured in DMSO for **3, 4** with a UNICAM UV2-100 UV/VISIBLE spectrometer.

[5'-6'-Bis(17',25',32'-trinitro-phthalocyaninyl) (1,4,7,10-tetrathia-12-crown)dizinc(II)] (3)

A mixture of tetracyanodibenzo-[1,4,7,10-tatrathia-12-crown] **(1)** (0.050 g, 0.115 mmol), 4-nitrophthalonitrile **(2)** (0.150 g, 0.690 mmol) and zinc(II) acetate (0.050 g, 0.230 mmol) was refluxed in amyl alcohol under argon for 6 h (Scheme 42.1). The reaction mixture was cooled down to room temperature and precipitated by adding methanol. After filtration, the product was washed with methanol, chloroform and acetone. This compound was soluble in tetrahydrofuran (THF), dimethylformamide (DMF) and dimethylsulfoxide (DMSO).

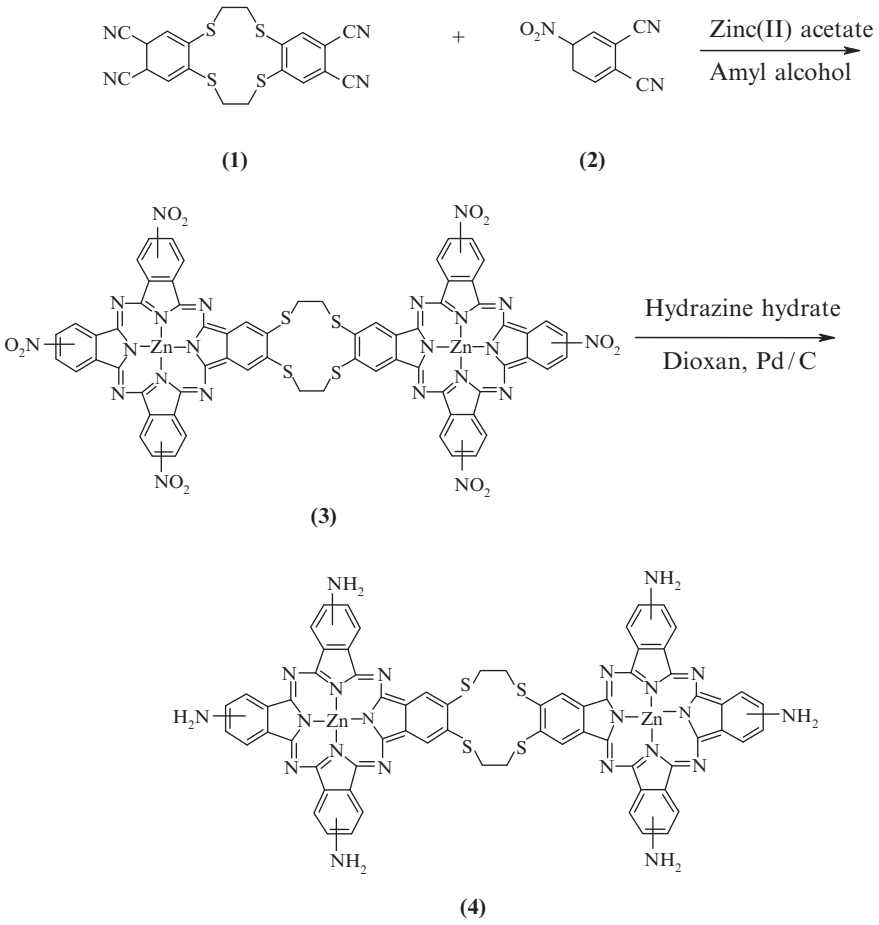

Scheme 42.1 Synthesis of Zn(II) dimeric phthalocyanines 3 and 4

Yield: 55 mg (30%). UV-vis (DMSO, λmax/nm (log ε)) 337 (5.090), 430 (sh) (4.080), 642 (sh) (4.610) and 682 (4.77); ^{1}H-NMR (400 MHz/DMSO) δ: 3.36 (s, 8H, CH_2), 7.75–8.25 (m, 22H, ArH); IR (KBr pellet) ν cm^{-1}: 3060, 2983, 2923, 2858, 1620, 1523, 1344, 1260, 1090, 902, 742; Found (%): C, 51.72; H, 1.70; N, 19.49; S, 7.95. Calc. for $C_{68}H_{30}N_{22}S_4O_{12}Zn_2$ (%): C, 51.56; H, 1.84; N, 19.55; S, 8.04.

[5,6,5',6'-Bis(17',25',32'-trisamino-pthalocyaninyl) (1,4,7,10-tetrathia-12-crown)dizinc (II)] (4)

A mixture of **3** (0.030 g, 0.019 mmol), hydrazine hydrate (8 mL) and catalytic amount of 10% Pd/C was refluxed in dry dioxan (30 mL) under argon atmosphere

for 24 h (Scheme 42.1). The reaction mixture was cooled and quickly suction filtered. The filtrate evaporated to dryness under vacuum and washed with methanol, THF and acetone. Dark green product was dried in vacuum. This compound is soluble in DMF and DMSO. Yield: 21.2 mg (79%). UV-vis(DMSO, λmax/nm (log ε) 358 (4.952), 643 (4.710) and 716 (4.897); ^{1}H-NMR (400 MHz/ DMSO) δ: 3.36 (s, 8H, CH_2), 7.75–8.25 (m, 22H, ArH); IR (KBr pellet) ν, cm^{-1}: 3,447, 3417, 3060, 2983, 2923, 2858, 1620,, 1560, 1540, 1420, 1344, 1260, 1090, 902,742; Found (%): C, 58.01; H, 2.79; N, 21.60; S, 9.18. Calc. for $C_{68}H_{42}N_{22}S_4Zn_2$ (%): C, 57.79; H, 2.97; N, 21.81; S, 8.36.

Results and Discussion

Initial compounds tetracyanodibenzo(1,4,7,10-tetrathia-(12-crown-4)) **1**, 4-nitro-1,2-dicyano benzene and 4,5-bis(hexylthio)phthalonitrile were available from earlier study. Nitro-substituted dimeric Co(II) phthalocyanine **3** was prepared by reaction of tetracyanodibenzol-(1,4,7,10-tetrathia-(12-crown-4)) **1**, 4-nitro-1,2-dicyanobenzene **2** and zinc(II) acetate in amyl alcohol.

Peripheral nitro substituents on the Pc offer a number of possibilities to obtain reactive binding sites, such as reduction to an amine. For this purpose, hydrazine hydrate is used as the reductant.

The IR spectra of both **3** and **4** taken with the KBr pellets. The stretching peaks at 2983, 2858 cm^{-1} confirmed the presence of –CH respectively for compounds **3**and **4**. The stretching peaks at around 1523–1344 cm^{-1} in the spectrum of **3** indicated the presence of a $–NO_2$ group that disappeared in case of the amine-substituted pc **4**. The presence of $–NH_2$- in the structure of **4** was observed at 3447–3417 cm^{-1}. The C-S-C ether chain was characterized by the an absorption at 1,090 cm^{-1} for all dimeric compounds.

The UV-Vis absorption spectra of the phthalocyanine system exhibited characteristic Q and B bands. All of them showed typical electronic spectra with two strong absorption regions, one in UV region at about 330 nm (B band) which attributed the transitions from the deeper π levels to LUMO. The other band was observed in visible region at 670–720 nm (Q band) with a weaker satellite band around 600–650 nm [10] which indicated the aggregation. The characteristic Q band for all compounds was ascribed to the π-π* transition from highest occupied molecular orbital (HUMO) to the lowest unoccupied molecular orbital (LUMO). The band broadening that accompanies the exciton (or Davydon coupling) effects changes the visible region (Fig. 42.1). In the spectra of **3** and **4**, Q bands shift from 682 to 716 nm. This is because the electron-donating ability of amino group [11].

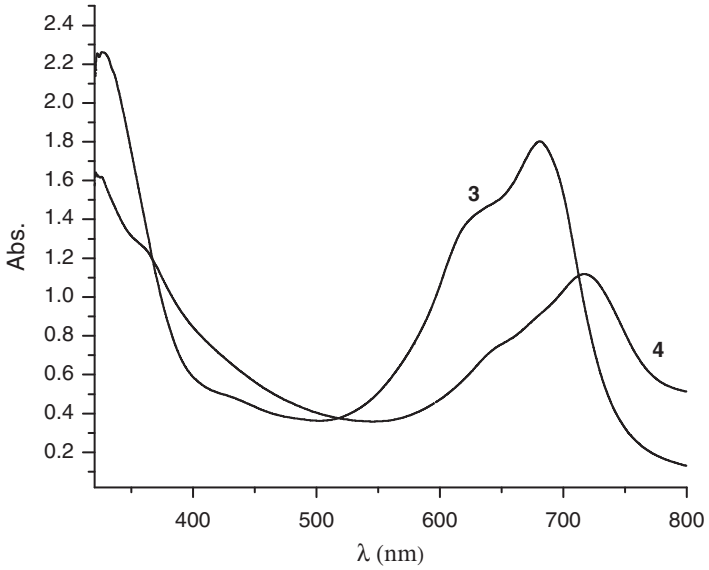

Fig. 42.1 UV/VIS spectra of 3 and 4

References

1. Nicholson, M.M., 1993, C.C. Leznoff and A.B.P. Lever, eds. In *The Phthalocyanines Properties and Applications* Vol. 3, VCH, New York, pp 76–117.
2. Schultz, H., Lehman, H., Rein, M. and Hanack, M., 1991, *Struct. Bond.,* **74,** 41–146.
3. (a) Musluoğlu, E., Gürek, A., Ahsen, V., Gül, A. and Bekarğlu, Ö., 1992, *Chem. Ber*., **125,** 2337–2339.
   (b) Dabak, S., Gül, A. Bekaroğlu, Ö., 1994, *Chem. Ber.,* **127,** 2009–2012.
4. Zhang, Y.J., Li, Y., Liu Q., Jin, J., Ding, B., Song, Y., Jiang, L., Du, X., Zhao, Y. and Li, T.J., 2002, *Synth. Met.,* **128,** 43–46.
5. (a) Gürek, A.G. and Bekaroğlu, Ö., 1997, *J. Porphyr. Phthalocyan.,* **1,** 67–76.
   (b) Gürek, A.G. and Bekaroğlu, Ö., 1997, *J. Porphyr. Phthalocyan.,* **1,** 227–237.
6. (a) Abdurrahmanoğlu, Ş., Altındal, A., Özkaya, A.R., Bulut, M. and Bekaroğlu, Ö., 2004, *Chem. Commun.*, 2096–2097.
   (b) Abdurrahmanoğlu, Ş., Özkaya, A.R., Bulut, M. and Bekaroğlu, Ö., 2004, *Dalton Trans.,* **23,** 4022–4029.
7. Perrin, D.D. and Armarego, W.L.F., 1980, *Purification of Laboratory Chemicals*, 2nd ed. Pregamon, Oxford.
8. Dabak, S. and Bekaroğlu, Ö., 1997, *New J. Chem.,* **21,** 267–271.
9 Young, J.G. and Onyebuago, W., 1990, *J. Org. Chem.,* **55,** 2155–2165.
10. Ozan, N. and Bekaroğlu, Ö., 2003, *Polyhedron,* **22,** 819–823.
11. Seelan, S., Srinivas, M.S. and Sivasenker, S., 2001, *J. Mol. Catal. A- Chem.,* **168,** 61–68.

Chapter 43
Synthesis and Characterization of N-[1,10-Phenanthroline]-N'-[(Benzo-15-Crown-5)yl] Thiourea and Its Complex with Copper(I)

Fikriye Tuncel Elmalı[1], Ulvi Avcıata[1], Nebahat Demirhan[1], and Ahmet Gül[2]

Abstract A new thiourea ligand, N-[1,10-phenanthroline]-N'-[(benzo-15-crown-5)yl]thiourea has been synthesized from the reaction of 5-amino-1,10-phenanthroline with 15-isothiocyanatobenzo[15-crown-5] and its Cu(I) complex has been prepared. The structures of the ligand and its complex have been characterized by elemental analysis, UV-vis, FTIR, ^{1}H NMR (DMSO-d_6), ^{13}C NMR (DMSO-d_6) and MS spectra (LC-MS).

Keywords Copper, ligand, phenanthroline, thiourea

Introduction

1,10,-Phenanthroline is a well-known N-heterocyclic chelating agent with a rigid planar structure [1]. Derivatives of 1,10-phenanthroline have played a major role in the development of polypyridyl metal complexes [2]. Thus 1,10-phenanthroline and its derivatives are one of the most versatile bridging ligands in this regard as these have pendant 1,10-phenanthroline and catechol as two chelating centers with well explored coordination chemistry of their respective mononuclear components [3]. The photochemical and redox properties of the complexes can be varied systematically through appropriate substitutions on the phenanthroline rings [4].

The chemistry of substituted thiourea derivatives has attracted attention because of their potential use as reagents for the separation of metal ions and in biological applications such as their use: as antibacterial, antiviral or antifungal agents. In addition to their applications, the ligands are of interest as they possess various potential donor sites [5].

[1]Yıldız Technical University, Faculty of Arts and Sciences, Department of Chemistry, 34210 Esenler-Istanbul, Turkey

[2]Istanbul Technical University, Department of Chemistry, Maslak, Istanbul, Turkey

B. Sener (ed.), *Innovations in Chemical Biology*, doi: 10.1007/978-1-4020-6955-0

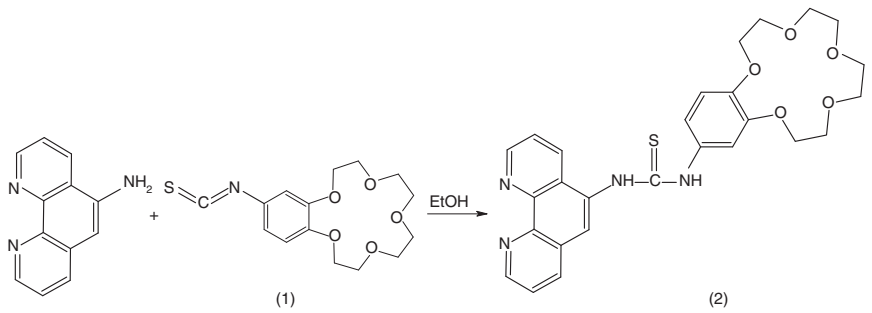

Fig. 43.1 Formation reaction of the ligand

In this study, we report synthesis of a new thiourea derivative **(2)** which contain crown ether and phenanthroline ring by the reaction of 5-amino-1,10-phenanthroline with 15-isothiocyanatobenzo[15-crown-5] **(1)** (Fig. 43.1) and its complex with Cu(I) is obtained. The structures of the ligand and the complex were determined by their elemental analysis, UV-vis, FTIR, ^{1}H NMR (DMSO-d_6), ^{13}C NMR (DMSO-d_6) and Mass spectra (LC-MS).

Experimental

The FTIR spectra (KBr discs) were recorded in the 4,000–400 cm^{-1} range on a Perkin Elmer Spectrum One Bv 5.0 spectrophotometer. Proton NMR and Carbon NMR spectra were recorded on a Varian^{UNITY} INOVA 500 MHz spectrometer. Mass spectra (LC-MS) were determined on a Finnigan™ LCQ™ Advantage MAX and (GC-MS) on a Agilent Technologies 6890N-5973 inert spectrometer. Electronic spectra were recorded on a Agilent 8453 UV-Vis. spectroscopy system. Elemental analyses were determined on a Thermo Finnigan Flash EA 112. Melting points were obtained with a Gallenkamp CAP MPD-350 apparatus in open capillaries.

All other chemicals employed were of the highest grade available. 5-Nitro-1,10-phenanthroline, 5-amino-1,10-phenanthroline [6] and benzo[15-crown-5], 15-nitrobenzo[15-crown-5], 15-aminobenzo[15-crown-5] were prepared according to the published methods [7, 8].

Synthesis

15-Isothiocyanatobenzo[15-crown-5] (1)

To a solution of 15-aminobenzo[15crown-5] (1 g, 3.5 mmol) in 25 mL of water was added solution 0.3 mL of $SCCl_2$ in 5 mL of $CHCl_3$. The mixture was stirred rapidly for 5 h at room temperature. The $CHCl_3$ layer was separated with separation funnel

from aqueous layer $CHCl_3$ layer washed with H_2O (2 × 5 mL) and was reduced to approximately 2–3 mL by rotary evaporation. The pale-yellow precipitate was filtered and dried. Yield, 1.128 g (98%), m.p 93°C. The product is soluble in chloroform, ethanol and methanol. FTIR (KBr): 3,080 (Ar-CH), 2,927, 2,876 (CH_2), 2,142 (N = C = S), 1,600 (Ar-C = C), 1,472 (CH_2), 1,268, 1,241 (Ar-OCH_2) and 1,140 (OCH_2) cm^{-1}. ^1H NMR ($CHCl_3$-d_6): δ: 6.8–6.7 (m, 3H, Ar-H), 4.2–3.6 (m, 16H, OCH_2). Anal Calcd. For $C_{15}H_{19}NO_5S$ (325.38 g/mol): C, 55.38; H, 5.84; N, 4.31; S, 9.85%. Found C, 55.12; H, 5.72; N, 4.25; S, 9.54%. GC-MS, m/z (abundance): 325 (M^+).

N-[1,10-phenanthroline]-N'-[(benzo-15-crown-5)yl] thiourea (2)

A solution of 5,6-diamino-1,10-phenanthroline (0.5 g, 2.38 mmol) in 50 mL of absolute ethanol was added into a solution of 15-isothiocyanatobenzo[15-crown-5] **(1)** (0.774, 2.38 mmol) in 50 mL of ethanol. The mixture was refluxed on a water bath under N_2 atmosphere for 5 h. Then, the solvent was evaporated and the oily product was dissolved 10 mL ethanol. A brown precipitate was obtained by the addition of diethyl ether. The mixture was filtered and washed with ethanol. Yield, 0.165 g (62%); m.p, 230–231°C. The product is soluble in methanol and DMSO. FTIR (KBr): 3,197,3,115 (NH), 3,032 (Ar-CH), 2,922,2,873 (CH_2), 1,624 (Ar-C = N), 1,592 (Ar-C = C), 1,508 (NH-CS), 1,454, 1,419 (CH_2), 1,359 (C = S), 1,225 (Ar-OCH_2), 1,128 (OCH_2) cm^{-1}.^1H NMR (DMSO-d_6): δ 10.9–9.5 (s, 2H, NH) (disappeared with D_2O), 9.2–7.7 (m, 6H, Ar-H), 7.2–6.8 (m, 3H, Ar-H), 4.2–3.2 (m, 16H, OCH_2).^{13}C NMR, δ: 182.32,180.31 (s, 1C, C = S), 150.56–101.18 (m, 18C, Ar-C), 71.12–69.19 (m, 8C, OCH_2). Anal. Calcd. For $C_{27}H_{28}N_4O_5S$ (520.61 g/mol); C, 62.29; H, 5.42; N, 10.76; S, 6.16%. Found: C, 61.90; H, 5.80; N, 10.50; S, 5.52%. LC-MS, m/z (%): 519.32 (M-1).

Cu(I) Complex

In order to prepare the Cu(I) complex, ligand **(2)** (0.02 g, 0.0385 mmol) was dissolved in 20 mL of absolute ethanol and CuCl (0.0019 g, 0.0192 mmol) in 10 mL absolute ethanol was added into this solution. After addition of 0.01 M KOH solution in ethanol to raise the pH to 7.0–7.5, the mixture was stirred at room temperature for 3 h. The solvent was evaporated to 1/3 of their volume. The dark-brown complex was precipitated. It was filtered, washed with ethanol and then dried. The complex is soluble in methanol and DMSO.Yield, 0.015 g (68%); m.p > 350°C. FTIR (KBr): 3,208 (NH), 3,060 (Ar-CH), 2,928, 2,867 (CH_2), 1,613 (Ar-C = N), 1,595 (Ar-C = C), 1,511 (NH-CS), 1,456, 1,426 (CH_2), 1,360 (C = S), 1,224 (Ar-OCH_2), 1,127 (OCH_2) cm^{-1}. ^1H NMR (DMSO-d_6), δ: 10.2–9.6 (s, 4H, NH) (disappeared with D_2O), 9.4–6.8 (m, 18H, Ar-H), 4.4–3.0 (m, 32H, OCH_2). Anal. Calcd. For $C_{54}H_{56}N_8O_{10}S_2ClCu$ (1,140.20 g/mol): C, 56.88; H, 4.95; N, 9.82; S, 5.62%. Found: C, 57.37; H, 4.64; N, 9.02; S, 5.18%.

Result and Discussion

The starting compounds, 5-amino-1,10-phenanthroline and 15-aminobenzo[15-crown-5] were synthesized according to reported procedures [6–8]. 15-Isothiocyanatobenzo [15-crown-5] **(1)** was obtained from the reaction of 15-aminobenzo[15-crown-5] with $SCCl_2$. The new ligand, N-[1,10-phenanthroline]-N'-[(benzo-15-crown-5)yl]thiourea **(2)** was synthesized from 5-amino-1,10-phenanthroline and 15-isothiocyanatobenzo[15-crown-5] with addition reaction (Fig. 43.1). This ligand was isolated as brown color in a good yield (ca. 62%). Its copper(I) complex was prepared by treating the ligand with the corresponding metal salts 1:2 (Fig. 43.2). The new compounds were characterized by elemental analysis, UV-vis, FTIR, ^{1}H NMR, ^{13}C NMR and Mass spectra.

The FTIR spectrum of the ligand **(2)** also provides additional data to confirm the structure given inv. 43.1. Respectively, NH, C = N and C = S stretching vibrations appear at 3,197–3,115, 1,624 and 1,359 cm^{-1}. The characteristic absorptions of aromatic and aliphatic ether groups of the crown ether moiety of 1,225 and 1,128 are also consistent with the reported values [9–12]. N = C = S stretching vibration at 2,142 cm^{-1} in 15-isothiocyanatobenzo[15-crown-5] disappeared the ligand spectrum. In the FTIR spectra of the Cu (I) complex 3,208 cm^{-1} NH stretching vibrations has appeared, suggesting that this NH group is not coordinated to the metal ion. Nitrogens of 1,10-phenanthroline stretching bands at 1,624 cm^{-1} shift to the lower or higher wave numbers indicate the formation of coordination bands between metal ion and these nitrogen atoms.

The ligand **(2)** is soluble in DMSO. The UV-vis spectra of the ligand and Cu(I) complex were recorded in methanol. In the electronic spectrum a band appears at 283 nm which can be assigned to the π-π^* transition of C = C, C = N group in the ligand. The electronic spectra of the complex are showed 290 nm.

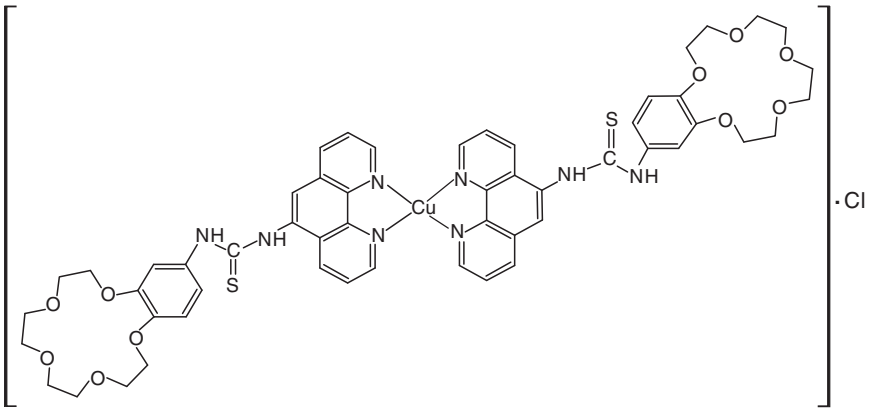

Fig. 43.2 Suggested structure of the Cu(I) complex

The ^{1}H NMR spectra of the ligand **(2)** (Fig. 43.3) in DMSO-d_6 confirmed the proposed structure showing two D_2O-exchangeable protons (Fig. 43.4) of δ 10.9–9.5 ppm as singlet for the NH groups. Two NH protons which is consistent with the presence of the rotational isomers appear at 10.9, 10.4, 9.9 and 9.5 ppm as a singlet [5, 12]. The chemical shifts of the aromatic protons 9.2–6.8 ppm as multiplet. The aliphatic ether protons appear as three multiplets between 4.2–3.2 ppm [10, 11]. The ^{1}H NMR spectra of the diamagnetic Cu(I) complex also provides additional data for this compound. The Cu(I) complex appears at 10.2–9.6 ppm as singlet D_2O exchangeable NH protons.

The ^{13}C NMR spectrum of the ligand **(2)** in DMSO-d_6 (Fig. 43.5) a singlet band at 182.32, 180.31 ppm are due to the C = S group[5]. The aromatic and crown ether carbon atoms appear 150.56–101.18 and 71.12–69.19 ppm [5, 9–11].

The molecular ion peak m/z 519 (M-1) of the free ligand **(2)** (Fig. 43.6) is present in the LC-MS spectra which supports the proposed structures. The important fragment has been appeared at m/z 487 corresponding to loss of SH. Mass spectral data confirm the proposed structure of the ligand **(2)**.

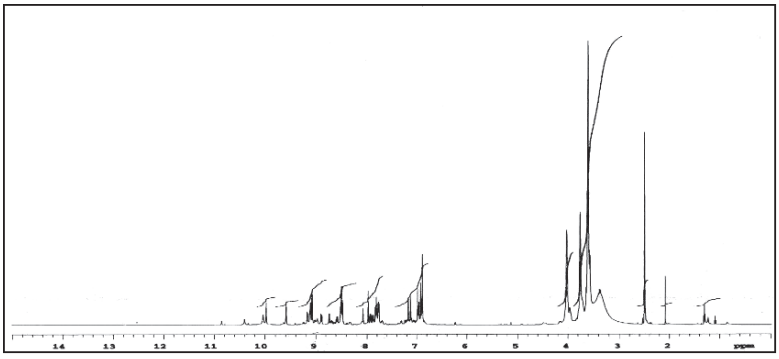

Fig. 43.3 ^{1}H NMR spectra of ligand **(2)**

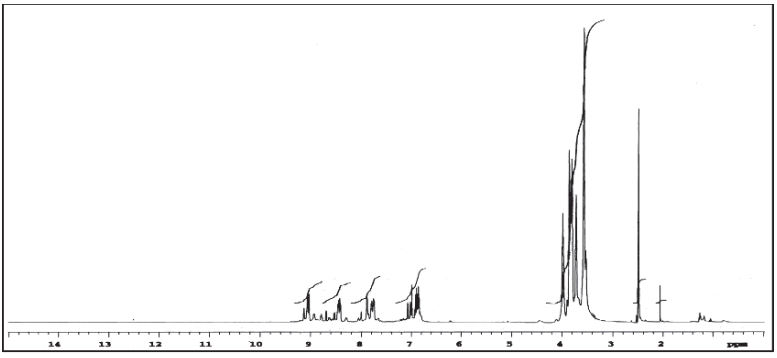

Fig. 43.4 ^{1}H NMR spectra (D_2O-Exch.) of ligand **(2)**

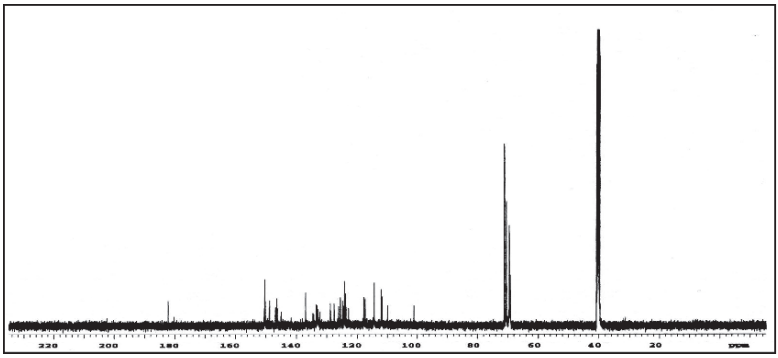

Fig. 43.5 ^{13}C NMR spectra of ligand **(2)**

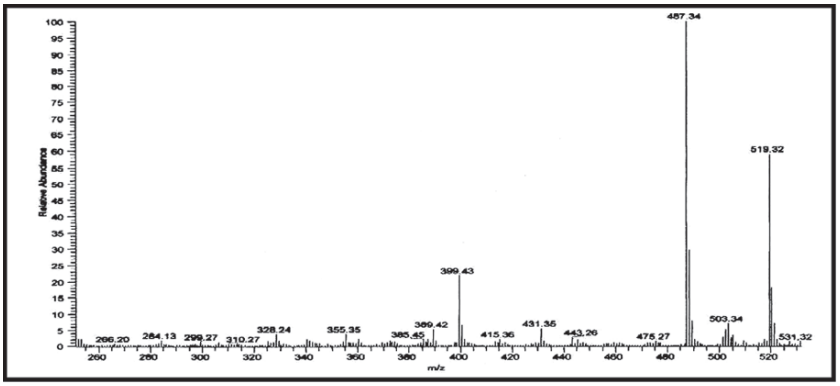

Fig. 43.6 LC-MS spectra of ligand **(2)**

Elemental analyses of the ligand **(2)** and its Cu(I) complex show good agreement with the proposed structures of the ligand and its complex.

Acknowledgement We wish to acknowledge the financial support by the "TUBITAK Research Fund" (Project no. TBAG-101T019).

References

1. Moghimi, A., Alizadeh, R., Shokrollahi, A., Aghabozorg, H., Shamsipur, M. and Shockravi, A., 2003, *Inorg. Chem.,* **42,** 1616.
2. Sammes, P.G. Yahioğlu, G., 1994, *Chem. Soc. Rev.,* **23,** 327–336.
3. Shukla, A.D. and Das, A., 2000, *Polyhedron,* **19,** 2605–2611.
4. Camren, H., Chang, M.Y., Zeng, L. and Mc Guire, M.E., 1996, *Synth. Commun.,* **26,** (6),1247–1252.

5. Moloto, M.J., Malik, M.A., O'Brien, P., Motrualli, M. and Kolawole, G.A., 2003, *Polyhedron,* **22,** 595–603.
6. Gillard, R.D. and Hill, R.E., 1974, *J.C.S. Dalton*, 1217–1236.
7. Shchori, E., Jagur-Grodzinski, J. and Shporer, M., 1973, *J. Am. Chem. Soc.,* **95,** 3842.
8. Ungaro, R., El Haj, B. and Smid, J., 1976, *J. Am. Chem. Soc.,* **98,** (17)5198–5202.
9. Yuan, Y.F., Wang, J.T., Gimeno, M.C., Laguna, A. and Jones, P.G., 2001, *Inorg. Chimica Acta,* **324,** 309–317.
10. Hayvalı, Z., Gündüz, N., Kılıç and Z. Weber, E., 1999, *J. Prakt. Chem.,* **341,** (6),568–573.
11. Hayvalı, Z., Hayvalı, M., Kılıç and Z. Hökelek, T., 2001, *J. Mol. Struct.,* **597,** 223–234.
12. Salman, A., Ateş, Ö., Cesur, N. and Ötük, G., 1991, *Arch. Pharm. (Weinheim),* **324,** 55–56.

Chapter 44
Synthesis and Characterization of New Type Soluble Porphyrazine Containing 1-Bromo-3-Methylbutan Group and Investigation of Its Complexes

Ali Erdoğmuş[1], Gülnur Keser Karaoğlan[1], Ulvi Avcıata[1] and Ahmet Gül[2]

Abstract Bis(3-methylbutantio) maleonitril has been obtained from the reaction of disodium salt, 1-bromo-3 methylbütan in acetone under nitrogen for 11 hours. MgPz has been synthesized through the cyclotetramerization reaction of magnesium and n-butanol with bis(3-methylbutantio) maleonitril. The metal free pophyrazine derivative was obtained by its treatment with trifluroacetic acid and further reaction of this product with cobalt(II) acetate, nickel(II) acetate and zinc(II) acetate led to the metal porphyrazine (MPz, M = Co, Ni ve Zn). These new compounds have been investigated and characterized by UV, FT-IR, ^{1}H NMR, GC-MS and elemental analysis methods.

Keywords Magnesium, nickel, pigment, phythalocyanines, porphyrazine, spectroscopy, synthesis

Introduction

Porphyrazines as a chemical class provide the dominant blue and blue-green pigments, due to their intense absorption at long wavelengths in the visible spectrum, to their excellent durability and their relatively low cos [1]. Tetrapyrrolitic macrocyclic ring systems are porphyrins, tetraazaporphyrins, phythalocyanines and porphyrazines. These compounds have been used electrophotography, optical data, photodynamic therapy of tumors, liquid crystals, pigments and dyes. Porphyrazines have been of considerable interest to spectroscopist and theoreticians for their high symmetrical, planar structure and electron delocalisation [2].

Yıldız Technical University, Faculty of Arts and Sciences, Department of Chemistry, 34210 Esenler- İstanbul, Turkey
İstanbul Technical University, Faculty of Arts and Sciences, Department of Chemistry, Maslak- İstanbul, Turkey

B. Sener (ed.), *Innovations in Chemical Biology*, doi: 10.1007/978-1-4020-6955-0

In the present work, our aim has been prepared to different peripheral porphyrazines which include eight 3-methylbutan and 3-phenylpropyl groups. Peripherally-functionalized porphyrazines have the potential to exhibit novel optical, magnetic and electronic properties [3].

Experimental Part

Instrumentation

The FTIR spectra (KBr discs) were recorded in the 4,000–400 cm^{-1} range on a Mattson 1000 FTIR spectrometer. The spectra and absorbance measurements were recorded on a Agilent 8453 UV-visible Spectroscopy System. Proton NMR spectra were recorded on a Brucker AC–400 MHz ($CDCl_3$) spectrometer. The elemental analyses and mass spectra (LC-MS) were determined in the TUBITAK Laboratory (Center of Science and Technology Research of Turkey). Melting points were obtained with a Gallenkamp CAP MPD–350 apparatus in open capillaries.

Preparation of Sodium Cyano Dithioformate

9.8 g (0.2 mol) of powdered and dried NaCN was mixed with 60 mL of DMF. 12.4 mL (0.2 mol) of CS_2 was added into that solution dropwise with stirring in ice bath for about 10 min. After removing ice bath, mixture was stirred 30 min more. Dark red-brown mixture was diluted to 200 mL with isobutanol and heated until all product was dissolved in it. Mixture was filtered while it was hot to remove unreacted NaCN. After that, filtrate was stood to cool and crystallize. Needle type Brown crystals formed and washed with ether and dried on P_2O_5. Yield was 20 g (80%).

Preparation of Dithiomaleonitrile Disodium Salt

Sodium Cyano Dithioformate was dissolved in 110 mL of $CHCl_3$ and filtrate dark-brown solution was formed. That solution was stood at room temperature for 4–5 days and then after, the precipitate which was formed from product and sulfur was dissolved in MeOH and by addition of ether crystallization occurred. Lemon yellow crystals were dried with vacuum until to the fixed weight. The product is slightly soluble in water and insoluble in diethylether, benzene and chloroform. Yield was 17.5 g (85%).

Preparation of Bis(3-metilbutantio) Maleonitrile (1)

One gram (15 mmol) of dithiomaleonitrile disodium salts was mixed with 1.35 mL (0.0108 mol) of 1-bromo3-metylbutane in 50 mL of acetone refluxed a 60°C for about 11 hours. The reaction time was controlled by TLC. When acetone was evaporated, the remain which was oil like product treated with $CHCl_3$ to remove insoluble salts by decantation. The $CHCl_3$ phase was extracted several times with

Na_2SO_4. The crude product obtained by evaporation of the solvent was chromatographed on a silica column (eluent: Chloroform). Yield 1.5 g (85%) The product is good soluble in $CHCl_3$, acetone and hexan.

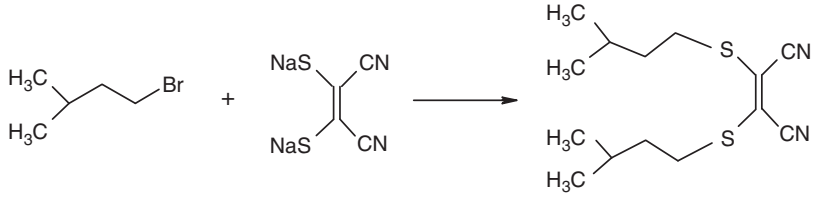

Compound 1	C	H	N	S
Calculated (%)	59.53	7.85	9.92	22.45
Experimental (%)	58.96	7.72	10.01	21.90

2,3,7,8,12,13,17,18 Oktakis(3-methylbutanethio) Porphyrazine, N^{21}, N^{22}, N^{23}, N^{24} Magnesium (2)

0.24 g (10 mmol) of magnesium and a small I_2 crystal was refluxed in 15 mL BuOH for about 12 hours. The prepared $(BuO)_2$ Mg solution and 2.82 (10 mmol) 1 was refluxed for 48 hours. The reaction time was controlled by TLC. At the end, the blue color product was obtained. Firstly, reaction mixture was filtered to remove unreacted Mg and BuOH was evaporated under reduced pressure and dried under vacuum. The crude product was chromatographed on a silica column (eluent: Chloroform). Yield 2.05 g (73%) as given in Scheme 44.1.

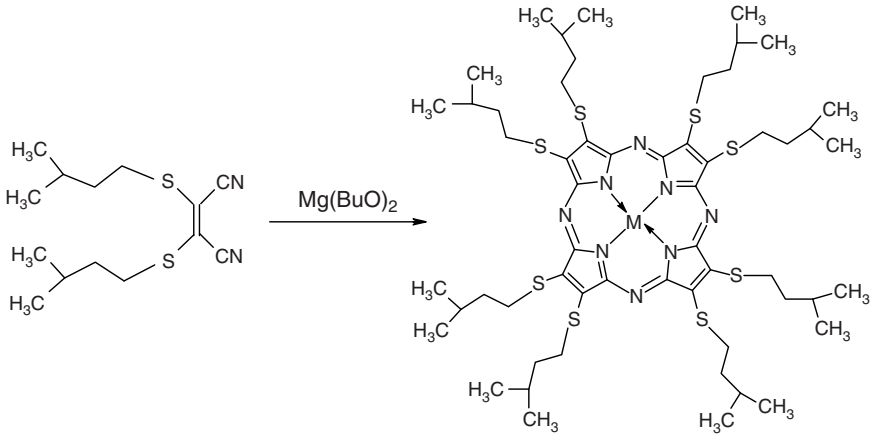

M=Mg, 2H, Ni

Scheme 44.1 Metal free prophyrazines

Compound 2	C	H	N	S
Teorik (%)	58.27	7.68	9.71	22.13
Deneysel (%)	58.99	7.79	9.90	20.33

[2,3,7,8,12,13,17,18-oktakis(3-methylbutanthio) H^{21},H^{23} Porphyrazine N^{21}, N^{22}, N^{23}, N^{24}] (3)

Two grams of MgPz dissolved in 18 mL of trifluoroaceticacid for 3 hours at room temperature under nitrogen. Then reaction mixture was dropped on to ice and neutralized with ammonia and stood in refrigerator for about 2 hours. After then, it was taken into chloroform phase and washed and then, was dried with Na_2SO_4. Then, Solvent was removed and the precipitate was washed with MeOH. Finally, the violent color metal-free porphyrazine was obtained. Yield 1.76 g (80%) as given in Scheme 44.1.

Compound 3	C	H	N	S
Teorik (%)	59.42	8.01	9.90	22.66
Deneysel (%)	58.76	7.89	9.60	21.76

{2, 3, 7, 8, 12, 13, 17, 18-oktakis (3-methylbutanethio) porfirazine $N^{21}N^{22}N^{23}N^{24}$}nickel (II) NiPz (4)

0.1 g (0.44 mmol) H_2Pz, was dissolved in 10 mL chloroform and added 0.11 g $Ni(Ac)_2$. $4H_2O$ which dissolved in 10 mL EtOH and refluxed for 12 hours under nitrogen. The reaction time was controlled by TLC. After completion of the reaction, the mixture was filtered and precipitate washed small amount cold hexan and water to remove unreacted metal free porphyrazine metal salts and dried under reduce pressure via P_2O_5. Yield 0.90 g (86%) as given in Scheme 44.1.

Compound 4	C	H	N	S
Teorik (%)	57.90	7.64	7.24	22.10
Deneysel (%)	57.26	7.43	7.11	21.13

Result and Discussion

The synthetic route to metals porphyrazines requires the preparation of porphyrazine core at the beginning. The starting material of porphyrazine was disodium salt of dithiomaleonitrile which was obtained from the reaction of carbondisulfide with sodiumcyanide in two steps. The results of IR spectrum and melting point (290°C) of compound supported the structure we aimed.

The alkylation process was accomplished by 1-bromo3-metylbutane in acetone. The alkylated dithiomaleonitrile is a very suitable starting material for porphyrazine derivatives. This compound is soluble in chloroform, acetone, hexane and dichloromethane. In the IR spectrum of this compounds, characteristic C-H stretching vibration due to CN group and CH_2 groups come out at 2,127 and 2,980 cm^{-1}. The band at 2,200 cm^{-1} in the IR spectrum of Ligand can be assigned to CN group in the structure. The elemental analyses and GC-MS (282 g/mol 95% abundance) result was compatible with proposed structure of ligand (**1**). The ^{1}H NMR spectrum of ligand in $CDCl_3$ shows that compatible with other results.

For the synthesis of MgPz (**2**), the alkylated maleonitrile was treated with Mg butanolate. Because of the template effect of magnesium, maleonitrile molecules cyclotetramerize to form magnesium porphyrazine. MgPz is soluble in number of common solvents like chloroform, acetone etc. and little soluble in ethanol and methanol. The absence of CN peaks in IR spectrum can easily be attributed to the cyclotetramerization, and the only strong peak was observed at 2,922 cm^{-1} for C-H stretching vibration of 3-metylbutane groups.

As in the case of phthalocyanines and porphyrazines, porphyrazines also give strong absorptions in both high and low energy regions of visible light. In the absorption spectrum of MgPz, the single peak appeared around 672 nm as Q band and another one appeared around 344 nm as B bands.

The metal-free porphyrazine, H_2Pz (**3**), was prepared by treatment of MgPz with minimum amount of triflouraaceticacid. When metal ion is removed from the center of core system, two N atoms in pyrrole ring are protonated. That was proved by both IR and UV/VIS spectra of the compound. In the IR spectrum, the peak around 3,240 cm^{-1} shows the presence N-H bonds in H_2Pz. There is splitting in the Q band absorptions of H_2Pz, because of the D_{2h} symmetry of molecule. The Q band absorptions appeared in 711 and 641 nm. For B band absorption, there is only one peak in 348 nm for porphyrazine. And also ^{1}H- NMR spectrum shows that a single peak at -1 ppm for N-H protons in the structure as given in Fig. 44.1.

In order to prepare NiPz (**4**) derivative, H_2Pz was reacted with $Ni(Ac)_2.4H_2O$ in the mixture of chloroform and ethanol to obtain NiPz. In the ^{1}H- NMR spectrum of NiPz, chemical shifts assignable to $–SCH_2$, $C\text{-}CH_2\text{-}C$, -CH and $-CH_3$ groups at 4.2,

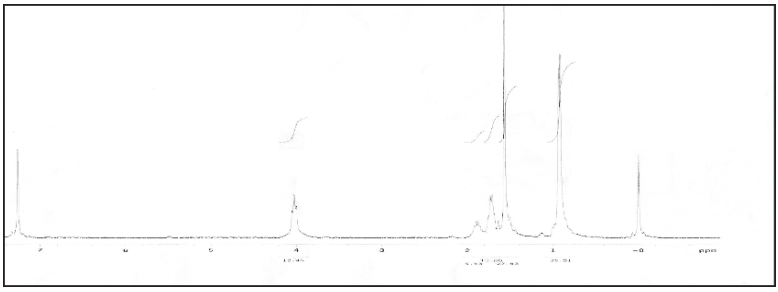

Fig. 44.1 ^{1}H-NMR spectrum of the compound (**3**)

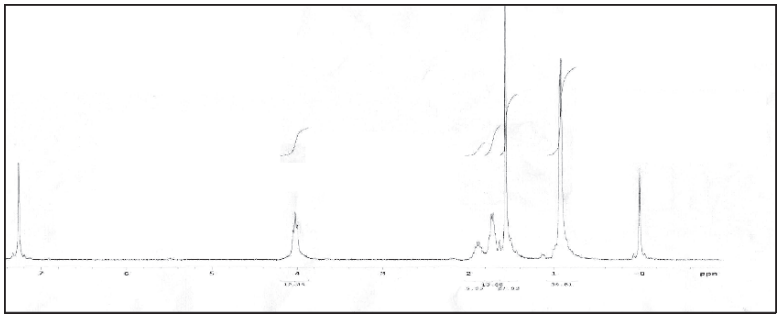

Fig. 44.2 [1]H-NMR spectrum of the compound (**4**)

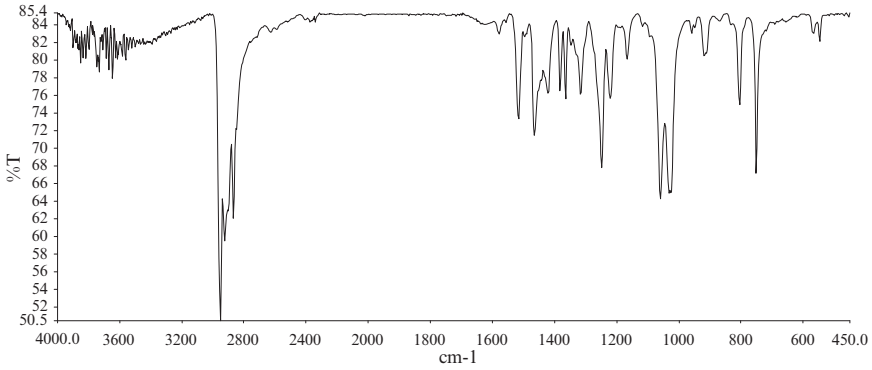

Fig. 44.3 IR spectrum of the compound (**4**)

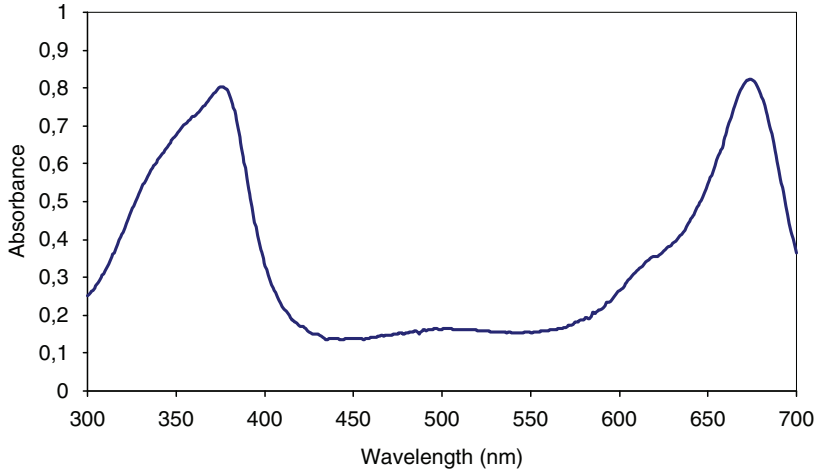

Fig. 44.4 UV spectrum of the compound (**4**)

1.6, 1.8 and 0.8 ppm respectively as given in Fig. 44.2. The IR spectra (Fig. 44.3) and elemental analyses results was compatible with proposed structure of NiPz. For the Ni porphyrazines Q and B band absorption are at 666 and 360 nm respectively (Fig. 44.4).

References

1. Smith, H.M. (1968), Phthalocyanines. In (P.A. Lewis, ed.), *The Pigment Handbook* **1**(2),Willey, New York, p. 663.
2. Anderson, M.E., Barrett, A.G.M. and Hoffman, B.M. (1999), *Inorg. Chem.,* **38,** 6143–6151.
3. Kobayashi, N. (2001), *Chem. Rev.,* **99,** 219.

Chapter 45
Synthesis and Characterization of New Type Soluble Porphyrazine Containing 3-Phenylpropyl Bromide Group and Investigation of Its Complexes

Ali Erdoğmuş[1], Ulvi Avcıata[1], and Ahmet Gül[2]

Abstract Oktakis (3-phenylpropyl) porphyrazinato nickel(II), $ZnPz(SCHCH_2R)_8$, Where R = C_7H_8, was synthesized and its structure and spectral properties were investigated in chloroform. Firstly, Bis(3-Phenylpropyl) maleonitril has been obtained from the reaction of disodium salt, in 3-Phenylproply bromide acetone under nitrogen for 20 hours. MgPz has been synthesized through the cyclotetramerization reaction of magnesium and n-butanol with bis(3-Phenylproplytio) maleonitril. The metal free porphyrazine derivative was obtained by its treatment with trifluroacetic acid and further reaction of this product with zinc(II) acetate led to the metal porphyrazine (MPz, M = Zn). These new compounds have been investigated and characterized by UV, FT-IR, ^{1}H NMR, GC-MS and elemental analysis methods.

Keywords Ligand, oktakis, 3-Phenylproply bromide, porphyrazine, spectroscopy, synthesis

Introduction

Intensive research interest in peripherally functionalized porphyrazines during the last decade has shown that these tetrapyrol derivatives should be considered as alternatives to the phthalocyanines that have found extensive applications in many fields. These include material science and the photodynamic therapy of tumors as well as pigments and dyes [1]. These compounds have been used electrophotography, optical data, photodynamic therapy of tumors, liquid crystals, pigments and dyes. Porphyrazines have been of considerable interest to spectroscopist and theoreticians for their high symmetrical, planar structure and electron delocalisation [2].

[1] Yildiz Technical University, Faculty of Arts and Sciences, Department of Chemistry, 34210 Esenler, Istanbul, Turkey

[2] Istanbul Technical University, Faculty of Arts and Sciences, Department of Chemistry, Masalk, Istanbul, Turkey

B. Sener (ed.), *Innovations in Chemical Biology*, doi: 10.1007/978-1-4020-6955-0

In the present work, our aim has been prepared to different peripheral porphyrazines which include eight 3-phenylpropyl groups. Peripherally-functionalized porphyrazines have the potential to exhibit novel optical, magnetic and electronic properties [3, 4].

Experimental Part

Instrumentation

The FTIR spectra (KBr discs) were recorded in the 4,000–400 cm^{-1} range on a Mattson 1000 FTIR spectrometer. The spectra and absorbance measurements were recorded on a Agilent 8453 UV-visible Spectroscopy System. Proton NMR spectra were recorded on a Brucker AC–200 MHz (DMSO-d_6) spectrometer. The elemental analyses and mass spectra (LC-MS) were determined in the TUBITAK Laboratory (Center of Science and Technology Research of Turkey). Melting points were obtained with a Gallenkamp CAP MPD–350 apparatus in open capillaries.

Preparation of sodium cyano dithioformate and dithiomaleonitrile disodium salt were synthesized according to the procedure revised [1].

Preparation of Bis(3-Fenilprophylthio) Maleonıtrile

One gram (0.0054 mol) of dithiomaleonitrile disodium salts was mixed with 1.65 mL (0.0108 mol) of 3-Phenylpropylbromide in 30 mL of acetone refluxed a 60°C for about 20 hours. The reaction time was controlled by TLC. When acetone was evaporated, the remain which was oil like product treated with $CHCl_3$ to remove insoluble salts by decantation. The $CHCl_3$ phase was extracted several times with Na_2SO_4. The crude oil product obtained by evaporation of the solvent was chromatographed on a silica column (eluent; Chloroform). Yield 2.1 g (89%) Mw: 378 g/mol (determined by GC-MS) The product is good soluble in $CHCl_3$, acetone and hexane. Elemental analysis results for; Calculated C 69.80, H 5.86, N 7.40, S 16.94, Experimental 69.27, H 5.8, N 7.33, S 16.32%.

[2,3,7,8,12,13,17,18 Oktakis(3-Fenilprophylthio) Porphyrazine, N^{21},N^{22},N^{23},N^{24}]

Magnesium

0.24 g (10 mmol) of magnesium and a small I_2 crystal was refluxed in 15 mL BuOH for about 12 hours. The prepared $(BuO)_2$ Mg solution and 3.78 g (10 mmol) (1) was refluxed for 12 hours. The reaction time was controlled by TLC. At the end, the

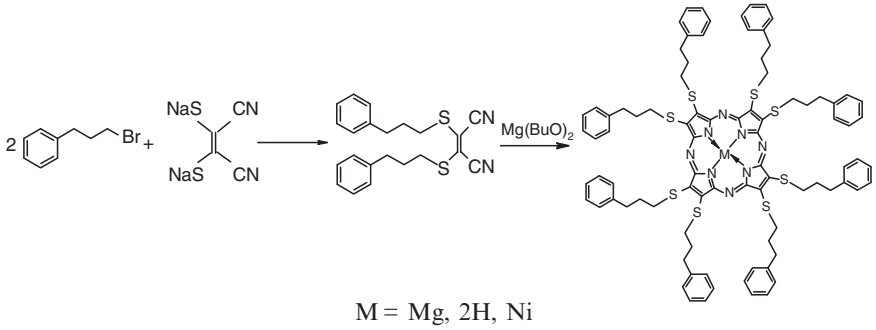

Scheme 45.1 Metal free pophyrazine derivatives

blue color product was obtained. Firstly, reaction mixture was filtered to remove unreacted Mg and BuOH was evaporated under reduced pressure and dried under vacuum. The crude product was chromatographed on a silica column (eluent: Chloroform). Yield 2.47 g (71%). Molecular formula as given in Scheme 45.1. Calculated C 68.70, H 5.77, N 7.28, S 16.67%, experimental 68.17%, H 5.61%, N 7.56%, S 15.92%.

[2,3,7,8,12,13,17,18-Oktakis(3-Fenilprophylthio) H^{21},H^{23} Porphyrazine N^{21}, N^{22}, N^{23}, N^{24}]

Two grams of MgPz dissolved in 18 mL of trifluoroaceticacid for 3 hours at room temperature under nitrogen. Then reaction mixture was dropped on to ice and neutralized with ammonia and stood in refrigerator for about 2 hours. After then, it was taken into chloroform phase and washed, and then was dried with Na_2SO_4. Then, Solvent was removed and the precipitate was washed with MeOH. Finally, the violent color metal-free porphyrazine was obtained. Yield 1.86 g (86%) as given in Scheme 45.1. Calculated C 67.44%, H 5.93%, N 6.79%, S 15.59%, experimental 67.71, H 5.98, N 7.09, S 16.92%.

[2, 3, 7, 8,12, 13, 17-oktakis (3-phenylpropylthio) Porphyrazine $N^{21}N^{22}N^{23}N^{24}$]Nickel

0.1 g (0.066 mmol) H_2Pz, was dissolved in 10 mL chloroform and added 0.165 g $Ni(Ac)_2$. $4H_2O$ (0.066 mmol) which dissolved in 10 mL EtOH and refluxed for 14 hours under nitrogen. The reaction time was controlled by TLC. After completion of the reaction, the mixture was filtered and precipitate was washed small amount

cold hexane and water to remove unreacted metal free porfirazine and metal salts, and then dried under reduce pressure via P_2O_5. Yield 0.92 g (91%) as given in Scheme 45.1. Calculated C 69.80, H 5.86, N 7.40, S 16.94%, experimental C 69.27, H 5.8, N 7.33, S 16.32%.

Result and Discussion

The synthetic route to metals porphyrazines requires the preparation of porphyrazine core at the beginning. The starting material of porphyrazine was disodium salt of dithiomaleonitrile which was obtained from the reaction of carbondisulfide with sodiumcyanide in two steps. The results of IR spectrum and melting point (290°C) of compound supported the structure we aimed.

The alkylation process was accomplished 3-Phenylpropylbromide in acetone. The alkylated dithiomaleonitrile is a very suitable starting material for porphyrazine derivatives. This compound is soluble in chloroform, acetone, hexane and dichloromethane. In the IR spectrum of this compounds, characteristic C-H stretching vibration due to CN group and CH_2 groups come out at 2,122 and 2,982 cm^{-1}. The band at 2,202 cm^{-1} in the IR spectrum of ligand can be assigned to CN group in the structure. The elemental analyses and GC-MS (378 g/mol 89% abundance) result was compatible with proposed structure of ligand. The ^1H NMR spectrum of ligand in $CDCl_3$ shows that compatible with other results. In the ^1H NMR spectrum of ligand, chemical shifts assignable to $–SCH_2$, $C\text{-}CH_2\text{-}C$, $\text{-}CH_2$ and benzen groups at 3.1, 2.05, 2.7 and 7.2 ppm, respectively.

For the synthesis of MgPz, the alkylated maleonitrile was treated with Mg butanolate. Because of the template effect of magnesium, maleonitrile molecules cyclotetramerize to form magnesium porphyrazine. MgPz is soluble in number of common solvents like chloroform, acetone etc. and little soluble in ethanol and methanol. The absence of CN peaks in IR spectrum can easily be attributed to the cyclotetramerization, and the only strong peak was observed at 2,922 cm^{-1} for C-H stretching vibration of fenilprophyl. And others characteristic peaks belonging to ligand.

As in the case of phthalocyanines and porphyrazines, porphyrazines also give strong absorptions in both high and low energy regions of visible light. In the absorption spectrum of MgPz, the single peak appeared around 673 nm as Q band and another one appeared around 378 nm as B bands.

The metal-free porphyrazine, H_2Pz, was prepared by treatment of MgPz with minimum amount of triflouraaceticacid. When metal ion is removed from the center of core system, two N atoms in pyrrole ring are protonated. That was proved by both IR and UV/VIS spectra of the compound. In the IR spectrum, the peak around 3,240 cm^{-1} shows the presence N-H bonds in H2Pz. There is splitting in the Q band absorptions of H_2Pz, because of the D_{2h} symmetry of molecule. The Q band absorptions appeared in 713 and 638 nm. For B band absorption, there is only one

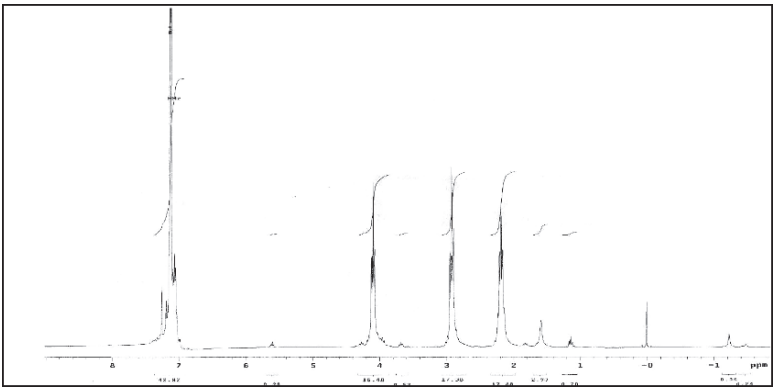

Fig. 45.1 ^{1}H NMR spectrum of H_2Pz

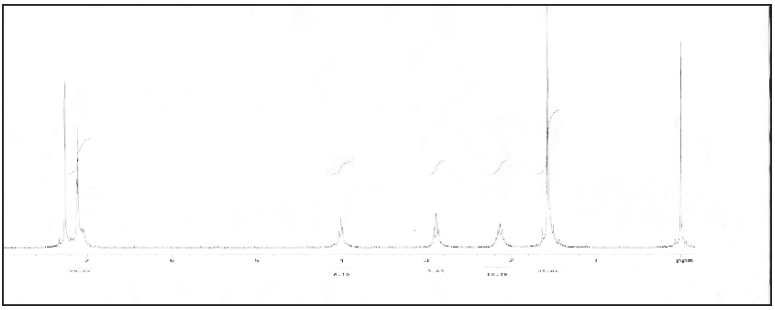

Fig. 45.2 ^{1}H NMR spectrum of NiPz

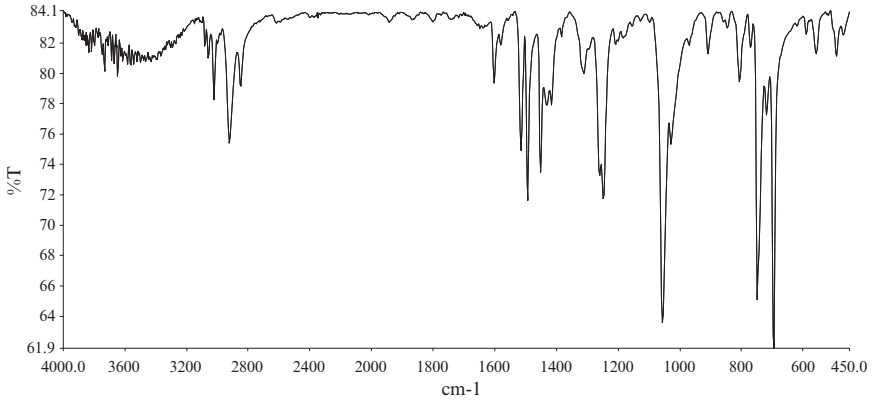

Fig. 45.3 IR spectrum of NiPz

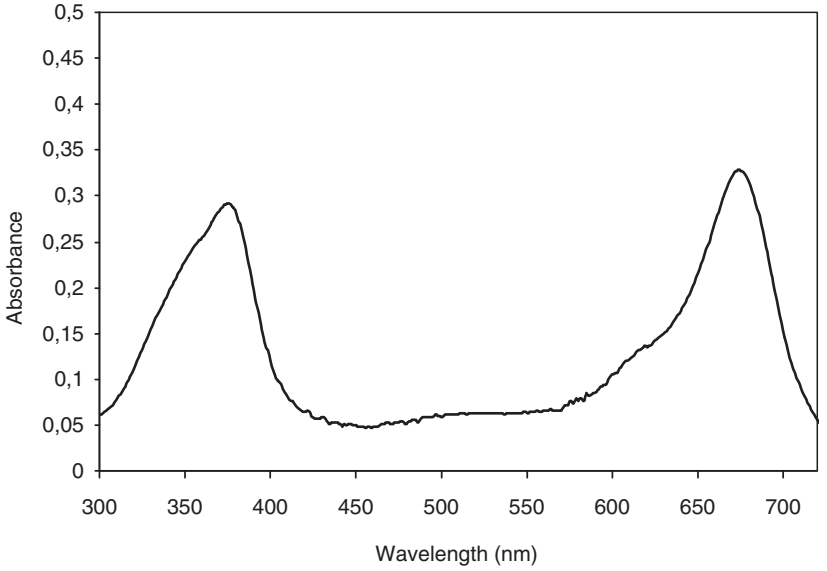

Fig. 45.4 UV spectrum of NiPz

peak in 350 nm for porphyrazine. And also ^{1}H- NMR spectrum shows that a single peak about at -1.2 ppm for N-H protons in the structure as given in Fig. 45.1.

In order to prepare NiPz derivative, H_2Pz was reacted with $Ni(Ac)_2.4H_2O$ in the mixture of chloroform and ethanol to obtain NiPz. In the ^{1}H NMR spectrum of NiPz, chemical shifts assignable to $–SCH_2$, C-CH_2-C, -CH and benzen groups at 4.0, 1.52, 2.2 and 7.2 ppm respectively as given in Fig. 45.2. The IR spectra (Fig. 45.3) and elemental analyses results was compatible with proposed structure of NiPz. For the Ni porphyrazines Q and B band absorption are at 666 and 360 nm respectively (Fig. 45.4).

References

1. Luk'yanets, E.A., 1992, *Mol. Mat.,* **1,** 209–216
2. Kopranenkov, V.N. and Lukyanets, E.A., 1995, *Izv. Akad. Nauk. Ser. Kim.,* **12,** 2320–2336.
3. Anderson, M.E., Barrett, A.G.M. and Hoffman, B.M., 1999, *Inorg. Chem.,* **38,** 6143–6151.
4. Kobayashi, N., 2001, *Chem. Rev.,* **99,** 219.

Chapter 46
Synthesis and Characterization of Novel Peripherally 3-Bromo-1-Phenyl-1-Propene Derivative of Porphyrazine

Bahadır Keskin[1], Ulvi Avcıata[1], and Ahmet Gül[2]

Abstract Magnesium porphyrazines substituted with eight (phenyl-propene) groups on the peripheral positions have been prepared by cyclotetramerization of 1,2-bis(3-phenyl-2-propenethio) maleonitrile and then achieved porphyrazine by 3-bromo-1-phenyl-1-propene. Metal-free derivative was obtained by its treatment with trifluoroacetic acid. The new compounds have been characterized by FT-IR, ^{1}H-NMR, UV-VIS and elemental analysis methods.

Keywords Macrocyclic, maleonitril, porphyrazine

Introduction

Tetrapyrrol macrocycles such as phthalocyanines, porphyrines and porphyrazines have been of great scientific interest in industries for their wide-spread applications in the fields of colouring material-pigment, energy conversion, electrophotography, gas sensors, liquid crystals, infrared dyes for laser technology, optical data storage. They have also been of considerable interest to theoreticians owing to their high symmetry, planarity and electronic delocalization [1, 2]. It has been found that functional groups fused to the peripheral positions of metal–Pz are integrated to the macrocyclic core more effectively than that of Pc [3–5]. The aim of the present work will be to synthesize novel soluble porphyrazine derivatives by making use of a substituted maleonitrile starting material namely 3-bromo-1-phenyl-1-propene.

Following the formation of novel ligand, Mg-porphyrazine will be prepared by using magnesium butanolate. Then treating Mg-Pz with CH_3COOH is produced

[1]Yildiz Technical University, Faculty of Arts and Sciences, Department of Chemistry, 34210, Istanbul, Turkey

[2]Istanbul Technical University, Faculty of Arts and Sciences, Department of Chemistry, 34469 Istanbul, Turkey

B. Sener (ed.), *Innovations in Chemical Biology*, doi: 10.1007/978-1-4020-6955-0

metal free porphyrazine. Molecular structure of metal free porphyrazine and magnesium porphyrazine will be clarified and characterized by UV, FT-IR, ^{1}H NMR, TLC and elemental analysis methods.

Experimental Part

Reagents

Chemicals employed were of the highest grade available. Unless specified other wise, reagent grade reactants and solvents were used as received from chemical suppliers. High purity potassium nitrate was used supporting electrolyte. The electronic spectra and absorbance measurements were recorded on a Agilent 8453 UV-Visible spectroscopy system. The FTIR Spectra (KBr discs) were recorded in the 4,000–400 cm^{-1} range on PerkinElmer Spectrum One spectrometer by using KBr pellets. Proton NMR spectra were recorded on a Brucker 400 MHz spectrometer using TMS as the reference. Elemental analyses were recorded on Thermo Flashea 1112 series equipment.

The disodium salt of dithiomaleonitrile (1) was prepared according to the previously reported procedures [6, 7].

Synthesis of 1,2-bis(3-phenyl-2-propenethio)maleonitrile (2)

Disodium salt of dithiomaleonitrile (**1**) 1.5 g in 40 ml EtOH and 3-bromo-1-phenyl-1-propene 3.15 g in 10 ml EtOH were mixed slowly under argon for about 15 min. The mixture was heated at 60°C under argon for about 20 h. The solid part was settled down from solution by cooling room temperature was filtered out and washed with ethanol. Finally pale yellow crystals were obtained which was soluble in chloroform, dichloromethane acetone. Yield: 1.66 g, 70% (Fig. 46.1). MF: $C_{22}H_{18}N_2S_2$.

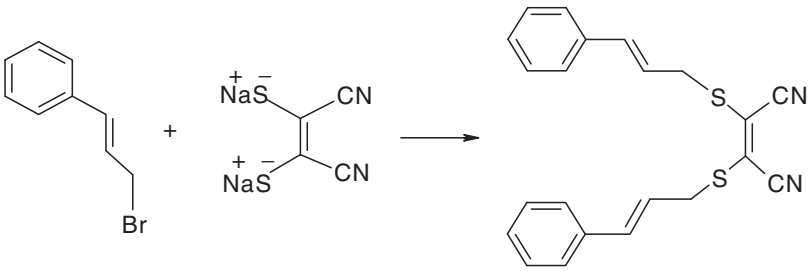

Fig. 46.1 1,2-bis(3-phenyl-2-propenethio)maleonitrile

[2,3,7,8,12,13,17,18-Octakis(3-phenyl-2-propenethio)-porphyrazinato]Mg(II) (3)

Mg turnings 0.033 g and a small I_2 crystal were refluxed in 7 ml of n-BuOH for about 20 h in to obtain $Mg(BuO)_2$ under nitrogen. 0.748 g of 1,2-bis(3-phenyl-2-propenethio)maleonitrile was added to this solution and the mixture was refluxed for about 7.5 h under nitrogen atmosphere, a dark green suspension was obtained. Then the mixture was filtered when hot, washed with n-BuOH and evaporated by rotary. The remaining oily product was dissolved in chloroform 30 ml. The blue-green product was filtered and washed with methanol. Yield: 0.426 g (65%) (Scheme 46.1). MF: $C_{81}H_{60}MgN_8S_8$.

2.4. [2,3,7,8,12,13,17,18-Octakis(3-phenyl-2-propenethio)^{21}H, ^{23}H porphyrazine] (4)

Nine hundred and eighty-five milligrams of the dinirile **3** was dissolved in minimum amount of CF_3COOH and stirred overnight at room temperature. The reaction mixture was added about 7 ml of NH_3 solution to neutralize it and cooled overnight in freezes. After the filtration of crude product, it was treated with $CHCl_3$ and extracted with water twice. The chloroform phase dried over anhydrous Na_2SO_4 and the solvent was evaporated in vacuum. The oily product was dissolved in diethyl ether and filtrated when cold. Finally pure violet color metal free porphyrazine was obtained. Yield: 0.341 g (%80) (Scheme 46.1). MF:$C_{81}H_{62}N_8S_8$.

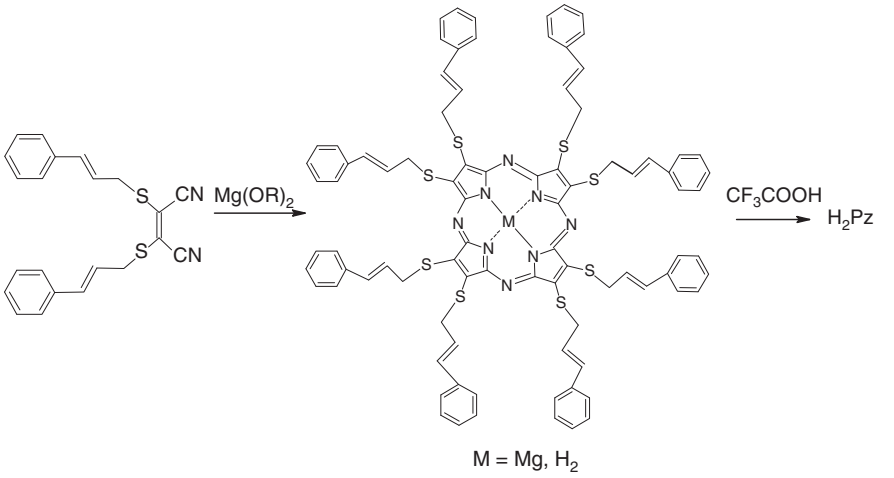

Scheme 46.1 Oktakis (3-phenyl-2-propenethio) porfirazinato magnezyum(II) and H_2Pz synthesis

Results and Discussion

FT-IR Spectra of the Molecules

The synthetic route followed in this work is shown in Scheme 46.1. To synthesize the symmetrically octakis-substituted porphyrazines, first disodium salt of dithiomaleonitrite **1** and then 1,2-bis(3-phenyl-2-propenethio)maleonitrile **2** were prepared. It is soluble in $CHCl_3$, dichloromethane and acetone, insoluble in diethyl ether, MeOH and apolar hydrocarbon solvents such as n-hexane. Elemental analyses correspond closely with the values calculated for (**2**–**4**) (Table 46.1). In the FT-IR spectrum of compound **2** stretching vibration of C≡N is observed at 2,208 cm^{-1}, the aliphatic C–H peaks are around 2,852–2,924 cm^{-1} and the characteristic substituted aromatic C–H peaks is observed at 3,026 cm^{-1} (Fig. 46.2). The presence of bulky electron-donating S-groups is expected to give porphyrazines absorbing electromagnetic radiation just in the same range as phthalocyanines [4, 8–11].

Conversion of the dinitrile into porphyrazine was achieved by the template effect of magnesium butanolate. By cyclotetramerization, the pure green porphyrazine

Table 46.1 Elemental analysis results of the porphyrazines[a]

Compound	C	H	N
2	70.90 (70.55)	4.95 (4.84)	7.56 (7.48)
3	68.43 (68.21)	4.37 (4.24)	7.94 (7.86)
4	69.54 (69.30)	4.63 (4.45)	7.89 (7.98)

[a]Required values are given in parentheses

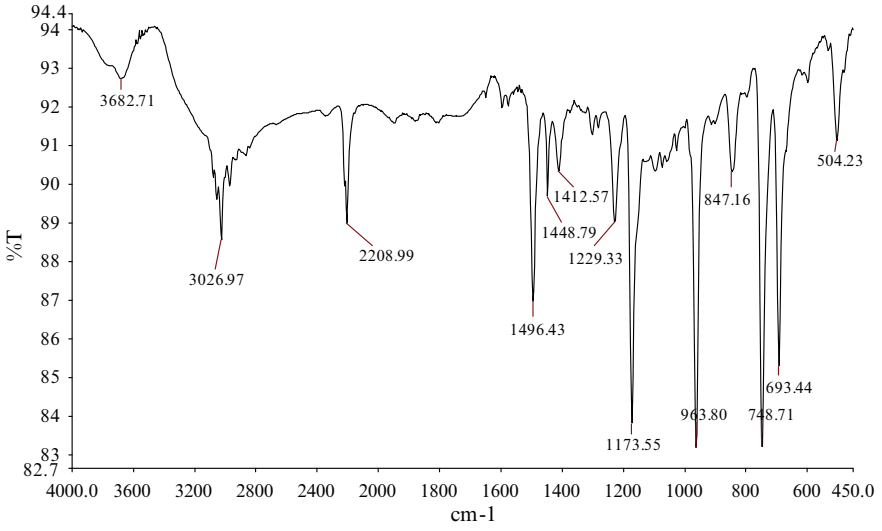

Fig. 46.2 FT-IR-spectrum 1,2-bis(3-phenyl-2-propenethio)maleonitrile

octakis(3-phenyl-2-propenethio)-porphyrazinatomagnesium **3** (Scheme 46.1) was obtained by drying in vacuum. It is dissolved in acetone, chloroform, dichloromethane but not dissolved in methanol, hexane and ethyl acetate. In the FT-IR spectrum of compound **2** stretching vibration of C≡N is observed at 2,208 cm^{-1}, the aliphatic C–H peaks are around 2,852–2,924 cm^{-1} and the characteristic substituted aromatic C–H peaks is observed at 3,025 cm^{-1}. After conversion of dinitrile derivative **2** to porphyrazine **3** was confirmed by the disappearance of the sharp C≡N vibration around 2,208 cm^{-1} of the precursor **2** and the appearing the same aromatic and aliphatic C-H peaks (Fig. 46.3).

The N–H stretching absorption of the inner core of the metal-free porphyrazine **4** was observed around 3,281 cm^{-1}. FT-IR spectra of all porphyrazines derivatives (**3**–**4**) showed the aliphatic C–H peaks are around 2,853–2,924 cm^{-1} and the aromatic characteristic peak is around 3,026 cm^{-1} (Fig. 46.4).

UV-Visible Spectra of Complexes

Electronic spectra are especially useful to establish the structure of the porphyrazines (**3**–**4**). UV–Vis spectra of porphyrazine core are dominated by two intense bands, the Q band around 660 nm and the B band in the near UV region of around 355 nm, both correlated to π→π* transitions [12, 13]. UV–Vis spectra of metalloporphyrazines (**3**, **4** in $CHCl_3$) prepared in the present work exhibited intense single Q band absorption of the π→π* transitions around 665 nm and B bands in the UV region around 341–373 nm. For metal-free derivative **4**, Q band is split into two

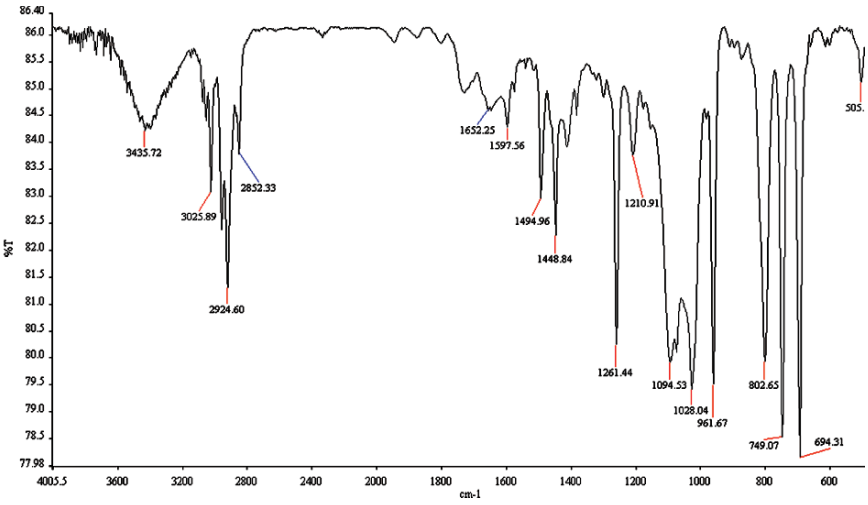

Fig. 46.3 FT-IR spectrum of [2,3,7,8,12,13,17,18-Octakis(3-phenyl-2-propenethio)-porphyrazinato] Mg(II)

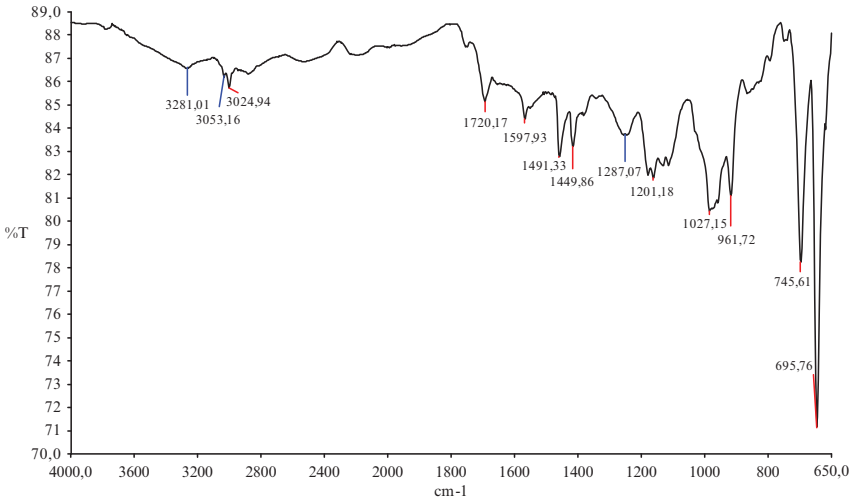

Fig. 46.4 FT-IR spectrum of [2,3,7,8,12,13,17,18-Octakis(3-phenyl-2-propenethio)^{21}H,^{23}H porphyrazine]

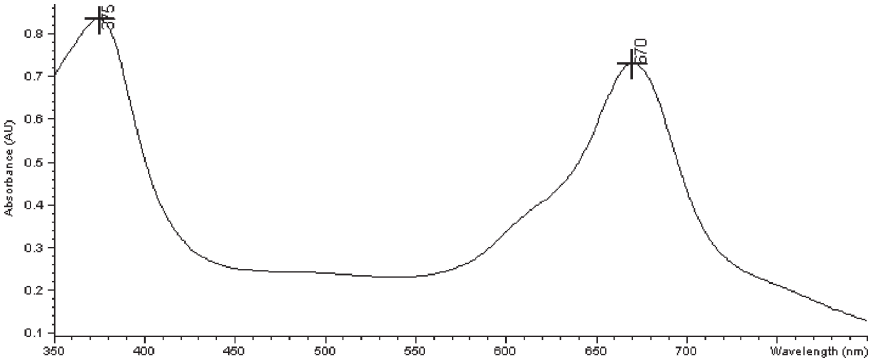

Fig. 46.5 UV–Vis spectrum of porphyrazine MgPz in $CHCl_3$

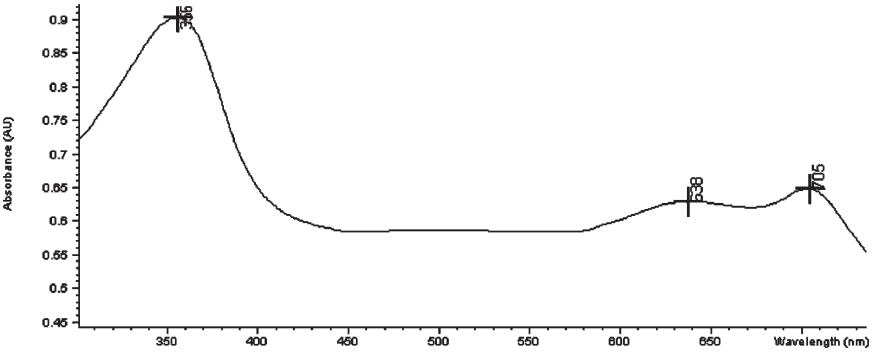

Fig. 46.6 UV–Vis spectrum of metal-free porphyrazine H2Pz in CHCl3

peaks at 638 and 735 nm as a consequence of the change in the symmetry of porphyrazine core from D_{4h} (in the case of metallo derivatives) to D_{2h} (Figs. 46.5 and 46.6). This result is proved the formation of metal free porphyrazine as reported early [2, 14].

^{1}H NMR Spectrum

The ^{1}H NMR spectrum of 1,2-bis(3-phenyl-2-propenethio)maleonitrile ligand four different types of protons are clearly seen: A multiplet around 7.2–7.4 ppm corresponding to Ar-H protons, S-CH_2 protons shifts at 3.92 ppm, a doublet around 6.7 ppm and a multiplet at 6.1–6.2 ppm for propene protons [2, 4–6].

Acknowledgement We express our sincere thanks to the TUBITAK (Project no. 106T392) for financial support

References

1. Luk'yanets, E.A., 1992, *Mol. Mat.,* **1,** 209–216.
2. Gonca, E. and Gül, A., 2005, *Inorg. Chem. Commun.,* **8,** 343–346.
3. Bellec, N., Montalkan, A.G. and Williams, B.M., 1999, *Inorg. Chem.,* **38,** 6143.
4. Polat, M. and Gül, A., 2000, *Dyes Pigments,* **45,** 195–199.
5. Öztürk, R. and Gül, A., 2004, *Tetrahedron Lett.,* **45,** 947–949.
6. Cook, A.H. and Linstead, R.P., 1937, *J. Chem. Soc*., 929.
7. Lindsay, J.K. and Hauser, C.R., 1957, *J. Org. Chem.,* **22,** 355.
8. Vagin, S., Barthel, M., Dini, D. and Hanack, M., 2003, *Inorg. Chem.,* **42,** 2683.
9. Öztürk, R. and Gül, A., 2004, *Tetrahedron Lett.,* **45,** 947.
10. Hasanov, B. and Gül, A., 2001, *Synth. React. Inorg. Met. Org. Chem.,* **31,** 673.
11. Öztürk, R., Güner, S., Aktaş, B. and Gül, A., 2001, *Synth. React. Inorg. Met. Org. Chem.,* **31,** 1623–1630.
12. van Nostrum, C.F. and Nolte, R.J.M., 1996, *Chem. Commun*., 2385–2392.
13. Pullen, A.E., Faulmann, C. and Cassoux, P., 1999, *Eur. J. Inorg. Chem*., 269–276.
14. Keskin, B., Köseoğlu, Y., Avciata, U., Gül, A., 2008, Polyhedron, **27**(4), 1155–1160.

Chapter 47
Lacunarity Analysis of TEM Images of Heat-Treated Hybrid Organosilica Materials

Raymond V. Rivera-Virtudazo[1], Alvin Karlo G. Tapia[1,4], Jesus Felix B. Valenzuela[4], Leonard Dela Cruz[2,3], Herman D. Mendoza[1], and Emily Valentin Castriciones[2,3]

Abstract The lacunarity of TEM images of heat-treated hybrid organosilica materials incorporating a biphenyl moiety was determined. The measured lacunarity of the samples correlated with the degree of observed clumping. Heat treatment was found to be desirable in decreasing the lacunarity of the samples, leading to an increase in the available surface area of the material.

Keywords Lacunarity analysis, organosilica materials

Introduction

Two classes of materials that have been extensively used as heterogeneous catalysts and adsorption media are microporous (pore diameter ≤ ~20 A) and mesoporous (~20–500 A) inorganic solids [1]. The recent developments in hybrid materials include synthesis of inorganic silica framework systems incorporating organic functionalities by surfactant-mediated polymerization method. The ordered hybrid materials developed have well defined structures which can be made amenable to continues tuning by incorporating various organic moieties, as well as organometallic species. The wide application of these materials in catalysis [2] is a consequence of the microstructures which allow molecules access to the large internal surfaces and cavities that enhance catalytic activity and adsorptive capacity. Morphological characterisation of hybrid materials generally involve various imaging techniques

[1] Materials Science Engineering Program-College of Engineering, University of the Philippines,, Diliman, Philippines

[2] Natural Sciences Research Institute, University of the Philippines, Diliman, Philippines

[3] Inorganic Synthesis and Computational Research Laboratory, Institute of Chemistry, University of the Philippines, Diliman, Quezon City, 1101 Philippines

[4] Materials Physics Laboratory, Physics Division, IMSP, CAS University of the Philippines-Los Baños, Laguna, Philippines

B. Sener (ed.), *Innovations in Chemical Biology*, doi: 10.1007/978-1-4020-6955-0

like transmission- and scanning electron microscopy (TEM/SEM), atomic force microscope (AFM), X-ray diffraction, and analysis based on adsorption isotherms to obtain pore size and pore size distribution. To our knowledge, lacunarity analysis of TEM images of mesoporous hybrid organosilica materials incorporating a biphenyl moiety has not been reported to date in the literature.

Lacunarity was originally developed to describe the connectedness of the void spaces of fractals [3]. The fractal dimension is a single parameter that describes the complexity or roughness of the spatial pattern [4]. It is a way of measuring qualities that otherwise have no clear definition such as the degree of roughness or brokenness or irregularity in an object [5]. Fractal analysis is a tool that is being applied to surface science so that one can enhance our ability to work with surfaces. Lacunarity analysis is a multiscale method for describing patterns of spatial dispersion. It can be considered a scale-dependent measure of heterogeneity or texture of an object, whether or not it is a fractal [6]. It can be used with both binary and quantitative data in one, two, and three dimensions. The method is more general and can be readily used to describe nonfractal and multifractal patterns [7].

In this work, lacunarity analysis of TEM images of a previously synthesized hybrid organosilica material incorporating a biphenyl moiety was carried out. The results obtained such as degree of connectedness of holes in sample material were correlated to the visually observed degree of roughness of the material's surface.

Methodology

In this research study an ordered, mesoporous hybrid organosilica material incorporating a biphenyl moiety was fabricated. The polymerization process was surfactant-mediated to ensure uniform pore pattern and narrow pore size distribution. The synthesis of the organosilica precursor was done and investigated by the research group of the Inorganic Synthesis and Computational Research Laboratory of Institute of Chemistry, Diliman, Quezon City.

The 4,4'-dibromobiphenyl was used as the starting material The strategy taken for the synthesis of the organosilica was to carry out Grignard-type reaction to incorporate tetraethyl orthosilicate (TEOS) to 4,4'-dibromobiphenyl to create 4,4'-Bis(triethoxysilyl)biphenyl. Materials from this procedure had been subjected to polymerization surfactant-mediated polymerization. The product obtained was a white powder aggregate. Shown in Table 47.1 are the formulations used for the samples and the heat treatment.

Table 47.1 Formulations used for the samples

Sample	Amount of surfactant (CTAB) in grams	Heat treatment and autoclaving
A	4.87350	Yes
B	2.58844	Yes
C	4.87350	No
D	2.58844	No

Surface characterization of the samples above was done using Transmitted Electron Microscopy (TEM). The TEM pictures were enhanced digitally using ImageJ software [8]. The images were converted to 8-bit images and threshold was applied. Lastly, the images were converted to binary image and were inverted. The digitally inverted binary images were the ones analyzed for lacunarity using the Sliding – Box Lacunarity Scan option of the FracLac 2.1 [9] plugin for Image J.

The sliding box algorithm of calculating the lacunarity is as follows: A box of side *r* was placed at the top left of the binary image, and the number of black pixels inside the box, *s*, was counted. This is also the "mass" of the box. The box was then moved five pixels to the right, and *s* is counted again. This process is repeated over the entire image, producing a frequency distribution of the box masses *n(s,r)*. This frequency distribution is converted into a probability distribution *Q(s,r)* by dividing by the total number of boxes *N(r)* of size *r*.

The lacunarity, Λ, for the given value of *r* is calculated as:

$$\Lambda(r) = \frac{Z_2}{(Z_1)^2}$$

This calculation is repeated over a range of box sizes, and a double – logarithmic plot of the lacunarity versus the size of the sliding box is then produced. FracLac then outputs a text file containing the values of *r* and Λ for each image.

Results and Discussion

The TEM images viewed along different directions of a representative experimental mesoporous organosilica are shown in Figs. 47.1–47.5 for samples A, B, C, and D, respectively. Hybrid hexagonal arrays of mesopores and straight lattice fringes can be seen from the images viewed along and perpendicular to the pore axis, confirming the existence of a 2D hexagonal structural of p6mm symmetry as shown in Fig. 47.1

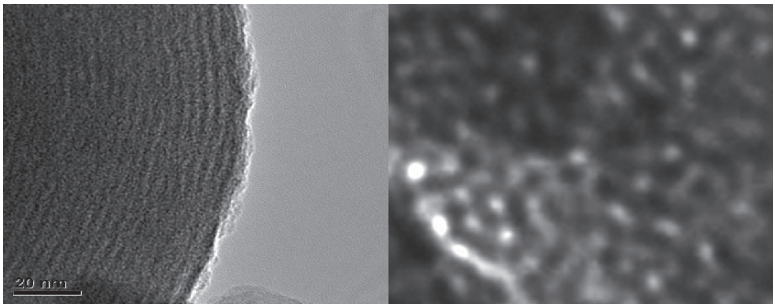

Fig. 47.1 TEM image of sample mesoporous organosilica (left) and cross sectional image (right)

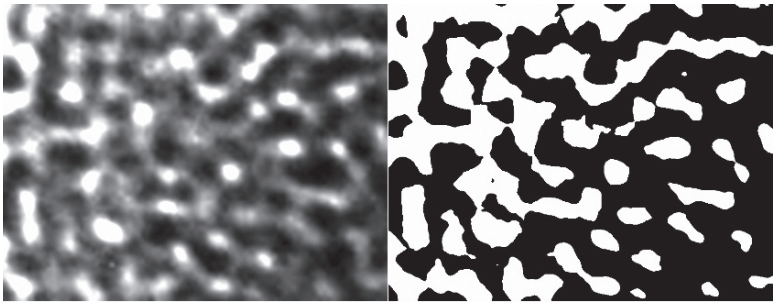

Fig. 47.2 TEM image of sample A (left) and the digitally inverted binary image (right)

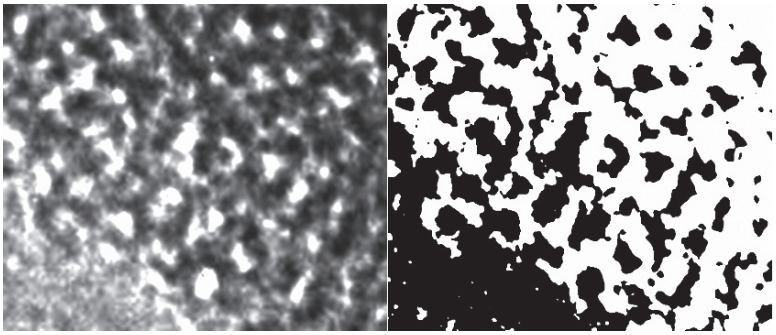

Fig. 47.3 TEM image of sample B (left) and the digitally inverted binary image (right)

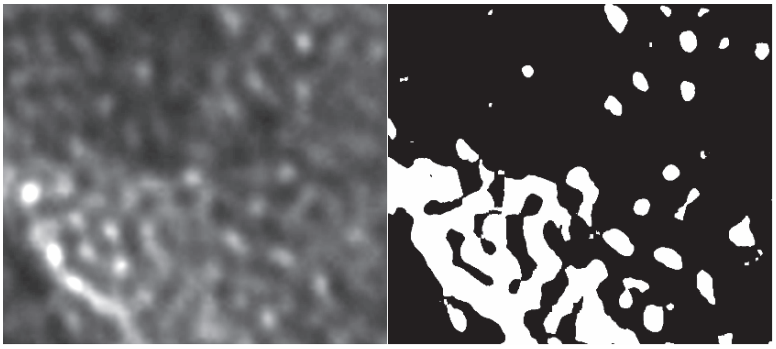

Fig. 47.4 TEM image of sample C (left) and the digitally inverted binary image (right)

(material with one dimensional channels arranged in a hexagonal net). These patterns are similar to those of mesoporous carbon [2], SBA-15 [3], MCM-41[4], demonstrating the long-range tubular order of the mesoporous materials.

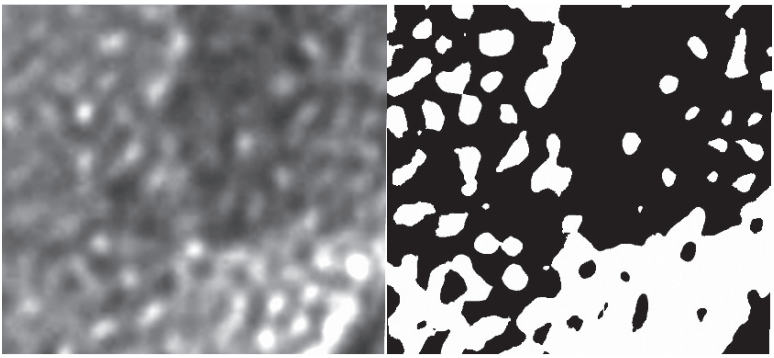

Fig. 47.5 TEM image of sample D (left) and the digitally inverted binary image (right)

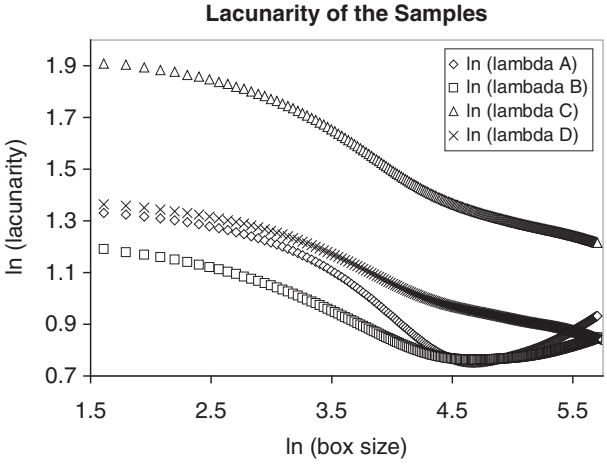

Fig. 47.6 Lacunarity analysis of the samples

Similar structures were found for all samples, but the textures are different. Though structures have hexagonal shape, it can be noticed that they are still heterogeneous. The lacunarity or degree of surface gaps can be used to describe the heterogeneity. Figure 47.6 shows the lacunarity of the samples in a double logarithmic plot.

When the samples were visually inspected, Samples C and D are more clumped together as compared to Samples A and B. As seen in Fig. 47.5, the lacunarity for Samples C and D are relatively higher compared to the lacunarity for Samples A and B. Also, the pores in Samples C and D are also more connected than those of Samples A and B; Samples C and D have more clumping than Samples A and B. These observations correlated with the plotted lacunarities.

It was noticed that the lacunarity of Sample A (heat – treated) is lower than that of Sample C (without heat treatment), which has the same amount of surfactant.

The same trend can be seen when comparing Samples B and D, which have the same amount of surfactant but treated differently (Sample B was heat – treated while Sample D was not). Evidently, the lacunarity is decreased by heat treatment. This indicates that, with heat treatment, the material becomes more homogeneous, and the holes tend to become evenly distributed throughout the material.

Another observation is that the lacunarity of Sample A is higher than that of Sample B. Both were heat-treated, but Sample B has less amount of surfactant than Sample A. The same trend can be observed when comparing Sample C (higher surfactant content) with Sample D (lower surfactant content). However, the difference between the lacunarities of Samples C and D is noticeably larger than that between Samples A and B. This indicates that the holes tend to be more clumped together when the surfactant content is high, although the degree of clumping decreases when the sample is heat-treated.

A high lacunarity indicates that the holes, or pores, are highly – interconnected with each other, and are clumped together. This implies that the surface area available for catalysis is small. A lower value of lacunarity, and therefore a high degree of homogeneity in the distribution of holes, is more desirable for the purposes of effective catalysis. Heat treatment of the sample is therefore desirable. While a lower surfactant concentration gives a lower value of lacunarity, heat treatment lessens the difference in the lacunarities of two sample preparations. Whether the difference would still be significant is a matter for further study.

Conclusion

Lacunarity analysis of TEM images of heat-treated hybrid organosilica materials incorporating a biphenyl moiety obtained in this study correlated well with the observed roughness or heterogeneity of the sample surfaces when visually inspected. Heat treatment of the materials was found to be desirable, as it decreases the heterogeneity of the materials (low lacunarity measured) and increases the effective surface area available for catalysis reactions. Lacunarity analysis of TEM images may be applied to characterize the degree of roughness or the gapiness of surfaces.

Acknowledgments The authors would like to acknowledge Miss Cheng (TEM in-charge with assistance of Yen-Yu Ou) and Judy Obliosca of the Material Science and Engineering at the National Tsing Hua University, 101, Section 2, Kuang Fu Road, Hsinchu 30013, Taiwan, Republic of China.

References

1. Li, C., 2004, *Chiral Synthesis on Catalysts Immobilized in Microporous and Mesoporous Materials*. (Rights Link) Marcel Dekker, New York.
2. Kresge, C.T., Leonowicz, M.E., Roth, W.J., Vartuli, J.C. and Beck, J.S., 1992, *Nature,* **359,** 710–712.

3. Mandelbrot, B., 1982, *The Fractal Geometry of Nature*. Freeman, San Francisco, CA.
4. Asefa, T., MacLachlan, M.J., Coombs, N. and Ozin, G.A., 1999, *Nature,* **402,** 867–871.
5. Gleick, J., 1987, *Chaos: Making a New Science*. Penguin Group, London.
6. Allain, C. and Cloitre, M., 1991, *Phys. Rev. A,* **44,** 3552–3558.
7. Plotnick, R.E. et al.1996, *Phys. Rev. E.,* **53,** 5461–5468.
8. Rasband, W., 2005, *Image J. 1.34n*. Available online at http://rsb.info.nih.gov/ij/
9. Karperien, A., 2004, *FracLac Advanced User's Manual (Frac_Lac.jar) Plugins/Fractal Analysis/FracLac.2005/03/23. version 2.0aF*. Charles Stuart University, Australia. Available online at http://www.geocities.com/akarpe@sbcglobal.net/usefraclac.html

Chapter 48
The Mechanical Properties of Water-Based Emulsion Polymers: Effect of Reaction Conditions

Ayfer Saraç and Kadir Turhan

Abstract Emulsion homopolymers and copolymers (latexes) are widely used in architectural interior and exterior paints, adhesives, and textile industries. Colloidal stabilizators in the emulsion polymerization strongly affect not only the colloidal properties of latexes but also the film and mechanical properties, in general. Additionally, the properties of polymer/copolymer latexes depend on the copolymer composition, polymer morphology, initiator, polymerization medium and colloidal characteristics of copolymer particles.

Copolymerization of vinyl acetate with acrylic monomers can lead to the production of latex having a wide range of mechanical and molecular properties depending on the molecular structure of the emulsifier, and also above parameters.

In this study, mechanical properties of emulsion copolymers of vinyl acetate and butyl acrylate, which consisted of a nonionic emulsifier (30 mol ethoxylated nonylphenol), an oligomeric stabilizator, and ammonium persulfate or potassium persulfate as initiators by changing monomer ratios from 90:10 to 10:90 for VAc:BuA, were determined by differential scanning calorimeter.

Keywords Copolymers, differential scanning calorimeter, emulsion homopolymers, latexes, oligomeric stabilizator, polymerization

Introduction

Water-borne coating systems have been the focus of significant research in recent years, which continues to be driven by tighter environmental regulations. Aqueous based dispersions of polymeric lattices provide a viable alternative to organic

Yıldız Technical University, Faculty of Arts and Sciences, Department of Chemistry
Davutpasa Campus, 34220, Esenler- Istanbul, Turkey

B. Sener (ed.), *Innovations in Chemical Biology*, doi: 10.1007/978-1-4020-6955-0

solvents based coatings by reducing the volatile organic content (VOC) of the final product. Major research areas in this field include studying the coalescence of particles during film formation, film forming ability of different polymeric lattices, interdiffusion of polymer segments during particle coalescence and mechanical and viscoelastic properties of latex coatings. A good collection of articles covering these areas of research interests is presented elsewhere [1].

Emulsion homopolymers and copolymers (latexes) are widely used in architectural interior and exterior paints, adhesives, and textile industries [2–4]. Colloidal stabilizators in the emulsion polymerization strongly affect not only the colloidal properties of latexes but also the film and mechanical properties, in general. Additionally, the properties of polymer/copolymer latexes depend on the copolymer composition, polymer morphology, initiator, polymerization medium and colloidal characteristics of copolymer particles.

Producing a polymer with a desired quality is a major goal in the polymer industry, but defining the reactor's operating conditions to produce a given polymer quality is a difficult task. Optimization of the process involves working with inverse modeling, i.e., search for the reactor's operating conditions based on information of the polymer quality. Emulsion homo and copolymers can be synthesized by applying different production process and using different reactors, such as continuous stirred tank reactor (CSTR), the multi-reactor train and the tubular or loop reactor (LR). Especially in the last 3 decade, many kinds of reactor had been developed by several researchers. LR is one of the most important and an attractive alternative production method for the emulsion homo and copolymers [5, 6]. In the LR continuous process, the reaction mixture is re-circulated by a pump through pipe work fitted with cooling jackets, or sprayed with variable water jets. The heat is removed throughout the piping. The ratio of water phase to monomer and the total input volume can be controlled, as can the rate of recirculation. The flow of cooling water is automatically controlled since overcooling may retard the reaction. If the built-up monomer suddenly polymerizes, it is not possible to control the exothermic reaction. If overheating is applied, the initiator decomposes too rapidly, leading to loss of reaction later in the process or even destabilization of the polymer particles. It is easier to control the reaction temperature in the loop process with such a small reaction volume and the absence of reflux.

The stabilizing of aqueous latexes succeeded by using emulsifiers (anionic, nonionic) and/or their mixture, steric stabilizators (polyvinyl alcohol (PVOH), hydroxyethyl cellulose, polyethylene glycol, new protective colloids etc.), and polymerizable surfaces active agents, in general. Vinyl acetate (VAc) emulsion homopolymers and copolymers (latexes) are widely used as binders in water-based interior and exterior architectural paints, coatings, and adhesives, since they have higher mechanical and water resistance properties than the homopolymers of both monomers [2, 4, 7].

Copolymerization of VAc with acrylic monomers can lead to the production of latex having a wide range of mechanical and molecular properties depending on the molecular structure of the emulsifier, copolymer composition, initiating system and protective colloid in the polymerization. One of the most important industrial

latexes, widely utilized in water-based architectural (exterior or interior) coatings, and adhesives market, is the VAc/butyl acrylate (BuA) emulsion copolymer [2, 5, 6], with a BuA composition of 15–30%, since they have higher mechanical and water resistance properties than the homopolymers of both monomers.

In this study, mechanical properties of emulsion copolymers of VAc and BuA were determined by differential scanning calorimeter (DSC).

Materials and Methods

Batch emulsion copolymerization of VAc and BuA was carried out using a nonionic emulsifier (30 mol ethoxylated nonylphenol, NP 30), a new oligomeric stabilizator (N-methylol acrylamide, AMOL), Nopco-1497 as antifoam agent, and ammonium persulfate (APS) as initiator by changing monomer ratios from 100:0 to 0:100 for VAc:BuA in the loop reactor. The monomer ratio of VAc and BuA were changed in the copolymerization (VAc:BuA 100:0, 90:10, 75:25, 60:40, 50:50, 40:60, 25:75, 10:90 and 0:100) at 70^0C and 400 rpm constant stirring rate in the loop reactor. Some detailed information about loop reactor was given in literature [7]. The effects of BuA (wt %) increased in the copolymer composition on the glass transition temperature of emulsion copolymers obtained were investigated. Glass transition temperature of all polymers was determined by using DSC Perkin Elmer Pyris 6 model. A sample of copolymerization recipe was given in Table 48.1.

Results and Discussion

T_g of the copolymers with both initiators showed similar trend to the homoBuA's T_g with increasing BuA percentage in the copolymer composition. T_g's of VAc-co-BuA latexes have decreased with BuA percentage in the copolymer composition for APS and PPS very regularly (Figs. 48.1 and 48.2).

Glass transition temperatures (T_gs) of either VAc-BuA homopolymers or copolymers obtaining by DSC were shown that in Figs. 48.1 and 48.2 related with changing BuA percentage in the copolymer composition. T_g of the copolymers with both initiators moves to the homoBuA's T_g with increasing BuA percentage in the copolymer composition. Because it is known that T_g's poly(VAc) and T_g's poly(BuA) are +32C and −54C, respectively [8]. It was shown that T_g's of polymers decrease linearly in this figure.

Table 48.1 Recipes used in copolymerization experiment

Substance	VAc	BuA	Oligomeric stabilizator	NP30	Initiator	$NaHCO_3$	Nopco-1497	Deionized water	Total (%)
Weight (%)	39.34	4.37	1.88	3.60	0.24	0.12	0.09	50.36	100.00

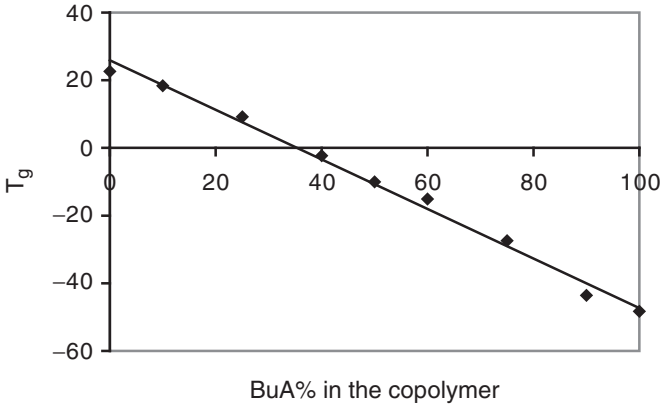

Fig. 48.1 Variation of Tg with BuA content in copolymer latexes in the presents of APS

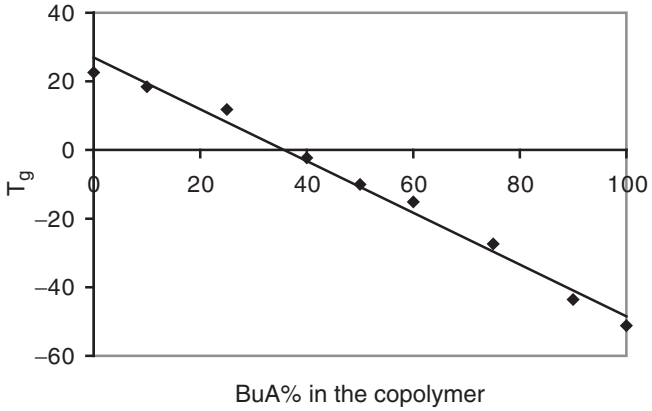

Fig. 48.2 Variation of Tg with BuA content in copolymer latexes in the presents of PPS

Copolymer (rich VAc) T_gs with PPS were found smaller than with APS. In these polymers T_g decreases because of the hydration shell formed at the end of grafting reactions of VAc with AMOL and APS on the polymer particles and obtaining branched structure [9]. Crosslinking happens during the forming films of latexes with AMOL, which is having functional end groups [10]. This structure of AMOL causes crosslinking and increasing of copolymer T_g. In other words crosslinking reaction takes place AMOL's molecules themselves, and also happens AMOL and PVAc chains. At the end of these reactions AMOL looses hydrophilic groups, having highly mechanical and water resist films are obtained compared with classical protective colloid such as PVOH.

Acknowledgements This research has been supported by State Planning Organization of Turkey (Project no. 24-DPT-01-02-01).

References

1. Agarwal, N. Farris, R.J., 2000, *Polym. Eng. Sci.,* **40,** 376–390.
2. Lovell, P.A. El-Aasser, M.S., 1997, *Emulsion Polymerization and Emulsion Polymers*, Wiley, Chichester, UK.
3. El-Aasser, M.S. Vanderhoff, J.W., 1981, *Emulsion Polymerization of Vinyl Acetate*, Applied Science Publishers, London.
4. Erbil, H.Y., 2000, *Vinyl Acetate Emulsion Polymerization and Copolymerization with Acrylic Monomers*, CRC, Boca-Raton, FL.
5. Geddes, K., 1983, The Loop Process, *Chem. Ind.,* **21,** 223–228.
6. Geddes, K., 1989, Start-up and Growth Mechanism in the Loop Continuous Reactor, *Brit. Polym. J.,* **21,** 434–441.
7. Sarac, A. Yildirim, H., 2003, Effect of Initiators and Ethoxylation Degree of Non-Ionic Emulsifiers on Vinyl Acetate and Butyl Acrylate Emulsion Copolymerization in the Loop Reactor. *J. Appl. Polym. Sci.,* **90**(2), 537–543.
8. Brandrup, J. and Immergut, E.H., 1989, *Polymer Handbook*, Wiley-Interscience/Wiley, New York.
9. Donescu, D., Ciupitoiu, A., Gosa, K. Languri, I., 1993, Water Polymer Interaction During Emulsion Polymerization of Vinyl Acetate, *Revue Roumaine de Chimie,* **38**(12), 1441–1448.
10. Bonardi, C., Christou, Ph., Llauro-Darricades, M.F., Guillot, J., Guyot, A. and Pichot, C., 1989, *Polymer Latex III International Conference, Characterization of Acrylic Latexes Functionalized by N-Methylol Acrylamide*, 6/1-6/14, Plastics and Rubber Institute, London.

Chapter 49
Investigation of Spectrophotometrical and Fluorescent Behavior of 1,3-Diethyl-5-(Quinoline-2-Ylmethylene)-2-Thioxodihydropyrimidine-4,6(1*H*,5*H*)-Dione in Various Solvents

Mevlüde Canlıca, H. Kerim Beker, İbrahim E. Özyiğit, Alper Akıncı, and Şeniz Kaban

Abstract Heterocyclic compounds containing atoms of the elements such as nitrogen, sulfur and oxygen as ring members are commonly used in various fields of industry as analytical reagents, ligands, dyestuffs, pharmaceutical substances and bioindicators.

In this study 5-(Quinoline-2-ylidene)-1,3-diethyl-2-thiobarbituric acid have been synthesized via Knoevenagel condensation reaction, the product solutions were prepared 10^{-3}–10^{-5} M in $CHCI_3$, THF, MeOH, DMF and DMSO. UV/VIS spectra recorded and then compared at each other. Absorbance of the solutions were measured at 200–300 nm. The maximum absorbance value increased and a new absorption appeared at 400–500 nm. The samples were excited at 337 nm in order to measure fluorescence. The maximum emission was observed in MeOH at 398 nm. These values increased by time; therefore, the samples were not stable in solution state.

Keywords Fluorescence, Heterocyclic compound, Knoevenagel condensation, Spectroscopy

Introduction

Heterocyclic compounds and their derivatives, which are developing quite rapidly and becoming more important day by day, constitute a branch of organic chemistry. Heterocyclic compounds containing atoms of the elements such as nitrogen, sulfur and oxygen as ring members are commonly used in various fields of industry as analytical reagents, ligands, dyestuffs, pharmaceutical substances and bioindicators [1–5].

Yıldız Technical University, Science and Art Faculty, Chemistry Department, 34220, Esenler-Istanbul, Turkey

B. Sener (ed.), *Innovations in Chemical Biology*, doi: 10.1007/978-1-4020-6955-0

1,3-Diethyl-5-(quinoline-2-ylmethylene)-2-thioxodihydropyrimidine-4,6(1*H*,5*H*)-dione has been synthesized by the reaction of 1,3-diethyl-2-thiobarbituric acid with quinoline-2-carboxaldehyde via Knoevenagel condensation [6–11].

In the present paper, the effect of various solvents on the absorption spectrum and the fluorescence spectrum of a heterocyclic compound was investigated.

Experimental

Reagent

All of chemicals were purchased from E. Merck: MeOH, $CHCI_3$, THF, DMF and DMSO. Bidistilled water was used.

Instrumentation

Routine electronic spectra were recorded on a Unicam UV/VIS spectrophotometer and routine fluorescence spectra were recorded on a PTI C71 Time Master Spectroflorometer including nanoflash nitrogen arc lamp and a stroboscopic detector by the Instrumental Analysis Laboratory of Chemistry Department, YTU.

Solutions

Compound solutions were prepared daily in 1.5×10^{-5} M, 10^{-4} M and 10^{-3} M of MeOH, $CHCI_3$, THF, DMF and DMSO.

Assay Procedure

Fluorescence spectra and UV/VIS spectra of compound solutions were recorded freshly, after one day and two months against its solvents and then they were compared to each other. Optimum fluorescence measurement settings were adjusted as λ_{ex} = *337 nm*, *ınt time: 0.1*, *step size: 0.5*, *averages: 3*, *slit with: completely open* and then they were compared to each other.

Results and Discussion

All organic compound are capable of absorbing electromagnetic radiation because all contain valence electrons that can be excited to higher energy levels. The electrons that contribute to absorption by an organic molecule are: (1) those that

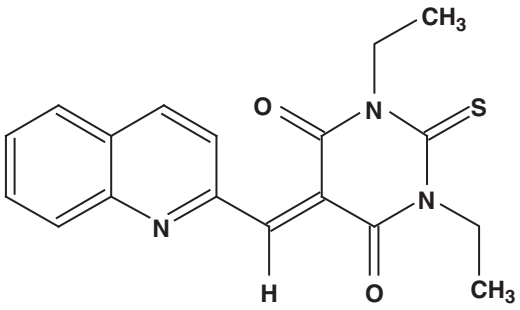

The Structure of Compound

participate directly in bond formation between atoms and are thus associated with more than one atom, (2) nonbonding or unshared outer electrons that are largely localized about such atoms as oxygen, the halogens, sulfur, and nitrogen. As n→π* and π→π* transitions, most applications of absorption spectroscopy to organic compounds are based upon transitions for n or ıı electrons to the π* excited state because the energies required for these processes bring the absorption peaks into an experimentally convenient spectral region (200–700 nm). Another characteristic difference between the two types of absorption is the effect exerted by the solvent on the wavelength of the peaks. Peaks associated with n→π* transition are generally shifted to shorter wavelengths (a hypsochromic or blue shift) with increasing polarity of the solvent. Usually, but not always, the reverse trend (a bathochromic or red shifted) is observed for π→π* transitions. The hypsochromic effect apparently arises from increased solvation of the unbonded electron pair, which lowers the energy of the n orbital. The most dramatic effects of this kind are seen with polar hydrolytic solvents, such as water or alcohols, in which hydrogen bond formation between the solvent protons and the nonbonded electron pair is extensive. A blue shift, also roughly corresponding to the energy of the hydrogen bond, is therefore observed. Thus, the energy of the n, π* excited state is not affected by this type of solvent interaction. A second solvent effect that undoubtedly influences both ıı→π* ve n→π* transition leads to a bathochromic shift with increased solvent polarity.

In choosing a solvent, consideration must be given not only to its possible effects upon the absorbing system. Quite generally, polar solvents tend to obliterate spectral fine structure arising from vibrational effects. In addition, the positions of absorption maxima are influenced by nature of the solvent. n→π* and π→π* transitions show electronic spectra with conjugated π electrons in the UV region at about 300–350 nm (B band) and in the visible portion at 500–600 nm.

It is important to note fluorescence seldom results from absorption of ultraviolet radiation of wavelengths lower than 250 nm because such radiation is sufficiently energetic to cause deactivation of the excited states by predissociation or dissociation. Fluorescence due to σ→σ* transitions is seldom observed; instead, such

emission is confined to the less energetic π*→π and π*→n processes. The most intense and the most useful fluorescence is found in compounds containing aromatic functional groups with low-energy π→π* transition levels. Highly conjugated double-bond structures may also exhibit fluorescence; on the other hand, fused ring structures ordinarily do.

The compound was dissolved in solvents that has various polarity. The optimum conditions for concentration were investigated with respect to maximum absorption. Increasing concentration as 10^{-5}, 10^{-4}, 10^{-3} M was lost spectral fine structure when there was hyperchromic effect in absorption spectra. Optimal conditions were chosen as 1.5 x 10^{-5} M, since this gives the highest absorbance value. The solutions of the compounds were prepared daily in 10^{-5} M of MeOH, $CHCI_3$, THF, DMF and DMSO.

As shown in Figs. 49.1–49.6, when the electronic spectra of the compound was investigated, the same peculiarities were observed as mentioned above. Increasing the polarity of the solvent as DMSO > DMF > MeOH > THF > $CHCI_3$ was shown to generally result in electronic spectra. Absorbance of the solutions were observed at 230–310 nm. The maximum absorbance value changed and a new absorption appeared at 510–550 nm as 1: fresh, 2: one day, 3: two months. The assay results obtained for each solvent are summarised in Table 49.1.

Fluorescence measurements of the compound were measured freshly, after an incubation of one day and two months in various solvents such as 1.5 x 10^{-3} M, 1.5 x 10^{-4} M and 1.5 x 10^{-5} M of MeOH, $CHCI_3$, THF, DMF and DMSO at room temperature. In the experiments, all the sample solutions were excited at 337 nm. As shown in Figs. 49.7–49.9, when the fluorescence spectra of the compound was investigated, the same peculiarities were observed as mentioned above. Optimum fluorescence yield was obtained in 1.5 x 10^{-4} M of MeOH, therefore, we decided to measure fluorescence in it (Fig. 49.9). Maximum fluorescence emission intensity was observed at 398 nm in the fluorescence spectra. The results showed that the fluorescence intensities increased by time. These observations are compatible with the other results obtained from UV/VIS spectrophotometer to clarify the behaviour of the molecule in solution state.

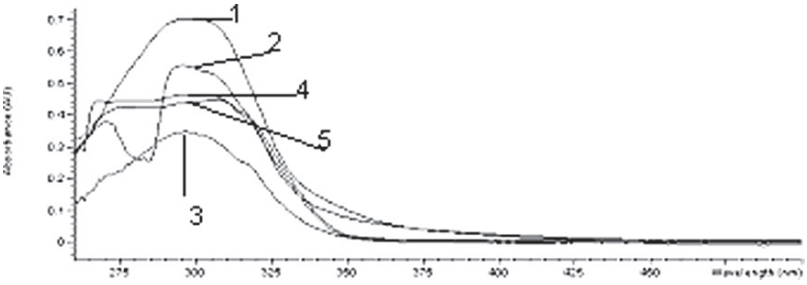

Fig. 49.1 Electronic spectra of 1.5 × 10^{-5} M compound in 1: $CHCI_3$, 2: THF, 3: MeOH, 4: DMF, 5: DMSO

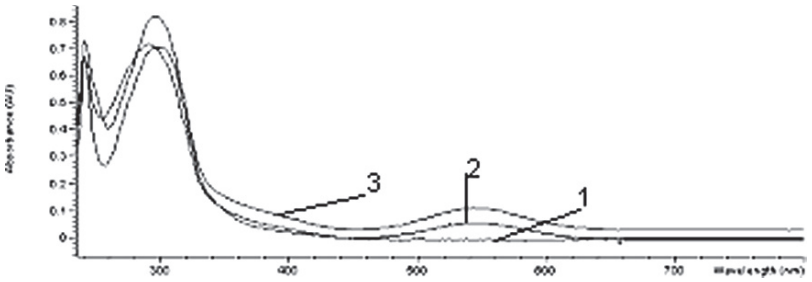

Fig. 49.2 Electronic spectrum of 1.5×10^{-5} M compound in $CHCI^3$

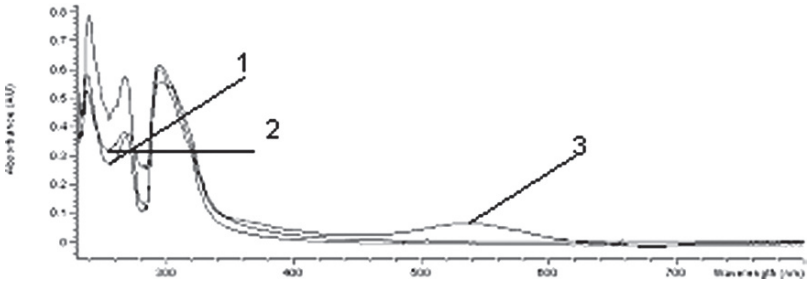

Fig. 49.3 Electronic spectrum of 1.5×10^{-5} M compound in THF

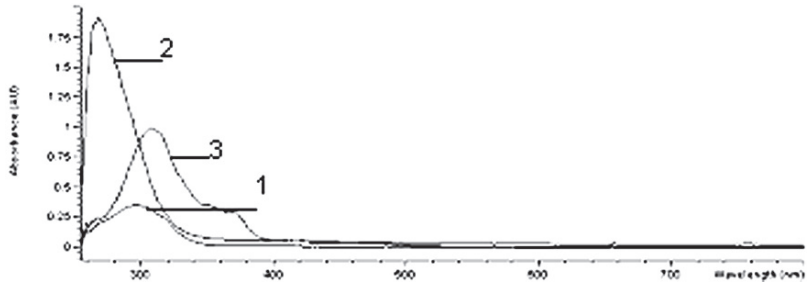

Fig. 49.4 Electronic spectrum of 1.5×10^{-5} M compound in MeOH

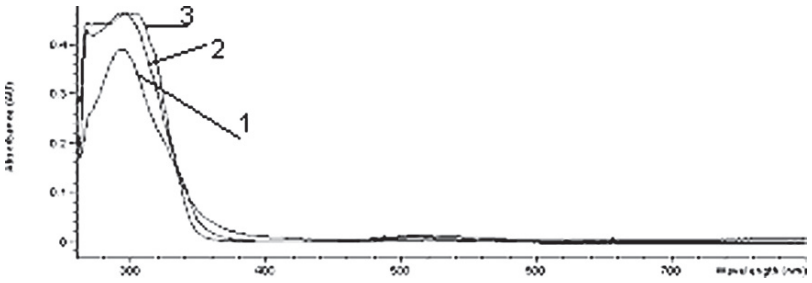

Fig. 49.5 Electronic spectrum of 1.5×10^{-5} M compound in DMF

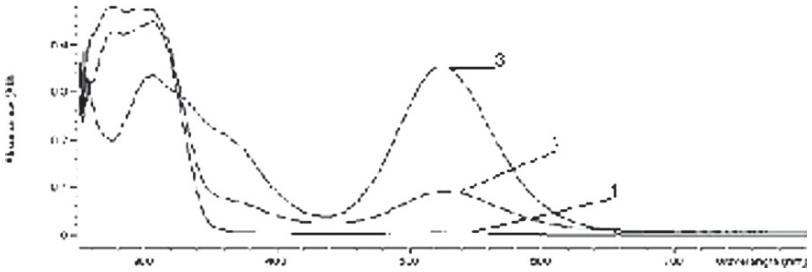

Fig. 49.6 Electronic spectrum of 1.5 × 10–5 M compound in DMSO

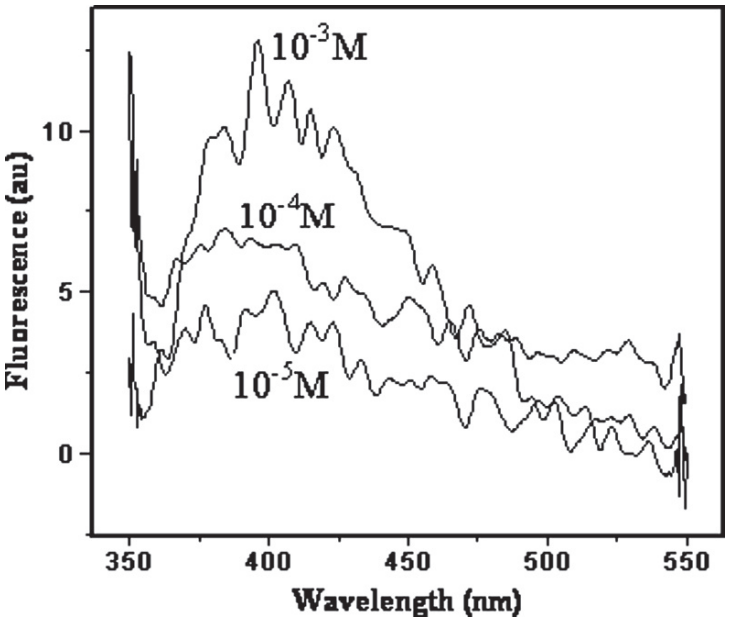

Fig. 49.7 Time resolved fluorescence spectra of the fresh sample solutions of MeOH in various concentrations

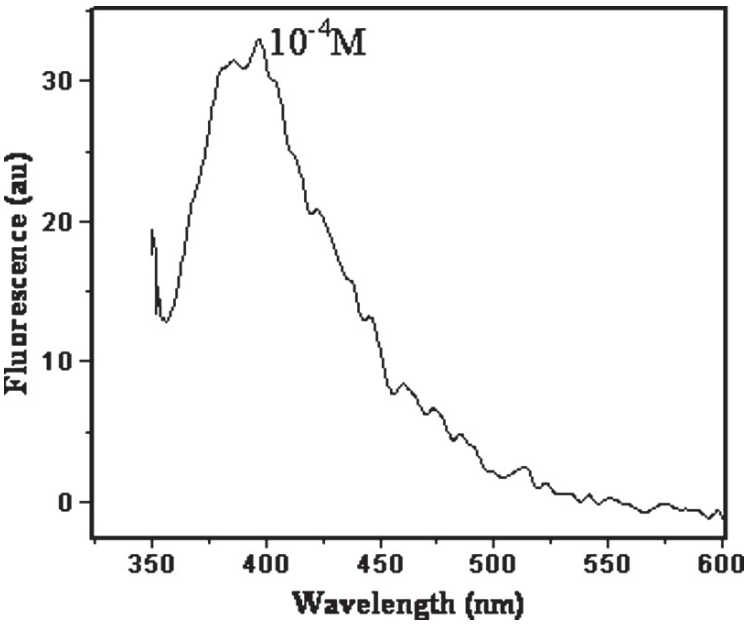

Fig. 49.8 Fluorescence spectrum of the sample solution of MeOH incubated for a day

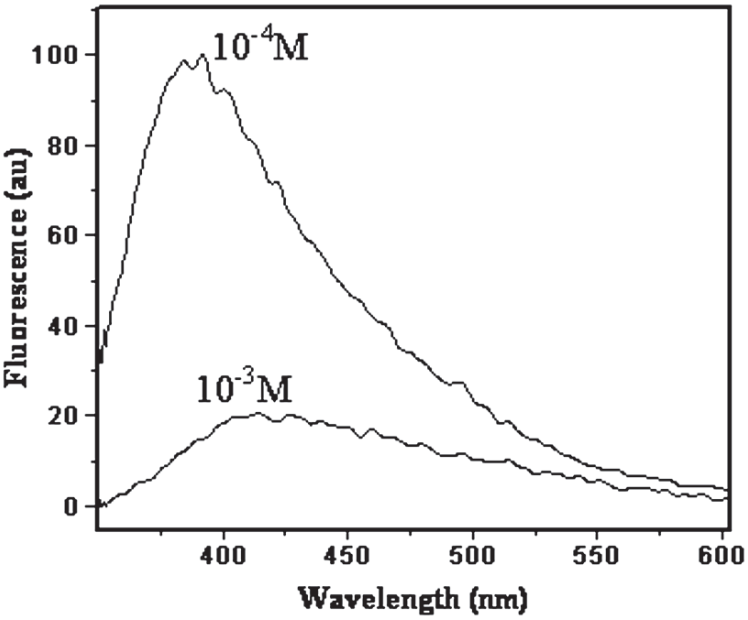

Fig. 49.9 Fluorescence spectra of the sample solutions of MeOH incubated for two months

Table 49.1 Spectral data of 1.5×10^{-5} M compound in solvents

Solvent		Fresh (1)			One Day (2)			Two Month (3)		
$CHCl_3$ (1)	λ(nm)	241	297	398	241	291	546	241	296	545
	Abc	0.0666	0.704	–	0.670	0.714	–	0.730	0.820	0.110
THF (2)	λ(nm)	238/270	295	430	238/267	295	488	239/267	0.294	537
	Abc	0.582/0.378	0.554	–	0.526/0.381	0.602	–	0.739/0.575	0.614	0.063
MEOH (3)	λ(nm)	–	297	485	268	–	399	–	308	369
	Abc	–	0.348	–	1.918	–	0.052	–	0.986	0.287
DMF (4)	λ(nm)		304			293			293	
	Abc		0.465			0.465			0.391	
DMSO (5)	λ(nm)	277	306		276	304	526	255	305	525
	Abc	0.425	0.448		0.480	0.474	0.091	0.317	0.335	0.353

References

1. htpp://www.unode.org/images/bulletin/bulletin_1957-01_1_pages_img001_small
2. htpp://www.sciencedaily.com/encyclopedia/emil-knoevenagel
3. htpp://people.bu.edu/jaylowe/Named%20reactions/K/Knoevenagel/Knoevenagel.htm
4. Beyer, H., 1963, Organic Chemistry, Verlag Harri Deutsch, Frankfurt, Germany.
5. Solomons, T.W.G., 1992, Organic Chemistry, 5th ed., Wiley, New York.
6. Rabjohn, N., 1976, *Org. React.,* **24,** 261.
7. March, J., 1985, Advanced Organic Chemistry, Reactions, Mechanisms and Structure, 3rd ed., John Wiley and Sons, Inc., New York.
8. Knoevenagel, E., 1898, *Condensation von Malonseaure mit Aromatischen Aldehyden Durch Ammoniak und Amine, Ber.,* **31,** 2596–2619.
9. Jursic, B.S., 2001, *J. Heterocyclic Chem.,* **38,** 655–657.
10. Jursic, B.S. Stevens, E.D., 2002, *Tetrahedron Lett.,* **43,** 5681–5683.
11. Akıncı, A., 2005, Kinolinil Substitüe Barbitürik ve Tiyobarbitürik Asit Türevlerinin Sentezi, FBE, Yıldız Technical University, Istanbul, Turkey. M.Sc. Thesis

Annex

Plenary lectures presented at the 9th Eurasia Conference on Chemical Sciences (EuAs C_2S-9) held in Antalya, Turkey during September 9–13, 2006 published in *Pure and Applied Chemistry*, Vol. 79, No. 12, pp. 2101–2177, 2007.

Index